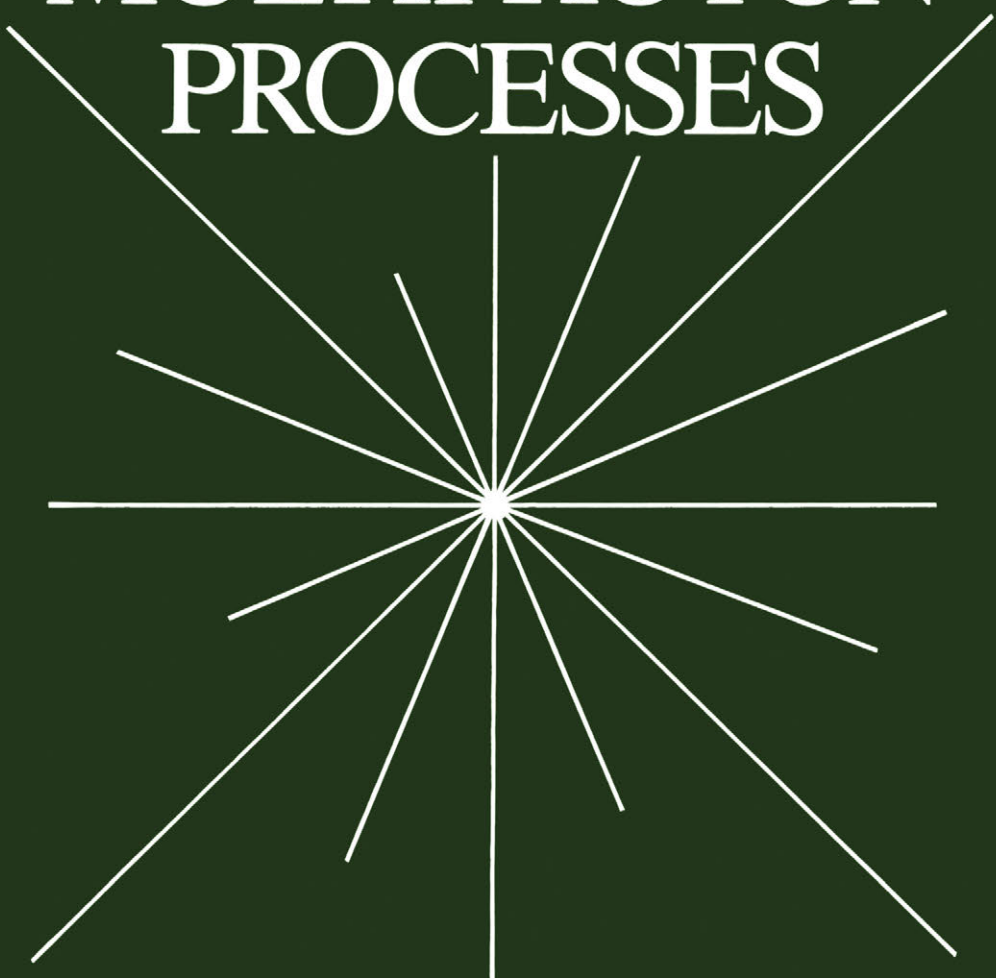


Physics of Atoms and Molecules

THEORY OF MULTIPHOTON PROCESSES



FARHAD H. M. FAISAL

THEORY OF
MULTIPHOTON
PROCESSES

PHYSICS OF ATOMS AND MOLECULES

Series Editors

P. G. Burke, *The Queen's University of Belfast, Northern Ireland*
H. Kleinpoppen, *Atomic Physics Laboratory, University of Stirling, Scotland*

Editorial Advisory Board

R. B. Bernstein (*New York, U.S.A.*)
J. C. Cohen-Tannoudji (*Paris, France*)
R. W. Crompton (*Canberra, Australia*)
J. N. Dodd (*Dunedin, New Zealand*)
G. F. Drukarev (*Leningrad, U.S.S.R.*)
W. Hanle (*Giessen, Germany*)

C. J. Joachain (*Brussels, Belgium*)
W. E. Lamb, Jr. (*Tucson, U.S.A.*)
P.-O. Löwdin (*Gainesville, U.S.A.*)
H. O. Lutz (*Bielefeld, Germany*)
M. R. C. McDowell (*London, U.K.*)
K. Takayanagi (*Tokyo, Japan*)

ATOM—MOLECULE COLLISION THEORY: A Guide for the Experimentalist

Edited by Richard B. Bernstein

ATOMIC INNER-SHELL PHYSICS

Edited by Bernd Crasemann

ATOMS IN ASTROPHYSICS

Edited by P. G. Burke, W. B. Eissner, D. G. Hummer, and I. C. Percival

AUTOIONIZATION: Recent Developments and Applications

Edited by Aaron Temkin

COHERENCE AND CORRELATION IN ATOMIC COLLISIONS

Edited by H. Kleinpoppen and J. F. Williams

COLLISIONS OF ELECTRONS WITH ATOMS AND MOLECULES

G. F. Drukarev

DENSITY MATRIX THEORY AND APPLICATIONS

Karl Blum

ELECTRON AND PHOTON INTERACTIONS WITH ATOMS

Edited by H. Kleinpoppen and M. R. C. McDowell

ELECTRON—ATOM AND ELECTRON—MOLECULE COLLISIONS

Edited by Juergen Hinze

ELECTRON-MOLECULE COLLISIONS

Edited by Isao Shimamura and Kazuo Takayanagi

INNER-SHELL AND X-RAY PHYSICS OF ATOMS AND SOLIDS

Edited by Derek J. Fabian, Hans Kleinpoppen, and Lewis M. Watson

INTRODUCTION TO THE THEORY OF LASER—ATOM INTERACTIONS

Marvin H. Mittleman

ISOTOPE SHIFTS IN ATOMIC SPECTRA

W. H. King

PROGRESS IN ATOMIC SPECTROSCOPY, Parts A, B, and C

Edited by W. Hanle, H. Kleinpoppen, and H. J. Beyer

THEORY OF MULTIPHOTON PROCESSES

Farhad H. M. Faisal

VARIATIONAL METHODS IN ELECTRON—ATOM SCATTERING THEORY

R. K. Nesbet

A Continuation Order Plan is available for this series. A continuation order will bring delivery of each new volume immediately upon publication. Volumes are billed only upon actual shipment. For further information please contact the publisher.

THEORY OF MULTIPHOTON PROCESSES

Farhad H. M. Faisal

*University of Bielefeld
Bielefeld, Federal Republic of Germany*

SPRINGER SCIENCE+BUSINESS MEDIA, LLC

Library of Congress Cataloging in Publication Data

Faisal, Farhad H. M.

Theory of multiphoton processes.

(Physics of atoms and molecules)

Includes bibliographical references and index.

1. Multiphoton processes. I. Title. II. Series.

QC793.5.P422F35 1986

539.7'217

86-22674

ISBN 978-1-4899-1979-3

ISBN 978-1-4899-1977-9 (eBook)

DOI 10.1007/978-1-4899-1977-9

© 1987 Springer Science+Business Media New York

Originally published by Plenum Press , New York in 1987

Softcover reprint of the hardcover 1st edition 1987

All rights reserved

No part of this book may be reproduced, stored in a retrieval system, or transmitted in any form or by any means, electronic, mechanical, photocopying, microfilming, recording, or otherwise, without written permission from the Publisher

To my mother,
who nourished my first interests in theoretical subjects,
and
to the memory of my father

Preface

My aim in this book has been to give an account of the theoretical methods of analysis of multiphoton processes in atomic physics. In this account I have emphasized systematic methods as opposed to ad hoc approaches. Both perturbative and nonperturbative methods are presented with illustrative results of concrete applications. The perturbation theory is the primary tool of analysis of nonresonant multiphoton processes. It is developed here in conjunction with a diagrammatic language and is also renormalized to free it from the unwanted divergences which accompany the ordinary treatment when higher-order corrections are considered. The nonperturbative methods (i.e., methods other than that of power series expansion in the field strength) become particularly important for consistent treatments of problems involving, for example, intermediate resonances, high field strengths, and finite pulse duration. The specifically nonperturbative methods for multiphoton transitions are presented in Chapters 6–11. The methods of resolvent equations and of effective Hamiltonians are developed for both the stationary and the time-dependent fields. The density matrix method is presented in conjunction with the problems of relaxation and of fluctuating fields. The Floquet theory is presented both in the energy domain and in the time domain. Also treated are the methods of continued fractions, recursive iterative equations, and chain Hamiltonians. Non-Hermitian Hamiltonian methods for multiphoton transitions are developed using the techniques of optical potential and rotation of coordinates. The book closes with a chapter on the theory of multiple emission and absorption of photons during electron-atom collisions in a laser field.

I have tried to give each chapter a somewhat autonomous character so that the reader may use a part of the book without necessarily having to read everything that precedes it. References to the literature sources used are provided throughout the text, and I hope these will be useful to the reader. I must add, however, that they are by no means meant to be exhaustive. The interested reader will find a comprehensive bibliography on

the subject in the excellent ongoing compilation *Multiphoton Bibliography*, edited by J. H. Eberly *et al.* (see, e.g., N.B.S. LP-92 suppl. 4/1984, University of Colorado and University of Rochester, edited by J. H. Eberly, N. D. Pitche, and J. W. Gallagher).

This book is primarily intended for those who plan to pursue active theoretical research in the subject. This group may include research students or more mature physicists to whom the subject may be new. Some of the extensions and developments that have not appeared in print before might be of interest to specialists in the subject.

During the period of writing this book I have benefited from numerous exchanges with many of my colleagues and students. I am especially thankful to Dr. J. T. Broad, Dr. M. Crance, Prof. A. Maquet, Prof. R. P. McEachran, and Dr. D. Miller for their helpful correspondence and/or comments on the manuscript. I am indebted to Prof. A. Maquet for sending me the original of Figure 22, to Mr. L. Dimou for Figures 52–64, to Mr. S. Jetzke for Appendix 2, and to Dr. D. Miller for preparing the index. I would like to thank Mr. H. Zerhau for typing the manuscript with exemplary patience. It is a pleasure to thank Dr. Ken Derham and the staff of Plenum Publishing Corporation for their excellent collaboration at various stages of producing this book. The research leading to this work has been supported by the Deutsche Forschungsgemeinschaft under Project No. SFB-216-M2. Finally, my special thanks are due to Prof. H. Kleinpoppen, whose friendly invitation and encouragements to write a monograph on the subject initiated this work.

F. H. M. Faisal

Contents

1. Electrons and Atoms in a Radiation Field	1
1.1. Introduction	1
1.2. The Minimum-Coupling Prescription	1
1.3. The First Quantization and the Semiclassical Approximation	4
1.4. The Gauge Invariance and Gauge Transformation of the Schrödinger Equation	5
1.5. The Hamiltonian of a Light Wave	6
1.6. The Dipole Approximation and Two Forms of the Interaction Hamiltonian	8
1.7. The Wave Function of a Free Electron in a Laser Field	10
1.7.1. The Wave Function in the “Velocity Gauge”	10
1.7.1.1. The Linearly Polarized Laser Field	10
1.7.1.2. The Circularly Polarized Laser Field	11
1.7.2. The Wave Function in the “Length Gauge”	12
1.8. From Light Waves to Photon Fields	12
1.8.1. The Second Quantization of Light Fields	14
1.9. The Hamiltonian of an Atom in a Monomode Laser Field in the Dressed-Oscillator Representation	18
1.10. The Dressed-Oscillator Atom–Field Hamiltonian with Multimode Laser Fields	22
1.11. Dressed Frequencies and Polarizations of a Two-Mode Field	25
1.12. The “Length-Form” Atom–Field Hamiltonian	27
2. The Perturbation Theory	29
2.1. Introduction	29
2.2. Time-Dependent Perturbation Theory	29
2.3. The Diagrammatic Method	34
2.4. Rules for Construction of the Diagrams	34
2.4.1. Two-Photon Absorption	36
2.4.2. Three-Photon Absorption	39
2.4.3. Four-Photon Absorption	39

2.4.4. Single-Photon Absorption	40
2.4.5. Two-Photon Absorption (Two-Mode Field)	41
2.4.6. Third-Harmonic Generation (Two-Mode Field)	42
2.4.7. Stimulated Emission of One Photon and Absorption of Two Photons in a Three-Mode Interaction	44
2.5. Rules for Writing Down the Transition Amplitude from a Diagram	45
2.5.1. Two-Photon Absorption	46
2.6. The Rate of Multiphoton Transition and the Generalized Cross Section	47
3. Renormalization of Perturbation Theory	53
3.1. Breakdown of Conventional Perturbation Theory	53
3.2. The Resolvent and the Wave Function	55
3.3. The T-Matrix and the “Linked Cluster” Expansion of T	57
3.4. Relation between True and Reduced T-Matrices	58
3.5. The Renormalized T-Matrix	59
3.6. Energy Renormalization of External States	60
3.7. Lagrange Expansion of the Energy Shift	61
3.8. Energy Shift from the Effective Hamiltonian	62
3.9. The Renormalized Rate of Multiphoton Transitions	63
3.9.1. The Singular ζ -Function	63
3.9.2. The Transition Rate	64
4. Methods for Evaluation of Generalized Cross Sections	67
4.1. Introduction	67
4.2. The Method of Green’s Function	68
4.2.1. The Radial Coulomb Green’s Function	69
4.2.1.1. The Closed-Form Representation	69
4.2.1.2. The Integral Representation	70
4.2.1.3. The Sturmian Representation	71
4.2.2. The Quantum-Defect Radial Green’s Function	73
4.2.2.1. The Closed-Form Representation	73
4.2.2.2. The Pseudopotential Green’s Function	77
4.3. The Method of Inhomogeneous Differential Equations	79
4.4. The Pseudocontinuum-Basis Method	82
4.5. The Truncated Summation Method	85
5. Nonresonant Multiphoton Ionization	89
5.1. Introduction	89
5.2. Multiphoton Ionization of the Hydrogen Atom	90
5.2.1. Two-Photon Ionization of the Hydrogen Atom	92
5.2.2. Three- and Many-Photon Ionization of Hydrogen	97
5.3. Multiphoton Ionization of Nonhydrogenic Atoms	102

6. The Method of Resolvent Equations	119
6.1. Introduction	119
6.2. Breakdown of Perturbation Theory at Resonance	119
6.3. Resolvent Equations: Monomode Semiclassical Field	121
6.4. Resolvent Equations: Monomode Quantum Field	124
6.5. Semiclassical Resolvent and Floquet Hamiltonian: Multimode Field	126
6.6. Resolvent Equations: Multimode Quantum Field	127
6.7. Correspondence between the Time-Dependent Wave Functions	128
6.8. A Model Hamiltonian and Explicit Solutions of the System of Resolvent Equations	130
6.8.1. Definition and Origin of the Model Hamiltonian	131
6.8.2. The Resolvent Equations and the Four Kinds of Transition	133
6.8.3. Solutions of the Resolvent Equations	134
6.8.4. Probability Distributions in Multiple Continua	137
6.8.5. Solutions of the Friedrichs–Fano Model	140
7. Theory of Effective Hamiltonians with Stationary and Time-Dependent Interactions	143
7.1. Introduction	143
7.2. The Effective Multiphoton Hamiltonian with One Intermediate Resonance	144
7.3. The One-Resonance Resolvent Equations	147
7.4. Time Dependence of Bound-Bound and Bound-Free Transitions	149
7.4.1. Application to Two-Photon Resonant Three-Photon Ionization of Cs	153
7.5. General Theory of Stationary Effective Hamiltonians	155
7.5.1. Separation of Resonant and Nonresonant States	159
7.5.2. Derivation of the Effective Hamiltonian	161
7.6. Theory of Time-Varying Effective Hamiltonians	168
7.6.1. The Quasi-Quantum Envelope Equations	170
7.6.2. Renormalized Perturbation Theory with Slowly Varying Fields and the Effective Hamiltonian	172
7.6.3. Probability Distributions Governed by the Slowly Varying Effective Hamiltonian	176
8. The Density Matrix Method	183
8.1. Introduction	183
8.2. The Pure State and Incoherent Mixtures	183
8.3. Equation of Motion of the Density Matrix	185
8.3.1. The Hermitian Case	186
8.3.2. The Non-Hermitian Case	186

8.4. Inclusion of Spontaneous Relaxation	188
8.5. Generalized Rotating Wave or Quasi-Energy-Shell Approximation	190
8.5.1. Density Matrix Equation for a Resonant Multiphoton Process	191
8.6. Theory of Multiphoton Transition in Stochastic Fields	194
8.6.1. Stochastic Differential Equations	194
8.6.2. The Kubo–Liouville Equation	195
8.6.3. Equation of the Marginal Averages	196
8.6.4. A Model of a “Monomode” Laser Field	198
8.6.5. Application to the Resonance Model	199
8.6.6. A Model of a Multimode Laser Field	205
8.6.7. Two-Photon Resonant Three-Photon Ionization	206
 9. Continued Fractions and Recursive-Iterative Perturbation Theory	213
9.1. Introduction	213
9.2. The Three-Term Recurrence Relation	214
9.3. The Continued-Fraction Representation	214
9.4. The Elastic Resolvent	216
9.5. The Resolvent for Emission and Absorption of n Photons	217
9.6. The Continued-Fraction Representation of the T-Matrix	218
9.6.1. Recursion Relation for the Reduced T-Matrix	219
9.6.2. The T-Matrix for Emission and Absorption of n Photons	220
9.7. Continued-Fraction Representation of a Stationary Wave Function	221
9.7.1. The n -Photon Wave Function	222
9.8. The Multiphoton Eigenvalue Problem	222
9.8.1. The Level-Shift Operator	223
9.9. Coupled Inhomogeneous Radial Equations for ψ_n	226
9.10. The Recursive-Iterative Wave Equations	228
9.11. Evaluation of the n -Photon Resolvent	231
9.12. The Case of Intermediate Resonances	234
9.13. The Two-Mode Problem	235
9.14. The Method of Chain Hamiltonians	237
9.14.1. Reduction of a Hamiltonian to a Chain	238
9.14.2. Eigenvalues and Eigenvectors of a Chain Hamiltonian	240
9.14.3. Matrix Elements of the Resolvent	241
9.14.4. The Transition Amplitude	243
 10. Floquet Theory of Multiphoton Transitions	245
10.1. Introduction	245
10.2. The Energy-Domain Floquet Method	245

10.2.1. The N -Electron Schrödinger Problem with a Multipolar Field	246
10.2.2. Structure of the Floquet Equations with Retardation	247
10.2.3. The Equivalent Solutions and the Independent Solutions	250
10.2.4. The Biorthonormal Properties and “Stationary” Solutions	252
10.2.5. The Evolution Matrix and the Transition Probabilities	254
10.2.6. The Floquet States and the “Floquet–Schrödinger Equation”	255
10.2.7. The Rovibrational Floquet Hamiltonian and the Multiphoton Infrared Excitation Spectra of CO	257
10.2.8. The Infinite System of Floquet Equations	264
10.2.9. Proof of the Existence of the Floquet Determinant and Its Analytic Properties	265
10.2.10. The “Floquet Zones” and the Irreducible Set of Poles	267
10.2.11. Polynomial Reduction of the Infinite-Order Secular Equation	267
10.2.11.1. The Nondegenerate Secular Polynomial	268
10.2.12. The Solution Vectors	271
10.2.12.1. Alternative Forms of Polynomial Coefficients in the Vicinity of Resonances	272
10.3. The Time-Domain Floquet Method	273
10.3.1. Introduction	273
10.3.2. Reduction of the Integration Interval	275
10.3.3. The Magnus Expansion of $U(t, 0)$	277
10.3.4. An Example of a Time-Domain Floquet Calculation	282
11. Non-Hermitian Hamiltonian Theory of Multiphoton Transitions	287
11.1. Introduction	287
11.2. Properties of Non-Hermitian Hamiltonians	288
11.3. The Solution Matrix	289
11.3.1. An Illustrative Case	291
11.4. Optical Potential Construction of Non-Hermitian Hamiltonians, Wave Functions, and Transition Amplitudes	293
11.4.1. The Causal and Anticausal Wave Equations	294
11.4.2. The Causal Wave Functions	296
11.4.3. Amplitudes for Bound–Bound and Bound–Free Transitions	298
11.4.4. Total Probability of Multiphoton-Induced Decay	299
11.4.5. Time Dependence of Multiphoton Transitions in Hydrogen	300
11.4.5.1. Two-Photon Transitions	300
11.4.5.2. Three-Photon Transitions	303
11.4.5.3. Field-Induced Quantum Beats in Multiphoton Ionization of H	304

11.5. The Multiphoton Non-Hermitian Hamiltonian Generated by Rotation of Coordinates	305
11.5.1. Rotated Hydrogenic Floquet Hamiltonian	307
11.5.2. Transition Amplitudes from the Rotated Hamiltonian	310
11.5.3. The Multiphoton Eigenvalue Problem and Inverse Iteration	312
11.5.4. An Effective Hamiltonian Generated by the Non-Hermitian Floquet Method	317
12. Theory of Radiative Electron–Atom Scattering	323
12.1. Introduction	323
12.2. Potential Scattering in a Laser Field	324
12.2.1. The Floquet Equation for Radiative Potential Scattering	325
12.2.2. Asymptotic Wave Functions	325
12.2.3. Green's Function for an Electron in a Dipole Radiation Field	327
12.2.4. The Scattered Wave and the Scattering Amplitude	329
12.2.5. Existence of the Stationary Cross Section in a Semiclassical Field	330
12.2.6. Radiative Scattering from a Pseudopotential	331
12.3. Multichannel Electron–Atom Scattering in a Laser Field	336
12.3.1. The Floquet Equation for Scattering	337
12.3.2. Eigenfunctions of the Reference Hamiltonian	338
12.3.3. Green's Function for the Reference Hamiltonian	339
12.3.4. Wave Functions of the Total System and the Scattering Amplitude	340
12.3.4.1. The Radiative First Born Amplitude	343
12.3.4.2. The Radiative Second Born Amplitude	344
12.3.5. Target State Distributions for Radiative Scattering	347
12.3.5.1. State Distribution: Pulsed Laser	348
12.3.5.2. Reduction of the Pure State to a Mixture	349
12.3.5.3. The Radiative “Elastic” Scattering Signal	350
12.3.5.4. The Scattering Signal for Adiabatic and Sudden Excitations	351
12.3.5.5. Steady-State Distribution: Continuous-Wave Case	352
12.3.5.6. A Typical Steady-State Distribution	353
12.3.6. The Amplitude Matrix in the Steady-State Case	355
12.3.7. A Multichannel Pseudopotential Model	357
12.3.7.1. The Scattering Singularities	360
12.3.7.2. Potential Scattering in a Laser Field	361
12.3.7.3. The Low-Frequency Limit	361
12.3.7.4. The Resonant Influence of Ground State H^- on Elastic Scattering	362

12.3.7.5. Target Excitation by Subthreshold Scattering	363
12.3.7.6. The Inelastic and Emission Cross Sections	365
12.3.7.7. Photon Amplification by Scattering	366
12.3.7.8. Low-Energy Angular Distribution	367
12.4. Direct, Rearrangement, and Fully Symmetrized Radiative Scattering Amplitudes	369
12.4.1. Direct and Rearrangement Amplitudes	371
12.4.2. The Radiative Rearrangement Scattering Amplitude	372
12.4.3. The Fully Symmetrized Radiative Scattering Amplitude	373
12.4.4. Spin-Flip and Related Amplitudes	377
12.5. Radiative Close-Coupling Equations	378
<i>Appendices</i>	385
1a. The Fifty-Six Topologically Distinct Eighth-Order Diagrams which Provide the Third Correction to Two-Photon Absorption	386
1b. The Twenty-One Topologically Distinct Seventh-Order Diagrams which Provide the Second Correction to Three-Photon Absorption	387
1c. The Twenty-Eight Topologically Distinct Eighth-Order Diagrams which Provide the Second Correction to Four-Photon Absorption	388
1d. The Thirty-Five Topologically Distinct Seventh-Order Diagrams which Provide the Third Correction to One-Photon Absorption	389
1e. Forty Additional Diagrams which Contribute in the Fourth-Order to the Two-Photon Absorption Amplitude for a Two-Mode Field When the Modes Are Distinct but Their Frequencies Are Degenerate	390
2. Two-Photon Matrix Elements τ for Hydrogen	391
<i>References</i>	393
<i>Index</i>	401

1

Electrons and Atoms in a Radiation Field

1.1. Introduction

A charged particle in a radiation field is the fundamental system from which the whole subject of multiphoton processes in atoms can be built up. In this chapter we shall briefly sketch the theory of an electron in a classical and a quantum radiation field. This will help to clarify the fundamental assumptions of our description and to introduce the basic theoretical approximations. Finally, it will permit us to write down the Hamiltonian of an N_a -electron atom in a monomode or in a multimode laser field. We also give two convenient renormalizations of the atom + field (quantum) interaction Hamiltonian within the widely used dipole approximation.

1.2. The Minimum-Coupling Prescription

The classical electrodynamics of an electron in a radiation field can be summarized by the Hamiltonian

$$H = \frac{1}{2\mu} \left(\mathbf{p} - \frac{e}{c} \mathbf{A} \right)^2 - e\phi \quad (1.2.1)$$

where e , μ , and \mathbf{p} are the charge, mass, and momentum of the electron and \mathbf{A} and ϕ are the vector potential and scalar potential of the radiation field, respectively. This Hamiltonian is obtained using the simple prescription of changing the momentum \mathbf{p} in the kinetic energy of the free electron by the

relation

$$\mathbf{p} \rightarrow \left(\mathbf{p} - \frac{e}{c} \mathbf{A} \right) \quad (1.2.2)$$

The potential energy $e\phi$ in the presence of the field is determined by the scalar potential ϕ . Before justifying this so-called “minimum-coupling prescription” we recall that the electric field \mathbf{E} and the magnetic field \mathbf{B} are obtained by simple differentiations of the potentials:

$$\mathbf{E} = -\frac{1}{c} \frac{\partial \mathbf{A}}{\partial t} + \nabla \phi \quad (1.2.3)$$

$$\mathbf{B} = \nabla \times \mathbf{A} \quad (1.2.4)$$

The minimum-coupling Hamiltonian (1.2.1) is justified because it correctly reproduces the equation of motion of the electron when substituted into the classical canonical equations.

To show this briefly we recall first that the classical motion of an electron in an electromagnetic field is governed by the Lorentz equation

$$\mu \frac{\partial \mathbf{v}}{\partial t} = \mathbf{F} \equiv e \left(\mathbf{E} + \frac{\mathbf{v}}{c} \times \mathbf{B} \right) \quad (1.2.5)$$

where \mathbf{v} is the velocity of the electron, c that of light, and \mathbf{F} is the Lorentz force.

Now if q_i and p_i are the canonical coordinates and momenta, then the canonical equations of dynamics are

$$\dot{q}_i = \frac{\partial H}{\partial p_i} \quad (1.2.6)$$

and

$$\dot{p}_i = -\frac{\partial H}{\partial q_i} \quad (1.2.7)$$

where the dot denotes differentiation with respect to time t . In cartesian coordinates

$$\left. \begin{aligned} (q_1, q_2, q_3) &\equiv (x, y, z) \equiv \mathbf{r} \\ (p_1, p_2, p_3) &\equiv (p_x, p_y, p_z) \equiv \mathbf{p} \end{aligned} \right\} \quad (1.2.8)$$

and

Thus when the Hamiltonian (1.2.1) is used, the x -component of Eq. (1.2.6) becomes

$$\dot{x} = \frac{\partial H}{\partial p_x} = \frac{1}{\mu} \left(p_x - \frac{e}{c} A_x \right) \quad (1.2.9)$$

When expression (1.2.1) is substituted in Eq. (1.2.7) we get

$$\begin{aligned} \dot{p}_x &= -\frac{\partial H}{\partial q_x} \\ &= e \frac{\partial \phi}{\partial x} + \frac{e}{\mu c} \left[\left(p_x - \frac{e}{c} A_x \right) \frac{\partial A_x}{\partial x} + \left(p_y - \frac{e}{c} A_y \right) \frac{\partial A_y}{\partial x} + \left(p_z - \frac{e}{c} A_z \right) \frac{\partial A_z}{\partial x} \right] \end{aligned} \quad (1.2.10)$$

Relationship (1.2.9) can be used to rewrite Eq. (1.2.10) in the form

$$\dot{p}_x = e \frac{\partial \phi}{\partial x} + \frac{e}{c} \left(\dot{x} \frac{\partial A_x}{\partial x} + \dot{y} \frac{\partial A_y}{\partial x} + \dot{z} \frac{\partial A_z}{\partial x} \right) \quad (1.2.11)$$

The total time derivative of A_x is given by

$$\frac{dA_x}{dt} = \frac{\partial A_x}{\partial t} + \dot{x} \frac{\partial A_x}{\partial x} + \dot{y} \frac{\partial A_x}{\partial y} + \dot{z} \frac{\partial A_x}{\partial z}$$

so Eq. (1.2.11) can be reexpressed as

$$\begin{aligned} \frac{d}{dt} \left(p_x - \frac{e}{c} A_x \right) &= e \left(\frac{\partial \phi}{\partial x} - \frac{1}{c} \frac{\partial A_x}{\partial t} \right) + \frac{e}{c} \left[\dot{y} \left(\frac{\partial A_y}{\partial x} - \frac{\partial A_x}{\partial y} \right) - \dot{z} \left(\frac{\partial A_z}{\partial x} - \frac{\partial A_x}{\partial z} \right) \right] \\ &= e \left(\frac{\partial \phi}{\partial x} - \frac{1}{c} \frac{\partial A_x}{\partial t} \right) + \frac{e}{c} [\mathbf{v} \times (\nabla \times \mathbf{A})]_x \end{aligned} \quad (1.2.12)$$

Since in the cartesian system the above steps leading to Eq. (1.2.12) are symmetric in x , y , and z , we can immediately write down the vector equation from the component equation (1.2.12) above:

$$\begin{aligned} \frac{d}{dt} \left(\mathbf{p} - \frac{e}{c} \mathbf{A} \right) &= e \left(\nabla \phi - \frac{1}{c} \frac{\partial \mathbf{A}}{\partial t} \right) + e \left[\frac{1}{c} \mathbf{v} \times (\nabla \times \mathbf{A}) \right] \\ &= e \left(\mathbf{E} + \frac{1}{c} \mathbf{v} \times \mathbf{B} \right) \end{aligned} \quad (1.2.13)$$

In the last line definitions (1.2.3) and (1.2.4) have been used. Similarly Eq.

(1.2.9) yields

$$\left(\mathbf{p} - \frac{e}{c} \mathbf{A} \right) = \mu \dot{\mathbf{r}} = \mu \mathbf{v} \quad (1.2.14)$$

By combining Eqs. (1.2.14) and (1.2.13) we have

$$\mu \frac{d\mathbf{v}}{dt} = e \left(\mathbf{E} + \frac{1}{c} \mathbf{v} \times \mathbf{B} \right)$$

which is the same as the Lorentz equation of motion (1.2.5) as required to fully justify the minimum-coupling prescription (1.2.2).

1.3. The First Quantization and the Semiclassical Approximation

The classical Hamiltonian (1.2.1) immediately allows us to quantize the electron's motion according to the principles of the first quantization:

$$\left. \begin{array}{l} \mathbf{p} \rightarrow -i\hbar \nabla \\ \mathbf{r} \rightarrow \mathbf{r} \\ H \rightarrow i\hbar \frac{\partial}{\partial t} \end{array} \right\} \quad (1.3.1)$$

In this scheme the potentials \mathbf{A} and ϕ are left, however, as classical functions (c numbers). We therefore obtain the “semiclassical” Schrödinger equation

$$\begin{aligned} i\hbar \frac{\partial}{\partial t} \psi(\mathbf{r}, t) &= \left\{ \frac{[-i\hbar \nabla - (e/c)\mathbf{A}]^2}{2\mu} + V \right\} \psi(\mathbf{r}, t) \\ &\equiv [H_0 + H'(t)]\psi(\mathbf{r}, t) \end{aligned} \quad (1.3.2)$$

which immediately provides the semiclassical electron–field interaction Hamiltonian $H'(t)$:

$$H'(\mathbf{r}, t) = \frac{e}{2\mu c} [2i\hbar \mathbf{A}(\mathbf{r}, t) \cdot \nabla + i\hbar (\nabla \cdot \mathbf{A}(\mathbf{r}, t))] + \frac{e^2}{2\mu c^2} \mathbf{A}(\mathbf{r}, t) \cdot \mathbf{A}(\mathbf{r}, t) \quad (1.3.3)$$

where the reference Hamiltonian is

$$H_0 = -\frac{\hbar^2}{2\mu} \nabla^2 + V \quad (1.3.4)$$

with

$$V = -e\phi \quad (1.3.5)$$

1.4. The Gauge Invariance and Gauge Transformation of the Schrödinger Equation

An interesting fact about the description of the electromagnetic field is that the field strengths are derivable from the potentials. At the same time, to a certain extent, the potentials can be chosen freely without changing the field strengths. Thus if we change

$$\mathbf{A} \rightarrow \mathbf{A}' = \mathbf{A} + \nabla\chi \quad (1.4.1)$$

and

$$\phi \rightarrow \phi' = \phi + \frac{1}{c} \dot{\chi} \quad (1.4.2)$$

in definitions (1.2.3) and (1.2.4), we find that the corresponding field strengths change as

$$\begin{aligned} \mathbf{E}' &= -\frac{1}{c} \dot{\mathbf{A}}' + \nabla\phi' \\ &= \left[-\frac{1}{c} \dot{\mathbf{A}} - \frac{1}{c} \frac{\partial}{\partial t} (\nabla\chi) \right] + \left(\nabla\phi + \frac{1}{c} \nabla \frac{\partial}{\partial t} \chi \right) \\ &= -\frac{1}{c} \dot{\mathbf{A}} + \nabla\phi = \mathbf{E} \end{aligned} \quad (1.4.3)$$

and

$$\begin{aligned} \mathbf{B}' &= \nabla \times \mathbf{A}' = \nabla \times (\mathbf{A} + \nabla\chi) = \nabla \times \mathbf{A} + \nabla \times \nabla\chi \\ &= \nabla \times \mathbf{A} = \mathbf{B} \end{aligned} \quad (1.4.4)$$

In other words the so-called gauge transformation of the first kind, Eqs. (1.4.1) and (1.4.2), involving an arbitrary scalar function $\chi = \chi(\mathbf{r}, t)$, leaves the field strengths unaltered. Often this allows one to choose the gauge suitably in order to simplify the mathematical description of the problem. One such choice, which is particularly suited for the pure radiation field (i.e., the light waves), is to select the gauge such that

$$\nabla \cdot \mathbf{A} = 0 \quad (1.4.5)$$

We shall use this “radiation gauge” (also called the “Coulomb gauge” or “transverse gauge”) in our description of radiation fields in this book. Transformations (1.4.1) and (1.4.2) change the Schrödinger equation (1.3.2) to

$$i\hbar \frac{\partial \psi}{\partial t} = \left[\frac{1}{2\mu} \left(-i\hbar \nabla - \frac{e}{c} \mathbf{A}' + \frac{e}{c} \nabla \chi \right)^2 - e\phi' + \frac{e}{c} \frac{\partial \chi}{\partial t} \right] \psi \quad (1.4.6)$$

Equation (1.4.6) can be rewritten as

$$i\hbar \frac{\partial}{\partial t} [e^{i(e/\hbar c)\chi} \psi] = \left[\frac{1}{2\mu} \left(-i\hbar \nabla - \frac{e}{c} \mathbf{A}' \right)^2 - e\phi' \right] [e^{i(e/\hbar c)\chi} \psi] \quad (1.4.7)$$

Therefore, the new solution of the Schrödinger equation after the gauge transformation is

$$\psi' \equiv e^{i(e/\hbar c)\chi} \psi \quad (1.4.8)$$

which differs from the old solution ψ by the phase factor $e^{i(e/\hbar c)\chi}$ only. We see that the Schrödinger equation is gauge “invariant”; it retains its form with respect to the potentials, provided also the wave function is phase transformed according to (1.4.8). Transformation (1.4.8) is sometimes referred to as the gauge transformation of the second kind.

1.5. The Hamiltonian of a Light Wave

The simplest formulation of the classical radiation field is obtained in the “radiation gauge” and is given by Maxwell’s wave equation of the vector potential in free space⁽¹⁾

$$\left(\nabla^2 - \frac{1}{c^2} \frac{\partial^2}{\partial t^2} \right) \mathbf{A} = 0 \quad (1.5.1)$$

supplemented by the radiation gauge condition

$$\left. \begin{aligned} \nabla \cdot \mathbf{A} &= 0 \\ \varphi &= 0 \end{aligned} \right\} \quad (1.5.2)$$

To solve Eq. (1.5.1) we write \mathbf{A} as a superposition of plane waves $e^{i\mathbf{k}\cdot\mathbf{r}}$ normalized in a large cubic volume of dimension $L^3 \rightarrow \infty$:

$$\mathbf{A} = \sum_{\mathbf{k}} \mathbf{\epsilon}_{\mathbf{k}} [q_{\mathbf{k}}(t) e^{i\mathbf{k}\cdot\mathbf{r}} + q_{\mathbf{k}}^*(t) e^{-i\mathbf{k}\cdot\mathbf{r}}] \quad (1.5.3)$$

where $\boldsymbol{\epsilon}_k$ is a unit polarization vector and \mathbf{k} is a propagation vector. Substitution of expression (1.5.3) in condition (1.5.2) immediately yields

$$\boldsymbol{\epsilon}_k \cdot \mathbf{k} = 0 \quad (1.5.4)$$

This is an equation of a plane passing through the origin and perpendicular to the direction of \mathbf{k} . Thus $\boldsymbol{\epsilon}_k$ is a planar vector with only two orthogonal (polarization) components. We should therefore associate

$$\boldsymbol{\epsilon}_k = \boldsymbol{\epsilon}_k^{(\lambda)} \quad \text{and} \quad q_k(t) = q_{k,\lambda}(t), \quad \lambda = 1, 2 \quad (1.5.5)$$

with each wave vector \mathbf{k} . For notational simplicity, however, we may omit the index λ when no confusion results.

We now substitute expression (1.5.3) in Eq. (1.5.1) and project onto a plane wave from the left. This gives the equation governing the unknowns $q_{k,\lambda}(t)$,

$$\frac{\partial^2 q_{k,\lambda}(t)}{\partial t^2} + c^2 k^2 q_{k,\lambda}(t) = 0 \quad (1.5.6)$$

and its complex conjugate

$$\frac{\partial^2 q_{k,\lambda}^*(t)}{\partial t^2} + c^2 k^2 q_{k,\lambda}^*(t) = 0 \quad (1.5.7)$$

Both Eqs. (1.5.6) and (1.5.7) can be satisfied by all complex $q_k(t)$, which are solutions of the simpler first-order equations

$$\frac{\partial q_{k,\lambda}(t)}{\partial t} = -i\omega_k q_{k,\lambda}(t) \quad (1.5.8)$$

where

$$\omega_k = ck \quad (1.5.9)$$

The last equation establishes the well-known dispersion relation of light waves in free space.

For a monomode constant-amplitude laser field the vector potential (1.5.3) takes the form

$$\mathbf{A}(\mathbf{r}, t) = \boldsymbol{\epsilon} A_0 \cos(\mathbf{k} \cdot \mathbf{r} - \omega t + \delta) \quad (1.5.10)$$

where

$$\boldsymbol{\epsilon}_k = \boldsymbol{\epsilon} \quad \text{and} \quad A_0 \equiv q_k(0) \quad (1.5.11)$$

$|\mathbf{k}| \equiv \omega/c$ is the wave number and δ is an arbitrary phase of the field.

1.6. The Dipole Approximation and Two Forms of the Interaction Hamiltonian

The dipole approximation of a radiation field consists of neglecting the “retardation” effect due to the wave vector \mathbf{k} and thus replacing the spatial modulation factor

$$e^{i\mathbf{k}\cdot\mathbf{r}} \approx 1 + \mathbf{k} \cdot \mathbf{r} + \dots \quad (1.6.1)$$

in expression (1.5.3) by the leading term, unity. Since the wavelength in the optical or suboptical region is almost always very large compared to any other characteristic length associated with the atomic system, effectively $|\mathbf{k}\mathbf{r}| \ll 1$ and hence the dipole approximation turns out nearly always to be very good in practice. The monomode laser field (1.5.10) in the dipole approximation simplifies to

$$\mathbf{A}(t) = \varepsilon_z A_0 \cos(\omega t + \delta) \quad (\text{linear polarization}) \quad (1.6.2)$$

or

$$\mathbf{A}(t) = A_0 [\varepsilon_x \cos(\omega t + \delta) - \varepsilon_y \sin(\omega t + \delta)] \quad (\text{circular polarization}) \quad (1.6.3)$$

where ε_x , ε_y , and ε_z are unit polarization vectors in the x , y , and z directions, respectively. Expression (1.6.2) or (1.6.3), because of the time independence of the amplitude A_0 , is appropriate for a continuous-wave (cw) laser. For a pulsed laser, on the other hand, we have

$$\mathbf{A}(t) = \varepsilon_z A_0(t) \cos(\omega t + \delta) \quad (\text{linear}) \quad (1.6.4)$$

or

$$\mathbf{A}(t) = A_0(t) [\varepsilon_x \cos(\omega t + \delta) - \varepsilon_y \sin(\omega t + \delta)] \quad (\text{circular}) \quad (1.6.5)$$

where $A_0(t)$ corresponds to the pulse-envelope function.

The so-called “velocity gauge” interaction Hamiltonian (1.3.3) with (1.4.5) in the dipole approximation becomes

$$H'(t) = \frac{ie\hbar}{\mu c} \mathbf{A}(t) \cdot \nabla + \frac{e^2}{2\mu c^2} A^2(t) \quad (1.6.6)$$

where $\mathbf{A}(t)$ is independent of the coordinates. Clearly, for the N_a -electron atom the semiclassical interaction Hamiltonian is the sum of (1.6.6) for the

N_a electrons, namely

$$H'(t) = \frac{ie\hbar}{\mu c} \sum_{j=1}^{N_a} \nabla_j \cdot \mathbf{A}(t) + \frac{e^2}{2\mu c^2} N_a A^2(t) \quad (1.6.7)$$

In the dipole approximation, it is also often convenient to use a transformed interaction Hamiltonian instead of expression (1.6.6), obtained by making a gauge transformation of the second kind

$$\psi(\mathbf{r}, t) = e^{i(e/\hbar c)\mathbf{r} \cdot \mathbf{A}(t)} \Psi(\mathbf{r}, t) \quad (1.6.8)$$

On substituting this expression in Eq. (1.3.2) one easily calculates

$$i\hbar \frac{\partial}{\partial t} \psi(\mathbf{r}, t) = e^{i(e/\hbar c)\mathbf{r} \cdot \mathbf{A}(t)} \left[i\hbar \frac{\partial}{\partial t} - \frac{e}{c} \mathbf{r} \cdot \frac{\partial \mathbf{A}(t)}{\partial t} \right] \Psi \quad (1.6.9).$$

$$\nabla \psi(\mathbf{r}, t) = e^{i(e/\hbar c)\mathbf{r} \cdot \mathbf{A}(t)} \left[\nabla + i \frac{e}{\hbar c} \mathbf{A}(t) \right] \Psi \quad (1.6.10)$$

and

$$\nabla^2 \psi(\mathbf{r}, t) = e^{i(e/\hbar c)\mathbf{r} \cdot \mathbf{A}(t)} \left[\nabla^2 + 2i \frac{e}{\hbar c} \mathbf{A}(t) \cdot \nabla - \frac{e^2}{\hbar^2 c^2} A^2(t) \right] \Psi \quad (1.6.11)$$

Then use of Eqs. (1.6.9)–(1.6.11) and the definition for the electric field strength, namely

$$\mathbf{E}(t) = -\frac{1}{c} \frac{\partial \mathbf{A}(t)}{\partial t} \quad (1.6.12)$$

in Eq. (1.3.2) easily yields the Schrödinger equation satisfied by $\Psi(\mathbf{r}, t)$,

$$i\hbar \frac{\partial}{\partial t} \Psi(\mathbf{r}, t) = \left[-\frac{\hbar^2}{2\mu} \nabla^2 + V - e\mathbf{r} \cdot \mathbf{E}(t) \right] \Psi(\mathbf{r}, t) \quad (1.6.13)$$

The semiclassical “electron + field” interaction Hamiltonian now takes the so-called “length form,”

$$H'(t) = -e\mathbf{r} \cdot \mathbf{E}(t) \quad (1.6.14)$$

Both forms of the interaction Hamiltonian, expressions (1.6.6) and (1.6.14), are widely used in analyses of multiphoton processes. We note in this context that when comparing results obtained using these two “forms,”

attention should be paid to transformation (1.4.8) for the basis functions employed in the calculations. Clearly, for an N_a -electron atom the “length-form” semiclassical interaction Hamiltonian is [cf. Eq. (1.6.7)]

$$H'(t) = -e \sum_{j=1}^{N_a} \mathbf{r}_j \cdot \mathbf{E}(t) \quad (1.6.15)$$

1.7. The Wave Function of a Free Electron in a Laser Field

As an example of the use of both forms of the semiclassical interaction Hamiltonian (1.6.6) and (1.6.14), we shall derive the wave function of a free electron in a dipole radiation field.

1.7.1. The Wave Function in the “Velocity Gauge”

The Schrödinger equation of the free electron in the “velocity gauge” is obtained from Eq. (1.3.2) by setting the static potential $V = 0$:

$$i\hbar \frac{\partial \psi(\mathbf{r}, t)}{\partial t} = \left[-\frac{\hbar^2}{2\mu} \nabla^2 + H'(t) \right] \psi(\mathbf{r}, t) \quad (1.7.1.1)$$

where $H'(t)$ is given by Eq. (1.6.6).

Remembering that a plane wave is an eigenvector of both the kinetic-energy operator $-(\hbar^2 \nabla^2)/(2\mu)$ and the momentum operator $-i\hbar \nabla$, a solution of Eq. (1.7.1.1) can be immediately written down in the form

$$\psi(\mathbf{r}, t) = \exp \left\{ -\frac{i}{2\mu\hbar} \int' \left[\hbar \mathbf{k} - \frac{e}{c} \mathbf{A}(t') \right]^2 dt' \right\} e^{i\mathbf{k} \cdot \mathbf{r}} \quad (1.7.1.2)$$

Equation (1.7.1.2) holds true for a vector potential $\mathbf{A}(t)$ with arbitrary time dependence.

1.7.1.1. The Linearly Polarized Laser Field

For the linearly polarized field (1.6.2) we obtain from Eq. (1.7.1.2)

$$\psi(\mathbf{r}, t) = \exp \left\{ -\frac{i}{\hbar} \left[\left(\varepsilon_k + \delta_e + \frac{\delta_e}{2\hbar\omega} \sin 2(\omega t + \delta) \right. \right. \right. \\ \left. \left. \left. - \boldsymbol{\alpha}_0 \cdot \mathbf{k} \sin(\omega t + \delta) \right) \right] + i\mathbf{k} \cdot \mathbf{r} \right\} \quad (1.7.1.1.1)$$

where $\varepsilon_k = \hbar^2 k^2 / 2\mu$ is the free kinetic energy, $\delta_e = e^2 A_0^2 / 4\mu c^2$ is an

average energy of interaction of the free electron with the field, and

$$\alpha_0 \equiv \frac{e\hbar A_0}{\mu c \omega} \epsilon \quad (1.7.1.1.2)$$

is a “radius of vibration” of the electron inside the field.

It is also of interest to expand expression (1.7.1.1.1) in the harmonics of the phase ($\omega t + \delta$) of the field. Using the well-known Jacobi–Anger formula⁽²⁾

$$e^{iz \sin \phi} = \sum_{n=-\infty}^{\infty} J_n(z) e^{in\phi} \quad (1.7.1.1.3)$$

we may expand the sinusoidal exponentials and obtain

$$\psi(\mathbf{r}, t) = \sum_{n=-\infty}^{\infty} J_n^L(\mathbf{A}_0, \mathbf{k}) e^{in(\omega t + \delta) - (i/\hbar)(\epsilon_k + \delta_e)t} e^{i\mathbf{k} \cdot \mathbf{r}} \quad (1.7.1.1.4)$$

where we have defined the generalized Bessel functions

$$J_n^L(\mathbf{A}_0, \mathbf{k}) \equiv \sum_{m=-\infty}^{\infty} J_m(\delta_e/2\hbar\omega) J_{n+2m}(\alpha_0 \cdot \mathbf{k}) \quad (1.7.1.1.5)$$

Remembering that

$$J_n(0) = \delta_{n,0} \quad (1.7.1.1.6)$$

for $\delta_e \ll \hbar\omega$ one may approximate

$$J_n^L(\mathbf{A}_0, \mathbf{k}) \approx J_n(\alpha_0 \cdot \mathbf{k}) \quad (1.7.1.1.7)$$

1.7.1.2. The Circularly Polarized Laser Field

We may use the circularly polarized laser field (1.6.3) in Eq. (1.7.1.2) to obtain the wave function

$$\psi(\mathbf{r}, t) = \exp \left\{ -\frac{i}{\hbar} [(\epsilon_k + 2\delta_e)t + (\alpha_0 k \sin \theta_k) \sin(\phi_k + \omega t + \delta)] + i\mathbf{k} \cdot \mathbf{r} \right\} \quad (1.7.1.2.1)$$

where

$$\mathbf{k} = (k_\rho, k_z, \phi_k) = (k \sin \theta_k, k \cos \theta_k, \phi_k) \quad (1.7.1.2.2)$$

The harmonic expansion of (1.7.1.2.1) is simply

$$\psi(\mathbf{r}, t) = \sum_{n=-\infty}^{\infty} J_n^C(\mathbf{A}_0, \mathbf{k}) \exp \left[in(\omega t + \delta) - \frac{i}{\hbar} (\epsilon_k + 2\delta_e) t \right] e^{i\mathbf{k}\cdot\mathbf{r}} \quad (1.7.1.2.3)$$

where

$$J_n^C(\mathbf{A}_0, \mathbf{k}) \equiv J_n(\alpha_0 k \sin \theta_k) e^{in\phi_k} \quad (1.7.1.2.4)$$

1.7.2. The Wave Function in the “Length Gauge”

The Schrödinger equation for a free electron in the “length gauge” is

$$i\hbar \frac{\partial \psi(\mathbf{r}, t)}{\partial t} = \left[-\frac{\hbar^2 \nabla^2}{2\mu} - e\mathbf{r} \cdot \mathbf{E}(t) \right] \psi(\mathbf{r}, t) \quad (1.7.2.1)$$

With the aid of Eq. (1.6.8) it is easily verified that

$$\Psi(\mathbf{r}, t) = \exp \left[-\frac{i}{\hbar} \frac{e}{c} \mathbf{r} \cdot \mathbf{A}(t) \right] \psi(\mathbf{r}, t) \quad (1.7.2.2)$$

is an exact solution of the above equation provided $\psi(\mathbf{r}, t)$ is given by Eq. (1.7.1.2) and $\mathbf{A}(t)$ is given by

$$\mathbf{A}(t) = -c \int' \mathbf{E}(t') dt' \quad (1.7.2.3)$$

One therefore expects that in problems with free electrons (such as radiative scattering) it is simpler to work with the velocity form of the wave equation rather than with the length form. The harmonic expansions of the free-electron wave function found above are closely related to the corresponding wave functions in the quantum field.

1.8. From Light Waves to Photon Fields

We first introduce a slight change of notation by normalizing the classical vector-potential amplitudes $q_{\mathbf{k}}(t)$ of Section 1.5 in the form

$$q_{\mathbf{k},\lambda}(t) = \left(\frac{2\pi\hbar c}{kL^3} \right)^{1/2} e^{i\delta} a_{\mathbf{k},\lambda}(t) \quad (1.8.1)$$

where δ is an arbitrary constant phase. Solutions of the light wave

equation (1.5.8) are

$$a_{\mathbf{k},\lambda}(t) = \exp(i\omega_k t) a_{\mathbf{k},\lambda} \quad (1.8.2)$$

where $a_{\mathbf{k},\lambda}$ are constants. The corresponding vector potential (1.5.3) becomes

$$\mathbf{A} = \sum_{\mathbf{k},\lambda} \left(\frac{2\pi\hbar c}{kL^3} \right)^{1/2} \mathbf{\epsilon}_{\mathbf{k}}^{(\lambda)} [e^{i\delta} a_{\mathbf{k},\lambda}(t) e^{i\mathbf{k}\cdot\mathbf{r}} + \text{c.c.}] \quad (1.8.3)$$

where c.c. stands for the complex conjugate of the term immediately preceding it. One easily calculates the field strengths from

$$\mathbf{E} \equiv -\frac{1}{c} \frac{\partial \mathbf{A}}{\partial t} = \sum_{\mathbf{k},\lambda} \left(\frac{2\pi\hbar c}{kL^3} \right)^{1/2} \mathbf{\epsilon}_{\mathbf{k}}^{(\lambda)} k [e^{i(\delta+\pi/2)} a_{\mathbf{k},\lambda}(t) e^{i\mathbf{k}\cdot\mathbf{r}} + \text{c.c.}] \quad (1.8.4)$$

and

$$\mathbf{B} \equiv \nabla \times \mathbf{A} = \sum_{\mathbf{k},\lambda} \left(\frac{2\pi\hbar c}{kL^3} \right)^{1/2} (\mathbf{\epsilon}_{\mathbf{k}}^{(\lambda)} \times \mathbf{k}) [e^{i(\delta+\pi/2)} a_{\mathbf{k},\lambda}(t) e^{i\mathbf{k}\cdot\mathbf{r}} + \text{c.c.}] \quad (1.8.5)$$

We are now in a position to write the Hamiltonian of the classical radiation field in the canonical form. The energy of the radiation field is given by the well-known⁽¹⁾ expression

$$U = \frac{1}{8\pi} \int (E^2 + B^2) d\mathbf{r} \quad (1.8.6)$$

where $d\mathbf{r}$ denotes an element of volume integration.

By substituting expressions (1.8.4) and (1.8.5) in Eq. (1.8.6) and simplifying the volume integrations with the help of the orthogonality relation,

$$(1/L^3) \int e^{i(\mathbf{k}-\mathbf{k}')\cdot\mathbf{r}} d\mathbf{r} = \delta_{\mathbf{kk}'} \quad (1.8.7)$$

and noting that

$$(\mathbf{\epsilon}_{\mathbf{k}}^{(\lambda)} \times \mathbf{k})(\mathbf{\epsilon}_{\mathbf{k}'}^{(\lambda')} \times \mathbf{k}) = k^2 \delta_{\lambda\lambda'} \quad (1.8.8)$$

we obtain

$$U = \sum_{\mathbf{k},\lambda} \hbar\omega_k a_{\mathbf{k},\lambda}^* a_{\mathbf{k},\lambda} \quad (1.8.9)$$

$$= \sum_{\mathbf{k},\lambda} \frac{1}{2} \hbar\omega_k [a_{\mathbf{k},\lambda}^* a_{\mathbf{k},\lambda} + a_{\mathbf{k},\lambda} a_{\mathbf{k},\lambda}^*] \quad (1.8.10)$$

The nonsymmetric and symmetric forms (1.8.9) and (1.8.10) are of course identical in the classical context but (as we shall soon see) in the second quantized version they lead to slightly different expressions. We note that the quantities $a_{\mathbf{k}}$ are not canonical variables. Therefore it is appropriate before quantization to change to canonical variables defined by linear combinations of the $a_{\mathbf{k}}$:

$$Q_{\mathbf{k}}^{(\lambda)} \equiv (a_{\mathbf{k},\lambda} + a_{\mathbf{k},\lambda}^*) \left(\frac{\hbar}{2\omega_{\mathbf{k}}} \right)^{1/2} \quad (1.8.11)$$

$$P_{\mathbf{k}}^{(\lambda)} \equiv -i(a_{\mathbf{k},\lambda} - a_{\mathbf{k},\lambda}^*) \left(\frac{\hbar\omega_{\mathbf{k}}}{2} \right)^{1/2} = \dot{Q}_{\mathbf{k}}^{(\lambda)} \quad (1.8.12)$$

The last equality ensures the canonical nature of variables $Q_{\mathbf{k},\lambda}$ and $P_{\mathbf{k},\lambda}$, in terms of which the field energy (1.8.6) becomes

$$U = \frac{1}{2} \sum_{\mathbf{k},\lambda} [(P_{\mathbf{k},\lambda})^2 + \omega_{\mathbf{k}}^2(Q_{\mathbf{k},\lambda})^2] \quad (1.8.13)$$

This is clearly the Hamiltonian of an ensemble of harmonic oscillators with frequencies $\omega_{\mathbf{k}}$, where each $\omega_{\mathbf{k}}$ is twofold degenerate with respect to the polarization index λ .

We may express the momentum of the radiation field in a similar way. The Poynting vector describing the flux of electromagnetic-field energy is

$$\mathbf{S} = c(\mathbf{E} \times \mathbf{B}) \quad (1.8.14)$$

Hence the momentum per unit volume⁽¹⁾ is given by

$$\mathbf{P} = \frac{1}{4\pi L^3} \frac{1}{c} \int (\mathbf{E} \times \mathbf{B}) d\mathbf{r} \quad (1.8.15)$$

Substitution of expressions (1.8.4) and (1.8.5) yields

$$\mathbf{P} = \sum_{\mathbf{k},\lambda} \hbar \mathbf{k} a_{\mathbf{k},\lambda}^* a_{\mathbf{k},\lambda} \quad (1.8.16)$$

$$= \frac{1}{2} \sum_{\mathbf{k},\lambda} \hbar \mathbf{k} (a_{\mathbf{k},\lambda}^* a_{\mathbf{k},\lambda} + a_{\mathbf{k},\lambda} a_{\mathbf{k},\lambda}^*) \quad (1.8.17)$$

1.8.1. The Second Quantization of Light Fields

According to the rules of quantization the canonical variables Q_{α} and P_{α} defined by relations (1.8.11) and (1.8.12) (α here denotes the set $\{\mathbf{k}, \lambda\}$)

are promoted to noncommutable operators, again denoted by Q_α and P_α , satisfying

$$\left. \begin{aligned} [P_\alpha, Q_\alpha] &= -i\hbar \\ \text{and} \\ [P_\alpha, Q_\alpha] &= [P_\alpha, P_{\alpha'}] = [Q_\alpha, Q_{\alpha'}] = 0 \end{aligned} \right\} \quad (1.8.1.1)$$

where $[\ , \]$ is the usual commutator bracket. Since the eigenvalues of the quantum oscillators are⁽³⁾

$$E_\alpha = (n_\alpha + \frac{1}{2})\hbar\omega_\alpha \quad (1.8.1.2)$$

we immediately see that the Hamiltonian of the pure radiation field is nothing but the sum of excitation energies of an infinite ensemble of oscillators. Using definitions (1.8.11) and (1.8.12) a little algebra shows that condition (1.8.1.1) is also equivalent to promoting quantities a_α to operators satisfying the normalized commutation rules

$$\left. \begin{aligned} [a_\alpha, a_\alpha^+] &= 1 \\ \text{and} \\ [a_\alpha, a_{\alpha'}^+] &= [a_\alpha, a_{\alpha'}] = [a_\alpha^+, a_{\alpha'}^+] = 0 \end{aligned} \right\} \quad (1.8.1.3)$$

where the complex-conjugate function a_k^* is promoted to the Hermitian conjugate operator a_k^+ . Operators a_α and a_α^+ are the “lowering” and “raising” operators of the quantum-mechanical oscillators and are referred to here as the photon annihilation and destruction operators, respectively. Correspondingly, the classical energy U goes over to the quantum Hamiltonian operator H_F . Thus if we quantize Eq. (1.8.9) we obtain

$$U \rightarrow H_F = \hbar\omega_k (a_{k,\lambda}^+ a_{k,\lambda}) \quad (1.8.1.4)$$

On the other hand if we quantize Eq. (1.8.10), which is classically identical to Eq. (1.8.9), we obtain

$$\begin{aligned} U \rightarrow H_F &= \frac{1}{2} \sum_{k,\lambda} \hbar\omega_k (a_{k,\lambda}^+ a_{k,\lambda} + a_{k,\lambda} a_{k,\lambda}^+) \\ &= \sum_{k,\lambda} \hbar\omega_k (a_{k,\lambda}^+ a_{k,\lambda} + \frac{1}{2}) \end{aligned} \quad (1.8.1.5)$$

We note that relations (1.8.1.4) and (1.8.1.5) are not quite identical but

differ by a constant amount

$$\frac{1}{2} \sum_{\mathbf{k}, \lambda} \hbar \omega_k \equiv w_0 \quad (1.8.1.6)$$

It would appear that the difference between the two versions is not substantial since a transformation of the origin of the scale of energy measurement could remove the difference. The constant w_0 , however, turns out to be infinite for the vacuum field and corresponds to the sum of the zero-point energies of the unexcited “vacuum oscillators.” The majority of, if not all, phenomena of interest involve essentially only the differences of the field energy, where the “zero-point energy” cancels out. Under such circumstances the choice of relation (1.8.1.4) or (1.8.1.5) becomes a formal one and either form may be used consistently throughout. Having established the equivalence of a pure-radiation field with an ensemble of harmonic oscillators above, we may adopt all the well-known results⁽³⁾ of quantum oscillators for our purpose. Thus the effect of the destruction (lowering) operator on the occupation state $|n_\alpha\rangle$ is

$$a_\alpha |n_\alpha\rangle = n_\alpha^{1/2} |n_\alpha - 1\rangle \quad (1.8.1.7)$$

and that of the creation operator on $|n_\alpha\rangle$ is

$$a_\alpha^+ |n_\alpha\rangle = (n_\alpha + 1)^{1/2} |n_\alpha + 1\rangle \quad (1.8.1.8)$$

Then the operator appearing in Hamiltonian (1.8.9),

$$\hat{N}_\alpha \equiv a_\alpha^+ a_\alpha \quad (1.8.1.9)$$

is easily shown from Eqs. (1.8.1.7) and (1.8.1.8) to satisfy the eigenvalue equation

$$\hat{N}_\alpha |n_\alpha\rangle = n_\alpha |n_\alpha\rangle \quad (1.8.1.10)$$

and has occupation number n_α for its eigenvalue, i.e., \hat{N}_α is the number operator. We see immediately that in terms of the number operator the radiation-field Hamiltonian (1.8.9),

$$H_F = \sum_{\mathbf{k}, \lambda} \hbar \omega_k \hat{N}_{\mathbf{k}, \lambda} \quad (1.8.1.11)$$

corresponds to the sum of energies of $n_{\mathbf{k}, \lambda}$ quanta each of which possesses energy $\hbar \omega_k$. By quantizing expression (1.8.16) for the field momentum \mathbf{P} we

also obtain the operator

$$\hat{P} = \sum_{\mathbf{k}, \lambda} \hbar \mathbf{k} a_{\mathbf{k}, \lambda}^+ a_{\mathbf{k}, \lambda} = \sum_{\mathbf{k}, \lambda} \hbar \mathbf{k} \hat{N}_{\mathbf{k}, \lambda} \quad (1.8.1.12)$$

This shows that the momentum of the radiation field comprises the sum of momenta of $n_{\mathbf{k}, \lambda}$ quanta, each of which possesses momentum $\hbar \mathbf{k}$. Thus the quantized radiation field is characterized, in the present representation, by an ensemble of field-excitation quanta, each of which has a definite energy $\hbar \omega_k$, momentum $\hbar \mathbf{k} = \hbar c \omega_k (\mathbf{k}/k)$, and two polarizations $\epsilon_k^{(\lambda)}$ ($\lambda = 1, 2$) for each \mathbf{k} and ω_k . Such excitations of the quantized light field are to be identified with the “photons.”⁽⁴⁾

The quantized vector potential and field strengths are also obtained in this representation almost automatically from expressions (1.8.3), (1.8.4), and (1.8.5), namely

$$\mathbf{A} = \sum_{\mathbf{k}, \lambda} \left(\frac{2\pi\hbar c}{kL^3} \right)^{1/2} \epsilon_k^{(\lambda)} [e^{i\delta} a_{\mathbf{k}, \lambda} e^{i\mathbf{k} \cdot \mathbf{r}} + e^{-i\delta} a_{\mathbf{k}, \lambda}^+ e^{-i\mathbf{k} \cdot \mathbf{r}}] \quad (1.8.1.13)$$

$$\mathbf{E} = \sum_{\mathbf{k}, \lambda} \left(\frac{2\pi\hbar\omega}{L^3} \right)^{1/2} \epsilon_k^{(\lambda)} [e^{i(\delta+\pi/2)} a_{\mathbf{k}, \lambda} e^{i\mathbf{k} \cdot \mathbf{r}} + e^{-i(\delta+\pi/2)} a_{\mathbf{k}, \lambda}^+ e^{-i\mathbf{k} \cdot \mathbf{r}}] \quad (1.8.1.14)$$

and

$$\mathbf{B} = \sum_{\mathbf{k}, \lambda} \left(\frac{2\pi\hbar\omega}{L^3} \right)^{1/2} (\mathbf{k} \times \epsilon_k^{(\lambda)}) [e^{i(\delta+\pi/2)} a_{\mathbf{k}, \lambda} e^{i\mathbf{k} \cdot \mathbf{r}} + e^{i(\delta+\pi/2)} a_{\mathbf{k}, \lambda}^+ e^{-i\mathbf{k} \cdot \mathbf{r}}] \quad (1.8.1.15)$$

It will be noted that all the creation and annihilation operators are time-independent (in the present Schrödinger representation) although they have been obtained by promoting the time-dependent classical variables $a_{\mathbf{k}, \lambda}(t)$. Heitler⁽⁵⁾ has noted explicitly that this is perfectly consistent with the usual quantization scheme in which, for example, the time-dependent classical momenta $\mathbf{p}(t)$ are promoted to the operators $-i\hbar \nabla$, which are time-independent. This avoids the roundabout procedure of first quantizing in the Heisenberg picture, which is time-dependent, and then returning to the Schrödinger picture to express the field operators in the time-independent form. The time dependence of the operators $a_{\mathbf{k}, \lambda}^+$ and $a_{\mathbf{k}, \lambda}$, when desired, is readily obtained from the quantization of Eq. (1.5.8):

$$\frac{\partial a_{\mathbf{k}, \lambda}^+}{\partial t} = i\omega_k a_{\mathbf{k}, \lambda}^+ \quad (1.8.1.16)$$

We note that in Eqs. (1.8.1.13)–(1.8.1.15) the choice of δ is arbitrary; a choice of $\delta = 0$ (which is most common) may be slightly more convenient

when working with vector potential \mathbf{A} , while it may be preferable to choose $\delta = -\pi/2$ when working with field strength \mathbf{E} .

1.9. The Hamiltonian of an Atom in a Monomode Laser Field in the Dressed-Oscillator Representation

The Hamiltonian H of an N_a -electron atom interacting with a quantum field can be easily written down using the quantized minimum-coupling prescription

$$-i\hbar\nabla \rightarrow \left(-i\hbar\nabla - \frac{e}{c} \mathbf{A} \right) \quad (1.9.1)$$

Thus

$$H = \frac{1}{2\mu} \sum_{j=1}^{N_a} \left[-i\hbar\nabla_j - \frac{e}{c} \mathbf{A}(\mathbf{r}_j) \right]^2 + V(\mathbf{r}_1, \mathbf{r}_2, \dots, \mathbf{r}_{N_a}) + H_F \quad (1.9.2)$$

where \mathbf{r}_j , $j = 1, 2, \dots, N_a$ are the coordinates of the atomic electrons and $V(\mathbf{r}_1, \mathbf{r}_2, \dots, \mathbf{r}_{N_a})$ is the static atomic interaction potential. The vector potential $\mathbf{A}(\mathbf{r}_j)$ is in general evaluated at the position of the electron \mathbf{r}_j , and H_F is the field Hamiltonian. In the dipole approximation the vector potential becomes independent of coordinates and we may write

$$\mathbf{A}(0) = \left(\frac{2\pi\hbar c^2}{\omega L^3} \right)^{1/2} (a + a^\dagger) \boldsymbol{\epsilon} \quad (1.9.3)$$

where a and a^\dagger are the (monomode) annihilation and creation operators, respectively.

Substitution of expression (1.9.3) in Eq. (1.9.2) yields the total atom + field system Hamiltonian in the form

$$H = H_a + H'_1 + H'_2 + H_F \quad (1.9.4)$$

where

$$H_a = -\frac{\hbar^2}{2\mu} \sum_{j=1}^{N_a} \nabla_j^2 + V(\mathbf{r}_1, \mathbf{r}_2, \dots, \mathbf{r}_{N_a}) \quad (1.9.5)$$

is the isolated atomic Hamiltonian. The interaction operator

$$H' \equiv H'_1 + H'_2 \quad (1.9.6)$$

consists of two parts,

$$H'_1 = \frac{ie\hbar}{\mu c} \sum_{j=1}^{N_a} \nabla_j \cdot \boldsymbol{\epsilon} s (a + a^+) \quad (1.9.7)$$

and

$$H'_2 = \frac{e^2 N_a}{2\mu c^2} s^2 (a + a^+)^2 \quad (1.9.8)$$

In Eqs. (1.9.7) and (1.9.8) we have denoted the field normalization constant by

$$s \equiv \left(\frac{2\pi\hbar c^2}{\omega L^3} \right)^{1/2} \quad (1.9.9)$$

It is noteworthy that the interaction term H'_2 (unlike the term H'_1) is completely free of electron coordinates and momenta. Yet its presence in the total interaction operator (1.9.6) leads to an awkward mixing of terms in the higher orders of perturbation calculations of multiphoton processes. For this and related reasons it is desirable to have alternative forms of the atom + field Hamiltonian, which may contain effectively only a single-term interaction operator.

For this purpose we first reduce Hamiltonian (1.9.4) into another equivalent form. This will allow us to absorb the interaction H'_2 into the field Hamiltonian H_F , leaving essentially the H'_1 term for the interaction. This modification will also help to clarify the relevance (or otherwise) of the interaction term H'_2 in the theory of multiphoton processes.

We reexpress the monomode operators a and a^+ in terms of the canonical coordinate and momentum operators

$$q \quad \text{and} \quad p \equiv -i\hbar \frac{d}{dq} \quad (1.9.10)$$

and rewrite

$$\left. \begin{aligned} a &= (2\hbar\omega)^{-1/2} (\omega q + ip) \\ a^+ &= (2\hbar\omega)^{-1/2} (\omega q - ip) \end{aligned} \right\} \quad (1.9.11)$$

In terms of these expressions the vector potential (1.9.3) becomes

$$\mathbf{A}(0) = \left(\frac{4\pi}{L^3} \right)^{1/2} cq \boldsymbol{\epsilon} \quad (1.9.12)$$

and the corresponding dipolar electric-field operator is given by

$$\begin{aligned}\mathbf{E}(0) &= i \left(\frac{2\pi\hbar\omega}{L^3} \right)^{1/2} (\mathbf{a} - \mathbf{a}^\dagger) \boldsymbol{\epsilon} \\ &= - \left(\frac{4\pi}{L^3} \right)^{1/2} \mathbf{p} \boldsymbol{\epsilon}\end{aligned}\quad (1.9.13)$$

Substituting Eqs. (1.9.11) in Eq. (1.8.1.11) we obtain the quantum oscillator form of the unperturbed field Hamiltonian

$$H = \frac{1}{2} \left(-\hbar^2 \frac{d^2}{dq^2} + \omega^2 q^2 \right) \quad (1.9.14)$$

Similarly, putting Eqs. (1.9.11) in operators (1.9.7) and (1.9.8) we derive

$$H'_1 = \frac{ie\hbar}{\mu} \sum_{j=1}^{N_a} \nabla_j \cdot \boldsymbol{\epsilon} \left(\frac{4\pi}{L^3} \right)^{1/2} q \quad (1.9.15)$$

and

$$H'_2 = \frac{1}{2} \omega_p^2 q^2 \quad (1.9.16)$$

where

$$\omega_p^2 \equiv 4\pi \frac{e^2}{\mu} \left(\frac{N_a}{L^3} \right) \quad (1.9.17)$$

We note that the above parameter ω_p corresponds to the well-known “plasma frequency” for an “electron gas” of density $\rho = (N_a/L^3)$. If Eqs. (1.9.14)–(1.9.16) are substituted in expression (1.9.4) and the last two terms added together, we obtain the desired alternative to the total Hamiltonian (1.9.4),

$$H = H_a + \frac{ie\hbar}{\mu} \left(\frac{4\pi}{L^3} \right)^{1/2} \left(\sum_{j=1}^{N_a} \nabla_j \right) \cdot \boldsymbol{\epsilon} q + \frac{1}{2} \left[-\hbar^2 \frac{d^2}{dq^2} + (\omega^2 + \omega_p^2) q^2 \right] \quad (1.9.18)$$

In Eq. (1.9.18) we observe that the unperturbed field Hamiltonian H_F is now replaced by the “dressed” (or renormalized) field Hamiltonian

$$H'_F \equiv \frac{1}{2} \left(-\hbar^2 \frac{d^2}{dq^2} + \omega'^2 q^2 \right) \quad (1.9.19)$$

with perturbed frequency

$$\omega' \equiv (\omega^2 + \omega_p^2)^{1/2} \quad (1.9.20)$$

where ω_p is given by relation (1.9.17). It is now clear that the role of the term H'_2 in Eq. (1.9.4) has been merely to perturb the photon energy $\hbar\omega$ into $\hbar\omega'$; this is due to back coupling of the field mode with itself via the atomic electrons. Later on we shall see that an analogous perturbation of an atomic energy level takes place due to back coupling of a level with itself via the photons.

The eigenstates of operator (1.9.19) satisfy the modified oscillator equation

$$H'_F |n\rangle = (n + \frac{1}{2})\hbar\omega' |n\rangle \quad (1.9.21)$$

and are given explicitly by⁽³⁾

$$|n\rangle = \left(\frac{\omega'}{\pi\hbar} \right)^{1/4} 2^{-n/2} (n!)^{-1/2} e^{-\omega' q^2/2\hbar} H_n [q(\omega'/\hbar)^{1/2}] \quad (1.9.22)$$

where H_n is the Hermite polynomial of order n . We may also introduce a pair of annihilation and creation operators corresponding to the dressed oscillator modes:

$$\left. \begin{aligned} a' &= (2\hbar\omega')^{-1/2}(\omega'q + ip) \\ a'^+ &= (2\hbar\omega')^{-1/2}(\omega'q - ip) \end{aligned} \right\} \quad (1.9.23)$$

Hence

$$H'_F = \hbar\omega'(a'^+ a' + \frac{1}{2}) \quad (1.9.24)$$

and the full Hamiltonian (1.9.18) assumes the desired alternative form

$$H = H_a + \hbar\omega'(a'^+ a' + \frac{1}{2}) + \frac{ie\hbar s'}{\mu c} \sum_{j=1}^{N_a} \nabla_j \cdot \boldsymbol{\epsilon}(a'^+ + a') \quad (1.9.25)$$

where

$$s' \equiv \left(\frac{2\pi\hbar c^2}{\omega' L^3} \right)^{1/2} \quad (1.9.26)$$

Comparison of Eq. (1.9.25) with Eqs. (1.9.4)–(1.9.9) shows that now the term H'_2 has disappeared from the Hamiltonian expressed in the dressed (primed) modes. The only parameter through which the primed quantities differ from the unprimed ones is the “plasma frequency,”

$$\omega_p = \left[4\pi \frac{e^2}{\mu} \left(\frac{N_a}{L^3} \right) \right]^{1/2} \quad (1.9.27)$$

One should note that the quantization volume L^3 of the laser field is usually of macroscopic dimension. Thus for processes involving interaction of the laser field with an individual atom (e.g., in a dilute gas), such that $L^3 \rightarrow \infty$, N_a fixed, ω_p is a vanishingly small quantity compared to ω since $(N_a/L^3)^{1/2} \rightarrow 0$ and ω_p may be neglected. On the other hand, if the laser interacts simultaneously with a macroscopic collection of electrons or atoms, as for example in a dense gas, then the thermodynamic limit $N_a \rightarrow \infty$, $L^3 \rightarrow \infty$, such that $N_a/L^3 = \rho$ (constant), can be important and ω_p need not be negligible compared to ω . In all cases, however, the dressed Hamiltonian, Eq. (1.9.25) or (1.9.18), can be used with advantage over the equivalent original Hamiltonian (1.9.4).

1.10. The Dressed-Oscillator Atom-Field Hamiltonian with Multimode Laser Fields

We now consider the atom-field Hamiltonian corresponding to an M -mode vector-potential field given by

$$\mathbf{A}(0) = \sum_{m=1}^M \mathbf{A}_m \quad (1.10.1)$$

where each component field

$$\mathbf{A}_m = \left(\frac{2\pi\hbar c^2}{\omega_m L^3} \right)^{1/2} (a_m + a_m^+) \boldsymbol{\epsilon}_m \quad (1.10.2)$$

has a distinct polarization vector $\boldsymbol{\epsilon}_m$, frequency ω_m , and amplitude.

In analogy with Eqs. (1.9.4)–(1.9.9), we may at once write down the total Hamiltonian in the M -mode case,

$$H(M) = H_a + H'_1(M) + H'_2(M) + H_F(M) \quad (1.10.3)$$

where

$$H'_1(M) = \frac{ie\hbar}{\mu c} \sum_{j=1}^{N_a} \sum_{m=1}^M \nabla_j \cdot \boldsymbol{\epsilon}_m s_m (a_m + a_m^+) \quad (1.10.4)$$

$$H'_2(M) = \frac{e^2 N_a}{2\mu c^2} \left[\sum_{m=1}^M \boldsymbol{\epsilon}_m s_m (a_m + a_m^+) \right]^2 \quad (1.10.5)$$

$$H_F(M) = \sum_{m=1}^M (a_m^+ a_m + \frac{1}{2}) \hbar \omega \quad (1.10.6)$$

and

$$s_m = \left(\frac{2\pi\hbar c^2}{\omega_m L^3} \right)^{1/2} \quad (1.10.7)$$

We may generalize the method of the previous section to reduce Hamiltonian (1.10.3) to one containing only the interaction operator $H'_1(M)$. It will be seen that now not only the photon energies $\hbar\omega_m$, but also the polarizations $\boldsymbol{\epsilon}_m$ are affected by the mutual interactions $H'_2(M)$ of the unperturbed modes.

For each mode m , we define

$$\left. \begin{aligned} q_m &= \left(\frac{\hbar}{2\omega_m} \right)^{1/2} (a_m + a_m^+) \\ p_m &= -i \left(\frac{\hbar\omega_m}{2} \right)^{1/2} (a_m - a_m^+) \equiv -i\hbar \frac{d}{dq_m} \end{aligned} \right\} \quad (1.10.8)$$

and

or

$$\left. \begin{aligned} a_m &= (2\hbar\omega_m)^{-\frac{1}{2}} (\omega_m q_m + ip_m) \\ a_m^+ &= (2\hbar\omega_m)^{-\frac{1}{2}} (\omega_m q_m - ip_m) \end{aligned} \right\} \quad (1.10.9)$$

and

On substituting expressions (1.10.8) and (1.10.9) in Eqs. (1.10.3)–(1.10.6), we obtain

$$H(M) = H_a + \frac{ie\hbar}{\mu} \left(\frac{4\pi}{L^3} \right)^{1/2} \sum_{j=1}^{N_a} \sum_{m=1}^M \nabla_j \cdot \boldsymbol{\epsilon}_m q_m + H'_F(M) \quad (1.10.10)$$

where

$$\begin{aligned} H'_F(M) &\equiv \frac{1}{2} \sum_{m=1}^M \left(-\hbar^2 \frac{d^2}{dq_m^2} + \omega_m^2 q_m^2 \right) \\ &\quad + \frac{1}{2} \omega_p^2 \sum_{m=1}^M \sum_{m'=1}^M \boldsymbol{\epsilon}_m \cdot \boldsymbol{\epsilon}_{m'} q_m q_{m'} \end{aligned} \quad (1.10.11)$$

We recognize relation (1.10.11) as the Hamiltonian of a system of coupled quantum oscillators. Hence it may be diagonalized using the well-known procedure of normal coordinates. To this end we first rewrite it as

$$H'_F(M) = \frac{1}{2} \left(\sum_{m=1}^M p_m^2 + \sum_{m=1}^M \sum_{m'=1}^M W_{mm'} q_m q_{m'} \right) \quad (1.10.12)$$

where the matrix $W_{mm'}$ is defined by

$$W_{mm'} \equiv \omega_m^2 \delta_{mm'} + \omega_p^2 \boldsymbol{\epsilon}_m \cdot \boldsymbol{\epsilon}_{m'}, \quad (m, m') = 1, 2, \dots, M \quad (1.10.13)$$

We note that $W_{mm'}$ is real and symmetric, so we may diagonalize it with the help of the transformation matrix $U_{\lambda,\lambda'}$, which satisfies the biorthonormal conditions

$$\sum_{m=1}^M U_{\lambda m} U_{\lambda' m} = \delta_{\lambda\lambda'} \quad (1.10.14)$$

and

$$\sum_{\lambda=1}^M U_{\lambda m} U_{\lambda m'} = \delta_{mm'} \quad (1.10.15)$$

The desired normal coordinates are therefore the eigenvectors

$$Q_\lambda = \sum_{m=1}^M U_{\lambda m} q_m \quad (1.10.16)$$

We also define the corresponding canonical momenta by

$$-i\hbar \frac{d}{dQ_\lambda} = P_\lambda = \sum_{m=1}^M U_{\lambda m} p_m = \sum_{m=1}^M U_{\lambda m} \left(-i\hbar \frac{d}{dq_m} \right) \quad (1.10.17)$$

The eigenvalues of the matrix W , Eq. (1.10.13), are denoted below by ω'_λ , where $\lambda = 1, 2, \dots, M$. It is easily verified, using the definitions above, that P_λ and Q_λ satisfy the required commutation relations

$$[P_\lambda, Q_{\lambda'}] = -i\hbar \delta_{\lambda\lambda'} \quad (1.10.18)$$

Besides, in view of definitions (1.10.14)–(1.10.17) one easily finds

$$\sum_{m=1}^M \sum_{m'=1}^M W_{mm'} q_m q_{m'} = \sum_{\lambda=1}^M \omega'^2_\lambda Q_\lambda^2 \quad (1.10.19)$$

and

$$\sum_{m=1}^M p_m^2 = \sum_{\lambda=1}^M P_\lambda^2 \quad (1.10.20)$$

When Eqs. (1.10.19) and (1.10.20) are substituted in expression (1.10.12), we get the dressed-oscillator Hamiltonian

$$H'_F(M) = \frac{1}{2} \sum_{\lambda=1}^M (P_\lambda^2 + \omega'^2_\lambda Q_\lambda^2) \quad (1.10.21)$$

with perturbed frequencies ω'_λ . Substitution of relation (1.10.16) in the

interaction $H'_i(M)$, Eq. (1.10.4), yields

$$H'_i(M) = \frac{ie\hbar}{\mu} \left(\frac{4\pi}{L^3} \right)^{1/2} \sum_{j=1}^{N_a} \sum_{\lambda=1}^M \nabla_j \cdot \boldsymbol{\epsilon}'_\lambda Q_\lambda \quad (1.10.22)$$

where the modified polarization vectors (of the dressed photon modes, Q_λ) are defined by

$$\boldsymbol{\epsilon}'_\lambda = \sum_{m=1}^M \boldsymbol{\epsilon}_m U_{m\lambda}, \quad \lambda = 1, 2, \dots, M \quad (1.10.23)$$

Thus finally the multimode Hamiltonian (1.10.3) reduces to exactly

$$H = H_a + H'_F(M) + H'_i(M) \quad (1.10.24)$$

where the individual terms on the right-hand side are given by Eqs. (1.9.5), (1.10.21), and (1.10.22), respectively.

We may also introduce the dressed annihilation and creation operators

$$\begin{aligned} a'_\lambda'^+ &\equiv (2\hbar\omega'_\lambda)^{-1/2} (\omega'_\lambda Q_\lambda + iP_\lambda) \\ a'_\lambda &\equiv (2\hbar\omega'_\lambda)^{-1/2} (\omega'_\lambda Q_\lambda - iP_\lambda) \end{aligned} \quad \left. \right\} \quad (1.10.25)$$

In terms of these quantities the reduced Hamiltonian (1.10.24) takes the alternative form

$$H = H_a + \sum_{\lambda=1}^M (a'_\lambda'^+ a'_\lambda + \frac{1}{2}) \hbar\omega'_\lambda + \frac{ie\hbar}{\mu c} \sum_{j=1}^{N_a} \sum_{\lambda=1}^M \nabla_j \cdot \boldsymbol{\epsilon}_\lambda s_\lambda (a'_\lambda + a'_\lambda'^+) \quad (1.10.26)$$

where the dressed-mode normalization constants are

$$s_\lambda = \left(\frac{2\pi\hbar c^2}{\omega'_\lambda L^3} \right)^{1/2} \quad (1.10.27)$$

1.11. Dressed Frequencies and Polarizations of a Two-Mode Field

To obtain a better insight into the nature of the multimode dressed-field frequencies and polarizations let us briefly consider the case of a two-mode field.

The matrix $W_{mm'}$ in Eq. (1.10.13) for $M = 2$ is

$$W_{mm'} \equiv \begin{vmatrix} (\omega_1^2 + \omega_p^2) & \omega_p^2 \boldsymbol{\epsilon}_1 \cdot \boldsymbol{\epsilon}_2 \\ \omega_p^2 \boldsymbol{\epsilon}_2 \cdot \boldsymbol{\epsilon}_1 & (\omega_2^2 + \omega_p^2) \end{vmatrix} \quad (1.11.1)$$

In terms of the eigenvalues of relation (1.11.1) we obtain the dressed photon energies

$$\left. \begin{aligned} \hbar\omega'_1 &= \hbar \left\{ \frac{\omega_1^2 + \omega_2^2 + 2\omega_p^2}{2} + \left[\left(\frac{\omega_1^2 - \omega_2^2}{2} \right)^2 + \omega_p^4 (\boldsymbol{\epsilon}_1 \cdot \boldsymbol{\epsilon}_2)^2 \right]^{1/2} \right\}^{1/2} \\ \hbar\omega'_2 &= \hbar \left\{ \frac{\omega_1^2 + \omega_2^2 + 2\omega_p^2}{2} - \left[\left(\frac{\omega_1^2 - \omega_2^2}{2} \right)^2 + \omega_p^4 (\boldsymbol{\epsilon}_1 \cdot \boldsymbol{\epsilon}_2)^2 \right]^{1/2} \right\}^{1/2} \end{aligned} \right\} \quad (1.11.2)$$

and

We note that the magnitude of the dressed photon energies depends characteristically on the angle between the polarization directions of the unperturbed modes.

The transformation matrix $U_{\lambda\lambda'}$ corresponding to relation (1.11.1) is

$$U_{\lambda\lambda'} \equiv \begin{pmatrix} \cos \theta & \sin \theta \\ -\sin \theta & \cos \theta \end{pmatrix} \quad (1.11.3)$$

where

$$\tan 2\theta = \frac{\omega_p^2 (\boldsymbol{\epsilon}_1 \cdot \boldsymbol{\epsilon}_2)}{\frac{1}{2}(\omega_1^2 - \omega_2^2)} \quad (1.11.4)$$

Hence the polarization vectors of the two dressed modes are explicitly

$$\boldsymbol{\epsilon}'_1 = \cos \theta \boldsymbol{\epsilon}_1 + \sin \theta \boldsymbol{\epsilon}_2 \quad (1.11.5)$$

$$\boldsymbol{\epsilon}'_2 = -\sin \theta \boldsymbol{\epsilon}_1 + \cos \theta \boldsymbol{\epsilon}_2 \quad (1.11.6)$$

Thus the perturbed polarization vectors in their turn depend on the frequencies.

We conclude this section by noting that in the case of the M -mode field, the importance of the interaction term $H_2'(M)$ is again determined by the size of the plasma frequency ω_p , Eq. (1.9.27). As before, we may conveniently use Hamiltonian (1.10.26) independently of the size of ω_p and interpret the results in terms of the unperturbed (unprimed) or perturbed (primed) frequencies and polarizations [such as Eqs. (1.11.2) and (1.11.5)]

depending on whether or not

$$\omega_p \ll \omega_m, \quad m = 1, 2, \dots, M \quad (1.11.7)$$

1.12. The “Length-Form” Atom–Field Hamiltonian

We consider another transformed form of the original atom–field Hamiltonian (1.9.4)–(1.9.9), which is also useful in the context of multiphoton processes in a laser field. To derive this dipole “length-form” quantum Hamiltonian we start not with Eq. (1.9.4) but with its exact equivalent, Eq. (1.9.18), in the oscillator representation:

$$H = -\frac{\hbar^2}{2\mu} \sum_{j=1}^{N_a} \nabla_j^2 + V(\mathbf{r}_1, \mathbf{r}_2, \dots, \mathbf{r}_{N_a}) + \frac{1}{2} \left(-\hbar^2 \frac{d^2}{dq^2} + \omega^2 q^2 \right) + \frac{ie\hbar}{\mu} \left(\frac{4\pi}{L^3} \right)^{1/2} \sum_{j=1}^{N_a} \nabla_j \cdot \boldsymbol{\epsilon} q + \frac{1}{2} \omega_p^2 q^2 \quad (1.12.1)$$

We consider the unitary transformation⁽⁶⁾

$$U = \exp \left[i \frac{e}{\hbar c} \sum_{j=1}^{N_a} \mathbf{r}_j \cdot \mathbf{A}(0) \right] = \exp \left[i \left(\frac{4\pi}{L^3} \right)^{1/2} \sum_{j=1}^{N_a} e \mathbf{r}_j \cdot \boldsymbol{\epsilon} q \right] \quad (1.12.2)$$

In the second line we have used the vector potential (1.9.12). The total state vector $|\psi\rangle$ satisfying the Schrödinger equation

$$i\hbar \frac{\partial |\psi\rangle}{\partial t} = H |\psi\rangle \quad (1.12.3)$$

may be transformed by U into $|\Psi\rangle$ where

$$|\psi\rangle = U |\Psi\rangle \quad (1.12.4)$$

Equations (1.12.3) and (1.12.4) can be used to easily calculate

$$\nabla_j |\psi\rangle = U \left[\nabla_j + \frac{ie}{\hbar} \left(\frac{4\pi}{L^3} \right)^{1/2} \boldsymbol{\epsilon} q \right] |\Psi\rangle \quad (1.12.5)$$

$$\nabla_j^2 |\psi\rangle = U \left[\nabla_j^2 + \frac{2ie}{\hbar} \left(\frac{4\pi}{L^3} \right)^{1/2} \nabla_j \cdot \boldsymbol{\epsilon} q - \frac{e^2}{\hbar^2} \left(\frac{4\pi}{L^3} \right) q^2 \right] |\Psi\rangle \quad (1.12.6)$$

and

$$\frac{d^2}{dq^2} |\psi\rangle = U \left[\frac{d^2}{dq^2} + \frac{2ie}{\hbar} \left(\frac{4\pi}{L^3} \right)^{1/2} \sum_{j=1}^{N_a} \mathbf{r}_j \cdot \mathbf{\epsilon} \frac{d}{dq} - \frac{e^2}{\hbar^2} \left(\frac{4\pi}{L^3} \right) \left(\sum_{j=1}^{N_a} \mathbf{r}_j \right)^2 \right] |\psi\rangle \quad (1.12.7)$$

Substituting Eqs. (1.12.6) and (1.12.7) in expression (1.12.1) and simplifying, one gets the Schrödinger equation for $|\Psi\rangle$:

$$\begin{aligned} i\hbar \frac{d}{dt} |\Psi\rangle = & \left[\sum_{j=1}^{N_a} -\frac{\hbar^2}{2\mu} \nabla_j^2 + V(\mathbf{r}_1, \mathbf{r}_2, \dots, \mathbf{r}_{N_a}) \right. \\ & + \frac{1}{2} \left(-\hbar^2 \frac{d^2}{dq^2} + \omega^2 q^2 \right) + \left(\frac{4\pi}{L^3} \right)^{1/2} e \sum_{j=1}^{N_a} \mathbf{r}_j \cdot \mathbf{\epsilon} \left(-i\hbar \frac{d}{dq} \right) \\ & \left. + \frac{2\pi}{L^3} \left(\sum_{j=1}^{N_a} e \mathbf{r}_j \right)^2 \right] |\Psi\rangle \end{aligned} \quad (1.12.8)$$

Remembering the definition of the electric-field operator $E(0)$, namely Eq. (1.9.13), we see that the above transformed Hamiltonian has the structure

$$H = H_a + H_F + \mathbf{D} \cdot \mathbf{E}(0) + \frac{2\pi}{L^3} [\mathbf{D}]^2 \quad (1.12.9)$$

where

$$\mathbf{D} \equiv \mathbf{D}(\mathbf{r}_1, \mathbf{r}_2, \dots, \mathbf{r}_{N_a}) = \left(-e \sum_{j=1}^{N_a} \mathbf{r}_j \right) \quad (1.12.10)$$

is the atomic dipole polarization operator. Operators H_a and H_F are the free-atom and free-field Hamiltonians, respectively.

We note from Eq. (1.12.9) that the interaction operator actually consists of two terms,

$$H' = +\mathbf{D} \cdot \mathbf{E}(0) \quad (1.12.11)$$

and

$$H'' = \frac{2\pi}{L^3} [\mathbf{D}]^2 \quad (1.12.12)$$

However, the “polarization energy” operator H'' is a quantity which depends, as does the plasma frequency ω_p given by Eq. (1.9.27), on the normalization volume of the laser field. For interactions of laser photons with an individual electron or atom (e.g., in a dilute gas) one may take the limit $L^3 \rightarrow \infty$, N_a fixed, so that $H'' \Rightarrow 0$. On the other hand, in the appropriate case of the thermodynamic limit (e.g., in a dense gas) where the effective electron number $N_a \rightarrow \infty$, $L^3 \rightarrow \infty$, such that $N_a/L^3 = \rho$ (constant), one should expect a significant contribution from the polarization energy term H'' .

2

The Perturbation Theory

2.1. Introduction

The essence of the theory of multiphoton processes proper lies in perturbation theory of one form or another. In this chapter we shall present a systematic development of perturbation theory and the relevant diagrammatic technique suitable for multiphoton processes. The simplest form of perturbation theory for multiphoton processes is that originally developed by Dirac⁽⁷⁾ for studying, among other things, the interaction of radiation with matter. This method is suitable for both time-dependent and time-independent interactions. We shall first derive the multiphoton transition amplitudes using the (time-dependent) semiclassical interaction. Later we shall see that use of quantum-field interaction generates completely equivalent results for virtually all processes in laser fields. This circumstance allows one to treat most multiphoton processes in a laser field using either the semiclassical or quantum-field formalism; the choice depends mainly on convenience in any particular situation.

2.2. Time-Dependent Perturbation Theory

The Schrödinger equation with an arbitrary time-dependent interaction $V(t)$ is

$$i\hbar \frac{\partial}{\partial t} \Psi(t) = [H_0 + V(t)]\Psi(t) \quad (2.2.1)$$

where H_0 is the “unperturbed” Hamiltonian. We shall also call H_0 a “reference Hamiltonian” in the sense that it is with reference to the states of H_0 that transition processes of physical interest are supposed to be

measured and hence defined and calculated. This definition requires that the states of the total Hamiltonian

$$H = H_0 + V(t) \quad (2.2.2)$$

approach the states of the reference Hamiltonian H_0 at asymptotically large time (or spatial) separations. We shall therefore develop the perturbation theory assuming that $V(t)$ is switched on and off adiabatically as $t \rightarrow \pm\infty$.

Let us rewrite the total wave function

$$\Psi(t) = \exp(-iH_0t/\hbar)\psi(t) \quad (2.2.3)$$

and substitute it in Eq. (2.2.1). This gives the new Schrödinger equation for $\psi(t)$ in the interaction picture

$$i\hbar \frac{\partial}{\partial t} \psi(t) = \hat{V}(t)\psi(t) \quad (2.2.4)$$

with modified interaction

$$\hat{V}(t) = \exp(iH_0t/\hbar)V(t)\exp(-iH_0t/\hbar) \quad (2.2.5)$$

We note in passing that the new perturbation $\hat{V}(t)$ is always time-dependent even if the old $V(t)$ was time-independent. The reference states of H_0 will be denoted $|j\rangle$ with energies $\varepsilon_j \equiv \hbar\omega_j$. We have introduced atomic eigenfrequencies ω_j for later convenience. In effect we assume that

$$H_0|j\rangle = \varepsilon_j |j\rangle = \hbar\omega_j |j\rangle \quad (2.2.6)$$

is a solved problem. The matrix elements of the modified interaction are

$$\langle j | \hat{V}(t) | i \rangle = \exp[i(\omega_i - \omega_j)t] \langle j | V(t) | i \rangle \quad (2.2.7)$$

which differ from that of $V(t)$ only by the phasor factor $\exp[i(\omega_i - \omega_j)t]$. A “solution” of Eq. (2.2.4) corresponding to the initial reference state $|i\rangle$ is

$$\psi_i(t) = |i\rangle + (-i/\hbar) \int_{-\infty}^t dt_1 V(t_1) | \psi_i(t_1) \rangle \quad (2.2.8)$$

This is easily verified by differentiating it once with respect to time. Clearly this solution reduces to the stationary reference state $|i\rangle$ in the remote past $t \rightarrow -\infty$. The quantity of primary interest is not the wave function but the probability amplitude for transition from the initial state $|i\rangle \rightarrow |f\rangle$, where

$|f\rangle$ is the final state of interest. This is of course given by the component of $\psi_i(t)$ containing $|f\rangle$, i.e., $\langle f | \psi_i(t) \rangle$. We may rewrite this amplitude

$$\langle f | \psi_i(t) \rangle \equiv \langle f | A(t) | i \rangle \quad (2.2.9)$$

in terms of an amplitude operator $A(t)$. By our definition (2.2.9), the transition amplitude at any time t between any two reference states $|i\rangle$ and $|f\rangle$ is merely the matrix element of $A(t)$ between these two states. Another simple way of looking at $A(t)$ is to undo the projection on the arbitrary final state $|f\rangle$ in relation (2.2.9). This gives

$$\psi_i(t) = A(t) | i \rangle \quad (2.2.10)$$

Equation (2.2.10) shows that $A(t)$ brings the unperturbed initial state $|i\rangle$ into the corresponding fully evolved “perturbed” state $\psi_i(t)$; $A(t)$ is therefore called the evolution operator. We may use Eq. (2.2.10) in both sides of Eq. (2.2.8) and undo the projection on the (arbitrary) initial state $|i\rangle$. This gives the equation for determining $A(t)$ in the form

$$A(t) = 1 + (-i/\hbar) \int_{-\infty}^t dt_1 V(t_1) A(t_1) \quad (2.2.11)$$

One way of solving Eq. (2.2.11) is by simple iteration, i.e., substituting $A(t_1)$ in the integral for the whole of the right-hand side evaluated at t_1 and repeating the process indefinitely. This gives the series solution

$$A(t) = 1 + \sum_{N=1}^{\infty} A^{(N)}(t) \quad (2.2.12)$$

where

$$A^{(1)}(t) = -i/\hbar \int_{-\infty}^t dt_1 V(t_1) \quad (2.2.13)$$

$$A^{(2)}(t) = (-i/\hbar)^2 \int_{-\infty}^t dt_1 V(t_1) \int_{-\infty}^{t_1} dt_2 V(t_2) \quad (2.2.14)$$

$$A^{(N)}(t) = (-i/\hbar)^N \int_{-\infty}^t dt_1 V(t_1) \int_{-\infty}^{t_1} dt_2 V(t_2) \cdots \int_{-\infty}^{t_{N-1}} dt_N V(t_N) \quad (2.2.15)$$

If the interaction is “weak,” then the series may be truncated to a finite term N and the N th-order transition amplitude $\langle f | A^{(N)}(t) | i \rangle$ evaluated.

The semiclassical dipole interaction in the “length gauge” and in the interaction picture is [see Eq. (1.6.15)]

$$\hat{V}(t) = \exp(iH_0 t/\hbar) [\mathbf{E}(t) \cdot \mathbf{D}] \exp(-iH_0 t/\hbar) \quad (2.2.16)$$

where

$$\mathbf{E}(t) = \left(\frac{\mathbf{E}}{2} e^{-i\omega t} + \frac{\mathbf{E}^*}{2} e^{i\omega t} \right) \quad (2.2.17)$$

and

$$\mathbf{D}_\lambda = \boldsymbol{\epsilon}_\lambda \cdot \mathbf{D} \quad (2.2.18)$$

$\mathbf{E}(t)$ is the electric field with maximum amplitude E , $\boldsymbol{\epsilon}_\lambda$ is the polarization vector in mode λ , and \mathbf{D} is the dipole operator of the atom. Let us start with the first-order term of series (2.2.12). By substituting expressions (2.2.16) and (2.2.17) in Eq. (2.2.13) and taking the matrix element between the initial and final states $|i\rangle$ and $|f\rangle$, one immediately obtains

$$\begin{aligned} \langle f | A^{(1)}(t) | i \rangle &= (-i/\hbar) \left[\int_{-\infty}^t dt_1 \exp[-i(\omega_i - \omega_f - \omega)t_1] \frac{E}{2} \langle f | D_\lambda | i \rangle \right. \\ &\quad \left. + \int_{-\infty}^t dt_1 \exp[-i(\omega_i - \omega_f + \omega)t_1] \frac{E^*}{2} \langle f | D_\lambda | i \rangle \right] \end{aligned} \quad (2.2.19)$$

On the assumption that the atom–field interaction time t is much larger than the characteristic atomic periods, we can take the limit $t \rightarrow +\infty$ and obtain the first-order amplitudes of interest

$$\begin{aligned} \langle f | A^{(1)}(\infty) | i \rangle &= -2\pi i/\hbar \left[\delta(\omega_i - \omega_f - \omega) \frac{E}{2} \langle f | D_\lambda | i \rangle \right. \\ &\quad \left. + \delta(\omega_i - \omega_f + \omega) \frac{E^*}{2} \langle f | D_\lambda | i \rangle \right] \end{aligned} \quad (2.2.20)$$

This elementary result already exhibits some of the basic properties of higher-order terms of the perturbation series to be discussed below. We note that Eq. (2.2.20) contains two amplitudes, which are completely independent of one another since they correspond to two different (energy-conserving) delta functions. Notwithstanding the semiclassical description of the radiation field, the first term in Eq. (2.2.20) may be interpreted as the amplitude for absorption of a photon. This term is nonzero only for $\varepsilon_i - \varepsilon_f = \hbar\omega$, which shows that the $i \rightarrow f$ transition occurs only if the atom absorbs the discrete amount of energy $\hbar\omega$ from the wave field. Similarly, the second term may be interpreted as an emission amplitude of a photon; it is nonzero for $\varepsilon_i - \varepsilon_f = -\hbar\omega$, which shows that in this transition the atom contributes an amount of energy $\hbar\omega$ to the wave field. The absorption amplitude corresponds to the field strength $E/2$ while the emission amplitude corresponds to the complex conjugate $E^*/2$. This

will be seen to have a direct parallel with the occurrence of the photon annihilation operator and the photon creation operator in the quantum-field description (we recall that the creation operator is simply the Hermitian conjugate of the annihilation operator). Finally, the one-photon amplitudes are simply proportional to the matrix element of the dipole operator projected onto the polarization vector. We shall see below that, in spite of their more involved nature, the higher-order amplitudes will maintain a similar external structure throughout.

We now consider the second-order term $A^{(2)}(t)$. On taking the matrix element between the initial and final states and inserting a complete set of unperturbed stationary states of H_0 , $\sum_j |j\rangle\langle j| = 1$ between the two interactions, we obtain

$$\begin{aligned} \langle f | A^{(2)}(t) | i \rangle &= (-i/\hbar)^2 \sum_j \int_{-\infty}^t dt_1 \exp[i(\omega_f - \omega_i)t_1] \\ &\quad \times \langle f | D_\lambda \left[\frac{E}{2} \exp(-i\omega t_1) + \frac{E^*}{2} \exp(i\omega t_1) \right] | j \rangle \\ &\quad \times \int_{-\infty}^{t_1} dt_2 \exp[i(\omega_i - \omega_f)t_2] \langle j | D_\lambda \left[\frac{E}{2} \exp(-i\omega t_2) + \frac{E^*}{2} \exp(i\omega t_2) \right] | i \rangle \end{aligned} \quad (2.2.21)$$

One may successively evaluate the time integrals from the right, set the time-dependent terms in the limit $t \rightarrow -\infty$ to zero (adiabatic switching-on condition), go over to the long-time limit $t \rightarrow +\infty$ in the final integral, and finally collect the terms belonging to the same delta functions. This gives

$$\begin{aligned} \langle f | A^{(2)(\infty)} | i \rangle &= -2\pi i (1/\hbar)^2 \left\{ \delta(\omega_i - \omega_f + 2\omega) \sum_j \frac{(E/2)\langle f | D_\lambda | j \rangle (E/2)\langle j | D_\lambda | i \rangle}{(\omega_i + \omega - \omega_j)} \right. \\ &\quad + \delta(\omega_i - \omega_f) \left[\sum_j \frac{(E^*/2)\langle f | D_\lambda | j \rangle (E/2)\langle j | D_\lambda | i \rangle}{(\omega_i + \omega - \omega_j)} \right. \\ &\quad \left. \left. + \sum_j \frac{(E/2)\langle f | D_\lambda | j \rangle (E^*/2)\langle j | D_\lambda | i \rangle}{(\omega_i - \omega - \omega_j)} \right] \right. \\ &\quad \left. + \delta(\omega_i - \omega_f - 2\omega) \sum_j \frac{(E^*/2)\langle f | D_\lambda | j \rangle (E^*/2)\langle j | D_\lambda | i \rangle}{(\omega_i - \omega - \omega_j)} \right\} \end{aligned} \quad (2.2.22)$$

By interpreting the energy-conserving delta functions as in the first-order case, we see that Eq. (2.2.22) contains:

1. A two-photon absorption amplitude

$$-2\pi i(1/\hbar^2)\delta(\omega_i - \omega_f + 2\omega)(E/2)^2\langle f | D_\lambda G(\omega_i + \omega)D_\lambda | i \rangle \quad (2.2.23)$$

2. A two-photon emission amplitude

$$-2\pi i(1/\hbar^2)\delta(\omega_i - \omega_f - 2\omega)(E^{*2}/2)\langle f | D_\lambda G(\omega_i - \omega)D_\lambda | i \rangle \quad (2.2.24)$$

3. An amplitude with no real emission or absorption of photons

$$\begin{aligned} -2\pi i(1/\hbar^2)\delta(\omega_i - \omega_f) & \left[|(E/2)|^2\langle f | D_\lambda G(\omega_i + \omega)D_\lambda | i \rangle \right. \\ & \left. + |(E/2)|^2\langle f | D_\lambda G(\omega_i - \omega)D_\lambda | i \rangle \right] \end{aligned} \quad (2.2.25)$$

In the above we have written $G(\omega_i \pm \omega)$ for the Green's function (also to be called the "propagator"):

$$G(\omega_i \pm \omega) \equiv \sum_j \frac{|j\rangle\langle j|}{(\omega_i \pm \omega - \omega_j)} \quad (2.2.26)$$

We note that amplitude (2.2.25) is nonzero only when $\omega_i = \omega_f$. Therefore the final state $|f\rangle$ must be either identical with the initial state $|i\rangle$, in which case expression (2.2.25) is the amplitude of the elastic scattering related to the dynamic Stark shift, or if $|f\rangle$ is different from $|i\rangle$ it must be degenerate with $|i\rangle$, in which case expression (2.2.25) gives the mixing amplitude between a degenerate pair of states, $|i\rangle$ and $|f\rangle$, due to the radiation field.

2.3. The Diagrammatic Method

The preceding section contains some examples of the fact that an algebraic evaluation of a given term of the perturbation series generates contributions to several distinct physical processes, not all of which may be of interest at the same time. For example, the second-order term (2.2.21) generates the amplitudes for the three physically distinct processes 1, 2, and 3 above. Therefore, it would appear to be useful if we had some *a priori* rules for selecting and writing down directly the amplitudes corresponding to a given multiphoton process of interest. Besides, the algebraic procedure becomes increasingly lengthy and awkward to manipulate with increasing orders. To this end it is usually convenient to translate the algebraic perturbation expansion in a diagrammatic language. For the problem at hand this language turns out to be very simple.

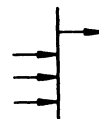
A diagram in the present context⁽⁸⁾ will consist of a vertical line representing the evolution of the atomic states and a number of arrows, each arrow representing a photon (i.e., a field mode with a specific field strength, polarization, wave number, or frequency). An arrow directed away from the line stands for the emission of a photon and an arrow directed into the line for the absorption of a photon. Figure 1 is a typical example of such a diagram, and shows that the atom absorbs three photons successively (reading from below upward) and then emits one photon.

The total number of arrows in a diagram corresponds to the total (real + virtual) number of photons participating in an amplitude. The “net number of arrows,” namely the difference between the numbers of outgoing and ingoing arrows, corresponds to the number of photons involved in the process of interest in a “real” sense, i.e., a long-time, energy-conserving sense, and the rest are considered to be participating only in a “virtual” sense, i.e., highly transient (energy-nonconserving) way. The perturbative (nominal) order of a diagram corresponds to the total number of arrows. The “net number” of arrows gives the physical or real photon order of the process to which the diagram contributes. Figure 1, for example, gives a (nominal) fourth-order contribution to a real two-photon absorption probability. At very high intensities there may be several diagrams of different perturbative (or nominal) orders, which contribute significantly to the same real photon or physical order of the process.

2.4. Rules for Construction of the Diagrams

A diagram containing N arrows (to be called an N th-order diagram) corresponds to an N th-order transition amplitude. Let Δn be the number of outgoing arrows minus the number of ingoing arrows, where $|\Delta n| \leq N$. Clearly, for $\Delta n > 0$, an N th-order diagram contributes to a real Δn -photon emission process assisted by $N - \Delta n$ virtual photons. Similarly, $\Delta n < 0$ corresponds to a real $|\Delta n|$ -photon absorption process assisted by $N - |\Delta n|$ virtual photons. The situation $\Delta n = 0$ corresponds to an elastic process with no real absorption or emission of photons. Thus, for example, the diagram in Figure 1 shows $N = 4$, $\Delta n = -2$; it therefore corresponds to a fourth-order amplitude and contributes to a “real” two-photon absorption,

Figure 1. A typical fourth-order diagram showing absorption of three photons followed by emission of one photon; it contributes to the net absorption of two photons. Changing the sense of all arrows in a diagram gives the corresponding diagram for the inverse process, in this case for the net emission of two photons.



assisted by $N - |\Delta n| = 2$ “virtual” photons. The following rules of thumb regarding diagrams of any order, in a monomode field, will be found to be useful:

1. The total number of diagrams in the N th order is 2^N .
2. To a $|\Delta n|$ -photon emission or absorption process in the N th order (out of 2^N diagrams) only

$$n_d \equiv \frac{N!}{\left(\frac{N + \Delta n}{2}\right)! \left(\frac{N - \Delta n}{2}\right)!} \quad (2.4.1)$$

diagrams contribute, provided $(N + \Delta n)/2$ is integral. When $(N + \Delta n)/2$ is nonintegral, there are no contributing diagrams at all.

3. The number of outgoing arrows in a diagram is $(N + \Delta n)/2$ and of ingoing arrows is $(N - \Delta n)/2$.
4. For even (odd) photon processes only even- (odd-) order diagrams contribute. Thus, for a two-photon emission process ($\Delta n = +2$), contributions arise from $N = 2, 4, 6, \dots$ orders.

The diagrammatic method is best clarified by working out examples. First we show how to draw all the appropriate diagrams for a given real photon process up to any given perturbative order. Then we state simple rules for writing down the analytic formula for the transition amplitude corresponding to a given diagram. The rules of thumb mentioned above will help in constructing the diagrams and also in ensuring that none of the relevant diagrams in a given order is omitted. All diagrams for a given emission process can be obtained from the diagrams of the corresponding absorption process by reversing the sense of all arrows appearing in the absorption diagrams, and vice versa.

2.4.1. Two-Photon Absorption

Let us consider the two-photon absorption process ($\Delta n = -2$). The diagrams contributing to this process occur in $N = 2, 4, 6, \dots$ orders.

The second-order diagrams. In this order the requirement that the total number of arrows must be two (since $N = 2$), and also that the number of ingoing arrows must be two (since $\Delta n = -2$), gives rise to the only diagram shown in Figure 2.



Figure 2. The lowest-order (second-order) diagram contributing to two-photon absorption.

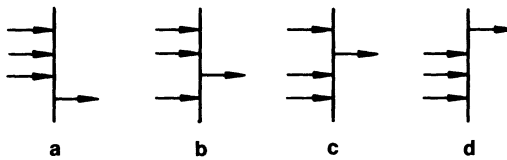


Figure 3. The four topologically distinct fourth-order diagrams which provide the first correction to the two-photon absorption amplitude.*

The fourth-order diagrams. The requirement $N = 4$ and $\Delta n = -2$ is satisfied by the four diagrams in Figure 3. Each of these diagrams contains four arrows in all ($N = 4$) with two “excess” ingoing arrows ($\Delta n = -2$). At this point it may be noted that according to rule 1 in the fourth order there are $2^4 = 16$ diagrams in all of which, according to rule 2, only

$$n_d = \frac{4!}{\left(\frac{4-2}{2}\right)!\left(\frac{4+2}{2}\right)!} = 4$$

contribute to the desired two-photon absorption process. This last number makes sure that no fourth-order diagram pertaining to the two-photon absorption process is omitted from our list of four topologically distinct diagrams shown in Figure 3.

If we wish to consider higher-order contributions to the two-photon absorption process, we must next go to the sixth order ($N = 6$). In this order there are in all $2^6 = 64$ diagrams of which, according to rule 2, only $n_d = 6!/(4!2!) = 15$ diagrams contribute to the two-photon absorption amplitude. They must each consist of six arrows ($N = 6$) and have two ingoing arrows in “excess” ($\Delta n = -2$). According to rule 3, therefore, there must be two outgoing and four ingoing arrows in each diagram. The 15 distinct diagrams in the sixth order are shown in Figure 4.

We note that it is usually not difficult to find a systematic way of drawing the necessary distinct diagrams. In the above case, for example, the first line shows that the diagrams with the necessary two outgoing arrows occur next to each other with no ingoing arrows between them. In the second line, there is one ingoing arrow occurring between them. Similarly, in the third and fourth lines there are respectively two and three ingoing arrows between them, until finally in the fifth line all the four ingoing arrows occur between the two outgoing arrows.

In the next-higher order, i.e., in the eighth order, there are altogether $2^8 = 256$ diagrams of which only $n_d = 8!/(5!3!) = 56$ diagrams contribute to the two-photon absorption process ($\Delta n = -2$). According to rule 3 there must be three outgoing and five ingoing arrows occurring in each of the diagrams. The 56 distinct diagrams are listed in Appendix 1a.

* Henceforth, vertical lines are assumed implicitly directed.

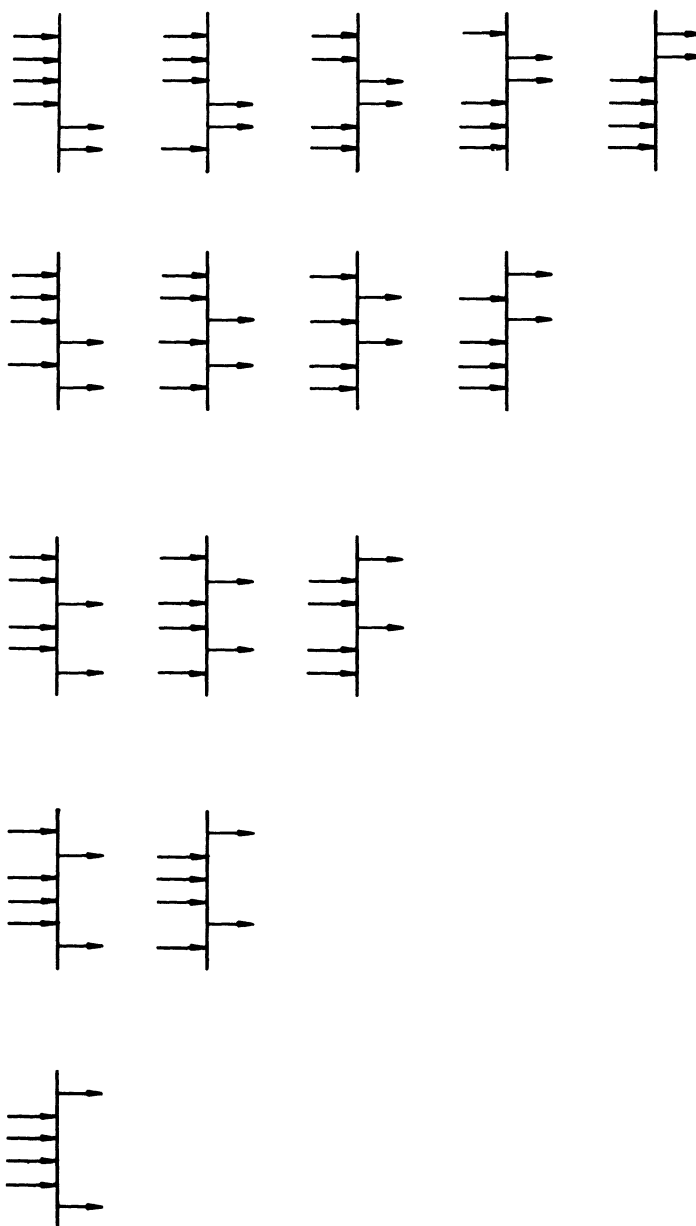


Figure 4. The fifteen topologically distinct sixth-order diagrams which provide the second correction to the two-photon absorption amplitude.

It should be remembered that for a Δn -photon emission process the necessary diagrams are obtained immediately from that of the n -photon absorption diagrams in any order by simply reversing the sense of the arrows.

2.4.2. Three-Photon Absorption

For the three-photon absorption, $\Delta n = -3$, contributions arise from $N = 3, 5, 7, \dots$ orders. The lowest-order diagram is given in Figure 5.

The first correction arises in the fifth order; the contributing five diagrams are shown in Figure 6. In the next-higher (seventh) order there are 21 contributing diagrams, which are given in Appendix 1b.

Figure 5. The lowest-order (third-order) diagram for three-photon absorption.

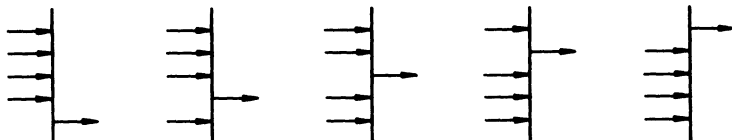
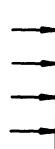


Figure 6. The five topologically distinct diagrams which provide the first correction to the three-photon absorption amplitude.

2.4.3. Four-Photon Absorption

The lowest-order contribution arises from the single diagram in Figure 7. The first correction occurs in the sixth order where there are six diagrams, as shown in Figure 8. In the next (eighth) order there are 28 diagrams, which are given in Appendix 1c.

Figure 7. The lowest-order (fourth-order) diagram for four-photon absorption.



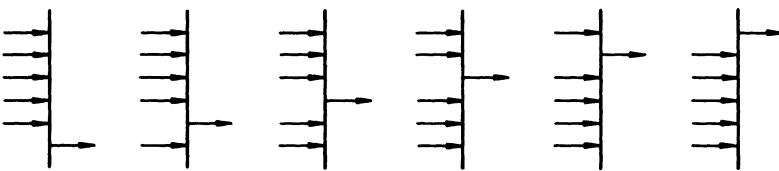


Figure 8. The six topologically distinct sixth-order diagrams which provide the first correction to the four-photon absorption amplitude.

2.4.4. Single-Photon Absorption

Although we are concerned here with multiphoton processes it is not quite out of context to consider the higher-order contributions to the single-photon absorption process. Certainly such contributions, which occur through virtual multiphoton processes, could be of significance at high laser intensities, currently available. The obvious first-order diagram is shown in Figure 9.

The first correction to the one-photon absorption amplitude is given by the three third-order diagrams, shown in Figure 10. In the next-higher (fifth) order there are 10 diagrams that contribute to the process. They are given in Figure 11. In the seventh order there are 35 diagrams, which can be found in Appendix 1d.

So far we have considered examples of diagrams for typical multiphoton processes involving only a monomode field. Multiphoton processes in fields of more than one mode are also of interest. Below we consider a few examples of diagrams with two- and three-mode interactions.



Figure 9. The lowest-order (first-order) diagram for one-photon absorption.

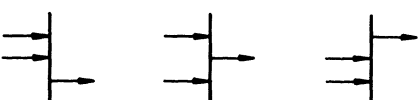


Figure 10. The three distinct third-order diagrams which provide the first correction to the one-photon absorption amplitude.

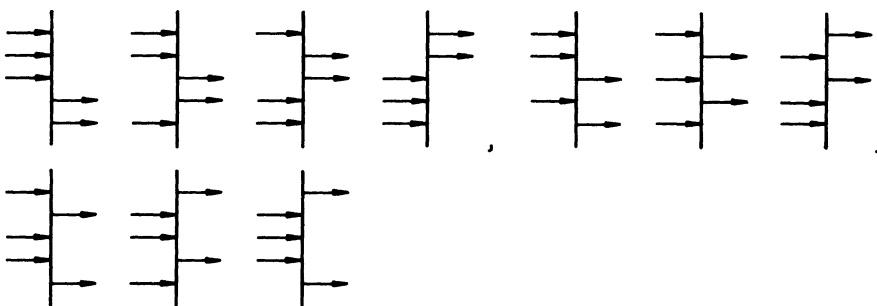


Figure 11. The ten topologically distinct diagrams which provide the second correction to the one-photon absorption amplitude.

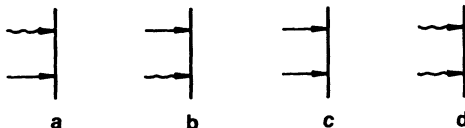
2.4.5. Two-Photon Absorption (Two-Mode Field)

Let us denote the photons of two distinct modes by two distinct arrows, \rightsquigarrow and \rightarrow . In the lowest nonvanishing order (second order) there are four distinct diagrams, shown in Figure 12.

We note that diagrams (c) or (d) correspond to absorption of two photons of the same mode, and therefore are of the same kind as in the monomode case in Figure 2. Diagrams (a) and (b) correspond to two-photon absorption with one photon of each kind. It is noteworthy that the sum of the two frequencies in cases (a) and (b) is equal and hence the two amplitudes may contribute coherently to the absorption process. If the frequencies of the two modes are not equal, then the sum of photon frequencies in cases (c) and (d) are different and differ from that of (a) and (b). Therefore they are not coherent with respect to one another. Consequently, for two-photon absorption from a two-mode field, the amplitude for the absorption of two different frequency photons differs from that of two photons with equal frequencies.

Higher-order corrections to these amplitudes can also be considered in a similar way. Let us consider the fourth-order contributions to two-photon absorption in this case. If the two frequencies are different, then the corrections arise from the 24 fourth-order diagrams with three photons of the kind \rightarrow and one photon of the kind \rightsquigarrow , and vice versa. These diagrams are shown in Figures 13(a) and (b), respectively.

Figure 12. The four topologically distinct lowest-order diagrams for two-photon absorption in a two-mode field. Photons of the two modes are denoted by \rightarrow and \rightsquigarrow .



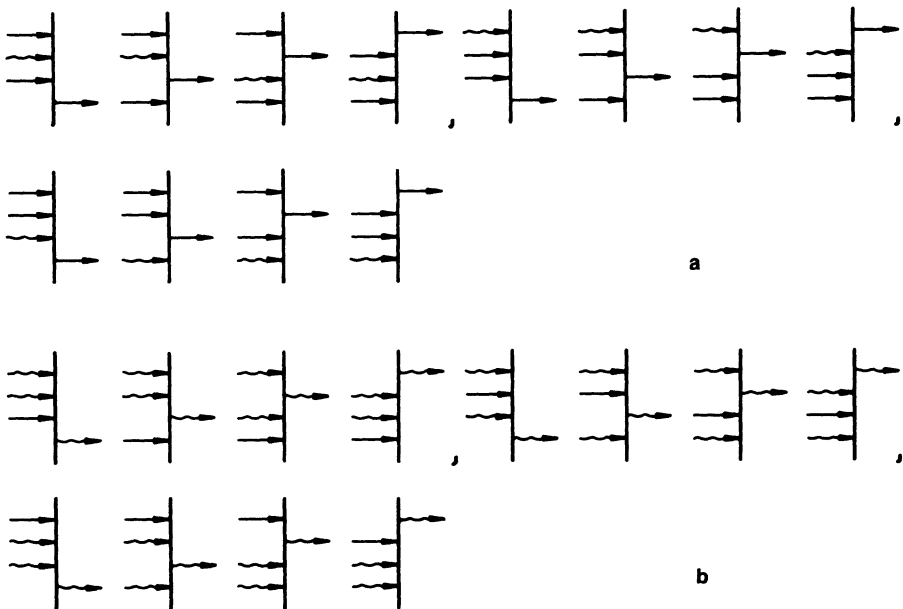


Figure 13. The twenty-four topologically distinct fourth-order diagrams which provide the first correction to the two-photon absorption amplitude in a two-mode field (or two fields) with two distinct frequencies. Diagram (b) can be obtained from diagram (a) by exchanging \rightarrow and \rightsquigarrow .

We note that the 12 diagrams in Figure 13(b) can be obtained from those in Figure 13(a) by exchanging the arrows \rightsquigarrow and \rightarrow .

If the two modes are distinct but their frequencies are identical, then one should add the 40 diagrams shown in Appendix 1e to the list in Figure 13.

2.4.6. Third-Harmonic Generation (Two-Mode Field)

In this process essentially three photons of one kind (\rightarrow) from an external field are absorbed and a new photon (\rightsquigarrow), having frequency three times that of an absorbed photon, is emitted spontaneously. The lowest-order contributions to the amplitude of the process therefore arise in the fourth order. They are given by the four diagrams in Figure 14.

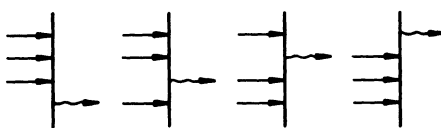


Figure 14. The four topologically distinct lowest-order diagrams for the third-harmonic generation. The third-harmonic photon is indicated by \rightsquigarrow and incident photons by \rightarrow .

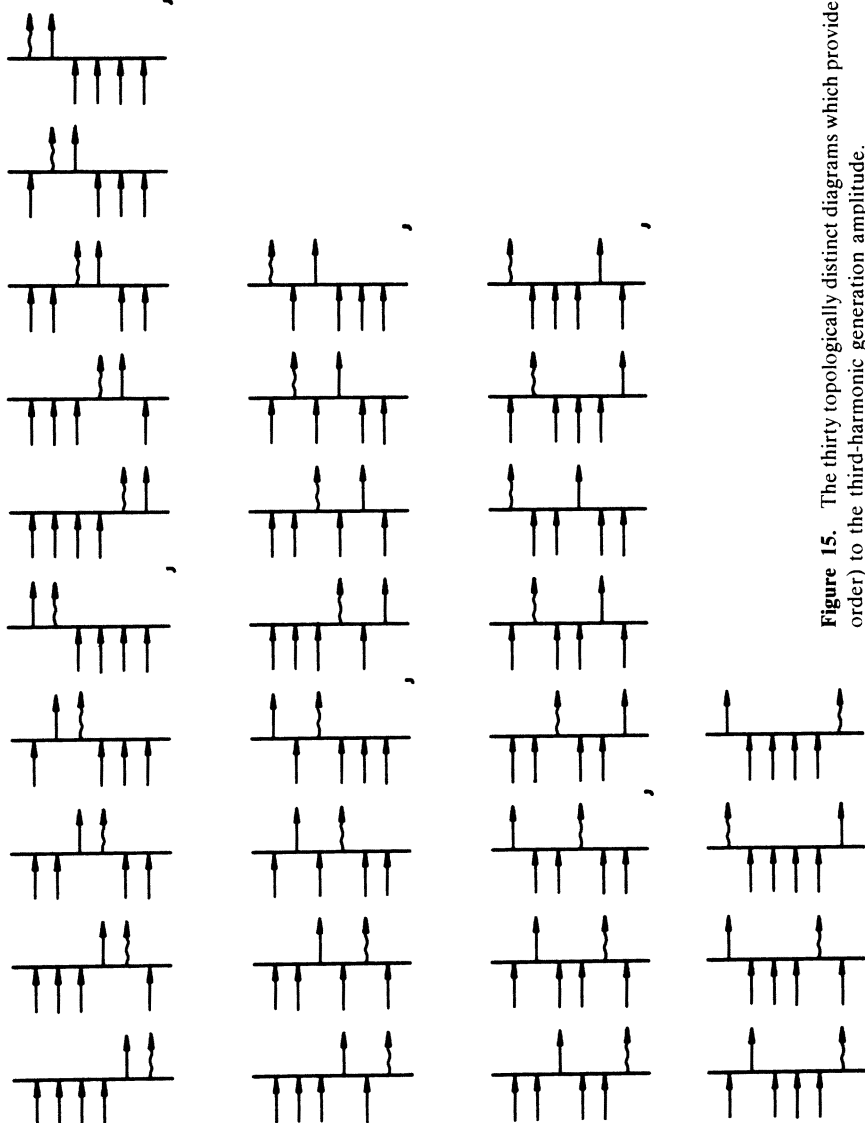


Figure 15. The thirty topologically distinct diagrams which provide the first correction (fifth order) to the third-harmonic generation amplitude.

The first higher-order correction to these amplitudes arises in the sixth order. In this order there are 30 diagrams in which five (three real and two virtual) external photons (\rightarrow) and one spontaneous photon (\rightsquigarrow) take part. They are listed in Figure 15.

We note further that there is another set of $4 \times 15 = 60$ diagrams in the sixth order, which involves three external photons (\rightarrow) and three spontaneous photons (\rightsquigarrow). Nevertheless, each of these diagrams involves three spontaneous photons (two virtual and one real), which makes its contributing strength negligibly small compared to the set of 30 diagrams shown in Figure 15 (involving only one spontaneous photon). They may therefore be quite safely neglected.

2.4.7. Stimulated Emission of One Photon and Absorption of Two Photons in a Three-Mode Interaction

We end our examples of diagrams by considering the case of a three-mode problem in which transition from an initial state of energy ε_i to a final state (energy ε_f) takes place due to three photons of distinct modes. We suppose the photons of the three modes are represented by the symbols \rightarrow (frequency ω_1), \rightsquigarrow (frequency ω_2), and \dashrightarrow (frequency ω_3). Figure 16 presents the 18 distinct third-order diagrams that contribute to the transition of interest.

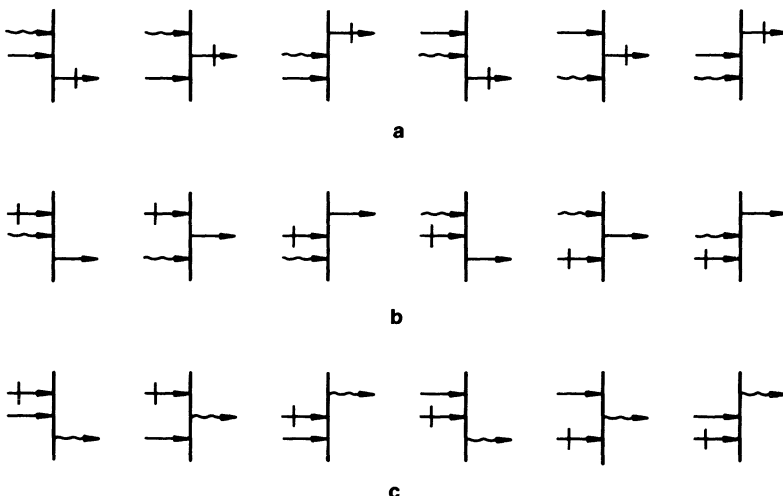


Figure 16. The eighteen topologically distinct lowest-order diagrams for a three-mode interaction process in which one photon is emitted and two photons absorbed.

We observe that the sets of diagrams (a), (b), and (c) are independent when the frequencies are different ($\omega_1 \neq \omega_2 \neq \omega_3$). In this case the set of six diagrams (a) alone contributes to the transition in which

$$\hbar(\omega_3 - \omega_1 - \omega_2) = \varepsilon_i - \varepsilon_f \quad (2.4.7.1)$$

Similarly, set (b) or (c) contributes to the transition process in which the transition energy satisfies respectively

$$\varepsilon_i - \varepsilon_f = \hbar(\omega_1 - \omega_2 - \omega_3) \quad (2.4.7.2)$$

or

$$\varepsilon_i - \varepsilon_f = \hbar(\omega_2 - \omega_1 - \omega_3) \quad (2.4.7.3)$$

Having considered the construction of diagrams of various complexities, we now give the means of converting them into analytic expressions for the transition amplitudes they represent. This can be achieved very simply from the rules given in the next section.

2.5. Rules for Writing Down the Transition Amplitude from a Diagram

Below we give four simple rules for writing down the transition amplitude corresponding to a given diagram. However, we first note the following definitions:

1. The point at which an arrow meets the line is to be called a “vertex.”
2. The “net frequency” $\Delta\Omega$ in any part (or whole) of a diagram is defined as $\Delta\Omega = (\text{sum of frequencies associated with the outgoing arrows}) - (\text{sum of frequencies associated with the ingoing arrows})$, in the considered part or whole of the diagram in question.
3. The “vertex strength” is denoted by V . In the dipole approximation $V = (E/2)D_\lambda$, where E is the electric-field vector, and D_λ is the projection along the field-polarization of the vector \mathbf{D} , the dipole operator of the target atom.
4. The unperturbed “propagator” is defined by

$$G(\omega_i - \Delta\Omega) \equiv \sum_j \frac{|j\rangle\langle j|}{\omega_i - \Delta\Omega - \omega_j} \quad (2.5.1)$$

where $\sum_j |j\rangle\langle j| = 1$ is the complete set of target states.

Rule 1. Read the diagram from below upward and assign a factor V at a vertex if the arrow at the vertex is ingoing, or a factor V^* if the arrow is outgoing.

Rule 2. Between any two neighboring vertices assign a propagator $G(\omega_i - \Delta\Omega)$, where the “net frequency” $\Delta\Omega$ is obtained from the entire portion of the diagram below the position of the propagator.

Rule 3. Multiply the vertex factors and propagator factors from right to left in the sequence of their occurrence from the bottom of the diagram upward. (This expression gives the transition operator.)

Rule 4. To obtain the transition amplitudes, put the initial ket $|i\rangle$ and final bra $\langle f|$, respectively, on the extreme right and left of the transition operator, and supply an overall factor

$$-2\pi i \left(\frac{1}{\hbar}\right)^N \delta(\omega_i - \Delta\Omega_0 - \omega_f) \quad (2.5.2)$$

where N is the total number of arrows and $\Delta\Omega_0$ is the “net frequency” for the whole diagram. (To obtain the full N th-order amplitude simply add similar individual amplitudes corresponding to all diagrams in the N th order with the same total “net frequency” Ω_0 .)

We illustrate the use of these rules below.

2.5.1. Two-Photon Absorption

For two-photon absorption the leading amplitude occurs in the second order, where there is only one diagram (see Figure 2).

Reading from below upward we assign the first vertex factor $(E/2)D_\lambda$ at the lowest vertex, which is followed by the propagator $G(\omega_i + \omega)$ and the last vertex factor $(E/2)D_\lambda$. Using rules 3 and 4 the two-photon absorption amplitude in the second order is simply found to be

$$A_{i \rightarrow f}^{(2)} = -2\pi i \left(\frac{1}{\hbar}\right)^2 \delta(\omega_i - \omega_f + 2\omega) \langle f | (E/2)D_\lambda G(\omega_i + \omega) (E/2)D_\lambda | i \rangle \quad (2.5.1.1)$$

This reproduces exactly Eq. (2.2.23) (which, of course, it must). The next higher-order correction comes from the fourth order, where there are four diagrams [see Figure 3(a), (b), (c), and (d)]. Consider the diagram in Figure 3(a).

Following rules 1 and 2 we assign a vertex factor $(E^*/2)D$ at the lowest vertex and then the propagator $G(\omega_i - \omega)$, and similarly for the rest

of the diagram. Use of rules 2 and 3 yields the transition operator

$$\frac{E}{2} D_\lambda G(\omega_i + \omega) \frac{E}{2} D_\lambda G(\omega_i) \frac{E}{2} D_\lambda G(\omega_i - \omega) \frac{E^*}{2} D_\lambda \quad (2.5.1.2)$$

while rule 4 gives the amplitude:

$$\begin{aligned} & -2\pi i \left(\frac{1}{\hbar} \right)^4 \delta(\omega_i - \omega_f + 2\omega) \langle f | \frac{E}{2} D_\lambda G(\omega_i + \omega) \\ & \times \frac{E}{2} D_\lambda G(\omega_i) \frac{E}{2} D_\lambda G(\omega_i - \omega) \frac{E^*}{2} D_\lambda | i \rangle \end{aligned} \quad (2.5.1.3)$$

By adding similar contributions from the other three diagrams one finds the full fourth-order amplitude corresponding to the two-photon absorption process:

$$\begin{aligned} A_{i \rightarrow f}^{(4)} = & -2\pi i \left(\frac{1}{\hbar} \right)^4 \delta(\omega_i - \omega_f + 2\omega) \\ & \times \left[\langle f | \frac{E}{2} D_\lambda G(\omega_i + \omega) \frac{E}{2} D_\lambda G(\omega_i) \frac{E}{2} D_\lambda G(\omega_i - \omega) \frac{E^*}{2} D_\lambda | i \rangle \right. \\ & + \langle f | \frac{E}{2} D_\lambda G(\omega_i + \omega) \frac{E}{2} D_\lambda G(\omega_i) \frac{E^*}{2} D_\lambda G(\omega_i + \omega) \frac{E}{2} D_\lambda | i \rangle \\ & + \langle f | \frac{E}{2} D_\lambda G(\omega_i + \omega) \frac{E^*}{2} D_\lambda G(\omega_i + 2\omega) \frac{E}{2} D_\lambda G(\omega_i + \omega) \frac{E}{2} D_\lambda | i \rangle \\ & \left. + \langle f | \frac{E^*}{2} D_\lambda G(\omega_i + 3\omega) \frac{E}{2} D_\lambda G(\omega_i + 2\omega) \frac{E}{2} D_\lambda G(\omega_i + \omega) \frac{E}{2} D_\lambda | i \rangle \right] \end{aligned} \quad (2.5.1.4)$$

where the last three lines correspond to the remaining three diagrams, Figure 3(b), (c), and (d), respectively. Clearly the transition amplitude corresponding to any diagram of the present theory, however complex, can be written down by the same simple procedure outlined above.

2.6. The Rate of Multiphoton Transition and the Generalized Cross Section

The probability of multiphoton transition from state $|i\rangle$ to state $|f\rangle$ is simply the square modulus of the corresponding transition amplitude

calculated to any desired order. The most common approximation is to consider an n -photon transition in the lowest nonvanishing order of perturbation theory, i.e., in the n th order. Thus, for example, the probability of absorption of n photons from a monomode laser field is given in the lowest order by

$$\begin{aligned} P_{i \rightarrow f}^{(n)} = & \left| -2\pi i \left(\frac{1}{\hbar}\right)^n \left(\frac{E}{2}\right)^n \delta(\omega_i + n\omega - \omega_f) \right. \\ & \times \langle f | D_\lambda G(\omega_i + (n-1)\omega) \\ & \times D_\lambda G(\omega_i + (n-2)\omega) \cdots D_\lambda G(\omega_i + \omega) D_\lambda | i \rangle \Big|^2 \end{aligned} \quad (2.6.1)$$

The rate (probability per unit interaction time T) of absorption of n photons is defined, when it exists, as

$$W_{i \rightarrow f}^{(n)} \equiv \lim_{T \rightarrow \infty} \frac{P_{i \rightarrow f}^{(n)}}{T} = 2\pi (2\pi\alpha F\omega/e^2)^n |T_{i \rightarrow f}^{(n)}|^2 \delta(\omega_i + n\omega - \omega_f) \quad (2.6.2)$$

In going from expression (2.6.1) to (2.6.2) we have made use of the relation

$$\begin{aligned} \delta(\omega_i + n\omega - \omega_f) &= \lim_{T \rightarrow \infty} \frac{1}{2\pi} \int_{-T/2}^{T/2} \exp[i(\omega_i + n\omega - \omega_f)t] dt \\ &= \lim_{T \rightarrow \infty} T/2\pi \quad \text{for } \omega_i + n\omega = \omega_f \end{aligned} \quad (2.6.3)$$

and the definition of the photon flux (the number of photons passing through unit area in unit time)

$$F \equiv \left(\frac{E^2}{8\pi}\right) \frac{1}{\hbar\omega} c \quad (2.6.4)$$

Often, instead of the flux F , we use the intensity I , defined by the amount of radiant energy flowing per second per unit area, $I \equiv F\hbar\omega$. The quantity $\alpha = e^2/\hbar c$ is the fine-structure constant. Finally, we have defined the compound matrix elements $T_{i \rightarrow f}^{(n)}$ as

$$T_{i \rightarrow f}^{(n)} \equiv \langle f | D_\lambda G[\omega_i + (n-1)\omega] D_\lambda G[\omega_i + (n-2)\omega] \cdots D_\lambda G(\omega_i + \omega) D_\lambda | i \rangle \quad (2.6.5)$$

As in the case of the ordinary “golden rule,” expression (2.6.2) for the n -photon absorption rate is not, as yet, due to the presence of the delta function, well defined. In fact, it says that the rate of transition to an

infinitely sharp final state is zero unless the energy of the final state agrees with that of the initial state infinitely closely; in that event, however, the rate becomes infinite! As has been pointed out by Dirac,⁽⁷⁾ the probability of detecting such a sharp final state is of measure zero and one is therefore led to consider the sum of probabilities in a small interval of energy in the vicinity of the final state. Two cases of interest arise.

1. Transition to a “discrete” final state with a line-shape function $S(\omega)$ given by

$$S(\omega) = \frac{1}{\pi} \frac{1/(2t_f)}{(\omega_i - \omega_f + n\omega)^2 + [1/(2t_f)]^2} \quad (2.6.6)$$

where t_f is the spontaneous lifetime associated with the transition $i \rightarrow f$.

2. Transition to a final continuum state with a density of states [with respect to the electron energy $\hbar\omega_{k_f} = \varepsilon_{k_f} = (\hbar^2 k_f^2)/(2\mu)$]

$$\rho(\varepsilon_{k_f}) = \frac{\mu k_f}{\hbar^2} \left(\frac{L}{2\pi} \right)^3 \quad (2.6.7)$$

where $\mathbf{k}_f = |\mathbf{k}_f| \hat{\mathbf{k}}_f$ is the wave vector of the electron and is determined by the energy conservation,

$$\frac{\hbar^2 k_f^2}{2\mu} = -\hbar\omega_i + n\hbar\omega \quad (2.6.8)$$

We note that the explicit expression for the density of states depends on the normalization convention of the continuum waves. In Eq. (2.6.7) we have assumed the continuum waves to be normalized to unit density in volume $L^3 \rightarrow \infty$. Integration of Eq. (2.6.2) over a small frequency interval $d(\omega_f)$ incorporating the line-shape function $S(\omega)$ yields for the rate of n -photon transition to a bound state

$$\frac{dW_{i \rightarrow f}^{(n)}}{d\Omega} = 2\pi (2\pi\alpha F\omega/e^2)^n |T_{i \rightarrow f}^{(n)}|^2 S(\omega) \quad (2.6.9)$$

Similarly integrating with respect to $d(\hbar\omega_{k_f})$ over the continuum spectrum and incorporating the density of final states we have, for the n -photon ionization rate,

$$\frac{dW_{i \rightarrow f}^{(n)}(\mathbf{k}_f)}{d\Omega} = 2\pi (2\pi\alpha F\omega/e^2)^n |T_{i \rightarrow f}^{(n)}(\mathbf{k}_f)|^2 \hbar\rho(\varepsilon_{k_f}) \quad (2.6.10)$$

The above rate corresponds to the probability of multiphoton ionization in

which the ionized electron is ejected in the direction $\Omega \equiv (\theta_{k_f}, \varphi_{k_f})$ within an element of solid angle $d\Omega \equiv \sin \theta_{k_f} d\theta_{k_f} d\varphi_{k_f}$ and therefore defines the “differential” rate of ionization. The “total” ionization rate per target atom is obtained from

$$W_{i \rightarrow f}^{(n)} = \int W_{i \rightarrow f}^{(n)}(k_f) d\hat{k}_f \quad (2.6.11)$$

The total n -photon ionization cross section is thus

$$\sigma_{i \rightarrow f}^{(n)} \equiv \frac{W_{i \rightarrow f}^{(n)}}{F} \quad (2.6.12)$$

From the above expressions it is clear that the leading-order contribution to the n -photon excitation or ionization probability is directly proportional to the n th power of the incident photon flux F (or the field intensity $I \equiv F\hbar\omega$). This suggests the definition of the so-called “generalized cross sections,”⁽⁹⁾ $\sigma_{i \rightarrow f}^{(n)}$, via the relation

$$W_{i \rightarrow f}^{(n)} \equiv \sigma_{i \rightarrow f}^{(n)} F^n \quad (2.6.13)$$

where $\sigma_{i \rightarrow f}^{(n)}$ is (like ordinary single-photon absorption or ionization cross sections) independent of photon flux and essentially represents a target (atomic) characteristic at off-resonant frequencies. One notes, however, that the dimension of $\sigma_{i \rightarrow f}^{(n)}$ is rather awkward; only when $\sigma_{i \rightarrow f}^{(n)}$ is multiplied by F^{n-1} does one obtain the total cross section $\sigma^{[n]}$ of usual dimension, namely (length)².

The main effort in calculating n -photon generalized cross sections therefore consists in evaluating the compound matrix elements (2.6.5). In Chapter 4 we shall consider various methods of doing the same. However, before that let us consider the structure of the generalized cross section when higher-order corrections to the lowest n -photon absorption process are taken into account. According to the diagrammatic method of the previous section the correction to the lowest n th-order amplitude consists of $(n+2)$ diagrams in the $(n+2)$ th order and $(n+3)(n+4)/2$ diagrams from the $(n+4)$ th order, etc. Thus the n -photon absorption amplitude may be written as

$$A_{i \rightarrow f}^{(n)} = -2\pi i \delta(\omega_i + n\omega - \omega_f) \left[\left(\frac{1}{\hbar} \right)^n \left(\frac{E}{2} \right)^n T_{i \rightarrow f}^{(n)} + \left(\frac{1}{\hbar} \right)^{n+2} \left(\frac{E}{2} \right)^{n+1} \left(\frac{E^*}{2} \right) T_{i \rightarrow f}^{(n+2)} \right. \\ \left. + \left(\frac{1}{\hbar} \right)^{n+4} \left(\frac{E}{2} \right)^{n+2} \left(\frac{E^*}{2} \right)^2 T_{i \rightarrow f}^{(n+4)} + \dots \right] \quad (2.6.14)$$

where each term of $T_{i \rightarrow f}^{(n+2)}$ is defined in an analogous way to that of $T_{i \rightarrow f}^{(n)}$, Eq. (2.6.5), the only difference being that each term of $T_{i \rightarrow f}^{(n+2)}$ contains extra operator factors $(GD_\lambda) \cdot (GD_\lambda)$ compared to those in $T_{i \rightarrow f}^{(n)}$. Similarly each term of $T_{i \rightarrow f}^{(n+4)}$ contains extra factors $(GD_\lambda) \cdot (GD_\lambda)$ compared to those in $T_{i \rightarrow f}^{(n+2)}$. With expression (2.6.14) the n -photon absorption rate becomes

$$\begin{aligned} W_{i \rightarrow f}^{(n)} = & 2\pi(2\pi\alpha F\omega/e^2)^n \{ |T_{i \rightarrow f}^{(n)}|^2 + (2\pi\alpha F\omega/e^2)(T_{i \rightarrow f}^{(n)} T_{i \rightarrow f}^{*(n+2)} + \text{c.c.}) \\ & + (2\pi\alpha F\omega/e^2)^2 [|T_{i \rightarrow f}^{(n+2)}|^2 + (T_{i \rightarrow f}^{(n)} T_{i \rightarrow f}^{*(n+4)} + \text{c.c.})] \\ & + \text{higher-order terms} \} \delta(\omega_i + n\omega - \omega_f) \end{aligned} \quad (2.6.15)$$

We can now estimate the region of applicability of the lowest (nonvanishing) order perturbation amplitude, which corresponds to retaining the first term in the braces in Eq. (2.6.15). One may reasonably demand that in this case the second term in the braces should be small (say $< 1\%$) compared to the first. Neglecting the details of the matrix elements and with restriction to nonresonant optical frequencies, $T_{i \rightarrow f}^{(n+2)} \approx (ea_0/\omega)^2 T_{i \rightarrow f}^{(n)}$. Therefore the second term in Eq. (2.6.15) becomes comparable to the first term when

$$2\pi\alpha F\omega \left(\frac{a_0}{\omega}\right)^2 = \left(\frac{I}{I_a}\right) \left(\frac{\omega_a}{2\omega}\right)^2 \approx O(1) \quad (2.6.16)$$

where

$$I_a = \frac{E_a^2}{8\pi} c \approx 3.5 \times 10^{16} \text{ W/cm}^2 \quad (2.6.17)$$

is the intensity corresponding to the atomic unit of field strength $E_a = e/a_0^2 = 5.1 \times 10^9 \text{ V/cm}$ and $\hbar\omega_a = e^2/a_0 = 27.2 \text{ eV}$ is the atomic unit of energy. This roughly corresponds to laser intensities in the region $I = F\hbar\omega \approx 10^{14} \text{ W/cm}^2$ for frequencies of the order of 1 eV. We therefore expect that the extensively used lowest-order calculations should be reliable for $I < 10^{12} \text{ W/cm}^2$ but higher-order terms should be investigated beyond such intensities. One notes, finally, that the next higher-order correction, namely the third term in Eq. (2.6.15), contains contributions from both the $(n+2)\text{th}$ - and $(n+4)\text{th}$ -order diagrams.

3

Renormalization of Perturbation Theory

3.1. Breakdown of Conventional Perturbation Theory

The rate of transition for multiphoton processes developed so far is valid, strictly speaking, only in the lowest nonvanishing order of perturbation theory. This is because, as we shall soon see, a straightforward effort to calculate the higher-order contributions (to a process permitted at a lower order), even in the simplest of cases, leads to the appearance of singular terms in the perturbation theory. These singularities and the associated divergence of the perturbation theory occur in spite of the assumed nonresonant character of the processes considered; in fact, they are related merely to the reappearance of the “external states” (the initial and final states of a given transition matrix element) in the summations over the complete set of intermediate states. They therefore have nothing to do with the physical resonances or the like, but are a pure artifact of the conventional perturbation expansion itself. Clearly, these singularities must be removed consistently if higher-order contributions to a given nonresonant multiphoton process are to be accounted for and the corresponding rate of transition calculated. To see how these singularities (which we shall also call “external divergencies”) arise, let us briefly calculate the third-order amplitude according to the conventional approach of Section 2.2. Proceeding exactly as for the second-order calculation outlined there, one finds the following expression for the third-order contributions:

$$\begin{aligned} \langle f | A^{(3)}(\infty) | i \rangle = & -2\pi i \left(\frac{1}{\hbar}\right)^3 [\delta(\omega_i + 3\omega - \omega_f) M_{i \rightarrow f}(3\omega) \\ & + \delta(\omega_i + \omega - \omega_f) M_{i \rightarrow f}(\omega) + \delta(\omega_i - 3\omega - \omega_f) M_{i \rightarrow f}(-3\omega) \\ & + \delta(\omega_i - \omega - \omega_f) M_{i \rightarrow f}(-\omega)] \end{aligned} \quad (3.1.1)$$

where

$$M_{i \rightarrow f}(3\omega) = \sum_{j_1 j_2} \frac{(E/2)\langle f | D_\lambda | j_2 \rangle (E/2)\langle j_2 | D_\lambda | j_1 \rangle (E/2)\langle j_1 | D_\lambda | i \rangle}{(\omega_i + 2\omega - \omega_n)(\omega_i + \omega - \omega_n)} \quad (3.1.2)$$

and

$$\begin{aligned} M_{i \rightarrow f}(\omega) = & \sum_{j_1 j_2} \left[\frac{(E^*/2)\langle f | D_\lambda | j_2 \rangle (E/2)\langle j_2 | D_\lambda | j_1 \rangle (E/2)\langle j_1 | D_\lambda | i \rangle}{(\omega_i + 2\omega - \omega_n)(\omega_i + \omega - \omega_n)} \right. \\ & + \frac{(E/2)\langle f | D_\lambda | j_2 \rangle (E^*/2)\langle j_2 | D_\lambda | j_1 \rangle (E/2)\langle j_1 | D_\lambda | i \rangle}{(\omega_i - \omega_n)(\omega_i + \omega - \omega_n)} \\ & \left. + \frac{(E/2)\langle f | D_\lambda | j_2 \rangle (E/2)\langle j_2 | D_\lambda | j_1 \rangle (E^*/2)\langle j_1 | D_\lambda | i \rangle}{(\omega_i - \omega_n)(\omega_i - \omega - \omega_n)} \right] \end{aligned} \quad (3.1.3)$$

Analogous expressions for $M_{i \rightarrow f}(-3\omega)$ and $M_{i \rightarrow f}(-\omega)$ are obtained from $M_{i \rightarrow f}(3\omega)$ and $M_{i \rightarrow f}(\omega)$, respectively, by interchanging $\omega \leftrightarrow -\omega$ and $(E/2) \leftrightarrow (E^*/2)$. From the energy-conserving delta functions in expression (3.1.1) one can easily identify $M_{i \rightarrow f}^{(3)}(3\omega)$ and $M_{i \rightarrow f}^{(3)}(\omega)$, respectively, as the third-order contribution to the three-photon and the third-order contribution to the single-photon absorption processes. An intermediate resonance is said to occur when one or more of the denominators, for example in relation (3.1.2) or (3.1.3), vanish (or nearly vanish) for an intermediate state $|j\rangle$ such that the equality

$$\omega_j = \omega_i + n\omega; \quad n = 0, \pm 1, \pm 2, \pm 3, \dots \quad (3.1.4)$$

is exactly (or nearly exactly) satisfied for any $j \neq i$ or f . These resonances are clearly of physical interest, for they correspond to large enhancement of the transition $i \rightarrow f$ (see Chapter 7). On the other hand, a look at, say, the last two terms of expression (3.1.3) shows that they contain vanishing denominators, which can occur for a very different reason, namely the reappearance of the initial state $|i\rangle$ or the final state $|f\rangle$ in the intermediate sum over states $|j\rangle$. Thus, for example, the second term of expression (3.1.3) diverges due to vanishing of the denominator when $|j_2\rangle = |i\rangle$ and also due to vanishing of the denominator when $|j_1\rangle = |f\rangle$ [in conjunction with $\delta(\omega_i - \omega_f + \omega)$ multiplying this amplitude in Eq. (3.1.1)]. They are cases of the breakdown of conventional perturbation theory due to external divergencies.

We shall recast the perturbation theory of nonresonant multiphoton processes below in such a way that the transition amplitudes and rates of transition to any order will be explicitly altogether free from external divergencies. At the same time, the energies of the external states (and

hence the energy shell on which the transition occurs) will be seen to be “renormalized.” In the process we shall also obtain the necessary conditions for the validity of the transition rate as a parameter for the description of “nonresonant” multiphoton transitions.

3.2. The Resolvent and the Wave Function

It is convenient to now use the quantum representation of the external field, since in this representation the Hamiltonian for the system of “atom + field” is stationary in the Schrödinger picture. We write (see Section 1.12) the total Hamiltonian as

$$H = H^0 + V \quad (3.2.1)$$

where

$$H^0 = H_{\text{atom}} + H_{\text{field}} \quad (3.2.2)$$

with

$$H_{\text{field}} = \hbar\omega a^+ a \quad (3.2.3)$$

and

$$V = \boldsymbol{\epsilon} \cdot \frac{\mathbf{D}}{2} (a^+ + a) \left(\frac{8\pi\hbar\omega}{L^3} \right)^{1/2} \quad (3.2.4)$$

is the interaction of the field

$$\mathbf{F} = \frac{1}{2}\boldsymbol{\epsilon}(a^+ + a)(8\pi\hbar\omega/L^3)^{1/2} \quad (3.2.5)$$

with atomic dipole operator \mathbf{D} . It is also convenient to introduce and make use of the resolvent operator⁽¹⁰⁾ for the resolution of the problem at hand.

The Schrödinger equation of the system defined by the stationary Hamiltonian (3.2.1) is

$$i\hbar \frac{\partial \psi(t)}{\partial t} = H\psi(t) \quad (3.2.6)$$

It has the formal time-dependent solution

$$\psi(t) = e^{-iHt/\hbar} \phi_i \quad (3.2.7)$$

which explicitly satisfies the initial condition $\psi(0) = \phi_i$, where ϕ_i is an

eigenstate of H^0 . We would like to express $\psi(t)$ in terms of its Laplace transform or in terms of its Fourier transform. The Laplace transformation of solution (3.2.7) is

$$L\psi(t) = \int_0^\infty e^{-st} \psi(t) dt = \frac{1}{s + iH/\hbar} \phi_i \quad (3.2.8)$$

The inverse transformation of Eq. (3.2.8) brings $\psi(t)$ into the form

$$\psi(t) = \frac{1}{2\pi i} \int_{\eta-i\infty}^{\eta+i\infty} ds e^{st} \frac{1}{s + iH/\hbar} \phi_i \quad (3.2.9)$$

where, as is usual for the Laplace integral, $\eta > 0$ and is large enough to exclude any singularity of $1/(s + iH/\hbar)$ on the right of the line $s = \eta$. To express $\psi(t)$ in terms of its Fourier transform we change the integration variable in Eq. (3.2.9) from s to a complex variable E , putting $s = -iE/\hbar$. Thus

$$\psi(t) = \frac{1}{2\pi i} \int_{i\eta'+\infty}^{i\eta'-\infty} dE e^{-iEt/\hbar} \frac{1}{E - H} \quad (3.2.10)$$

where again $i\eta'$ is large enough to avoid any singularity of $1/(E - H)$ above the line $E = i\eta'$. One observes that for all Hermitian H , the eigenvalues of H , and hence the singularities of $1/(E - H)$, lie simply on the real axis. It is therefore possible and worthwhile to simplify Eq. (3.2.10) further by moving to the limit $i\eta' \rightarrow 0$. Hence, defining $1/(E - H)$ uniquely by the relation

$$\lim_{\eta' \rightarrow \infty} \frac{1}{E + i\eta' - H} \equiv G^+(E) = \frac{1}{E - H + i0} \quad (3.2.11)$$

Eq. (3.2.10) may be replaced by the integral along the real E -axis

$$\psi(t) = -\frac{1}{2\pi i} \int_{-\infty}^{\infty} dE G^+(E) e^{-iEt/\hbar} \phi_i \quad (3.2.12)$$

It is clear from this equation that the system wave function is essentially nothing but the Fourier transform of the resolvent, $G^+(E)$, defined by relation (3.2.11). Thus, for a conservative system, every piece of information contained in the wave function $\psi(t)$ that is time-dependent can be obtained from knowledge of the resolvent $G(E)$, which is stationary. Because of its stationarity it is more convenient for many purposes to deal with the resolvent than with the wave function itself. For example, by using Eq. (3.2.12) the transition amplitude is expressed in terms of the resolvent

as

$$A_{fi}(t) = -\frac{1}{2\pi i} \int_{-\infty}^{\infty} dE \langle \phi_f | G^+(E) | \phi_i \rangle \exp[-i(E - E_f)t/\hbar] \quad (3.2.13)$$

where E_f is the unperturbed energy of state $|\phi_f\rangle$. Equation (3.2.13) can be used in a variety of ways for calculating multiphoton transition amplitudes. In this chapter we shall make use of it only in solving the problem of external divergencies within the nonresonant perturbation theory.

3.3. The T-Matrix and the “Linked Cluster” Expansion of T

For the nonresonant multiphoton transition problem the most convenient approach is to first expand resolvent (3.2.11) in powers of interaction V . To this effect we also introduce the corresponding unperturbed resolvent

$$G_0^+(E) = \frac{1}{E - H^0 + i0} \quad (3.3.1)$$

Substituting expression (3.2.1) in Eq. (3.2.11), expanding the denominator, and using relation (3.3.1), we obtain

$$\begin{aligned} G^+(E) &= \frac{1}{E - H^0 + i0 - V} = (1 - G_0^+ V)^{-1} G_0^+ \\ &= G_0^+ + G_0^+ V G_0^+ + G_0^+ V G_0^+ V G_0^+ V + \dots \end{aligned} \quad (3.3.2)$$

The transition matrix, or T-matrix, may now be defined by the infinite series

$$T = T(E) = V + V G_0^+ V + V G_0^+ V G_0^+ V + \dots \quad (3.3.3)$$

Substitution of this expression in Eq. (3.3.2) yields the relation between the resolvent and the T-matrix, namely

$$G^+(E) = G_0^+ + G_0^+ T(E) G_0^+ \quad (3.3.4)$$

It is clear from Eq. (3.3.3) that increasingly higher-order terms in Eq. (3.3.3) give rise to the correspondingly higher-order amplitudes (or diagrams) in the elementary perturbation theory considered before. Hence the higher-order terms in expansion (3.3.3) are plagued by the same problem of divergence due to the reappearance of external states (the

initial and final states) in the intermediate sums, as in the elementary theory. We may, however, define a new transition operator, τ , analogous to the true transition operator (3.3.3) but in which external states are deliberately excluded from all intermediate states. To this end we write the identity operator in terms of the complete set of states $|\phi_i\rangle$ of H^0 in two parts,

$$1 = \sum_{\text{all } i} |\phi_i\rangle\langle\phi_i| = (|\phi_i\rangle\langle\phi_i| + |\phi_f\rangle\langle\phi_f|) + q \quad (3.3.5)$$

where

$$q \equiv \sum_{i \neq f} |\phi_i\rangle\langle\phi_i| \quad (3.3.6)$$

With the help of q , we define the reduced T-matrix, τ , by the series

$$\tau = \tau(E) = V + VG_0^+ q V + VG_0^+ q V G_0^+ q V + \dots \quad (3.3.7)$$

In view of definition (3.3.6) of q (it is the projection operator that excludes states $|i\rangle$ and $|f\rangle$), τ is obviously free from the unwanted external states. In the language of the many-body (Bruckner–Bethe–Goldstone) perturbation theory,⁽¹¹⁾ such expansions are referred to as “linked cluster” expansions in which clusters of so-called “unlinked” diagrams (or terms) containing, e.g., the initial state as an intermediate state, are absent.

Our problem of the removal of external divergencies now reduces to the problem of expressing the matrix elements $T_f(E) = \langle\phi_f|T|\phi_i\rangle$ of the true T-matrix, Eq. (3.3.3), in terms of the matrix elements of the divergence-free reduced $\tau(E)$, defined by Eq. (3.3.7).

3.4. Relation between True and Reduced T-Matrices

One easily deduces from Eq. (3.3.3) that

$$\begin{aligned} T &= V + VG_0^+(V + VG_0^+ V + VG_0^+ V G_0^+ V + \dots) \\ &= V + VG_0^+ T \end{aligned} \quad (3.4.1)$$

By introducing the completeness relation (3.3.5) we rewrite Eq. (3.4.1) in the form

$$T = V + VG_0^+(\langle\phi_i|\phi_i| + \langle\phi_f|\phi_f|)T + VG_0^+ q T \quad (3.4.2)$$

$$= VS + VG_0^+ q T \quad (3.4.3)$$

where

$$S = 1 + G_0^+ (\langle \phi_i | \phi_i \rangle + \langle \phi_f | \phi_f \rangle) T \quad (3.4.4)$$

Equation (3.4.3) may be iterated starting with the first term, VS , on the right-hand side. Hence

$$\begin{aligned} T &= (V + VG_0^+ qV + VG_0^+ qVG_0^+ qV + \dots) S \\ &= \tau S \end{aligned} \quad (3.4.5)$$

where τ is the reduced T-matrix defined in Eq. (3.3.7). Taking the diagonal matrix element of Eq. (3.4.5) with respect to the initial state $|\phi_i\rangle$ and using definition (3.4.4) for S , we get the algebraic equation

$$T_u = \tau_u + \tau_u G_0^+(i) T_u + \tau_{uf} G_0^+(f) T_{fu} \quad (3.4.6)$$

where, for the sake of brevity, we have written

$$G_0^+(i) = \langle \phi_i | G_0^+ | \phi_i \rangle = \frac{1}{E - E_i + i0} \quad (3.4.7)$$

$$T_{fu} = \langle \phi_f | T | \phi_i \rangle \quad (3.4.8)$$

$$\tau_{fu} = \langle \phi_f | \tau | \phi_i \rangle \quad (3.4.9)$$

and similarly for the remaining matrix elements.

We take also the matrix element of Eq. (3.4.5) between the initial and final states $|\phi_i\rangle$ and $|\phi_f\rangle$ to find the important relation

$$T_{fu} = \tau_{fu} + \tau_{fi} G_0^+(i) T_u + \tau_{ff} G_0^+(f) T_{fu} \quad (3.4.10)$$

3.5. The Renormalized T-Matrix

Equations (3.4.6) and (3.4.10) constitute a simple pair of algebraic equations for the two unknowns T_u and T_{fu} and can be easily solved. Thus, finally, for the renormalized transition matrix element of interest T_{fu} , where $|f\rangle \neq |i\rangle$, we have the solution

$$T_{fu} = \frac{\tau_{fu}}{[1 - G_0^+(i)\tau_u][1 - G_0^+(f)\tau_{ff}] - \tau_{fu}\tau_{if}G_0^+(i)G_0^+(f)} \quad (3.5.1)$$

If this expression is substituted in Eq. (3.3.4), we also obtain the corre-

sponding renormalized matrix element of the resolvent,

$$G_{fi}^+(E) = \frac{\tau_{fi}(E)}{[E - E_i - \tau_u(E) + i0][E - E_f - \tau_{ff}(E) + i0] - \tau_{fi}(E)\tau_{if}(E)} \quad (3.5.2)$$

where we have explicitly indicated the E -dependence of all the quantities involved.

3.6. Energy Renormalization of External States

The poles of the resolvent [cf. Eq. (3.2.11)], and hence the zeros of the denominator of matrix element (3.5.2), give the energy eigenvalues of interest in the presence of the interaction. One may easily factorize the denominator in Eq. (3.5.2), namely

$$\begin{aligned} & \{[E - E_i - \tau_u(E) + i0][E - E_f - \tau_{ff}(E) + i0] - \tau_{fi}(E)\tau_{if}(E)\} \\ & \equiv (E - E'_i + i0)(E - E'_f + i0) \end{aligned} \quad (3.6.1)$$

where E'_i and E'_f are expressed in the symmetric form

$$E'_i = E_i + \Delta_i(E) \quad (3.6.2)$$

and

$$E'_f = E_f + \Delta_f(E) \quad (3.6.3)$$

The nominal “energy shifts” of the external states are

$$\Delta_i(E) = \tau_u(E) + \phi_{if}(E) \quad (3.6.4)$$

and

$$\Delta_f(E) = \tau_{ff}(E) - \phi_{if}(E) \quad (3.6.5)$$

The function $\phi_{if}(E)$, which arises due only to the mutual interaction between the external states, is given by

$$\phi_{if}(E) = \Delta_{if} \left[\left(1 + \frac{\tau_{if}\tau_{fi}}{(\Delta_{if})^2} \right)^{1/2} - 1 \right] \quad (3.6.6)$$

$$= \sum_{n=0}^{\infty} (-1)^n \frac{(2n-1)!!}{(2n+2)!!} \frac{(\tau_{if}\tau_{fi})^{n+1}}{(\Delta_{if})^{2n+1}} \quad (3.6.7)$$

where $\Delta_{if} = E_i + \tau_u(E) - E_f - \tau_{ff}(E)$. We have also used the notations $(2n-1)!! = 1 \cdot 3 \cdot 5 \cdots (2n-1)$ [with $(-1)!! = 1$] and $(2n+2)!! = 2 \cdot 4 \cdot 6 \cdots (2n+2)$. It is clear that the eigenvalue equations

$$E'_i = E_i + \Delta_i(E) \quad (3.6.8)$$

and

$$E'_f = E_f + \Delta_f(E) \quad (3.6.9)$$

are transcendental equations in E . We shall denote as the principal roots those roots of Eqs. (3.6.8) and (3.6.9), which go over to the unperturbed energies E_i and E_f , respectively, when the interaction $V \rightarrow 0$. The renormalized energies of external states $|i\rangle$ and $|f\rangle$ will be accordingly identified with the respective principal roots of Eqs. (3.6.8) and (3.6.9).

3.7. Lagrange Expansion of the Energy Shift

Let $\Delta_i(E)$, appearing above, stand for its expansion as a perturbation series in V up to a fixed desired order. We assume that the expansion of $\Delta_i(E)$, considered as a function in the complex E -plane, satisfies the analytic conditions of the Lagrange theorem.⁽¹²⁾ Then Eq. (3.6.8) may be inverted about E_i to obtain the Lagrange series for the principal root,

$$E'_i = E_i + \sum_{n=1}^{\infty} \frac{d^{n-1}}{dE_i^{n-1}} [\Delta_i(E_i)]^n \quad (3.7.1)$$

This equation yields the change in energy of the initial state,

$$\Delta'_i = \sum_{n=1}^{\infty} \frac{d^{n-1}}{dE_i^{n-1}} [\Delta_i(E_i)]^n \quad (3.7.2)$$

The correction $\Delta'_i(E_i)$ is in general complex due to the presence of $G_0^+(i)$ in the expansion of $\Delta_i(E_i)$. In fact

$$\Delta'_i = \operatorname{Re} \Delta'_i - i \operatorname{Im} \Delta'_i \quad (3.7.3)$$

where the relation $\operatorname{Im} \Delta'_i \geq 0$ is guaranteed by the outgoing (retarded) boundary condition on $G_0^+(i)$. The real part of Δ'_i therefore gives the “shift,” while the imaginary part may be interpreted as the “width” of the renormalized initial state. In a completely analogous way one obtains, from the second factor of Eq. (3.6.1), the renormalized final state energy

$$E'_f = E_f + \Delta'_f \quad (3.7.4)$$

where

$$\Delta'_f = \sum_{n=1}^{\infty} \frac{d^{n-1}}{dE_f^{n-1}} [\Delta_f(E_f)]^n \equiv \operatorname{Re} \Delta'_f - i \operatorname{Im} \Delta'_f \quad (3.7.5)$$

with $\operatorname{Im} \Delta'_f \geq 0$. A similar interpretation of the real and imaginary parts of E'_f , such as the “shift” and “width” of the final state, holds.

We observe that for an N -photon process the off-diagonal matrix elements τ_{if} or τ_{fi} are at least of order $(F_0)^N$, F_0 being the peak field strength, so that the product $\tau_{if}\tau_{fi}$ in ϕ_{if} [see Eq. (3.6.6) or (3.6.7)] is $O(F_0)^{2N}$. The diagonal matrix elements τ_u and τ_{ff} are $O(F_0)^2$ for $N \geq 2$. Hence expansion (3.6.7) should converge rapidly with increasing $N \geq 2$.

3.8. Energy Shift from the Effective Hamiltonian

An alternative way of obtaining the shifted energies E'_i and E'_f is to use the explicitly renormalized effective matrix elements obtained in Chapter 7. For the case of two near-degenerate states $|\phi_i\rangle$ and $|\phi_f\rangle$ the energy-determining secular equation is

$$\begin{vmatrix} [E - H_u(W^0)] & H_{if}(W^0) \\ H_{fi}(W^0) & [E - H_{ff}(W^0)] \end{vmatrix} = 0 \quad (3.8.1)$$

where H_{ab} are the matrix elements of the effective Hamiltonian, Eq. (7.5.2.9), evaluated at a fixed energy W^0 . The two solutions of Eq. (3.8.1) give directly

$$\left. \begin{aligned} E'_i &= \frac{1}{2}[H_u(W^0) + H_{ff}(W^0)] + L_{if}(W^0) \\ E'_f &= \frac{1}{2}[H_u(W^0) + H_{ff}(W^0)] - L_{if}(W^0) \end{aligned} \right\} \quad (3.8.2)$$

where

$$L_{if}(W^0) = \left[\left(\frac{H_u(W^0) - H_{ff}(W^0)}{2} \right)^2 + H_{if}(W^0)H_{fi}(W^0) \right]^{1/2} \quad (3.8.3)$$

In the above one may choose W^0 equal to either E_i or E_f .

3.9. The Renormalized Rate of Multiphoton Transitions

The amplitude of transition from state $|i\rangle$ to $|f\rangle$ is given in terms of matrix elements $G_{fi}^+(E)$. Thus from Eqs. (3.2.13), (3.5.2), and (3.6.1) we get

$$A_{f \rightarrow i}(t) = -\frac{1}{2\pi i} \int_{-\infty}^{\infty} dE \exp[-i(E - E_f)t/\hbar] \frac{\tau_f(E)}{(E - E'_i + i0)(E - E'_f + i0)} \quad (3.9.1)$$

Although in general a knowledge of $\tau_f(E)$ for all E is necessary to determine the detailed time dependence of amplitude $A_{fi}(t)$, we shall see that for nonresonant processes, under conditions to be specified below, a constant probability of transition per unit time or the rate of transition exists and is determined by a fixed value of E , namely that on the (renormalized) energy shell.

The constant rate of transition, as a parameter to describe the nonresonant multiphoton transitions, is of interest for an interaction time larger than typical atomic periods but still small enough to satisfy the requirement that the total probability of transition during the period of interaction remains small compared to unity, i.e., provided⁽¹³⁾

$$\frac{\text{Im } \Delta'_i t}{\hbar} \ll 1 \quad \text{and} \quad \frac{\text{Im } \Delta'_f t}{\hbar} \ll 1 \quad (3.9.2)$$

For the “atom + field” interaction time t_p typically satisfying

$$10^{-6} \text{ s} > t_p > 10^{-16} \text{ s} \quad (3.9.3)$$

this may be ensured, provided

$$\text{Im } \Delta'_i \ll \Delta_{\min} \quad \text{and} \quad \text{Im } \Delta'_f \ll \Delta_{\min} \quad (3.9.4)$$

where Δ_{\min} is the smallest of the intermediate detunings. Under the above restrictions we may formally let

$$\text{Im } \Delta'_i \rightarrow 0 \quad \text{and} \quad \text{Im } \Delta'_f \rightarrow 0 \quad (3.9.5)$$

For nonresonant processes Δ_{\min} is roughly on the order of the atomic frequencies and the above conditions are respected for a considerable range of incident intensities.

3.9.1. The Singular ζ -Function

In the derivation of the transition rate to follow below, it will be helpful to introduce the singular $\zeta(E)$ -function⁽¹³⁾ of the real variable E ,

defined variously but equivalently by

$$\zeta(E) = -\frac{i}{\hbar} \int_0^\infty e^{iEt/\hbar} dt = \lim_{\eta \rightarrow 0} \frac{1}{E + i\eta} = \frac{(P)}{E} - i\pi\delta(E) \quad (3.9.1.1)$$

$$= \lim_{t \rightarrow \infty} \frac{1 - e^{-iEt/\hbar}}{E} \quad (3.9.1.2)$$

with the property

$$E\zeta(E) = 1 \quad (3.9.1.3)$$

and

$$\zeta(E) - \zeta^*(E) = -2\pi i \delta(E) \quad (3.9.1.4)$$

The function $\zeta(E)$ also possesses the useful limiting property

$$\lim_{t \rightarrow \infty} \zeta(E) e^{-iEt/\hbar} = \begin{cases} -2\pi i \delta(E), & t \rightarrow +\infty \\ 0, & t \rightarrow -\infty \end{cases} \quad (3.9.1.5)$$

This is easily proved using the integral representation (3.9.1.1):

$$\begin{aligned} \lim_{t \rightarrow \pm\infty} \zeta(E) e^{-iEt/\hbar} &= -\frac{i}{\hbar} \int_0^\infty e^{iE(t'-t)/\hbar} dt' \Big|_{t=\pm\infty} \\ &= -\frac{i}{\hbar} \int_{-t}^{\infty} e^{iE\tau/\hbar} d\tau \Big|_{t=\pm\infty} = \begin{cases} -2\pi i \delta(E), & t \rightarrow +\infty \\ 0, & t \rightarrow -\infty \end{cases} \end{aligned} \quad (3.9.1.6)$$

3.9.2. The Transition Rate

Taking the limit (3.9.5) and using the second relation of (3.9.1.1) in Eq. (3.9.1), the amplitude can be expressed in the form

$$A_{fi}(t) = -\frac{1}{2\pi i} \int_{-\infty}^{\infty} dE \tau_{fi}(E) \zeta(E - E') \zeta(E - E_f) \exp[-i(E - E_f)t/\hbar] \quad (3.9.2.1)$$

The product of the ζ -functions in this equation are now separated in partial fractions,

$$\zeta(E - E') \zeta(E - E_f) = \zeta(E' - E_f) [\zeta(E - E') - \zeta(E - E_f)] \quad (3.9.2.2)$$

If relation (3.9.2.2) is substituted in Eq. (3.9.2.1), suitable time-dependent factors extracted, and the limit $t \rightarrow +\infty$ taken, then the limiting property

(3.9.1.5) can be applied and integration over dE carried out trivially. This manipulation yields

$$\begin{aligned} \lim_{t \rightarrow \infty} A_{fi}(t) &= \lim_{t \rightarrow \infty} \{\tau_{fi}(E')\zeta(E' - E_i)\exp[-i(E' - E_f)t/\hbar] \\ &\quad - \tau_{fi}(E_f)\exp[-i(E' - E_f)t/\hbar]\}\zeta(E' - E_i)\exp[+i(E' - E_f)t/\hbar]\} \end{aligned} \quad (3.9.2.3)$$

In the limit $t \rightarrow +\infty$ the last term in this relation does not contribute [cf. Eq. (3.9.1.5)] and can be omitted. Therefore we may define

$$\begin{aligned} C_f(t) &\equiv \exp[i(E_f - E_f)t/\hbar]A_{fi}(t \rightarrow \infty) \\ &= \tau_{fi}(E')\zeta(E' - E_f)\exp[-i(E' - E_f)t/\hbar] \end{aligned} \quad (3.9.2.4)$$

The time derivative of Eq. (3.9.2.4) gives

$$\dot{C}_f(t) = (-i/\hbar)\tau_{fi}(E')\exp[-i(E' - E_f)t/\hbar] \quad (3.9.2.5)$$

since $x\zeta(x) = 1$. In the long-time limit of interest, provided $(E_f - E_f)$ is real the rate of transition $R_{i \rightarrow f}$ per unit time is

$$\begin{aligned} R_{i \rightarrow f} &\equiv \frac{d}{dt}|A_{fi}(t \rightarrow \infty)|^2 = \frac{d}{dt}|C_f(t)|^2 \\ &= C_f(t)\dot{C}_f^*(t) + \dot{C}_f(t)C_f^*(t) \end{aligned} \quad (3.9.2.6)$$

By using expressions (3.9.2.4) and (3.9.2.5) in Eq. (3.9.2.6) and remembering property (3.9.1.4), the desired renormalized rate of transition can be obtained in the form

$$R_{i \rightarrow f} = \frac{2\pi}{\hbar}|\tau_{fi}(E')|^2\delta(E' - E_f) \quad (3.9.2.7)$$

The transition rate is therefore controlled by the reduced τ -matrix element evaluated at a single value of $E = E'$. Moreover, it vanishes outside the (renormalized) energy shell $E' = E'$. For $|f\rangle$ in the continuum with state density $\rho_f(E')$, the measured rate corresponds as usual to the sum of expression (3.9.2.7) over the final states in the interval E_f and $E_f + dE_f$ and the average over the initial states:

$$R_{i \rightarrow f} \Rightarrow \frac{2\pi}{\hbar} \sum_i \frac{1}{S_i} |\tau_{fi}(E')|^2 \rho_f(E') \quad (3.9.2.8)$$

where S_i^{-1} is the statistical weight of the initial states.

For transitions to a final discrete state, the density of states in relation (3.9.2.8) should be replaced by the relevant line-shape function, such as Eq. (2.6.6). We also observe that the basic result (3.9.2.7) derived here is symmetric in form with respect to the initial and final states; consequently no further adjustments⁽¹³⁾ are necessary to ensure this desirable property.

We may summarize the result of the renormalization procedure carried out in this chapter, in the context of the diagrammatic perturbation theory, as follows. All the diagrams generated by the reduced T-matrix $\tau_{if}(E')$ [see Eq. (3.3.7)] are the same as the usual ones generated by the unrenormalized $T_{if}(E_i)$; however (1) the undesirable external states as intermediate states are automatically excluded from $\tau_{if}(E')$, and (2) the unperturbed external energies E_i and E_f are replaced by the real parts of the renormalized energies E'_i and E'_f given by Eqs. (3.7.2) and (3.7.3), respectively, or (3.8.2) and (3.8.3). Finally, the constant rate of transition $R_{i \rightarrow f}$ [given by Eq. (3.9.2.8)] and hence the cross section, $\sigma_{i \rightarrow f} \equiv (1/F)R_{i \rightarrow f}$, where F is the photon flux, are useful valid concepts for nonresonant multiphoton processes only as long as restrictions (3.9.2)–(3.9.4) are respected.

4

Methods for Evaluation of Generalized Cross Sections

4.1. Introduction

Actual evaluation of a multiphoton transition amplitude involves compound matrix elements of the form

$$T_{i \rightarrow f}^{(n)} = \langle f | D_\lambda G(\omega_i + (n-1)\omega) D_\lambda G(\omega_i(n-2)\omega) \cdots D_\lambda G(\omega_i + \omega) D_\lambda | i \rangle \quad (4.1.1)$$

where

$$G(\omega_i + \Omega) = \sum_j \frac{|j\rangle\langle j|}{(\omega_i + \Omega - \omega_j)} \quad (4.1.2)$$

One therefore needs to evaluate the matrix elements of the dipole operator between complete sets of states $\{|j\rangle\}$ of the target atom. Such sets invariably contain (besides a denumerable set of discrete states) a non-denumerable set of continuum states. It is the integration over the continuum which as a rule poses some difficulty in practice. Here we shall discuss exact methods of performing this sum that bypass the problem of explicit integration over the continuum. The first method consists of using various alternative representations of Green's function and is in fact most convenient for the important case of Coulomb systems as well as for the alkalis. The method is mainly analytic in nature. The second method is that of the inhomogeneous differential equation; it is in principle applicable to any system of interest and is fully numerical in nature. A third method, the pseudocontinuum-basis approach, replaces the true continuum by appropriately chosen square-integrable functions, which accurately reproduce the continuum functions in the effective range of distances by matching

procedures. Besides these essentially “exact” methods we shall consider an approximate method, which is often useful in providing a first estimate, particularly for more complex targets where detailed information on the properties of the isolated system is unavailable or difficult to obtain *ab initio*.

4.2. The Method of Green’s Function

The one-electron atomic Green’s function of the model Hamiltonian H_a , in the coordinate representation, is completely defined by the inhomogeneous differential equation

$$\begin{aligned} [H_a - E]G(E; \mathbf{r}, \mathbf{r}') &= \left[-\frac{\hbar^2}{2\mu} \nabla_{\mathbf{r}}^2 - \frac{Ze^2}{r} + U(r) - E \right] G(E; \mathbf{r}, \mathbf{r}') \\ &= -\delta(\mathbf{r} - \mathbf{r}') \end{aligned} \quad (4.2.1)$$

where $\nabla_{\mathbf{r}}^2$ is the Laplacian operator, $-(Ze^2)/r$ is the long-range attractive Coulomb interaction with residual charge Z , and $U(r)$ is a short-range effective central potential.

Taking advantage of the central symmetry of the Hamiltonian it is easy to separate the radial part of Green’s function from the angular part by expanding in spherical harmonics:

$$G(E; \mathbf{r}, \mathbf{r}') = \sum_{l=0}^{\infty} g_l(E; r, r') \sum_{m=-l}^l Y_{lm}(\hat{r}) Y_{lm}^*(\hat{r}') \quad (4.2.2)$$

Using

$$\delta(\mathbf{r} - \mathbf{r}') = \frac{\delta(r - r')}{rr'} \sum_{lm} Y_{lm}(\hat{r}) Y_{lm}^*(\hat{r}') \quad (4.2.3)$$

and remembering

$$\nabla_{\mathbf{r}}^2 = \frac{1}{r} \frac{d^2}{dr^2} r - \frac{\hat{L}^2}{r^2} \quad (4.2.4)$$

with

$$\hat{L}^2 Y_{lm}(\hat{r}) = l(l+1) Y_{lm}(\hat{r}) \quad (4.2.5)$$

substitution of expression (4.2.2) in Eq. (4.2.1) and projection onto $Y_{lm}^*(\hat{r})$ immediately gives the equation for the radial Green’s function in the form

$$\left\{ \frac{\hbar^2}{2\mu} \left[\frac{1}{r} \frac{d^2}{dr^2} r - \frac{l(l+1)}{r^2} \right] + \frac{Ze^2}{r} - U(r) + E \right\} g_l(E; r, r') = \frac{\delta(r - r')}{rr'} \quad (4.2.6)$$

We shall now consider a number of explicit forms of Green's function for the Coulomb case and for the effective potentials suitable for model alkali atoms, which have been found to be useful in multiphoton calculations.

4.2.1. The Radial Coulomb Green's Function

4.2.1.1. The Closed-Form Representation

In the pure Coulomb case, $U(r) \equiv 0$ in Eq. (4.2.6). The transformations

$$g_l(E; r, r') = \frac{f_l(E; r, r')}{rr'}, \quad \rho = \frac{2Z}{va_0} r \quad (4.2.1.1)$$

and

$$v = \frac{Ze}{(-2Ea_0)^{1/2}} \quad (4.2.1.2)$$

yield Whittaker's standard form⁽¹⁴⁾

$$\left[\frac{d^2}{d\rho^2} - \frac{1}{4} + \frac{v + \frac{1}{4} - (l + \frac{1}{2})^2}{\rho^2} \right] f_l(E; \rho, \rho') = \left(\frac{v}{Ze^2} \right) \delta(\rho - \rho') \quad (4.2.1.3)$$

The solutions of the homogeneous part of Eq. (4.2.1.3) are the well-known regular and irregular Whittaker functions,⁽¹⁴⁾ $M_{v,l+1/2}(\rho)$ and $W_{v,l+1/2}(\rho)$. According to the usual method^(15,16) of constructing the solution of the inhomogeneous equation, with the help of regular and irregular solutions of the homogeneous equation, one has

$$f_l(E; \rho, \rho') = \left(\frac{v}{Ze^2} \right) \frac{1}{W} M_{v,l+1/2}(\rho_<) W_{v,l+1/2}(\rho_>) \quad (4.2.1.4)$$

where

$$W \equiv W\{M_{v,l+1/2}, W_{v,l+1/2}\} = -\frac{\Gamma(2l+2)}{\Gamma(1+l-v)} \quad (4.2.1.5)$$

is the Wronskian and where we have used the symbols

$$\rho_> \equiv \text{greater of } (\rho, \rho') \quad \text{and} \quad \rho_< \equiv \text{lesser of } (\rho, \rho') \quad (4.2.1.6)$$

By using relations (4.2.1.4) and (4.2.1.5) and transforming back to r and r' we obtain the closed-form representation of the Coulomb Green's

function,

$$g_l(E; r, r') = -\frac{v/(Ze^2)}{rr'} \frac{\Gamma(1+l-v)}{\Gamma(2l+2)} M_{v,l+1/2} \left(\frac{2Z}{va_0} r_> \right) W_{v,l+1/2} \left(\frac{2Z}{va_0} r_< \right) \quad (4.2.1.7)$$

One of the beautiful properties of Green's functions is that the energy eigenvalues of the Hamiltonian appear automatically at the position of the simple poles while the corresponding residues at the eigenvalues yield the "square" of the normalized wave functions. Thus, for example, one can easily verify that Rydberg energy levels appear at the poles of the gamma function in Eq. (4.2.1.7) which occur at the negative integral values of its argument, including zero. Since the poles of $\Gamma(1+l-v)$ occur for $v = n$ where $n \geq l+1$ is an integer, the definition (4.2.1.2), namely $v = Ze/(-2Ea_0)^{1/2} = n$, yields immediately the hydrogenic eigenvalues $E = E_{nl} = -Z^2 e^2 / (2n^2 a_0)$. Similarly one notes that the residue of $\Gamma(1+l-v)$ at $E = E_{nl}$, as $v \rightarrow n (\geq l+1)$, is

$$\frac{(-1)^{n-l-1}}{(n-l-1)!} \frac{Z^2 e^2}{n^3 a_0} \quad (4.2.1.8)$$

From Eq. (4.2.1.7) one easily reobtains the normalized hydrogenic wave functions when one remembers that⁽¹⁷⁾

$$\lim_{v \rightarrow n} M_{v,l+1/2}(x) = e^{-x/2} x^{l+1} {}_1F_1(-n+l+1; 2l+2; x) \quad (4.2.1.9)$$

and

$$\lim_{v \rightarrow n} W_{v,l+1/2}(x) = (-1)^{n-l-1} \frac{\Gamma(n+l+1)}{\Gamma(2l+2)} e^{-x/2} (x)^{l+1} {}_1F_1(-n+l+1; 2l+2; x) \quad (4.2.1.10)$$

where ${}_1F_1(a; c; x)$ is the confluent hypergeometric function. We shall soon use these properties of Green's function in extending⁽¹⁸⁾ the present approach to alkali-like model atoms by incorporating the quantum-defect theory.⁽¹⁹⁻²¹⁾

4.2.1.2. The Integral Representation

The form of Coulomb Green's function (4.2.1.7) has been known for a long time. It is noteworthy that the dependent ranges of the r -coordinates in Eq. (4.2.1.7), while perfectly simple to handle in numerical calculations, make it inconvenient for analytic calculations. An interesting restate-

ment⁽²²⁾ of the above form has been useful for two-photon transition problems (see Chapter 5). To derive the new form we make use of the integral representation^(23,24)

$$\begin{aligned} & \int_0^\infty \exp[-\frac{1}{2}(a_1 + a_2)t \cosh x] [\coth(x/2)]^{2\nu} I_{2l+1}(t(a_1 a_2)^{1/2} \sinh x) dx \\ &= \frac{\Gamma(l+1-\nu)}{t(a_1 a_2)^{1/2} \Gamma(2l+2)} W_{\nu, l+1/2}(a_1 t) M_{\nu, l+1/2}(a_2 t) \end{aligned} \quad (4.2.1.11)$$

where $a_1 > a_2$ and $\operatorname{Re}(l+1-\nu) > 0$. Substitution of relation (4.2.1.11) in Eq. (4.2.1.7) yields the desired result

$$\begin{aligned} g_l(E; r, r') &= -\frac{2\mu}{\hbar^2} (rr')^{-1/2} \int_0^\infty dx \exp\left\{-\frac{Z}{\nu a_0} (r+r')\right\} \cosh x \\ &\times (\coth x/2)^{2\nu} I_{2l+1}\left[\frac{2Z}{\nu a_0} (rr')^{1/2} \sinh x\right] \end{aligned} \quad (4.2.1.12)$$

The usefulness of this representation largely stems from the fact that the necessary matrix elements of the multipole operators with respect to the hydrogenic or Slater orbitals can be evaluated exactly⁽²⁵⁾ in terms of the following integral and its derivatives with respect to the exponential parameters:

$$\begin{aligned} J_l(\beta, \beta') &\equiv \int_0^\infty dr \int_0^\infty dr' (rr')^{l+1} \exp\left[-\frac{z}{\nu a_0} (\beta r + \beta' r')\right] g_l(E; r, r') \\ &= -\frac{2\mu}{\hbar^2} \frac{2^{l+1} (2l+1)! (\nu a_0 / Z)^{2l+3}}{(l+1-\nu)[(1+\beta)(1+\beta')]^{2l+2}} \\ &\times {}_2F_1\left(2l+2, l+1-\nu; l+2-\nu; \frac{(1-\beta)(1-\beta')}{(1+\beta)(1+\beta')}\right) \end{aligned} \quad (4.2.1.13)$$

where ${}_2F_1(a, b; c; x)$ is the Gauss hypergeometric function. Representation (4.2.1.12) has also been successfully used⁽²⁶⁾ in accounting for retardation effects in two-photon radiative transitions.

4.2.1.3. The Sturmian Representation

We now consider a completely separable and denumerable product representation^(27,28) of the radial Coulomb Green's functions, which has been found to be most useful in higher-order multiphoton calculations in hydrogenic systems. It turns out to be an expansion over the complete denumerable set of functions, the so-called "Sturmian" functions.⁽²⁹⁻³¹⁾ For

our purpose this Green's function is more conveniently obtained^(32,33) by using integral representation (4.2.1.12) and replacing the Bessel function by the well-known Hille-Hardy formula⁽³⁴⁾ (for the generating functions of products of Laguerre polynomials):

$$\begin{aligned} & I_{2l+1}(2(RR')^{1/2}y^{1/2}/(1-y)) \\ &= (RR')^{l+1/2} \exp\left[\frac{y}{1-y}(R+R')(1-y)\right] \sum_{p=0}^{\infty} \frac{p!}{\Gamma(p+2l+2)} \\ & \quad \times L_p^{2l+1}(R)y^{p+l+1/2}L_p^{2l+1}(R') \end{aligned} \quad (4.2.1.14)$$

We set $R = 2Zr/(va_0)$, $R' = 2Zr'/(va_0)$, and $2y^{1/2}/(1-y) = \sinh x$, and note the elementary relations

$$\frac{1+y}{1-y} = \cosh x, \quad \frac{1}{y} = \coth^2(x/2)$$

and

$$\int_0^\infty dx [\dots] = \int_0^1 dy y^{-1/2} (1-y)^{-1} [\dots] \quad (4.2.1.15)$$

Substitution of Eq. (4.2.1.14) in relation (4.2.1.12) and use of the above transformations (4.2.1.15) lead to an elementary integration in y and one easily obtains

$$\begin{aligned} g_l(E; r, r') &= -\frac{2\mu}{\hbar^2} \left(\frac{2Z}{va_0}\right) \sum_{p=0}^{\infty} \left\{ \left[\exp\left(-\frac{zr}{va_0}\right) \left(\frac{2z}{va_0}r\right)^l L_p^{2l+1}\left(\frac{2z}{va_0}r\right) \right] \right. \\ & \quad \times \left. \frac{p!}{\Gamma(p+2l+2)} \frac{1}{(p+l+1-v)} \left[\exp\left(-\frac{zr'}{va_0}\right) \left(\frac{2zr'}{va_0}\right)^l L_p^{2l+1}\left(\frac{2z}{va_0}r'\right) \right] \right\} \end{aligned} \quad (4.2.1.16)$$

where, as before,

$$v = \frac{Ze}{(-2Ea_0)^{1/2}}$$

Using the relation between the Laguerre polynomials and the confluent hypergeometric functions,⁽³⁵⁾ namely

$$L_p^{2l+1}(x) = \frac{(p+2l+1)!}{p!(2l+1)!} {}_1F_1(-p, 2l+2; x) \quad (4.2.1.17)$$

and changing p to the “principal quantum number” $n \equiv p + l + 1$, expres-

sion (4.2.1.16) can be rewritten in the alternative form

$$\begin{aligned}
 g(E; r, r') &= -\frac{2\mu}{\hbar^2} \left(\frac{2Z}{va_0} \right) \sum_{n=l+1}^{\infty} \left[\exp \left(-\frac{zr}{va_0} \right) \left(\frac{2z}{va_0} r \right)^l {}_1F_1 \left(-n + l + 1; 2l + 2; \frac{2z}{va_0} r \right) \right] \\
 &\times \frac{(n+l)!}{[(2l+1)!]^2(n-l-1)!} \frac{1}{(n-v)} \\
 &\times \left[\exp \left(-\frac{zr'}{va_0} \right) \left(\frac{2zr'}{va_0} \right)^l {}_1F_1 \left(-n + l + 1; 2l + 2; \frac{2z}{va_0} r' \right) \right] \quad (4.2.1.18)
 \end{aligned}$$

Before concluding this section on the radial Coulomb Green's function we note that a number of other representations in the coordinate space,^(36,37) in the momentum space,⁽³⁸⁻⁴⁰⁾ as well as in the hyperspherical space⁽⁴¹⁾ are available for the full three-dimensional Coulomb Green's function. They have been successfully used for actual calculations^(26,42-45) in lower orders. On the other hand, radial representations appear to be particularly convenient for evaluation of multiphoton compound matrix elements to any order.

4.2.2. The Quantum-Defect Radial Green's Function

4.2.2.1. The Closed-Form Representation

It is interesting that the usefulness of Coulomb Green's function can be extended to include the system of alkali-like effective one-electron atoms whose spectra are known to be closely reproduced by the modified Rydberg formula

$$E_{nl} = -\frac{Z^2 e^2}{2n^{*2} a_0} \quad (4.2.2.1)$$

where $n^* = n - \mu_l(E_{nl})$ is the effective principal quantum number and $\mu_l(E_{nl})$ is the so-called quantum defect. The quantum-defect method⁽¹⁹⁻²¹⁾ is well known in connection also with the ordinary photoelectric effect and the problem of electron scattering from isoelectronic sequences of neutral atoms. Here we give the construction⁽¹⁸⁾ of the closed-form radial Green's function by incorporating the principal results of the quantum-defect method (QDM). We observe that although the QDM assumes a single-electron approximation, the empirical use of the experimental spectrum of the atom effectively accounts for some many-body effects.

We consider the radial equation of Green's function (4.2.6), where

$U(r)$ is taken as the non-Coulomb part of the interaction with the property $U(r) \rightarrow 0$ for $r > r_c$, where r_c is a hypothetical radius of the “atomic core.” The explicit form of $U(r)$, $r < r_c$, can be left unspecified provided $r^2 U(r) \rightarrow 0$ as $r \rightarrow 0$.

The general solution^(15,16,18) of Eq. (4.2.6) can be constructed from the solutions of the corresponding homogeneous equations:

$$g_l(E; r, r') = \frac{v}{Ze^2} \frac{1}{rr'} \frac{\Gamma(l+1-v)}{\Gamma(2l+2)} M_{v,l+1/2} \left(\frac{2z}{va_0} r_- \right) W_{v,l+1/2} \left(\frac{2z}{va_0} r_+ \right) + A \frac{v}{Ze^2} \frac{1}{rr'} W_{v,l+1/2} \left(\frac{2z}{va_0} r_- \right) W_{v,l+1/2} \left(\frac{2z}{va_0} r' \right) \quad (4.2.2.2)$$

where

$$v = \frac{Ze}{(-2Ea_0)^{1/2}}$$

and we define for subsequent use

$$k = i \frac{Z}{va_0} = (2\mu E/\hbar^2)^{1/2} \quad (4.2.2.3)$$

The first term on the right-hand side of Eq. (4.2.2.2) is Green’s function of the Coulomb problem while the last term is merely the solution of the homogeneous equation, which is regular at infinity. Since we are considering the outgoing Green’s function, the solution regular at zero does not enter. The arbitrary constant A is to be determined by matching expression (4.2.2.2) at $r = r_c$ with the solution of Eq. (4.2.6) in the inner region $r < r_c$. Since a positive-energy Green’s function is to be regular at infinity, one merely includes the solution $W_{vl+1/2}$ in the second term. Let us consider the asymptotic form for the outgoing radial Green’s function $g_l(E, r, r')$, $r, r' \rightarrow \infty$:

$$g_l(E, r, r') \rightarrow \frac{2}{krr'} \exp \left[i \left(kr_+ + \frac{Z \ln 2kr_+}{ka_0} - \frac{l\pi}{2} + \sigma_l + \delta_l \right) \right] \times \sin \left(kr_- + \frac{z \ln 2kr_-}{ka_0} - \frac{l\pi}{2} + \sigma_l + \delta_l \right) \frac{1}{e^2 a_0} \quad (4.2.2.4)$$

where $\sigma_l = \arg \Gamma(l+1-v)$ is the Coulomb phase shift and δ_l is the phase shift due to the residual interaction.

If the asymptotic form of Eq. (4.2.2.2) is computed as $r, r' \rightarrow \infty$ and compared with Eq. (4.2.2.4), one finds

$$A = \exp\{i[2\sigma_l - \pi(l-v)]\} [\exp(2i\delta_l) - 1] \quad (4.2.2.5)$$

Hence given the phase shifts $\delta_l(E)$, Eqs. (4.2.2) and (4.2.2.4) determine the Green's function at positive energies $E > 0$. For negative energies, $E < 0$, it is possible to continue analytically the positive-energy Green's function (4.2.2.2) by using the basic QDM continuation formula⁽¹⁹⁻²¹⁾

$$\cotg \delta_l(E) \rightarrow (1 - e^{2\pi i v}) \left[\cotg \pi \mu_l(E) - \frac{i}{e^{-2\pi i v} - 1} \right] \quad (4.2.2.6)$$

where the quantum defects $\mu_l(E)$ are obtained by fitting to corresponding values of the Rydberg formula (4.2.2.1). With relation (4.2.2.6), the constant A is continued to $E < 0$:

$$A = \frac{\Gamma(l+1-v)}{\Gamma(l+1+v)} \frac{\sin \pi[l + \mu_l(v)]}{\sin \pi[v + \mu_l(v)]} \quad (4.2.2.7)$$

On combining Eqs. (4.2.2.7) and (4.2.2.2) the closed-form QDM Green's function for $E < 0$ is therefore found to be given by

$$g_l(E, r, r') = \frac{Z}{v e^2} \Gamma(l+1+v) \Gamma(l+1-v) M_{v,l}(r_<) W_{v,l}(r_>) \quad (4.2.2.8)$$

where we have used the definitions

$$M_{v,l}(r) \equiv \frac{1}{(2l+1)!} M_{v,l+1/2} \left(\frac{2Z}{va_0} r \right) + \frac{\sin \pi[l + \mu_l(v)]}{\sin \pi[v + \mu_l(v)]} W_{v,l}(r) \quad (4.2.2.9)$$

and

$$W_{v,l}(r) \equiv \frac{1}{\Gamma(l+1+v)} W_{v,l+1/2} \left(\frac{2z}{va_0} r \right) \quad (4.2.2.10)$$

The bound-state energies and normalized discrete wave functions according to the QDM are readily found by locating the poles of Green's function (4.2.2.8) and calculating the residues at the eigenenergies. It is seen from expression (4.2.2.9) that the poles occur at the zeros of $\sin \pi[\mu_l(v) + v]$, namely $\mu_l(v) + v = n$, an integer; use of the definition of v confirms the eigenvalues given by Eq. (4.2.2.1). The residues at these eigenvalues give the quantum-defect eigenfunctions⁽²⁰⁾ for $E < 0$:

$$R_{nl}(r) = \frac{(z/a_0)^{1/2}}{vr} \left[\Gamma(l+1+v) \Gamma(v-l) \left(1 + \frac{\partial \mu_l(v)}{\partial v} \right) \right]^{-1/2} W_{v,l+1/2} \left(\frac{2z}{va_0} r \right) \quad (4.2.2.11)$$

The change in $\mu_l(v)$ is often small and the above term $\partial \mu_l(v)/\partial v$ may be neglected. One should note further that the residues at the pure Coulomb

poles, i.e., the poles of the gamma function in the first and second terms of Eq. (4.2.2.9), cancel out, as they should.

The usefulness of the closed-form Green's function (4.2.2.8) [or (4.2.2.2)] can be seen most simply from the evaluation, for example, of a typical second-order radial matrix element

$$M^{(2)}(2\omega) = \langle R_{n'l'}(r) g_L(\omega_i \pm \omega; r, r') r' R_{nl}(r') \rangle \quad (4.2.2.12)$$

Substitution for g_L from relation (4.2.2.8) gives

$$M^{(2)}(2\omega) = \frac{Ze}{ve^2} \Gamma(l+1+v) \Gamma(l+1-v) I \quad (4.2.2.13)$$

with

$$v = \frac{Ze}{[2\hbar(\omega_i \pm \omega)a_0]^{1/2}} \quad (4.2.2.14)$$

and

$$I \equiv \int_{r_0}^{\infty} dr \int_{r_0}^{\infty} dr' R_{n'l'}(r) r \mathcal{M}_{v,L}(r_-) \mathcal{W}_{v,L}(r_>) R_{nl}(r') \quad (4.2.2.15)$$

where r_0 [$\approx (v/2)$] is chosen to eliminate the nonphysical divergence in the wave function (due to the presence of the irregular Whittaker functions) at the origin. We may convert the above double integral into the sum of two terms of the same form,

$$I = I_1 + I_2$$

where

$$I_1 = \int_{r_0}^{\infty} dr \left[R_{n'l'}(r) r \mathcal{W}_{v,L}(r) \int_{r_0}^r \mathcal{M}_{v,L}(r') R_{nl}(r') r' dr' \right] \quad (4.2.2.16)$$

and

$$\begin{aligned} I_2 &= \int_{r_0}^{\infty} dr R_{n'l'}(r) r \mathcal{M}_{v,L}(r) \int_r^{\infty} \mathcal{W}_{v,L}(r') R_{nl}(r') r' dr' \\ &= \int_{r_0}^{\infty} dr \left[R_{nl}(r) r \mathcal{W}_{v,L}(r) \int_{r_0}^r R_{n'l'}(r') r' \mathcal{M}_{v,L}(r') dr' \right] \end{aligned} \quad (4.2.2.17)$$

(Integrals I_1 and I_2 are in fact equal for a diagonal matrix element.) In this form I_1 or I_2 is most economically evaluated numerically using equal steps. As a result of the single infinite range of the integrals, the double integral in practice⁽¹⁸⁾ reduces to a single integral and the time taken to evaluate it becomes comparable to that for calculating merely a first-order matrix element.

We note that the irregular Whittaker functions appearing above are calculated, as is usual in quantum-defect theory,^(19,20) from the asymptotic expansion

$$W_{v,l+1/2} \left(\frac{2r}{v} \right) = \left(\frac{2r}{v} \right)^v e^{-r/v} \sum_{t=0}^{t_0} b_t r^{-t} \quad (4.2.2.18)$$

with

$$b_0 = 1 \quad \text{and} \quad b_t = \frac{v}{2t} [l(l+1) - (v-t)(v-t+1)] b_{t-1} \quad (4.2.2.19)$$

and the cutoff t_0 is chosen to terminate the asymptotic series (4.2.2.18) at the usual minimum term.

The regular function may be calculated from the series expansion

$$M_{v,l+1/2} \left(\frac{2r}{v} \right) = e^{-r/v} \left(\frac{2r}{v} \right)^{l+1} \sum_{t=0}^{\infty} a_t r^t \quad (4.2.2.20)$$

with

$$a_0 = 1 \quad \text{and} \quad a_t = \frac{2}{vt} \left(\frac{l+t-v}{2l+1+t} \right) a_{t-1} \quad (4.2.2.21)$$

4.2.2.2. The Pseudopotential Green's Function

Finally, we consider the radial Green's function of one-particle alkali-like systems represented by a pseudopotential

$$V(\mathbf{r}) = \sum_{l=0}^{\infty} \frac{B_l}{r^2} \hat{P}_l - \frac{Ze^2}{r} \quad (4.2.2.22)$$

where B_l is a constant to be determined from the experimental energy eigenvalues with given values of l . This choice^(33,46-48) of the pseudopotential has the advantage over the usual quantum-defect theory insofar as both the wave functions and Green's function are now given analytically throughout the configuration space:

$$\hat{P}_l \equiv \sum_m |Y_{lm}\rangle\langle Y_{lm}|$$

If Eq. (4.2.2.22) is introduced in the equation for Green's function (4.2.6) and we project as before on the spherical harmonics, we obtain

$$\left\{ -\frac{\hbar^2}{2\mu} \left[\frac{1}{r} \frac{d^2}{dr^2} r - \frac{\lambda_l(\lambda_l+1)}{r^2} \right] - \frac{Ze^2}{r} - E \right\} g_l(E; r, r') = -\frac{\delta(r-r')}{rr'} \quad (4.2.2.23)$$

This equation is very similar to the equation in the pure Coulomb case, except that now the integral angular-momentum quantum numbers l are replaced in general by “nonintegral quantum numbers” λ_l , where

$$\lambda_l(\lambda_l + 1) \equiv l(l + 1) + \frac{2\mu}{\hbar^2} B_l \quad (4.2.2.24)$$

The Coulomb Sturmian-like Green's function of this system can be readily written down⁽³³⁾ on comparison with Eq. (4.2.1.18), if everywhere in the latter equation l is analytically continued to λ_l . To this end the factorials containing l are continued by the gamma function to their nonintegral values λ_l while the degenerate hypergeometric function, with $l \rightarrow \lambda_l$, automatically continues the finite polynomials to the convergent infinite series. Thus we have the result

$$\begin{aligned} g_l(E; r, r') = & -\frac{2\mu}{\hbar^2} \left(\frac{2Z}{va_0} \right) \sum_{n=l+1}^{\infty} \left[\exp\left(-\frac{R}{2}\right) R^{\lambda_l} {}_1F_1(-n + \lambda_l + 1; 2\lambda_l + 2; R) \right] \\ & \times \frac{\Gamma(n + \lambda_l + 1)}{\Gamma(2\lambda_l + 2)\Gamma(n - \lambda_l)} \frac{1}{(n - v)} \\ & \times \left[\exp\left(-\frac{R'}{2}\right) (R')^{\lambda_l} {}_1F_1(-n + \lambda_l + 1; 2\lambda_l + 2; R') \right] \end{aligned} \quad (4.2.2.25)$$

where

$$R \equiv \frac{2Z}{va_0} r, \quad R' \equiv \frac{2Z}{va_0} r', \quad \text{and} \quad v = \frac{Ze}{(-2Ea_0)^{1/2}} \quad (4.2.2.26)$$

Similarly the closed-form representation of Eq. (4.2.2.25), analogous to Eq. (4.2.1.7), is

$$g_l(E; r, r') = \frac{v}{Ze^2} \frac{1}{rr'} \frac{\Gamma(1 + \lambda_l - v)}{\Gamma(2\lambda_l + 2)} M_{v, \lambda_l + 1/2} \left(\frac{2Z}{va_0} r \right) W_{v, \lambda_l + 1/2} \left(\frac{2Z}{va_0} r' \right) \quad (4.2.2.27)$$

The energy spectrum of the system is obtained from the simple poles of $\Gamma(1 + \lambda_l - v)$ which occur when $1 + \lambda_l - v = -n_r$ with $n_r = 0, 1, 2, 3, \dots$.

Thus the energy level with quantum numbers nl of this model is

$$E_{n_r l} = -\frac{Z^2 e^2 / a_0}{2(n_r + \lambda_l + 1)^2} \quad (4.2.2.28)$$

where n_r is the radial quantum number. The principal quantum number for

the valence electron can be defined as

$$n = n_r + l + 1 + p_l \quad (4.2.2.29)$$

where p_l is the number of filled shells of the core. Equation (4.2.2.28) allows us to determine the constants λ_l (or, equivalently, the potential parameters B_l) on comparison with the experimental spectrum E_{nl} . In this way B_l becomes weakly energy-dependent, and the pseudopotential (4.2.2.22) in principle becomes of the nonlocal (or “velocity-dependent”) type. We note also that

$$\lambda_l(E) = p_l + l - \mu_l(E) \quad (4.2.2.30)$$

and therefore $\lambda_l(E)$ can be defined for energies E other than the bound-state energies E_{nl} , by the extrapolation–interpolation method of the usual quantum-defect theory.^(19–21)

4.3. The Method of Inhomogeneous Differential Equations

A rather powerful method of performing the ubiquitous intermediate sums exactly is the indirect numerical approach of inhomogeneous differential equations (IDE).^(49–51) This method has been applied to calculations of a number of second-order processes^(51–54) in the H atom, before being adopted to the two-photon ionization calculation.⁽⁵⁴⁾ Subsequently it was generalized^(55,56) to treat many-photon ionization problems. The major usefulness of the method lies in its ability to treat systems which, as a rule, are nonhydrogenic and hence cannot be treated analytically. For multiphoton-ionization calculations IDEs have been developed first in the momentum representation,^(54,55) but are perhaps more convenient to apply, especially for nonhydrogenic systems, in the configuration-space⁽⁵⁶⁾ representation. We shall describe the latter, more direct approach below.

The $(N + 1)$ th-order T-matrix element can be written in the suggestive form

$$T_{i \rightarrow f}^{(N+1)} = \langle f | V | \psi_i^{(N)} \rangle \quad (4.3.1)$$

where

$$| \psi_i^{(N)} \rangle = \oint_{j_N} \frac{| j_N \rangle \langle j_N | V}{(E_i^{(N)} - \epsilon_{j_N})} \dots \oint_{j_2} \frac{| j_2 \rangle \langle j_2 | V}{(E_i^{(2)} - \epsilon_{j_2})} \oint_{j_1} \frac{| j_1 \rangle \langle j_1 | V | i \rangle}{(E_i^{(1)} - \epsilon_{j_1})} \quad (4.3.2)$$

$| \psi_i^{(N)} \rangle$ is recognized as a component of the N th-order perturbed wave function evolving from the initial state $| i \rangle$. The propagator sums \oint run over

the spectrum of the atom avoiding, where necessary, the outer states of the matrix element. The propagator energies are $E_i^{(n)} \equiv \varepsilon_i + \hbar\Omega_n$, $n = 1, 2, 3, \dots, N$. Beginning with the extreme right-hand sum in Eq. (4.3.2) one defines

$$|\psi_i^{(1)}\rangle = \sum_{j_1}' |j_1\rangle\langle j_1| V |i\rangle \frac{1}{E_i^{(1)} - \varepsilon_{j_1}}$$

Operating with $(E_i^{(1)} - H_a)$ on the left and recalling that $H_a |j\rangle = \varepsilon_j |j\rangle$, where H_a is the target Hamiltonian, one obtains $|\psi_i^{(1)}\rangle$ as a solution of the differential equation

$$(E_i^{(1)} - H_a) |\psi_i^{(1)}\rangle = \sum_{j_1}' |j_1\rangle\langle j_1| V |i\rangle \quad (4.3.3)$$

If the closure property of the atomic states is used, then one may reduce the inhomogeneous terms on the right-hand side of relation (4.3.3) to a single or at most a few known terms:

$$(E_i^{(1)} - H_a) |\psi_i^{(1)}\rangle = Q_{(1)} V |i\rangle \quad (4.3.4)$$

with

$$Q_{(1)} \equiv 1 - P_{(1)} \quad (4.3.5)$$

where

$$P_{(1)} \equiv |i\rangle\langle i| \delta_{\varepsilon_i, E_i^{(1)}} + |f\rangle\langle f| \delta_{\varepsilon_f, E_i^{(1)}} \quad (4.3.6)$$

(Often $P_{(1)}$ does not contribute at all due to selection rules of the matrix element of V .)

Now the IDE given by Eq. (4.3.4) can be solved numerically to obtain $|\psi_i^{(1)}\rangle$ explicitly. Once $|\psi_i^{(1)}\rangle$ is known, the above procedure is repeated to construct the equation satisfied by the second-order perturbed function.

$$|\psi_i^{(2)}\rangle \sum_{j_2}' \frac{|j_2\rangle\langle j_2| V |\psi_i^{(1)}\rangle}{E_i^{(2)} - \varepsilon_{j_2}} \quad (4.3.7)$$

This equation is

$$(E_i^{(2)} - H_a) |\psi_i^{(2)}\rangle = (1 - P_{(2)}) V |\psi_i^{(1)}\rangle \quad (4.3.8)$$

with

$$P_{(2)} \equiv |i\rangle\langle i| \delta_{\varepsilon_i, E_i^{(2)}} + |f\rangle\langle f| \delta_{\varepsilon_f, E_i^{(2)}} \quad (4.3.9)$$

Again the right-hand side of Eq. (4.3.8) is known and the IDE can be

solved numerically for $|\psi_i^{(2)}\rangle$. Continuing this process one therefore obtains the final perturbed function $|\psi_i^{(N)}\rangle$ from the solution of the N th-order IDE:

$$(E_i^{(N)} - H_a) |\psi_i^{(N)}\rangle = (1 - P_{(N)}) V |\psi_i^{(N-1)}\rangle \quad (4.3.10)$$

where

$$P_{(N)} \equiv |i\rangle\langle i| \delta_{\epsilon_i, E_i^{(N)}} + |f\rangle\langle f| \delta_{\epsilon_f, E_i^{(N)}} \quad (4.3.11)$$

The numerical solution of Eq. (4.3.10), $|\psi_i^{(N)}\rangle$, is substituted in expression (4.3.1) and the desired $(N+1)$ th-order amplitude is obtained by a final quadrature.

To summarize, starting with the unperturbed initial state $|i\rangle$ one builds up the final perturbed solution $|\psi_i^{(N)}\rangle$ by solving step by step a chain of IDEs. It must be noted that the angular parts of the matrix elements are first integrated out in expression (4.3.2) in order to work only with the radial Hamiltonian in a single variable r , which generally permits numerical solution of the radial IDEs for effective one-electron systems without difficulty.

As an illustration, we consider the unperturbed states of H_a to have the form

$$|j\rangle \equiv |jl\rangle = \frac{F_{jl}^{(0)}(r)}{r} Y_{lm}(\hat{r}) \quad (4.3.12)$$

where $F_{jl}^{(0)}(r)$ are radial eigenfunctions. It is convenient to choose the z -axis, for a linearly polarized radiation, along the polarization direction ϵ of the field \mathbf{E} , or along the direction of propagation of radiation, for a circularly polarized field. With this convention the interaction V becomes simply

$$\frac{1}{2}\mathbf{E} \cdot \mathbf{D} = \frac{1}{2}ED_\lambda \quad (4.3.13)$$

where

$$D_\lambda = -er(4\pi/3)^{1/2} Y_{1\lambda}(\hat{r}) \quad (4.3.14)$$

with

$$\lambda = 0, \quad \text{linear polarization}$$

$$\lambda = +1, \quad \text{left circular polarization}$$

$$\lambda = -1, \quad \text{right circular polarization}$$

The angular integrals that now appear in Eq. (4.3.2) are⁽⁵⁷⁾

$$\begin{aligned}
 & \left(\frac{4\pi}{3} \right)^{1/2} \langle Y_{l'm'}(\hat{r}) | Y_{1\lambda}(\hat{r}) | Y_{lm}(\hat{r}) \rangle \\
 &= \left[\frac{l_{>}^2 - m^2}{(2l+1)(2l'+1)} \right]^{1/2} \delta_{m'm} ; \quad l_{>} = \text{greater}(l, l'); \quad \lambda = 0 \\
 &= \left\{ \left[\frac{(l+1+m)(l'+1+m)}{2(2l+1)(2l'+1)} \right]^{1/2} \delta_{l',l+1} \delta_{m',m+1} \right. \\
 &\quad \left. + \left[\frac{(l-1-m)(l'+1-m)}{2(2l+1)(2l'+1)} \right]^{1/2} \delta_{l',l-1} \delta_{m',m+1} \right\} ; \quad \lambda = 1 \quad (4.3.15)
 \end{aligned}$$

The corresponding radial IDEs are of the same form as Eqs. (4.3.4), (4.3.8), and (4.3.10), but with the simple replacements

$$\begin{aligned}
 H_a \rightarrow H_e &= -\frac{\hbar^2}{2\mu} \left[\frac{d}{dr^2} - \frac{l(l+1)}{r^2} \right] + \frac{U(r)}{r} \quad (4.3.16) \\
 \psi_i^{(N)} &\rightarrow F_{il_i}^{(N)}(r) \\
 |j_n\rangle &\rightarrow |j_nl_n\rangle \\
 E_i^{(n)} &\rightarrow E_{il_i}^{(n)} \\
 \varepsilon_{jn} &\rightarrow \varepsilon_{jnl_n}
 \end{aligned}$$

$U(r)/r$ is the effective one-electron target (model) potential.

The inhomogeneous radial equations are solved by specifying the boundary conditions of the perturbed radial functions. The following four cases can arise in practice⁽⁵⁶⁾:

1. $E_{il_i}^{(n+1)} < 0$ and $F_{jnl_n}^{(n)}(r)$ exponentially decreasing.
2. $E_{il_i}^{(n+1)} > 0$ and $F_{jnl_n}^{(n)}(r)$ exponentially decreasing.
3. $E_{il_i}^{(n+1)} < 0$ and $F_{jnl_n}^{(n)}(r)$ oscillating.
4. $E_{il_i}^{(n+1)} > 0$ and $F_{jnl_n}^{(n)}(r)$ oscillating.

4.4. The Pseudocontinuum-Basis Method

Direct evaluations of multiphoton perturbative matrix elements involve intermediate summations over the discrete, and integrations over the continuum, wave functions of the target. Numerical handling of the intermediate continuum integrations usually presents a difficult calculational problem. A rather general and practical numerical approach to avoid this problem extends the logic of the widely used discrete-basis configuration-interaction (CI) calculations for the bound-state problems to

the continuum problem. This method is best explained with the help of a specific example. We outline the method in connection with the two-photon ionization of the He atom, as was done originally.⁽⁵⁸⁾ The basic idea is to enlarge the discrete basis set of one-electron functions by an additional subset of one-electron “pseudocontinuum” functions of the form

$$f_{l,m}(k, \mathbf{r}) = N_l a_l(r) r^l \cos(kr) Y_{lm}(\hat{\mathbf{r}}) \quad (4.4.1)$$

where

$$a_l(r) = \sum_i c_{i,l} \exp(-q_i r) \quad (4.4.2)$$

The adjustable constants q_i and $c_{i,l}$ are chosen such that Eq. (4.4.2) behaves approximately like

$$a_l(r) \sim \frac{1}{r^{l+1}} \quad (a < r < b) \quad (4.4.3)$$

within an (intermediately large) interval $[a, b]$. This approximately ensures that the radial behavior of the “pseudocontinuum” orbitals (4.4.1) in the interval becomes similar to the r -dependence of the continuum functions

$$f_l(r) \sim \frac{\cos(kr)}{r} \quad (4.4.4)$$

in the same interval. Clearly, the range $[a, b]$ has to be chosen judiciously and by a trial-and-error approach for any given problem. The calculational steps, with illustrative numbers for the He case quoted in parentheses, are as follows:

1. A range $[a, b]$ is chosen ($a = 2$ au and $b = 30$ au).
2. A set of “localized bases” of Slater-type orbitals plus a number of Rydberg hydrogenic orbitals are selected in order to obtain a reasonable representation of the discrete part of the spectrum ($l \leq 6$, number of configurations, 70 to 80).
3. Some “pseudocontinuum” bases of the form (4.4.1) are added with k values, for each l ($l \leq 4$), equally spaced over a range of energy ($k = 0.1$ to 2 au). Some extra configurations containing the “pseudocontinuum” orbitals are added [mostly of the $(1s f_l)$ type for the manifold of total angular momentum l].
4. The matrix of the resulting configuration space is diagonalized and the most redundant linear combinations identified and eliminated for the rest of the calculation.

5. The Hamiltonian in the remaining configuration space is diagonalized to yield a set of (unity-normalized) “packet states”

$$\phi_{n,l}(x_1, x_2, \dots)$$

where $x_i \equiv (\mathbf{r}_i, \sigma_i)$ stands for the position and spin coordinates of the i th electron [about 130 to 140 states $\phi_{n,l}(x_1, x_2)$].

6. The discrete states $\phi_{n,l}$ with eigenvalues $E_{n,l}$ lying above the ionization threshold ($E_{n,l} > -2$ au) are selected and the corresponding one-electron densities $P_{n,l}(r_1)$ (i.e., the spinless radial diagonal elements of the one-electron density matrix) are calculated from $r = 0$ up to a large value $r = r_{\max}$ ($r_{\max} = 60$ au):

$$P_{n,l}(r_1) = 2 \int d\hat{r}_1 d\sigma_1 dx_2 |\phi_{n,l}(x_1, x_2)|^2 \quad (4.4.5)$$

7. Assuming that the “packet states” $\phi_{n,l}$ obtained from this extended CI calculation are sufficiently narrow, one expects that at distances larger than the atomic size (but not too large!) $P_{n,l}(r)$ should closely mimic the behavior of the usual continuum asymptotic density. Thus at the larger end of the range $r = [0, r_{\max}]$, one sets

$$r^2 P_{\epsilon,l}(r) = \left(\frac{2}{\pi \epsilon^{1/2}} \right) \{ \cos \delta_l(\epsilon) [F_{\epsilon,l}(r) + \operatorname{tg} \delta_l(\epsilon) G_{\epsilon,l}(r)] \}^2 \quad (4.4.6)$$

where $F_{\epsilon,l}(r)$ and $G_{\epsilon,l}(r)$ are the well-known regular and irregular Coulomb radial waves, $\delta_l(\epsilon)$ is the continuum phase shift, and $\epsilon = E_{n,l} + E_{\text{ion}}$, where E_{ion} is the ionization energy.

8. The radial density (4.4.5) is compared with Eq. (4.4.6) at the upper end of the range $r = [0, r_{\max}]$ (20 au to 50 au) to determine the phase shifts $\delta_l(\epsilon)$ and normalization constants required to energy δ -normalize the “packet states” ϕ_{nl} . From these functions not only can the usual continuum wave behavior be reproduced in the range $r = 0$ to r_{\max} , but also the possible resonant states at particular energies may be detected. Figure 17 shows the result of the densities at three energies for the state $\text{He}({}^1p^0)$. It is seen from this figure that curves A ($E = -1.78426$ au) and B ($E = -0.71725$ au) correspond to usual oscillatory-type continuum states while curve C ($E = -0.68963$ au) is already a quasi-localized state around the nucleus, revealing itself as a resonant state. The state functions so obtained have been found also to reproduce reliably⁽⁵⁸⁾ the usual one-photon ionization cross section of 2^1S and 2^1P states of He at low ionization energies.

9. The pseudocontinuum states ϕ_{nl} can actually be rather narrow

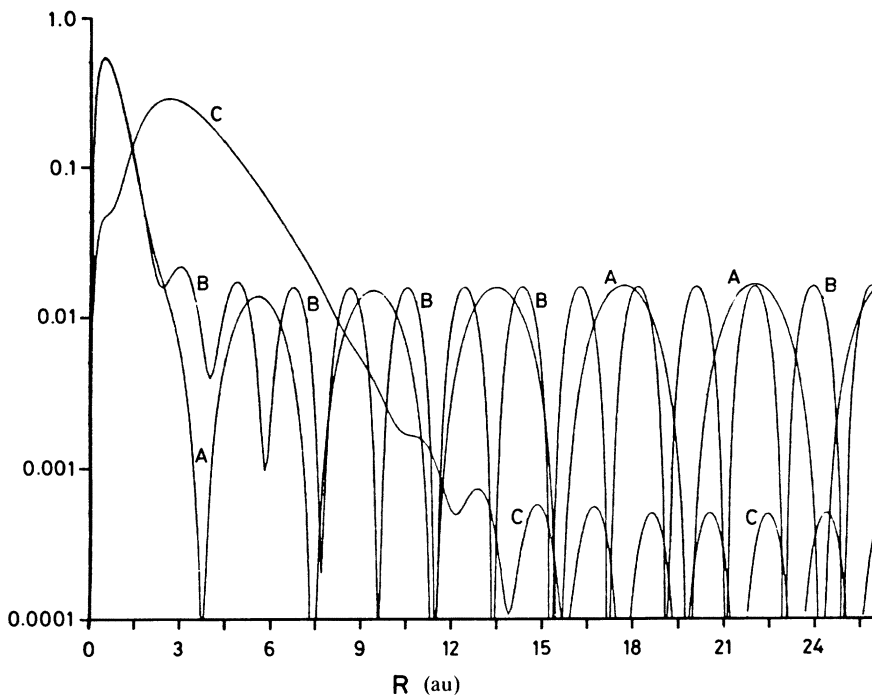


Figure 17. Radial densities for three pseudocontinuum p -states of He at energies $E = -1.78426$ (au) (curve A), -0.71725 au (curve B), and -0.68963 au (curve C). We note that state C behaves like a quasi-localized state reflecting the presence of resonance at this energy (after Cacelli *et al.*⁽⁵⁸⁾).

wave packets. Hence the required integration over the unperturbed intermediate continuum states of the target atom is rather well represented by simply summing over the set of discrete pseudocontinuum states ϕ_{nl} .

4.5. The Truncated Summation Method

For complex atomic systems it is not always practicable to use the previous exact summation methods. The truncated summation method is an approximate method for estimating the intermediate sum or Green's function, which has often been employed⁽⁵⁹⁻⁶²⁾ to calculate few-photon ionization cross sections in alkali atoms.

The method simply takes a finite number of discrete eigenstates of the target Hamiltonian (usually a model Hamiltonian) and neglects the rest of the intermediate states on the expectation that their contribution is

negligible. We give an approximate method of estimating the error, which should provide some guidance to the situation regarding when the method may be useful. Consider the second-order amplitude

$$T_{i \rightarrow f}^{(2)} = \sum_{j=1}^{\infty} \frac{\langle f | D_{\lambda} | j \rangle \langle j | D_{\lambda} | i \rangle}{(\omega_i - \omega_j - \omega)} = \langle f | D_{\lambda} G(\omega_i - \omega) D_{\lambda} | i \rangle \quad (4.5.1)$$

where

$$G(\omega_i - \omega) = \sum_{j=1}^{\infty} \frac{|j\rangle \langle j|}{(\omega_i - \omega_j - \omega)} \quad (4.5.2)$$

One may split an exact Green's function $G(\Omega_i)$ into two parts,

$$G(\Omega_i) = G_p(\Omega_i) + C_p(\Omega_i) \quad (4.5.3)$$

where

$$G_p(\Omega_i) = \sum_{j=1}^p \frac{|j\rangle \langle j|}{(\Omega_i - \omega_j)} \quad (4.5.4)$$

contains the sum over the first p discrete states and a “correction term”

$$C_p(\Omega_i) = \sum_{j=p+1}^{\infty} \frac{|j\rangle \langle j|}{(\Omega_i - \omega_j)} \quad (4.5.5)$$

which contains the rest. An attempt to evaluate this “correction” exactly would be tantamount to evaluating expression (4.5.1) exactly; hence the desired approximation method consists in estimating $C_p(\Omega_i)$ with the help of an “average frequency.”⁽⁵⁹⁾ Thus one assumes

$$C_p(\Omega_i) \approx \sum_{j=p+1}^{\infty} \frac{|j\rangle \langle j|}{\Omega_i - \langle \omega \rangle} = \frac{1-P}{\Omega_i - \langle \omega \rangle} \quad (4.5.6)$$

where $\langle \omega \rangle$ is an “average frequency,” which may be set equal to the ionization energy when ω_p ($\equiv \omega_{j=p}$) in Eq. (4.5.4) is close to the ionization threshold. In the above equation

$$P = \sum_{j=1}^p |j\rangle \langle j| \quad (4.5.7)$$

is the projector onto the p discrete states of interest. By combining relations (4.5.6) and (4.5.3) one obtains the approximate Green's function

$$G(\Omega_i) \approx G_p(\Omega_i) + \frac{1-P}{\Omega_i - \langle \omega \rangle} \quad (4.5.8)$$

Use of this approximation in Eq. (4.5.1) gives, for the second-order transition amplitude,

$$T_{i \rightarrow f}^{(2)} \approx \langle f | D_\lambda G_p(\Omega_i) D_\lambda | i \rangle + \langle f | D_\lambda (1 - P) D_\lambda | i \rangle \frac{1}{(\Omega_i - \langle \omega \rangle)} \quad (4.5.9)$$

with $\Omega_i = \omega_i - \omega$. Only a finite number of matrix elements appear in this relation and hence it may be computed directly. We note that in the second term of expression (4.5.9) matrix elements of both D_λ and D_λ^2 appear. The approximation (4.5.9) is likely to be a good one when the modulus of the “correction part” [the second term in relation (4.5.9)] is small compared to the modulus of the first term. This is often the case when one or a few of the intermediate bound states are in “near resonance” with respect to one or several photon absorptions. A generalization of the method to higher-order matrix elements is straightforward; one merely replaces each of the sequence of exact Green’s functions appearing in the N th-order amplitude, Eq. (4.1.1), by the corresponding truncated Green’s function, Eq. (4.5.8), as often as required.

5

Nonresonant Multiphoton Ionization

5.1. Introduction

Ionization is perhaps the most common multiphoton phenomenon that occurs when a strong enough radiation field, virtually of any frequency, is made to interact with gas atoms. As the sum of energies of the absorbed photons exceeds the ionization threshold-energy, the continuum states of the atom allow for both the necessary energy conservation and the satisfaction of the angular-momentum selection rules which give rise to a nonvanishing ionization probability. The degree of ionization, however, depends in significant and characteristic ways on the strength, polarization, and frequency of the field.

A typical nonresonant multiphoton ionization occurs through simultaneous absorption of several photons. Figure 18 shows a schematic of multiphoton ionization through nonresonant absorption of four photons. A multiphoton transition is said to be nonresonant if there are no intermediate atomic levels whose energy coincides (or almost coincides) with a multiple of the photon energy. In such cases perturbation theory may be used to calculate the generalized cross sections.

In this chapter we shall consider specific cases of multiphoton ionization cross sections calculated by various methods introduced in Chapter 4. In the prototype case of the hydrogen atom it is possible to obtain the generalized cross section entirely in terms of known (hypergeometric) functions to any order of interest. For nonhydrogenic systems, the Green's-function method or the inhomogeneous differential equation and pseudocontinuum-basis methods can be applied effectively.

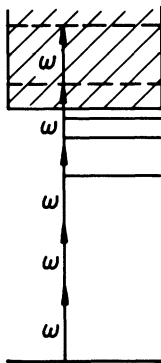


Figure 18. A schematic showing the process of nonresonant ionization by absorption of four or more photons from the ground state of an atom.

5.2. Multiphoton Ionization of the Hydrogen Atom

The initial state of the target hydrogen atom can be taken as an arbitrary bound state with quantum numbers (n, l, m) :

$$|i\rangle = R_{nl}(r)Y_{lm}(\hat{r}) \quad (5.2.1)$$

where

$$R_{nl}(r) = C_{nl} \exp(-r/n) r^l {}_1F_1(-n + l + 1; 2l + 2; 2r/n) \quad (5.2.2)$$

with

$$C_{nl} = 2^{2l+1} n^{-(l+2)} \frac{1}{(2l+1)!} \left[\frac{(n+l)!}{(n-l-1)!} \right]^{1/2} \quad (5.2.3)$$

The final state for ionization must be the ingoing Coulomb continuum state

$$|f^{(-)}\rangle = \left(\frac{8\pi^3}{k} \right)^{1/2} \sum_{LM} i^L \exp(-i\sigma_L) R_{e,L}(r) Y_{LM}(\hat{r}) Y_{LM}^*(\hat{k}) \quad (5.2.4)$$

where $\delta_L = \arg \Gamma(L + 1 - i/k)$ is the Coulomb phase shift, and the energy-scale delta-normalized radial wave functions

$$R_{e,L}(r) = C_{k,L} \exp(-ikr) r^L {}_1F_1(i/k + L + 1; 2L + 2; 2ikr) \quad (5.2.5)$$

$$\sim_{r \rightarrow \infty} \left(\frac{2}{\pi k} \right)^{1/2} \frac{1}{r} \sin \left(kr + \frac{1}{k} \ln kr + \sigma_L - \frac{1}{2} l\pi \right) \quad (5.2.6)$$

$$C_{k,L} = \frac{2^{L+1}}{(2L+1)!} k^L \left[\frac{\prod_{s=1}^L (s^2 + k^{-2})}{1 - e^{-2\pi/k}} \right]^{1/2} \quad (5.2.7)$$

with $\varepsilon = k^2/2$. In this chapter atomic units ($e = \hbar = m = 1$) are used except where stated explicitly otherwise.

The lowest-order N -photon amplitude is of the form

$$T_{i \rightarrow f}^{(N)} = \langle f^{(-)} | D_\lambda G(\omega_i + (N-1)\omega) D_\lambda G(\omega_i + (N-2)\omega) D_\lambda \cdots D_\lambda (\omega_i + \omega) D_\lambda | i \rangle \quad (5.2.8)$$

This is first reduced to the radial form by using the angular-momentum selection rules. In the absence of spin-orbit coupling, the multiphoton selection rule is obtained by applying successively the ordinary dipole selection rules [see Eq. (4.3.15)]:

$$\begin{aligned} \Delta l &= \pm 1, \quad \Delta m = 0 \quad \text{for } \lambda = 0 \quad (\text{linear polarization}) \\ \Delta l &= \pm 1, \quad \Delta m = +1 \quad \text{for } \lambda = +1 \quad (\text{left circular polarization}) \\ \Delta l &= \pm 1, \quad \Delta m = -1 \quad \text{for } \lambda = -1 \quad (\text{right circular polarization}) \end{aligned} \quad (5.2.9)$$

This is shown schematically in Figure 19.

For example, in the case of two-photon transition from an initial state (l, m) , relation (5.2.9) may be applied twice, as shown schematically in Figure 20, to obtain the angular quantum numbers of the intermediate states as well as of the final state.

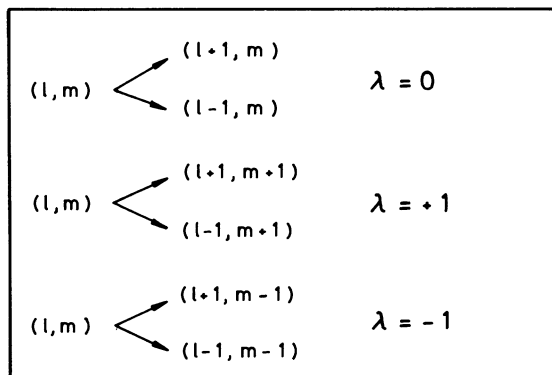


Figure 19. Coupling of states obeying single-photon dipole selection rule: $\lambda = 0$ corresponds to linear polarization and $\lambda = \pm 1$ to left (+) and right (-) circular polarizations; $l = 0, 1, 2, 3, \dots$ and $|m| \leq l$.

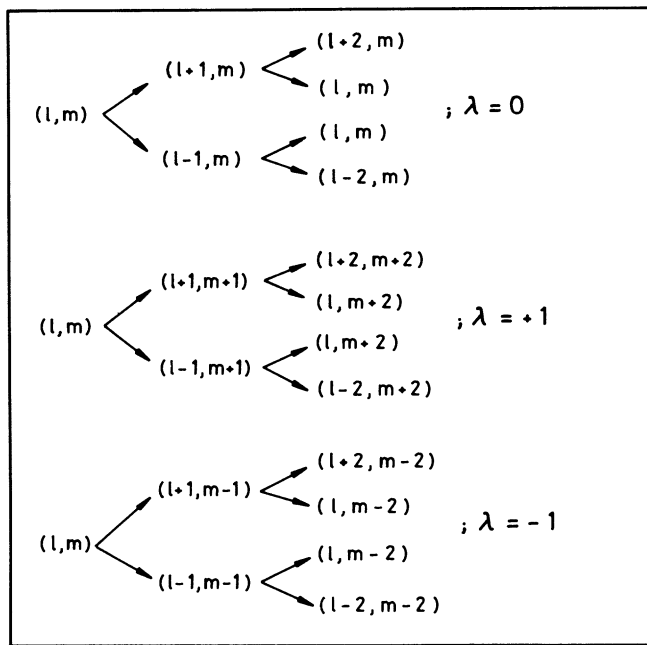


Figure 20. Coupling of states obeying two-photon dipole selection rule: $\lambda = 0$ corresponds to linear polarization and $\lambda = \pm 1$ to left (+) and right (-) circular polarizations; $l = 0, 1, 2, 3, \dots$ and $|m| \leq l$.

5.2.1. Two-Photon Ionization of the Hydrogen Atom

The two-photon differential ionization cross section

$$\frac{d\sigma^{(2)}}{d\Omega} = \frac{1}{F} \frac{dW^{(2)}}{d\Omega} \quad (5.2.1.1)$$

can be obtained from the rate [Eq. (2.6.10)]

$$\frac{dW^{(2)}}{d\Omega} = (2\pi)^3 \alpha^2 \omega^2 \sum_j \left| \frac{\langle f | \boldsymbol{\epsilon} \cdot \mathbf{r} | j \rangle \langle j | \boldsymbol{\epsilon} \cdot \mathbf{r} | i \rangle}{\omega_i - \omega_j + \omega} \right|^2 F^2 \quad (5.2.1.2)$$

where F is the photon flux. For the ground state of the hydrogen atom $|i\rangle = 2e^{-r} Y_{00}(\hat{\mathbf{r}})$; the final state $|f\rangle$ is the ingoing continuum Coulomb wave function [Eq. (5.2.4)] and the state density $\rho(E_f) = 1$. Use of the selection rules (Figure 20) for linear polarization ($\lambda = 0$) with $l = 0$, $m = 0$, and Eq. (4.3.15) allows easy evaluation of the angular integrals.

The differential cross section may then be expressed as

$$\frac{1}{I} \frac{d\sigma^{[2]}}{d\Omega} = \frac{\pi^2}{8I_0} \alpha\omega |T_0 + T_2|^2 \quad (5.2.1.3)$$

where

$$T_0 = \frac{2}{3\sqrt{\pi}} \exp(i\sigma_0) M_0(\omega) \quad (5.2.1.4)$$

and

$$T_2 = \frac{2}{3\sqrt{\pi}} (1 - 3 \cos^2 \theta) \exp(i\sigma_2) M_2(\omega) \quad (5.2.1.5)$$

$M_0(\omega)$ and $M_2(\omega)$ are the second-order radial matrix elements

$$M_L(\omega) = \sum_{J,p} \frac{\langle R_{eL}(r) r R_{J,p}(r) \rangle \langle R_{J,p}(r) r R_{1s}(r) \rangle}{\omega_{1s} - \omega_{J,p} + \omega} \quad (5.2.1.6)$$

with $L = 0$ and 2 ; $R_{eL}(r)$ is the radial Coulomb wave function with asymptotic behavior given by Eq. (5.2.6), σ_0 and σ_2 are the s - and d -wave Coulomb phase shifts, I is the external field intensity, I_0 ($= 7.019 \times 10^{16}$ W/cm 2) is a characteristic hydrogenic intensity, and

$$\sigma_L \equiv \arg \Gamma(L + 1 + i/k)$$

The radial matrix elements may be evaluated by any one of the methods described in Chapter 4. The result is best expressed in the form⁽⁶³⁾

$$\frac{1}{I} \frac{d\sigma^{[2]}}{d\Omega} = A + B \cos^2 \theta + C \cos^4 \theta \quad (\text{cm}^4/\text{W/Sr}) \quad (5.2.1.7)$$

where I is in W/cm 2 and θ is the angle of ejection of the ionized electron with respect to the direction of (linear) polarization, ϵ . The total cross section integrated over all directions is then given by

$$\frac{\sigma^{[2]}}{I} = 4\pi(A + B/3 + C/5) \quad (\text{cm}^4/\text{W}) \quad (5.2.1.8)$$

The angular distribution parameters A , B , and C can be written explicitly⁽⁶³⁾ in terms of generalized hypergeometric or Appell functions, which are rather complicated. Table 1 gives numerical values of the parameters and integrated cross sections for a range of incident photon wavelengths.

It is interesting to observe that the total two-photon ionization cross section, in the wavelength region above the one-photon ionization threshold (13.6 eV), varies monotonically (roughly as λ^6). In this domain

Table 1. Parameters of Angular Distribution for Two-Photon Ionization of H(1s) and Total Cross Section per Unit Intensity $\sigma^{[2]}/I$ in cm^4/W and I in W/cm^2 (from Klarsfeld⁽⁶³⁾)^a

λ (nm)	A	B	C	$\sigma^{[2]}/I$
60.0	4.694(37)	-5.118(36)	1.657(35)	2.611(35)
70.0	1.469(36)	-1.542(35)	4.542(35)	6.801(35)
80.0	3.991(36)	-4.032(35)	1.098(34)	1.572(34)
90.0	9.748(36)	-9.474(35)	2.413(34)	3.321(34)
95.0	1.140(32)	-5.523(32)	7.462(32)	9.950(32)
96.4	1.001(36)	-4.055(36)	1.666(35)	1.507(34)
100.3	1.214(35)	-1.448(35)	3.537(35)	1.808(34)
110.0	3.382(35)	-1.606(34)	2.597(34)	4.049(34)
112.2	2.310(35)	-3.113(35)	5.709(35)	3.034(34)
120.0	5.616(33)	-2.790(32)	4.152(32)	5.803(32)
130.0	1.239(33)	-7.413(33)	1.126(32)	1.283(32)
140.0	8.350(34)	-5.026(33)	7.566(33)	8.453(33)
145.0	8.307(34)	-4.948(33)	7.372(33)	8.240(33)
160.0	1.010(33)	-5.690(33)	8.072(33)	9.143(33)
170.0	1.230(33)	-6.592(33)	8.907(33)	1.024(32)
182.352	1.607(33)	-7.994(33)	9.944(33)	1.170(32)

^a The entry 4.694(37) is an abbreviation for 4.694×10^{-37} , etc

therefore expression (5.2.1.8) may be written as

$$\frac{\sigma^{[2]}}{I} = (1.572 \times 10^{-45}) g_2 \lambda^6 \quad (\text{cm}^4/\text{W}) \quad (5.2.1.9)$$

where λ is in nanometers and I in W/cm^2 . Equation (5.2.1.9) thus provides a second-order correction g_2 to the Gaunt factor.^(63,64) Variation of g_2 is very slow as a function of ejected electron energy and is shown in Figure 21.

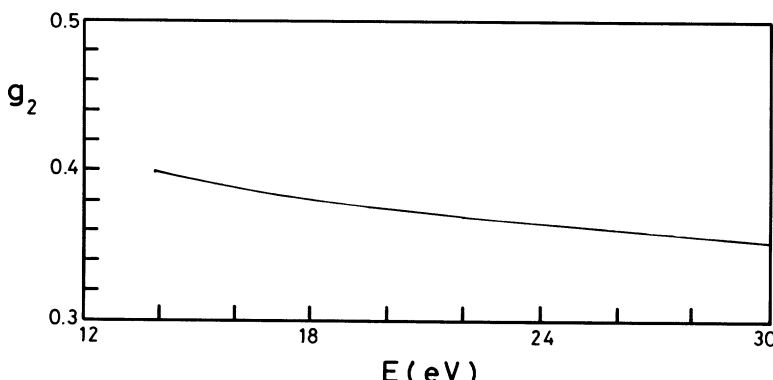


Figure 21. The two-photon Gaunt factor (from Klarsfeld⁽⁶³⁾).

The two-photon ionization cross section for the metastable H(2s) can be evaluated in a similar way. Equations (5.2.1.3)–(5.2.1.5) are obtained with

$$M_L = \sum_j \int \frac{\langle R_{\epsilon L}(r) r R_{jp}(r) \rangle \langle R_{jp}(r) r R_{2s}(r) \rangle}{\omega_{2s} - \omega_{jp} + \omega}, \quad L = 0, 2 \quad (5.2.1.10)$$

where

$$R_{2s}(r) = (\frac{1}{2})^{3/2} (2 - r) e^{-r/2}$$

Table 2. Angular Distribution Parameters A , B , C (in 10^{-28}) and Total Two-Photon Ionization Cross Section for Metastable Hydrogen H(2s) (from Zernik⁽⁵⁴⁾)^a

λ (nm)	M_s	M_d	A	B	C	$\sigma^{[2]} / I$
729.01	-1.719(3)	-8.506(3)	0.01463	-0.1100	0.2068	0.2427
711.92	-2.197(3)	-9.708(3)	0.01871	-0.1434	0.2758	0.3278
700.00	-2.731(3)	-1.114(4)	0.02432	-0.1887	0.3696	0.4437
694.35	-3.094(3)	-1.215(4)	0.02871	-0.2242	0.4430	0.5346
680.04	-4.753(3)	-1.689(4)	0.05436	-0.4314	0.8740	1.073
666.13	-1.083(4)	-3.472(4)	2.224	-1.808	3.770	4.719
647.20	1.125(4)	3.083(4)	0.1697	-1.394	3.061	3.987
630.00	3.503(3)	8.102(3)	0.01111	-0.09215	0.2171	0.2991
620.00	2.379(3)	4.881(3)	0.003870	-0.03196	0.08006	0.1160
607.51	1.614(3)	2.748(3)	0.001160	-0.009137	0.02591	0.04140
600.00	1.314(3)	1.935(3)	0.0005635	-0.004028	0.01301	0.02288
590.00	1.014(3)	1.148(3)	0.0002159	-0.0009888	0.004653	0.01026
580.00	7.865(2)	5.736(2)	0.0001068	0.00002613	0.001182	0.004422
569.54	5.978(2)	1.172(2)	0.0001090	0.00009208	0.00005025	0.001882
560.00	4.543(2)	-2.156(2)	0.0001626	-0.0002896	0.0001729	0.001266
550.00	3.223(2)	-5.100(2)	0.0002500	-0.0009473	0.0009855	0.001650
536.04	1.526(2)	-8.764(2)	0.0004196	-0.002224	0.002986	0.003460
530.00	7.841(1)	-1.035(3)	0.0005176	-0.002949	0.004212	0.004734
520.00	-5.796(1)	-1.331(3)	0.0007464	-0.004602	0.007102	0.007948
510.00	-2.422(2)	-1.750(3)	0.001177	-0.007622	0.01251	0.01432
500.00	-5.956(2)	-2.605(3)	0.002437	-0.01624	0.02827	0.03364
491.51	-1.738(3)	-5.505(3)	0.01040	-0.06974	0.1285	0.1613
487.30	-7.613(3)	-2.064(4)	0.1434	-0.9549	1.822	2.380
485.23	1.286(4)	3.221(4)	0.3463	-2.287	4.455	5.970
481.13	2.057(3)	4.351(3)	0.006257	-0.04000	0.08200	0.1171
470.00	5.751(2)	5.905(2)	0.0001522	-0.0004832	0.001546	0.003774
464.93	3.935(2)	1.514(2)	0.00005676	0.00002674	0.0001028	0.001084
460.00	2.681(2)	-1.436(2)	0.00006690	-0.0001233	0.00009338	0.0005590
455.63	1.748(2)	-3.587(2)	0.0001138	-0.0004910	0.0005885	0.0008519

^a M_s and M_d are the s and d components of the compound radial matrix elements, Eq. (5.2.1.10), with $L = 0$ and 2 ; values of $\sigma^{[2]} / I$ are given in 10^{-28} cm 4 /W and I in W/cm 2 . The entry -1.719(3) is an abbreviation for -1.719×10^{-3} , etc.

is the radial $2s$ wave function. The differential and integrated cross sections for two-photon ionization of $H(2s)$ can again be expressed in the form (5.2.1.7) and (5.2.1.8), respectively.

Table 2 gives numerical values⁽⁵⁴⁾ of the corresponding parameters A , B , C and the cross section $\sigma^{[2]}/I$ as a function of wavelength. Second-order radial matrix elements M_s and M_d are also included for this case.

It is of interest to observe that the two-photon ionization cross section for a hydrogenic ion of nuclear charge Z could be easily obtained from that of $Z = 1$ according to the simple scaling law⁽⁵⁴⁾

$$\sigma^{[2]}(\omega, Z) = Z^{-8} \sigma^{[2]}(\omega/Z^2, 1) \quad (5.2.1.11)$$

This can be easily verified from Eq. (5.2.1.2) by remembering that the length in Coulomb problems scales as Z while the energy scales as Z^2 .

Equation (5.2.1.11) shows that with increasing ionic charge the two-photon ionization of the ion at the corresponding reduced frequency will be lowered dramatically.

Virtually all available methods of calculation have been used for the two-photon ionization of hydrogen. Table 3 presents a comparison⁽⁶⁵⁾ of results using inhomogeneous-differential-equation (IDE) methods and various representations of Coulomb Green's function (GF).

IDE1⁽⁶⁶⁾ and IDE2⁽⁶⁷⁾ are obtained by the method of inhomogeneous differential equations and GF1 to GF4 are obtained by using various representations of Coulomb Green's function (GF1,⁽⁶⁸⁾ integral representa-

Table 3. Two-Photon Ionization Cross Section of $H(1s)$ Calculated by Different Methods (from Morellec *et al.*⁽⁶⁵⁾)^a

λ (nm)	IDE1	IDE2	GF1	GF2	FG3	GF4
92.5	—	—	—	1.29	2.04	2.03
97.5	51.5	—	—	67.7	49.2	49.1
102	67.5	55.2	55.2	55.2	70.8	70.9
110	4.01	4.05	4.05	4.05	4.04	4.0
120	630.0	580.0	580.0	580.0	642.0	642.0
130	128.0	128.0	128.0	128.0	128.0	127.0
140	84.5	84.5	84.5	84.5	84.7	84.5
160	91.5	91.4	91.4	91.4	91.8	91.5
170	103	102.0	102.0	102.0	103.0	103.0
Ref.	Chan and Tang ⁽⁶⁶⁾	Teague and Lambropoulos ⁽⁶¹⁾	Klarsfeld ⁽⁶⁸⁾	Kristenko and Vetchinkin ⁽⁶⁹⁾	Laplanche <i>et al.</i> ⁽⁷¹⁾	Karule ⁽⁷⁰⁾

^a Scaled cross sections $\sigma^{[2]}/I$ are in units of 10^{-34} cm⁴/W, I is intensity in W/cm⁻².

tion; GF2⁽⁶⁹⁾ and GF4,⁽⁷⁰⁾ Sturmian representation; GF3,⁽⁷¹⁾ closed-form representation).

Agreement among the three different calculations IDE2, GF1, and GF2 is highly satisfactory and should provide a numerical bench mark for such calculations. The slight discrepancy of the other calculations with respect to this set, especially at shorter wavelengths, is presumably due to computational fluctuations in those calculations.

Multiphoton bound-bound transition matrix elements are easily obtained in a similar way; they occur often as intermediate steps in multiphoton ionization calculations. Appendix 2 gives a sample of two-photon matrix elements between bound states of the hydrogen atom.

5.2.2. Three- and Many-Photon Ionization of Hydrogen

The angular algebra can always be handled by successive application of the selection rules (5.2.9) as discussed in connection with the two-photon case. The significant theoretical quantity for three-photon ionization is the radial matrix element

$$M_{\lambda_1 \lambda_2 L} = \langle R_{\epsilon L}(r) r g_{\lambda_2}(\omega_i + 2\omega) r g_{\lambda_1}(\omega_i + \omega) R_{nl}(r) \rangle \quad (5.2.2.1)$$

where (nl) is an arbitrary initial state of the hydrogen atom and (ϵL) is the corresponding continuum state with $\epsilon = k^2/2 = 3\omega - 1/(2n^2)$. Equation (5.2.2.1) is most conveniently evaluated^(45,72,73) by using the Sturmian representation of Green's function.

Substitution of Sturmian Green's functions g_{λ_1} and g_{λ_2} from Eq. (4.2.1.18) permits one to express Eq. (5.2.2.1) explicitly in terms of sums of Gordon-type integrals⁽⁷⁴⁾

$$\begin{aligned} J(n, \lambda, \kappa | n', \lambda', \kappa') &= \int_0^\infty dr r^{3+\lambda+\lambda'} e^{-(\kappa+\kappa')r} {}_1F_1(\lambda + 1 - n, 2\lambda + 2, 2\kappa r) \\ &\quad \times {}_1F_1(\lambda' + 1 - n', 2\lambda' + 2, 2\kappa' r) \\ &= (-1)^{\lambda_1} \frac{(\lambda_2 + 1)!}{2\kappa_2^2 (\kappa_1 - \kappa_2)^{2\lambda_2 + 2}} \left(\frac{\kappa_2 - \kappa_1}{\kappa_2 + \kappa_1} \right)^{n_1} \left(\frac{\kappa_2 - \kappa_1}{\kappa_2 + \kappa_1} \right)^{n_2} \\ &\quad \times \sum_{q=0}^2 \binom{2}{q} [\kappa_2(n_2 - 1 + q) - \kappa_1 n_1] \left(\frac{\kappa_2 - \kappa_1}{\kappa_2 + \kappa_1} \right)^q \\ &\quad \times {}_2F_1(\lambda_2 + 1 - n_2 - q, \lambda_1 + 1 - n_1; 2\lambda_2; -4\lambda_1\lambda_2/(\kappa_2 - \kappa_1)^2) \end{aligned} \quad (5.2.2.2)$$

where λ_2 and λ_1 are the greater and lesser of the values (λ, λ') , respectively;

(n_2, κ_2) and (n_1, κ_1) are values of (n, κ) which correspond to λ_2 and λ_1 , respectively.

When n, κ or n', κ' are complex, as in the present case of ionization, a convenient real polynomial representation⁽⁷⁵⁾ of the integral is

$$\begin{aligned} J\left(n_2, \lambda_2, \kappa_2 \mid \frac{1}{ik}, \lambda_2 - 1, ik\right) &= \frac{(2\lambda_2 + 1)! \exp[k^{-1}(2 \operatorname{tg}^{-1} \rho - \pi)]}{2\kappa_2^2 \rho^{2\lambda_2 + 2} (1 + \rho^2)^{n_2 + 2}} \\ &\times \sum_{q=0}^2 (-1)^q \binom{2}{q} (1 + \rho^2)^q [\kappa_2(n_2 + 1 - q) - 1] G_{\lambda_2}\left(\lambda_2 + q - 1 - n_2; \frac{1}{k}; \rho\right) \end{aligned} \quad (5.2.2.3)$$

and

$$\begin{aligned} J\left(n_2, \lambda_2, \kappa_2 \mid \frac{1}{ik}, \lambda_2 + 1, ik\right) &= -2 \frac{(2\lambda_2 + 1)! \exp\left[\frac{1}{k}(2 \operatorname{tg}^{-1} \rho - \pi)\right]}{k^{2\lambda_2 + 6} (1 + \rho^2)^{n_2 + 2}} \\ &\times \sum_{q=0}^2 \binom{2}{q} \alpha \beta (1 + \rho^2)^q [1 - \kappa_2(n_2 + 1 - q)] G_{\lambda_2 + 2}\left(\lambda_2 + q + 1 - n_2; \frac{1}{k}; \rho\right) \end{aligned} \quad (5.2.2.4)$$

where

$$\begin{aligned} \rho &= \kappa_2/k, \quad \alpha = \lambda_2 + 1 - n_2(q^2 - q - 1) \\ \beta &= \lambda_2 + 2 + (n_2 + 1)q^2 - (3n_2 + 2)q + n_2 \end{aligned}$$

and

$$G_l(-n, \eta, \rho) = \sum_{l=0}^{2n} b_l \rho^l$$

with

$$b_0 = 1, \quad b_1 = 2n\eta/l$$

$$b_j = -\frac{1}{j} (2l + j + 1)^{-1} [4\eta(j - 1 - n)b_{j-1} + (2n + 2 - j)(2l + 2n + 1 - j)b_{j-2}] \quad (5.2.2.5)$$

Finally, in terms of the quantities J the explicit result for the radial matrix element is^(45,72,73)

$$\begin{aligned} M_{\lambda_1 \lambda_2, L} &= C_{n,l} C_{k,L} 2^2 \prod_{j=1}^2 \frac{(2\kappa_j)^{2\lambda_j + 1}}{[(2\lambda_j + 1)!]^2} \sum_{n_1=\lambda_1+1}^{\infty} K_1 J\left(n, l, \frac{1}{n} \mid n_1, \lambda_1, \kappa_1\right) \\ &\times \sum_{n_2=\lambda_2+1}^{\infty} K_2 J(n_1, \lambda_1, \kappa_1 \mid n_2, \lambda_2, \kappa_2) J\left(n_2, \lambda_2, \kappa_2 \mid \frac{1}{ik}, L, ik\right) \end{aligned} \quad (5.2.2.6)$$

where

$$\kappa_j = \left[\frac{1}{n^2} - 2j\omega \right]^{1/2} \quad \text{and} \quad K_j = \left(n_j - \frac{1}{\kappa_j} \right)^{-1} \frac{(n_j + \lambda_j)!}{(n_j - \lambda_j - 1)!} \quad (5.2.2.7)$$

We note that in expression (5.2.2.6) for the present three-photon case there are only two intermediate sums over n_1 and n_2 .

There is no difficulty in extending the analysis to the case of N -photon transition. The n th-order amplitude contains $(N - 1)$ such intermediate Green's functions as in Eq. (5.2.2.1). Thus one finds^(45,72)

$$\begin{aligned}
 M_{\lambda_1 \dots \lambda_{N-1}} &= \langle R_{\epsilon L} | r g_{\lambda_{N-1}}(\epsilon_n + (N-1)\omega) \cdots r g_{\lambda_2}(\epsilon_n + 2\omega) r g_{\lambda_1}(\epsilon_n + \omega) r | R_{nl} \rangle \\
 &= C_{nl} C_{\epsilon L} 2^{N-1} \prod_{q=1}^{N-1} \frac{(2\kappa_q)^{2\lambda_q+1}}{[(2\lambda_q + 1)!]^2} \\
 &\times \sum_{m_1=\lambda_1+1}^{\infty} K_1 J\left(n, l, \frac{1}{n} | m_1, \lambda_1, \kappa_1\right) \sum_{m_2=\lambda_2+1}^{\infty} K_2 J(m_1, \lambda_1, \kappa_1 | m_2, \lambda_2, \kappa_2) \cdots \\
 &\times \sum_{m_{N-1}=\lambda_{N-1}+1}^{\infty} K_{N-1} J(m_{N-2}, \lambda_{N-2}, \kappa_{N-2} | m_{N-1}, \lambda_{N-1}, \kappa_{N-1}) \\
 &\times J\left(m_{N-1}, \lambda_{N-1}, \kappa_{N-1} | \frac{1}{ik}, L, ik\right) \quad (5.2.2.8)
 \end{aligned}$$

The three-photon ionization cross section of the H(1s) state calculated using this method is shown for both linear (dashed line) and circular (solid line) polarization of light in Figure 22 (for wavelengths between 190 and 270 nm).

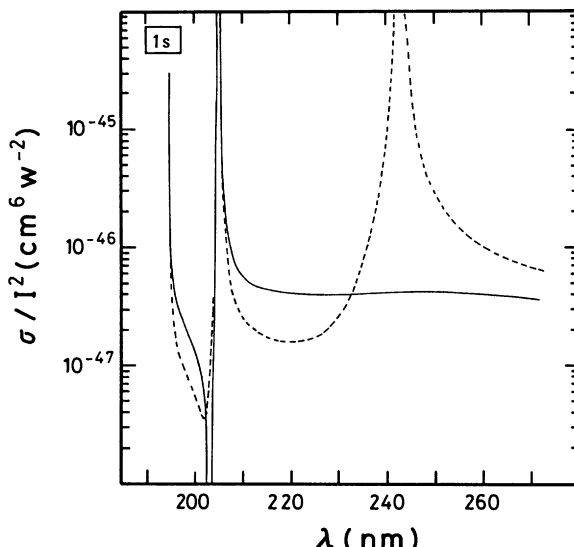


Figure 22. Three-photon ionization cross section σ for H(1s) with circularly (solid line) and linearly (dashed line) polarized light (from Maquet⁽⁴⁵⁾).

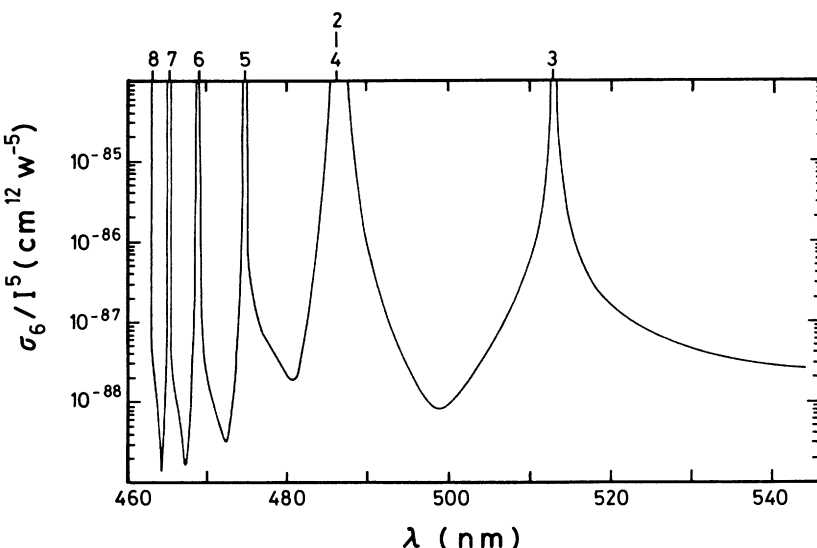


Figure 23. Frequency dependence of the six-photon ionization cross section σ_6 of H(1s) for a linearly polarized field (after Karule⁽⁷³⁾).

These cross sections exhibit typical dispersion phenomena near the intermediate resonant Rydberg levels. The dramatic difference between the linear (dashed line) and circular (solid line) polarization at about 240 nm is due to the presence of a two-photon intermediate resonance in the case of linear polarization with the $n = 2, l = 0, m = 0$ state. In the circular case the selection rule ($\lambda = 1$) would require a resonant ($l = 2, m = 2$) state, which does not exist in this region. This explains the qualitative difference in the two cases. The second peak at shorter wavelength is due to two-photon resonance with ($n = 3, l = 0, 2, m = 0$) states for linear polarization and ($n = 3, l = 2, m = 2$) state for circular ($\lambda = 1$) polarization, respectively.

We note the deep minimum between the two peaks at shorter wavelengths. Such regions of transparency are common; they are due to the destructive interference between intermediate subamplitudes having opposite signs in the regions between pairs of adjacent resonances.

Figure 23 shows the six-photon ionization cross sections of the ground-state hydrogen atom between 460 and 540 nm with a linearly polarized field, calculated⁽⁷³⁾ using the Sturmian Green's function. They are in excellent agreement with that obtained by the fully numerical IDE method.^(66,67) Actual calculations of the hydrogen atom up to 16-photon ionization has been performed,⁽⁷³⁾ however experimental data for such cross sections in the hydrogen atom are as yet unavailable for comparison. We note that besides the lowest-allowed-order multiphoton ionization

cross sections one may employ higher-order perturbation theory to calculate the so-called above-threshold ionization cross sections. These are cross sections for ionization by absorption of n photons, where n is larger than the minimum number of photons required to overcome the ionization threshold. Results are obtained using analytic continuation of the Green's function^(63,64,76,77,79) and by the IDE method.^(78,80) Results for above-threshold ionization cross sections of H(1s) by two- and three-photon absorption are given in Tables 4 and 5, respectively. It should be pointed out that the IDE method can be readily applied to atoms others than the hydrogen atom (see Section 5.3) and it seems to facilitate⁽⁷⁸⁾ the calculation of the Above-Threshold-Ionization (ATI) cross section from excited states of hydrogen more readily than the analytic-continuation technique, which may suffer from slow to poor convergence near the threshold. ATI rates $W^{(N+S)}$ for ($N + S$)-photon ionization, in which S additional photons are absorbed above the N -photon ionization threshold, have been calculated⁽⁸⁰⁾ also for a set of N and S using the IDE method, for the ionization of H(1s). Table 6 shows the result in terms of $W^{(N+S)}/I^{N+S}$, where I is the intensity in W/cm². These results are consistent with the presence of a critical intensity $I_c \sim 10^{14}$ W/cm², beyond which the first-allowed ionization probability and the probabilities of ionization by absorption of additional photons tend to be comparable.

Table 4. Above-Threshold Two-Photon Ionization Cross Section of the H(1s) State for a Circularly Polarized Field Calculated by the IDE Method (from Aymar and Crance⁽⁷⁸⁾)^a

λ (nm)	$\sigma_{(2)}^c/I$ (cm ⁴ /W)		
	a	b	c
2	1.10(44)	1.11(44)	1.10(44)
10	3.02(40)	2.99(40)	3.02(40)
30	3.22(37)	3.22(37)	3.22(37)
40	2.03(36)	2.02(36)	2.03(36)
50	8.54(36)	8.52(36)	8.53(36)
60	2.79(36)	2.77(36)	2.79(36)
70	7.64(35)	7.64(35)	7.64(35)
80	1.85(34)	1.85(34)	1.85(34)
90	4.06(34)	—	4.06(34)
91.127	4.41(34)	—	—

^a Column a is from Aymar and Crance⁽⁷⁸⁾ compared with the analytic continuation technique, column b and c, from Klarsfeld and Maquet.^(77,79) The entry 1.10(44) is an abbreviation for 1.10×10^{-44} , etc.

Table 5. Total Cross Section for Above-Threshold Three-Photon Ionization of H(1s) in Units of cm^6/W^2 for Linearly ($\sigma_{(3)}^L$) and Circularly ($\sigma_{(3)}^C$) Polarized Light (from Klarsfeld and Maquet⁽⁷⁷⁾)^a

λ (nm)	$\sigma_{(3)}^L/I^2$	$\sigma_{(3)}^C/I^2$
20	1.16(56)	6.38(57)
40	6.60(54)	4.72(54)
60	2.65(53)	2.39(52)
80	3.68(51)	4.04(51)
100	—	—
120	5.55(48)	4.67(48)
140	1.00(48)	2.39(48)
160	2.03(48)	5.07(48)
180	4.67(48)	1.13(47)

^a I is intensity in W/cm^2 . The entry 1.16(56) is an abbreviation for 1.16×10^{-56} , etc.

Table 6. Above-Threshold Ionization Rates $W^{(N+S)}/I^{(N+S)}$ for $(N+S)$ -Photon Ionization of H(1s) in Which S Photons are Absorbed Above the N -photon Ionization Threshold (from Gontier and Trahin⁽⁸⁰⁾)^a

S	$N = 6$ $\lambda = 530$ (nm)	$N = 7$ $\lambda = 650$ (nm)	$N = 10$ $\lambda = 910$ (nm)	$N = 12$ $\lambda = 1082$ (nm)
0	1.39 (69)	1.49 (97)	4.51(123)	3.46(149)
1	2.84 (83)	9.85(111)	7.78(136)	9.81(162)
2	2.92 (97)	2.53(124)	5.35(149)	1.10(174)
3	2.80(111)	5.84(138)	2.61(162)	1.08(187)
4	2.66(125)	1.35(151)	1.89(175)	9.87(201)
5	2.32(139)	2.75(165)	1.04(188)	8.91(214)

^a The entry 1.39(69) is an abbreviation for 1.39×10^{-69} , etc.

5.3. Multiphoton Ionization of Nonhydrogenic Atoms

An effective one-electron model of alkali atoms permits calculation of multiphoton ionization cross sections of these atoms in a completely analogous way to that for the hydrogen atom. Table 7 compares calculated results for two-photon ionization generalized cross sections, $\sigma^{(2)} = W^{(2)}/F^2$, where $W^{(2)}$ is the two-photon ionization rate and F is the incident photon flux, for a number of alkali atoms. [We shall use the notation $\sigma^{(N)} =$

Table 7. Two-Photon Generalized Ionization Cross Section $\sigma^{(2)}$ (in cm^4 s) for Alkali Atoms Calculated at Comparable Wavelengths by Different Methods (after Morellec *et al.*⁽⁶⁵⁾)^a

Atom	λ (nm)	TSM	$\text{GF}_{(1)}$	$\text{GF}_{(2)}$	$\text{GF}_{(3)}$
Li	347.1	7.8(50)	2.42(49)	1.14(49)	1.0(49)
Na	347.1	6.0(53)	6.25(52)	5.52(52)	4.0(51)
K	347.1	3.1(50)	3.08(50)	7.24(50)	—
	530.0	—	1.61(49)	1.12(49)	5.0(49)
Rb	347.1	5.1(50)	2.53(50)	4.16(49)	1.5(50)
	530.0	2.9(49)	1.08(49)	1.55(48)	4.0(49)
Cs	347.1	2.6(49)	2.52(49)	4.16(49)	—
	530.0	9.0(50)	7.41(49)	1.55(48)	2.0(49)

^a TSM denotes the truncated summation method with quantum-defect wave function (after Bebb⁽⁸¹⁾), $\text{GF}_{(1)}$ the quantum-defect Green's function (after Manakov *et al.*⁽⁶²⁾), $\text{GF}_{(2)}$ the model Fuess-potential Green's function (after Manakov *et al.*⁽⁶³⁾), $\text{GF}_{(3)}$ the quantum-defect closed-form Green's function (after McGuire⁽⁶⁴⁾). The entry 7.8(50) is an abbreviation for 7.8×10^{-50} , etc.

$W^{(N)}/F^{(N)}$ in $\text{cm}^{2N} \text{s}^{N-1}$ (where $W^{(N)}$ is the N -photon ionization rate in s^{-1}) for the generalized cross section, with F in $\text{cm}^{-2} \text{s}^{-1}$.]

Generalized cross sections for three-, four-, and five-photon ionization of alkali atoms calculated by different methods at comparable wavelength are shown in Table 8.

The spread among the various calculations in Tables 7 and 8 is roughly of one order of magnitude, indicating how the sensitivity of multiphoton-ionization calculations depends on the accuracy of bound and continuum wave functions (or Green's functions) used. For calculations using quantum-defect wave functions (or Green's functions) the inaccuracy may stem mainly from a few lowest-lying states (which are usually rather poorly accounted for in QDM). The very large discrepancy in four-and five-photon ionization cross sections of alkali atoms (see Table 8) calculated by QDM and pseudopotential Green's-function methods should warn the reader of the increasing sensitivity of higher-order processes on the choice of the necessarily approximate wave functions. In Table 9 we quote the above-threshold two-photon ionization cross section for Li($2s$), calculated⁽⁷⁸⁾ using a model-potential IDE method.

Of the rare-gas atoms, theoretical calculations of multiphoton ionization cross sections for He(2^1S) and He(2^3S) states have received most attention.^(58,86-92) Calculation of the two-photon ionization cross section of argon⁽⁹³⁻⁹⁵⁾ and neon⁽⁹⁵⁾ using many-body perturbation theory⁽⁹³⁾ and random-phase approximation (RPA)⁽⁹⁵⁾ have also been performed.

These calculated results for alkali atoms and noble gases mostly show rather large dispersions with respect to the method used and/or the gauge ("length" or "velocity" gauge) utilized. Thus, in order to be able to

Table 8. Three-, Four-, and Five-Photon Generalized Ionization Cross Sections of Alkali Atoms Calculated by Different Methods (after Morellec *et al.*⁽⁶⁵⁾)^a

$\sigma^{(3)}$: in $\text{cm}^6 \text{s}^2$						
Atom	λ (nm)	TMS	$\text{GF}_{(1)}$	$\text{GF}_{(2)}$	$\text{GF}_{(3)}$	$\text{GF}_{(4)}$
Li	530.0	—	—	7.14(82)	—	2.0(81)
Na	530.0	9.0(81)	2.33(78)	—	—	2.0(81)
	694.3	4.3(77)	9.33(78)	9.31(78)	1.05(77)	1.0(77)
K	694.3	7.0(80)	1.87(79)	3.72(79)	2.00(79)	5.0(80)
Rb	694.3	9.0(78)	1.14(78)	1.17(77)	3.68(78)	4.0(78)
Cs	694.3	6.3(78)	9.57(78)	1.00(77)	1.02(77)	1.0(77)

 $\sigma^{(N)}: \sigma^{(4)}$ (in $\text{cm}^8 \text{s}^3$) and $\sigma^{(5)}$ (in $\text{cm}^{10} \text{s}^4$)

Atom	λ (nm)	N	$\text{GF}_{(1)}$	$\text{GF}_{(2)}$
Li	694.3	4	3.52(106)	—
	1060.0	5	1.37(137)	—
Na	1060.0	5	3.96(138)	5.14(142)
K	1060.0	4	4.38(107)	9.18(108)
Rb	1060.0	4	1.32(107)	2.14(108)
Cs	1060.0	4	5.16(107)	7.14(108)

^a $\sigma^{(N)}$ is in $\text{cm}^{2N} \text{s}^{N-1}$. TSM denotes the truncated summation method with QDM wave function (from Bebb⁽⁸¹⁾), and $\text{GF}_{(1)}$, $\text{GF}_{(2)}$, $\text{GF}_{(3)}$, and $\text{GF}_{(4)}$ the Green's-function methods (from Manakov *et al.*,⁽⁶²⁾ Manakov *et al.*,⁽⁸³⁾ McGuire,⁽⁸⁴⁾ and Laplanche *et al.*,⁽⁸⁵⁾ respectively). The entry 9.0(81) is an abbreviation for 9.0×10^{-81} , etc.

Table 9. Above-Threshold Ionization Cross Section $\sigma_{(3)}^C$ for Li(2s) by Circularly Polarized Light (from Aymar and Crance⁽⁷⁸⁾)^a

λ/ν^2 (nm)	λ (nm)	$\sigma_{(3)}^C/I$ (cm^4/W)
10	25.23	1.64(37)
20	50.47	7.44(36)
30	75.70	6.32(35)
40	100.94	2.77(34)
50	126.17	8.52(34)
60	151.41	2.10(33)
70	176.64	4.44(33)
90	227.11	1.49(32)
91.127	229.95	1.58(32)

^a $\nu = 1.58853$ is the effective quantum number of the Li(2s) state. I is in W/cm^2 . The entry 1.64(37) is an abbreviation for 1.6×10^{-37} , etc.

discriminate to a certain extent among the methods of calculation, experimental data on absolute measurements of multiphoton ionization cross sections of both alkali atoms and noble gases appear to be indispensable.

In Table 10 we quote selected data on absolute measurements of multiphoton ionization of various atoms (with linearly polarized photons). Figure 24 compares⁽⁶⁵⁾ calculated (horizontal line) and measured (vertical bars) values of three-photon ionization cross sections of alkali atoms and excited-state singlet and triplet helium atoms.

The difference between the two theoretical calculations (Lom. a and b) of He(2^1S) at 694.5 nm is noteworthy. The agreement with experiment and calculation, which takes account of the dynamic Stark-shift of a near-resonant state (Lom. b), is much better than the calculation (Lom. a) which takes no account of it. The near-resonance in question (2^1S - 6^1S transition) is dynamically Stark-shifted away from the two-photon energy (unperturbed position 40.5 cm^{-1} from two-photon energy at $\lambda = 694.5\text{ cm}$), thereby decreasing the cross section toward the experimental value. This result is obtained⁽⁹²⁾ using model-potential wave functions for the singlet

Table 10. Experimental Data on Generalized Ionization Cross Sections $\sigma^{(N)}$ ($\text{cm}^{2N}\text{ s}^{N-1}$) for Selected Atoms (after Morellec *et al.*⁽⁶⁵⁾)^a

N	λ (nm)	Atom	$\sigma^{(N)}$	Ref.
2	347.26	He(2^1S)	$2.7 (\pm 2.0) \times 10^{-49}$	Lompré <i>et al.</i> ⁽⁹¹⁾
2	347.26	He(2^3S)	$1.5 (\pm 1.4) \times 10^{-49}$	Lompré <i>et al.</i> ⁽⁹¹⁾
2	528.0	Cs	$6.7 (\pm 1.9) \times 10^{-50}$	Normand and Morellec ⁽⁹⁷⁾
3	693.7	He(2^1S)	$5 \times 10^{-80} - 4 \times 10^{-77}$	Bakos <i>et al.</i> ⁽⁸⁷⁾
3	694.5	He(2^1S)	$3.3 (\pm 1.9) \times 10^{-80}$	Lompré <i>et al.</i> ⁽⁹¹⁾
3	694.5	He(2^3S)	$3.0 (\pm 2.2) \times 10^{-81}$	Lompré <i>et al.</i> ⁽⁹¹⁾
3	694.5	Na	$5.4 \begin{pmatrix} +1.3 \\ -1.1 \end{pmatrix} \times 10^{-77}$	Cervenan <i>et al.</i> ⁽⁹⁸⁾
3	694.5	K	$3.5 \begin{pmatrix} +0.9 \\ -0.7 \end{pmatrix} \times 10^{-79}$	Cervenan <i>et al.</i> ⁽⁹⁸⁾
3	694.5	Rb	$1.44 \begin{pmatrix} +0.53 \\ -0.34 \end{pmatrix} \times 10^{-77}$	Cervenan <i>et al.</i> ⁽⁹⁸⁾
3	694.5	Cs	$1.8 \begin{pmatrix} +1.1 \\ -0.7 \end{pmatrix} \times 10^{-77}$	Cervenan <i>et al.</i> ⁽⁹⁸⁾
4	1056.0	Cs	$7.5 (\pm 2.8) \times 10^{-104}$	Normand and Morellec ⁽⁹⁷⁾
4	1060.0	Cs	$1.0 \begin{pmatrix} +0.60 \\ -0.37 \end{pmatrix} \times 10^{-107}$	Arslandbekov <i>et al.</i> ⁽⁹⁹⁾
5	1060.0	Na	$1.26 \begin{pmatrix} +2.74 \\ -0.86 \end{pmatrix} \times 10^{-137}$	Arslandbekov <i>et al.</i> ⁽⁹⁹⁾
6	693	Xe	$10^{-176 \pm 1.7}$	Voronov and Delone ⁽⁹⁶⁾
11	1060.0	Xe	$10^{-338} - 10^{-334}$	Arslandbekov and Delone ⁽¹⁰⁰⁾

^a Incident photon flux F is in $\text{cm}^{-2}\text{ s}^{-1}$.

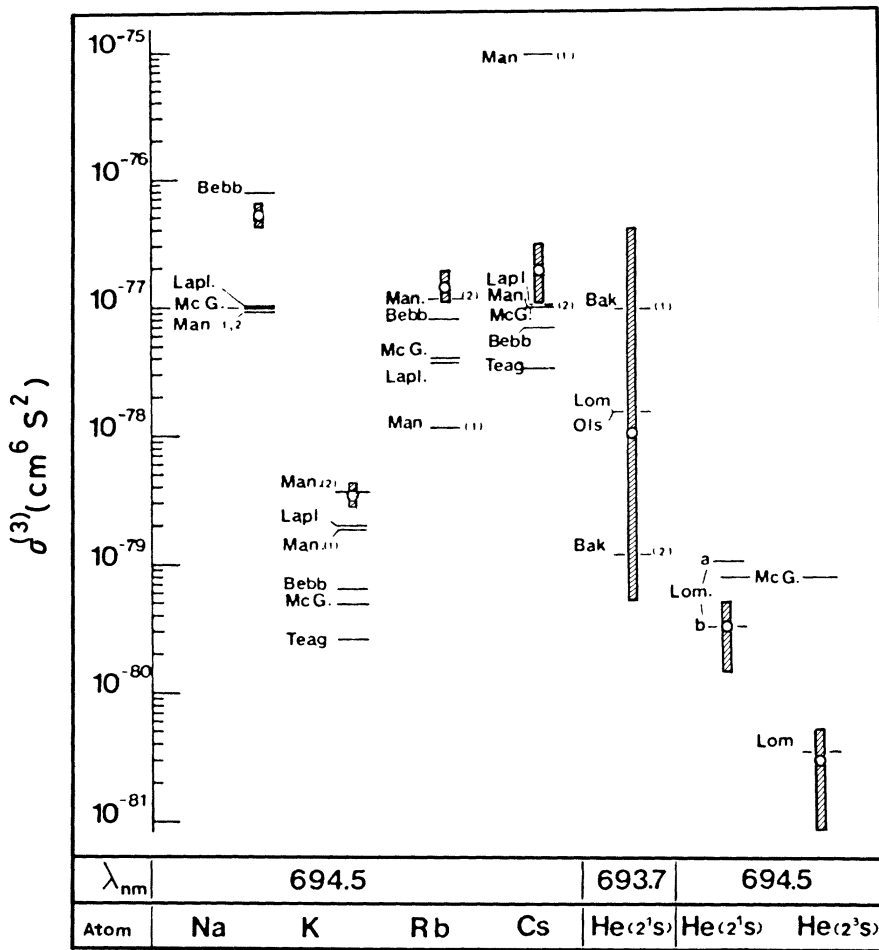


Figure 24. Comparison of theoretical calculations (horizontal lines) of three-photon ionization of alkali atoms and $\text{He}(2^1S)$ and $\text{He}(2^3S)$ with experimental data (vertical bars). Bak. denotes results of Bakos *et al.*⁽⁸⁷⁾ ((1), QDM; (2), HF), Bebb, Bebb,⁽⁸¹⁾ Lapl., Laplanche *et al.*,⁽⁸⁵⁾ Lom., Lompré *et al.*⁽⁹¹⁾ (a, lowest order; b, higher order), Man. (1), Manakov *et al.*,⁽⁸²⁾ Man. (2), Manakov *et al.*,⁽⁸³⁾ Mc G., McGuire,⁽⁸⁴⁾ Ols., Olsen *et al.*,⁽⁸⁸⁾ Teag., Teague and Lambopoulos⁽⁶¹⁾ (from Morellec *et al.*⁽⁶⁵⁾).

and triplet states of helium; these have been shown⁽⁹²⁾ also to reproduce the one-photon photoionization cross sections, oscillator strength, and resonance energies, in the helium atom, generally in a highly satisfactory manner. Numerical values for the cross sections of two-photon ionization of $\text{He}(2^1S)$ and $\text{He}(2^3S)$ for a wide range of frequencies are listed in Tables 11 and 12, while the corresponding three-photon ionization cross sections

Table 11. He(2^1S): Two-Photon Generalized Ionization Cross Section $\sigma^{(2)}$ vs. Incident Frequency ω (from Aymar and Crance⁽⁹²⁾)^a

ω (cm $^{-1}$)	$\sigma^{(2)}$ (cm 4 s)	ω (cm $^{-1}$)	$\sigma^{(2)}$ (cm 4 s)
16007	8.2(-49)	27000	1.1(-49)
18000	1.5(-48)	27400	5.7(-49)
19500	1.9(-47)	27600	3.5(-47)
19700	1.2(-46)	27650	2.1(-47)
19900	1.6(-46)	27700	2.2(-48)
20000	3.2(-47)	27800	2.8(-49)
20500	1.4(-48)	28000	1.7(-50)
21000	2.0(-49)	28100	6.7(-51)
21500	3.1(-50)	28400	3.1(-50)
21875	1.1(-50)	28800	3.0(-49)
22500	3.3(-50)	28900	1.4(-48)
23000	7.0(-50)	28955	4.9(-47)
24000	2.2(-49)		
24500	5.0(-49)	28980	1.9(-47)
25000	5.3(-48)	29000	3.2(-48)
25100	4.0(-47)	29100	1.0(-49)
		29200	1.1(-50)
25200	3.7(-47)	29250	6.0(-51)
25300	3.3(-48)	29500	4.8(-50)
25500	3.7(-49)	29700	4.6(-49)
25800	3.7(-50)	29750	3.3(-48)
26000	9.6(-51)		
26100	7.8(-51)	29800	2.0(-48)
26400	2.1(-50)	29850	1.4(-49)
26600	3.9(-50)	30000	8.4(-51)

Experimental and Calculated Resonance Frequencies and Threshold (in cm $^{-1}$)

	ω_{exp}	ω_{th}	$\omega_{\text{exp}} - \omega_{\text{th}}$
Threshold	16017	16007	10
3^1P	19932	19811	121
4^1P	25215	25151	64
5^1P	27665	27623	42
6^1P	28997	28965	32
7^1P	29802	29774	28

^a The entry 8.2(-49) is an abbreviation for 8.2×10^{-49} , etc.

Table 12. He(2^3S): Two-Photon Generalized Ionization Cross Section $\sigma^{(2)}$ vs. Incident Frequency ω (from Aymar and Crance⁽⁹²⁾)^a

ω (cm $^{-1}$)	$\sigma^{(2)}$ (cm 4 s)	ω (cm $^{-1}$)	$\sigma^{(2)}$ (cm 4 s)
19221	2.8(-49)	33200	5.1(-50)
20500	2.6(-49)	33600	1.6(-49)
22000	2.9(-49)	33800	7.1(-49)
24000	5.1(-49)	33900	1.4(-47)
25000	1.6(-48)		
25500	1.6(-47)	33950	9.7(-48)
25600	8.5(-47)	34000	9.3(-49)
		34100	1.0(-49)
25700	3.5(-46)	34250	7.7(-51)
25800	1.8(-47)	34375	1.4(-51)
26000	2.2(-48)	34500	5.1(-51)
26500	1.5(-49)	35000	6.1(-50)
27000	1.5(-50)	35200	2.6(-49)
27450	2.1(-51)	35300	6.3(-48)
28000	1.0(-50)		
29000	3.9(-50)	35350	1.9(-48)
30000	9.1(-50)	35400	1.8(-49)
31000	5.9(-49)	35500	9.8(-51)
31200	2.7(-48)	35575	1.4(-51)
31300	3.6(-47)	35700	7.6(-51)
		36000	7.8(-50)
31350	1.2(-46)	36100	3.8(-49)
31400	7.1(-48)	36150	2.3(-47)
31500	1.0(-48)		
31750	6.3(-50)	36200	2.4(-49)
32000	5.7(-51)	36250	2.3(-50)
32150	1.7(-51)	36325	1.4(-51)
32400	5.8(-51)	36400	7.1(-51)
32750	1.9(-50)	36500	2.5(-50)

Experimental and Calculated Resonance Frequencies and Threshold (in cm $^{-1}$)

	ω_{exp}	ω_{th}	$\omega_{\text{exp}} - \omega_{\text{th}}$
Threshold	19227	19221	6
3^3P	25709	25668	41
4^3P	31361	31333	28
5^3P	33945	33924	21
6^3P	35337	35319	18
7^3P	36171	36156	15

^a The entry 2.8(-49) is an abbreviation for 2.8×10^{-49} , etc.

Table 13. He(2^1S): Three-Photon Generalized Ionization Cross Section $\sigma^{(3)}$ vs. Incident Frequency ω (from Aymar and Crance⁽⁹²⁾)^a

ω (cm $^{-1}$)	$\sigma^{(3)}$ (cm 6 s 2)	ω (cm $^{-1}$)	$\sigma^{(3)}$ (cm 6 s 2)
10700	3.1(-81)	13840	7.1(-79)
11000	7.5(-81)	13900	3.9(-80)
11500	2.1(-80)	13950	7.9(-81)
12000	4.8(-80)	14020	1.5(-81)
12200	9.2(-80)	14200	8.6(-81)
12270	2.0(-79)	14350	3.9(-80)
12290	4.7(-79)	14400	7.0(-79)
12300	1.3(-78)		
		14410	1.2(-78)
12320	2.0(-78)	14430	1.3(-79)
12330	5.0(-79)	14450	2.4(-79)
12370	1.8(-79)	14480	1.9(-77)
12500	7.3(-79)		
12550	4.7(-78)	14490	4.0(-78)
		14500	5.7(-79)
12600	6.2(-79)	14550	1.5(-80)
12650	4.5(-79)	14580	3.6(-81)
12800	1.7(-80)	14620	1.4(-81)
12970	1.7(-81)	14700	6.1(-81)
13200	6.9(-81)	14800	3.3(-80)
13500	2.7(-80)	14830	1.7(-79)
13600	5.6(-80)	14835	6.0(-79)
13650	1.4(-79)		
13670	1.0(-78)	14840	1.2(-77)
		14855	1.2(-79)
13680	1.1(-77)	14870	3.0(-79)
13690	3.9(-79)	14880	1.4(-78)
13710	1.4(-79)		
13760	3.3(-79)	14890	1.2(-77)
13800	4.4(-76)	14900	3.8(-79)
		14920	3.5(-80)
13820	1.1(-77)	14950	3.4(-81)

Experimental and Calculated Resonance Frequencies and Threshold (in cm $^{-1}$)

	ω_{exp}	ω_{th}	$\omega_{\text{exp}} - \omega_{\text{th}}$
Threshold	10678	10672	6
4^1S	12331	12311	20
4^1D	12584	12578	6
5^1S	13693	13678	15
5^1D	13820	13813	7
6^1S	14419	14405	14
6^1D	14492	14483	9
7^1S	14851	14839	12
7^1D	14896	14888	8

^a The entry 3.1(-81) is an abbreviation for 3.1×10^{-81} , etc.

are listed in Tables 13 and 14. Quoted cross sections have been obtained using the theoretically calculated energies. Since the cross sections vary rapidly near the resonance peaks, in this region the predicted cross section for a given frequency must be found by translating the theoretical curve along the frequency axis in order to bring the theoretical and experimental

Table 14. He(2^3S): Three-Photon Generalized Ionization Cross Section $\sigma^{(3)}$ vs. Incident Frequency ω (from Aymar and Crance⁽⁹²⁾)^a

ω (cm $^{-1}$)	$\sigma^{(3)}$ (cm $^6 s^2$)	ω (cm $^{-1}$)	$\sigma^{(3)}$ (cm $^6 s^2$)
12815	1.1(-78)	17000	2.4(-79)
13000	4.6(-78)		
13100	8.1(-77)	17050	4.8(-79)
		17100	2.3(-80)
13200	8.8(-78)	17200	1.3(-81)
13500	1.5(-79)	17250	7.0(-82)
14000	4.7(-81)	17400	2.2(-81)
14200	2.6(-81)	17500	1.1(-80)
14500	4.2(-81)	17520	3.7(-80)
15000	1.5(-80)	17530	1.8(-79)
15150	7.6(-80)		
15200	1.5(-78)	17540	1.7(-78)
		17550	7.0(-80)
15220	1.7(-78)	17560	2.6(-80)
15250	2.1(-79)	17590	1.3(-80)
15400	3.1(-80)	17640	2.3(-80)
15600	6.4(-80)	17670	6.6(-80)
15700	2.0(-79)	17690	3.7(-79)
15750	9.3(-79)		
		17710	8.5(-79)
15800	7.5(-77)	17720	1.3(-79)
15900	7.5(-80)	17740	2.1(-80)
16000	1.1(-80)	17780	2.5(-81)
16100	2.7(-81)	17800	1.1(-81)
16250	1.0(-81)	17840	5.8(-82)
16400	1.8(-81)	17900	1.4(-81)
16600	5.6(-81)	17960	4.2(-81)
16700	2.8(-80)	17990	2.0(-80)
16725	1.5(-79)	17995	4.2(-80)
16750	5.0(-79)	18010	1.2(-79)
16775	4.2(-80)	18020	2.0(-80)
16850	1.6(-80)	18040	1.1(-80)
16950	4.7(-80)	18080	3.6(-80)
		18090	7.8(-80)

Table 14 (continued)

Experimental and Calculated Resonance Frequencies and Threshold (in cm^{-1})

	ω_{exp}	ω_{th}	$\omega_{\text{exp}} - \omega_{\text{th}}$
Threshold	12818	12814	4
3^3D	13123	13121	2
4^3S	15221	15207	14
4^3D	15794	15790	4
5^3S	16745	16735	10
5^3D	17030	17026	4
6^3S	17540	17532	8
6^3D	17702	17697	5
7^3S	18006	17999	7
7^3D	18107	18101	6

^a The entry $1.1(-78)$ is an abbreviation for 1.1×10^{-78} , etc.

resonance frequencies into coincidence. The differences between the experimental and theoretically calculated resonance energies are supplemented below each table.

The results of two-photon ionization cross sections (in the leading nonvanishing second-order perturbation theory) for the 2^1S state of He, calculated⁽⁵⁸⁾ by the pseudocontinuum basis method, are shown by the dots and curves in Figure 25. The lines (solid line denotes the length gauge and dashed line the velocity gauge) are obtained using only a single configuration approximation for the final continuum states. A single configuration approximation has been found to be remarkably sufficient to describe the final states at photon energies off the resonances and the antiresonance (interference minimum). The role played by electron correlation effects is discernible only when the resonances and the antiresonance are approached. We note that near the antiresonance the discrepancy between the "velocity-gauge" (square dot) and "length-gauge" (round dot) predictions is not completely negligible. Over the wide range of nonresonant frequencies, however, they are completely indistinguishable from one another in the scale of the figure. Figures 26 and 27 show the frequency dependence of two-photon ionization cross sections for Ne and Ar, respectively, calculated⁽⁹⁵⁾ within a version of the RPA approximation for the target wave functions and a set of pseudocontinuum final states. The calculated cross sections away from the resonances are noted to depend strongly on the gauge of the interaction form chosen; this is mainly attributed to the sensitivity of the matrix elements between the inter-

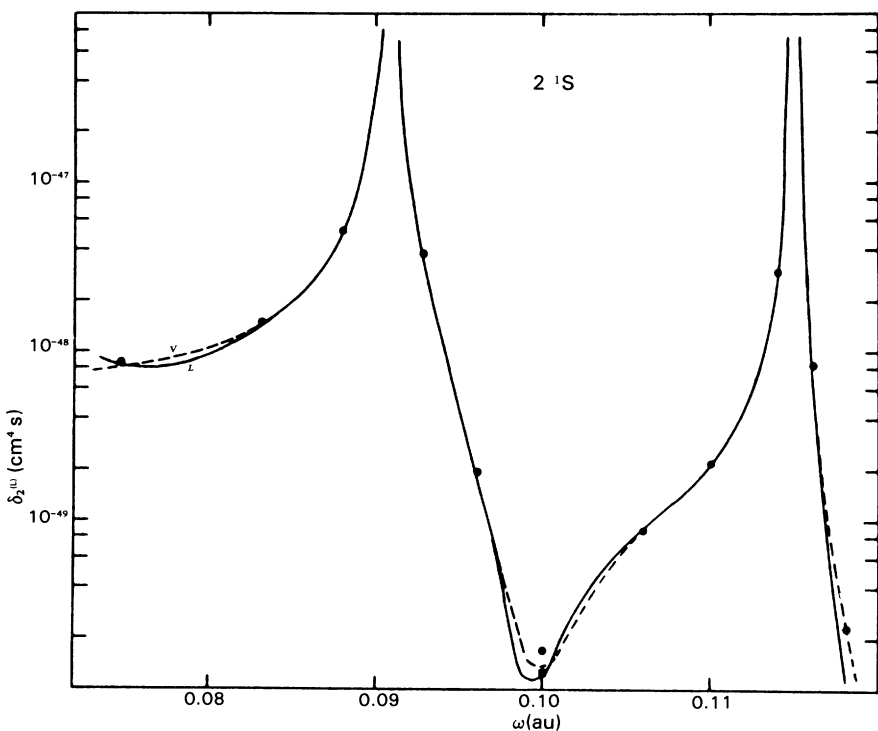


Figure 25. Two-photon ionization cross sections for He(1S) in a linearly polarized field calculated using a CI basis extended by a set of pseudocontinuum basis states. Round dots refer to length gauge and the square dot to the velocity gauge. Lines are a one configuration approximation for the final state, with the solid line referring to the length gauge, the dashed line to the velocity gauge (from Cacelli *et al.*⁽⁸⁸⁾).

mediate and final states. The two-photon (partial) ionization cross section for Ar has also been calculated⁽⁹³⁾ using many-body perturbation theoretical wave functions for Ar. In this calculation too, a significant dependence of the (partial) cross sections on the gauge of the interaction operator chosen is found. It should be observed that the many-body calculation⁽⁹³⁾ for Ar uses a set of HF wave functions in the intermediate sum thus neglecting electron-electron correlation in the intermediate states. In the RPA calculation,⁽⁹⁵⁾ on the other hand, the intermediate excited states contain combinations of one-electron states involving transitions $ns \rightarrow n's$ and $np \rightarrow n'd$. However, the above-mentioned many-body perturbation calculation treats the continuum states probably more comprehensively than the continuum matched square-integrable functions employed in RPA

calculations. These results clearly indicate that accurate measurements of the two (or more) photon ionization cross sections in noble gases could provide a very sensitive test of the models of wave functions of complex atoms (which may only be calculated approximately).

The importance of higher than the lowest nonvanishing-order terms of the perturbation series has been investigated in four-photon ionization of Cs atoms.⁽¹⁰¹⁾ In the case studied the $6S^{1/2}$ – $6F^{5/2,3/2}$ transition energies are dynamically Stark-shifted toward the intermediate three-photon energy (unperturbed position 79 cm^{-1} from the three-photon energy at $\lambda = 1056\text{ nm}$). This brings the four-photon ionization cross section at 1056 nm (in contrast with that given by the lowest-order amplitude only) with the error margin of the experimental data.⁽⁹⁷⁾

A very sensitive test of the accuracy of theoretical calculations is provided by the cross sections in the region of interference minima. These minima or transparency regions between resonances are common in multiphoton ionization cross sections and are due mainly to cancellation of dominant contributions of nearby intermediate atomic states. They are referred to as antiresonances.

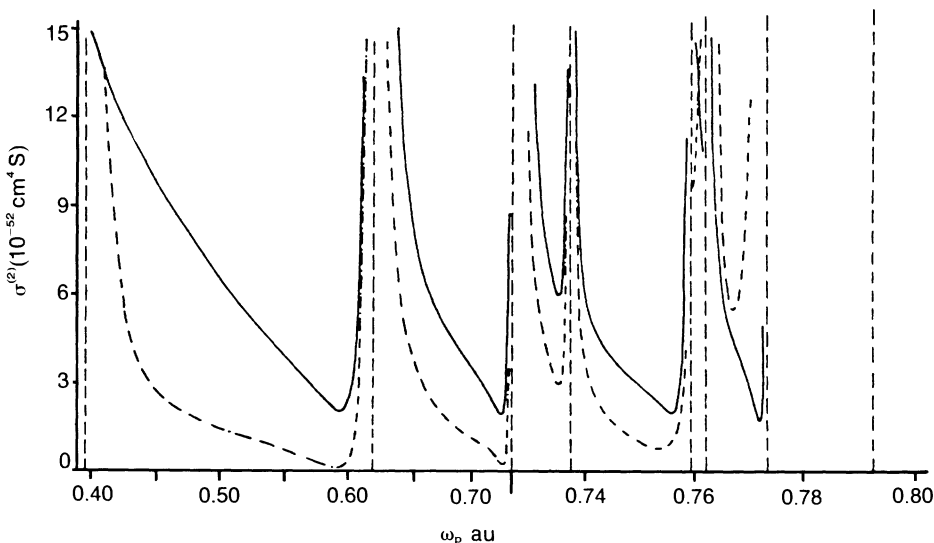


Figure 26. Generalized cross section of two-photon ionization of Ne calculated with RPA wave functions, shown as a function of photon energy (in au) for linear polarization. The solid line refers to the velocity gauge, the chain curve to the length gauge. Vertical dashed lines indicate unperturbed resonance energies and ionization threshold. Different energy scales have been used to enlarge the right-hand part of the figure (from Moccia *et al.*⁽⁹⁵⁾).

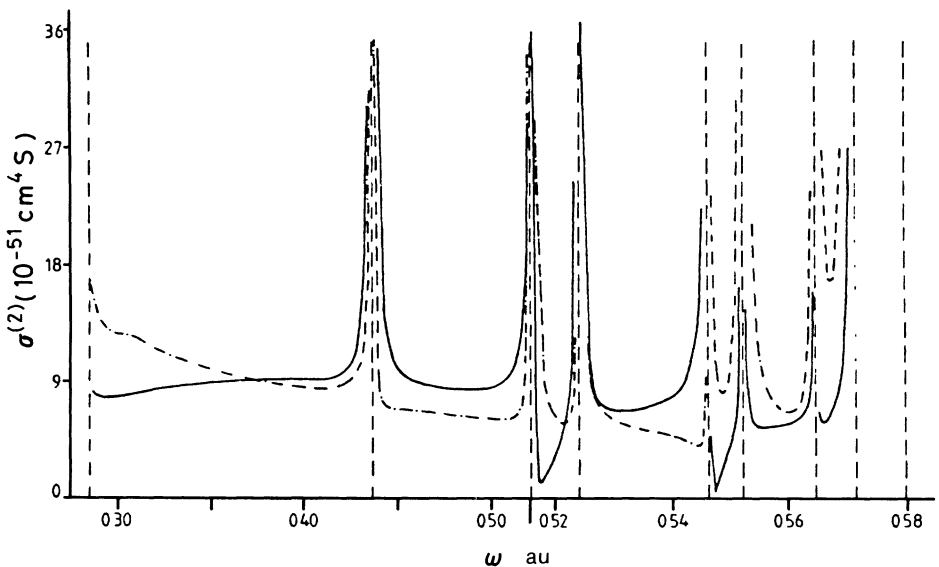


Figure 27. Generalized cross section of two-photon ionization of Ar calculated with RPA wave functions, shown as a function of photon energy (in au), for linear polarization. The solid curve refers to the velocity gauge, the chain curve to the length gauge. Vertical dashed lines indicate unperturbed resonance energies and ionization threshold. Different energy scales have been used to enlarge the right-hand part of the figure (from Moccia *et al.*⁽⁹⁵⁾).

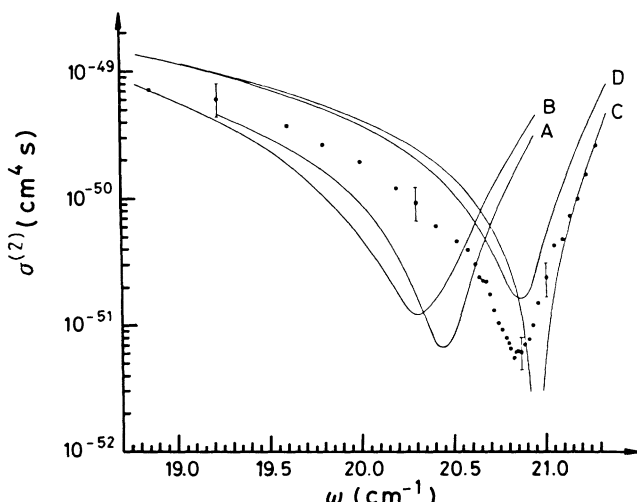


Figure 28. Two-photon ionization cross section of Cs near an antiresonance at about 20,800 cm^{-1} . Dots denote experimental data of Morellec *et al.*⁽¹⁰²⁾. Theoretical calculations are represented by curves A (from Lambropoulos and Teague⁽⁶⁰⁾), B (from Declercy *et al.*⁽¹⁰³⁾), C (from Teague *et al.*⁽¹⁰⁴⁾), and D (from Aymar and Crance⁽¹⁰⁵⁾).

Extreme care and ingenuity are necessary in measuring the cross sections at antiresonances, particularly for alkali atoms, as they are liable to be swamped by the larger contribution of even a trace amount of molecular species (dimers) present in the interaction volume. Theoretically, the cancellation of contributions from terms with opposite signs near the minimum frequency makes the result for the magnitude as well as the position of the antiresonant cross section very sensitive to the approximation used.

Two-photon ionization of Cs around the antiresonance near 20.800 cm⁻¹ has been studied both experimentally⁽¹⁰²⁾ and theoretically.^(60,103-105) Figure 28 compares the results.

Table 15. Calculated Generalized Cross Sections for Two-Photon Ionization of K, Na, and Li Atoms (from Mizuno⁽¹⁰⁷⁾)^a

ω (eV)	Potassium		Sodium		Lithium	
	$\sigma_L^{(2)}$	R_c	$\sigma_L^{(2)}$	R_c	$\sigma_L^{(2)}$	R_c
2.2	33.9	1.10	—	—	—	—
2.3	17.9	1.07	—	—	—	—
2.3456*	13.9	1.06	—	—	—	—
2.4	9.91	1.04	—	—	—	—
2.5	5.60	1.02	—	—	—	—
2.6	3.12	1.00	36.0	1.06	—	—
2.7	1.59	0.98	17.1	1.00	—	—
2.8	0.58	0.99	8.65	0.94	20.1	1.29
2.9	0.00848	1.46	4.54	0.87	15.8	1.28
3.0	4.01	0.80	2.43	0.79	12.7	1.28
3.1	35.8	0.82	1.30	0.70	10.5	1.27
3.2	4.73	0.82	0.673	0.59	9.04	1.27
3.3	2.15	0.82	0.314	0.46	8.05	1.26
3.4	1.18	0.82	0.109	0.27	7.44	1.26
3.5	0.518	0.84	0.0121	0.09	7.23	1.25
3.57152 [†]	0.0205	0.05	0.0362	1.20	7.42	1.24
3.6	41.13	0.65	0.0953	0.93	7.62	1.24
3.7	1.30	0.74	1.71	0.55	9.80	1.22
3.8	—	—	47.1	0.39	37.1	1.17
3.9	—	—	1.82	0.29	0.206	0.47
4.0	—	—	0.624	0.21	0.976	1.34
4.1	—	—	0.291	0.15	1.72	1.28
4.2	—	—	—	—	2.20	1.26
4.3	—	—	—	—	2.72	1.24

^a $\sigma_L^{(2)}$ (in 10^{-50} cm⁴s) refers to linearly polarized light. $R_c = \sigma_c^{(2)} / \sigma_L^{(2)}$ is the circular polarization efficiency.

[†] refers to the second harmonic of the ruby laser ($\lambda = 347.15$ nm) and * to the second harmonic of the Nd-glass laser ($\lambda = 529.5$ nm).

We note that the calculations for curves C and D use a sophisticated model potential, which includes the spin-orbit interaction and the effect of core polarization of the Cs atom. The calculations for curves A and C use truncated sums. The difference between the positions of minima in each pair of curves (A, B) or (C, D) may be interpreted as indicating that the effect of inclusion of the complete set of states (particularly the continuum) is to shift the minimum toward the lower frequency.

In spite of the existing difference in absolute magnitude between theory (D) and experimental data, the reproduction of the antiresonance frequency and the trend of the data over the entire region speak highly in favor of the accurate model-potential calculation pertaining to curve D.

Generalized cross sections $\sigma^{(2)}$ for two-photon ionization of the lighter alkali atoms, Li, Na, and K, have also been calculated using model potentials^(106,107) (without spin-orbit interaction) and the IDE method. Table 15 presents $\sigma_L^{(2)}$ with linear polarization and the ratio (sometimes called the “circular polarization efficiency”) $R_c = \sigma_c^{(2)} / \sigma_L^{(2)}$, where $\sigma_c^{(2)}$ is the cross section with circular polarization for these atoms.

Finally, we observe that in general, if the incident light is circularly polarized, then the electrons emitted during multiphoton ionization, in which the photon frequency is varied between a pair of fine-structure levels (e.g., of alkali atoms), can be highly spin-polarized.⁽⁶¹⁾ Figure 29 shows a

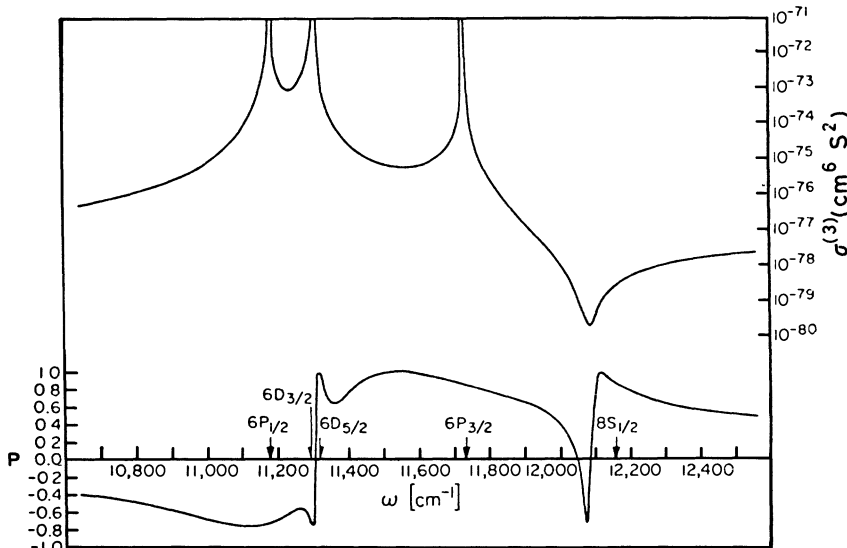


Figure 29. Photoelectron spin-polarization P and generalized cross section $\sigma^{(3)}$ for three-photon ionization of Cs with (right) circularly polarized light. The photon frequency range is around the $6S \rightarrow 6P$ transition. A two-photon resonance with the $6D$ state occurs for a photon frequency of about 11.300 cm^{-1} (from Teague and Lambropoulos⁽⁶¹⁾).

typical result of the frequency dependence of the polarization fraction

$$P = \frac{\sigma^{\parallel} - \sigma^{\perp}}{\sigma^{\parallel} + \sigma^{\perp}}$$

with obvious notation, for the three-photon ionization of Cs. The corresponding generalized three-photon ionization cross section $\sigma^{(3)}$ is also shown. These calculations were carried out⁽⁶¹⁾ using the truncated-summation method. The circularly polarized laser frequency is varied in the frequency range of the 6S–6P transition in Cs. It should be noted that there is a two-photon resonance with the 6D state at $\omega \approx 11,300 \text{ cm}^{-1}$.

The presence of two closely-lying fine-structure resonances (such as the 6D_{3/2} and 6D_{5/2} states in this example) can lead to additional structures⁽⁶¹⁾ in the electron spin-polarization. In general, there exists a frequency between the fine structures where P tends to 100%.

6

The Method of Resolvent Equations

6.1. Introduction

Generally speaking, the perturbation theory which forms the heart of theoretical methods for treating off-resonant phenomena cannot be applied directly in the case of resonant multiphoton processes. Modifications are called for to correctly and conveniently approach the problem of resonance breakdown of ordinary perturbation theory. This is most easily carried out by adopting⁽¹⁰⁸⁻¹¹²⁾ the powerful method of resolvent equations^(1,10,113,114) to the multiphoton transition problem. In this chapter a system of algebraic equations satisfied by the matrix elements of the resolvent for the semiclassical as well as for the number-state description of the multiphoton Hamiltonian is developed. Both monomode and multimode resolvent equations are constructed. A rather general model-Hamiltonian for multiphoton processes is introduced, and the resulting resolvent equations are solved explicitly for the four kinds of multiphoton transition of physical interest. Probability distributions of occupation of the above-threshold continuum states by multiphoton absorption from a bound state are also given.

6.2. Breakdown of Perturbation Theory at Resonance

A multiphoton process is said to be resonant whenever an intermediate state of the target spectrum is closely reached from the initial state by absorption (or emission) of an integral number of photons. Figure 30 shows schematically a three-photon ionization process via two intermediate resonances.

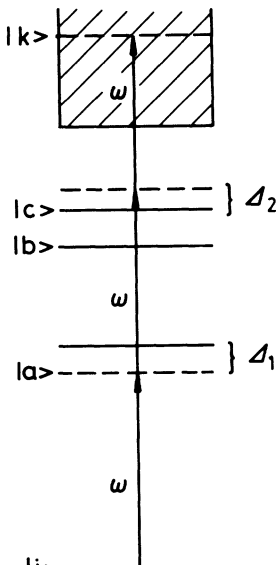


Figure 30. Schematic diagram of a resonant-ionization process via two intermediate (near-) resonances.

The first resonance in Figure 30 is seen to occur with respect to the state $|a\rangle$ with a small detuning Δ_1 , due to absorption of one photon from the initial ground state $|i\rangle$, and the second resonance with a detuning Δ_2 with respect to the state $|c\rangle$, due to absorption of two photons from the ground state. The detunings are defined by

$$\hbar\Delta_1 = (\varepsilon_a - \varepsilon_i) - \hbar\omega \quad \text{and} \quad \hbar\Delta_2 = (\varepsilon_c - \varepsilon_i) - 2\hbar\omega$$

where ε_i , ε_a , and ε_c are the energies of the initial and of the near-resonant intermediate states, respectively. They should be very small compared to the atomic transition energies involved, or identically zero, for the process to be significantly described as resonant. If the resonances are to be isolated, then the detunings should also be small compared to typical separations among the neighboring levels (primarily of the same parity) in the spectral region of interest.

Let us consider the lowest-order two-photon transition amplitude

$$T_{i \rightarrow f}^{(2)} = \sum_j \frac{\langle f | \frac{\mathbf{E}}{2} \cdot \mathbf{D} | j \rangle \langle j | \frac{\mathbf{E}}{2} \cdot \mathbf{D} | i \rangle}{(\omega_i - \omega_j + \omega)} \quad (6.2.1)$$

The denominator $\omega_i - \omega_j + \omega = \Delta$ is just the one photon detuning with respect to the intermediate state $|j\rangle$.

For a resonant (or near-resonant) process with some small Δ , (which need not be zero) the transition amplitude (6.2.1) can be exceedingly large, so much so that the corresponding probability of transition $|i\rangle \rightarrow |f\rangle$ will exceed unity, signaling a breakdown of the (unmodified) perturbation theory. Physically, of course, no such violation of unitarity occurs and the perturbation theory requires general modification. We note that if the lowest-order amplitude breaks down at a resonance, then all higher-order amplitudes contributing to the process of interest will also break down individually. In fact, in the vicinity of a resonance, renormalization of the unperturbed states of the atom becomes significant (particularly due to its interaction with the external field). The resulting field-dependent shift and broadening of the resonant levels prevent the resonance breakdown of the theory. There are varieties of ways in which perturbation theory may be modified to account for the shift and broadening of multiphoton resonances. The selection of an approach is usually guided by the particular features of the problem at hand and the methods are often equivalent in substance. One of the most powerful and systematic methods of treating resonant multiphoton processes is that of resolvent equations.

This method is generally applicable to systems described by stationary Hamiltonians and is thus usually employed for multiphoton problems in connection with the quantum treatment of the field, since, in the Schrödinger representation, the total Hamiltonian of atom + quantum field is stationary. We shall show that there is in fact no difficulty in making this method available to the semiclassical treatment of the field, which is time periodic in nature. Indeed, it will be seen below that both the quantum and semiclassical treatments are virtually equivalent; they give the same result with high accuracy except perhaps when the effects of spontaneous emission must be treated *ab initio* and hence using the quantum field.

6.3. Resolvent Equations: Monomode Semiclassical Field

We may start with the Schrödinger equation of an atom in the presence of a single-mode semiclassical field [$\mathbf{E}(t) = \epsilon F_0 \cos(\omega t + \delta)$]

$$i\hbar \frac{\partial}{\partial t} \psi(t) = [H_a + H_i(t)]\psi(t) \quad (6.3.1)$$

where the atom-field interaction is given by

$$H_i(t) = V[e^{i(\omega t + \delta)} + e^{-i(\omega t + \delta)}] \quad (6.3.2)$$

with $V = F_0 \mathbf{e} \cdot \mathbf{D}/2$, F_0 denoting the peak-field strength, \mathbf{e} the unit polarization vector, and \mathbf{D} the dipole operator; H_a is the atomic Hamiltonian with $H_a \phi_i = \varepsilon_i \phi_i$.

Generally speaking, we are interested in solutions of Eq. (6.3.1) satisfying given initial conditions. These solutions are usually obtained rather indirectly: first by finding the general solution $\psi(t)$ and then imposing the initial condition on the general solution to arrive at the particular solutions of interest. It is therefore interesting and useful to generate the particular solution of interest directly by incorporating the initial condition in the Schrödinger equation (6.3.1) (and retaining its differential form!).

For most purposes we are interested in the initial condition given by

$$\psi(t) = \begin{cases} 0, & t < 0 \\ \psi(0), & t = +0 \end{cases} \quad (6.3.3)$$

Condition (6.3.3) defines all retarded solutions that start at a finite time $t = 0$ with value $\psi(0)$ and evolve toward the future, $t > 0$. It is most convenient to incorporate condition (6.3.3) by adding an inhomogeneous term, $i\hbar\delta(t)\psi(0)$, to Eq. (6.3.1). This gives the Heitler–Ma version^(1,115) of the Schrödinger equation:

$$i\hbar \frac{\partial}{\partial t} \psi(t) = [H_a + H_i(t)]\psi(t) + i\hbar\delta(t)\psi(t) \quad (6.3.4)$$

We note parenthetically [by integration of Eq. (6.3.4) in the vicinity of $t \approx 0$] that the jump implied by condition (6.3.3) at $t = +0$ is fully accounted for in Eq. (6.3.4). Let us reduce Eq. (6.3.4), without approximation, to a completely stationary system. For this purpose we develop $\psi(t)$ in a generalized Fourier “integral + series” expansion of the form

$$\psi(t) = -\frac{1}{2\pi i} \sum_{n=-\infty}^{\infty} \int_{-\infty}^{\infty} dE G_{n|0}(E) \psi(0) e^{-i(E-n\hbar\omega)t/\hbar + in\delta} \quad (6.3.5)$$

where $G_{n|0}(E)$ are time-independent quantities. The second suffix “0” of $G_{n|0}(E)$ is introduced to remind us of the initial condition $\psi(0)$, at $t = 0$. The delta function in Eq. (6.3.4) can be rewritten similarly as

$$i\hbar\delta(t) = -\frac{1}{2\pi i} \sum_{n=-\infty}^{\infty} \int_{-\infty}^{\infty} dE \delta_{n|0} e^{-i(E-n\hbar\omega)t/\hbar + in\delta} \quad (6.3.6)$$

Substitution of Eqs. (6.3.6) and (6.3.5) in Eq. (6.3.4) easily gives

$$\begin{aligned}
& \sum_{n=-\infty}^{\infty} \int_{-\infty}^{\infty} dE [E - H_a - n\hbar\omega] G_{n|0}(E) e^{-i(E-n\hbar\omega)t/\hbar + in\delta} \\
&= \sum_{n=-\infty}^{\infty} \int_{-\infty}^{\infty} dE V G_{n|0}(E) [e^{-i[E-(n+1)\hbar\omega]t/\hbar + i(n+1)\delta} + e^{-i[E-(n-1)\hbar\omega]t/\hbar + i(n-1)\delta}] \\
&\quad + \sum_{n=-\infty}^{\infty} \delta_{n|0} e^{-i(E-n\hbar\omega)t/\hbar + in\delta} \tag{6.3.7}
\end{aligned}$$

In order that Eq. (6.3.4) should be satisfied by Eq. (6.3.5) for all t , it is sufficient that the coefficients of $e^{-i(E-n\hbar\omega)t/\hbar}$, $n = 0, \pm 1, \pm 2, \pm 3, \dots$, remain equal on both sides of relation (6.3.7). Thus we obtain

$$[E - H_a - n\hbar\omega] G_{n|0}(E) = V[G_{n-1|0}(E) + G_{n+1|0}(E)] + \delta_{n|0} \tag{6.3.8}$$

The necessity of Eq. (6.3.8) is established by the fact that the unique solution of Eq. (6.3.4) follows from Eq. (6.3.8).

For the sake of brevity let us introduce “index shifters” S_n^{\pm} by the simple definitions

$$S_n^{\pm} G_{n|0} = G_{n\pm 1|0} \tag{6.3.9}$$

In other words, S_n^{\pm} merely shifts the suffix n of $G_{n|0}$ by ± 1 , respectively. Using relation (6.3.9), Eq. (6.3.8) may be written as

$$[E - H_n] G_{n|0}(E) = \delta_{n|0} \tag{6.3.10}$$

where

$$H_n = H_a + n\hbar\omega + V(S_n^+ + S_n^-), \quad n = 0, \pm 1, \pm 2, \dots, \pm \infty \tag{6.3.11}$$

We note that the stationary operator H_n depends only on the atomic variables. The only trace of the time dependence of the field is now to be found in the subscript n . It is possible also to interpret n as the change in photon occupation number, as well shall find subsequently.

The matrix representation of H_n , in which form the equivalence of the time-dependent and stationary formulations were first demonstrated clearly,⁽¹¹⁶⁾ can be expressed conveniently in the form

$$\sum_{jj'} |j\rangle [H_n]_{jj'} \langle j'| = \sum_{jj'} |j\rangle [(\epsilon_j + n\hbar\omega)\delta_{jj'} + V_{jj'}(S_n^+ + S_n^-)] \langle j'| \tag{6.3.12}$$

where $|j\rangle$ is the complete set of eigenfunctions of H_a . We shall often use the term multiphoton “Floquet Hamiltonian” interchangeably to mean either the operator form (6.3.11) or the matrix form (6.3.12).

The essential equivalence of the semiclassical resolvent equations (6.3.10) developed here with the resolvent equations of the quantum Hamiltonian is considered in the next section.

6.4. Resolvent Equations: Monomode Quantum Field

The Schrödinger equation for the combined “atom + field” system (including the initial condition) is

$$\begin{aligned} i\hbar \frac{\partial}{\partial t} |\psi(t)\rangle &= \left[H_a + \hbar\omega a^+ a + \epsilon \cdot \mathbf{D}(a^+ + a) \left(\frac{2\pi\hbar\omega}{L^3} \right)^{1/2} \right] |\psi(t)\rangle \\ &+ i\hbar\delta(t) |\psi(t)\rangle \end{aligned} \quad (6.4.1)$$

where $|\psi(0)\rangle = |n_0\rangle\phi_i$ is the initial state at $t=0$, with the field in the number state $|n_0\rangle$ and the atom in the state ϕ_i . Let us expand $|\psi(t)\rangle$ in terms of the complete set of number states $|n+n_0\rangle$ as

$$|\psi(t)\rangle = \sum_n \psi_{n|n_0,i}(t) |n+n_0\rangle \quad (6.4.2)$$

where n is obviously the change in the field occupation number from its initial value n_0 , and the suffix n_0, i on $\psi_{n|n_0,i}(t)$ is supplied to remind us of the initial condition. We substitute expression (6.4.2) in Eq. (6.4.1) and project onto $\langle n' + n_0 |$ to find

$$\begin{aligned} i\hbar \frac{\partial}{\partial t} \psi_{n|n_0,i}(t) &= [H_a + (n + n_0)\hbar\omega] \psi_n(t) + \frac{\epsilon \cdot \mathbf{D}}{2} [F_{n+1}\psi_{n+1}(t) + F_n\psi_{n-1}(t)] \\ &+ i\hbar\delta(t)\delta_{n|n_0}\phi_i \end{aligned} \quad (6.4.3)$$

where we have defined

$$\frac{F_n}{2} \equiv \left(\frac{2\pi\hbar\omega(n+n_0)}{L^3} \right)^{1/2} \quad (6.4.4)$$

We have also used the relations $a^+ |n\rangle = (n+1)^{1/2} |n+1\rangle$ and $a |n\rangle = n^{1/2} |n-1\rangle$ (and interchanged the indices, $n \leftrightarrow n'$, at the end).

We may further expand $\psi_{n|n_0,i}(t)$ as a Fourier integral

$$\psi_{n|n_0,i}(t) = -\frac{1}{2\pi i} \int_{-\infty}^{\infty} dE e^{-iEt/\hbar} G_{n|n_0}(E) \phi_i \quad (6.4.5)$$

and use the identity

$$i\hbar\delta(t) = -\frac{1}{2\pi i} \int_{-\infty}^{\infty} dE e^{-iEt/\hbar} \quad (6.4.6)$$

When expressions (6.4.5) and (6.4.6) are substituted in Eq. (6.4.3), we find as before that $G_{n|n_0}(E)$ must satisfy the equations

$$[E - H_a - (n + n_0)\hbar\omega]G_{n|n_0}(E) = \frac{\epsilon \cdot \mathbf{D}}{2} [F_{n+1}G_{n+1|n_0}(E) + F_nG_{n-1|n}(E)] + \delta_{n|n_0} \quad (6.4.7)$$

Equations (6.4.7) are the exact quantum resolvent equations and are shown below to be essentially equivalent to the semiclassical equations (6.3.11) derived earlier.

Virtually for all external fields (such as laser fields) the initial occupation number $n_0 \gg |n|$, where n is the change in the field occupation number due to interaction with the atomic system. The factors F_n in Eq. (6.4.7) may therefore be readily approximated by

$$F_n \approx F_{n+1} \approx F_0 = \left(\frac{8\pi\hbar\omega n_0}{L^3} \right)^{1/2}, \quad \frac{n_0}{L^3} \gg \frac{n}{L^3} \quad (6.4.8)$$

to within an accuracy of $1:n/n_0$.

In approximation (6.4.8) we may identify F_0 with the classical peak field strength (since $F_0^2/8\pi$ equals the initial energy density $n_0\hbar\omega/L^3$ of the photon field). As an example of the accuracy of relation (6.4.8), we note that even for a moderate laser intensity of 1 W/cm^2 (say at optical frequencies) the initial number density n_0/L^3 is about $10^7/\text{cm}^3$, while the significant number of photons exchanged $|n|$ ($n < 0$ absorption, $n > 0$ emission) at this density would hardly exceed several tens or hundreds, if at all. Approximation (6.4.8) is sometimes referred to as the “laser approximation.” We note also that with increasing field strength (for a fixed frequency) relation (6.4.8) becomes more accurate and the quantum field tends to behave more like a classical one. This tendency of a radiation field at high quantum density to behave like a classical time-dependent field has been noted since the beginning of quantum mechanics.⁽¹¹⁷⁾

We note that only the relative change in the eigenvalues of the field Hamiltonian, $H_{\text{rad}} = \hbar\omega a^\dagger a$, appears in any transition amplitude. We may therefore always simplify the notation by counting all photon energies with reference to the initial occupation number of the field (i.e., one might think of the initial state of the field as the new “ground state” or the new “vacuum”); this may be easily done by formally setting $n_0 = 0$ in Eq. (6.4.7). With this convention in mind and using the “laser approximation,”

namely Eq. (6.4.8), one can rewrite relation (6.4.7) in the form

$$[E - H_n]G_{n|0}(E) = \delta_{n|0} \quad (6.4.9)$$

where H_n is identical with the Floquet Hamiltonian defined by Eq. (6.3.11).

Equation (6.4.9) can in fact be obtained, in the “laser approximation,” directly from the quantum resolvent operator G defined by

$$G(E) = \frac{1}{E - H} \quad (6.4.10)$$

where H is the Hamiltonian of the total atom + field system defined by the square brackets on the right-hand side of Eq. (6.4.1). If expression (6.4.10) is rewritten as $(E - H)G = 1$ and the matrix elements taken between $\langle n |$ and $| 0 \rangle$, then, with the aid of approximation (6.4.8), one immediately finds that

$$(E - H_n)\langle n | G | 0 \rangle = \delta_{n|0} \quad (6.4.11)$$

where H_n has the same significance as before. The identity of Eq. (6.4.11) or (6.4.9) in the “laser approximation” with relation (6.3.10) shows that

$$G_{n|0}(E) = \langle n | G | 0 \rangle$$

i.e., the semiclassical resolvents $G_{n|0}(E)$ defined by Eq. (6.3.5) are just the matrix elements between the number states $| n \rangle$ and $| 0 \rangle$ of the quantum resolvent operator (6.4.10), in the “laser approximation” Eq. (6.4.8).

6.5. Semiclassical Resolvent and Floquet Hamiltonian: Multimode Field

The method of Section 6.3 can be easily generalized to obtain stationary resolvent equations and Floquet Hamiltonians in the case of a multimode semiclassical field.

Let a p -mode field be defined by

$$\mathbf{F}(t) = \sum_{i=1}^p F_i \boldsymbol{\epsilon}_i \cdot \mathbf{D} \cos(\omega_i t + \delta_i) \quad (6.5.1)$$

where $\boldsymbol{\epsilon}_i$, ω_i , and δ_i refer to the i th mode. The total wave function $\psi(t)$ of the Schrödinger equation

$$i\hbar \frac{\partial}{\partial t} \psi(t) = [H_a + \mathbf{F}(t) \cdot \mathbf{D}] \psi(t) \quad (6.5.2)$$

may now be expanded as Fourier “integral + series” of the form

$$\psi(t) = -\frac{1}{2\pi i} \sum_{n_1, n_2, \dots, n_p=-\infty}^{\infty} \int_{-\infty}^{\infty} dE \exp[-iEt/\hbar + i(n_1\omega_1 + n_2\omega_2 + \dots + n_p\omega_p)t] \\ \times \exp[i(n_1\delta_1 + n_2\delta_2 + \dots + n_p\delta_p)] G_{n_1, n_2, \dots, n_p|0}(E) \psi(0) \quad (6.5.3)$$

with initial condition (6.3.3) accounted for by $\psi(0)$. Substitution of expression (6.5.3) in Eq. (6.5.2) and comparison of the coefficients of $\exp\{-iEt/\hbar + i(n_1\omega_1 + n_2\omega_2 + \dots + n_p\omega_p)t\}$ on both sides of the resulting equation immediately yields the following stationary resolvent equation:

$$[E - H_{n_1, n_2, \dots, n_p}] G_{n_1, n_2, \dots, n_p|0}(E) = \delta_{n_1, 0} \delta_{n_2, 0} \cdots \delta_{n_p, 0} \quad (6.5.4)$$

with the multimode Floquet Hamiltonian

$$H_{n_1, n_2, \dots, n_p} = \left[H_a + \sum_{i=1}^p n_i \hbar \omega_i + \sum_{i=1}^p V_i (S_{n_i}^+ + S_{n_i}^-) \right] \quad (6.5.5)$$

The index shifters $S_{n_i}^\pm$ are defined exactly as in Section 6.3 for the i th mode. Thus

$$S_{n_i}^\pm G_{n_1, n_2, \dots, n_p|0}(E) \equiv G_{n_1, n_2, \dots, n_i \pm 1, \dots, n_p|0}(E) \quad (6.5.6)$$

and

$$V_i = F_i \frac{\boldsymbol{\epsilon}_i \cdot \mathbf{D}}{2}, \quad i = 1, 2, \dots, p \quad (6.5.7)$$

6.6. Resolvent Equations: Multimode Quantum Field

It is virtually certain that in the number-state representation one obtains an analogous set of resolvent equations as in the semiclassical case. Let us briefly derive the resolvent equations with a multimode quantum field and compare them with Eq. (6.5.4). The total Hamiltonian in this case can be written as

$$H = \left[H_a + \sum_{i=1}^p \hbar \omega_i a_i^+ a_i + \sum_{i=1}^p \left(\frac{2\pi\hbar\omega_i}{L^3} \right)^{1/2} \boldsymbol{\epsilon}_i \cdot \mathbf{D} (a_i^+ + a_i) \right] \quad (6.6.1)$$

By taking the matrix elements of the resolvent equation

$$(E - H) G = 1 \quad (6.6.2)$$

between any state

$$\langle n_1 + n_0^1, n_2 + n_0^2, \dots, n_i + n_0^i, \dots, n_p + n_0^p |$$

and the initial state

$$|n_0^1, n_0^2, \dots, n_0^i, \dots, n_0^p\rangle$$

where n_0^i is the initial occupation number in the i th mode, one immediately finds that

$$\begin{aligned} & \left[E - H_a - \sum_{i=1}^p \hbar\omega_i (n_i + n_0^i) \right] \\ & \times \langle n_1 + n_0^1, \dots, n_i + n_0^i, \dots, n_p + n_0^p | G | n_0^1, \dots, n_0^i, \dots, n_0^p \rangle \\ & + \frac{1}{2} \mathbf{\epsilon}_i \cdot \mathbf{D} [F_{n+1} \langle n_1 + n_0^1, \dots, n_i + 1 + n_0^i, \dots, n_p + n_0^p | G | n_0^1, \dots, n_0^i, \dots, n_0^p \rangle \\ & + F_n \langle n_1 + n_0^1, \dots, n_i - 1 + n_0^i, \dots, n_p + n_0^p | G | n_0^1, \dots, n_0^i, \dots, n_0^p \rangle] n \\ & = \delta_{n_1,0} \delta_{n_2,0} \cdots \delta_{n_i,0} \cdots \delta_{n_p,0} \end{aligned} \quad (6.6.3)$$

where

$$F_{n_i} = \left[\frac{(8\pi\hbar\omega)(n_i + n_0^i)}{L^3} \right]^{1/2} \quad (6.6.4)$$

If, as before, the “laser approximation” is used for each mode, we may replace F_{n_i} by the classical peak field strength

$$F_i = \left(\frac{8\pi\hbar\omega_i}{L^3} n_0^i \right)^{1/2} \quad (6.6.5)$$

and, adopting as before the convention of referring all photon occupation numbers to the initial state, we may replace the matrix elements

$$\langle n_1 + n_0^1, n_2 + n_0^2, \dots, n_i + n_0^i, \dots, n_p + n_0^p | G | n_0^1, n_0^2, \dots, n_0^i, \dots, n_0^p \rangle$$

by

$$\langle n_1, \dots, n_i, \dots, n_p | G | 0, \dots, 0, \dots, 0 \rangle \equiv G_{n_1, \dots, n_i, \dots, n_p | 0}(E) \quad (6.6.6)$$

Use of relations (6.6.5) and (6.6.6) reduces Eqs. (6.6.3) at once to the semiclassical equations (6.5.4), as expected.

6.7. Correspondence between the Time-Dependent Wave Functions

It is noteworthy that the above quantum treatment gives rise to the time-dependent state function [see Eqs. (6.4.2)–(6.4.5)]

$$|\psi(t)\rangle = -\frac{1}{2\pi i} \sum_n \int_{-\infty}^{\infty} dE e^{-iEt/\hbar} |n\rangle G_{n|0}(E) \phi_i \quad (6.7.1)$$

This apparently differs from the time-dependent wave function obtained in the semiclassical treatment, namely Eq. (6.3.5), in spite of the essential equivalence between the respective resolvents, $G_{n|0}(E)$.

To complete the correspondence, we therefore observe that the above difference is only one of “pictures.” Remembering that the quantum $|\psi(t)\rangle$ has been obtained in the stationary Schrödinger picture, we transform $|\psi(t)\rangle$ in an “intermediate picture” in which the unperturbed radiation Hamiltonian $\hbar\omega a^+a$ is eliminated by the transformation

$$|\psi(t)\rangle \Rightarrow e^{-ia^+a\omega t} |\psi_I(t)\rangle \quad (6.7.2)$$

On applying relation (6.7.2) to Eq. (6.4.1) we obtain

$$i\hbar \frac{\partial}{\partial t} |\psi_I(t)\rangle = \left\{ H_a + \left(\frac{2\pi\hbar\omega}{L^3} \right)^{1/2} \boldsymbol{\epsilon} \cdot \mathbf{D} [e^{ia^+a\omega t} (a^+ + a) e^{-ia^+a\omega t}] \right\} |\psi_I(t)\rangle \quad (6.7.3)$$

We note that

$$e^{ia^+a\omega t} a^+ = a^+ e^{iaa^+\omega t} \quad \text{and} \quad a e^{-ia^+a\omega t} = e^{-iaa^+\omega t} a$$

and the commutator $[a, a^+] = 1$. Hence Eq. (6.7.3) can be immediately simplified to read

$$i\hbar \frac{\partial}{\partial t} |\psi_I(t)\rangle = \left\{ H_a + \left(\frac{2\pi\hbar\omega}{L^3} \right)^{1/2} \boldsymbol{\epsilon} \cdot \mathbf{D} [a^+ e^{i\omega t} + e^{-i\omega t} a] \right\} |\psi_I(t)\rangle \quad (6.7.4)$$

The corresponding state function from (6.7.1) and (6.7.2) is

$$|\psi_I(t)\rangle = -\frac{1}{2\pi i} \sum_n \int_{-\infty}^{\infty} dE e^{-iEt/\hbar + in\omega t} |n\rangle G_{n|0}(E) \phi_i \quad (6.7.5)$$

The “intermediate picture” quantum Schrödinger equation (6.7.4) and the state function (6.7.5) therefore correspond directly to the semiclassical equation (6.3.1) and the wave function (6.3.5), respectively.

Furthermore, we note that the amplitude of the occurrence of the number state $|n\rangle$ in the wave function (6.7.5) corresponds to the coefficient of the phasor, $e^{in\delta}$, in the semiclassical solution (6.3.5). Thus the inner product between the number states corresponds to the normalized phase integral over δ :

$$\langle m | n \rangle \leftrightarrow \frac{1}{2\pi} \int_0^{2\pi} d\delta e^{-i(m-n)\delta} \quad (6.7.6)$$

Equation (6.7.6) is, in fact, in agreement with the explicit “phase representation”⁽¹¹⁸⁾ of the quantum field, in the “laser approximation.”

The m -photon transition amplitude as a function of the interaction time may be obtained semiclassically from Eq. (6.3.5) through the prescription

$$A_{i \rightarrow f}^{(m)}(t) = \frac{1}{2\pi} \int_0^{2\pi} d\delta e^{-im\delta} \langle \phi_f | \psi_\delta^i(t) \rangle \quad (6.7.7)$$

$$= -\frac{1}{2\pi i} \int_{-\infty}^{\infty} dE \langle \phi_f | G_{m|0}(E) | \phi_i \rangle e^{-iEt/\hbar + im\omega t} \quad (6.7.8)$$

where we have explicitly indicated the initial index i and the phase dependence of the wave function $\psi(t)$.

The quantum m -photon transition amplitude in the interaction representation is also given by the same expression (6.7.8), since it follows from the definition:

$$A_{i \rightarrow f}^{(m)}(t) = \langle m | \langle \phi_f | \psi_i(t) \rangle \rangle \quad (6.7.9)$$

where $\psi_i(t)$ is given by the wave function (6.7.5). The problem of determining the time dependence of multiphoton transitions, either in the semiclassical or in the number-state representation, is thus reduced to the problem of determining the resolvent matrix elements $G_{m|0}(E)$, which appear in the transition amplitudes (6.7.8). In the next section we consider an explicit case.

6.8. A Model Hamiltonian and Explicit Solutions of the System of Resolvent Equations

In this section we introduce a model Hamiltonian that may be used to study various kinds of multiphoton process, including above-threshold processes in the continuum. We evaluate the four classes of matrix elements of physical interest of the corresponding resolvent operator, exactly. We assume a space spanned by an arbitrary but finite number of discrete states $|B\rangle$ with energy E_B and a finite set of continuum states $|E_F, F\rangle$ with energy E_F . The discrete set of quantum numbers uniquely specifies the states $|B\rangle$ and $|E_F, F\rangle$, respectively. For example, we may have states of the form

$$|B\rangle = \phi_b |n\rangle \quad \text{and} \quad |F\rangle \equiv |E_F, F\rangle = \phi_f(\varepsilon_F) |n\rangle \quad (6.8.1)$$

Here, ϕ_b is a bound atomic wave function (say of an electron in a central field) with energy ε_{jl} , so that $b = (j, l, m)$ where j is the principal and l and m are the angular-momentum quantum numbers, respectively; $|n\rangle$ stands for a (discrete) photon number state. Hence, in this case

$$(b, n) = (j, l, m, n) \quad \text{and} \quad E_B = \varepsilon_{jl} + n\hbar\omega \quad (6.8.2)$$

Similarly, $\phi_f(\varepsilon_l)$ may be a partial-wave continuum wave function with angular momentum l and energy ε_l . Hence

$$(f, m) = (\varepsilon_l, l, m, n) \quad \text{and} \quad E_F = \varepsilon_{fl} + n\hbar\omega \quad (6.8.3)$$

6.8.1. Definition and Origin of the Model Hamiltonian

We define our model Hamiltonian as follows:

$$H \equiv H_0 + V \quad (6.8.1.1)$$

where

$$\langle B' | H | B \rangle = E_B \delta_{B'B} + V_{B'B} \quad (\text{bound-bound}) \quad (6.8.1.2)$$

$$\langle F | H | B \rangle = V_{FB}(E_F) \quad (\text{bound-free}) \quad (6.8.1.3)$$

$$\langle B | H | F \rangle = V_{BF}(E_F) \quad (\text{free-bound}) \quad (6.8.1.4)$$

$$\langle F' | E - H | F \rangle = (E - E_F)(\delta_{F'F} + i\pi V_{F'F}(E_{F'}, E_F))\delta(E_{F'} - E_F) \quad (\text{free-free}) \quad (6.8.1.5)$$

with

$$H_0 | B \rangle = E_B | B \rangle \quad \text{and} \quad H_0 | E_F, F \rangle = E_F | E_F, F \rangle \quad (6.8.1.6)$$

and the normalizations

$$\langle B' | B \rangle = \delta_{BB'} \quad \text{and} \quad \langle E_{F'}, F' | E_F, F \rangle = \delta(E_{F'} - E_F)\delta_{F'F} \quad (6.8.1.7)$$

and

$$B = 1, 2, \dots, B_{\max} \quad \text{and} \quad F = 1, 2, \dots, F_{\max}$$

where the matrix elements of the interaction Hamiltonian are denoted by

$$V_{CD} \equiv \langle C | V | D \rangle \quad (6.8.1.8)$$

We note that the free-free matrix elements (6.8.1.5) are modeled by the

so-called “optical potentials” restricted onto the energy shell. We observe that in the special case in which the continuum–continuum coupling matrix elements $V_{FF'}$ in Eq. (6.8.1.5) are altogether omitted, our model Hamiltonian reduces formally to a Friedrichs–Fano-type Hamiltonian.^(119,120)

The origin of the free–free matrix elements of the model Hamiltonian may be understood as follows. In the continuum space we may expand the wave function $|\psi_c\rangle$ satisfying

$$(E - H_c)|\psi_c\rangle = 0 \quad (6.8.1.9)$$

where $H_c = H_0^c + V_c$ is the continuum projected part of the total Hamiltonian describing the free–free transitions, as

$$|\psi_c\rangle = \sum_{F'} \int dE_{F'} c_{F'} |E_{F'}\rangle \quad (6.8.1.10)$$

where $|E_{F'}\rangle$ are the continuum eigenfunctions of H_0 with energy $E_{F'}$. By substituting expression (6.8.1.10) in relation (6.8.1.9) and projecting onto $\langle E_F|$, one gets

$$(E - E_F)c_F = \sum_{F''} \int dE_{F''} V_{FF''} c_{F''} \quad (6.8.1.11)$$

Similarly,

$$(E - E_{F''})c_{F''} = \sum_{F'} \int dE_{F'} V_{F''F'} c_{F'} \quad (6.8.1.12)$$

We eliminate $c_{F''}$ from Eq. (6.8.1.11) by substituting from Eq. (6.8.1.12); this yields

$$(E - E_F)c_F = \sum_{F'} \int dE_{F'} M_{FF'} c_{F'} \quad (6.8.1.13)$$

where the matrix elements are given by

$$M_{FF'} \equiv \sum_{F''} \int dE_{F''} V_{FF''} \frac{1}{E - E_{F''} + i0} V_{F''F'} \quad (6.8.1.14)$$

We now approximate the exact matrix element (6.8.1.14) by an estimate in the vicinity of the energy shell (energy-conserving points in the multiphoton continua):

$$E = E_F = E_{F'} \quad (6.8.1.15)$$

By neglecting the shift due to the principal value of (6.8.1.14) on the energy shell we have

$$\begin{aligned} M_{FF'} &\approx -i\pi \sum_{F''} \int dE_{F''} V_{FF''} \delta(E - E_{F''}) V_{F''F'} \\ &= -i\pi \langle E_F | V_c \delta(E - H_0^c) V_c | E_{F'} \rangle \\ &= -i\pi \langle E_F | V_c \delta(E - H_0^c)(H_c - H_0^c) | E_{F'} \rangle \end{aligned} \quad (6.8.1.16)$$

In view of expression (6.8.1.15) we finally approximate the right-hand side of relation (6.8.1.16) by

$$\begin{aligned} M_{FF'} &\approx -i\pi \langle E_F | V_c \delta(E_F - H_0^c)(E - H_0^c) | E_{F'} \rangle \\ &= -i\pi \langle E_F | V | E_{F'} \rangle \delta(E_F - E_{F'}) (E - E_{F'}) \end{aligned} \quad (6.8.1.17)$$

Substitution of relation (6.8.1.17) in Eq. (6.8.1.13) gives

$$\sum_{F'} \int dE_{F'} [(E - E_{F'}) (\delta_{FF'} + i\pi V_{FF'}) \delta(E_F - E_{F'})] c_{F'} = 0 \quad (6.8.1.18)$$

The free-free part of the model Hamiltonian, namely Eq. (6.8.1.5), is thus a direct consequence of relation (6.8.1.18). The resulting Hamiltonian is non-Hermitian and the sign of the imaginary term in Eq. (6.8.1.5) defines a “retarded” Hamiltonian, which is appropriate for the initial-value problems. The corresponding conjugate Hamiltonian H^+ , on the other hand, defines an “advanced” Hamiltonian appropriate for the final-value problems.

6.8.2. The Resolvent Equations and the Four Kinds of Transitions

Using Hamiltonian (6.8.1.1) we write the equation of the resolvent operator as

$$(E - H_0)G = VG + I \quad (6.8.2.1)$$

There are two pairs of independent sets of equations for the matrix elements of G , depending on whether the initial state is in the bound part, $|B_0\rangle$, or in the free part, $|E_{F_0}, F_0\rangle$, of the spectrum of H_0 . Thus taking matrix elements on both sides of Eq. (6.8.2.1) we obtain the four systems of

equations

$$(E - E_B)G_{B|B_0} = \sum_{B'} V_{BB'} G_{B'|B_0} + \sum_F \int dE_F V_{BF}(E_F) G_{F|B_0} + \delta_{B|B_0} \quad (6.8.2.2)$$

$$\begin{aligned} (E - E_F)G_{F|B_0} &= \sum_B V_{FB}(E_F) G_{B|B_0} - i\pi \sum_{F'} \int dE_{F'} V_{FF'}(E_F, E_{F'}) \delta(E_F - E_{F'}) (E - E_{F'}) G_{F'|B_0} \\ &\quad (6.8.2.3) \end{aligned}$$

and

$$(E - E_B)G_{B|F_0} = \sum_{B'} V_{BB'} G_{B'|F_0} + \sum_F \int dE_F V_{BF}(E_F) G_{F|F_0} \quad (6.8.2.4)$$

$$\begin{aligned} (E - E_F)G_{F|F_0} &= \sum_B V_{FB}(E_F) G_{B|F_0} - i\pi \sum_{F'} \int dE_{F'} V_{FF'}(E_F, E_{F'}) \delta(E_F - E_{F'}) \\ &\quad \times (E - E_{F'}) G_{F'|F_0} + \delta(E_F - E_{F_0}) \delta_{FF_0} \quad (6.8.2.5) \end{aligned}$$

They describe four types of physical process:

$G_{B|B_0} \Rightarrow$ bound–bound transition (excitation)

$G_{F|B_0} \Rightarrow$ bound–free transition (ionization)

$G_{B|F_0} \Rightarrow$ free–bound transition (capture)

$G_{F|F_0} \Rightarrow$ free–free transition (scattering)

6.8.3. Solution of the Resolvent Equations

To solve the pair of equations (6.8.2.2) and (6.8.2.3), we first introduce an intermediate quantity

$$S_{F|B_0} \equiv (E - E_F)G_{F|B_0} \quad (6.8.3.1)$$

and define the matrix W by

$$W_{FF'} = \delta_{FF'} + i\pi V_{FF'}(E_F, E_{F'}) \quad (6.8.3.2)$$

In terms of Eqs. (6.8.3.1) and (6.8.3.2), Eq. (6.8.2.3) can be rewritten easily as

$$\sum_{F'} W_{FF'} S_{F'|B_0} = \sum_B V_{FB}(E_F) G_{B|B_0} \quad (6.8.3.3)$$

Hence

$$S_{F|B_0} = \sum_{F'B} [W^{-1}]_{FF'} V_{F'B}(E_{F'}) G_{B|B_0} \quad (6.8.3.4)$$

Using relations (6.8.2.4) and (6.8.3.1) in the second term on the right-hand side of Eq. (6.8.2.2) we obtain

$$\sum_B P_{BB'}(E) G_{B'|B_0} = \delta_{B|B_0} \quad (6.8.3.5)$$

where the matrix $P = P(E)$, which depends parametrically on E , is given by

$$[P(E)]_{BB'} = [(E - E_B) \delta_{BB'} - V_{BB'} - L_{BB'}(E)] \quad (6.8.3.6)$$

with

$$L_{BB'}(E) \equiv \sum_{FF'} \int dE_F \frac{V_{BF}(E_F)}{E - E_F + i0} [W^{-1}]_{FF'} V_{F'B'}(E_{F'}) \quad (6.8.3.7)$$

Hence from Eq. (6.8.3.5), we get explicitly the *bound–bound* (or excitation) matrix elements of G :

$$G_{B|B_0} = \sum_{B'} [P^{-1}(E)]_{BB'} \delta_{B'|B_0} = [P^{-1}(E)]_{BB_0} \quad (6.8.3.8)$$

Combining relation (6.8.3.1) with Eqs. (6.8.3.4) and (6.8.3.8) we also have the *bound–free* (or ionization) matrix elements of G :

$$G_{F|B_0} = \frac{1}{E - E_F + i0} \sum_{F'B} [W^{-1}]_{FF'} V_{F'B}(E_{F'}) [P^{-1}(E)]_{BB_0} \quad (6.8.3.9)$$

We note that the diagonal matrix elements $L_{BB}(E)$ obtained from relation (6.8.3.7) introduce part of the “shifts” and “widths” of the bound states due to their coupling to the continua. In general, assuming again the outgoing boundary condition for the inverse operator, namely

$$\frac{1}{E - E_F + i0} = \frac{P}{E - E_F} - i\pi\delta(E - E_F) \quad (6.8.3.10)$$

expression (6.8.3.7) can be rewritten in the form

$$L_{BB'}(E) = \hbar [\Delta_{BB'}(E) - \frac{1}{2}i\Gamma_{BB'}(E)] \quad (6.8.3.11)$$

where

$$\hbar\Delta_{BB'}(E) = \sum_{FF'}(\text{P}) \int dE_F \frac{V_{BF}(E_F)}{E - E_F} [W^{-1}]_{FF'} V_{F'B'}(E_{F'}) \quad (6.8.3.12)$$

and

$$\hbar\Gamma_{BB'}(E) = 2\pi \sum_{FF'} V_{BF}(E_F) [W^{-1}]_{FF'} V_{F'B'}(E_{F'}) \quad (6.8.3.13)$$

(P) $\int dE_F$ stands for the principal-value integral.

To solve Eqs. (6.8.2.4) and (6.8.2.5), we set

$$S_{F|F_0} \equiv (E - E_F) G_{F|F_0} \quad (6.8.3.14)$$

and use Eq. (6.8.3.2) for W to rewrite Eq. (6.8.2.5) as

$$\sum_{F'} W_{FF'} S_{F'|F_0} = \sum_B V_{FB}(E_F) G_{B|F_0} + \delta(E_F - E_{F_0}) \delta_{FF_0} \quad (6.8.3.15)$$

Hence

$$S_{F|F_0} = \sum_{F'B} [W^{-1}]_{FF'} V_{F'B}(E_{F'}) G_{B|F_0} + [W^{-1}]_{FF_0} \delta(E_F - E_{F_0}) \quad (6.8.3.16)$$

Substituting expressions (6.8.3.16) and (6.8.3.14) in Eq. (6.8.2.4) and using definitions (6.8.3.7) and (6.8.3.6) for the matrix $P(E)$, one finds that

$$\sum_{B'} [P(E)]_{BB'} G_{B'|F_0} = \sum_F V_{BF}(E_F) [W^{-1}]_{FF_0} \frac{1}{E - E_{F_0} + i0} \quad (6.8.3.17)$$

Hence the *free-bound* (or capture) matrix elements of G are given by

$$G_{B|F_0} = \sum_{B'F} [P^{-1}(E)]_{BB'} V_{B'F}(E_F) [W^{-1}]_{FF_0} \frac{1}{E - E_{F_0} + i0} \quad (6.8.3.18)$$

Finally, by substituting Eq. (6.8.3.18) in Eq. (6.8.3.16) and using relation (6.8.3.14), one also obtains the *free-free* (or scattering) matrix elements of G :

$$\begin{aligned} G_{F|F_0} &= \frac{1}{E - E_F + i0} \\ &\times \sum_{B,B_1,F_1,F_2} [W^{-1}]_{FF_1} V_{F_1B}(E_{F_1}) [P^{-1}(E)]_{BB_1} V_{B_1F_2}(E_{F_2}) [W^{-1}]_{F_2F_0} \frac{1}{E - E_{F_0} + i0} \\ &+ \frac{1}{E - E_F + i0} [W^{-1}]_{FF_0} \delta(E_F - E_{F_0}) \end{aligned} \quad (6.8.3.19)$$

Expressions (6.8.3.8), (6.8.3.9), (6.8.3.18), and (6.8.3.19) are the four desired exact solutions of the resolvent equation (6.8.2.1), defined by the model Hamiltonian, Eqs. (6.8.1.1)–(6.8.1.5).

6.8.4. Probability Distributions in Multiple Continua

As an application of the above results we determine the probability distributions of occupation of the continuum states, due to multiphoton transitions from a bound state. This problem is of particular interest in connection with the nonperturbative behavior of infrared multiphoton dissociation⁽¹²¹⁾ and for the formally rather analogous problem of above-threshold ionization (ATI), which are being vigorously studied both experimentally^(122–127) and theoretically.^(80,128–136)

We write the time-dependent amplitude for the *bound-free* transition

$$|B_0\rangle \equiv |\phi_0\rangle |0\rangle \rightarrow |E_F, F\rangle \equiv |\phi_F\rangle |n_F\rangle \quad (6.8.4.1)$$

as

$$\begin{aligned} A_{F|B_0}(t) &= -\frac{1}{2\pi i} \int_{-\infty}^{\infty} dE G_{F|B_0}(E) \exp[-i(E - E_F)t/\hbar] \\ &= -\frac{1}{2\pi i} \int_{-\infty}^{\infty} dE \frac{\exp[-i(E - E_F)t/\hbar]}{E - E_F + i0} \\ &\times \sum_{F'B} [W^{-1}]_{FF'} V_{F'B}(E_F) [P^{-1}(E)]_{BB_0} \end{aligned} \quad (6.8.4.2)$$

Equation (6.8.3.9) has been used to write the second line of Eq. (6.8.4.2). We observe parenthetically that Eq. (6.8.4.2) has a reduced dimension, due to the energy-delta normalization of the states $|E_F, F\rangle$; these states are related to the unity normalized continuum states (in a large box), say $\Phi_{\mathbf{k}_F}^{(-)}$, by the relation

$$\Phi_{\mathbf{k}_F}^{(-)} |n_F\rangle = \frac{1}{\rho(E_F)^{1/2}} \sum_{L_{FM_F}} |E_F, F\rangle Y_{L_{FM_F}}^*(\hat{K}_F) \quad (6.8.4.3)$$

where

$$\rho(E_F) = \frac{\mu K_F}{\hbar^2} \left(\frac{L}{2\pi}\right)^3$$

is the density of final states [see Eqs. (2.6.7)–(2.6.8)]. The bound-free transition probability distributions (including those to be derived below) are in fact independent of the normalization volume L^3 of the continuum states.

To proceed with the main point we recall the second equality in expression (3.9.1.1) and the identity (3.9.1.6). By taking the long-time limit $t \rightarrow +\infty$ in Eq. (6.8.4.2) we find that the first factor in the integral of this equation reduces to $-2\pi i\delta(E - E_F)$. Thus one obtains

$$A_{F|B_0}(t \rightarrow +\infty) = \sum_{F'B} [W^{-1}]_{FF'} V_{F'B}(E_F) [P^{-1}(E_F)]_{BB_0} \quad (6.8.4.4)$$

Therefore, the steady-state (differential) probability distribution of the occupation of the continuum states between E_F and $E_F + dE_F$ is

$$\frac{d}{dE_F} P_{B_0 \rightarrow E_F}(\infty) = \sum_{F(L_F M_F)} \left| \sum_{F'B} [W^{-1}]_{FF'} V_{F'B}(E_F) [P^{-1}(E_F)]_{BB_0} \right|^2 \quad (6.8.4.5)$$

This is the total probability obtained, as usual, by summing the contributions of partial probabilities from relation (6.8.4.4) over the countable set of degenerate partial waves F ($\equiv L_F M_F$), where the final states $|E_F, F\rangle$ are assumed to be associated with (partial) spherical waves of angular momenta ($L_F M_F$) of the free particle. The angular distribution of the free particle propagating in a direction \hat{K}_F within the solid angle $d\hat{K}_F$ (or momentum within \mathbf{K}_F and $\mathbf{K}_F + d\mathbf{K}_F$) from Eq. (6.8.4.4) becomes

$$\frac{d^2 P_{B_0 \rightarrow \mathbf{K}_F}}{d\hat{K}_F dE_F} = \left| \sum_{F(L_F M_F)} \sum_{F'B} Y_{L_F M_F}(\hat{K}_F) [W^{-1}]_{FF'} V_{F'B}(E_F) [P^{-1}(E_F)]_{BB_0} \right|^2 \quad (6.8.4.6)$$

We observe that the above distributions (6.8.4.5) and (6.8.4.6) are determined exactly by a fixed value of $E, E = E_F$, for each set of final states of energy E_F . This is consistent with the character of long-time distributions in general.

In the special case in which one may need to consider only one bound state in the discrete space, one has from Eqs. (6.8.3.6) and (6.8.3.11)

$$[P^{-1}(E_F)]_{B_0 B_0} = \left[E_F - E_{B_0} - V_{B_0 B_0} - \hbar\Delta_{B_0 B_0}(E_F) + \frac{\hbar}{2} i\Gamma_{B_0 B_0}(E_F) \right]^{-1} \quad (6.8.4.7)$$

In this case therefore the differential probability distribution (6.8.4.5) reduces to

$$\frac{d}{dE_F} P_{B_0 \rightarrow E_F}(\infty) = \frac{\sum_{F'(L_F M_F)} \left| \sum_{F'} [W^{-1}]_{FF'} V_{F'B_0}(E_F) \right|^2}{[\hbar\Delta_0(E_F)]^2 + [\hbar\Gamma_{B_0 B_0}(E_F)/2]^2} \quad (6.8.4.8)$$

where

$$\hbar\Delta_0(E_F) = E_F - E_{B_0} - V_{B_0 B_0} - \hbar\Delta_{B_0 B_0} \quad (6.8.4.9)$$

Correspondingly, the angular distribution (6.8.4.6) simplifies to

$$\frac{d^2 P_{B_0 \rightarrow K_F}}{d \hat{K}_F d E_F} = \frac{\left| \sum_F \sum_{F'} Y_{LFMF}(\hat{K}_F) [W^{-1}]_{FF'} V_{F'B_0}(E_F) \right|^2}{[\hbar \Delta_0(E_F)]^2 + [\hbar \Gamma_{B_0 B_0}(E_F)/2]^2} \quad (6.8.4.10)$$

The probability distribution (6.8.4.8) or (6.8.4.10) has a Lorenzian structure centered around

$$E_F = E'_0 \equiv E_{B_0} + V_{B_0 B_0} + \hbar \Delta_{B_0 B_0} \quad (6.8.4.11)$$

which is the total energy shifted by an amount $V_{B_0 B_0} + \hbar \Delta_{B_0 B_0}$ from the unperturbed position E_{B_0} , and has the width $\hbar \Gamma_{B_0 B_0}$. Furthermore, if the width $\hbar \Gamma_{B_0 B_0}$ is sufficiently narrow, then the matrix elements involving the final state of energy E_F may be assumed to vary only negligibly in the significant range of integration over dE_F , and hence may be taken outside the energy integration sign. The integration over dE_F of function (6.8.4.8) or (6.8.4.10) may then be performed in the range $-\infty$ to $+\infty$. Alternatively and more formally, in the energy-conserving approximation with sufficiently narrow $\hbar \Gamma_{B_0 B_0}$, we may introduce

$$\frac{1}{(E_F - E'_0)^2 + (\frac{1}{2} \hbar \Gamma_{B_0 B_0})^2} \rightarrow \frac{2\pi}{\hbar \Gamma_{B_0 B_0}} \delta(E_F - E'_0) \quad (6.8.4.12)$$

In either approach, Eq. (6.8.4.8) yields the useful result for the integrated probability:

$$P_{B_0 \rightarrow E_F}(\infty) = \frac{2\pi}{\hbar} \sum_{F(LFM_F)} |R_{FB_0}(E_F)|^2 \frac{1}{\Gamma_{B_0 B_0}} \quad (6.8.4.13)$$

where

$$R_{FB_0}(E_F) = \sum_{F'} [W^{-1}]_{FF'} V_{F'B_0}(E_F) \quad (6.8.4.14)$$

Similarly, Eq. (6.8.4.10) gives the energy-integrated angular distribution of the free particle in the form

$$\frac{d}{d \hat{K}_F} P_{B_0 \rightarrow K_F} = \frac{2\pi}{\hbar} \left| \sum_F Y_{LFMF}(\hat{K}_F) R_{FB_0}(E_F) \right|^2 \frac{1}{\Gamma_{B_0 B_0}} \quad (6.8.4.15)$$

An approach to steady-state distributions (6.8.4.8) and (6.8.4.10) may also be determined explicitly using the approximation in which the E -dependence of the shift and width of the bound state, $\Delta_{B_0 B_0}(E)$ and

$\Gamma_{B_0B_0}(E)$, are assumed to be negligible. In this case Eq. (6.8.4.2) becomes

$$A_{F|B_0}(t) = -\frac{1}{2\pi i} R_{FB_0}(E_F) \int_{-\infty}^{\infty} dE \frac{\exp[-i(E-E_F)t/\hbar]}{[E-E_F+i0]} \\ \times \left[E - E_{B_0} - V_{B_0B_0} - \hbar\Delta_{B_0B_0}(E_F) + \frac{\hbar}{2}i\Gamma_{B_0B_0}(E_F) \right]^{-1} \quad (6.8.4.16)$$

By closing the contour in the lower-half complex E -plane, this can be easily integrated by the residue theorem to yield

$$A_{F|B_0}(t) = R_{FB_0}(E_F) \frac{1 - \exp[i\Delta_0(E_F)t - \frac{1}{2}\Gamma_{B_0B_0}(E_F)t]}{[\hbar\Delta_0(E_F) + (\hbar/2)i\Gamma_{B_0B_0}(E_F)]} \quad (6.8.4.17)$$

Hence the differential probability distribution of the continuum states F in the range E_F to $E_F + dE_F$, to be occupied after an interaction time t_p (e.g., a “step pulse” of duration t_p), is

$$\frac{d}{dE_F} P_{B_0 \rightarrow E_F}(t_p) = \frac{\sum_{F(L_F M_F)} |R_{FB_0}(E_F)|^2}{[\hbar\Delta_0(E_F)]^2 + [\hbar\Gamma_{B_0B_0}(E_F)/2]^2} \\ \times \{1 + \exp[-\Gamma_{B_0B_0}(E_F)t_p] \\ - 2 \exp[-\frac{1}{2}\Gamma_{B_0B_0}(E_F)t_p] \cos[\Delta_0(E_F)t_p]\} \quad (6.8.4.18)$$

The time dependence of the angular distribution corresponding to Eq. (6.8.4.10) is given by

$$\frac{d^2 P_{B_0 \rightarrow E_F}(t_p)}{d\hat{\mathbf{K}}_F dE_F} = \frac{\left| \sum_F Y_{L_F M_F}(\hat{\mathbf{K}}_F) R_{FB_0}(E_F) \right|^2}{[\hbar\Delta_0(E_F)]^2 + [\hbar\Gamma_{B_0B_0}(E_F)/2]^2} \\ \times \{1 + \exp[-\Gamma_{B_0B_0}(E_F)t_p] \\ - 2 \exp[-\frac{1}{2}\Gamma_{B_0B_0}(E_F)t_p] \cos[\Delta_0(E_F)t_p]\} \quad (6.8.4.19)$$

In the limit of long interaction time, $t_p \rightarrow \infty$ (such as a cw laser), Eqs. (6.8.4.18) and (6.8.4.19) approach exactly to the distributions (6.8.4.8) and (6.8.4.10), respectively.

6.8.5. Solutions of the Friedrichs–Fano Model

In the special case in which the off-diagonal matrix elements $V_{FF'}$ in Eq. (6.8.1.5) are formally set equal to zero, our Hamiltonian reduces to the special case of the Friedrichs–Fano Hamiltonian.^(119,120) The four kinds of

solution of the Friedrichs–Fano model can therefore be immediately written down from the more general results derived earlier [see Eqs. (6.8.3.8)–(6.8.3.9) and (6.8.3.18)–(6.8.3.19)] by the simple replacement

$$[W^{-1}]_{FF'} \rightarrow \delta_{FF'} \quad (6.8.5.1)$$

This procedure yields the solutions

$$G_{B|B_0} = [P^{-1}(E)]_{BB_0} \quad (\text{bound–bound transition}) \quad (6.8.5.2)$$

$$G_{F|B_0} = \frac{1}{E - E_F + i0} \sum_B V_{FB}(E_F) [P^{-1}(E)]_{BB_0} \quad (\text{bound–free transition}) \quad (6.8.5.3)$$

$$G_{B|F_0} = \sum_{B'} [P^{-1}(E)]_{BB'} V_{B'F_0}(E_{F_0}) \frac{1}{E - E_{F_0} + i0} \quad (\text{free–bound transition}) \quad (6.8.5.4)$$

and

$$\begin{aligned} G_{F|F_0} = & \frac{1}{E - E_F + i0} \sum_{BB'} V_{FB}(E_F) [P^{-1}(E)]_{BB'} V_{B'F_0}(E_{F_0}) \frac{1}{E - E_{F_0} + i0} \\ & + \frac{1}{E - E_F + i0} \delta_{FF_0} \delta(E_F - E_{F_0}) \quad (\text{free–free transition}) \end{aligned} \quad (6.8.5.5)$$

In these equations the matrix elements $[P^{-1}(E)]_{BB'}$ are defined by relation (6.8.3.6), but with $L_{BB'}$ replaced by

$$U_{BB'} \equiv \sum_F \int dE_F V_{BF}(E_F) \frac{1}{E - E_F + i0} V_{FB'}(E_F) \quad (6.8.5.6)$$

These solutions of the Friedrichs–Fano model and the correspondingly simplified probability distributions become directly applicable only when the continuum is prediagonalized.

We note that the inverse matrices $[W^{-1}]$ and $[P^{-1}(E)]$ appearing in all the previous equations are nonsingular finite matrices and hence can be evaluated without difficulty. Finally, it is useful to observe that the matrix elements $V_{BB'}$ and $V_{BF}(E_F)$ in relations (6.8.1.2)–(6.8.1.4) can also be interpreted as the corresponding “effective matrix elements” (see Chapter 7). Clearly, the solutions of the resulting effective Hamiltonian problem are again given by the same equations as derived above in Sections 6.8.2–6.8.5 with the new meaning of quantities $V_{BB'}$ and $V_{BF}(E_F)$ understood.

7

Theory of Effective Hamiltonians with Stationary and Time-Dependent Interactions

7.1. Introduction

One of the most useful methods of treating resonant multiphoton processes consists in reducing the full original Hamiltonian to an “effective Hamiltonian,” which couples explicitly only the most “relevant states” of the problem of interest. In this chapter we shall give a systematic method of constructing the effective Hamiltonian for both stationary as well as time-dependent fields. At first, however, we shall give an intuitive description of such Hamiltonians that will help to understand the physical basis underlying the systematic theory to follow in Sections 7.5 and 7.6.

The basic idea behind an effective multiphoton Hamiltonian^(109,137-139) is to divide the whole set of states of the unperturbed system into two complementary sets, one of which consists of the “quasi-resonant” states, e.g., the initial, final, and near-resonant states, which are treated explicitly. The other set includes the rest of the “nonresonant” states and is used only to determine the coupling matrix elements between all pairs of states of the first set, using higher-order nonresonant perturbation theory. This is appropriate so long as the external field strength $F < F_{\max}$, where F_{\max} is approximately the field for which the interaction energy, equal to about eFa_0 , becomes comparable to the minimum energy difference $\hbar\Delta_{\min}$ among the nonresonant states, or

$$eF_{\max}a_0 = \hbar\Delta_{\min} = |\varepsilon_i \pm n\hbar\omega - \varepsilon_f|_{\min} \quad (7.1.1)$$

where ε_i is the initial energy of the atom, n is the number of photons

virtually (i.e., nonresonantly) absorbed or emitted, and ϵ , is the energy of any nonresonant state. Hence in this approach the actual field strength should be restricted to

$$F < \frac{\hbar\Delta_{\min}}{ea_0} \quad (7.1.2)$$

which, in the optical-frequency region, may reach a few percent of the atomic field strength $F_a = 5.142 \times 10^9$ V/cm.

7.2. The Effective Multiphoton Hamiltonian with One Intermediate Resonance

The structure of the effective Hamiltonian will be seen to depend essentially only on the number of intermediate resonances. Below we consider the frequently occurring case of a single intermediate resonance. To be specific we first consider a two-photon resonant process when the three-photon ionization channels are open. A schematic diagram depicting the process is shown in Figure 31. Three states, namely 1, 2, and C, are marked and taken as the “resonant” states of the problem. We are interested in the time evolution of these states under the action of the radiation field. In state 1 the atom is in its level $|1\rangle$ and no photon is emitted or absorbed. In state 2 the atom is in the level $|2\rangle$ and two photons are absorbed. Finally in state C, the atom is in the continuum state $|\mathbf{k}\rangle$ with three photons absorbed. For the two-photon resonant three-photon ionization of alkali atoms, for example, states $|1\rangle$ and $|2\rangle$ can be the ground state and the first excited s -state, respectively, in which case $|\mathbf{k}\rangle$ is a single p -wave continuum. In general, $|\mathbf{k}\rangle$ is composed of a sum of partial waves at energy $\hbar^2 k^2 / 2\mu$.

In Figure 31 there is a quasi-resonant path (solid arrows) and a nonresonant path (dashed line) to the continuum. The nonresonant path merely excludes the quasi-resonant intermediate state $|2\rangle$. The effective two-photon coupling between the bound levels $|1\rangle$ and $|2\rangle$ may be described, as expected intuitively, by the second-order two-photon absorp-

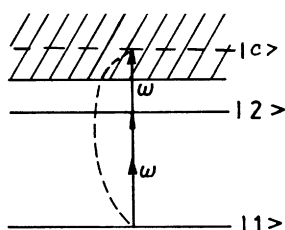


Figure 31. Schematic of a two-photon resonant three-photon ionization process indicating the resonant (solid arrows) path and the direct (nonresonant) path (dashed line) to the continuum.

tion matrix element

$$V_{12}^{(2)} = \sum_j' \frac{\langle 1 | \frac{\mathbf{F}}{2} \cdot \mathbf{D} | j \rangle \langle j | \frac{\mathbf{F}}{2} \cdot \mathbf{D} | 1 \rangle}{\omega_1 + \omega - \omega_j} \quad (7.2.1)$$

where the prime indicates that the intermediate states $|j\rangle = |1\rangle, |2\rangle$, and $|\mathbf{k}\rangle$ are excluded from the sum. (The perturbative order of any effective matrix element V is indicated explicitly by the superscript on V .) The effective coupling between the quasi-resonant level $|2\rangle$ and the continuum $|\mathbf{k}\rangle$ is given by the one-photon absorption matrix element (of photoionization) from the level $|2\rangle$,

$$V_{2\mathbf{k}}^{(1)} = \langle 2 | \frac{\mathbf{F}}{2} \cdot \mathbf{D} | \mathbf{k} \rangle \quad (7.2.2)$$

The nonresonant three-photon coupling between the ground level $|1\rangle$ and $|\mathbf{k}\rangle$ (as shown by the dashed line) is similarly expected to be given by the three-photon absorption matrix element

$$V_{1\mathbf{k}}^{(3)} = \sum_{j_1}' \sum_{j_2}' \frac{\langle 1 | \frac{\mathbf{F}}{2} \cdot \mathbf{D} | j_1 \rangle \langle j_1 | \frac{\mathbf{F}}{2} \cdot \mathbf{D} | j_2 \rangle \langle j_2 | \frac{\mathbf{F}}{2} \cdot \mathbf{D} | k \rangle}{(\omega_1 + \omega - \omega_{j_1})(\omega_1 + 2\omega - \omega_{j_2})} \quad (7.2.3)$$

where again primes indicate that the sums must exclude the three states treated explicitly. We note that the off-diagonal coupling matrix $V_{12}^{(2)}$ between the bound states is of second order. Hence, to be self-consistent one must also include the second-order contribution to the diagonal matrix elements of the bound states (which give the dynamic Stark shifts of the levels). Thus we have

$$V_{11}^{(2)} = \sum_{j_1}' \frac{\langle 1 | \frac{\mathbf{F}}{2} \cdot \mathbf{D} | j_1 \rangle \langle j_1 | \frac{\mathbf{F}}{2} \cdot \mathbf{D} | 1 \rangle}{\omega_1 + \omega - \omega_{j_1}} + \sum_{j_1}' \frac{\langle 1 | \frac{\mathbf{F}}{2} \cdot \mathbf{D} | j_1 \rangle \langle j_1 | \frac{\mathbf{F}}{2} \cdot \mathbf{D} | 1 \rangle}{\omega_1 - \omega - \omega_{j_1}} \quad (7.2.4)$$

An expression similar to Eq. (7.2.4), where only the outer levels are changed to $|2\rangle$, gives the diagonal matrix elements $V_{22}^{(2)}$.

In this context one usually neglects both the diagonal matrix element for the continuum $|\mathbf{k}\rangle$ as well as the nondiagonal continuum-continuum matrix elements, primarily for mathematical convenience. This may be justified at sufficiently low field strengths provided the effect of the neglected coupling terms on the density of states and/or the phases of the continuum wave function is small compared to those in the absence of the

field. It is noteworthy that the next higher-order perturbative contribution to the diagonal matrix elements is of fourth order and is, therefore, neglected altogether. A third-order coupling $V_{2k}^{(3)}$ should, in principle, be added to the $V_{2k}^{(1)}$ matrix element, but this is also usually neglected because of its smallness. The effective Hamiltonian of interest is thus now given by the set of dominant coupling matrix elements considered together,

$$\begin{aligned} H &\equiv \begin{pmatrix} H_{11} & H_{12} & H_{1C} \\ H_{21} & H_{22} & H_{2C} \\ H_{C1} & H_{C2} & H_{CC} \end{pmatrix} \\ &= \begin{pmatrix} \varepsilon_1 + V_{11}^{(2)} & V_{12}^{(2)} & V_{1k}^{(3)} \\ V_{21}^{(2)} & \varepsilon_2 - 2\hbar\omega + V_{22}^{(2)} & V_{2k}^{(1)} \\ V_{k1}^{(3)} & V_{k2}^{(1)} & E_\epsilon (\equiv \varepsilon - 3\hbar\omega) \end{pmatrix} \end{aligned} \quad (7.2.5)$$

It is understood also that the continuum index \mathbf{k} on the bound-free matrix element implies integration over $d\mathbf{k}$ when H operates on its wave function. The essential feature of the effective matrix elements is their insensitive dependence on ω (since in these matrix elements ω remains within the nonresonant space). They may therefore be calculated for a fixed frequency and used as fixed parameters, while the ionization process is inspected for its dependence on detuning in the vicinity of the resonance (which is treated explicitly). It is often good practice, however, to calculate the effective matrix elements for a number of frequency points in the domain of interest and obtain them at the required frequencies by simple extrapolation. Clearly, the range of detuning over which the same effective Hamiltonian may be used is limited by the requirement of near-constant or slowly varying behavior of the effective matrix elements with respect to the incident frequency. This property must therefore be ensured (if possible, by appropriately enlarging the set of “resonant” states) for reliable use of the effective Hamiltonians.

Effective Hamiltonians of the same structure as display (7.2.5) often arise for different physical situations. Thus, for example, exactly the same Hamiltonian structure is also obtained for the two-photon ionization process with one-photon intermediate resonance. In this case the effective Hamiltonian matrix is clearly

$$\begin{pmatrix} H_{11} = \varepsilon_1 + V_{11}^{(2)}, & H_{22} = \varepsilon_2 - \hbar\omega + V_{22}^{(2)}, & H_{kk} \equiv E_\epsilon = \varepsilon - 2\hbar\omega \\ H_{12} = V_{12}^{(1)} = H_{21}^*, & H_{1k} = V_{1k}^{(2)} = H_{k1}^*, & H_{2k} = V_{2k}^{(1)} = H_{k2}^* \end{pmatrix} \quad (7.2.6)$$

It should be noted that a Hamiltonian of form (7.2.5) or (7.2.6) is a simple special case of the more general model Hamiltonian of Section 6.8.1.

These special cases, however, are frequently encountered and in fact

constitute prototypes for all resonant processes. We shall therefore give an *ab initio* analysis leading to the complete time-dependent solutions of the transition probabilities governed by them.

7.3. The One-Resonance Resolvent Equations

Let us assume that the atom is initially in state $|1\rangle$ and introduce the following simplifying notations for the matrix elements of the resolvent $G(E)$:

$$\langle j | G(E) | i \rangle = g_j(E) = g_j \quad (7.3.1)$$

for all $j = |1\rangle, |2\rangle$, and $|\mathbf{k}\rangle$. By building the matrix elements of the resolvent equation corresponding to Hamiltonians (7.2.5) or (7.2.6),

$$[E - H]G(E) = 1 \quad (7.3.2)$$

between the initial state $|1\rangle$ and the three “resonant” states $|j\rangle$ in turn, we obtain

$$\left. \begin{aligned} (E - H_{11})g_1 &= H_{12}g_2 + \sum_{\mathbf{k}} H_{1\mathbf{k}}g_{\mathbf{k}} \\ (E - H_{22})g_2 &= H_{21}g_1 + \sum_{\mathbf{k}} H_{2\mathbf{k}}g_{\mathbf{k}} \\ (E - E_{\epsilon})g_{\mathbf{k}} &= H_{\mathbf{k}1}g_1 + H_{\mathbf{k}2}g_2 \end{aligned} \right\} \quad (7.3.3)$$

We have introduced the symbol

$$\sum_{\mathbf{k}} \underset{\text{lim } L \rightarrow \infty}{\equiv} \frac{L^3}{(2\pi)^3} \int k^2 dk \sin \theta_k d\theta_k d\phi_k$$

where L^3 is the normalization volume of the continuum states $|\mathbf{k}\rangle$ and the wave vector $\mathbf{k} \equiv (k, \theta_k, \phi_k)$.

Equations (7.3.3) are easily solved by eliminating $g_{\mathbf{k}}$ from the first two equations with the aid of the third. It is immediately clear on substitution of the last equation of the set (7.3.3) into the first two that this introduces parameters of the form

$$\sum_{\mathbf{k}} H_{\mathbf{k}} \frac{1}{E - E_{\epsilon}} H_{\mathbf{k}j}, \quad j = 1, 2 \quad (7.3.4)$$

They are uniquely defined only on specifying the boundary condition,

which we assume to be the outgoing condition. Hence

$$\sum_{\mathbf{k}} H_{i\mathbf{k}} \frac{1}{E - E_e + i0} H_{\mathbf{k}\nu} = \hbar\delta_{ii}(E) - \frac{1}{2}i\hbar\gamma_{ii}(E) \quad (7.3.5)$$

where

$$\hbar\delta_{ii}(E) = (P) \sum_l \int dE_{\epsilon} \frac{H_{ie}^l H_{e\epsilon}^l}{E - E_e} \rho(\epsilon) \quad (7.3.6)$$

and

$$\hbar\gamma_{ii}(E) = 2\pi \sum_l H_{ie}^l H_{e\epsilon}^l \rho(\epsilon) \Big|_{E=E_e} \quad (7.3.7)$$

The summation over l corresponds to the angular-momentum components of $|\mathbf{k}\rangle$ and $\rho(\epsilon)$ is the density of states at $\epsilon = \hbar^2 k^2/(2\mu)$. The diagonal elements $\hbar\delta_{ii}(E)$ and $\hbar\gamma_{ii}(E)$ may be interpreted as contributions respectively to the shift and width of the discrete level $|i\rangle$ due to its interaction with the continuum $|\mathbf{k}\rangle$. The off-diagonal elements may be thought of as the dispersive and the dissipative contributions to the correlation between states $|i\rangle$ and $|j\rangle$ caused by their mutual interaction with the continuum $|\mathbf{k}\rangle$.

In general these parameters depend, as indicated, on the total energy E of the interacting “atom + field” system. This dependence around the initial unperturbed total energy E_0 is often weak and the parameters are conveniently evaluated at $E = E_0$, i.e., their slow variation with E is neglected. Henceforth we shall assume

$$\delta_{ii} = \delta_{ii}(E) \Big|_{E=E_0} \quad \text{and} \quad \gamma_{ii} = \gamma_{ii}(E) \Big|_{E=E_0} \quad (7.3.8)$$

If $g_{\mathbf{k}}$ is eliminated from the first two of Eqs. (7.3.3) by substituting from the third equation, we obtain the pair of equations

$$\left. \begin{aligned} (E - H'_{11} + \frac{1}{2}i\hbar\gamma_1)g_1 &= (H'_{12} - \frac{1}{2}i\hbar\gamma_{12})g_2 + 1 \\ (E - H'_{22} + \frac{1}{2}i\hbar\gamma_2)g_2 &= (H'_{21} - \frac{1}{2}i\hbar\gamma_{21})g_1 \end{aligned} \right\} \quad (7.3.9)$$

where

$$H'_{ii} \equiv H_{ii} + \hbar\delta_{ii} \quad \text{and} \quad \gamma_i \equiv \gamma_{ii} \quad (7.3.10)$$

The resolvent matrix elements g_1 and g_2 are readily obtained by solving the pair of algebraic equations (7.3.9), and $g_{\mathbf{k}}(E)$ is obtained from the last of Eqs. (7.3.3). Thus, explicitly, we obtain

$$g_1(E) = \frac{(E - H'_{22} + \frac{1}{2}i\hbar\gamma_2)}{D(E)} \quad (7.3.11)$$

$$g_2(E) = \frac{H'_{21} - \frac{1}{2}i\hbar\gamma_{21}}{D(E)} \quad (7.3.12)$$

and

$$g_k(E) = \frac{H_{k1}(E - H'_{22} + \frac{1}{2}i\hbar\gamma_2) + H_{k2}(H'_{21} - \frac{1}{2}i\hbar\gamma_{21})}{(E - E_k)D(E)} \quad (7.3.13)$$

where

$$D(E) \equiv (E - H'_{11} + \frac{1}{2}i\hbar\gamma_1)(E - H'_{22} + \frac{1}{2}i\hbar\gamma_2) - (H'_{12} - \frac{1}{2}i\hbar\gamma_{12})(H'_{21} - \frac{1}{2}i\hbar\gamma_{21}) \quad (7.3.14)$$

with

$$H'_{ij} = H_{ij} + \hbar\delta_{ij} \equiv \hbar V'_{ij}, \quad (i, j) = 1, 2 \quad (7.3.15)$$

After extracting the roots of expression (7.3.14), it is useful to factorize $D(E)$ in the form

$$D(E) \equiv (E - E_+)(E - E_-) \quad (7.3.16)$$

where

$$E_{\pm} = \frac{\hbar}{2}(\omega_+ - i\Gamma \pm \Omega) \quad (7.3.17)$$

We have introduced here the “complex Rabi frequency”

$$\Omega = [(\delta - i\gamma)^2 + 4(V'_{12} - \frac{1}{2}i\gamma_{12})(V'_{21} - \frac{1}{2}i\gamma_{21})]^{1/2} \quad (7.3.18)$$

and defined

$$\begin{aligned} \omega_+ &= \frac{H'_{11} + H'_{22}}{\hbar}, & \delta &= \frac{H'_{11} - H'_{22}}{\hbar} \\ \gamma &= \frac{\gamma_1 - \gamma_2}{2}, & \Gamma &= \frac{\gamma_1 + \gamma_2}{2} \end{aligned} \quad (7.3.19)$$

7.4. Time Dependence of Bound-Bound and Bound-Free Transitions

The explicit expressions of the resolvent matrix elements, namely Eqs. (7.3.11)–(7.3.13), make it possible to find the detailed time dependence⁽¹⁰⁹⁾ of the corresponding transition amplitudes $b_i(t)$ from their Fourier transforms:

$$b_i(t) = -\frac{1}{2\pi i} \int_{-\infty}^{\infty} dE g_i(E) e^{-iEt/\hbar} \quad (7.4.1)$$

These integrals are most readily evaluated using contour integration. To this end we choose a closed contour running clockwise along the real axis and around the lower-half complex E -plane and observe that the poles of $g_-(E)$ occur at the roots of $D(E)$, Eq. (7.3.1.7). The residue theorem and elementary algebra easily yield the time dependence of the bound-state amplitudes in the form

$$b_2(t) = \frac{e^{-\Gamma t/2}}{\Omega} \left[(-2i)(V'_{21} - \frac{1}{2}i\gamma_{21}) \sin \frac{\Omega t}{2} \right] e^{-i\omega_+ t/2} \quad (7.4.2)$$

and

$$b_1(t) = \frac{e^{-\Gamma t/2}}{\Omega} \left[\Omega \cos \frac{\Omega t}{2} - (\gamma + i\delta) \sin \frac{\Omega t}{2} \right] e^{-i\omega_+ t/2} \quad (7.4.3)$$

These amplitudes closely resemble the well-known “Rabi formula.”⁽¹⁴⁰⁾ In fact, in the absence of ionization and for single-photon transition between states $|1\rangle$ and $|2\rangle$, they reduce to that formula. In the present, more general case involving ionization, the probability of excitation of the intermediate resonance is

$$|b_2(t)|^2 = \frac{|W_{21}|^2}{|\Omega|^2} (e^{-\Gamma_1 t} + e^{-\Gamma_2 t} - 2e^{-\Gamma t} \cos \Delta t) \quad (7.4.4)$$

The constants in this expression are given by the real and imaginary parts of the complex Rabi frequency

$$\Omega \equiv \Delta + i\lambda \quad (7.4.5)$$

where

$$\Delta = |\Omega| \cos \phi, \quad \lambda = |\Omega| \sin \phi \quad (7.4.6)$$

$$\tan 2\phi = -\frac{2(\delta\gamma + \gamma_1\gamma_2 q)}{\delta^2 + 4|V'_{21}|^2 - (\gamma^2 + |\gamma_{12}|^2)} \quad (7.4.7)$$

and

$$|\Omega|^2 = \{[\delta^2 + 4|V'_{21}|^2 - (\gamma^2 + |\gamma_{12}|^2)]^2 + 4(\delta\gamma + \gamma_1\gamma_2 q)^2\}^{1/2} \quad (7.4.8)$$

We have also defined the off-diagonal complex coupling constant

$$W_{21} \equiv V'_{21} - \frac{1}{2}i\gamma_{21} \quad (7.4.9)$$

and the two decay constants

$$\Gamma_1 = \Gamma - \lambda \quad \text{and} \quad \Gamma_2 = \Gamma + \lambda \quad (7.4.10)$$

It is clear from the above that the real and imaginary parts of the complex Rabi frequency are responsible for the oscillation of the resonance and its spreading, respectively. We note that the long time decay of the excitation is inevitable because of the constraint $\Gamma > \lambda$. The parameter

$$q \equiv \frac{2 \operatorname{Re}(V'_{12} \gamma_{21})}{\gamma_1 \gamma_2} \quad (7.4.11)$$

is an analog of the ‘‘Fano asymmetry parameter,’’ well known in the theory of autoionization.⁽¹²⁰⁾ For future reference [see Eq. (7.4.15)] we also define here the sum

$$s^2 \equiv \delta^2 + \gamma^2 + 4|W_{21}|^2 \quad (7.4.12)$$

The probability of finding the atom back in the initial state after some time t is, from Eq. (7.4.3),

$$\begin{aligned} |b_1(t)|^2 = & \frac{1}{4|\Omega|^2} \{ [|\Omega|^2 + \delta^2 + \gamma^2 + 2(\Delta\delta - \lambda\gamma)] e^{-\Gamma_1 t} \\ & + [(|\Omega|^2 + \delta^2 + \gamma^2) - 2(\Delta\delta - \lambda\gamma)] e^{-\Gamma_2 t} \\ & - 2[(\delta^2 + \gamma^2 - |\Omega|^2) \cos \Delta t \\ & + 2(\Delta\gamma + \lambda\delta) \sin \Delta t] e^{-\Gamma_1 t} \} \end{aligned} \quad (7.4.13)$$

As expected, the ground-state probability also eventually decays into the continuum.

The probability of finding the system at all (in the model space) must, however, be preserved at all times and equals unity, the initial probability. Hence the total probability of resonant ionization may be conveniently obtained from the equality

$$P_{\text{ion}}(t) = 1 - |b_1(t)|^2 - |b_2(t)|^2 \quad (7.4.14)$$

The combination of Eqs. (7.4.4), (7.4.13), and (7.4.14) therefore yields

$$\begin{aligned} P_{\text{ion}}(t) = & 1 - \frac{1}{4|\Omega|^2} \{ [|\Omega|^2 + s^2 + 2(\Delta\delta - \lambda\gamma)] e^{-\Gamma_1 t} \\ & + [|\Omega|^2 + s^2 - 2(\Delta\delta - \lambda\gamma)] e^{-\Gamma_2 t} \\ & - 2[(s^2 - |\Omega|^2) \cos \Delta t + 2(\Delta\gamma + \lambda\delta) \sin \Delta t] e^{-\Gamma_1 t} \} \end{aligned} \quad (7.4.15)$$

This prototype result describes the time dependence of resonant ionization due to pulsed radiation, here assumed to be a step pulse of duration t .

The probability $P_{\text{ion}}(t)$ can also be used to investigate the line shape of the ionization induced by a pulsed laser on putting $t = t_{\text{pulse}}$ and varying the detuning δ .

In the case of continuous excitation, for example with cw lasers, the ionization probability is conveniently studied in terms of the steady-state ionization spectrum $S_{\text{ion}}(\omega)$, which may be defined by the relation

$$S_{\text{ion}}(\omega) \equiv \sum_{j=1}^2 \gamma_j \int_0^\infty |b_j(t)|^2 dt \quad (7.4.16)$$

A simple calculation using Eqs. (7.4.4) and (7.4.13) yields the explicit result

$$\begin{aligned} S_{\text{ion}}(\omega) &= \frac{\Gamma}{(\Gamma^2 + \Delta^2)(\Gamma^2 - \lambda^2)} \\ &\times \left\{ 2\gamma_2 |W_{21}|^2 + \gamma_1 \left[\Gamma\gamma_2 + \frac{1}{2}(\delta^2 + \gamma^2 + \Delta^2 - \lambda^2) + \frac{\Delta\delta\lambda}{\Gamma} \right] \right\} \end{aligned} \quad (7.4.17)$$

The first term on the right-hand side of this equation gives the major resonant contribution to the ionization signal. The second term involving the square brackets arises from the nonresonant (direct) contribution from the initial state and from the interference between the resonant and nonresonant processes. This term is usually smaller in magnitude than the first term, but may at times significantly influence the shape of the spectrum.

It is clear from Eq. (7.4.15) that, in general, the ionization probability exhibits a much more involved dependence on t than that expected from a constant (in time) rate of ionization $W_{\text{ion}}^{(n)}$ or from the existence of an n -photon ionization cross section $\sigma_{\text{ion}}^{(n)} = W_{\text{ion}}^{(n)} / (\text{photon flux})$. In the latter situation one expects $P_{\text{ion}}(t)$ to depend on t as

$$P_1(t) \approx 1 - \exp(-W_{\text{ion}}^{(n)}t) \quad (7.4.18)$$

Such behavior is only realized approximately under conditions of large detunings δ , or for weak bound-bound transition strength V_{21} (compared to the strength of the bound-free coupling γ_2). In particular, when $V_{21} \approx \gamma_2$ there exists no time domain⁽¹⁰⁹⁾ in which the ionization probability $P_{\text{ion}}(t)$ may be even approximately described in terms of $P_1(t)$ and hence by a constant rate of transition. In this situation, therefore, the cross section for the multiphoton ionization cannot exist and $P_{\text{ion}}(t)$ ought to be used.

This is clearly seen in Figure 32, where a graph of $P_{\text{ion}}(t)$ is shown at an interaction time $t = T$ (in units of γ_2^{-1}). It is assumed that the nonresonant transition strength is one-hundredth of the resonant transition strength γ_2 . The asymmetry parameter is $q = 24$ and the detuning $\delta = 0$. The perturba-

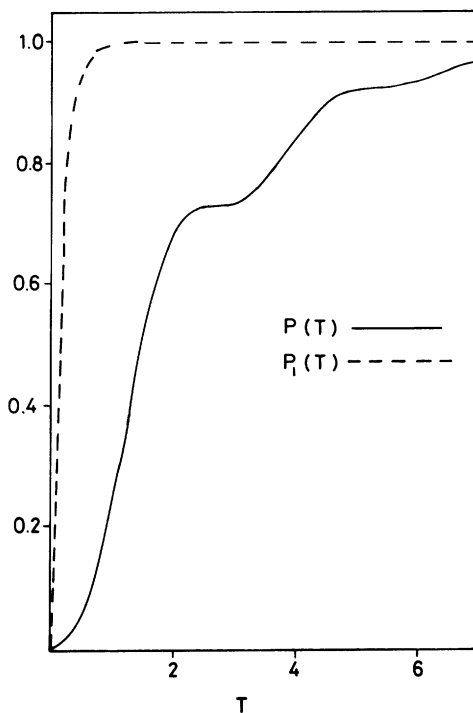


Figure 32. Time dependence of resonant bound-free transition probability $P_{\text{ion}}(T)$ as a function of interaction time T (in units of γ_2^{-1}) for $\delta = 0$, $q = 24$, and $\gamma_1 = 0.01 \gamma_2$. The rate model using perturbation theory, $P_i(T)$, is shown for comparison (from Beers and Armstrong⁽¹⁰⁹⁾).

tion theoretical probability $P_i(T)$ is also shown for comparison. The step-like modulation of $P_{\text{ion}}(T)$ reflects essentially the effect of competition between Rabi oscillation and ionization decay.

In the next section we give a typical example of two-photon resonant three-photon ionization, which has been studied experimentally⁽¹⁴¹⁾ and analyzed theoretically⁽¹⁴²⁾ using an effective Hamiltonian.

7.4.1. Application to Two-Photon Resonant Three-Photon Ionization of Cs

Consider a two-photon quasi-resonant transition between the $6^2P_{3/2}$ state and the $16P_J$ state (where $J = \frac{1}{2}$ or $\frac{3}{2}$) of neutral Cs. The resonant $16P_J$ state is coupled by a one-photon transition with the continuum. Here the state $6^2P_{3/2}$ corresponds to the initial state $|1\rangle$ and the $16P_J$ state to the state $|2\rangle$. In the actual experiment the initial state has been prepared by a linearly polarized cw laser saturating the $6^2S_{1/2}-6^2P_{3/2}$ transition from the ground ($6^2S_{1/2}$) state. The three-photon ionization of the “initial state”

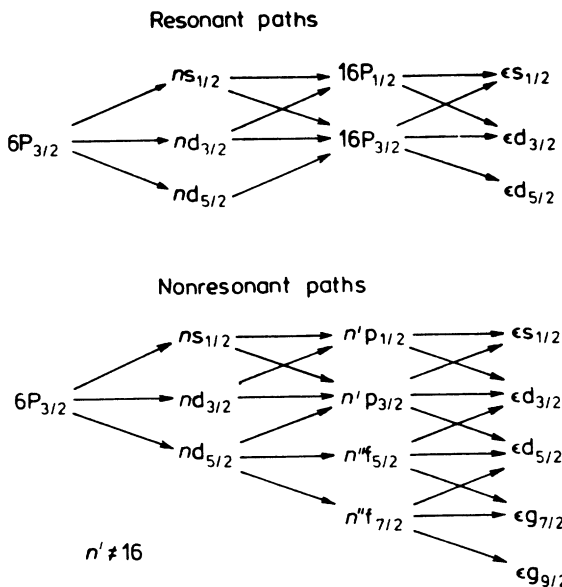


Figure 33. Resonant and nonresonant quantum paths for two-photon resonant three-photon ionization of $\text{Cs}(6P_{3/2})$ (from Crance and Aymar⁽¹⁴²⁾).

$6^2P_{3/2}$ has been achieved with a Q-switched Nd-glass laser, which was linearly polarized and yielded pulses of duration $t_p = 37$ ns. The essential calculational work consists in constructing the effective matrix elements. To this end it is useful first to isolate both the resonant and the important nonresonant quantum paths that couple the initial $6^2P_{3/2}$ state to the final continuum states. Figure 33 shows these paths schematically. Since the ground level of CsI is a $2S_{1/2}$ state, only the states $m_j = \pm \frac{1}{2}$ of the level $6^2P_{3/2}$ are prepared initially. Also, only the states with $m_j = \pm \frac{1}{2}$ are involved in the ionization process (the quantization axis is chosen parallel to the unique direction of polarizations). The paths for $m_j = +\frac{1}{2}$ and $m_j = -\frac{1}{2}$ are therefore equivalent and their contributions equal. The discrete levels $6P_{3/2}$ and $16P_{3/2}$ or $16P_{5/2}$, being P -levels, the (nonresonant) three-photon and (resonant) one-photon transitions to the continuum couple only the s - and d -components of the continuum ($\epsilon J J'$). They can be designated $\epsilon s_{1/2}$, $\epsilon d_{3/2}$, and $\epsilon d_{5/2}$ in the jj -coupling scheme. Clearly the projection of the total angular momentum remains fixed along a path.

Let us denote by K' the two-photon matrix element $V_{12}^{(2)}$ connecting the states $6P_{3/2}$ and $16P_J$. Then

$$V_{12}^{(2)} \equiv K' = \sum_{nl} \int \frac{\langle 6p | r | nl \rangle \langle nl | r | 16p \rangle}{\omega_0 - \omega_{nl}} \langle (\frac{1}{2}1)_{\frac{3}{2}\frac{1}{2}} | (C_0^{(1)})^2 | (\frac{1}{2}1)J_{\frac{1}{2}}^1 \rangle I \quad (7.4.1.1)$$

where the first factor gives the radial part and the second factor the angular part of the matrix element of interest. The summation is over the discrete and continuum states. The off-resonant frequency in the effective matrix element has been conveniently set at

$$\omega_0 \equiv \frac{1}{2\hbar} (\varepsilon_{16p} - \varepsilon_{6p}) \quad (7.4.1.2)$$

The field intensity is denoted by I . The radial wave functions are designated $|nl\rangle$ and $c_q^{(k)}$ are the spherical tensors.⁽¹⁴³⁾

The matrix element coupling the state $16P_J$ to the continuum $\varepsilon l'J'$ is given by

$$L_J^{J'} \equiv \langle 16p | r | \varepsilon l \rangle \langle (\frac{1}{2}1) J_{\frac{1}{2}}^1 | C_0^{(1)} | (\frac{1}{2}l) J'_{\frac{1}{2}} \rangle I^{1/2} \quad (7.4.1.3)$$

Thus

$$\gamma_2 \equiv \sum_J |L_J^{J'}|^2 \quad (7.4.1.4)$$

Similarly, $M^{J'}$ is the matrix element coupling the “initial” state $6P_{3/2}$ and the continuum $\varepsilon l''J'$, where

$$M^{J'} = \sum_{\substack{nl \\ n'l' \neq 16p}} \frac{\langle 6p | r | nl \rangle \langle nl | r | n'l' \rangle \langle n'l' | r | \varepsilon l''J' \rangle}{(\omega_0 - \omega_{nl})(2\omega_0 - \omega_{n'l'})} \times \langle (\frac{1}{2}1)_{\frac{3}{2}\frac{1}{2}}^3 | (C_0^{(1)})^3 | (\frac{1}{2}l'') J'_{\frac{1}{2}} \rangle I^{3/2} \quad (7.4.1.5)$$

Then

$$\gamma_1 = \sum_{J'} |M_J^{J'}| \quad (7.4.1.6)$$

where

$$M_J^{J'} = M^{J'} + K^{J''} \frac{1}{\omega_J - \omega_{J''}} L_{J''}^{J'} \quad (7.4.1.7)$$

The second term in expression (7.4.1.7) is added in order to take account of the two intermediate states $16P_J$ and $16P_{J''}$ when the resonance $16P_J$ is being investigated. Thus the second state ($16P_{J''}$) is treated as an off-resonant state as well. This is reasonable so long as the separation between them is much larger than the laser linewidth. In the present system the separation between states $16P_{1/2}$ and $16P_{3/2}$ is about an order of magnitude larger than the widths of the laser lines used in the experiment. The effective matrix elements K , L , and M as well as the diagonal Stark shifts

for the states $6P_{3/2(1/2)}$, $6P_{3/2(3/2)}$, $16P$, and $12F$ have been calculated using a single electron nonrelativistic parametric central potential. The intermediate sums were performed by the method of inhomogeneous differential equations. To avoid spurious detunings, at resonance, $\hbar\omega$ was replaced self-consistently by the calculated energy difference $(\varepsilon_{16P} - \varepsilon_{6P})/2$. The results of the calculations are given in Tables 16–19.

Table 16. Transition Matrix Elements K^J between $6P_{3/2M}$ and $16P_{JM}$ in Units of $s^{-1} W^{-1} cm^2$ (from Crance and Aymar⁽¹⁴²⁾)

$J \setminus M $	$\frac{1}{2}$	$\frac{3}{2}$
$\frac{1}{2}$	0.280	0.0
$\frac{3}{2}$	-0.335	-0.731

Table 17. Transition Matrix Elements L_J' between $16P_{JM}$ and εl_{JM} in Units of $(s^{-1} W^{-1} cm^2)^{1/2}$ (from Crance and Aymar⁽¹⁴²⁾)

$JM \setminus l_{JM'}$	$s_{1/2 \ 1/2}$	$d_{3/2 \ 1/2}$	$d_{5/2 \ 1/2}$	$d_{3/2 \ 3/2}$	$d_{5/2 \ 5/2}$
$\frac{1}{2} \frac{1}{2}$	0.162	-0.447	0	0	0
$\frac{3}{2} \frac{1}{2}$	0.230	-0.0632	-0.465	0	0
$\frac{3}{2} \frac{3}{2}$	0	0	0	-0.190	-0.379

Table 18. Transition Matrix Elements M^J between $6P_{3/2M}$ and εl_{JM} in Units of $(s^{-1} W^{-3} cm^6)^{1/2}$ (from Crance and Aymar⁽¹⁴²⁾)

$M \setminus l_J$	$d_{3/2}$	$d_{5/2}$	$g_{7/2}$	$g_{9/2}$
$\frac{1}{2}$	$1.39 \ 10^{-13}$	$7.33 \ 10^{-13}$	$-3.02 \ 10^{-13}$	$-1.35 \ 10^{-12}$
$\frac{3}{2}$	$2.77 \ 10^{-13}$	$5.55 \ 10^{-13}$	$-6.77 \ 10^{-13}$	$-9.59 \ 10^{-12}$

Table 19. Dynamic Stark Shifts in Units of $s^{-1} W^{-1} cm^2$ (from Crance and Aymar⁽¹⁴²⁾)

$6P_{3/2 \ 1/2}$	$6P_{3/2 \ 3/2}$	$16P$	$12F$
76.1	-2.30	29.0	29.1

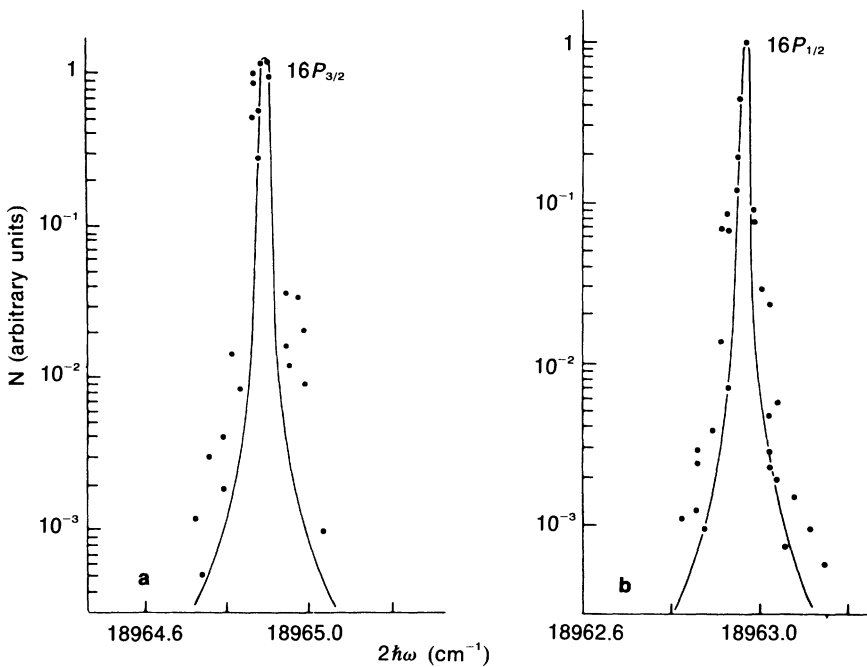


Figure 34. Three-photon resonant ionization signal from Cs as a function of frequency in the region of two-photon intermediate resonance $16P_{3/2}$ or $16P_{1/2}$ at a laser intensity of 5×10^6 W/cm². Dots refer to experimental data and solid lines to theoretical calculation of Crance and Aymar⁽¹⁴²⁾ (from Crance and Aymar⁽¹⁴²⁾).

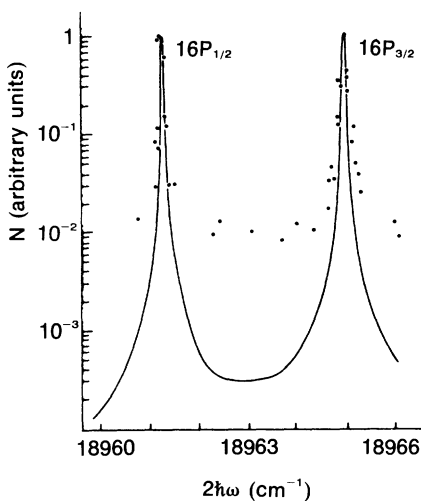


Figure 35. Three-photon resonant ionization signal from Cs as a function of laser frequency in the region of two-photon intermediate resonance $16P_{3/2}$ or $16P_{1/2}$ at a laser intensity of 10^8 W/cm². Dots refer to experimental data of Normand *et al.*⁽¹⁴¹⁾ and solid lines to theoretical calculation of Crance and Aymar⁽¹⁴²⁾ (from Crance and Aymar⁽¹⁴²⁾).

In actual comparison of the experiments with analysis, the Doppler effect at room temperature was taken into account by convoluting the $P_{\text{ion}}(t)$ with a Gaussian Doppler profile at 300 K. Figures 34 and 35 compare the experimental and calculated ionization signals as a function of laser frequency at two different intensities.

7.5. General Theory of Stationary Effective Hamiltonians

A systematic method for constructing the effective Hamiltonian, valid to any order for a general stationary Hamiltonian, will now be presented. In fact, the method at the same time provides a general means of obtaining higher-order perturbative matrix elements in the presence of any finite number of intermediate resonances.

The time-dependent Schrödinger equation of the interacting system of “atom + field” is, as usual,

$$i\hbar \frac{\partial}{\partial t} \Psi(t) = H\Psi(t) \quad (7.5.1)$$

where

$$H = H_0 + V, \quad H_0 = H_{\text{atom}} + H_{\text{field}} \quad (7.5.2)$$

and V is the stationary “atom + field” interaction (in the quantum-field representation). It is convenient at this stage to introduce a suitable scaling constant W^0 , with respect to which all the energies may be measured, through the phase transformation

$$\Psi(t) = e^{-iW^0 t/\hbar} \psi(t) \quad (7.5.3)$$

Substitution of this expression in Eq. (7.5.1) yields

$$i\hbar \frac{\partial}{\partial t} \psi(t) = [H^0 + V]\psi(t) \quad (7.5.4)$$

where

$$H^0 = H_0 - W^0 \quad (7.5.5)$$

Below, we shall let H stand for $H^0 + V$.

For the conservative system at hand it suffices for our purpose to deal with the stationary equation corresponding to Eq. (7.5.4):

$$E\psi = H\psi = (H^0 + V)\psi \quad (7.5.6)$$

where E is the total-energy parameter. The time-dependent solution of Eq. (7.5.4) can be obtained from

$$\psi(t) = e^{-iHt/\hbar} \psi(0) \quad (7.5.7)$$

7.5.1. Separation of Resonant and Nonresonant States

We shall now separate the resonant or “quasi-resonant” states with zero or small detunings, from the “nonresonant” states with large detunings, making use of projection operators⁽¹⁴⁴⁾ p and q such that

$$p = \sum_j' |\phi_j\rangle\langle\phi_j| \quad (7.5.1.1)$$

and

$$q = 1 - p$$

where $H^0 |j\rangle = E_j |j\rangle$ provide the complete set of eigenstates $\{|j\rangle\}$ and eigenvalues $\{E_j\}$. The sum in expression (7.5.1.1) is only over the “quasi-resonant” product states $|\phi_j\rangle$ of H^0 , indicated by the prime on the summation sign.

We recall that the projection operators are by nature idempotent,

$$p^2 = p \quad \text{and} \quad q^2 = q \quad (7.5.1.2)$$

and orthogonal,

$$pq = 0 = qp \quad (7.5.1.3)$$

To separate the quasi-resonant from the nonresonant states we use the identity $p + q = 1$ on the left of ψ on both sides of Eq. (7.5.6) and operate from the left with p . This yields

$$E\psi_p = H_{pp}\psi_p + H_{pq}\psi_q \quad (7.5.1.4)$$

where the projected wave functions and Hamiltonians are given by

$$p\psi \equiv \psi_p, \quad q\psi \equiv \psi_q$$

and

$$pH_p \equiv H_{pp}, \quad pH_q \equiv H_{pq}$$

By operating similarly with q instead of p on the left side of Eq. (7.5.6), we get

$$E\psi_q = H_{qq}\psi_q + H_{qp}\psi_p \quad (7.5.1.6)$$

where

$$qHq \equiv H_{qq} \quad \text{and} \quad qHp \equiv H_{qp} \quad (7.5.1.7)$$

We may now use Eq. (7.5.1.6) to eliminate adiabatically the nonresonant part of the wave function ψ_q from Eq. (7.5.1.4) and obtain the wave equation for the “quasi-resonant” part ψ_p only. To this end Eq. (7.5.1.6) is first solved for ψ_q :

$$\psi_q = \frac{1}{E - H_{qq} \pm i0} H_{pq}\psi_p \quad (7.5.1.8)$$

where, as usual, the limit symbols $\pm i0$ are meant to be associated with the outgoing and ingoing boundary conditions, respectively. It should be understood below that the corresponding state vector ψ_q is also distinct, i.e., ψ_q^+ or ψ_q^- , respectively, and similarly for ψ_p . We shall, however, omit these signs unless an explicit distinction is necessary. It is also understood that the initial state, in the absence of the interaction, is included in the p -space and no homogeneous term is necessary to add on the right-hand side of Eq. (7.5.1.8). Substitution of solution (7.5.1.8) in Eq. (7.5.1.4) yields

$$E\psi_p = \hat{H}_{pp}(E)\psi_p \quad (7.5.1.9)$$

where

$$\hat{H}_{pp}(E) = H_{pp} + H_{pq} \frac{1}{E - H_{qq}} H_{qp} \quad (7.5.1.10)$$

Since in the present representation

$$H_{qq} = H_{qq}^0 + V_{qq} \quad (7.5.1.11)$$

and

$$H_{pq} = V_{pq} \quad (7.5.1.12)$$

[cf. Eq. (7.5.1.3): $H_{pq}^0 = 0$], therefore Eq. (7.5.1.10) actually reduces to

$$\hat{H}_{pp}(E) = H_{pp}^0 + V_{pp} + V_{pq} \frac{1}{E - H_{qq}^0 - V_{qq}} V_{qp} \quad (7.5.1.13)$$

It is tempting to interpret this expression as the effective Hamiltonian in the p -space of interest, since it has nonvanishing matrix elements only between the states in that space, and to consider Eq. (7.5.1.9) as the corresponding effective Schrödinger equation. In fact it is easily verified that the intuitively obtained effective Hamiltonians, Eqs. (7.2.5) or (7.2.6), can be obtained by expanding expression (7.5.1.13) in powers of V_{qq} and making the following approximations:

1. The energy parameter in expression (7.5.1.13) is approximated everywhere by $E = E_i$ (total initial energy).
2. The third- and higher-order terms in V are neglected.
3. The continuum-continuum coupling is dropped.

7.5.2. Derivation of the Effective Hamiltonian

Strictly speaking, however, $\hat{H}_{pp}(E)$ of expression (7.5.1.13) is not a Hamiltonian and Eq. (7.5.1.9) is not a Schrödinger equation, since the energy parameter E appears on both sides of Eq. (7.5.1.9) through its presence in $\hat{H}_{pp}(E)$. We shall see below that it is precisely the requirement of the removal of the E -dependence from the right-hand side of Eq. (7.5.1.9) that will generate the desired effective Hamiltonian to any given order of interest [and at the same time render Eq. (7.5.1.9) into a proper Schrödinger equation].

We set

$$D_q(E) \equiv E - H_{qq}^0 \quad (7.5.2.1)$$

and expand the third term of $\hat{H}_{pp}(E)$ on the right-hand side of Eq. (7.5.1.13) in the form

$$\begin{aligned} V_{pq} \frac{1}{E - H_{qq}^0 - V_{qp}} V_{qp} \\ = \left[V_{pq} \frac{1}{D_q(E)} V_{qp} + V_{pq} \frac{1}{D_q(E)} V_{qq} \frac{1}{D_q(E)} V_{qp} + \dots \right] \end{aligned} \quad (7.5.2.2)$$

Hence

$$\begin{aligned} \hat{H}_{pp}(E) = \left[H_{pp}^0 + V_{pp} + V_{pq} \frac{1}{D_q(E)} V_{qp} + V_{pq} \frac{1}{D_q(E)} V_{qq} \frac{1}{D_q(E)} V_{qp} + \dots \right] \\ (7.5.2.3) \end{aligned}$$

We may choose the scale constant W^0 equal to or on the order of any one of the unperturbed energies of the quasi-resonant states (in the p -space). Hence $H_{pp}^0 = (H_0 - W^0)_{pp}$ will be generally small, including the value zero.

On the other hand

$$\frac{1}{H_{qq}^0} = \frac{1}{(H_0 - W^0)_{qq}} \quad (7.5.2.4)$$

which has matrix elements only in the nonresonant q -space, is characterized by large denominators compared to both the interaction strength V and matrix elements $H_{pq}^0 = (H_0 - W^0)_{pq}$ (for a significantly wide range of intensities of practical interest). We may therefore usefully further expand the operator $\hat{H}_{pp}(E)$ given by Eq. (7.5.2.3) in powers of $1/H_{qq}^0$ to any desired order. To this end we first expand

$$\frac{1}{D_q(E)} = \frac{1}{E - H_{qq}^0} \quad (7.5.2.5)$$

in inverse forms of H_{qq}^0 :

$$\frac{1}{D_q(E)} = - \left[\frac{1}{H_{qq}^0} + \frac{1}{H_{qq}^0} E \frac{1}{H_{qq}^0} + \frac{1}{H_{qq}^0} E \frac{1}{H_{qq}^0} E \frac{1}{H_{qq}^0} + \dots \right] \quad (7.5.2.6)$$

We note that in terms of Eq. (7.5.2.3), Eq. (7.5.1.9) has the structure

$$E\psi_p = \left[H_{pp}^0 + V_{pp} + V_{pq} \frac{1}{D_q(E)} V_{qp} + V_{pq} \frac{1}{D_q(E)} V_{qq} \frac{1}{D_q(E)} V_{qp} + \dots \right] \psi_p \quad (7.5.2.7)$$

Application of expansion (7.5.2.6) everywhere on the right-hand side of Eq. (7.5.2.7) evidently leads to the operation of E on ψ_p on the extreme right. Repeated operations of E on ψ_p of the form $E\psi_p$, $E^2\psi_p$, etc., appear with increasingly higher orders in $1/H_{qq}^0$. Now $E\psi_p$, $E^2\psi_p$, etc., can be eliminated by successive use of the same equation (7.5.2.7) (the left-hand side gives $E\psi_p$, and hence it can be replaced by the right-hand side as many times as necessary). By this iteration procedure the right-hand operator in Eq. (7.5.2.7) is easily replaced by an equivalent operator \hat{H}_{pp} , which does not include the energy parameter E . In this way Eq. (7.5.2.7) reduces to a Schrödinger equation

$$E\psi_p = \hat{H}_{pp}\psi_p \quad (7.5.2.8)$$

where the desired effective Hamiltonian \hat{H}_{pp} is given by a perturbation

expansion

$$\hat{H}_{pp} = \sum_{n=0}^{\infty} H^{(n)} = H_{pp}^0 + \hat{V}_{pp} \quad (7.5.2.9)$$

where

$$\hat{V}_{pp} = \sum_{n=1}^{\infty} H^{(n)}$$

is the effective interaction operator. In terms of the unperturbed propagator in the q -space defined by

$$q \frac{1}{H_{qq}^0} q \equiv q \frac{1}{(H_0 - W^0)_{qq}} q \equiv G_{qq}^0(W^0) \equiv G_q^0 \quad (7.5.2.10)$$

we have the explicit result:

$$H^{(0)} = H_{pp}^0 \quad (7.5.2.11)$$

$$H^{(1)} = V_{pp}; \quad H_{pp} \equiv H^{(0)} + H^{(1)} \quad (7.5.2.12)$$

$$H^{(2)} = (VG_q^0 V)_{pp} \quad (7.5.2.13)$$

$$H^{(3)} = (VG_q^0 VG_q^0 V)_{pp} - (V(G_q^0)^2 V)_{pp} H_{pp} \quad (7.5.2.14)$$

$$\begin{aligned} H^{(4)} = & (VG_q^0 VG_q^0 VG_q^0 V)_{pp} - (V(G_q^0)^2 V)_{pp} (VG_p^0 V)_{pp} \\ & - (V(G_q^0)^2 VG_q^0 V)_{pp} H_{pp} - (VG_q^0 V (G_q^0)^2 V)_{pp} H_{pp} \\ & + (V(G_q^0)^3 V)_{pp} H_{pp} H_{pp} \end{aligned} \quad (7.5.2.15)$$

There is no basic difficulty in obtaining still higher-order contributions to the effective Hamiltonian. We quote results only up to $H^{(6)}$ in order to avoid excessive length:

$$\begin{aligned} H^{(5)} = & (VG_q^0 VG_q^0 VG_q^0 VG_q^0 V)_{pp} \\ & - \{(V(G_q^0)^2 VG_q^0 VG_q^0 V)_{pp} H_{pp} + (VG_q^0 V (G_q^0)^2 VG_q^0 V)_{pp} H_{pp} \\ & \quad + (VG_q^0 VG_q^0 V (G_q^0)^2 V)_{pp} H_{pp}\} - (V(G_q^0)^2 V)_{pp} (VG_q^0 VG_q^0 V)_{pp} \\ & - \{V(G_q^0)^2 VG_q^0 V)_{pp} (VG_q^0 V)_{pp} + (VG_q^0 V (G_q^0)^2 V)_{pp} (VG_q^0 V)_{pp}\} \\ & + (V(G_q^0)^2 V)_{pp} (V(G_q^0)^2 V)_{pp} H_{pp} \\ & + \{(V(G_q^0)^3 VG_q^0 V)_{pp} H_{pp} H_{pp} + (V(G_q^0)^2 V (G_q^0)^2 V)_{pp} H_{pp} H_{pp} \\ & \quad + (VG_q^0 V (G_q^0)^3 V)_{pp} H_{pp} H_{pp}\} + (V(G_q^0)^3 V)_{pp} H_{pp} (VG_q^0 V)_{pp} \\ & + (V(G_q^0)^3 V)_{pp} (VG_q^0 V)_{pp} H_{pp} - (V(G_q^0)^4 V)_{pp} H_{pp} H_{pp} H_{pp} \end{aligned} \quad (7.5.2.16)$$

and

$$\begin{aligned}
H^{(6)} = & (VG_q^0 VG_q^0 VG_q^0 VG_q^0 VG_q^0 V)_{pp} \\
& - \{(V(G_q^0)^2 VG_q^0 VG_q^0 VG_q^0 V)_{pp} H_{pp} + (VG_q^0 V(G_q^0)^2 VG_q^0 VG_q^0 V)_{pp} H_{pp} \\
& \quad + (VG_q^0 VG_q^0 V(G_q^0)^2 VG_q^0 V)_{pp} H_{pp} + (VG_q^0 VG_q^0 VG_q^0 V(G_q^0)^2 V)_{pp} H_{pp}\} \\
& - (V(G_q^0)^2 V)_{pp} (VG_q^0 VG_q^0 VG_q^0 V)_p \\
& - \{(V(G_q^0)^2 VG_q^0 V)_{pp} (VG_q^0 VG_q^0 V)_{pp} + (VG_q^0 V(G_q^0)^2 V)_{pp} (VG_q^0 VG_q^0 V)_{pp}\} \\
& - \{(V(G_q^0)^2 VG_q^0 VG_q^0 V)_{pp} (VG_q^0 V)_{pp} + (VG_q^0 V(G_q^0)^2 VG_q^0 V)_{pp} (VG_q^0 V)_{pp} \\
& \quad + (VG_q^0 VG_q^0 V(G_q^0)^2 V)_{pp} (VG_q^0 V)_{pp}\} \\
& + \{(V(G_q^0)^2 V)_{pp} (V(G_q^0)^2 VG_q^0 V)_{pp} H_{pp} + (V(G_q^0)^2 V)_{pp} (VG_q^0 V(G_q^0)^2 V)_{pp} H_{pp}\} \\
& + \{(V(G_q^0)^2 VG_q^0 V)_{pp} (V(G_q^0)^2 V)_{pp} H_{pp} + (VG_q^0 V(G_q^0)^2 V)_{pp} (V(G_q^0)^2 V)_{pp} H_{pp}\} \\
& + (V(G_q^0)^2 V)_{pp} (V(G_q^0)^2 V)_{pp} (VG_q^0 V)_{pp} - (V(G_q^0)^2 V)_{pp} (V(G_q^0)^3 V)_{pp} H_{pp} H_{pp} \\
& + \{(V(G_q^0)^3 VG_q^0 VG_q^0 V)_{pp} H_{pp} H_{pp} + (V(G_q^0)^2 V(G_q^0)^2 VG_q^0 V)_{pp} H_{pp} H_{pp} \\
& \quad + (V(G_q^0)^2 VG_q^0 V(G_q^0)^2 V)_{pp} H_{pp} H_{pp} + (VG_q^0 V(G_q^0)^3 VG_q^0 V)_{pp} H_{pp} H_{pp}\} \\
& + (V(G_q^0)^3 V)_{pp} H_{pp} (VG_q^0 VG_q^0 V)_{pp} \\
& + \{(V(G_q^0)^3 VG_q^0 V)_{pp} H_{pp} (VG_q^0 V)_{pp} + (V(G_q^0)^2 V(G_q^0)^2 V)_{pp} H_{pp} (VG_q^0 V)_{pp} \\
& \quad + (VG_q^0 V(G_q^0)^3 V)_{pp} H_{pp} (VG_q^0 V)_{pp}\} \\
& - (V(G_q^0)^3 V)_{pp} H_{pp} (V(G_q^0)^2 V)_{pp} H_{pp} + (V(G_q^0)^3 V)_{pp} (VG_q^0 VG_q^0 V)_{pp} H_{pp} \\
& + \{(V(G_q^0)^3 VG_q^0 V)_{pp} (VG_q^0 V)_{pp} H_{pp} + (V(G_q^0)^2 V(G_q^0)^2 V)_{pp} (VG_q^0 V)_{pp} H_{pp} \\
& \quad + (VG_q^0 V(G_q^0)^3 V)_{pp} (VG_q^0 V)_{pp} H_{pp}\} \\
& + (V(G_q^0)^3 V)_{pp} (VG_q^0 V)_{pp} (VG_q^0 V)_{pp} - (V(G_q^0)^3 V)_{pp} (V(G^0)^2 V)_{pp} H_{pp} H_{pp} \\
& - \{(V(G_q^0)^4 VG_q^0 V)_{pp} H_{pp} H_{pp} H_{pp} + (V(G_q^0)^3 V(G_q^0)^2 V)_{pp} H_{pp} H_{pp} H_{pp} \\
& \quad + (V(G_q^0)^2 V(G_q^0)^3 V)_{pp} H_{pp} H_{pp} H_{pp} + (VG_q^0 V(G_q^0)^4 V)_{pp} H_{pp} H_{pp} H_{pp}\} \\
& - (V(G_q^0)^4 V)_{pp} H_{pp} H_{pp} (VG_q^0 V)_{pp} - (V(G_q^0)^4 V)_{pp} H_{pp} (VG_q^0 V)_{pp} H_{pp} \\
& - (V(G_q^0)^4 V)_{pp} (VG_q^0 V)_{pp} H_{pp} H_{pp} + (V(G_q^0)^5 V)_{pp} H_{pp} H_{pp} H_{pp} H_{pp}
\end{aligned} \tag{7.5.2.17}$$

Thus there are 14 and 42 terms in the fifth and sixth orders, respectively. It is noteworthy that they may be expressed also in terms of the derivatives of the Green's function in the q -space: this could be useful for higher-order computations. Thus using the notation

$$V^{(n)} \equiv (VG_q^0 VG_q^0 VG_q^0 V \cdots VG_q^0 V) \tag{7.5.2.18}$$

where $G_q^0 = G_q^0(W_0)$ [which depends on the energy constant W_0 , see Eq. (7.5.3)] appears $(n - 1)$ times, the terms collected together in the curly brackets in expressions (7.5.2.16) and (7.5.2.17) may be expressed in terms of the derivatives of $V^{(n)}(W_0)$ with respect to the energy W_0 . Thus expressed, $H^{(5)}$ reduces to the sum of nine terms, namely

$$\begin{aligned}
 H^{(5)} = & V_{pp}^{(5)} + \left(\frac{\partial}{\partial W_0} V^{(4)} \right)_{pp} H_{pp} + \left(\frac{\partial}{\partial W_0} V^{(2)} \right)_{pp} V_{pp}^{(3)} + \left(\frac{\partial}{\partial W_0} V^{(3)} \right)_{pp} V_{pp}^{(2)} \\
 & + \left(\frac{\partial}{\partial W_0} V^{(2)} \right)_{pp} \left(\frac{\partial}{\partial W_0} V^{(2)} \right)_{pp} H_{pp} + \frac{1}{2!} \left(\frac{\partial^2}{\partial W_0^2} V^{(3)} \right)_{pp} (H_{pp})^2 \\
 & + \frac{1}{2!} \left(\frac{\partial^2}{\partial W_0^2} V^{(2)} \right)_{pp} H_{pp} V_{pp}^{(2)} + \frac{1}{2!} \left(\frac{\partial^2}{\partial W_0^2} V^{(2)} \right)_{pp} V_{pp}^{(2)} H_{pp} \\
 & + \frac{1}{3!} \left(\frac{\partial^3}{\partial W_0^3} V^{(2)} \right)_{pp} (H_{pp})^3
 \end{aligned} \tag{7.5.2.19}$$

Similarly, $H^{(6)}$ reduces to the following sum of 22 terms only:

$$\begin{aligned}
 H^{(6)} = & V_{pp}^{(6)} + \left(\frac{\partial}{\partial W_0} V^{(5)} \right)_{pp} H_{pp} + \left(\frac{\partial}{\partial W_0} V^{(2)} \right)_{pp} V_{pp}^{(4)} + \left(\frac{\partial}{\partial W_0} V^{(3)} \right)_{pp} V_{pp}^{(3)} \\
 & + \left(\frac{\partial}{\partial W_0} V^{(4)} \right)_{pp} V_{pp}^{(2)} + \left(\frac{\partial}{\partial W_0} V^{(2)} \right)_{pp} \left(\frac{\partial}{\partial W_0} V^{(3)} \right)_{pp} H_{pp} \\
 & + \left(\frac{\partial}{\partial W_0} V^{(3)} \right)_{pp} \left(\frac{\partial}{\partial W_0} V^{(2)} \right)_{pp} H_{pp} + \left(\frac{\partial}{\partial W_0} V^{(2)} \right)_{pp} \left(\frac{\partial}{\partial W_0} V^{(2)} \right)_{pp} V_{pp}^{(2)} \\
 & + \left(\frac{\partial}{\partial W_0} V^{(2)} \right)_{pp} \frac{1}{2!} \left(\frac{\partial^2}{\partial W_0^2} V^{(2)} \right)_{pp} (H_{pp})^2 + \frac{1}{2!} \left(\frac{\partial^2}{\partial W_0^2} V^{(4)} \right)_{pp} (H_{pp})^2 \\
 & + \frac{1}{2!} \left(\frac{\partial^2}{\partial W_0^2} V^{(2)} \right)_{pp} H_{pp} V_{pp}^{(3)} + \frac{1}{2!} \left(\frac{\partial^2}{\partial W_0^2} V^{(3)} \right)_{pp} H_{pp} V_{pp}^{(2)} \\
 & + \frac{1}{2!} \left(\frac{\partial^2}{\partial W_0^2} V^{(2)} \right)_{pp} H_{pp} \left(\frac{\partial}{\partial W_0} V^{(2)} \right)_{pp} H_{pp} + \frac{1}{2!} \left(\frac{\partial^2}{\partial W_0^2} V^{(2)} \right)_{pp} V_{pp}^{(3)} H_{pp} \\
 & + \frac{1}{2!} \left(\frac{\partial^2}{\partial W_0^2} V^{(3)} \right)_{pp} V_{pp}^{(2)} H_{pp} + \frac{1}{2!} \left(\frac{\partial^2}{\partial W_0^2} V^{(2)} \right)_{pp} V_{pp}^{(2)} V_{pp}^{(2)} \\
 & + \frac{1}{2!} \left(\frac{\partial^2}{\partial W_0^2} V^{(2)} \right)_{pp} \left(\frac{\partial}{\partial W_0} V^{(2)} \right)_{pp} (H_{pp})^2 + \frac{1}{3!} \left(\frac{\partial^3}{\partial W_0^3} V^{(3)} \right)_{pp} (H_{pp})^3 \\
 & + \frac{1}{3!} \left(\frac{\partial^3}{\partial W_0^3} V^{(2)} \right)_{pp} (H_{pp})^2 V_{pp}^{(2)} + \frac{1}{3!} \left(\frac{\partial^3}{\partial W_0^3} V^{(2)} \right)_{pp} H_{pp} V_{pp}^{(2)} H_{pp} \\
 & + \frac{1}{3!} \left(\frac{\partial^3}{\partial W_0^3} V^{(2)} \right)_{pp} V_{pp}^{(2)} (H_{pp})^2 + \frac{1}{4!} \left(\frac{\partial^4}{\partial W_0^4} V^{(2)} \right)_{pp} (H_{pp})^4
 \end{aligned} \tag{7.5.2.20}$$

It is now easy to see that the intuitively derived effective Hamiltonians, Eq. (7.2.5) or (7.2.6), are reobtained from the general expansion (7.5.2.9), truncated up to second order:

$$\hat{H}_{pp} \approx H_{pp}^0 + V_{pp} + V_{pq} G_q^0(E_i) V_{qp} \quad (7.5.2.21)$$

where we have chosen $W_0 = E_i$.

It is interesting that the expressions for $H^{(n)}$ as such also provide the perturbed energy of an arbitrarily given state in the p -space. Thus, for example, retaining a single state ϕ_i in the p -space and assuming that the perturbation V (e.g., the dipole interaction) is of odd parity and state ϕ_i possesses a definite parity, we have

$$H_u^{(0)} = (E_i - W_0) = 0 \quad (7.5.2.22)$$

and

$$H_u^{(1)} = V_u = 0 \quad (7.5.2.23)$$

and hence, from relations (7.5.2.12),

$$H_u \equiv H_u^{(0)} + H_u^{(1)} = 0 \quad (7.5.2.24)$$

Thus for the case of a single state in the p -space, the choice $W^0 = E_i$ is most economical in that all terms involving H_u automatically drop out, in all orders. The first nonvanishing correction to the energy of a state ϕ_i arises in the second order. Expression (7.5.2.13) yields

$$H_u^{(2)} = \sum_{j \neq i} V_{ij} \frac{1}{E_i - E_j} V_{ji} \quad (7.5.2.25)$$

which is the well-known result. Furthermore, the first term of $H_u^{(3)}$ in Eq. (7.5.2.14) vanishes because of the parity conditions, and the second term of Eq. (7.5.2.14) vanishes due to Eq. (7.5.2.24). Hence, as expected, in this case

$$H_u^{(3)} = 0 \quad (7.5.2.26)$$

The fourth-order correction now simplifies, because of Eq. (7.5.2.24), to the first two terms in expression (7.5.2.15):

$$H_u^{(4)} = \sum_{\substack{(j_1, j_2, j_3) \\ (\neq i)}} V_{ij_1} \frac{1}{E_i - E_{j_1}} V_{j_1 j_2} \frac{1}{E_i - E_{j_2}} V_{j_2 j_3} \frac{1}{E_i - E_{j_3}} V_{j_3 i} - \left[\sum_{j \neq i} \left(V_{ij} \frac{1}{(E_i - E_j)^2} V_{ji} \right) \right] \left[\sum_{j \neq i} \left(V_{ij} \frac{1}{E_i - E_j} V_{ji} \right) \right] \quad (7.5.2.27)$$

Hence we may rewrite

$$H_u^{(4)} = V_u^{(4)} + \left(\frac{\partial}{\partial E_i} V_u^{(2)} \right) V_u^{(2)} \quad (7.5.2.28)$$

where $V_u^{(4)}$ stands for the triple sum in expression (7.5.2.27) and $V_u^{(2)}$ is the same as $H_u^{(2)}$ of Eq. (7.5.2.25). Equation (7.5.2.28) exactly reproduces the fourth-order energy correction⁽¹⁴⁵⁾ to a given state ϕ_i in the nonresonant situation. Similarly, the fifth- and sixth-order energies are obtained from expressions (7.5.2.19) and (7.5.2.20), reduced by setting $H_u = 0$ throughout.

Thus the present method provides a generalization of the Rayleigh-Schrödinger perturbation theory for a single nondegenerate state to a group of degenerate (or quasi-degenerate) states (i.e., for the states in p). In fact, the effective Hamiltonian developed here can be viewed as a general formulation of the usual degenerate perturbation theory.

Clearly this theory applies formally to any interaction Hamiltonian V . For the multiphoton-interaction Hamiltonian of interest, such as Eqs. (3.2.1)–(3.2.5), the following special situation and resulting simplification are worth noting. Let us restrict ourselves to only two states, ϕ_i and ϕ_f , in the p -space. Let $\phi_i = |\varepsilon_i\rangle|n_i\rangle$ and $\phi_f = |\varepsilon_f\rangle|n_f\rangle$, where n_i and n_f are the photon occupation numbers and $|\varepsilon_i\rangle$ and $|\varepsilon_f\rangle$ are the atomic states. If $n_i - n_f \neq \pm 1$, for instance in the case of transitions involving absorption or emission of more than one photon or for no net absorption or emission of photons, the latter case occurs in the process of dynamic Stark effects,^(146–149) then the matrix elements are given by

$$V_{fi} = \langle \varepsilon_f | \mathbf{D} \cdot \frac{\mathbf{e}}{2} | \varepsilon_i \rangle \left(\frac{2\pi\hbar\omega}{L^3} \right)^{1/2} \langle n_f | (a^+ + a) | n_i \rangle = 0 \quad (7.5.2.29)$$

since

$$\langle n_f | a^+ + a | n_i \rangle = 0 \quad \text{for } n_i - n_f \neq \pm 1 \quad (7.5.2.30)$$

and $V_u = V_{ff} = 0$ due to the fixed parity of states ϕ_i and ϕ_f and of operator \mathbf{D} . Also,

$$H_{fi}^0 = (W^0 - H_0)_{fi} = (W^0 - E_i)\delta_{if} = 0 \quad \text{for } i \neq f \quad (7.5.2.31)$$

$$H_u^0 = 0 \quad \text{for the choice } W_0 = E_i \quad (7.5.2.32)$$

$$H_{ff}^0 = 0 \quad \text{on the energy shell } E_i = E_f = W_0 \quad (7.5.2.33)$$

Hence $H_{pp} = 0$ with $p = |\phi_i\rangle\langle\phi_i| + |\phi_f\rangle\langle\phi_f|$ and the expression for the effective Hamiltonian (7.5.2.9) simplifies considerably, particularly at higher orders. Thus we obtain the following fully renormalized perturbative matrix elements for transitions ($n_i - n_f \neq \pm 1$) between states ϕ_i and ϕ_f

considered on the unperturbed energy shell, $E_i = E_f$:

$$H_{pp} \equiv H^{(0)} + H^{(1)} = 0 \quad (7.5.2.34)$$

$$H^{(2)} = (VG_q^0 V)_{pp} \quad (7.5.2.35)$$

$$H^{(3)} = (VG_q^0 VG_q^0 V)_{pp} \quad (7.5.2.36)$$

$$H^{(4)} = (VG_q^0 VG_q^0 VG_q^0 V)_{pp} - (V(G_q^0)^2 V)_{pp} (VG_q^0 V)_{pp} \quad (7.5.2.37)$$

$$\begin{aligned} H^{(5)} &= (VG_q^0 VG_q^0 VG_q^0 VG_q^0 V)_{pp} - (V(G_q^0)^2 V)_{pp} (VG_q^0 VG_q^0 V)_{pp} \\ &\quad - \{(V(G_q^0)^2 VG_q^0 V)_{pp} + (VG_q^0 V(G_q^0)^2 V)_{pp}\} (VG_q^0 V)_{pp} \end{aligned} \quad (7.5.2.38)$$

$$\begin{aligned} H^{(6)} &= V_{pp}^{(6)} + \left(\frac{\partial}{\partial W_0} V^{(2)} \right)_{pp} V_{pp}^{(4)} + \left(\frac{\partial}{\partial W_0} V^{(3)} \right)_{pp} V_{pp}^{(3)} \\ &\quad + \left(\frac{\partial}{\partial W_0} V^{(4)} \right)_{pp} V_{pp}^{(2)} + \left(\frac{\partial}{\partial W_0} V^{(2)} \right)_{pp} \left(\frac{\partial}{\partial W_0} V^{(2)} \right)_{pp} V_{pp}^{(2)} \\ &\quad + \frac{1}{2!} \left(\frac{\partial^2}{\partial W_0^2} V^{(2)} \right)_{pp} V_{pp}^{(2)} V_{pp}^{(2)} \end{aligned} \quad (7.5.2.39)$$

7.6. Theory of Time-Varying Effective Hamiltonians

Until now we have considered radiation fields with constant amplitudes and phases of the form

$$\mathbf{F}(t) = \epsilon F_0 \cos(\omega t + \delta) \quad (7.6.1)$$

or its quantum version

$$\mathbf{F}(t) = \epsilon \left(\frac{2\pi\hbar\omega}{L^3} \right)^{1/2} (a^+ + a) \quad (7.6.2)$$

Sometimes it becomes essential to consider the effect of the time variation of amplitude F_0 and phase δ of the radiation field. For example, pulsed laser radiation often has the form

$$\mathbf{F}(t) = \epsilon E(t) \cos(\omega t + \phi(t)) \quad (7.6.3)$$

where $E(t)$ and $\phi(t)$ are slowly varying functions of time and describe the envelopes of the real amplitude and phase, respectively. It is also common to write Eq. (7.6.3) in the alternative form

$$\mathbf{F}(t) = \frac{\epsilon}{2} [e(t) e^{i\omega t} + e^*(t) e^{-i\omega t}] \quad (7.6.4)$$

where

$$e(t) \equiv E(t) e^{i\phi(t)} \quad \text{or} \quad e^*(t) \equiv E(t) e^{-i\phi(t)} \quad (7.6.5)$$

is known as the “complex envelope” of the field $\mathbf{F}(t)$.

The time variation of the envelope functions are generally slow compared to the time variation of the field with respect to the central frequency ω . For many pulsed lasers, typical time periods of significant change of the complex envelope $e(t)$ may lie in the region, say, 10^{-7} – 10^{-12} s. This is very much larger than a typical optical period $1/\omega \approx 10^{-16}$ s. The envelope functions are thus generally assumed to satisfy the conditions

$$\frac{\dot{E}(t)}{E(t)} \ll \omega \quad \text{and} \quad \dot{\phi} \ll \omega \quad (7.6.6)$$

where the dot implies derivative with respect to time t , or, in terms of the complex envelope $e(t)$, it is assumed that

$$\frac{1}{\omega} \left| \frac{\dot{e}(t)}{e(t)} \right| \ll 1 \quad (7.6.7)$$

The Schrödinger equation for an atom in a time-dependent field $\mathbf{F}(t)$ of the form (7.6.4) is

$$i\hbar \frac{\partial}{\partial t} \psi(t) = \left\{ H_{\text{atom}} + \boldsymbol{\epsilon} \cdot \frac{\mathbf{D}}{2} [e(t) e^{i\omega t} + e^*(t) e^{-i\omega t}] \right\} \psi(t) \quad (7.6.8)$$

One may reduce Eq. (7.6.8) to a set of “slowly varying envelope equations” whose time dependence will be governed by the slowly varying complex envelope functions only.

Let us expand $\psi(t)$ as

$$\psi(t) = \sum_{n=-\infty}^{\infty} \psi_n(t) e^{in\omega t} \quad (7.6.9)$$

where quantities $\psi_n(t)$ depend on the time parameter t , but slowly. By substituting expansion (7.6.9) in Eq. (7.6.8) and collecting the coefficients of $e^{in\omega t}$ in the resulting equations, one easily finds that

$$\begin{aligned} \sum_{n=-\infty}^{\infty} e^{in\omega t} & \left\{ i\hbar \frac{\partial}{\partial t} \psi_n(t) - (H_{\text{atom}} + n\hbar\omega) \psi_n(t) \right. \\ & \left. - \boldsymbol{\epsilon} \cdot \frac{\mathbf{D}}{2} [e(t) \psi_{n-1}(t) + e^*(t) \psi_{n+1}(t)] \right\} = 0 \end{aligned} \quad (7.6.10)$$

Thus to satisfy Eq. (7.6.8) it is sufficient that the quantity in the curly brackets in Eq. (7.6.10) vanishes for each $n = 0, \pm 1, \pm 2, \pm 3, \dots$, etc. The particular solutions thus obtained [the above condition is not necessary for Eq. (7.6.8) to be satisfied generally] are governed by the equation

$$i\hbar \frac{\partial}{\partial t} \psi_n(t) = (H_{\text{atom}} + n\hbar\omega)\psi_n(t) + \frac{\boldsymbol{\epsilon} \cdot \mathbf{D}}{2} [e(t)\psi_{n-1}(t) + e^*(t)\psi_{n+1}(t)] \quad (7.6.11)$$

with

$$n = 0, \pm 1, \pm 2, \pm 3, \dots, \pm \infty$$

They are physically justified due to the presence of two usually very different time scales of change in the field and its envelope. Equations (7.6.11) will be referred to as the “slowly varying envelope equations,” since the perturbation terms now contain only the slowly varying envelope functions. Before proceeding to develop the time-dependent effective Hamiltonian it is useful to compare a quasi-quantum analog of the semiclassical Eq. (7.6.11).

7.6.1. The Quasi-Quantum Envelope Equations

We consider the following quantum “field + atom” equation in the Schrödinger representation

$$i\hbar \frac{\partial}{\partial t} |\psi(t)\rangle = \left\{ H_{\text{atom}} + a^+ a \hbar\omega + \boldsymbol{\epsilon} \cdot \mathbf{D} \left(\frac{2\pi\hbar\omega}{L^3} \right)^{1/2} [\tilde{e}(t)a + \tilde{e}^*(t)a^+] \right\} |\psi(t)\rangle \quad (7.6.1.1)$$

where $\tilde{e}(t)$ is a dimensionless slowly varying function of time with unit maximum, and $\tilde{e}^*(t)$ is the complex conjugate of $\tilde{e}(t)$.

Let us expand the state vector $|\psi(t)\rangle$ in the complete set of number states $\{|n'\rangle\}$, which are generated by

$$H_{\text{rad}} |n'\rangle = a^+ a \hbar\omega |n'\rangle = n' \hbar\omega |n'\rangle \quad (7.6.1.2)$$

Thus

$$|\psi(t)\rangle = \sum_n \psi_n(t) |n' + n_0\rangle \quad (7.6.1.3)$$

where n_0 is the “initial mean occupation number,” which is generally very

large compared to any relevant departure n from n_0 , namely

$$\left(\frac{n_0}{L^3}\right) \gg \left(\frac{n}{L^3}\right) \quad (7.6.1.4)$$

If expansion (7.6.1.3) is substituted in Eq. (7.6.1.1) and we project onto the state $\langle n + n_0 |$, we get

$$\begin{aligned} i\hbar \frac{\partial}{\partial t} \psi_n(t) &= [H_{\text{atom}} + (n_0 + n)\hbar\omega] \psi_n(t) \\ &+ \boldsymbol{\epsilon} \cdot \frac{\mathbf{D}}{2} [F_{n+1}^0 \tilde{e}(t) \psi_{n+1}(t) + F_n^0 \tilde{e}^*(t) \psi_{n-1}(t)] \end{aligned} \quad (7.6.1.5)$$

where

$$F_n^0 = \left(\frac{8\pi\hbar\omega(n_0 + n)}{L^3}\right)^{1/2} \quad (7.6.1.6)$$

Comparison of Eqs. (7.6.11) and (7.6.1.5) shows immediately that they are equivalent, provided we choose functions $\tilde{e}(t)$ such that

$$e(t) = F_0 \tilde{e}(t) \quad (7.6.1.7)$$

where

$$F_0 = \left(\frac{8\pi\hbar\omega n_0}{L^3}\right)^{1/2} \approx F_n^0 \approx F_{n+1}^0 \quad (7.6.1.8)$$

In this relation we assume as usual the validity of the excellent “laser approximation,” Eq. (7.6.1.4), and adopt the convention of measuring the photon occupation energy on a scale in which the initial occupation energy is the origin.

In general, we may introduce an arbitrary (real) scaling constant W^0 (which may be fixed in the end according to convenience) by the phase transformation

$$\psi(t) \Rightarrow e^{-iW^0 t/\hbar} \psi(t) \quad (7.6.1.9)$$

and write Eq. (7.6.1.1) in the form

$$i\hbar \frac{\partial}{\partial t} \psi(t) = [H^0 + V(t)] \psi(t) \equiv H(t) \psi(t) \quad (7.6.1.10)$$

where

$$H^0 \equiv H_0 - W^0 = H_{\text{atom}} + a^+ a \hbar\omega - W^0 \quad (7.6.1.11)$$

and

$$V(t) \equiv \epsilon \cdot \frac{\mathbf{D}}{2} \left(\frac{8\pi\hbar\omega}{L^3} \right)^{1/2} [\tilde{e}(t)a + \tilde{e}^*(t)a^+] \quad (7.6.1.12)$$

Equation (7.6.1.10) is obviously the analog of the stationary equation (7.5.3) to which it reduces in the special case where $\tilde{e}(t)$ is replaced throughout by its maximum value, unity. Equation (7.6.1.10) along with Eqs. (7.6.1.11) and (7.6.1.12) are to be referred to as the “quasi-quantum envelope equation.”

7.6.2. Renormalized Perturbation Theory with Slowly Varying Fields and the Effective Hamiltonian

We generalize the method of Section 7.5 to the present time-dependent case. It consists of a systematic way of getting higher-order “on-shell” matrix elements between arbitrary pairs of states, which are automatically renormalized. The result will provide the necessary time-dependent generalization of the effective Hamiltonian in the presence of an arbitrary (but finite) number of intermediate resonances. Because of its compactness, it is now more convenient to work directly with the quasi-quantum envelope equation (7.6.1.10) than with its semiclassical equivalent, Eqs. (7.6.11).

We divide the reference states into “quasi-resonant” and “nonresonant” parts. In spite of the nonconservative nature of Eq. (2.6.1.10) there is no need to introduce explicitly time-dependent projection operators for this purpose (since H^0 itself is stationary). We therefore use the same projectors p and q for projecting onto the “quasi-resonant” space (p) and onto the “nonresonant” space ($q = 1 - p$), as defined in Eqs. (7.5.1.2) and (7.5.1.3). By inserting, as before, the identity operator $p + q = 1$ on the left of $\psi(t)$ in both sides of Eq. (7.6.1.10) and projecting onto the left with p or with q , we obtain the pair of time-dependent equations

$$i\hbar \frac{\partial}{\partial t} \psi_p(t) = H_{pp}(t)\psi_p(t) + H_{pq}(t)\psi_q(t) \quad (7.6.2.1)$$

$$i\hbar \frac{\partial}{\partial t} \psi_q(t) = H_{qq}(t)\psi_q(t) + H_{qp}(t)\psi_p(t) \quad (7.6.2.2)$$

in which we have introduced the following abbreviations:

$$\begin{aligned} p | \psi(t) \rangle &\equiv \psi_p(t), & pH(t)p &\equiv H_{pp}(t), & pH(t)q &\equiv H_{pq}(t) \\ q | \psi(t) \rangle &\equiv \psi_q(t), & qH(t)q &\equiv H_{qq}(t), & qH(t)p &\equiv H_{qp}(t) \end{aligned}$$

The above operators reduce in the present representation to

$$H_{pp}(t) = H_{pp}^0 + V_{pp}(t), \quad H_{pq}(t) = V_{pq}(t) \quad (7.6.2.3)$$

and

$$H_{qq}(t) = H_{qq}^0 + V_{qq}(t), \quad H_{qp}(t) = V_{qp}(t) \quad (7.6.2.4)$$

We may proceed further by formally solving for $\psi_q(t)$. Equation (7.6.2.2) yields

$$\psi_q(t) = \frac{1}{i\hbar\partial/\partial t - H_{qq}(t)} V_{qp}(t)\psi_p(t) \quad (7.6.2.5)$$

In writing the above “solution” $\psi_q(t)$ it is supposed that the initial state (or states) are included in the p -space, hence no homogeneous part is added to Eq. (7.6.2.5). The nonresonant wave function $\psi_q(t)$ is now eliminated (adiabatically) by substituting expression (7.6.2.5) in relation (7.6.2.1). We obtain the projected equation in the space of the “quasi-resonant” states only:

$$i\hbar \frac{\partial}{\partial t} \psi_p(t) = \left[H_{pp}(t) + V_{pq}(t) \frac{1}{i\hbar\partial/\partial t - H_{qq}(t)} V_{qp}(t) \right] \psi_p(t) \quad (7.6.2.6)$$

This is the generalization of the conservative equation (7.5.1.9). The explicitly time-dependent operator

$$\hat{H}_{pp}(t) = \left[H_{pp}(t) + V_{pq}(t) \frac{1}{i\hbar\partial/\partial t - H_{qq}(t)} V_{qp}(t) \right] \quad (7.6.2.7)$$

is the analog of Eq. (7.5.1.10). It is important to note that Eq. (7.6.2.6) is not, strictly speaking, a Schrödinger equation since the energy operator $i\hbar\partial/\partial t$ arises not only on the left-hand side but also on the right-hand side of Eq. (7.6.2.6) and, indeed, in a rather involved way through the generator $\hat{H}_{pp}(t)$. One may, however, eliminate the time-derivative operator from $\hat{H}_{pp}(t)$ in a systematic way at arbitrarily higher orders of the perturbation theory, in a manner rather analogous to the procedure adopted in the stationary case. Care must naturally now be taken of the effect of the operator $i\hbar\partial/\partial t$ on the interaction $V(t)$ as well as on the wave function $\psi_p(t)$ during the elimination procedure.

Let us define

$$D_q(t) = \left(i\hbar \frac{\partial}{\partial t} - H_{qq}^0 \right) \quad (7.6.2.8)$$

and expand the inverse operator in Eq. (7.6.2.6) as

$$\begin{aligned}\frac{1}{i\hbar \frac{\partial}{\partial t} - H_{qq}^0 - V_{qq}(t)} &= \frac{1}{D_q(t) \left[1 - \frac{1}{D_q(t)} V_{qq}(t) \right]} \\ &= \frac{1}{D_q(t)} + \frac{1}{D_q(t)} V_{qq}(t) \frac{1}{D_q(t)} \\ &\quad + \frac{1}{D_q(t)} V_{qq}(t) \frac{1}{D_q(t)} V_{qq}(t) \frac{1}{D_q(t)} + \dots \quad (7.6.2.9)\end{aligned}$$

We also develop $1/D_q(t)$ in inverse powers of H_{qq}^0 . From Eq. (7.6.2.8) we obtain

$$\begin{aligned}\frac{1}{D_q(t)} &= \frac{1}{i\hbar \frac{\partial}{\partial t} - H_{qq}^0} = - \left(1 - \frac{1}{H_{qq}^0} \delta_t \right)^{-1} \frac{1}{H_{qq}^0} \\ &= - \left(\frac{1}{H_{qq}^0} + \frac{1}{H_{qq}^0} \delta_t \frac{1}{H_{qq}^0} + \frac{1}{H_{qq}^0} \delta_t \frac{1}{H_{qq}^0} \delta_t \frac{1}{H_{qq}^0} + \dots \right) \quad (7.6.2.10)\end{aligned}$$

where

$$\delta_t \equiv i\hbar \frac{\partial}{\partial t} \quad (7.6.2.11)$$

Using Eqs. (7.6.2.9) and (7.6.2.10) in Eq. (7.6.2.6) we may operate successively on the right with δ_t and express the right-hand side of Eq. (7.6.2.6) in terms of the derivatives of $V(t)$ [$\dot{V}(t)$, $\ddot{V}(t)$, etc.] and $\delta_t \psi_p(t)$, $(\delta_t)^2 \psi_p(t)$, etc., occurring with increasing powers of $1/H_{qq}^0$. But $\delta_t \psi_p(t)$ is the left-hand side of Eq. (7.6.2.6). Therefore it may be replaced by the right-hand side again and the process iterated as many times as necessary. The reader will notice the analogy of the process of eliminating $\delta_t \psi_p(t)$, $(\delta_t)^2 \psi_p(t)$, etc., in the present case with the manner of eliminating $E\psi_p$, $E^2 \psi_p$, etc., in the stationary case. In this way one may finally obtain the proper Schrödinger equation in the p -space, to an arbitrary order,

$$i\hbar \frac{\partial}{\partial t} \psi_p(t) = \sum_{n=0}^{\infty} H^{(n)}(t) \psi_p(t) \quad (7.6.2.12)$$

where

$$\hat{H}_{pp}(t) = \sum_{n=0}^{\infty} H^{(n)}(t) \equiv H_{pp}^0 + \hat{V}_{pp}(t) \quad (7.6.2.13)$$

and

$$\hat{V}_{pp}(t) \equiv \sum_{n=1}^{\infty} H^{(n)}(t) \quad (7.6.2.14)$$

are the desired time-dependent effective Hamiltonian and effective interaction operator, respectively. We quote below the first few terms of $H^{(n)}(t)$ explicitly [with $\delta_i V(t) \equiv \dot{V}(t)$, $\delta_i^2 V(t) \equiv \ddot{V}(t)$, etc.]:

$$H^{(0)}(t) = H_{pp}^0 \quad (7.6.2.15)$$

$$H^{(1)}(t) = V_{pp}(t); \quad H^{(0)}(t) + H^{(1)}(t) = H_{pp}(t) \quad (7.6.2.16)$$

$$H^{(2)}(t) = (V(t)G_q^0 V(t))_{pp} \quad (7.6.2.17)$$

$$\begin{aligned} H^{(3)}(t) = & (V(t)G_q^0 V(t)G_q^0 V(t))_{pp} - (V(t)(G_q^0)^2 V(t))_{pp} H_{pp}(t) \\ & - (V(t)(G_q^0)^2 \dot{V}(t))_{pp} \end{aligned} \quad (7.6.2.18)$$

$$\begin{aligned} H^{(4)}(t) = & [(V(t)G_q^0 V(t)G_q^0 V(t)G_q^0 V(t))_{pp} \\ & - (V(t)(G_q^0)^2 V(t))_{pp} (V(t)G_q^0 V(t))_{pp} \\ & - (V(t)(G_q^0)^2 V(t)G_q^0 V(t))_{pp} H_{pp}(t) \\ & - (V(t)G_q^0 V(t)(G_q^0)^2 V(t))_{pp} H_{pp}(t) \\ & + (V(t)(G_q^0)^3 V(t))_{pp} H_{pp}(t) H_{pp}(t)] \\ & + [-(V(t)G_q^0 V(t)(G_q^0)^2 \dot{V}(t))_{pp} - (V(t)(G_q^0)^2 \dot{V}(t)(G_q^0) V(t))_{pp} \\ & - (V(t)(G_q^0)^2 V(t)G_q^0 \dot{V}(t))_{pp} + (V(t)(G_q^0)^3 V(t))_{pp} (\dot{V}(t))_{pp} \\ & + 2(V(t)(G_q^0)^3 \dot{V}(t))_{pp} H_{pp}(t) + (V(t)(G_q^0)^3 \ddot{V}(t))_{pp}] \end{aligned} \quad (7.6.2.19)$$

We note that in Eqs. (7.6.2.17)–(7.6.2.19) only the unperturbed stationary Green's function in the q -space, G_q^0 , defined in Eq. (7.5.2.10), appears. This causes only the nonresonant stationary states to appear in the intermediate sums in all orders. Expansion (7.6.2.14) should therefore converge rapidly for most pulse intensities of interest. We should observe that, generally speaking, $V(t)$ is a quantity of second order of smallness, due to the slowly varying condition (7.6.7). Similarly, $\dot{V}(t)$ is of the third order of smallness and so on. For a stationary interaction the terms involving the derivatives $\dot{V}(t)$, $\ddot{V}(t)$, etc., of course vanish and the results (7.6.2.15)–(7.6.2.19) go over exactly to those obtained in the stationary case, namely Eqs. (7.5.2.11)–(7.5.2.15). The terms appearing above in $H^{(n)}(t)$ and containing no derivatives of $V(t)$ may be called the adiabatic part, while the diabatic (nonadiabatic) corrections are given by the terms containing the derivatives of $V(t)$. A comparison of Eqs. (7.6.2.15)–(7.6.2.19) with the stationary case Eqs. (7.5.2.11)–(7.5.2.15) in fact shows

that the adiabatic (part of the) effective Hamiltonians $H^{(n)}(t)$ are correctly reproduced by simply promoting the time-independent interaction V in the stationary effective Hamiltonians $H^{(n)}$, to become the time-dependent $V(t)$. The diabatic corrections, however, are nonzero in the third order and beyond.

7.6.3. Probability Distributions Governed by the Slowly Varying Effective Hamiltonian

A major hindrance to the numerical solution of the slowly varying envelope equation with time-dependent effective Hamiltonian, Eq. (7.6.2.12), occurs due to nonnegligible coupling to the continuum states of the atomic system. We may, however, solve them approximately, without difficulty, by following⁽¹⁵⁰⁾ an extension of the energy-conserving approximation for the stationary Hamiltonian (e.g., Section 6.8.1) to the time-dependent case. We note parenthetically that for pulses defined in the entire time domain $t = [-\infty, \infty]$, the higher-order effective interaction operators $\hat{V}_{pp}(t)$ must be understood as defined with respect to the principal value of the unperturbed propagator G_q^0 , given in Eq. (7.5.2.10).

We denote the discrete eigenstates of H_{pp}^0 , consisting of the bound atomic states ϕ_B with energy ε_B and the photon number states $|n_B\rangle$ with energy $n_B\hbar\omega$, by $|B\rangle = |\phi_B\rangle|n_B\rangle$ with total energy $E_B = \varepsilon_B + n_B\hbar\omega$. Similarly, the atomic continuum states are denoted by $|\phi_{F(L_F M_F)}\rangle$ with atomic energy ε_F so that the continuum of eigenstates of H_{pp}^0 is denoted by $|F\rangle = |E_F, F\rangle = |\phi_{F(L_F M_F)}\rangle|n_F\rangle$ with $E_F = \varepsilon_F + n_F\hbar\omega$. We shall assume that the dominant continuum states occur essentially near the energy-conserving points in the atomic continua, $E_F = E_{B_0}$ or $\varepsilon_F = E_{B_0} - n_F\hbar\omega$, with an energy spread η . This spread would in fact depend on the intensity of the field as well as on the strength of the atomic transition matrix elements. Also, the spread η would be usually larger than the characteristic widths $\Delta\varepsilon$ of the ionization peaks in the continuum. Thus with respect to the ordinary atomic continua, and not too large field intensity, one may assume⁽¹⁵⁰⁾

$$\Delta\varepsilon \ll \eta \ll \hbar\omega \quad (7.6.3.1)$$

such that the bound-free and free-free matrix elements vary only negligibly in the domain η . Before proceeding further, we note that effects⁽¹⁵¹⁻¹⁵³⁾ of the presence of structures in the continuum, e.g., due to autoionization states, on multiphoton ionization must be examined⁽¹⁵⁴⁻¹⁵⁹⁾ individually. The same remark applies to the formally analogous problem of predissociation⁽¹⁶⁰⁻¹⁶²⁾ in a laser field. Assuming relation (7.6.3.1) we may approximate

the total wave function in the p -space by

$$\psi_p(t) = \sum_B b_B(t) |B\rangle + \sum_F \int_{E_F-\eta}^{E_F+\eta} dE_F b_{EF}(t) |E_F, F\rangle \quad (7.6.3.2)$$

Substitution of approximation (7.6.3.2) in Eq. (7.6.2.12) and subsequent projection on $\langle B |$ and $\langle F |$ yield the equations for the amplitudes in the form

$$i\hbar \frac{\partial b_B(t)}{\partial t} - E_B b_B(t) = \sum_{B'} \hat{V}_{BB'}(t) b_{B'}(t) + \sum_F \int_{E_F-\eta}^{E_F+\eta} dE_F \hat{V}_{BE_F}(t) b_{EF}(t) \quad (7.6.3.3)$$

and

$$i\hbar \frac{\partial b_{EF}(t)}{\partial t} - E_F b_{EF}(t) = \sum_B \hat{V}_{EFB}(t) b_B(t) + \sum_{F'} \int_{E_F-\eta}^{E_F+\eta} dE_{F'} \hat{V}_{EFE_F}(t) b_{E_F}(t) \quad (7.6.3.4)$$

We shall now reduce the equations for the amplitudes $b_B(t)$ and $b_{EF}(t)$ to a countable set involving amplitudes $b_B(t)$ of the discrete states only. To this end we define

$$a_{EF}(t) \equiv \exp(iE_F t/\hbar) b_{EF}(t) \quad (7.6.3.5)$$

and

$$S_F(t) \equiv i\hbar \frac{\partial b_{EF}(t)}{\partial t} - E_F b_{EF}(t) \quad (7.6.3.6)$$

By substituting expression (7.6.3.5) in relation (7.6.3.6) one obtains

$$a_{EF}(t) = -\frac{i}{\hbar} \int_{-\infty}^t \exp(iE_F t'/\hbar) S_F(t') dt' \quad (7.6.3.7)$$

so that, from definition (7.6.3.5),

$$b_{EF}(t) = -\frac{i}{\hbar} \int_{-\infty}^t \exp[-iE_F(t-t')/\hbar] S_F(t') dt' \quad (7.6.3.8)$$

In view of relation (7.6.3.1) one may take the bound-free and free-free matrix elements in Eqs. (7.6.3.3) and (7.6.3.4) outside the energy integrals and let η tend formally to infinity afterward. We are thus led to consider

the integral

$$\begin{aligned} \int_{E_F - \eta}^{E_F + \eta} dE_F b_{E_F}(t) &= -\frac{i}{\hbar} \int_{-\infty}^t \int_{E_F - \eta}^{E_F + \eta} dE_F \exp[-iE_F(t-t')/\hbar] S_F(t') dt' \\ &= -2\pi i \int_{-\infty}^t \delta(t-t') S_F(t') dt' \\ &= -i\pi S_F(t) \end{aligned} \quad (7.6.3.9)$$

The first line of Eq. (7.6.3.9) is obtained by substituting Eq. (7.6.3.8) and interchanging the order of the energy and time integrations; the second line follows on letting $\eta \rightarrow \infty$. In view of the above result Eqs. (7.6.3.3) and (7.6.3.4) simplify to

$$i\hbar \frac{\partial}{\partial t} b_B(t) - E_B b_B(t) = \sum_{B'} \hat{V}_{BB'}(t) b_{B'}(t) - i\pi \sum_F \hat{V}_{BE_F}(t) S_F(t) \quad (7.6.3.10)$$

and

$$\sum_{F'} [\delta_{FF'} + i\pi \hat{V}_{EF_E F'}(t)] S_{F'}(t) = \sum_B \hat{V}_{EF_B}(t) b_B(t) \quad (7.6.3.11)$$

Equation (7.6.3.11) can be solved to obtain

$$S_F(t) = \sum_{F'B'} [W^{-1}(t)]_{FF'} \hat{V}_{EF'B'}(t) b_{B'}(t) \quad (7.6.3.12)$$

where the matrix $[W(t)^{-1}]$ is the inverse of the matrix defined by

$$[W(t)]_{FF'} \equiv [\delta_{FF'} + i\pi \hat{V}_{EF_E F'}(t)] \quad (7.6.3.13)$$

Substitution of relation (7.6.3.12) in Eq. (7.6.3.10) yields also

$$i\hbar \frac{\partial}{\partial t} b_B(t) - E_B b_B(t) = - \sum_{B'} Z_{BB'}(t) b_{B'}(t) \quad (7.6.3.14)$$

where

$$-Z_{BB'}(t) = \hat{V}_{BB'}(t) - i\pi L_{BB'}(t) \quad (7.6.3.15)$$

with

$$L_{BB'}(t) = \sum_{FF'} \hat{V}_{BE_F}(t) [W^{-1}(t)]_{FF'} \hat{V}_{EF'B'}(t) \quad (7.6.3.16)$$

Equations (7.6.3.14) constitute a countable set of first-order differential equations for the amplitudes of the discrete states only and can be solved

by the usual numerical methods, for any finite number of (near-resonant) states in the p -space. We note that these equations are the time-dependent analogs of the equation of the resolvent matrix elements obtained from the stationary model Hamiltonian of Sections 6.8.1 and 6.8.2. The time-dependent probability of occupation of the continuum state $|E_F F\rangle$ is

$$\begin{aligned} P_{E_F}(t) &\equiv \int_{E_F-\eta}^{E_F+\eta} dE_F |b_{E_F}(t)|^2 \\ &= \frac{1}{\hbar^2} \int_{-\infty}^t \int_{-\infty}^t dt' dt'' \int_{E_F-\eta}^{E_F+\eta} dE_F \exp[-iE_F(t'-t'')/\hbar] S_F^*(t') S_F(t'') \\ &= \frac{2\pi}{\hbar} \int_{-\infty}^t \int_{-\infty}^t dt' dt'' \delta(t'-t'') S_F^*(t') S_F(t'') \\ &= \frac{2\pi}{\hbar} \int_{-\infty}^t dt' |S_F(t')|^2 \end{aligned} \quad (7.6.3.17)$$

The second line of this relation is obtained by substitutions from Eq. (7.6.3.9) and assuming that the energy and time integrations are interchangeable. The third line follows on taking the limit $\eta \rightarrow \infty$.

Once the discrete state amplitudes $b_B(t)$ are calculated from the finite set of equations (3.7.3.14), $S_F(t)$ is immediately given by expression (7.6.3.12) and the probability (7.6.3.17) can be evaluated by quadrature. Equation (7.6.3.17) yields the rate of transition per unit time

$$\frac{d}{dt} P_{E_F}(t) = \frac{2\pi}{\hbar} |S_F(t)|^2 \quad (7.6.3.18)$$

which shows that $S_F(t)$ given by expression (7.6.3.12) is a time-dependent analog of the S -matrix (or T -matrix) usually defined only for stationary systems.

Finally, we consider the specially simple but important case of a single discrete state $|B_0\rangle$ ionizing toward a set of continuum states $|F\rangle$. Assuming that initially (at $t = t_0$) the system is in the state $|B_0\rangle$, Eq. (7.6.3.14) can be immediately solved to give

$$b_{B_0}(t) = \exp \left(-\frac{i}{\hbar} \left[E_{B_0}(t - t_0) - \int_{t_0}^t Z_{B_0 B_0}(t') dt' \right] \right) \quad (7.6.3.19)$$

Thus the probability of finding the system in the initial state at some time t is

$$P_{B_0}(t) = |b_{B_0}(t)|^2 = \exp \left(-\frac{2}{\hbar} \int_{t_0}^t \text{Im } Z_{B_0 B_0}(t') dt' \right) \quad (7.6.3.20)$$

In general, this probability will be a finite (nonzero and noninfinite) quantity at the end of the pulse duration (also we recall that the slowly varying pulse envelope vanishes at large times).

If expression (7.6.3.20) is substituted in Eq. (7.6.3.12) in this case, one obtains

$$|S_F(t)|^2 = |R_{FB_0}(t)|^2 P_{B_0}(t) \quad (7.6.3.21)$$

with

$$R_{FB_0}(t) = \sum_F [W^{-1}(t)]_{FF'} \hat{V}_{F'B_0}(t) \quad (7.6.3.22)$$

Hence the rate of multiphoton ionization (or dissociation) into the state $|E_F, F\rangle$ is, from Eqs. (7.6.3.21) and (7.6.3.18),

$$\frac{d}{dt} P_{B_0 \rightarrow F}(t) = \frac{2\pi}{\hbar} |R_{FB_0}(t)|^2 P_{B_0}(t) \quad (7.6.3.23)$$

We assume that initially the number density of atoms in the interaction volume is n_0 . The populations in the bound and continuum states, namely

$$N_0(t) \equiv n_0 P_{B_0}(t) \quad \text{and} \quad N_{E_F}(t) \equiv n_0 \sum_{L_F M_F} P_{B_0 \rightarrow F}(t) \quad (7.6.3.24)$$

are thus found to satisfy the equations

$$\frac{d}{dt} N_0(t) = - \left[\frac{2}{\hbar} \operatorname{Im} Z_{B_0 B_0}(t) \right] N_0(t) \quad (7.6.3.25)$$

and

$$\frac{d}{dt} N_{E_F}(t) = \frac{2\pi}{\hbar} \sum_{F(L_F M_F)} |R_{F(L_F M_F) B_0}(t)|^2 N_0(t) \quad (7.6.3.26)$$

These equations follow in a straightforward manner from Eqs. (7.6.3.20) and (7.6.3.23) and definitions (7.6.3.24).

From the definition (7.6.3.15) of $Z_{B_0 B_0}(t)$ we note that the real part of $Z_{B_0 B_0}(t)$ determines the “shift” of the energy level of $|B_0\rangle$ due to the dynamic Stark-effect and the imaginary part gives its “width” due to the decay into the continua. Equation (7.6.3.25) enables us to actually interpret $(2/\hbar)\operatorname{Im} Z_{B_0 B_0}(t)$ as the total rate of decay of the initial population at time t .

Similarly, Eq. (7.6.3.26) shows that the quantity $(2\pi/\hbar)\sum_F |R_{FB_0}(t)|^2$, where $R_{FB_0}(t)$ is defined by relation (7.6.3.22), corresponds to the (time-dependent) rate of transfer of population from the bound state to the continuum states at energy E_F , at time t .

Finally, we write down the angular distribution (cf. Section 6.8.4) of the ejected particle, propagating with energy ε_F and momentum between \mathbf{K}_F and $\mathbf{K}_F + d\hat{\mathbf{K}}_F$ (within an element of solid angle $d\hat{\mathbf{K}}_F$):

$$\frac{d}{d\hat{\mathbf{K}}_F} P_{B_0 \rightarrow E_F}(t) = \frac{2\pi}{\hbar} \int_{t_0}^t \left| \sum_{F(L_F M_F)} Y_{L_F M_F}(\hat{\mathbf{K}}_F) R_{F(L_F M_F) B_0}(t') \right|^2 P_{B_0}(t') dt' \quad (7.6.3.27)$$

This is the analog of the stationary-field result (6.8.4.15). The total probability of transition in a state of energy E_F is obtained by integrating over $d\hat{\mathbf{K}}_F$, and taking the limits $t_0 \rightarrow -\infty$, $t \rightarrow \infty$:

$$P_{B_0 \rightarrow E_F} = \frac{2\pi}{\hbar} \sum_{F(L_F M_F)} \int_{-\infty}^{\infty} |R_{F(L_F M_F) B_0}(t')|^2 P_{B_0}(t') dt' \quad (7.6.3.28)$$

This result is of course consistent with the “rate equation” (7.6.3.26) for the population, $N_{E_F}(t)$. It is also the analog of the stationary-field long-time result, Eq. (6.8.4.13). In fact all the results obtained for the slowly-varying-pulse case in this section have their counterparts in the “step-pulse” case dealt with in Section 6.8.4.

We conclude this chapter by observing that the probability distribution of the inverse process of stimulated capture^(163,164) can be derived if desired for the “step pulse” or for a “slowly varying pulse” in a completely similar way by the method of Section 6.8.4 or of this section, respectively.

8

The Density Matrix Method

8.1. Introduction

Analysis of multiphoton processes under the influence of a “larger environment,” such as the relaxation of excitations by spontaneous emission due to interaction with the vacuum field or the effects of laser fluctuation, is often most conveniently treated not within the framework of the amplitude equations but rather using the more general method of the density matrix. In this chapter we outline the method with examples of typical applications to problems of spontaneous relaxation⁽¹⁶⁵⁾ and field fluctuations^(166–170) in multiphoton transitions.

8.2. The Pure State and Incoherent Mixtures

Let us consider an ideally isolated quantum system that is found at a certain time in a certain state i . The isolated system in state i is completely described in terms of its normalized wave function $|\psi_i\rangle$. The latter may be represented as a coherent superposition of any complete orthonormal set of functions $\{|\phi\rangle\}$ which can span the Hilbert space of interest. Thus

$$|\psi_i\rangle = \sum_n a_n^{(i)} |\phi_n\rangle \quad (8.2.1)$$

with coefficients

$$a_n^{(i)} = \langle \phi_n | \psi_i \rangle \quad (8.2.2)$$

In this event the isolated system is said to be in a “pure state” $|\psi_i\rangle$, which permits one to obtain full information about the system, i.e., it allows one to determine the maximum possible number of independent physical

quantities characterizing the system in this state. The mean value of any observable O of the system in the pure state $|\psi_i\rangle$ is simply the quantum expectation value

$$\langle O \rangle = \langle \psi_i | O | \psi_i \rangle \quad (8.2.3)$$

Let us now assume that the system is not completely isolated but (as is generally the case in the real world) is an interacting part of a larger system (the “whole”). Due to this interaction it is no longer possible to fully specify the state of the system (of interest) in terms of its isolated pure-state wave functions $|\psi_i\rangle$; one would need to know the wave function of the “whole” for the complete characterization. This wave function (of the “whole”) is, however, often unavailable or may not be calculable in practice. What may be known (or may need to be known!) is only the relative frequency w_i of occurrence of the isolated pure states $|\psi_i\rangle$ in the enlarged whole. In this case we may only specify the state of the system (of interest) statistically. A nonisolated system described by the (isolated) pure states $|\psi_i\rangle$ plus the statistical weights w_i of the occurrence of $|\psi_i\rangle$ is said to be in a state of incoherent “mixture.” The statistical weights w_i , being relative frequencies, are clearly real numbers such that

$$w_i \geq 0 \quad \text{and} \quad \sum_i w_i = 1 \quad (8.2.4)$$

The definition of the mean value of an observable of the system in a state of incoherent mixture is naturally extended to be the quantum expectation value with respect to the pure states $|\psi_i\rangle$ weighted by w_i :

$$\langle O \rangle \equiv \sum_i w_i \langle \psi_i | O | \psi_i \rangle \quad (8.2.5)$$

Substitution of expansion (8.2.1) in relation (8.2.5) therefore yields

$$\langle O \rangle = \sum_i \sum_{n,n'} w_i a_n^{*(i)} O_{n,n'} a_{n'}^{(i)} \quad (8.2.6)$$

where

$$O_{n,n'} = \langle \phi_n | O | \phi_{n'} \rangle \quad (8.2.7)$$

We may now define the density matrix ρ in the $\{|\phi_n\rangle\}$ representation by its matrix elements

$$\langle \phi_{n'} | \rho | \phi_n \rangle = \rho_{n'n} = \sum_i a_n^{*(i)} w_i a_{n'}^{(i)} \quad (8.2.8)$$

In terms of $\rho_{n'n}$ Eq. (8.2.6) becomes

$$\langle O \rangle = \sum_{n,n'} O_{nn'} \rho_{n'n} = \sum_n [O\rho]_{nn} = \text{Tr}[O\rho] \quad (8.2.9)$$

where $\text{Tr}[\dots]$ stands for the trace of $[\dots]$. Since operators commute under the trace operation we note that

$$\langle O \rangle = \text{Tr}[O\rho] = \text{Tr}[\rho O] \quad (8.2.10)$$

We see that knowledge of ρ permits one to obtain all relevant physical information pertaining to a system in a state of “incoherent mixture.”

If relation (8.2.2) is introduced in Eq. (8.2.8) one easily finds that

$$\langle \phi_{n'} | \rho | \phi_n \rangle = \sum_i \langle \phi_{n'} | \psi_i \rangle w_i \langle \psi_i | \phi_n \rangle \quad (8.2.11)$$

Since this equation holds for arbitrary ϕ_n and $\phi_{n'}$ we may remove the projections on both sides and express ρ directly in terms of $|\psi_i\rangle$:

$$\rho = \sum_i |\psi_i\rangle w_i \langle \psi_i| \quad (8.2.12)$$

We note that the pure-state density matrix is merely a special case of expression (8.2.12) in which all but one of the w_i are equal to zero. The only nonzero w_i must therefore be equal to unity [cf. Eq. (8.2.4)]. Hence in the pure state i , the density matrix is

$$\rho = |\psi_i\rangle \langle \psi_i| \quad (8.2.13)$$

It is noteworthy that for a pure state $[\rho]^2 = \rho$, while for an incoherent “mixture” $[\rho]^2 \neq [\rho]$.

8.3. Equation of Motion of the Density Matrix

With the change of time the states $|\psi_i\rangle$ of the system in general also change. Thus the density operator (8.2.12) becomes

$$\rho(t) = \sum_i |\psi_i(t)\rangle w_i \langle \psi_i(t)| \quad (8.3.1)$$

The equation of motion of $\rho(t)$ is obtained by considering the eigenstates

of the Hamiltonian of the system that may be governed by a Hermitian or by a non-Hermitian Hamiltonian.

8.3.1. The Hermitian Case

If H is the Hamiltonian, assumed to be Hermitian, with eigenvectors $|E_n\rangle$ at energies E_n , then

$$H|E_n\rangle = E_n|E_n\rangle \quad (8.3.1.1)$$

and we have the expansion

$$|\psi_i(0)\rangle = \sum_n |E_n\rangle\langle E_n| \psi_i(0)\rangle \quad (8.3.1.2)$$

The time evolution of Eq. (8.3.1.2) is easily obtained from that of the eigenstates $|E_n\rangle$ in the form

$$|\psi_i(t)\rangle = \sum_n \exp(-iE_n t/\hbar) |E_n\rangle\langle E_n| \psi_i(0)\rangle \quad (8.3.1.3)$$

Use of Eqs. (8.3.1.1) and (8.3.1.3) in Eq. (8.3.1) readily yields

$$\rho(t) = e^{-iHt/\hbar} \rho(0) e^{iHt/\hbar} \quad (8.3.1.4)$$

where we have used the closure relation

$$\sum_n |E_n\rangle\langle E_n| = 1 \quad (8.3.1.5)$$

to sum over n and n' ; the initial value of $\rho(t=0)$ is given by

$$\rho(0) = \sum_i |\psi_i(0)\rangle w_i \langle \psi_i(0)| \quad (8.3.1.6)$$

Differentiation of Eq. (8.3.1.4) with respect to time yields the desired equation of motion of $\rho(t)$, namely

$$i\hbar \frac{\partial \rho}{\partial t} = H\rho - \rho H = [\rho, H] \quad (8.3.1.7)$$

8.3.2. The Non-Hermitian Case

We assume that the system of interest is governed by the non-Hermitian Hamiltonian \hat{H} . Then \hat{H} and its adjoint \hat{H}^+ satisfy the eigen-

value equations (see Section 11.2)

$$\hat{H} |\lambda_n\rangle = \lambda_n |\lambda_n\rangle \quad (8.3.2.1)$$

and

$$\langle X_n | \hat{H}^+ = \langle X_n | \lambda_n^* \quad (8.3.2.2)$$

The resolution of the identity takes the form

$$\sum_n |\lambda_n\rangle\langle X_n| = 1 \quad (8.3.2.3)$$

With the aid of this relation we obtain the expansion

$$|\psi_i(0)\rangle = \sum_n |\lambda_n\rangle\langle X_n| \psi_i(0) \quad (8.3.2.4)$$

Its time evolution is

$$|\psi_i(t)\rangle = \sum_n \exp(-i\lambda_n t/\hbar) |\lambda_n\rangle\langle X_n| \psi_i(0) = e^{-i\hat{H}t/\hbar} |\psi_i(0)\rangle \quad (8.3.2.5)$$

Similarly we obtain

$$\langle\psi_i(0)| = \sum_n \langle\psi_i(0)| \lambda_n |\lambda_n\rangle\langle X_n| \quad (8.3.2.6)$$

and its time evolution

$$\langle\psi_i(t)| = \sum_n \langle\psi_i(0)| \lambda_n |\lambda_n\rangle\langle X_n| \exp(+i\lambda_n^* t/\hbar) \quad (8.3.2.7)$$

$$= \langle\psi_i(0)| e^{i\hat{H}^+ t/\hbar} \quad (8.3.2.8)$$

Substitution of Eqs. (8.3.2.5) and (8.3.2.8) in expression (8.2.12) yields the analog of relation (8.3.1.4), namely

$$\rho(t) = e^{-i\hat{H}t/\hbar} \rho(0) e^{i\hat{H}^+ t/\hbar} \quad (8.3.2.9)$$

Differentiating with respect to t we have

$$i\hbar \frac{\partial \rho(t)}{\partial t} = \hat{H}\rho - \rho\hat{H}^+ \quad (8.3.2.10)$$

Equation (8.3.2.10) clearly shows that in the non-Hermitian case the motion of the system is governed by the simultaneous influence of \hat{H} and \hat{H}^+ .

8.4. Inclusion of Spontaneous Relaxation

For multiphoton processes in an external field the effect of spontaneous emission is incorporated into the theory via approximate extension of the density matrix equation (8.3.2.10). From the quantum statistical theory⁽¹⁶⁵⁾ of spontaneous emission of a many-level atomic system we know that, to a high degree of accuracy, it can be accounted for by considering the following three effects: (1) broadening of the levels due to spontaneous decay, the rate of which equals Einstein's (total) A -coefficient for that level; (2) displacement of the levels due to Lamb shifts; and (3) the internal relaxation effect, namely the gain in the probability of occupation of each lower level due to spontaneous transition from the upper levels, at time t .

We may describe the first two effects (the widths and shifts) in terms of a complex diagonal Hamiltonian

$$H^{(s)} = \hbar(\Delta^{(s)} - \frac{1}{2}i\Gamma^{(s)}) \quad (8.4.1)$$

where $\Delta^{(s)}$ is a diagonal matrix (in the representation of the unperturbed atomic states) whose element $\Delta_{jj}^{(s)}$ is equal to the Lamb shift of the level j , and $\Gamma^{(s)}$ is a diagonal decay matrix whose element $\Gamma_{jj}^{(s)}$ is equal to Einstein's (total) A -coefficient of that level. The internal relaxation effect may be described by a diagonal "supply" matrix $\Lambda^{(s)}$ the elements of which are given by

$$\Lambda_{ii}^{(s)} = \sum_{j>i} \gamma_j \rho_{jj}(t), \quad i, j = 1, 2, 3, \dots, j_{\max} \quad (8.4.2)$$

where the levels are numbered in increasing order of their energies starting with the ground state $j = 1$ and ending with the highest-lying state j_{\max} ; γ_j is Einstein's (partial) A -coefficient for the transition $(j) \rightarrow (i)$. Thus, for example,

$$\Lambda_{11}^{(s)} = \gamma_{12} \rho_{22}(t) + \gamma_{13} \rho_{33}(t) + \dots + \gamma_i \rho_{ii}(t) + \dots \quad (8.4.3)$$

is the rate at which state 1 is supplied with (occupation) probability or "population" via spontaneous relaxation of all states lying energetically above it. In terms of the dipole transition matrix elements D_{ij} one has

$$\hbar \gamma_j = \frac{4}{3} |D_{ij}|^2 \left(\frac{\omega_i}{c} \right)^3 \quad (8.4.4)$$

where $\hbar\omega_{ji} = \varepsilon_j - \varepsilon_i$ is the energy difference of the levels of interest. We note also that

$$\Gamma_{ji}^{(s)} = \sum_{j' < j} \gamma_{ji}' \quad (8.4.5)$$

The Lamb shifts $\Delta_{ji}^{(s)}$ are given by

$$\hbar\Delta_{ji}^{(s)} = - \sum_l \sum_{k,s} |D_{jl}\varepsilon_{ks}|^2 \left(\frac{2\pi ck}{L^3}\right) \frac{1}{\omega_{ks} + \omega_{lj}} \quad (8.4.6)$$

The shift integrals (8.4.6) are divergent and need to be renormalized before use. We note, however, that the absolute magnitude of the Lamb shifts are often negligibly small compared to the shifts (and widths) introduced by most external laser fields. On the other hand, the observed Lamb shifts of a transition $(i) \leftrightarrow (j)$, when available, may be directly identified with $\hbar(\Delta_{ji}^{(s)} - \Delta_{jj}^{(s)})$ and hence incorporated without difficulty. This is possible since it is only the difference of energies between levels which enter, as we shall see below, and not their individual values. The density matrix equation for the spontaneous emission in a multilevel atom may now be written down using the effective Hamiltonian $H^{(s)}$ following essentially Eq. (8.3.2.10):

$$i\hbar \frac{\partial \rho}{\partial t} = H^{(s)}\rho - \rho H^{+(s)} + i\hbar\Lambda^{(s)} \quad (8.4.7)$$

The last term in this equation takes account of “supply” of probabilities due to the relaxation. The above intuitive construction of Eq. (8.4.7) can be justified rigorously within the Markov–Born Rotating Wave (M–B R) approximation (which is an excellent approximation for the weak, resonant, and essentially incoherent process of spontaneous emission). Equation (8.4.7) is, in fact, identical with the quantum statistical Master equation for spontaneous emission in a multistate atom as derived⁽¹⁶⁵⁾ subject to the M–B R approximation.

If now

$$H = H^0 + V(t) \quad (8.4.8)$$

is the total Hamiltonian of the system atom + field, where $V(t)$ is the slowly varying interaction Hamiltonian (Section 7.6.2) due to the external field, then the shifts and widths of the atomic levels due to the spontaneous emission considered above may be thought of as changing the Hermitian atomic Hamiltonian H^0 into a non-Hermitian Hamiltonian, i.e.,

$$H_0 \equiv H^0 + \hbar(\Delta^{(s)} - \frac{1}{2}i\Gamma^{(s)}) \quad (8.4.9)$$

The total Hamiltonian including the effect of coupling to the vacuum field now becomes

$$\hat{H} = H_0 + V(t) \quad (8.4.10)$$

The density matrix equation of the combined non-Hermitian system may therefore be written as [cf. Eq. (8.4.7)]

$$i\hbar \frac{\partial \rho}{\partial t} = \hat{H}\rho - \rho\hat{H}^+ + i\hbar\Lambda^{(s)} \quad (8.4.11)$$

The supposition here is that the change in the combined density matrix ρ during a short time interval Δt is due to the change induced by the external interaction and the change induced by the spontaneous emission, which are, to first order in Δt , additive. The simplicity with which the shift, the decay, and above all the relaxation effect are easily and correctly incorporated in the equation of motion of the system (8.4.11) justifies adoption of the density matrix representation [rather than the (Schrödinger) amplitude-equation representation] in such and all analogous circumstances. Equation (8.4.11) can also be rewritten in the alternative form

$$i\hbar \frac{\partial \rho}{\partial t} = [H, \rho] + \hbar[\Delta^{(s)}, \rho] - \frac{\hbar}{2} i[\Gamma^{(s)}, \rho]_+ + i\hbar\Lambda^{(s)} \quad (8.4.12)$$

where $[\Gamma^{(s)}, \rho]_+$ is the anticommutator $\Gamma^{(s)}\rho + \rho\Gamma^{(s)}$.

8.5. Generalized Rotating Wave or Quasi-Energy-Shell Approximation

One of the most useful approximations of the dynamical equations (8.4.12) for multiphoton processes is obtained by employing a “quasi-energy-shell” (or generalized “rotating wave”) approximation. In this approximation one retains only states (coupled by matrix elements of the effective Hamiltonian) for which the unperturbed energies $E_i'' = \epsilon_i + (n_0 + n)\hbar\omega$ are nearly equal (or equal) to the unperturbed energy of the initial state, $E_i'''' = \epsilon_i + n_0\hbar\omega$. This “quasi-energy-shell” (QES) approximation in the number state (or in the semiclassical Floquet picture) is equivalent to a generalized “rotating wave approximation” (RWA) of the fully time-dependent equations. In the generalized RWA only those terms of the dynamical equations (expressed in the interaction picture) are retained which oscillate (exponentially) with the smallest of frequencies,

i.e., least rapidly. For the elementary problem of a two-level atom, near-resonant with a one-photon transition, this amounts to retaining one of the two exponentially oscillating (or rotating) terms of the $F_0 \cos(\omega t + \delta)$ wave, which gives the difference of frequencies with respect to the frequency separation of the two levels and of the field. The neglected term, on the other hand, rotates very rapidly because of its dependence on the sum of the two frequencies; consequently its contribution in the mean is small compared to that of the term retained. Thus arose, originally in the context of magnetic-resonance studies, the name RWA for the said approximation. This popular approximation is currently applied to a whole class of near-resonant multiphoton processes in multilevel systems, in the generalized sense defined above. We note that the effective Hamiltonian method of Sections 7.5 and 7.6 may be viewed as a rigorous systematization of the RWA.

8.5.1. Density Matrix Equation for a Resonant Multiphoton Process

This class of multiphoton transition problems has been previously discussed (cf. Sections 7.3 and 7.4) without taking account of spontaneous relaxation. In the present problem, an upper bound state is assumed to be coupled to the ground state by an N -photon (near-) resonant transition. The upper state is also coupled to a break-up continuum (ionization, dissociation, etc.) by a p -photon transition. Furthermore, the ground state is allowed to be coupled to the continuum also through the off-resonant states, and indirectly (via the continuum) to the upper resonant state. In the presence of a time-dependent slowly varying envelope of the field, the Hamiltonian of the system still has a structure similar to the constant-amplitude case [cf. Eqs. (7.2.5) and (7.2.6)] but the matrix elements are now defined in accordance with the theory of slowly varying effective Hamiltonians of order N . As before, the coupling between the two bound states is given by a (2×2) -non-Hermitian matrix Hamiltonian $H \equiv H^0 + V$:

$$H = \begin{pmatrix} h_{11}(t) & h_{12}(t) \\ h_{21}(t) & h_{22}(t) \end{pmatrix} \quad (8.5.1.1)$$

where $h_{ij}(t)$ are slowly varying functions of time. If the field is assumed to be represented by

$$\mathbf{F}(t) = \boldsymbol{\epsilon} e(t) \cos(\omega t + \phi(t)) \quad (8.5.1.2)$$

where $\boldsymbol{\epsilon}$ is the polarization vector and the complex envelope function is

$$F(t) = e(t) e^{-i\phi(t)} \quad (8.5.1.3)$$

then the matrix elements $h_{ij}(t)$ can be expressed more explicitly in the form

$$\left. \begin{aligned} h_{11}(t) &= \hbar [\omega_1 + \delta_1(t) - \frac{1}{2}i\gamma_1(t)] \\ h_{22}(t) &= \hbar [\omega_2 - N\omega + \delta_2(t) - \frac{1}{2}i\gamma_2(t)] \\ h_{12}(t) &= \hbar [\Omega_{12}(t) - \frac{1}{2}i\gamma_{12}(t)] \\ h_{21}(t) &= \hbar [\Omega_{21}(t) - \frac{1}{2}i\gamma_{21}(t)] \end{aligned} \right\} \quad (8.5.1.4)$$

From the known field dependence of the lowest order slowly varying matrix elements we may exhibit the time-dependence of (8.5.1.4) explicitly. Thus

$$\delta_1(t) = \alpha_1 [e(t)]^2 \quad (8.5.1.5)$$

$$\delta_2(t) = \alpha_2 [e(t)]^2 \quad (8.5.1.6)$$

which are the dynamic Stark shifts of levels 1 and 2. Also,

$$\gamma_1(t) = \lambda_1 [e(t)]^{2(N+p)} \quad (8.5.1.7)$$

and

$$\gamma_2(t) = \lambda_2 [e(t)]^{2p} \quad (8.5.1.8)$$

which are the $(N+p)$ - and p -photon transition rates into the break-up continuum (from ground state 1 and upper state 2, respectively). Furthermore,

$$\Omega_{12}(t) = \beta_{12} [e(t)]^N e^{-iN\phi(t)} \quad (8.5.1.9)$$

$$\Omega_{21}(t) = \beta_{21} [e(t)]^N e^{+iN\phi(t)} \quad (8.5.1.10)$$

are the matrix elements of the direct N -photon coupling of states 1 and 2. Finally,

$$\gamma_{12}(t) = \lambda_{12} [e(t)]^{N+2p} e^{-iN\phi(t)} \quad (8.5.1.11)$$

$$\gamma_{21}(t) = \lambda_{21} [e(t)]^{N+2p} e^{+iN\phi(t)} \quad (8.5.1.12)$$

are the indirect $(N+2p)$ -order coupling of states 1 and 2 via the continuum. The constants (α_1, α_2) , (λ_1, λ_2) , (β_{12}, β_{21}) , and $(\lambda_{12}, \lambda_{21})$ are the lowest-nonvanishing-order perturbative matrix elements (the order being the same as the power of $[e(t)]$ appearing with them) as for the constant-amplitude field. Alternatively, these constants may be obtained from the numerical method of Section 11.5.4, provided the powers of the field

dependence are found to check appropriately. We should add here that the fourth- or higher-order Stark shifts, which are usually negligible compared to the quadratic terms retained in $\delta_1(t)$ and $\delta_2(t)$, may be needed to be added to the matrix elements (8.5.1.4) in higher-order problems. As with constant-amplitude fields, contributions of $\gamma_{12}(t)$ or $\gamma_{21}(t)$ are usually small compared to that of $\Omega_{12}(t)$ or $\Omega_{21}(t)$; they may however affect the shape of the transition spectrum through interference effects. The spontaneous decay matrix is

$$\Gamma^{(s)} = \begin{pmatrix} 0 & 0 \\ 0 & \gamma_s \end{pmatrix} \quad (8.5.1.13)$$

where γ_s is the spontaneous decay rate of the upper level 2. The spontaneous relaxation matrix $\Lambda^{(s)}$ is simply given by

$$\Lambda^{(s)} = \begin{pmatrix} \gamma_s \rho_{22}(t) & 0 \\ 0 & 0 \end{pmatrix} \quad (8.5.1.14)$$

We neglect below the small Lamb shifts $\Lambda^{(s)}$ [see Eq. (8.4.1)]. Substitution of Eqs. (8.5.1.1), (8.5.1.13), and (8.5.1.14) in Eq. (8.4.12) yields the effective density matrix equation, which can be expressed as a set of four equations for the elements of ρ :

$$i \begin{bmatrix} i\Gamma_{11}(t) & -i\gamma_s & V_{21}(t)e^{-iN\phi(t)} & -V_{12}(t)e^{iN\phi(t)} \\ 0 & i\Gamma_{22}(t) & -V_{21}(t)e^{-iN\phi(t)} & V_{12}(t)e^{iN\phi(t)} \\ V_{12}(t)e^{iN\phi(t)} & -V_{12}(t)e^{iN\phi(t)} & -\Delta^*(t) & 0 \\ -V_{21}(t)e^{-iN\phi(t)} & V_{21}(t)e^{-iN\phi(t)} & 0 & \Delta(t) \end{bmatrix} \begin{bmatrix} \rho_{11}(t) \\ \rho_{22}(t) \\ \rho_{12}(t) \\ \rho_{21}(t) \end{bmatrix} = \begin{bmatrix} \dot{\rho}_{11}(t) \\ \dot{\rho}_{22}(t) \\ \dot{\rho}_{12}(t) \\ \dot{\rho}_{21}(t) \end{bmatrix} \quad (8.5.1.15)$$

where

$$\Gamma_{11}(t) = \lambda_1[e(t)]^{2(N+p)} \quad (8.5.1.16)$$

$$\Gamma_{22}(t) = \gamma_s + \lambda_2[e(t)]^{2p} \quad (8.5.1.17)$$

$$V_{12}(t) = \beta_{12}[e(t)]^N - \frac{1}{2}i\lambda_{12}[e(t)]^{N+2p} \quad (8.5.1.18)$$

and

$$\Delta(t) = \{N\omega - (\omega_2 - \omega_1) + (\alpha_2 - \alpha_1)[e(t)]^2 + \frac{1}{2}i(\Gamma_{11}(t) + \Gamma_{22}(t))\} \quad (8.5.1.19)$$

The slowly varying effective density matrix equations (8.5.1.15) can be clearly used directly to study the effect of laser pulses. We shall see in the next section that they also provide a convenient basis for the study of multiphoton processes in fluctuating (stochastic) fields.

8.6. Theory of Multiphoton Transition in Stochastic Fields

Until now we have considered the radiation field to be a deterministic variable. Sometimes it is necessary to consider the effect of the inherent fluctuations either in the phase, or in the amplitude, or in both the phase and amplitude of the external field. Thus, for example, when dealing with a “monomode” laser (operating much above the laser threshold), although the field intensity is essentially stable, the phase (if not the amplitude) can be a fluctuating quantity. This gives rise to a small but finite bandwidth to the otherwise monomode field. The actual field is therefore, strictly speaking, a stochastic variable rather than an exactly deterministic object. An intensity-stable single-mode laser has been modeled^(166–170) as a fluctuation in which the phase of the field undergoes a diffusion process.⁽¹⁷¹⁾ A “multimode” field with many uncorrelated modes, on the other hand, exhibits more complex fluctuations involving both the phase and amplitude. Such a field is modeled^(172,173) as a chaotic Gaussian process.⁽¹⁷⁴⁾ The chaotic Gaussian fluctuations lead to the finite bandwidths of laser lines observed in all multimode lasers. The fluctuation properties of the field are systematically described in terms of the various orders of correlation functions⁽¹⁷⁴⁾ of the field.

8.6.1. Stochastic Differential Equations

A systematic analytic treatment of multiphoton processes in fluctuating fields is provided by enlarging the scope of the deterministic equations (used so far) to stochastic differential equations. A stochastic differential equation is defined to be a differential equation whose coefficients contain random functions of the independent variables. They are clearly well suited for the study of the effect of external sources of fluctuations on a dynamical system, since one may directly interpret the perturbation Hamiltonian as a random function of the external field with given stochastic properties. Thus, for example, the density matrix equations (8.5.1.15) in which the interaction Hamiltonian

$$V(t) = \frac{1}{2} \mathbf{D} \cdot \mathbf{F}(t) \quad (8.6.1.1)$$

contains the external field $\mathbf{F}(t)$ becomes a stochastic differential equation

due to the assumed stochastic nature of $\mathbf{F}(t)$. In general, the actual problem of finding the solution of stochastic differential equations poses considerably greater mathematical difficulty compared to that posed by the deterministic equations. There is hardly a general method of solution of stochastic differential equations available. However, within certain restrictive assumptions about the stochastic process involved, a systematic study of multiphoton processes can be made. One such systematic method, which we shall consider here, is the method of Kubo–Liouville equations. This is a nonperturbative method.

8.6.2. The Kubo–Liouville Equation

In the presence of field fluctuations, multiphoton transition probabilities become stochastic objects. Therefore, the quantities of observational interest are their ensemble averages (or other moments). This theory provides a means of generating them from the solutions of a set of equations, which are derived starting from the stochastic differential equations. Let us consider a system of linear stochastic differential equations for a vector of N dependent variables

$$\mathbf{x}(t) = \{x_i(t)\}, \quad i = 1, 2, \dots, N \quad (8.6.2.1)$$

$$\frac{\partial}{\partial t} x_i(t) = \sum_{j=1}^N A_{ij}(\boldsymbol{\epsilon}(t), t)x_j(t), \quad i = 1, 2, 3, \dots, N \quad (8.6.2.2)$$

where $\boldsymbol{\epsilon}(t)$ denotes the given (external) stochastic processes and $A_{ij}(\boldsymbol{\epsilon}(t), t)$ is the coefficient matrix. Equation (8.6.2.2) can be viewed as a flow in the x -space. One may therefore write the continuity equation of the generalized density $D(\mathbf{x}, t)$ of this flow in the form

$$\frac{\partial D(\mathbf{x}, t)}{\partial t} = - \sum_{i,j} \frac{\partial}{\partial x_i} [A_{ij}(\boldsymbol{\epsilon}, t)x_j D(\mathbf{x}, t)] \quad (8.6.2.3)$$

To make further progress it is now necessary to assume that the external stochastic processes of interest are Markovian and hence that their joint probability distribution $p(\boldsymbol{\epsilon}, t)$ satisfies the Master equation⁽¹⁷⁵⁾

$$\frac{\partial}{\partial t} p(\boldsymbol{\epsilon}, t) = Wp(\boldsymbol{\epsilon}, t) \quad (8.6.2.4)$$

where W is the “Master operator” governing the given Markov process $\boldsymbol{\epsilon}(t)$. A basic observation is that even if the process $\mathbf{x}(t)$ of interest is not Markovian, it may be considered as a projection⁽¹⁷⁶⁾ of an enlarged process

$(\mathbf{x}, \boldsymbol{\epsilon})$, which is Markovian in character. The continuity equation of the generalized density $P(\mathbf{x}, \boldsymbol{\epsilon}, t)$ of the joint flow of $(\mathbf{x}, \boldsymbol{\epsilon})$ is then obtained by combining Eqs. (8.6.2.3) and (8.6.2.4). Thus

$$\frac{\partial P(\mathbf{x}, \boldsymbol{\epsilon}, t)}{\partial t} = - \sum_{i,j} \frac{\partial}{\partial x_i} A_{ij}(\boldsymbol{\epsilon}, t) x_j P(\mathbf{x}, \boldsymbol{\epsilon}, t) + W P(\mathbf{x}, \boldsymbol{\epsilon}, t) \quad (8.6.2.5)$$

In writing this equation one observes that the change in $P(\mathbf{x}, \boldsymbol{\epsilon}, t)$ is additive, to first order in Δt , with respect to the separate changes in \mathbf{x} and $\boldsymbol{\epsilon}$. We shall refer to Eq. (8.6.2.5) as a Kubo–Liouville equation.⁽¹⁷⁷⁾ The distribution function $P(\mathbf{x}, \boldsymbol{\epsilon}, t)$ with a fixed initial condition is the solution of Eq. (8.6.2.5) with the requirement

$$P(\mathbf{x}, \boldsymbol{\epsilon}, 0) = \delta(\mathbf{x} - \mathbf{x}^0) P_1(\boldsymbol{\epsilon}, 0) \quad (8.6.2.6)$$

where \mathbf{x}^0 is the given initial value of the “output” vector process \mathbf{x} and $P_1(\boldsymbol{\epsilon}, 0)$ is the initial distribution function of the “input” (Markov) process $\boldsymbol{\epsilon}$.

8.6.3. Equation of the Marginal Averages

The physical quantity of interest in multiphoton processes is often the ensemble average $\langle x_i(t) \rangle$ of a component x_i ,

$$\langle x_i(t) \rangle = \int x_i P(\mathbf{x}, \boldsymbol{\epsilon}, t) d\mathbf{x} d\boldsymbol{\epsilon} \quad (8.6.3.1)$$

Thus, for example, x_i could be an element of the “atom + field” density matrix ρ satisfying Eq. (8.4.11). For such purposes one may actually avoid solving directly the Kubo–Liouville density equation (8.6.2.5) in favor of a simpler set of equations of the marginal averages $y_k(\boldsymbol{\epsilon}, t)$ defined by

$$y_k(\boldsymbol{\epsilon}, t) \equiv \int x_k P(\mathbf{x}, \boldsymbol{\epsilon}, t) d\mathbf{x}, \quad k = 1, 2, \dots, N \quad (8.6.3.2)$$

where

$$d\mathbf{x} \equiv dx_1 dx_2 \cdots dx_N \quad (8.6.3.3)$$

The equation satisfied by $y_k(\boldsymbol{\epsilon}, t)$ may be derived as follows.⁽¹⁷⁵⁾ We multiply Eq. (8.6.2.5) by x_k and integrate with respect to $d\mathbf{x}$ to obtain

$$\frac{\partial y_k(\boldsymbol{\epsilon}, t)}{\partial t} = - \sum_{i,j} x_k A_{ij}(\boldsymbol{\epsilon}, t) \frac{\partial}{\partial x_i} [x_j P(\mathbf{x}, \boldsymbol{\epsilon}, t)] dx + W y_k(\boldsymbol{\epsilon}, t) \quad (8.6.3.4)$$

where we have used the definition (8.6.3.2) on the left-hand side as well as for the last term of Eq. (8.6.3.4). To simplify the remaining term we integrate partially once with respect to dx_i and find

$$\begin{aligned} & - \sum_{i,j} A_{ij}(\boldsymbol{\varepsilon}, t) \int d\mathbf{x}_i [x_k x_j P(\mathbf{x}, \boldsymbol{\varepsilon}, t) \Big|_{x_i = -\infty}^{x_i = +\infty}] \\ & + \sum_{i,j} A_{ij}(\boldsymbol{\varepsilon}, t) \int \frac{\partial x_k}{\partial x_i} [x_j P(\mathbf{x}, \boldsymbol{\varepsilon}, t)] d\mathbf{x} \end{aligned} \quad (8.6.3.5)$$

where $d\mathbf{x}_i \equiv d\mathbf{x}$ (without the increment dx_i). The first term of expression (8.6.3.5) vanishes for all “healthy” distributions $P(\mathbf{x}, \boldsymbol{\varepsilon}, t)$, which vanish at the end points of integration with respect to the variables x_i . The contribution from the second term is [using the definition (8.6.3.2)] simply

$$\sum_j A_{kj}(\boldsymbol{\varepsilon}, t) y_j(\boldsymbol{\varepsilon}, t) \quad (8.6.3.6)$$

Hence Eq. (8.6.3.4) reduces to

$$\frac{\partial y_i(\boldsymbol{\varepsilon}, t)}{\partial t} = \sum_j A_{ij}(\boldsymbol{\varepsilon}, t) y_j(\boldsymbol{\varepsilon}, t) + W y_i(\boldsymbol{\varepsilon}, t) \quad (8.6.3.7)$$

for all $(i, j) = 1, 2, \dots, N$. The initial condition for $y_i(\boldsymbol{\varepsilon}, t)$ is readily found from Eqs. (8.6.3.2) and (8.6.2.6):

$$y_i(\boldsymbol{\varepsilon}, 0) = x_i^0 P_i(\boldsymbol{\varepsilon}, 0) \quad (8.6.3.8)$$

Finally, the desired ensemble average $\langle x_i \rangle$ of x_i is easily found from Eqs. (8.6.3.1) and (8.6.3.2) to be

$$\langle x_i(t) \rangle = \int y_i(\boldsymbol{\varepsilon}, t) d\boldsymbol{\varepsilon} \quad (8.6.3.9)$$

Clearly, it is necessary only to solve Eq. (8.6.3.7) with boundary condition (8.6.3.8) to obtain any $\langle x_i(t) \rangle$ from relation (8.6.3.9).

Actual solutions of the marginal average equations satisfied by the elements of the multiphoton “atom + field” density matrix equation (8.4.12) pose a nontrivial problem. For a variety of multiphoton-transition problems, such as near-resonant two-photon transitions in the double-optical-resonance, dynamical-Stark-effect, resonant three-photon ionization, this problem has been tackled successfully in terms of an eigenfunction-expansion method,^(173,178) which employs the eigenfunctions of the “Master operator” W [see Eq. (8.6.2.4)]. Below we consider two

applications of this method with models of both “monomode” and “multimode” lasers.

8.6.4. A Model of a “Monomode” Laser Field

In this model⁽¹⁷⁹⁾ the laser field

$$\mathbf{E}(t) = \epsilon \epsilon_0 \cos(\omega t + \phi(t)) \quad (8.6.4.1)$$

is considered to possess a constant amplitude ϵ_0 and a fluctuating phase $\phi(t)$. The phase is assumed to satisfy a Langevin equation of the form

$$\frac{d\phi}{dt} = f(t) \quad (8.6.4.2)$$

where $f(t)$ is a Gaussian random “force” with two-point stationary autocorrelation function

$$\langle f(t_1)f(t_2) \rangle = b\gamma \exp(-\gamma |t_1 - t_2|) \quad (8.6.4.3)$$

Function $f(t)$ in its turn may be thought of as satisfying the equation

$$\frac{d}{dt} f(t) + \gamma f(t) = F(t) \quad (8.6.4.4)$$

where $F(t)$ is a Gaussian “ δ -force,” i.e., having the correlation function

$$\langle F(t_1)F(t_2) \rangle = 2b\gamma^2 \delta(t_1 - t_2) \quad (8.6.4.5)$$

corresponding to a “white-noise” (or flat) spectrum. Thus the phase $\phi(t)$ can be regarded as a projection of a two-dimensional Markov process relating to the two parameters b and γ . The constants γ and b can be interpreted from Eqs. (8.6.4.2)–(8.6.4.5). Thus $1/\gamma$ is a “correlation time” of the phase derivative $\partial\phi/\partial t = \dot{\phi}(t)$ and b is a bandwidth.

They may be related to the system constants, which appear in the theory of monomode lasers,⁽¹⁸⁰⁾ but can be assumed as given for the present purpose. The two-time correlation function $G(t_1, t_2)$ of the field (8.6.4.1) is⁽¹⁷⁹⁾

$$\begin{aligned} G(t_1, t_2) &\equiv \frac{\langle E(t_1), E(t_2) \rangle}{\langle E(t_1), E(t_1) \rangle} = \langle \exp(i\phi(t_1) - i\phi(t_2)) \rangle \\ &= \exp\{-b |t_1 - t_2| + [\exp(-\gamma |t_1 - t_2|) - 1]/\gamma\} \end{aligned} \quad (8.6.4.6)$$

The Fourier transform of this equation therefore gives the spectrum of the “monomode” laser. There are two limits of interest: (1) $\gamma \gg b$, for which the spectrum is Lorenzian and has width $\Delta\omega = b$, and (2) $\gamma \rightarrow 0$ and $b \rightarrow \infty$ while keeping $(\gamma b)^{1/2}$ constant, for which the spectrum is Gaussian and has width $\Delta\omega = (\gamma b)^{1/2}$. In the limit $\gamma \rightarrow \infty$, the phase derivative $\dot{\phi}(t)$ becomes δ -correlated and the phase $\phi(t)$ becomes a diffusion⁽¹⁷¹⁾ process.

Finally, the Master equation corresponding to the Langevin equation (8.6.4.4) is just the Fokker–Planck equation⁽¹⁷⁸⁾

$$\frac{\partial}{\partial t} P(f, t) = WP(f, t) \quad (8.6.4.7)$$

where the Master operator (or Fokker–Planck operator) is given by

$$W = - \left(\gamma \frac{\partial}{\partial f} + \gamma^2 b \frac{\partial^2}{\partial f^2} \right) \quad (8.6.4.8)$$

Therefore the stationary distribution $P(f)$ is obtained from the solution of the stationary form of Eq. (8.6.4.7), namely

$$WP_0(f) = \left(\gamma \frac{\partial}{\partial f} + \gamma^2 b \frac{\partial^2}{\partial f^2} \right) P_0(f) = 0 \quad (8.6.4.9)$$

Thus

$$P(f) = P_0(f) = \frac{1}{(2b\gamma\pi)^{1/2}} e^{-f^2/(2b\gamma)} \quad (8.6.4.10)$$

8.6.5. Application to the Resonance Model

Let us consider the effective density matrix equations (8.5.1.15) along with the stochastic field (8.6.4.1). We first introduce the simple transformation of variables

$$\left. \begin{aligned} x_1(t) &= \rho_{11}(t) \\ x_2(t) &= \rho_{22}(t) \\ x_3(t) &= e^{-iN\phi(t)} \rho_{12}(t) \\ x_4(t) &= e^{iN\phi(t)} \rho_{21}(t) \end{aligned} \right\} \quad (8.6.5.1)$$

Substitution of expressions (8.6.5.1) into Eq. (8.5.1.15) gives a convenient general vector equation for $\mathbf{x} = (x_1, x_2, x_3, x_4)$:

$$\frac{d\mathbf{x}(t)}{dt} + [A(0) + i\dot{\phi}(t)B(0)]\mathbf{x}(t) = 0 \quad (8.6.5.2)$$

where $A(0)$ and $B(0)$ are constant matrices;

$$A = \begin{pmatrix} \Gamma_{11} & -\gamma_s & -iV_{21} & iV_{12} \\ 0 & \Gamma_{22} & iV_{21} & -iV_{12} \\ -iV_{12} & iV_{12} & i\Delta^* & 0 \\ iV_{21} & -iV_{21} & 0 & -i\Delta \end{pmatrix} \quad (8.6.5.3)$$

where the matrix elements here have the same significance as in Eq. (8.5.1.15) except that $[e(t)]$, according to our assumption of a constant-amplitude field, is replaced everywhere by the constant ε_0 .

The matrix B is a (sparse) diagonal matrix

$$B(0) = \begin{pmatrix} 0 & 0 & 0 & 0 \\ 0 & 0 & 0 & 0 \\ 0 & 0 & N & 0 \\ 0 & 0 & 0 & -N \end{pmatrix} \quad (8.6.5.4)$$

The equation for the marginal averages can be written out immediately by combining Eqs. (8.6.5.3), (8.6.5.4), and (8.6.5.2) as in Eq. (8.6.3.7):

$$\left[\frac{d}{dt} - W + A + ifB \right] \mathbf{y}(f, t) = 0 \quad (8.6.5.5)$$

The desired averages are therefore given by Eq. (8.6.3.9),

$$\langle \mathbf{x}(t) \rangle = \int_{-\infty}^{\infty} df \mathbf{y}(f, t) \quad (8.6.5.6)$$

where $\mathbf{y}(f, t)$ is the solution of Eq. (8.6.5.5) with initial condition

$$\mathbf{y}(f, 0) = \mathbf{x}^0 P_0(f) \quad (8.6.5.7)$$

To solve Eq. (8.6.5.5) systematically one expands $\mathbf{y}(f, t)$ in the complete set of left and right eigenfunctions of W ,

$$WP_n(f) = \lambda_n P_n(f) \quad (8.6.5.8)$$

and

$$W^+ \phi_n(f) = \lambda_n^* \phi_n(f) \quad (8.6.5.9)$$

For the operator $-W$, Eq. (8.6.4.4),

$$\lambda_n = n\gamma \quad (8.6.5.10)$$

and $P_0(f) = [1/(2b\gamma\pi)^{1/2}] \exp(-f^2/2b\gamma)$

$$P_n(f) = P_0(f)\phi_n(f) \quad (8.6.5.11)$$

where

$$\phi_n(f) = \frac{1}{(2^n n!)^{1/2}} H_n(f/(2b\gamma)^{1/2}), \quad n = 0, 1, 2, \dots \quad (8.6.5.12)$$

and H_n are the Hermite polynomials. Thus

$$\mathbf{y}(f, t) = \sum_n \mathbf{c}_n(t) \phi_n(f) \quad (8.6.5.13)$$

where

$$\mathbf{c}_n(t) = \int_{-\infty}^{\infty} df \phi_n(f) \mathbf{y}(f, t) \quad (8.6.5.14)$$

with

$$\mathbf{c}_n(0) = \mathbf{x}^0 \delta_{n,0} \quad (8.6.5.15)$$

The ensemble average of $\mathbf{y}(f, t)$ is thus simply given by Eqs. (8.6.5.6) and (8.6.5.13),

$$\begin{aligned} \langle \mathbf{x}(t) \rangle &= \int \left(\sum_n \mathbf{c}_n(t) \phi_n(f) \right) df \\ &= \sum_n \mathbf{c}_n(t) \delta_{n,0} \\ &= \mathbf{c}_0(t) \end{aligned} \quad (8.6.5.16)$$

In the second line of this relation we have used the fact that $\phi_0(t) = 1$ and the orthogonality condition

$$\int_0^{\infty} df \phi_0^*(f) \phi_n(f) = \delta_{n,0} \quad (8.6.5.17)$$

The coefficient vectors $\mathbf{c}_n(t)$ are determined by substituting expression (8.6.5.13) in Eq. (8.6.5.5), multiplying by function $\phi_m(f)$, and integrating with respect to f . This procedure yields

$$\begin{aligned} \left(\frac{d}{dt} + m\gamma + A \right) \dot{c}_m(t) + iB[b\gamma(m+1)]^{1/2} c_{m+1}(t) \\ + iB[b\gamma m]^{1/2} c_{m-1}(t) = 0, \quad m = 0, 1, 2, \dots \end{aligned} \quad (8.6.5.18)$$

The eigenvalues $\lambda_m = m\gamma$ and the orthogonality of function $\phi_n(f)$ are employed as usual in writing out Eq. (8.6.5.18), which completely determines coefficients $\mathbf{c}_0(t)$ and hence the desired averages. It is convenient to transform Eq. (8.6.5.18) into a set of algebraic equations by employing the Laplace transform of $c_m(t)$:

$$L_s \mathbf{c}_m(t) \equiv \mathbf{d}_m(s) \equiv \int_0^\infty \mathbf{c}_m(t) e^{-st} dt \quad (8.6.5.19)$$

On taking the Laplace transform of Eq. (8.6.5.18) we obtain⁽¹⁷⁹⁾

$$(s + m\gamma + A)\mathbf{d}_m(s) + iB[b\gamma(m+1)]^{1/2}\mathbf{d}_{m+1}(s) + iB[b\gamma m]^{1/2}\mathbf{d}_{m-1}(s) = \mathbf{x}^0 \delta_{n,0} \quad (8.6.5.20)$$

where we have used the initial value given by Eq. (8.6.5.15). This is a three-term matrix recurrence relation for the vector $\mathbf{d}_m(s)$ and is easily solved for $d_0(s)$ by the matrix continued-fractions technique (cf. Sections 9.2 and 9.3). Thus

$$\mathbf{d}_0(s) = \frac{1}{s + A + k(s)} \mathbf{x}^0 \quad (8.6.5.21)$$

where $k(s)$ is the matrix continued-fraction defined by

$$k(s) = B \cfrac{\gamma b}{s + \gamma + A + B \cfrac{2\gamma b}{s + 2\gamma + A + B \cfrac{3\gamma b}{s + 3\gamma + A + \dots}}} \quad (8.6.5.22)$$

The explicit time dependence of the averages $\langle \mathbf{x}(t) \rangle$ may be calculated from the inverse transform of $\mathbf{d}_0(s)$,

$$\langle \mathbf{x}(t) \rangle = \mathbf{c}_0(t) = \frac{1}{2\pi i} \int_{a-i\infty}^{a+i\infty} ds \mathbf{d}_0(s) e^{st} \quad (8.6.5.23)$$

where a is such that on the right of the line $s = a$ there are no poles of $\mathbf{d}_0(s)$. The other coefficient can be found similarly, if desired, from the transforms

$$\mathbf{d}_n(s) = -i \frac{(\gamma b n)^{1/2}}{R_n(s)} B \mathbf{d}_{n-1}(s) \quad (8.6.5.24)$$

for $n = 1, 2, 3, \dots$, where $R_n(s)$ is the matrix continued-fraction,

$$R_n(s) \equiv s + n\gamma + A + B \frac{(n+1)\gamma b}{R_{n+1}(s)} B \quad (8.6.5.25)$$

We note that $k(s)$ in expression (8.6.5.21) is related to $R_1(s)$ by

$$k(s) = B \frac{\gamma b}{R_1(s)} B \quad (8.6.5.27)$$

In the stationary case $(d/dt)c_m(t) = 0$, Eq. (8.6.5.18) may be easily solved as above in terms of the matrix continued-fractions; one obtains

$$[A + k(0)]\langle \mathbf{x}(\infty) \rangle = 0 \quad (8.6.5.28)$$

where $k(0) \equiv k(s=0)$ is given by relation (8.6.5.22) and $\langle \mathbf{x}(\infty) \rangle$ denotes the stationary value of $\langle \mathbf{x}(t) \rangle$.

It is of interest also to enquire to what extent a differential equation, applying directly to the averages $\langle \mathbf{x}(t) \rangle$, may be obtained for this system. To this end one inverts the Laplace transform of $\mathbf{d}_0(s)$, Eq. (8.6.5.21), and finds

$$\left(\frac{d}{dt} + A \right) \langle \mathbf{x}(t) \rangle + \int_0^t \tilde{K}(t-t') \langle \mathbf{x}(t') \rangle dt' = 0 \quad (8.6.5.29)$$

Clearly, this equation exhibits a finite correlation time through the shifted kernel $\tilde{K}(t'-t)$, where \tilde{K} is the inverse Laplace transform of $K(s)$. However, in the limit the phase derivative $\dot{\phi}(t)$ becomes a rapidly fluctuating object, one expects a negligibly small effect of the memory or correlation time. Thus in the “memoryless approximation” Eq. (8.6.5.2) reduces to a simple differential equation of the averages⁽¹⁷⁹⁾:

$$\left[\frac{d}{dt} + A + B \frac{b\gamma}{\gamma + A} B \right] \langle \mathbf{x}(t) \rangle = 0 \quad (8.6.5.30)$$

Furthermore, we note [Eq. (8.6.4.3)] that in the limit $\gamma \rightarrow \infty$ the phase derivatives $\dot{\phi}(t)$ indeed become delta correlated. Hence, on taking the limit $\gamma \rightarrow \infty$ in Eq. (8.6.5.30) one arrives at the well-known result, which is exactly valid^(181,182) for the delta-correlated phase-diffusion model:

$$\left[\frac{d}{dt} + A + bB^2 \right] \langle \mathbf{x}(t) \rangle = 0 \quad (8.6.5.31)$$

When applying Eq. (8.6.5.31) to the class of resonant multiphoton pro-

cesses described by Eq. (8.6.5.2), we first observe from matrix (8.6.5.4) that

$$bB^2 = N^2 b \begin{pmatrix} 0 & 0 & 0 & 0 \\ 0 & 0 & 0 & 0 \\ 0 & 0 & 1 & 0 \\ 0 & 0 & 0 & 1 \end{pmatrix} \quad (8.6.5.32)$$

Hence the equation of the average density matrix elements $\langle x(t) \rangle$ given by Eq. (8.6.5.3) reduces simply to

$$\left[\frac{d}{dt} + A(0) \right] \langle x(t) \rangle = 0 \quad (8.6.5.33)$$

where $A(0)$ is the same as A in Eq. (8.6.5.3), except that two of the diagonal matrix elements change as

$$i\Delta^* \rightarrow i\Delta^* + N^2 b \quad (8.6.5.34)$$

and

$$-i\Delta \rightarrow -i\Delta + N^2 b \quad (8.6.5.35)$$

This amounts to merely an increase in the decay constant $(\Gamma_{11} + \Gamma_{22})/2$ of the two off-diagonal density matrix elements $x_3(t)$ and $x_4(t)$, namely

$$\frac{1}{2}(\Gamma_{11} + \Gamma_{22}) \rightarrow \frac{1}{2}(\Gamma_{11} + \Gamma_{22}) + N^2 b \quad (8.6.5.36)$$

everything else remaining the same.

We therefore see that the theory of multiphoton processes using deterministic monomode (constant-amplitude) fields is essentially justified in the presence of diffusive phase fluctuations, provided the laser bandwidth is small enough such that

$$N^2 b \ll \frac{1}{2}(\Gamma_{11} + \Gamma_{22}) \quad (8.6.5.37)$$

We note that the increase (8.6.5.36) in the transverse (off-diagonal) decay constant is related directly to the decay constant of the N th-order correlation function (associated with the N -photon resonance transition), since for the diffusive process one has⁽¹⁶⁶⁾

$$\langle [E^*(t_1)]^N [E(t_2)]^N \rangle = |\varepsilon_0|^{2N} \exp[-N^2 b |t_1 - t_2|] \quad (8.6.5.38)$$

which decays exponentially with the same constant $N^2 b$. Finally, it should be observed that for non-delta-correlated phase fluctuations the desired

averages are obtained from Eq. (8.6.5.29) and determined by the inverse of Laplace transform (8.6.5.21).

8.6.6. A Model of a Multimode Laser Field

A multimode laser field exhibits both phase and amplitude fluctuations and may be considered to represent⁽¹⁸³⁾ a chaotic Gaussian process. Study of its influence on multiphoton processes presents a correspondingly more difficult mathematical problem. We shall assume⁽¹⁷³⁾ that the complex envelope function

$$E(t) = e(t)e^{-i\phi(t)} \equiv x(t) + iy(t) \quad (8.6.6.1)$$

is a two-dimensional Gaussian Markov process and satisfies the Langevin equations

$$\left. \begin{aligned} \frac{\partial x(t)}{\partial t} &= -bx(t) + F_x(t) \\ \frac{\partial y(t)}{\partial t} &= -by(t) + F_y(t) \end{aligned} \right\} \quad (8.6.6.2)$$

and

where $F_x(t)$ and $F_y(t)$ are independent δ -correlated Gaussian forces

$$\begin{aligned} \langle F_x(t_1)F_y(t_2) \rangle &= 0 \\ \langle F_x(t_1)F_x(t_2) \rangle &= bI_0\delta(t_1 - t_2) = \langle F_y(t_1)F_y(t_2) \rangle \end{aligned} \quad (8.6.6.3)$$

When we pass over to the amplitude variable $e = I^{1/2}$ and phase ϕ , we may also describe the process (8.6.6.1) by the Fokker–Planck (Master) equation corresponding to relations (8.6.6.2):

$$\frac{\partial}{\partial t} P[I, \phi, t] = W(I, \phi)P(I, \phi, t) \quad (8.6.6.4)$$

where

$$W(I, \phi) = 2b \left[\frac{\partial}{\partial I} (I - I_0) + I_0 \frac{\partial^2}{\partial I^2} I + \frac{I_0}{4I} \frac{\partial^2}{\partial \phi^2} \right] \quad (8.6.6.5)$$

The two-point N th-order correlation function for this process is given by⁽¹⁸⁵⁾

$$\begin{aligned} G^{(N)}(t_1, t_2) &= \langle [E^*(t_1)E(t_2)]^N \rangle \\ &= N! I_0^N \exp(-Nb|t_1 - t_2|) \end{aligned} \quad (8.6.6.6)$$

This may be compared with correlation function (8.6.5.38) for the (Brownian-) phase diffusion process.

Equation (8.6.6.6) enables us to identify parameters b and I_0 , respectively, with the bandwidth and mean intensity of the multimode field. We note that the Gaussian Markov assumption for the process (8.6.6.1) leads to an exponential autocorrelation function [Eq. (8.6.6.6) with $N = 2$] whose Fourier transform restricts the theory to fields with only Lorenzian spectra. On the other hand, it is this assumption that also permits one to employ the systematic method of the Kubo–Liouville equation (8.6.2.5) to this more complex problem involving amplitude fluctuations.

8.6.7. Two-Photon Resonant Three-Photon Ionization

We shall illustrate the method of solution following the analysis of a specific problem,^(173,184) namely the problem of two-photon resonant three-photon ionization in a multimode field. The density matrix equation is now a special case of Eq. (8.5.1.15) with $N = 2$ and $p = 1$. [It is also assumed that the higher-order matrix elements of order $(e(t))^{N+2p}$ in Eqs. (8.5.1.16)–(8.5.1.19) are negligible.]

Let us define the four-component vector $\mathbf{x}(t)$ by

$$\left. \begin{array}{l} x_1(t) = \rho_{11}(t), \\ x_2(t) = \rho_{22}(t) \\ x_3(t) = \rho_{12}(t), \\ x_4(t) = \rho_{21}(t) \end{array} \right\} \quad (8.6.6.7)$$

The field (8.6.6.1) depends on a set of two stochastic variables $\boldsymbol{\epsilon} \equiv (I, \phi)$. The Kubo–Liouville probability density $P(\mathbf{x}, I, \phi, t)$ therefore depends on both I and ϕ and satisfies Eq. (8.6.2.5), where A is the matrix obtained from the (Liouville) matrix on the left-hand side of Eq. (8.5.1.15):

$$A(I, \phi) = - \begin{pmatrix} 0 & \gamma_s & iV(I)e^{-i2\phi} & -iV(I)e^{i2\phi} \\ 0 & -(\gamma_s + \lambda_2 I) & -iV(I)e^{-i2\phi} & iV(I)e^{i2\phi} \\ iV(I)e^{i2\phi} & -iV(I)e^{i2\phi} & -i\Delta^*(I) & 0 \\ -iV(I)e^{-i2\phi} & iV(I)e^{i2\phi} & 0 & i\Delta(I) \end{pmatrix}$$

where

$$I = e^2 \quad (8.6.6.9)$$

and

$$\left. \begin{array}{l} V(I) = \beta I \\ \Delta(I) = \delta_0 - s(I) + \frac{1}{2}i(\gamma_s + \gamma(I)) \\ s(I) = (s_2 - s_1)I \\ \gamma(I) = \lambda_2 I \end{array} \right\} \quad (8.6.6.10)$$

and

$$\delta_0 = 2\omega - \omega_2 + \omega_1 \quad (8.6.6.11)$$

$$\hbar\beta = \sum_j \frac{\langle 2 | \mathbf{\epsilon} \cdot \frac{\mathbf{D}}{2} | j \rangle \langle j | \mathbf{\epsilon} \cdot \frac{\mathbf{D}}{2} | 1 \rangle}{\omega_1 - \omega_j - \omega} \quad (8.6.6.12)$$

$$\hbar s_i = \sum_j \left| \langle i | \mathbf{\epsilon} \cdot \frac{\mathbf{D}}{2} | j \rangle \right|^2 \left[\frac{1}{\omega_i - \omega_j + \omega} + \frac{1}{\omega_i - \omega_j - \omega} \right] \quad (i = 1, 2) \quad (8.6.6.13)$$

$$\hbar\lambda_2 = 2\pi \sum_{k_f} \left| \langle \mathbf{k}_f | \frac{\mathbf{\epsilon} \cdot \mathbf{D}}{2} | 2 \rangle \right|^2 \quad (8.6.6.14)$$

where $|\mathbf{k}_f\rangle$ is the continuum state of interest. The corresponding equations for the vector of the marginal averages $\mathbf{y}(t)$, where now

$$y_i(I, \phi; t) \equiv \int x_i P(\mathbf{x}, I, \phi; t) d\mathbf{x} \quad (i = 1, \dots, 4) \quad (8.6.6.15)$$

are obtained immediately from Eq. (8.6.3.7):

$$\left[\frac{\partial}{\partial t} - W(I, \phi) \right] \mathbf{y}(t) = A(I, \phi) \mathbf{y}(t) \quad (8.6.6.16)$$

$W(I, \phi)$ is given by Eq. (8.6.6.5). Equation (8.6.6.16) must be solved subject to the initial condition

$$y_i(I, \phi, t) = x_i^0 P_{00}(I, \phi) \quad (8.6.6.17)$$

where $P_{00}(I, \phi)$ is the stationary solution of

$$W(I, \phi) P_{00}(I, \phi) = 0 \quad (8.6.6.18)$$

This is given explicitly by

$$P_{00}(I, \phi) = \frac{1}{2\pi I_0} e^{-I/I_0} \quad (8.6.6.19)$$

The biorthonormal set of solutions of the left and right eigenvectors of the operator (8.6.6.5) are^(180,185)

$$\left. \begin{aligned} WP_n^m(I, \phi) &= \lambda_{nm} P_n^m(I, \phi) \\ W^+ \Phi_n^m(I, \phi) &= \lambda_{nm} \Phi_n^m(I, \phi) \end{aligned} \right\} \quad (8.6.6.20)$$

and

where

$$P_n^m(I, \phi) = \frac{e^{im\phi}}{2\pi I} \left[\frac{n!}{(n+|m|)!} \right]^{1/2} e^{-\chi} \chi^{|m|/2} L_n^{|m|}(\chi) \quad (8.6.6.21)$$

and

$$\Phi_n^m(I, \phi) = \left[\frac{n!}{(n+|m|)!} \right]^{1/2} \chi^{|m|/2} L_n^{|m|}(\chi) e^{im\phi} \quad (8.6.6.22)$$

In Eqs. (8.6.6.21) and (8.6.6.22) we have defined $\chi = I/I_0$; $L_n^{|m|}(\chi)$ are Laguerre polynomials. The eigenvalues of W are

$$\lambda_{nm} = b(2n + |m|) \quad (8.6.6.23)$$

The completeness relation

$$\sum_{nm} |P_n^m\rangle \langle \Phi_n^m| = 1 \quad (8.6.6.24)$$

is now used to expand $y_i(I, \phi; t)$ as

$$y_i(I, \phi, t) = \sum_{nm} c_{nm}^{(i)}(t) P_n^m(I, \phi) \quad (8.6.6.25)$$

Any desired average $\langle x_i(t) \rangle$ is obtained on substitution of Eq. (8.6.6.25) in relation (8.6.3.3):

$$\begin{aligned} \langle x_i(t) \rangle &= \int_0^\infty \int_0^{2\pi} y_i(I, \phi; t) dI d\phi \\ &= \sum_{nm} c_{nm}^{(i)}(t) \delta_{n,0} \delta_{m,0} = c_{00}^{(i)}(t) \end{aligned} \quad (8.6.6.26)$$

In the second line here we have used the fact that $\Phi_0^0(I, \phi) = 1$ along with the orthogonality relation

$$\begin{aligned} \langle \Phi_{n'}^m(I, \phi) | P_n^m(I, \phi) \rangle &= \int_0^\infty \int_0^{2\pi} \Phi_{n'}^m(I, \phi) P_n^m(I, \phi) dI d\phi \\ &= \delta_{n,n'} \delta_{m,m'} \end{aligned} \quad (8.6.6.27)$$

Finally, the equations determining the coefficients

$$c_i^{(n,m)}(t) = \langle \Phi_n^m | y_i(I, \phi; t) \rangle \quad (8.6.6.28)$$

are found by substituting Eq. (8.6.6.25) into Eq. (8.6.6.16), multiplying by function $\Phi_n^{m*}(I, \phi)$, and integrating over dI and $d\phi$. By using the orthogonality relation (8.6.6.27), eigenvalues (8.6.6.23), and well-known integrals involving Laguerre functions, one obtains⁽¹⁸⁴⁾

$$\left(\frac{d}{dt} + 2bn \right) (c_2^{n,0} + c_1^{n,0}) = -\gamma(I_0)(2n+1)c_2^{n,0} + \gamma(I_0)[(n+1)c_2^{n+1,0} + nc_2^{n-1,0}] \quad (8.6.6.29)$$

$$\begin{aligned} & \left[\frac{d}{dt} + 2bn + \gamma(I_0)(2n+1) + \gamma_s \right] c_2^{n,0} \\ &= \gamma(I_0)[(n+1)c_2^{n+1,0} + nc_2^{n-1,0}] \\ &+ iV(I_0)\{[(n+1)(n+2)]^{1/2}(c_4^{n,-2} - c_3^{n,2}) - 2[n(n+1)]^{1/2}(c_4^{n-1,-2} - c_3^{n-1,2}) \\ &+ [n(n-1)]^{1/2}(c_4^{n-2,-2} - c_3^{n-2,2})\} \end{aligned} \quad (8.6.6.30)$$

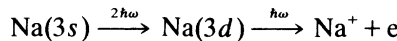
and

$$\begin{aligned} & \left[\frac{d}{dt} + i\delta_0 + is(I_0)(2n+3) + b(2n+1) + \gamma(I_0)(n+3/2) + \gamma_s/2 \right] c_3^{n,2} \\ &= iV(I_0)[(n+1)(n+2)]^{1/2}\{(c_2^{n,0} - c_1^{n,0}) - 2(c_2^{n+1,0} - c_1^{n+1,0}) + (c_2^{n+2,0} - c_1^{n+2,0})\} \end{aligned} \quad (8.6.6.31)$$

for all $n = 0, 1, 2, 3, \dots, \infty$. The infinite set of differential equations for the quantities $c_i^{n,m}(t)$ can be reduced to an infinite set of algebraic equations for their Laplace transforms, which, however, cannot be solved in closed form. Physically speaking, the lowest level of approximation, $n = 0$, would correspond to neglecting all correlation between the atom and the field (the so-called decorrelation approximation⁽¹⁸⁶⁾). This limit is obviously reached as the field “coherence time” $\approx 1/b \rightarrow 0$. Maintaining increasingly higher values of n in the system of equations (8.6.6.29)–(8.6.6.31) amounts to retaining the effect of mutual correlation between the atom and the field. This becomes increasingly significant for increasing field coherence time, e.g., for $1/b$ greater than the typical interaction periods involved in the system, or

$$\frac{1}{b} \gg [V(I_0)]^{-1}, [\gamma(I_0)]^{-1}, [s(I_0)]^{-1} \quad (8.6.6.32)$$

Detailed numerical calculations using finite truncations of Eqs. (8.6.6.29)–(8.6.6.31) have been carried out⁽¹⁸⁴⁾ for the resonant three-photon ionization of Na:



They reveal the difference in the ionization (or excitation) signals in Na due to a multimode (chaotic field model) vs. a single-mode (phase-diffusion model) laser field of the same intensity, as well as their dependence on the field correlation time and on the laser-atom interaction time.

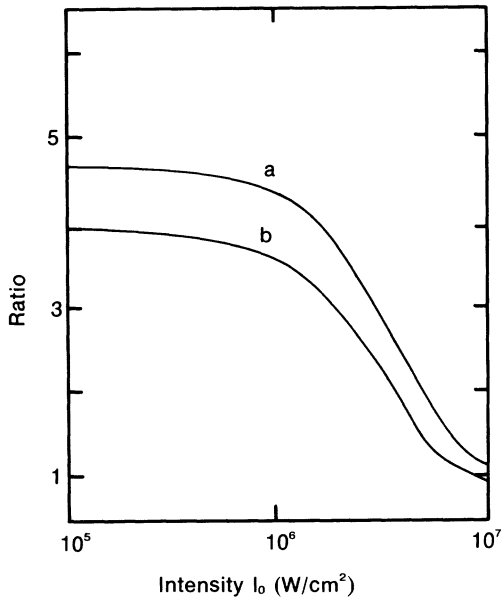


Figure 36. Ratio of on-resonance ionization (curve a) probabilities due to chaotic and phase-diffusive fields as a function of laser intensity (W/cm^{-2}) for the process of two-photon resonant three-photon ionization of $\text{Na}(3s)$. The corresponding ratio for the population of the intermediate excited state, $\text{Na}(3d)$, is given by curve b. The bandwidth $b = 0.09/2$ (cm^{-1}) and interaction time $t_p = 1$ ns (from Zoller and Lambropoulos⁽¹⁸⁴⁾).

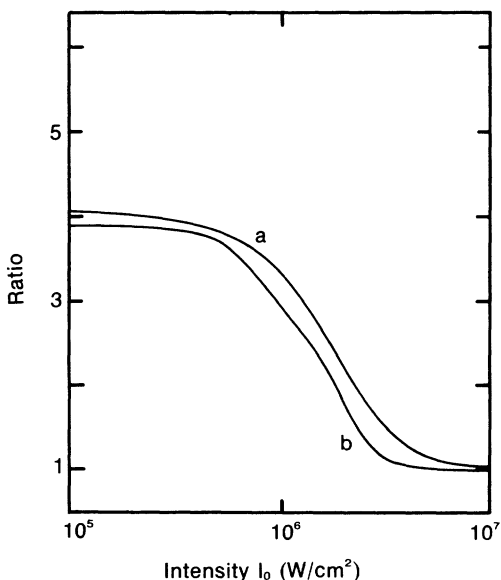


Figure 37. Ratio of on-resonance ionization (curve a) probabilities due to chaotic and phase-diffusive fields as a function of laser intensity (W/cm^{-2}) for the process of two-photon resonant three-photon ionization of $\text{Na}(3s)$. The corresponding ratio for the population of the intermediate excited state, $\text{Na}(3d)$, is given by curve b. The bandwidth $b = 0.09/2$ (cm^{-1}) and interaction time $t_p = 5$ ns (from Zoller and Lambropoulos⁽¹⁸⁴⁾).

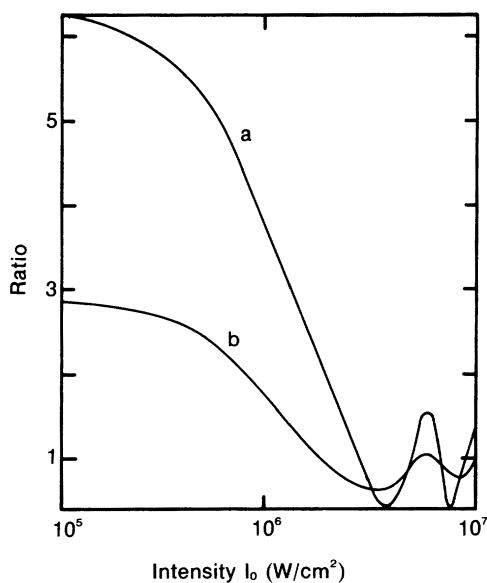


Figure 38. Ratio of on-resonance ionization (curve a) probabilities due to chaotic and phase-diffusive fields as a function of laser intensity (W cm^{-2}) for the process of two-photon resonant three-photon ionization of $\text{Na}(3s)$. The corresponding ratio for the population of the intermediate excited state, $\text{Na}(3d)$, is given by curve b. The bandwidth $b = 0.009/2$ (cm^{-1}) and interaction time $t_p = 1$ ns (from Zoller and Lambropoulos⁽¹⁸⁴⁾).

Figures 36–38 exhibit the ratios of on-resonance ionization probabilities (curve a) due to multimode vs. monomode laser fields of different bandwidths b and interaction times t_p . Similar ratios for the intermediate excited-state populations are given by the curves marked b.

An interesting result of this calculation is that at higher intensities and with the onset of saturation of the resonant transition, the ionization and excitation probabilities may become smaller in a multimode field than in a monomode field. This is in contrast to the low-intensity behavior. In the latter case the N -photon transition rate depends simply on the N th-order correlation function of light and hence it is $N!$ times larger [cf. Eqs. (8.6.5.38) and (8.6.6.6)] for a multimode (chaotic) field than for a single-mode (phase-diffusive) field. Another interesting result is that in the large-bandwidth limit the Stark-shift in the multimode case is found to be a factor of 3 larger than in the monomode case. However, this relation changes with increasing intensity and can therefore significantly affect the power-law dependence^(187,188) of the resonant ionization probability. Generally speaking one finds that, with large-bandwidth multimode fields of lower intensities, the ionization process becomes statistically independent of the resonant excitation step. However, as expected, a correlation between the two stages becomes manifest with increasing field correlation time, i.e., with decreasing bandwidth b .

9

Continued Fractions and Recursive-Iterative Perturbation Theory

9.1. Introduction

For high field strengths, the number of photons effectively exchanged between the atom and the field becomes rather large and it is necessary to find methods for evaluating the resolvent amplitudes or state vectors that can be extended arbitrarily in the photon space.

For strong-field processes in a monomode field one such method is provided by the matrix continued-fraction representation of the resolvent that describes the net emission or absorption of n photons. Originally, this was obtained^(8,189) by carefully counting and classifying the sequence of higher-order perturbation diagrams for an n -photon process and inferring their rule of composition that allowed the diagrams to be summed in terms of continued fractions of suitable operators. Analytic expressions of n -photon transition probabilities in special cases^(111,190-192) in terms of continued fractions and continued-fraction perturbation theory⁽¹⁹³⁻¹⁹⁵⁾ are also known. The technique of projection operators has been used⁽¹⁹⁶⁾ ingeniously to retrieve the general diagrammatic results. A rederivation of these results using the theory of determinants and matrix-partition techniques has also been given⁽¹⁹⁷⁾ and the relation with the Floquet method elucidated. Perhaps the simplest and most obvious way of deriving the continued-fraction representation of the multiphoton resolvent operator or any other related quantity, such as the multiphoton wave vector, is to use the following algebraic approach based on a three-term recurrence relation.

9.2. The Three-Term Recurrence Relation

We consider the resolvent equation

$$(E - H)G(E) = 1 \quad (9.2.1)$$

with the total Hamiltonian

$$H = H_{\text{atom}} + a^+ a \hbar \omega + \left(\frac{8\pi\hbar\omega}{L^3} \right)^{1/2} \boldsymbol{\epsilon} \cdot \frac{\mathbf{D}}{2} (a^+ + a) \quad (9.2.2)$$

For the matrix elements of the resolvent between a pair of number states we use the simplifying notation

$$\langle n_0 + n | G(E) | n_0 \rangle = G_n(E) = G_n \quad (9.2.3)$$

For the sake of brevity we also define the coupling strength

$$V_n = \left[\frac{2\pi\hbar\omega(n_0 + n)}{L^3} \right]^{1/2} \boldsymbol{\epsilon} \cdot \mathbf{D} \quad (9.2.4)$$

and the unperturbed Hamiltonian

$$H_n = H_{\text{atom}} + (n_0 + n)\hbar\omega \quad (9.2.5)$$

The matrix element of Eq. (9.2.1) between number states $\langle n_0 + n |$ and $| n_0 \rangle$ therefore reads simply

$$(E - H_n)G_n - V_{n+1}G_{n+1} - V_nG_{n-1} = \delta_{n,0} \quad (9.2.6)$$

Equation (9.2.6) provides the basis for the continued-fraction representation of G_n .

9.3. The Continued-Fraction Representation

For $n > 0$ [the delta part in relation (9.2.6) vanishes] we may multiply the homogeneous three-term recurrence relation (9.2.6) from the right by G_n^{-1} and obtain

$$\begin{aligned} V_n G_{n-1} G_n^{-1} &= E - H_n - V_{n+1} G_{n+1} G_n^{-1} \\ &= E - H_n - V_{n+1} G_{n+1} G_n^{-1} (V_{n+1}^{-1} V_{n+1}) \\ &= E - H_n - V_{n+1} \frac{1}{V_{n+1} G_n G_{n+1}^{-1}} V_{n+1} \end{aligned} \quad (9.3.1)$$

In the second line we have merely inserted the identity $(V_{n+1}^{-1} V_{n+1}) = 1$, while the third line follows at once from the elementary algebraic relation

$$G_{n+1} G_n^{-1} V_{n+1}^{-1} = (V_{n+1} G_n G_{n+1}^{-1})^{-1} \quad (9.3.2)$$

Let us set

$$R_n = R_n(E) = V_n G_{n-1} G_n^{-1} \quad (n > 0) \quad (9.3.3)$$

in relation (9.3.1) and we have already the generating equation for the continued fractions,

$$R_n(E) = E - H_n - V_{n+1} \frac{1}{R_{n+1}(E)} V_{n+1} \quad (9.3.4)$$

By taking the inverse of relation (9.3.1) and multiplying from the right by $V_n G_{n-1}$ and substituting Eq. (9.3.4), we in fact obtain the desired continued-fraction representation of the resolvent

$$G_n(E) = \frac{1}{R_n(E)} V_n G_{n-1}(E), \quad n > 0 \quad (9.3.5)$$

We may conveniently iterate $R_n(E)$ in the denominator of this equation with the aid of Eq. (9.3.4). This yields the continued fraction G_n free from the operator R_n :

$$\begin{aligned} G_n(E) = & \frac{1}{E - H_n - V_{n+1} \frac{1}{E - H_{n+1} - V_{n+2} \frac{1}{E - H_{n+2} - V_{n+3} \frac{1}{E - H_{n+3} \dots}} V_{n+1} V_{n+2} V_{n+3} \dots}} V_n G_{n-1}(E) \\ & \ddots \end{aligned} \quad (9.3.6)$$

In practice, however, the indefinite iterations in Eq. (9.3.6) must be truncated at a suitable level determined by simple numerical convergence.

An analogous derivation holds for $n < 0$. Thus, starting with the first line of Eq. (9.3.1) but retaining now the term with V_{n+1} on the left (instead of the term with V_n) and proceeding exactly as before, we obtain the continued-fraction representation of G_n for $n < 0$:

$$G_n(E) = \frac{1}{L_n(E)} V_{n+1} G_{n+1}(E), \quad n < 0 \quad (9.3.7)$$

where

$$L_n(E) = E - H_n - V_n \frac{1}{L_{n-1}(E)} V_{n-1} \quad (9.3.8)$$

is the analog of $R_n(E)$ given by Eq. (9.3.4).

9.4. The Elastic Resolvent

For $n = 0$ we have, directly from expression (9.2.6), the “connection equation”

$$(E - H_0)G_0(E) - V_1 G_1(E) - V G_{-1}(E) = 1 \quad (9.4.1)$$

Use of Eqs. (9.3.5) and (9.3.7) respectively for $G_1(E)$ and $G_{-1}(E)$ in Eq. (9.4.1) permits one to find $G_0(E)$ explicitly:

$$\begin{aligned} G_0(E) &= \left[E - H_0 - V_1 \frac{1}{R_1(E)} V_1 - V_0 \frac{1}{L_{-1}(E)} V_0 \right]^{-1} \\ &\equiv [E - H_0 - R^0(E) - L^0(E)]^{-1} \end{aligned} \quad (9.4.2)$$

where $R^0(E)$ and $L^0(E)$ are infinite continued fractions given by

$$R^0(E) \equiv V_1 \frac{1}{R_1(E)} V_1 \quad (9.4.3)$$

$$\begin{aligned} &= \frac{1}{E - H_1 - V_2 \frac{1}{E - H_2 - V_3 \frac{1}{E - H_3 - V_4 \frac{1}{E - H_4 \dots}}}} V_1 \\ &\quad V_2 \\ &\quad V_3 \\ &\quad V_4 \end{aligned} \quad (9.4.4)$$

$$L^0(E) \equiv V_0 \frac{1}{L_{-1}(E)} V_0 \quad (9.4.5)$$

$$\begin{aligned} &= \frac{1}{E - H_{-1} - V_{-1} \frac{1}{E - H_{-2} - V_{-2} \frac{1}{E - H_{-3} - V_{-3} \frac{1}{E - H_{-4} \dots}}}} V_0 \\ &\quad V_{-1} \\ &\quad V_{-2} \\ &\quad V_{-3} \end{aligned} \quad (9.4.6)$$

Equation (9.4.2) for $G_0(E)$ thus provides the elastic scattering of the

incident photons from the atomic target (with no net emission or absorption of photons). The poles of $G_0(E)$ also provide the perturbed eigenvalues of the atomic system in the presence of the field.

9.5. The Resolvent for Emission and Absorption of n Photons

The inelastic resolvent for the emission of n photons can be readily expressed as an explicit continued fraction. Thus by iterating Eq. (9.3.5) to replace $G_{n-1}(E)$ appearing on the right-hand side, in favor of $G_0(E)$, we get

$$G_n(E) = \frac{1}{R_n(E)} V_n \frac{1}{R_{n-1}(E)} V_{n-1} \cdots V_2 \frac{1}{R_1(E)} V_1 \frac{1}{E - H_0 - R^0(E) - L^0(E)} \quad (n > 0) \quad (9.5.1)$$

Similarly, Eq. (9.3.7) yields the resolvent operator for the absorption of n photons:

$$G_n(E) = \frac{1}{L_n(E)} V_{n+1} \frac{1}{L_{n+1}(E)} V_{n+2} \cdots V_{-1} \frac{1}{L_{-1}(E)} V_0 \frac{1}{E - H_0 - R^0(E) - L^0(E)} \quad (n < 0) \quad (9.5.2)$$

The main feature of transition operators (9.5.1) and (9.5.2) as well as of elastic amplitude (9.5.2) is that they are defined explicitly merely on the atomic Hilbert space, the need for the evaluation of all higher-order number-space intermediate matrix elements at every level of the continued fractions having been already disposed of due to relation (9.2.6). We note that the order of the virtual photon processes to be included for a given problem may be increased by merely retaining deeper levels of the fractions and calculating step by step. This eliminates the necessity of directly dealing with the increased total dimension of the product space, $|j\rangle |n\rangle$. It should be observed that the monomode semiclassical Floquet equations (6.3.8), being a three-term recursion relation like Eq. (9.2.6), can be treated in the same way. It is also obvious that this will give rise to exactly the same results for the resolvent amplitudes as given by Eqs. (9.4.2), (9.5.1), and (9.5.2) except that all quantities V_n will be equal to each other and will be given simply by the semiclassical interaction operator

$$V = \frac{F_0}{2} \boldsymbol{\epsilon} \cdot \mathbf{D} \quad (9.5.3)$$

where F_0 is the peak field strength.

9.6. The Continued-Fraction Representation of the T-Matrix

For nonresonant ionization processes and for the continuum-continuum transitions, the rate or cross section of multiphoton transitions should generally exist as a good parameter and the rate of the transition of interest [Eq. (3.9.2.7)] is governed by the reduced transition matrix τ , defined by Eq. (3.3.7). The method developed in the preceding sections will now be applied to obtain a continued-fraction representation of τ :

$$\tau = V + VqG_0^+V + VqG_0^+VqG_0^+V + \dots \quad (9.6.1)$$

We recall that G_0^+ is the unperturbed outgoing resolvent, Eq. (3.3.1) [not to be confused with the elastic resolvent $G_0(E)$, Eq. (9.4.2)], and that the projection operator q [see Eq. (3.3.6)] removes the external divergencies associated with the initial and final states. Thanks to the presence of q , the n -photon continued-fraction representation of the transition amplitudes, to be derived below, will also be free from such divergencies. Clearly, the infinite series (9.6.1) can be effectively “summed” as

$$\begin{aligned} \tau &= V + VqG_0^{(+)}(V + VqG_0^+V + \dots) \\ &= V + VqG_0^{(+)}\tau \end{aligned} \quad (9.6.2)$$

In analogy with the definitions in the previous section we define the matrix elements of τ between number states $\langle n_0 + n |$ and $| n_0 \rangle$ as

$$\tau_n = \langle n_0 + n | \tau | n_0 \rangle \quad (9.6.3)$$

Similarly we shall denote the expectation value of the unperturbed resolvent ($qG_0^{(+)}$) as simply

$$\begin{aligned} g_n^0 &= g_n^0(E) = \langle n_0 + n | qG_0^{(+)} | n_0 + n \rangle \\ &= \lim_{\eta \rightarrow 0} \frac{q_n}{E - H_{\text{atom}} - (n_0 + n)\hbar\omega + i\eta} \\ &= \lim_{\eta \rightarrow 0} \frac{q_n}{E - H_n + i\eta} \end{aligned} \quad (9.6.4)$$

with H_n given by expression (9.2.5). Since

$$q \equiv 1 - | n_0 + n_f \rangle | f \rangle \langle f | \langle n_0 + n_f | - | n_0 \rangle | i \rangle \langle i | \langle n_0 | \quad (9.6.5)$$

therefore

$$q_n = \begin{cases} 1 & \text{for } n \neq 0, n_f \\ 1 - | f \rangle \langle f | & \text{for } n = n_f \\ 1 - | i \rangle \langle i | & \text{for } n = 0 \end{cases} \quad (9.6.6)$$

9.6.1. Recursion Relation for the Reduced T-Matrix

On taking the matrix elements on both sides of Eq. (9.6.2) between states $|n + n_0\rangle$ and $|n_0\rangle$ and using the definitions just introduced, we obtain the (inhomogeneous) three-term recursion relation:

$$\tau_n = V_n g_{n-1}^0 \tau_{n-1} + V_{n+1} g_{n+1}^0 \tau_{n+1} + V_0 \delta_{n,-1} + V_1 \delta_{n,1} \quad (9.6.1.1)$$

where V_n is given as before by Eq. (9.2.4).

For $n \neq \pm 1$, Eq. (9.6.1.1) reduces to a three-term matrix recurrence relation and the method applied in the previous section can be used in a similar way without difficulty. Thus after some simple algebra we arrive at the result

$$\tau_n = \frac{1}{1 - V_{n+1} \frac{1}{R_{n+1}} V_{n+1} g_n^0} V_n g_{n-1}^0 \tau_{n-1} \quad (9.6.1.2)$$

for $n \geq 0, \neq 1$ and

$$\tau_n = \frac{1}{1 - V_n \frac{1}{L_{n-1}} V_n g_n^0} V_{n+1} g_{n+1}^0 \tau_{n+1} \quad (9.6.1.3)$$

for $n \leq 0, \neq -1$.

The expressions for τ_1 or τ_{-1} may be found by setting $n = 1$ or $n = -1$ in Eq. (9.6.1.1). Thus

$$\tau_1 = V_1 g_0^0 \tau_0 + V_2 g_2^0 \tau_2 + V_1 \quad (9.6.1.4)$$

and

$$\tau_{-1} = V_{-1} g_{-2}^0 \tau_{-2} + V_0 g_0^0 \tau_0 + V_0 \quad (9.6.1.5)$$

On letting $n = 0$ or 2 in Eq. (9.6.1.2) we get

$$\tau_0 = \frac{1}{1 - V_1 \frac{1}{R_1} V_1 g_0^0} V_0 g_{-1}^0 \tau_{-1} \quad (9.6.1.6)$$

and

$$\tau_2 = \frac{1}{1 - V_3 \frac{1}{R_3} V_3 g_2^0} V_2 g_1^0 \tau_1 \quad (9.6.1.7)$$

Also, from Eq. (9.6.1.3) for $n = 0$ or -2 we get

$$\tau_0 = \frac{1}{1 - V_0 \frac{1}{L_{-1}} V_0 g_0^0} V_1 g_1^0 \tau_1 \quad (9.6.1.8)$$

and

$$\tau_{-2} = \frac{1}{1 - V_{-2} \frac{1}{L_{-3}} V_{-2} g_{-2}^0} V_{-1} g_{-1}^0 \tau_{-1} \quad (9.6.1.9)$$

Substitution for τ_0 and τ_{-2} from Eqs. (9.6.1.8) and (9.6.1.7) into Eq. (9.6.1.4) yields the reduced one-photon emission amplitude,

$$\tau_1(E) = \frac{1}{1 - \left(V_1 \frac{1}{E - H_0 - L^0(E)} V_1 + V_2 \frac{1}{R_2(E)} V_2 \right) g_1^0(E)} V_0 \quad (9.6.1.10)$$

Similarly, substitution for τ_0 and τ_{-2} from Eqs. (9.6.1.6) and (9.6.1.9) into Eq. (9.6.1.5) yields

$$\tau_{-1}(E) = \frac{1}{1 - \left(V_{-1} \frac{1}{L_{-2}(E)} V_{-1} + V_0 \frac{1}{E - H_0 - R^0(E)} V_0 \right) g_{-1}^0(E)} V_0 \quad (9.6.1.11)$$

9.6.2. The T-Matrix for Emission and Absorption of n Photons

Finally, by iterating Eq. (9.6.1.2) the reduced n -photon emission amplitude τ_n is obtained for all $n \geq 3$, starting with τ_1 and τ_{-2} given by (9.6.1.10) and (9.6.1.7), respectively.

Similarly the n -photon absorption amplitudes τ_n are obtained from Eq. (9.6.1.3) by iteration for all $n \leq -3$, starting with τ_{-1} and τ_{-2} given by (9.6.1.11) and (9.6.1.9), respectively. The resulting expressions can be used in connection with Eq. (3.9.2.7) to determine the transition rate. We note that the reduced versions of the n -photon resolvents (9.5.1) and (9.5.2), if needed, may also be obtained from Eqs. (9.6.1.2) and (9.6.1.3) in combination with definition (3.3.4) relating the resolvent G to the T -matrix.

9.7. Continued-Fraction Representation of a Stationary Wave Function

The stationary Schrödinger equation

$$(E - H) |\psi\rangle = 0 \quad (9.7.1)$$

satisfied by the Hamiltonian (9.2.2) may be projected onto the number state $\langle n + n_0 |$, in the same way as we have projected the resolvent equation (9.2.1). Defining the n -photon component of the wave vector $|\psi\rangle$ by

$$\langle n + n_0 | \psi \rangle = \psi_n \quad (9.7.2)$$

one easily finds from Eq. (9.7.1) that

$$(E - H_n) \psi_n = V_{n+1} \psi_{n+1} + V_n \psi_{n-1} \quad (n = 0, \pm 1, \pm 2, \pm 3, \dots) \quad (9.7.3)$$

This is again a three-term (matrix) recurrence relation, similar to relation (9.2.6) for the resolvent G_n , except that Eq. (9.7.3) is homogeneous. Clearly, the wave function ψ_n for any n -photon process possesses the same form of the continued-fraction representation as that of the resolvent $G_n(E)$ obtained before. Proceeding exactly as in Section 9.3, one therefore obtains

$$\psi_n = \frac{1}{R_n(E)} V_n \psi_{n-1} \quad (n > 0) \quad (9.7.4)$$

and

$$\psi_n = \frac{1}{L_n(E)} V_{n+1} \psi_{n+1} \quad (n < 0) \quad (9.7.5)$$

where R_n and L_n are the same as in Eqs. (9.3.4) and (9.3.8) respectively. If we set $n = 0$ in Eq. (9.7.3) and express ψ_1 and ψ_{-1} in terms of ψ_0 with the help of Eqs. (9.7.4) and (9.7.5) respectively, we obtain

$$[E - H_0 - \mu^0(E)] \psi_0 = 0 \quad (9.7.6)$$

with

$$\mu^0(E) \equiv R^0(E) + L^0(E) \quad (9.7.7)$$

where R^0 and L^0 are given by Eqs. (9.4.4) and (9.4.6). In view of the homogeneous nature of Eq. (9.7.6) (while the wave functions ψ_n may be determined to within ψ_0) ψ_0 is uniquely specified only by imposing a suitable initial condition and normalization requirements.

9.7.1. The n -Photon Wave Function

The wave function ψ_n containing all information regarding the emission of n photons thus assumes the form

$$\psi_n = \frac{1}{R_n(E)} V_n \frac{1}{R_{n-1}(E)} V_{n-1} \cdots V_2 \frac{1}{R_1(E)} V_1 \psi_0 \quad (n > 0) \quad (9.7.1.1)$$

which is an exact analog of Eq. (9.5.1) for the resolvent G_n . Similarly, the wave function containing all information about the absorption of n photons is

$$\psi_n = \frac{1}{L_n(E)} V_{n+1} \frac{1}{L_{n+1}(E)} V_{n+2} \cdots V_{-1} \frac{1}{L_{-1}(E)} V_0 \psi_0 \quad (n < 0) \quad (9.7.1.2)$$

This is the analog of Eq. (9.5.2).

9.8. The Multiphoton Eigenvalue Problem

Determination of the perturbed eigenvalues in the presence of the field is often the crux of the calculational problem of multiphoton processes of interest. A formulation of the problem within the framework of the continued-fraction theory and a method of solution based on a recursive-iterative approach are developed below.

The Schrödinger equation for the Hamiltonian (9.2.2) is conveniently projected onto the subspace p . We let $\psi_p = p |\psi\rangle$ be the projected wave function, where p is a projection operator which projects onto any specified state (such as the initial state) of the system. Then, as in Section 7.5.1, we readily find the equation [cf. Eqs. (7.5.1.9) and (7.5.1.13)] satisfied by ψ_p :

$$\left[E - H^0 - V_{pp} - V_{pq} \frac{1}{E - H^0 - V_{qq}} V_{qp} \right] \psi_p = 0 \quad (9.8.1)$$

where

$$H^0 = H_{\text{atom}} + a^+ a \hbar \omega \quad (9.8.2)$$

$$V = \left(\frac{2\pi\hbar\omega}{L^3} \right)^{1/2} \boldsymbol{\epsilon} \cdot \mathbf{D} (a^+ + a) \quad (9.8.3)$$

and

$$V_{pq} = pVq \quad \text{etc.} \quad (9.8.4)$$

with

$$q = 1 - p \quad (9.8.5)$$

In order to find the eigenvalue equation, it is convenient to choose

$$p = |A\rangle\langle A|, \quad q = 1 - |A\rangle\langle A| \quad (9.8.6)$$

where

$$|A\rangle = |a\rangle |n_0 + 0\rangle \quad (9.8.7)$$

is the initial state, with the atom in state $|a\rangle$ with energy ε_a and the field in state $|n_0 + 0\rangle$.

If we project on the left of Eq. (9.8.1) with $\langle A|$ and use expression (9.8.7), then we obtain the eigenvalue equation

$$\left[E - E_A - \langle A | V | A \rangle - \langle A | V \frac{q}{E - H^0 - V_{qq}} V | A \rangle \right] \langle A | \psi \rangle = 0 \quad (9.8.8)$$

where

$$E_A = \varepsilon_a + n_0 \hbar \omega \quad (9.8.9)$$

9.8.1. The Level-Shift Operator

Equation (9.8.8) is an ordinary homogeneous algebraic equation whose condition of solution gives the perturbed eigenvalue $E = E'_\lambda$ (say) corresponding to the unperturbed eigenvalue E_A , namely

$$E = E_A + \langle A | V | A \rangle + \langle A | V \frac{q}{E - H^0 - V_{qq}} V | A \rangle \quad (9.8.1.1)$$

Thus the problem of finding the eigenvalues of the system reduces essentially to the evaluation of the diagonal matrix element of the “level-shift” operator^(10,11,13) $M(E)$ defined by

$$M(E) \equiv V \frac{q}{E - H^0 - V_{qq}} V \quad (9.8.1.2)$$

One notes that for the interaction V , given by expression (9.8.3), the diagonal matrix elements vanish and the q in the numerator of Eq. (9.8.8) can be replaced by unity [see Eq. (9.8.6)]. In this case, therefore, Eq. (9.8.1.1) further reduces to

$$E = E_A + \langle A | M(E) | A \rangle \quad (9.8.1.3)$$

with

$$\langle A | M(E) | A \rangle = \langle A | V \frac{1}{E - H^0 - V_{qq}} V | A \rangle \quad (9.8.1.4)$$

It should be observed that if one lets $V_{qq} = 0$ then, as expected, the change in energy $\Delta E_A \equiv E - E_A$ is given by the well-known second-order dynamic Stark-shift term

$$\langle A | V \frac{q}{E - H^0} V | A \rangle \quad (9.8.1.5)$$

Furthermore, if one expands the propagator $1/(E - H^0 - V_{qq})$ of the level-shift operator $M(E)$ in powers of V_{qq} , then one generates the (Brillouin–Wigner) perturbation expansion for the adiabatic energy of the state A .

For high incident field strength the perturbation expansion may not be applicable. If, however, the space of the given problem may be truncated to a finite set $\{|A\rangle\}$, then it is most convenient to determine the eigenvalues from direct diagonalization of the matrix representation of H , Eq. (9.2.2), in the truncated space. On the other hand, if the set $\{|A\rangle\}$ is infinite (or very large) and/or it may contain the atomic continuum explicitly, then the said matrix representation is of little use. The problem of finding the perturbed eigenvalues could then turn out to be formidable. We shall nevertheless show below that the eigenvalue equation (9.8.1.3) may be used to divide the problem into a sequence of subproblems, each of which may then be tackled one at a time and a finite number of eigenvalues may be evaluated using a step-by-step iterative procedure. To this end we shall relate the matrix element of the level-shift operator $M(E)$ to an inhomogeneous system of differential equations for the wave vectors ψ_n and calculate the matrix elements of $M(E)$ in terms of the solutions ψ_n . The system of wave equations for the functions ψ_n will be first treated using a generalized coupled-equation version⁽¹⁹⁸⁾ of the Dalgarno–Lewis IDE method (Section 4.3). It may conveniently be applied numerically if the effective number of photons exchanged is not too large. At a very high field strength, when the number of photons exchanged is rather large, the number of such coupled differential equations to be solved simultaneously

may however turn out to be impractically large. Clearly, in that event it will be worthwhile to recover the fundamental simplicity of the Dalgarno–Lewis IDE method in which no more than a single inhomogeneous differential equation (IDE) has to be solved simultaneously. This may be accomplished at the price of a recursive-iterative solution of a system of essentially uncoupled wave equations given below (Section 9.10). Once the matrix elements of $M(E)$ are known (corresponding to the unperturbed energy E_A) the desired perturbed eigenvalue $E = E'_A$ must then be obtained from the successive iterative solution of Eq. (9.8.1.3) until convergence.

Let us define a state vector $|\psi\rangle$ associated with the level-shift operator $M(E)$ by

$$|\psi\rangle \equiv \frac{1}{E - H^0 - V_{qq}} V |A\rangle \quad (9.8.1.6)$$

and develop $|\psi\rangle$ on the basis set of the number states $\{|n_0 + n\rangle\}$:

$$|\psi\rangle = \sum_{n=-n_0}^{\infty} |n_0 + n\rangle \psi_n \quad (9.8.1.7)$$

Equation (9.8.1.6) is the same as the inhomogeneous equation

$$(E - H^0 - V_{qq}) |\psi\rangle = V |A\rangle \quad (9.8.1.8)$$

Substitution of expansion (9.8.1.7) in Eq. (9.8.1.8) and projection onto the state $\langle n_0 + n |$ immediately gives

$$\begin{aligned} (E - H_n) \psi_n &= (V_{qq})_{n+1} \psi_{n+1} + (V_{qq})_n \psi_{n-1} + V_1 \langle n_0 + n | n_0 + 1 \rangle |a\rangle \\ &\quad + V_0 \langle n_0 + n | n_0 - 1 \rangle |a\rangle \end{aligned} \quad (9.8.1.9)$$

where we have used definitions (9.2.4) and (9.2.5) for the matrix elements of V_n and H_n respectively, as well as Eq. (9.8.7) for $|A\rangle$. For the sake of notational simplicity, in this section we shall omit the projection notation q from (V_{qq}) and simply write (V) and remember that the matrix element of $(V_{qq}) \equiv (V)$ with respect to the initial state $|A\rangle = |a\rangle |n_0\rangle$ is to be omitted (if it arises at all). This should cause no confusion in what follows. Thus Eq. (9.8.1.9), which is defined entirely on the atomic space, now reads

$$(E - H_n) \psi_n = (V)_{n+1} \psi_{n+1} + (V)_n \psi_{n-1} + V_1 |a\rangle \delta_{n,1} + V_0 |a\rangle \delta_{n,-1} \quad (9.8.1.10)$$

Comparison of Eq. (9.8.1.10) with Eq. (9.7.3) shows that the wave functions ψ_n are essentially the same as obtained earlier except that the particular

boundary condition is now fixed by the inhomogeneous terms in Eq. (9.8.1.10). Clearly, therefore, we can readily convert functions ψ_n into continued fractions of the kind (9.7.1.1) and (9.7.1.2) with initial solutions determined by the inhomogeneous term. This is, however, not necessary since the method for evaluating the energy matrix elements is more conveniently based on the recurrence equation (9.8.1.1) than on the fractions themselves.

Substitution of Eqs. (9.8.1.6) and (9.8.1.7) in relation (9.8.1.4) allows us to evaluate the matrix element of the level-shift operator $M(E)$ in terms of the wave functions ψ_1 and ψ_{-1} . Thus

$$\begin{aligned}\langle A | M(E) | A \rangle &= \langle a | \langle n_0 | V | \psi \rangle \\ &= \langle a | \langle n_0 | V \sum_n | n + n_0 \rangle | \psi_n \rangle \\ &= \langle a | V_1 | \psi_1 \rangle + \langle a | V_0 | \psi_{-1} \rangle\end{aligned}\quad (9.8.1.11)$$

The third line of this relation follows from the matrix elements of V with respect to the number states.

9.9. Coupled Inhomogeneous Radial Equations for ψ_n

Equation (9.8.1.10) shows that ψ_1 and ψ_{-1} are coupled to all the higher-order wave functions ψ_n through ψ_2 and ψ_{-2} , and so on. In view of the simplicity of the dipole operator V_n , and an assumed central (model) potential $V(r)$ for the optical electron, we may conveniently expand the wave functions ψ_n in terms of the eigenfunctions $| L, M_L \rangle$ of the total angular-momentum operator \hat{L}^2 satisfying the eigenvalue equation

$$\hat{L}^2 | L, M_L \rangle = L(L+1) | L, M_L \rangle \quad (9.9.1)$$

where L is the angular-momentum quantum number and M_L its projection. We shall denote the radial components of ψ_n as

$$\langle L, M_L \rangle | \psi_n \rangle = \psi_{LM_L}^n = F_L^n \quad (9.9.2)$$

where in the last term the projection index M_L is omitted for the sake of notational simplicity. In fact, choice of the linear polarization direction in V as the quantization axis makes $M_L = 0$ everywhere if the initial state (as is usual) is an S state. (If necessary the M_L index may be restored, without difficulty.) Assuming the coordinate representation of H_{atom} we may project the wave equation (9.8.1.10) onto $\langle LM_L |$ to obtain at once the

inhomogeneous radial coupled differential equations for the F_L^n :

$$[E_n - h_L] F_L^n = (V)_{n+1}^{L,L\pm 1} F_{L\pm 1}^{n+1} + (V)_n^{L,L\pm 1} F_{L\pm 1}^{n-1} \\ + (V)_r^{L,L\pm 1} |f_{L_a}\rangle \delta_{L\pm 1, L_a} \delta_{n,1} + (V)_0^{L,L\pm 1} |f_{L_a}\rangle \delta_{L\pm 1, L_a} \delta_{n,-1} \quad (9.9.3)$$

where the radial differential operator

$$h_L \equiv -\frac{\hbar^2}{2\mu} \left[\frac{d^2}{dr^2} + \frac{2}{r} - \frac{L(L+1)}{r^2} \right] + V(r) \quad (9.9.4)$$

and E_n is the “channel energy” given by

$$E_n = E - (n + n_0)\hbar\omega < 0 \quad (9.9.5)$$

Alternatively, when $E - (n + n_0)\hbar\omega > 0$,

$$E_n \equiv \frac{\hbar^2 K_n^2}{2\mu} = \left[\frac{2\mu}{\hbar^2} (E - (n + n_0)\hbar\omega) \right]^{1/2} \quad (9.9.6)$$

where K_n is the “channel momentum” in the “photon channel” n .

In Eq. (9.9.3), $(V)_n^{L,L\pm 1} \equiv (V_{qq})_n^{L,L\pm 1}$ are the angular-momentum matrix elements of $(V_{qq})_n$. A product term in Eq. (9.9.3) with index sign \pm is to be understood as the sum of two terms with the two signs; for example,

$$(V)_{n+1}^{L,L\pm 1} F_{L\pm 1}^{(n+1)} \equiv (V)_{n+1}^{L,L+1} F_{L+1}^{n+1} + (V)_{n+1}^{L,L-1} F_{L-1}^{(n+1)} \quad (9.9.7)$$

Finally, we let

$$|f_{L_a}\rangle \equiv \langle L_a | a \rangle \quad (9.9.8)$$

be the radial component of the initial state $|a\rangle$ and L_a be the initial angular momentum. If now the photon space is truncated such that

$$n_{\min} \leq n \leq n_{\max} \quad (9.9.9)$$

where n_{\max} is a positive and n_{\min} a negative integer, then the resulting finite system of coupled radial equations (9.9.3) may be integrated simultaneously and all F_L^n in the range (9.9.9) determined. The coupled wave equations (9.9.3), which are quite general, were originally obtained⁽¹⁹⁸⁾ by inverting the continued-fraction representation of $G_n(E)$.

Once the wave functions $F_L^n(r)$ are solved, virtually every quantity of physical interest (such as the transition amplitudes) may be calculated with their help. Thus, for example, we may construct ψ_1 and ψ_{-1} using the

expansions ($M_L = 0$)

$$\psi_1 = \sum_L |L, 0\rangle F_L^1(r) \quad (9.9.10)$$

and

$$\psi_{-1} = \sum_L |L, 0\rangle F_L^{-1}(r) \quad (9.9.11)$$

and evaluate the level-shift matrix element (9.8.1.11), for a given energy E , as a sum of four radial matrix elements,

$$\begin{aligned} \langle A | M(E) | A \rangle &= \langle f_a | (V)_1^{L_a L_a+1} | F_{L_a+1}^1 \rangle + \langle f_a | (V)_1^{L_a L_a-1} | F_{L_a-1}^1 \rangle \\ &\quad + \langle f_a | (V)_0^{L_a L_a+1} | F_{L_a+1}^{-1} \rangle + \langle f_a | (V)_0^{L_a L_a-1} | F_{L_a-1}^{-1} \rangle \end{aligned} \quad (9.9.12)$$

The matrix elements are finally calculated by simple numerical quadrature.

9.10. The Recursive-Iterative Wave Equations

As pointed out earlier, at high field strength the number of coupled equations may turn out as impractically large to be solved simultaneously. The original Dalgarno–Lewis (IDE) method (see Section 4.3) does not suffer from this difficulty since the perturbative equations are hierarchically solved one after another. We shall therefore give an alternative method of constructing the n -photon wave functions F_L^n (or ψ_n) that does not require the simultaneous solution of more than one inhomogeneous radial differential equation but generates the whole set of solutions F_L^n at the cost of recursive iterations. The method is best discussed with the help of examples. Below, we illustrate this in terms of the radial equations (9.9.3).

In this method the coupled system of equations (9.9.3) are replaced by the following recursive-iterative system in which $F_L^{(n,i)}$ is the i th iterate of F_L^n :

$$\begin{aligned} n < 0: \quad [E_n - h_L] F_L^{(n,i)} &= (V)_{n+1}^{L,L\pm 1} F_{L\pm 1}^{(n+1,i)} + (V)_n^{L,L\pm 1} F_{L\pm 1}^{(n-1,i-1)} \\ &\quad + (V)_0^{L,L\pm 1} |f_{L_a}\rangle \delta_{L\pm 1, L_a} \delta_{n,-1} \delta_{i,0} \\ n = 0: \quad [E_0 - h_L] F_L^{(0,i)} &= (V)_1^{L,L\pm 1} F_{L\pm 1}^{(1,i-1)} + (V)_0^{L,L\pm 1} F_{L\pm 1}^{(-1,i-1)} \\ n > 0: \quad (E_n - h_L) F_L^{(n,i)} &= (V)_{n+1}^{L,L\pm 1} F_{L\pm 1}^{(n+1,i-1)} + (V)_n^{L,L\pm 1} F_{L\pm 1}^{(n-1,i)} \\ &\quad + (V)_1^{L,L\pm 1} |f_{L_a}\rangle \delta_{L\pm 1, L_a} \delta_{n,1} \delta_{i,0} \end{aligned} \quad (9.10.1)$$

The iteration is assumed to be at most of finite order, $i = 0, 1, 2, \dots, i_{\max}$.

Physically speaking, the zeroth-order equations [Eq. (9.10.1) with $i = 0$] correspond to neglect of photon back-coupling effects. The back-coupling is restored in all orders starting with the first, i.e., for $i \geq 1$.

Equations (9.10.1) for $i \geq 1$ have the same structure as the coupled equations (9.9.3), which they replace.

Let us consider the zeroth-order ($i = 0$) and first-order ($i = 1$) equations explicitly. From relations (9.10.1) with $i = 0$ we obtain

$$\begin{aligned} n &\leq -2: & (E_n - h_L) F_L^{(n,0)} &= (V)_{n+1}^{L,L\pm 1} F_{L\pm 1}^{(n+1,0)} \\ n &= -1: & (E_{-1} - h_L) F_L^{(-1,0)} &= (V)_0^{L,L\pm 1} F_{L\pm 1}^{(0,0)} + (V)_0^{L,L\pm 1} |f_{L_a}\rangle \delta_{L\pm 1, L_a} \\ n &= 0: & (E_0 - h_L) F_L^{(0,0)} &= 0 \\ n &= 1: & (E_1 - h_L) F_L^{(1,0)} &= (V)_1^{L,L\pm 1} F_{L\pm 1}^{(0,0)} + (V)_1^{L,L\pm 1} |f_{L_a}\rangle \delta_{L\pm 1, L_a} \\ n &\geq 2: & (E_n - h_L) F_L^{(n,0)} &= (V)_n^{L,L\pm 1} F_{L\pm 1}^{(n-1,0)} \end{aligned} \quad (9.10.2)$$

Similarly with $i = 1$, we have from relations (9.10.2)

$$\begin{aligned} n &= -2: & (E_{-2} - h_L) F_L^{(-2,1)} &= (V)_{-1}^{L,L\pm 1} F_{L\pm 1}^{(-1,1)} + (V)_{-2}^{L,L\pm 1} F_{L\pm 1}^{(-3,0)} \\ n &= -1: & (E_{-1} - h_L) F_L^{(-1,1)} &= (V)_0^{L,L\pm 1} F_{L\pm 1}^{(0,1)} + (V)_{-1}^{L,L\pm 1} F_{L\pm 1}^{(-2,0)} \\ n &= 0: & (E_0 - h_L) F_L^{(0,1)} &= (V)_1^{L,L\pm 1} F_{L\pm 1}^{(1,0)} + (V)_0^{L,L\pm 1} F_{L\pm 1}^{(-1,0)} \\ n &= 1: & (E_1 - h_L) F_L^{(1,1)} &= (V)_2^{L,L\pm 1} F_{L\pm 1}^{(2,0)} + (V)_1^{L,L\pm 1} F_{L\pm 1}^{(0,1)} \\ n &= 2: & (E_2 - h_L) F_L^{(2,1)} &= (V)_3^{L,L\pm 1} F_{L\pm 1}^{(3,0)} + (V)_2^{L,L\pm 1} F_{L\pm 1}^{(1,1)} \end{aligned} \quad (9.10.3)$$

(We note that at high field strength, subscript n on all the V_n above may be neglected and V_n set equal to $(F_0/2)(\mathbf{\epsilon} \cdot \mathbf{D})$ everywhere.)

The structure of the first-order equations (9.10.3) is clearly maintained at all higher orders ($i \geq 2$) and hence need not be discussed separately.

The hierarchical solution begins with the zeroth-order set (9.10.2) and with the equation for $n = 0$. This is a homogeneous equation and merely specifies the radial wave functions of the unperturbed problem with respect to the (model) potential $V(r)$ and provides the set of unperturbed initial wave functions $|f_{L_a}\rangle$.

The initial solution is fed into the right-hand side of the equations for $n = +1$. Since the inhomogeneous term in the equation for $n = 1$ is thus known we may solve for $F_L^{(1,0)}$ independently of the other equations. We note that only those partial solutions are generated which possess the opposite parity of the driving inhomogeneity (starting with the initial state f_{L_a} in the equation for $n = 0$), as dictated by the odd parity of the dipole interaction. The result is substituted in the right-hand side of the next equation with $n = 2$ and the equation solved independently for $F_L^{(2,0)}$. This

scheme is repeated with higher $n \geq 3$ and up to a desired n_{\max} . A similar treatment of the equations with $n = -1$ and $n = -2$ (starting with the known solution of the equation for $n = 0$ in the zeroth-order solution) generates $F_L^{(-1,0)}$ and $F_L^{(-2,0)}$ successively. This process, when repeated with $n \leq -3$, generates the desired solutions up to a predetermined n_{\min} . We are now prepared to start with the solution of the set (9.10.3) beginning again with the equation for $n = 0$. The inhomogeneity of this equation is given by the already calculated solutions $F_{L\pm 1}^{(\pm 1,0)}$ and hence it may be solved for $F_L^{(0,1)}$ independently. The solutions $F_L^{(0,1)}$ thus found and the old solutions $F_{L\pm 1}^{(2,0)}$ may clearly be used to generate the inhomogeneity of the equation with $n = +1$. This equation may be solved independently of other equations to find $F_L^{(1,1)}$. Use of $F_{L\pm 1}^{(1,1)}$ and the old solution $F_{L\pm 1}^{(3,0)}$ allows calculation of $F_L^{(2,1)}$ from the equation with $n = +2$ and the process continues for $n \geq 3$. It is clear that an analogous process will generate the solutions $F_L^{(-1,1)}$ and $F_L^{(-2,1)}$ from the successive but otherwise independent solutions of the equations with $n = -1$, $n = -2$, and so on. This will provide all the solutions necessary to proceed with the solution of the next set of equations for $i = 2$. This set has the same structure as the set with $i = 1$ and hence can be solved analogously if required. The method closely resembles the original Dalgarno–Lewis (IDE) method of solving hierarchical equations requiring no more than the solution of one differential equation at a time; it may therefore be carried out in principle to arbitrarily high values of n (in either direction). In practice, this would be limited ultimately by the propagation of the rounding-off errors with increasing levels of iteration. We note that one may test the convergence (or otherwise) of the solutions with respect to higher n_{\max} or n_{\min} by increasing them in steps and solving the extra equations, starting essentially with the solutions of the previous set. The stable solutions $F_L^{(n,i_{\max})} \equiv F_L^{(n)}$ thus generated are assumed to be converged approximants of the desired true wave functions F_L^n , which may be used to calculate the physical quantities of interest.

Thus, for example, one may use solutions $F_L^{(1)}$ and $F_L^{(-1)}$ to calculate the energy shift given by Eq. (9.9.12), where E is chosen at first to be the unperturbed value $E = E^{(0)} = E_A$. Thus we get the first-order energy shift

$$\Delta E^{(1)} = \langle A | M(E^{(0)}) | A \rangle \quad (9.10.4)$$

We may start the process of solving system (9.10.1), but now with E replaced by

$$E = E^{(1)} = E^{(0)} + \Delta E^{(1)} \quad (9.10.5)$$

The new solutions $F_L^{(1)}$ and $F_L^{(-1)}$ may be substituted in an obvious way in

Eq. (9.9.12) to generate the level shift in the second order,

$$\Delta E^{(2)} = \langle A | M(E)^{(1)} | A \rangle \quad (9.10.6)$$

which yields the second estimate of the eigenvalue

$$E = E^{(2)} = E^{(1)} + \Delta E^{(2)} \quad (9.10.7)$$

Obviously the higher-order estimates $E^{(n)}$, $n > 3$ may be calculated analogously and the numerical convergence of the result tested at the cost of more of the same calculational routine. The same arguments evidently hold true for finding a different eigenvalue starting with the unperturbed eigenvalue $E = E^{(0)} = E_B$, belonging to the unperturbed state $|B\rangle \equiv |b\rangle|n_0=0\rangle$.

It is noteworthy that for an N -electron atom, the radial equation analogous to Eqs. (9.9.3) or (9.10.1) can be derived in close analogy with the well-known derivation of the “close-coupling” equations for the scattering electron in the theory of electron–atom collision.⁽¹⁹⁹⁾ In essence, the N -electron atom in this context is to be considered formally as an “($N - 1$)-electron ‘core’ + one ‘optical’ electron” system; the equation for the N th “optical” electron will then be analogous to the “close-coupling” equations for the scattering electron in collision theory.

9.11. Evaluation of the n -Photon Resolvent

The method of the previous section may be applied equally well to the evaluation of matrix elements of other operators of interest. We shall briefly outline the evaluation of the resolvent amplitude for the absorption (or emission) of n photons.

The equation for the resolvent operator in the subspace p is clearly given by

$$\left[E - H^0 - V_{pp} - V_{pq} \frac{q}{E - H^0 - V_{qq}} V_{qp} \right] G_{pp} = p \quad (9.11.1)$$

where

$$G_{pp} \equiv p \frac{1}{E - H} p \quad (9.11.2)$$

and H is given by Eq. (9.2.2). Let

$$p = |A\rangle\langle A| + |F\rangle\langle F| \quad (9.11.3)$$

where

$$|A\rangle = |a\rangle |n_0 + 0\rangle \quad (9.11.4)$$

is the initial state and

$$|F\rangle = |f\rangle |n_0 + n_f\rangle \quad (9.11.5)$$

is the final state. Hence now

$$q = 1 - |A\rangle\langle A| - |F\rangle\langle F| \quad (9.11.6)$$

Use of expression (9.2.2) in Eq. (9.11.1) and projections from the left onto $\langle A|$ and $\langle F|$ and from the right onto $|A\rangle$ yield

$$[E - \varepsilon_a - n_0\hbar\omega - V_{AA} - M_{AA}(E)]G_{AA} - [V_{AF} + M_{AF}(E)]G_{FA} = 1 \quad (9.11.7)$$

and

$$[E - \varepsilon_f - (n_0 + n_f)\hbar\omega - V_{FA} - M_{FA}(E)]G_{AA} - [V_{FF} + M_{FF}(E)]G_{FA} = 0 \quad (9.11.8)$$

This is a pair of algebraic equations for the matrix elements $\langle A|G|A\rangle \equiv G_{AA}$ and $\langle F|G|A\rangle \equiv G_{FA}$, which depend essentially on the matrix elements of the operator $M(E)$, Eq. (9.8.1.2), where

$$M_{FA}(E) = \langle F|M(E)|A\rangle \quad (9.11.9)$$

with

$$V_{FA}(E) = \langle F|V|A\rangle \quad (9.11.10)$$

and similar definitions for the other quantities. The diagonal element $M_{AA}(E)$ is the same as expression (9.8.1.5) (except that q now excludes both the initial and final states, which are assumed to be different); clearly, $M_{AA}(E)$ can be evaluated by the method of the last section. The same holds true for the evaluation of the off-diagonal matrix element $M_{FA}(E)$, as seen below.

If the atomic state $|f\rangle$ associated with the final state $|F\rangle$ corresponds to that of the ionized electron, then $|f\rangle$ is given by a linear combination of the angular-momentum states $|L_f M_f\rangle$ and has the form

$$|f\rangle \rightarrow |c\rangle = \sum_{L_c M_c} |f_{L_c}\rangle |L_c M_c\rangle \quad (9.11.11)$$

Sometimes (e.g., for the free-free transitions) the initial atomic state may

also be a linear combination of angular-momentum states of the form

$$|a\rangle = \sum_{L_a M_a} |f_{L_a}\rangle |L_a M_a\rangle \quad (9.11.12)$$

In the above $|f_{L_c}\rangle$ and $|f_{L_a}\rangle$ are the radial functions.

We therefore consider the matrix element of $M(E)$ with respect to the rather general states

$$|A\rangle = |a\rangle |n_0 + n_c\rangle \quad (9.11.13)$$

and

$$|C\rangle = |c\rangle |n_0 + n_c\rangle \quad (9.11.14)$$

where $|a\rangle$ and $|c\rangle$ are given by relations (9.11.12) and (9.11.11), respectively, and n_a and n_c are occupation numbers with respect to n_0 . We have

$$\begin{aligned} M_{CA}(E) &\equiv \langle c | V \frac{q}{E - H^0 - V_{qq}} V | A \rangle \\ &= \langle c | \langle n_0 + n_c | V \frac{q}{E - H^0 - V_{qq}} V | n_0 + n_a \rangle | a \rangle \end{aligned} \quad (9.11.15)$$

Let us introduce, as before, a state vector

$$|\psi\rangle = \frac{q}{E - H^0 - V_{qq}} V |A\rangle \quad (9.11.16)$$

so that

$$(E - H^0 - V_{qq}) |\psi\rangle = q V |n_0 + n_a\rangle \sum_{L_a M_a} |L_a M_a\rangle |f_{L_a}\rangle \quad (9.11.17)$$

We introduce the expansion

$$|\psi\rangle = \sum_{nLM} |n_0 + n\rangle F_L^n |LM\rangle \quad (9.11.18)$$

substitute it in Eq. (9.11.17), and project from the left onto $\langle n_0 + n | \langle LM |$ to obtain the recurrence radial wave equations

$$\begin{aligned} (E_n - h_L) F_{L,L_a}^{n,n_a} &= (V_{qq})_{n+1}^{L,L\pm 1} F_{L\pm 1,L_a}^{n+1,n_a} + (V_{qq})_n^{L,L\pm 1} F_{L\pm 1,L_a}^{n-1,n_a} \\ &\quad + (qV)_{n_a+1}^{L,L\pm 1} |f_{L_a}\rangle \delta_{n,n_a+1} \delta_{L\pm 1,L_a} \\ &\quad + (qV)_{n_a}^{L,L\pm 1} |f_{L_a}\rangle \delta_{n,n_a-1} \delta_{L\pm 1,L_a} \end{aligned} \quad (9.11.19)$$

Here, F_{L,L_a}^{n,n_a} denotes the radial function F_L^n with quantum number L ; L_a of the initial partial wave f_{L_a} and the initial photon state $|n_0 + n_a\rangle$ are indicated explicitly by the second sub- and superscripts. Otherwise, the same notational convention is used as in Eq. (9.9.3). Clearly Eq. (9.11.19) may be treated numerically in a manner completely analogous to that described in Section 9.10. Finally, in terms of F_{L,L_a}^{n,n_a} one may calculate, from Eq. (9.11.15),

$$\begin{aligned} M_{CA}(E) = & \sum_{L_c L_a} [\langle f_c | (V)_{n_c+1}^{L_c, L_c+1} | F_{L_c+1, L_a}^{n_c+1, n_a} \rangle + \langle f_c | (V)_{n_c+1}^{L_c, L_c-1} | F_{L_c-1, L_a}^{n_c+1, n_a} \rangle] \\ & + \sum_{L_c L_a} [\langle f_c | (V)_{n_c}^{L_c, L_c+1} | F_{L_c+1, L_a}^{n_c-1, n_a} \rangle + \langle f_c | (V)_{n_c}^{L_c, L_c-1} | F_{L_c-1, L_a}^{n_c-1, n_a} \rangle] \quad (9.11.20) \end{aligned}$$

Thus the matrix element of $M(E)$ is reduced again to ordinary quadrature using the numerical radial wave functions F_{L,L_a}^{n,n_a} . The index M_c or M_a for the azimuthal quantum number is suppressed in writing expression (9.11.20). We observe also that in the “laser approximation” the matrix elements of V in the second line of Eq. (9.11.20) is identical to those in the first line.

9.12. The Case of Intermediate Resonances

If intermediate states $|B\rangle$ exist and are energetically close to the total energy of the initial or final state, then it is useful to include them in the p -space. For example, if there is one intermediate state $|B\rangle = |b\rangle|n_0 + n_b\rangle$, which is close to or exactly in resonance, then one gets

$$q = 1 - |A\rangle\langle A| - |B\rangle\langle B| - |F\rangle\langle F| \quad (9.12.1)$$

Projection of Eq. (9.11.1) from the left onto the states $\langle A|$, $\langle B|$, and $\langle F|$ in turn, and from the right on $|A\rangle$, easily yields the three algebraic equations

$$\begin{aligned} [E - \varepsilon_a - n_0 \hbar\omega - V_{AA} - M_{AA}(E)]G_{AA} - [V_{AB} + M_{AB}(E)]G_{BA} \\ - [V_{AF} + M_{AF}(E)]G_{FA} = 1 \quad (9.12.2) \end{aligned}$$

$$\begin{aligned} [E - \varepsilon_b - (n_0 + n_b) \hbar\omega - V_{BA} - M_{BA}(E)]G_{BA} - [V_{BB} + M_{BB}(E)]G_{BB} \\ - [V_{BF} + M_{BF}(E)]G_{FB} = 0 \quad (9.12.3) \end{aligned}$$

and

$$\begin{aligned} [E - \varepsilon_f - (n_0 + n_f) \hbar\omega - V_{FA} - M_{FA}(E)]G_{FA} - [V_{FF} + M_{FF}(E)]G_{FF} \\ - [V_{FB} + M_{FB}(E)]G_{FB} = 0 \quad (9.12.4) \end{aligned}$$

The algebraic equations governing the amplitudes for the elastic, resonant, and inelastic transition amplitudes (G_{AA} , G_{BA} , and G_{FA} , respectively) may be solved essentially in the same way as for the matrix elements $M_{CA}(E)$ discussed in the previous section. It is worth observing that (up to moderately high intensities) the E -dependence of the above operator $M(E)$ would be rather weak. This is because the resonant state $|B\rangle$ as well as the external states $|A\rangle$ and $|F\rangle$ do not enter into $M(E)$ thanks to the projector q , given by Eq. (9.12.1). The perturbed eigenvalues E of the initial, final, and resonant states are determined by the solution of the secular equation, $\text{Det}(E) = 0$, where $\text{Det}(E)$ is the secular determinant formed by the 3×3 coefficient matrix (without E) on the left-hand side of the above system of three algebraic equations. For more than one resonance an appropriately extended system of equations can be easily constructed and treated in an identical way. We note also that the same method may be applied to the calculation of matrix elements of the reduced T-matrix without difficulty.

9.13. The Two-Mode Problem

The method of the recurrence relation outlined in the last section may be extended to the case of more than one field or field modes without any logical difficulty (although no straightforward continued-fraction representation of the amplitudes may be obtained in this case). We shall briefly indicate the approach with a two-field (mode) problem. The Hamiltonian now reads

$$H = H^{(0)} + V + U \quad (9.13.1)$$

with

$$H^{(0)} = H_{\text{atom}} + a_1^+ a_1 \hbar \omega_1 + a_2^+ a_2 \hbar \omega_2 \quad (9.13.2)$$

$$V = \left(\frac{2\pi\hbar\omega_1}{L^3} \right)^{1/2} \boldsymbol{\epsilon}_1 \cdot \mathbf{D} (a_1^+ + a_1) \quad (9.13.3)$$

and

$$U = \left(\frac{2\pi\hbar\omega_2}{L^3} \right)^{1/2} \boldsymbol{\epsilon}_2 \cdot \mathbf{D} (a_2^+ + a_2) \quad (9.13.4)$$

In general, unit polarization vectors $\boldsymbol{\epsilon}_1$ and $\boldsymbol{\epsilon}_2$ are nonidentical and frequencies ω_1 and ω_2 are noncommensurate (not multiples of one another).

The resolvent $G = 1/(E - H)$ may again be projected onto the p -space. If we take the matrix element of G with respect to a state

$$|A\rangle = |f_{L_a}\rangle |L_a M_a\rangle |n_a + n_0\rangle |m_a + m_0\rangle \quad (9.13.5)$$

where $|a\rangle$ is an atomic state, and $n_a + n_0$ and $m_a + m_0$ are the occupation numbers of modes 1 and 2, then we obtain the elastic resolvent

$$G_{AA}(E) = \frac{1}{E - \varepsilon_a - (n + n_0)\hbar\omega_1 - (m + m_0)\hbar\omega_2 - V_{AA} - U_{AA} - M_{AA}(E)} \quad (9.13.6)$$

where in the dipole case

$$V_{AA} = U_{AA} = 0 \quad (9.13.7)$$

and

$$\begin{aligned} M_{AA}(E) &= \langle A | (V + U) \frac{q}{E - H^{(0)} - V_{qq} - U_{qq}} (V + U) | A \rangle \\ &= \langle A | (V + U) | \psi \rangle \end{aligned} \quad (9.13.8)$$

with

$$| \psi \rangle \equiv \frac{q}{E - H^{(0)} - V_{qq} - U_{qq}} (V + U) | A \rangle \quad (9.13.9)$$

The poles of any matrix element of the resolvent can provide the eigenvalues of the corresponding Hamiltonian. The energy shift of the state $|A\rangle$ in the presence of the two fields (modes) can therefore be determined from the zeros of the denominator of the elastic resolvent (9.13.6):

$$E = \varepsilon_a + (n + n_0)\hbar\omega_1 + (m + m_0)\hbar\omega_2 + \langle A | (V + U) | \psi \rangle \quad (9.13.10)$$

where Eq. (9.13.8) has been used in the last term. We can analyze Eq. (9.13.8) by expanding the wave function $|\psi\rangle$ in the form

$$| \psi \rangle = \sum_{n=-n_0}^{\infty} \sum_{m=-m_0}^{\infty} F_L^{(n,m)}(r) | L, M \rangle | n + n_0 \rangle | m + m_0 \rangle \quad (9.13.11)$$

Substitution of expansion (9.13.11) in Eq. (9.13.8) and projection onto $|n + n_0\rangle \langle m + m_0|$ then gives the system of inhomogeneous radial equa-

tions for the two-mode problem of interest:

$$\begin{aligned}
 & [E - (n + n_0)\hbar\omega_1 - (m + m_0)\hbar\omega_2 - h_L] F_L^{(n,m)} \\
 &= (V)_{n+1}^{L,L\pm 1} F_{L\pm 1}^{(n+1,m)} + (V)_n^{L,L\pm 1} F_{L\pm 1}^{(n-1,m)} \\
 &\quad + (U)_{m+1}^{L,L\pm 1} F_{L\pm 1}^{(n,m+1)} + (U)_m^{L,L\pm 1} F_{L\pm 1}^{(n,m-1)} \\
 &\quad + [(V)_{n+1}^{L,L\pm 1} \delta_{n,n_a-1} + (V)_n^{L,L\pm 1} \delta_{n,n_a+1}] |f_{L_a}\rangle \delta_{L\pm 1,L_a} \\
 &\quad + [(U)_{m+1}^{L,L\pm 1} \delta_{m,m_a-1} + (U)_m^{L,L\pm 1} \delta_{m,m_a+1}] |f_{L_a}\rangle \delta_{L\pm 1,L_a} \quad (9.13.12)
 \end{aligned}$$

where the matrix elements of (V_{qq}) for the two modes have been expressed separately as

$$(V)_n \equiv \left[\frac{2\pi\hbar\omega_1}{L^3} (n_0 + n) \right]^{1/2} (\boldsymbol{\varepsilon}_1 \cdot \mathbf{D}) \quad (9.13.13)$$

$$(U)_m \equiv \left[\frac{2\pi\hbar\omega_2}{L^3} (m_0 + m) \right]^{1/2} (\boldsymbol{\varepsilon}_2 \cdot \mathbf{D}) \quad (9.13.14)$$

Equations (9.13.12) are fully analogous to Eqs. (9.9.3) obtained in the monomode case, except that now the photon channels are characterized by the two independent quantum numbers n and m instead of n alone. In the absence of mode m , Eqs. (9.13.12) reduce to Eqs. (9.9.3) with $n_a \equiv 0$, as they must. It should be obvious now how they may be extended to account for more than two modes. Finally, we note that use of the radial functions in the matrix element (9.13.8) reduces the latter to

$$\begin{aligned}
 M_{AA}(E) &= \langle A | (V + U) | \psi \rangle \\
 &= \langle f_{L_a} | (V)_{n_a+1}^{L_a,L_a\pm 1} | F_{L_a\pm 1}^{(n_a+1,m_a)} \rangle + \langle f_{L_a} | (V)_n^{L_a,L_a\pm 1} | F_{L_a\pm 1}^{(n_a-1,m_a)} \rangle \\
 &\quad + \langle f_{L_a} | (U)_{m_a+1}^{L_a,L_a\pm 1} | F_{L_a\pm 1}^{(n_a,m_a+1)} \rangle + \langle f_{L_a} | (U)_m^{L_a,L_a\pm 1} | F_{L_a\pm 1}^{(n_a,m_a-1)} \rangle \quad (9.13.15)
 \end{aligned}$$

The off-diagonal elements of the two-mode “level-shift” operator can obviously be reduced in an analogous manner.

9.14. The Method of Chain Hamiltonians

The Lanczos method⁽²⁰⁰⁾ of tridiagonalization of an arbitrary square matrix has been developed^(201,202) into a powerful tool for solving Schrödinger equations algebraically. This method can be conveniently applied to calculate matrix elements of the resolvent and to determine the

time dependence of multiphoton evolution operators. The method derives its practical strength from its ability to handle a large number of basis states with economic storage requirements. In this section we describe the fundamentals of the method and derive the time dependence of the transition amplitude for excitation of a system with many but discrete degrees of freedom.

The basic idea of the method is to reduce the true Hamiltonian into a tridiagonal recurrence relation — the “chain Hamiltonian” — in such a way that the physical importance of the most relevant states, namely the initial and final states, is built into the reduction process from the beginning. Each step of the reduction to the chain Hamiltonian will be seen to incorporate contributions from more and more remote neighborhoods (in the state space) of these two states only. This is why the size of the initial basis set that may be used to represent a given Hamiltonian in matrix form could be very large in this method, and yet the effective vector space of the reduced tridiagonal Hamiltonian (the “chain”) appropriate for a given transition is expected to be significantly smaller in size. The physical properties of interest (such as the eigenvalues or transition probabilities) can be obtained from the eigenvalues and eigenvectors of the chain Hamiltonian only. We shall see below that the transition amplitude can in fact be obtained⁽²⁰³⁾ without explicit knowledge of the eigenvectors and only in terms of the eigenvalues (of the chain Hamiltonian and of two additional “reduced chains”). A “reduced chain” is defined by removing the first row and column of a given (tridiagonal) chain Hamiltonian.

9.14.1. Reduction of a Hamiltonian to a Chain

A Hamiltonian H is assumed first to be represented as a square matrix on a set of basis functions $\{|\alpha\rangle\}$:

$$H \Rightarrow H_{\alpha\alpha'}, \quad \text{all } (\alpha, \alpha') = 1, 2, 3, \dots, \alpha_{\max} \quad (9.14.1.1)$$

The Lanczos method of tridiagonalization⁽²⁰⁰⁾ is now applied with a special initial condition to (9.14.1.1) to convert it into the form

$$H |U_n\rangle = a_n |U_n\rangle + b_{n+1} |U_{n+1}\rangle + b_n |U_{n-1}\rangle \quad (9.14.1.2)$$

Thus the problem is essentially to find the constants a_n , b_n , and the vectors $|U_n\rangle$ for $n = 0, 1, 2, 3, \dots$; $|U_{-1}\rangle = 0$.

We may imagine that each $|U_n\rangle$ is given by an expansion in the basis $\{|\alpha\rangle\}$ of the form

$$|U_n\rangle = \sum_{\alpha} U_{\alpha\alpha'}^{(n)} |\alpha'\rangle \quad (9.14.1.3)$$

with coefficients $U_{\alpha\alpha}^{(n)}$. The vector $|U_0\rangle$ is chosen to coincide with a given state of physical interest, such as the initial or final state or any linear combination of the two. Successively distant neighbors of $|U_0\rangle$, namely $|U_1\rangle, |U_2\rangle, \dots$, are found recursively as follows.

We put $n = 0$ in Eq. (9.14.1.2) and obtain

$$b_1|U_1\rangle = H|U_0\rangle - a_0|U_0\rangle \quad (9.14.1.4)$$

We assume normalization of $|U_0\rangle$, i.e.

$$\langle U_0|U_0\rangle = 1 \quad (9.14.1.5)$$

and demand orthogonality of $|U_1\rangle$ with $|U_0\rangle$, namely

$$\langle U_1|U_0\rangle = 0 \quad (9.14.1.6)$$

By projecting with $\langle U_0|$ on Eq. (9.14.1.4) and using relations (9.14.1.5) and (9.14.1.6) we find

$$a_0 = \langle U_0|H|U_0\rangle \quad (9.14.1.7)$$

Quantities b_1 and $|U_1\rangle$ can be determined by demanding normalization of $|U_1\rangle$,

$$\langle U_1|U_1\rangle = 1 \quad (9.14.1.8)$$

This procedure yields

$$b_1^2 = [(H - a_0)|U_0\rangle]^\dagger[(H - a_0)|U_0\rangle] \quad (9.14.1.9)$$

Hence the normalized

$$|U_1\rangle = \frac{1}{+b_1}(H - a_0)|U_0\rangle \quad (9.14.1.10)$$

where the positive root of Eq. (9.14.1.9) is chosen. The next pair of constants a_1 and b_2 , and the vector $|U_2\rangle$ can be determined in a similar way by requiring $n = 1$ in Eq. (9.14.1.2) with

$$\langle U_2|U_2\rangle = 1, \quad \langle U_2|U_1\rangle = 0, \quad \text{and} \quad \langle U_2|U_0\rangle = 0 \quad (9.14.1.11)$$

Hence

$$a_1 = \langle U_1|H|U_1\rangle \quad (9.14.1.12)$$

$$b_2^2 = [(H - a_1)|U_1\rangle - b_1|U_0\rangle]^\dagger[(H - a_1)|U_1\rangle - b_1|U_0\rangle] \quad (9.14.1.13)$$

and

$$|U_2\rangle = \frac{1}{+b_2} ((H - a_1)|U_1\rangle - b_1|U_0\rangle) \quad (9.14.1.14)$$

In general, we therefore require only that $|U_n\rangle$ be normalized and orthogonal to its two neighbors $|U_{n-1}\rangle$ and $|U_{n-2}\rangle$, in order to find the general result successively, for all $n > 1$:

$$a_n = \langle U_n | H | U_n \rangle \quad (9.14.1.15)$$

$$|b_{n+1}|^2 = [(H - a_n)|U_n\rangle - b_n|U_{n-1}\rangle]^+[(H - a_n)|U_n\rangle - b_n|U_{n-1}\rangle] \quad (9.14.1.16)$$

and

$$|U_{n+1}\rangle = \frac{1}{+b_{n+1}} [(H - a_n)|U_n\rangle - b_n|U_{n-1}\rangle] \quad (9.14.1.17)$$

It is easy to verify by induction that all $|U_n\rangle$, so obtained up to a given n , are in fact normalized and orthogonal to all others. The full set of constants a_n and b_n and the orthonormal vectors $|U_n\rangle$, for $n = 0, 1, 2, 3, \dots$, define the chain Hamiltonian (9.14.1.2) “based” on the initial state $|U_0\rangle$. The chain Hamiltonian assumes a symmetric Jakobi tridiagonal form

$$H = \begin{pmatrix} a_0 & b_1 & 0 & 0 & \cdots \\ b_1 & a_1 & b_2 & 0 & \cdots \\ 0 & b_2 & a_2 & b_3 & \cdots \\ 0 & 0 & b_3 & a_3 & \cdots \\ \vdots & \vdots & \vdots & \vdots & \ddots \end{pmatrix} \quad (9.14.1.18)$$

9.14.2. Eigenvalues and Eigenvectors of a Chain Hamiltonian

If the eigenfunction with eigenenergy E of Hamiltonian H is expressed as a linear combination $\sum_n P_n |U_n\rangle$ of the chain vectors $|U_n\rangle$, then the Schrödinger equation is given by

$$H \sum_n P_n |U_n\rangle = E \sum_n P_n |U_n\rangle \quad (9.14.2.1)$$

Replacing $H |U_n\rangle$ by the chain (9.14.1.2) and equating coefficients of $|U_n\rangle$ one finds the matrix eigenvalue problem

$$\begin{pmatrix} E - a_0 & -b_1 & 0 & 0 & \cdots \\ -b_1 & E - a_1 & -b_2 & 0 & \cdots \\ 0 & -b_2 & E - a_2 & -b_3 & \cdots \\ 0 & 0 & -b_3 & E - a_3 & \cdots \\ \vdots & \vdots & \vdots & \vdots & \ddots \end{pmatrix} \begin{pmatrix} P_0 \\ P_1 \\ P_2 \\ P_3 \\ \vdots \end{pmatrix} = 0 \quad (9.14.2.2)$$

We suppose $\Delta_n(E)$ is the determinant of the matrix defined by the first n rows and columns of the matrix on the left-hand side of problem (9.14.2.2); also $\Delta_{-1}(E) = 0$ and $\Delta_0(E) = 1$. By expanding $\Delta_{n+1}(E)$ one easily obtains

$$\Delta_{n+1}(E) = (E - a_n)\Delta_n(E) - b_n^2\Delta_{n-1}(E) \quad (9.14.2.3)$$

These determinants are obviously polynomials in E and the required eigenvalues are the zeros of the last member [say $\Delta_N(E)$] of the sequence for a finite (or truncated) chain.

Equation (9.14.2.2) also yields the recurrence relation of the coefficients $P_n(E)$:

$$EP_n(E) = a_n P_n(E) + b_{n+1} P_{n+1}(E) + b_n P_{n-1}(E) \quad (9.14.2.4)$$

The functions $P_n(E)$ are related to determinants $\Delta_n(E)$ by

$$\Delta_n(E) = b_1 b_2 b_3 \cdots b_n P_n(E) \quad (9.14.2.5)$$

For a finite chain at an eigenvalue $E = E_\alpha$, $\Delta_N(E_\alpha) = 0$ and one has the two-term relation

$$(E_\alpha - a_{N-1})P_{N-1}(E_\alpha) - b_{N-1}P_{N-2}(E_\alpha) = 0 \quad (9.14.2.6)$$

For an infinite chain the values of the determinants between any two eigenvalues can diverge. The zeros of $\Delta_n(E)$ with increasing n , however, converge to the eigenvalues of the chain Hamiltonian. Instead of discussing further the many known⁽²⁰²⁾ analytic properties of the finite and infinite chains, we observe that they are closely related to and often complementary to the results obtained within the independently developed⁽²⁰⁴⁻²⁰⁸⁾ J-matrix method of scattering theory. This is because the analytic foundation of both these theories lies in the tridiagonal recurrence relation (satisfied by the Hamiltonian) and the connection of the latter with the well-developed theories of orthogonal polynomials⁽²⁰⁹⁾ and continued fractions.⁽²¹⁰⁾

9.14.3. Matrix Elements of the Resolvent

We now consider the method of obtaining the transition matrix elements. Any matrix element between a pair of initial and final states, $|\phi_i\rangle$ and $|\phi_f\rangle$, is to be obtained in terms of the diagonal matrix elements between linear combinations of the pairs $|\phi_i\rangle$ and $|\phi_f\rangle$. To this end one constructs⁽²⁰²⁾ the four linear combinations

$$|u_0\rangle = (\frac{1}{2})^{1/2} [|\phi_i + \phi_f\rangle] \quad (9.14.3.1)$$

$$|v_0\rangle = \left(\frac{1}{2}\right)^{1/2} [|\phi_i - \phi_f\rangle] \quad (9.14.3.2)$$

$$|w_0\rangle = \left(\frac{1}{2}\right)^{1/2} [|\phi_i + i\phi_f\rangle] \quad (9.14.3.3)$$

and

$$|z_0\rangle = \left(\frac{1}{2}\right)^{1/2} [|\phi_i - i\phi_f\rangle] \quad (9.14.3.4)$$

In terms of the above combinations, the matrix element of the resolvent $G = 1/(E - H)$ is given by

$$\begin{aligned} \langle \phi_f | G(E) | \phi_i \rangle &= \frac{1}{2} [\langle u_0 | G(E) | u_0 \rangle - \langle v_0 | G(E) | v_0 \rangle] \\ &\quad + \frac{1}{2} i [\langle w_0 | G(E) | w_0 \rangle - \langle z_0 | G(E) | z_0 \rangle] \end{aligned} \quad (9.14.3.5)$$

If $|\phi_i\rangle$ and $|\phi_f\rangle$ are real (or may be made real by properly choosing the phases) then one may work with the combinations $|u_0\rangle$ and $|v_0\rangle$ only so that

$$\langle \phi_f | G(E) | \phi_i \rangle = \frac{1}{2} [\langle u_0 | G(E) | u_0 \rangle - \langle v_0 | G(E) | v_0 \rangle] \quad (9.14.3.6)$$

For the sake of simplicity we shall assume that $|\phi_i\rangle$ and $|\phi_f\rangle$ are real. Equation (9.14.3.6) shows that an arbitrary matrix element of $G(E)$ is calculated from two different diagonal matrix elements of the resolvent of the chain Hamiltonian “based” on states $|u_0\rangle$ and $|v_0\rangle$. We shall denote them explicitly in terms of the following notation:

$$\langle u_0 | G(E) | u_0 \rangle = \langle u_0 | \frac{1}{E - H} | u_0 \rangle \equiv G(E | u_0) \quad (9.14.3.7)$$

It is evident from this relation that $G(E | u_0)$ is the leading element of the inverse of $[E - H]$, so that

$$G(E | u_0) = [E - H]_{0,0}^{-1} = \frac{D_1(E)}{D_0(E)} = \frac{1}{D_0(E) | D_1(E)} \quad (9.14.3.8)$$

where $D_0(E)$ is the full determinant of $[E - H]$ and $D_1(E)$ is the determinant obtained by deleting the first row and column of the matrix $[E - H]$. Similarly, we define $D_n(E)$ to be the determinant obtained by deleting the first n rows and columns of $[E - H]$. The right-hand side of Eq. (9.14.3.8) can be reexpressed by successively expanding the determinants by the usual rules in the form

$$\begin{aligned} D_0(E) &= (E - a_0)D_1(E) - b_1^2 D_2(E) \\ D_1(E) &= (E - a_1)D_2(E) - b_2^2 D_3(E) \\ &\vdots \end{aligned} \quad (9.14.3.9)$$

Substitution of expressions (9.14.3.9) in Eq. (9.14.3.8) yields the continued fraction

$$G(E \mid u_0) = \frac{1}{E - a_0 - b_1^2/E - a_1 - b_2^2/E - a_2 - b_3^2/\cdots b_{N-1}^2/E - a_N \cdots} \quad (9.14.3.10)$$

Expression (9.14.3.10) is a purely algebraic quantity and can be evaluated easily once E is known. Combining Eq. (9.14.3.10) and a similar expression for $G(E \mid v_0)$ along with relation (9.14.3.6) gives finally

$$\langle \phi_f \mid G(E) \mid \phi_i \rangle = \tfrac{1}{2}[G(E \mid u_0) - G(E \mid v_0)] \quad (9.14.3.11)$$

$$= \frac{1}{2} \left[\frac{1}{E - a_0 - b_1^2 \mid E - a_1 - b_2^2 \mid E - a_2 \cdots} \right. \\ \left. - \frac{1}{E - a'_0 - b'_1 \mid E - a'_1 - b'^2_2 \mid E - a'_2 \cdots} \right] \quad (9.14.3.12)$$

where a'_n and b'_n are the constants of the chain Hamiltonian “based” on $|v_0\rangle$. One sees that the matrix element of the resolvent is given by the difference of two algebraic continued fractions defined in terms of the constants of the two chain Hamiltonians “based” on the two states $|u_0\rangle$ and $|v_0\rangle$ alone.

9.14.4. The Transition Amplitude

The transition amplitude at time t is usually given by the matrix element of the evolution operator

$$U(t \mid 0) = e^{-iHt/\hbar} \quad (9.14.4.1)$$

We intend to express the amplitude entirely in terms of only the eigenvalues of the chain H and two related chains. Let us for a moment assume that the exact eigenvalues and eigenvectors of H are E_α and $|E_\alpha\rangle$. Then

$$A_{i \rightarrow f}(t) = \langle \phi_f \mid U(t \mid 0) \mid \phi_i \rangle = \sum_{\alpha} \langle \phi_f \mid E_\alpha \rangle \langle E_\alpha \mid \phi_i \rangle e^{-iE_{\alpha}t/\hbar} \quad (9.14.4.2)$$

We shall assume that $\langle \phi_f \mid E_\alpha \rangle$ and $\langle E_\alpha \mid \phi_i \rangle$ are real [if they are not, then we must use all the four combinations, Eqs. (9.14.3.1)–(9.14.3.4), instead of only the first two in an analogous way]. In terms of Eqs. (9.14.3.1) and (9.14.3.2) we may clearly write

$$\langle \phi_f \mid E_\alpha \rangle \langle E_\alpha \mid \phi_i \rangle = \tfrac{1}{2}[\langle u_0 \mid E_\alpha \rangle^2 - \langle v_0 \mid E_\alpha \rangle^2] \quad (9.14.4.3)$$

If the matrix element of the resolvent is expressed in the form

$$G(E | u_0) = \langle u_0 | G(E) | u_0 \rangle = \sum_{\alpha} \langle u_0 | E_{\alpha} \rangle^2 \frac{1}{E - E_{\alpha}} \equiv \sum_{\alpha} \frac{R_{\alpha}(u_0)}{E - E_{\alpha}} \quad (9.14.4.4)$$

then it is immediately seen that

$$\langle u_0 | E_{\alpha} \rangle^2 = R_{\alpha}(u_0) = \lim_{E \rightarrow E_{\alpha}} (E - E_{\alpha}) G(E | u_0) \quad (9.14.4.5)$$

is simply the residue of the resolvent $G(E | u_0)$ at the pole $E = E_{\alpha}$. Substitution of Eq. (9.14.4.5) in relation (9.14.4.2) yields

$$A_{i \rightarrow f}(t) = \frac{1}{2} \sum_{\alpha} [R_{\alpha}(u_0) - R_{\alpha}(v_0)] e^{-iE_{\alpha}t/\hbar} \quad (9.14.4.6)$$

Furthermore, from Eq. (9.14.3.8) we have

$$G(E | u_0) = \frac{D_1(E)}{D_0(E)} = \frac{\det[E - H_r]}{\det[E - H]} = \frac{\prod_{\beta=1}^{N-1} [E - E_{\beta}(u_0)]}{\prod_{\beta=1}^N (E - E_{\beta})} \quad (9.14.4.7)$$

where H_r is the “reduced-chain” matrix obtained by deleting the first row and column of the chain Hamiltonian H (“based” on $|u_0\rangle$); $E_{\beta}(u_0)$ are the eigenvalues of H_r and E_{β} are the eigenvalues of H , the chain (9.14.1.18). Hence from Eq. (9.14.4.5) and (9.14.4.7) we obtain for the residues

$$R_{\alpha}(u_0) = \lim_{E \rightarrow E_{\alpha}} (E - E_{\alpha}) \frac{D_1(E)}{D_0(E)} = \frac{\prod_{\beta=1}^{N-1} [E_{\alpha} - E_{\beta}(u_0)]}{\prod_{\beta \neq \alpha}^N (E_{\alpha} - E_{\beta})} \quad (9.14.4.8)$$

Finally, by inserting the latter relation in Eq. (9.14.4.6), we obtain the desired result⁽²⁰³⁾

$$A_{i \rightarrow f}(t) = \frac{1}{2} \sum_{\alpha=1}^N \frac{\prod_{\beta=1}^{N-1} [E_{\alpha} - E_{\beta}(u_0)] - \prod_{\beta=1}^{N-1} [E_{\alpha} - E_{\beta}(v_0)]}{\prod_{\beta \neq \alpha}^N (E_{\alpha} - E_{\beta})} e^{-iE_{\alpha}t/\hbar} \quad (9.14.4.9)$$

Clearly, one requires nothing more than the eigenvalues of the tridiagonal chain Hamiltonian H , given by Eq. (9.14.1.18), and of the two “reduced chains” H_r , based on $|u_0\rangle$ and $|v_0\rangle$, to completely determine the transition amplitude at any time t .

10

Floquet Theory of Multiphoton Transitions

10.1. Introduction

In Chapter 6 we saw how the Floquet Hamiltonian for multiphoton processes arises from the semiclassical resolvent theory and how this Hamiltonian was found to be essentially equivalent to the projection of the quantum Hamiltonian onto the space of the occupation numbers. The fundamental property of the system that permits such a development is the periodicity of the semiclassical Hamiltonian in time and/or the periodicity of the stationary Hamiltonian in energy. In this chapter the Floquet theory of multiphoton transition amplitudes is developed in both the energy and time domains. We begin the energy-domain analysis with the construction of a general Floquet Hamiltonian applicable to an N -electron system and to multipolar interactions.

10.2. The Energy-Domain Floquet Method

Until now we have remained within the framework of the “dipole” or “long-wavelength” approximation of the atom–field interaction. This is in fact an excellent approximation for most problems occurring in the region of optical (or lower) frequencies. However, there is no essential difficulty in removing this limitation and incorporating the multipolar contributions directly into the theory. We shall take into account the full minimum coupling interaction with an N -electron system below and point out the simplifications that ensue from the “long-wavelength” approximation, at appropriate places.

10.2.1. The N -Electron Schrödinger Problem with a Multipolar Field

The Schrödinger equation for an N_a -electron atom in an external electromagnetic field is

$$i\hbar \frac{\partial}{\partial t} \Psi(\mathbf{x}, t) = \left\{ H_0 + \left[-\frac{e}{\mu c} \sum_{i=1}^{N_a} \mathbf{A}(\mathbf{r}_i, t) \cdot \mathbf{p}_i + \frac{e^2}{2\mu c^2} \sum_{i=1}^{N_a} A^2(\mathbf{r}_i, t) \right] \right\} \Psi(\mathbf{x}, t)$$

$$\equiv H(t)\Psi(x, t) \quad (10.2.1.1)$$

where H_0 is the N_a -particle Hamiltonian of the isolated atom and provides a complete set of eigenstates $\{|j\rangle\}$ and eigenvalues $\{\varepsilon_j\}$ satisfying

$$H_0 |j\rangle = \varepsilon_j |j\rangle \quad (10.2.1.2)$$

We assume that the set $\{j\}$ denotes all the quantum numbers necessary to uniquely specify the state $|j\rangle$.

In Eq. (10.2.1.1), $\mathbf{p}_i \equiv -i\hbar\nabla_i$ corresponds to the momentum operator of the i th electron and \mathbf{x} represents the set of coordinates of the N_a electrons $\{\mathbf{r}_1, \mathbf{r}_2, \dots, \mathbf{r}_{N_a}\}$. The vector potential at the position of the i th electron is

$$\mathbf{A}(\mathbf{r}_i, t) = \boldsymbol{\epsilon} \left\{ \frac{A_0}{2} \exp[i(\mathbf{k} \cdot \mathbf{r}_i - \omega t - \delta)] + \text{c.c.} \right\} \quad (10.2.1.3)$$

where $\boldsymbol{\epsilon}$ and \mathbf{k} are respectively the unit polarization and propagation vector of the field such that $\boldsymbol{\epsilon} \cdot \mathbf{k} = 0$, δ is the initial phase, A_0 the peak strength, and ω is the frequency. The phase of $\boldsymbol{\epsilon}$ may be absorbed into δ .

We note at the outset that an important consequence of the monomode field (10.2.1.3) in Eq. (10.2.1.1) is that the total Hamiltonian $H(t)$ is a periodic function of time with period $\tau = 2\pi/\omega$:

$$H(t + \tau) = H(t) \quad (10.2.1.4)$$

Using Eq. (10.2.1.3) we write

$$-\frac{e}{\mu c} \sum_{i=1}^{N_a} \mathbf{A}(\mathbf{r}_i, t) \mathbf{p}_i = V^{(1)}(\mathbf{x}) e^{-i(\omega t + \delta)} + V^{(-1)}(\mathbf{x}) e^{i(\omega t + \delta)} \quad (10.2.1.5)$$

where

$$V^{(\pm 1)}(\mathbf{x}) = -\frac{eA_0}{2\mu c} \sum_{i=1}^{N_a} \boldsymbol{\epsilon} \cdot \mathbf{p}_i \exp(\pm i\mathbf{k} \cdot \mathbf{r}_i) \quad (10.2.1.6)$$

We also have

$$\frac{e^2}{2\mu c^2} \sum_{i=1}^{N_a} A^2(\mathbf{x}_i, t) = V^{(0)} + V^{(2)}(\mathbf{x}) e^{-2i(\omega t + \delta)} + V^{(-2)}(\mathbf{x}) e^{2i(\omega t + \delta)} \quad (10.2.1.7)$$

where

$$V^{(0)} = \frac{N_a e^2 A_0^2}{4\mu c^2} \quad (10.2.1.8)$$

and

$$V^{(\pm 2)}(\mathbf{x}) = \frac{e^2 A_0^2}{8\mu c^2} \sum_{i=1}^{N_a} \exp(\pm 2i\mathbf{k} \cdot \mathbf{r}_i) \quad (10.2.1.9)$$

The constant $V^{(0)}$ may be interpreted as the mean interaction energy of the atom with the field. We note that the interaction operators $V^{(\pm 1)}(\mathbf{x})$ and $V^{(\pm 2)}(\mathbf{x})$ are simple sums of one-electron operators only; their matrix elements may therefore be obtained without undue difficulty once the wave functions $|j\rangle$ are available. Substitution of relations (10.2.1.5) and (10.2.1.7) in Eq. (10.2.1.1) gives

$$i\hbar \frac{\partial}{\partial t} \Psi(\mathbf{x}, t) = [H_0 + V^{(0)} + V^{(1)}(\mathbf{x}) e^{-i(\omega t + \delta)} + V^{(-1)}(\mathbf{x}) e^{i(\omega t + \delta)} + V^{(2)}(\mathbf{x}) e^{-2i(\omega t + \delta)} + V^{(-2)}(\mathbf{x}) e^{2i(\omega t + \delta)}] \Psi(\mathbf{x}, t) \quad (10.2.1.10)$$

10.2.2. Structure of the Floquet Equations with Retardation

Floquet's theorem^(211,212) on differential equations with periodic coefficients requires that the solutions $\psi(\mathbf{x}, t)$ of Eq. (10.2.1.1) or (10.2.1.10) have the form

$$\Psi(\mathbf{x}, t) = e^{-iEt/\hbar} \phi(\mathbf{x}, t) \quad (10.2.2.1)$$

where the “characteristic exponent” E/\hbar is a parameter independent of time and is, in general, noncommensurate with respect to the frequency ω , and $\phi(\mathbf{x}, t)$ is a periodic function of t and reflects the periodicity of the total Hamiltonian $H(t)$. In other words

$$\phi(\mathbf{x}, t + \tau) = \phi(\mathbf{x}, t) \quad (10.2.2.2)$$

Hence we may expand $\phi(\mathbf{x}, t)$ in a Fourier series

$$\phi(\mathbf{x}, t) = \sum_{n=-\infty}^{\infty} \phi_n(\mathbf{x}) e^{in(\omega t + \delta)} \quad (10.2.2.3)$$

Substitution of Eqs. (10.2.2.3) and (10.2.2.1) in Eq. (10.2.1.10) easily yields (as in Chapter 6) an equation with terms depending on the Fourier exponentials $e^{in(\omega t+\delta)}$. This equation must, however, be satisfied for all times t and hence we may equate the coefficients of equal powers of $e^{i(\omega t+\delta)}$ to obtain the set of stationary Floquet equations

$$[E - H_0 - V^{(0)} - n\hbar\omega] \phi_n(\mathbf{x}) = V^{(1)}(\mathbf{x})\phi_{n+1}(\mathbf{x}) + V^{(-1)}(\mathbf{x})\phi_{n-1}(\mathbf{x}) \\ + V^{(2)}(\mathbf{x})\phi_{n+2}(\mathbf{x}) + V^{(-2)}(\mathbf{x})\phi_{n-2}(\mathbf{x}) \quad (10.2.2.4)$$

where

$$n = 0, \pm 1, \pm 2, \dots, \pm \infty$$

In analogy with the index shifters defined in Chapter 6, we may introduce shift operators

$$S_n^{(\pm 1)} \phi_n \equiv \phi_{n \pm 1} \quad (10.2.2.5)$$

and

$$S_n^{(\pm 2)} \phi_n \equiv \phi_{n \pm 2} \quad (10.2.2.6)$$

These operators permit Eq. (9.2.2.4) to be expressed in the form of a stationary Schrödinger equation

$$E\phi_n(\mathbf{x}) = H_{(n)}^F \phi_n(\mathbf{x}) \quad (10.2.2.7)$$

where

$$H_{(n)}^F = [H_0 + V^{(0)} + n\hbar\omega + S_n^{(1)}V^{(1)}(\mathbf{x}) + S_n^{(-1)}V^{(-1)}(\mathbf{x}) \\ + S_n^{(2)}V^{(2)}(\mathbf{x}) + S_n^{(-2)}V^{(-2)}(\mathbf{x})] \quad (10.2.2.8)$$

Equation (10.2.2.8) is the Floquet Hamiltonian with the full effect of retardation included. We shall denote the matrix representation of $H_{(n)}^F$ on the basis of H_0 and for all n simply as H^F , and absorb the constant $V^{(0)}$ in the unperturbed energy $\{\epsilon_i\}$ of H_0 . The only formal difference between the present, more general equation (10.2.2.4) and that obtained in the dipole approximation before [cf. Eq. (6.3.8)] is that Eq. (10.2.2.4) consists of a five-term matrix recurrence relation as opposed to a three-term relation valid for the dipole case. In the dipole approximation it is perhaps more convenient, for problems involving discrete states, to work in the “ $\mathbf{E} \cdot \mathbf{D}$ gauge” rather than by omitting $V^{(\pm 2)}$ and the \mathbf{k} -dependence of the $V^{(\pm 1)}$ terms in Eq. (10.2.2.8).

The retardation (or multipolar) effect is also conveniently included in a similar manner for the case of a quantum field. In the number-state

representation the Schrödinger equation, including retardation, is given by

$$E |\psi\rangle = \left[H_0 + a^+ a \hbar\omega - \frac{e}{\mu c} \left(\frac{2\pi\hbar\omega}{L^3} \right)^{1/2} \sum_{i=1}^{N_a} (A^+(\mathbf{r}_i) + A(\mathbf{r}_i)) \mathbf{\epsilon} \cdot \mathbf{p}, \right. \\ \left. + \frac{e^2}{2\mu c^2} \left(\frac{2\pi\hbar\omega}{L^3} \right)^{1/2} \sum_{i=1}^{N_a} (A^+(\mathbf{r}_i) + A(\mathbf{r}_i))^2 \right] |\psi\rangle \quad (10.2.2.9)$$

where

$$A(\mathbf{r}_i) = \exp(i\mathbf{k} \cdot \mathbf{r}_i) a \quad (10.2.2.10)$$

and

$$A^+(\mathbf{r}_i) = \exp(-i\mathbf{k} \cdot \mathbf{r}_i) a^+ \quad (10.2.2.11)$$

In analogy with the demonstration for the dipole case in Chapter 6, it is easily found that the projection of Eq. (10.2.2.9) onto the number states $|n\rangle$ goes over exactly to the Floquet equations (10.2.2.4) provided, of course, the “laser approximation,” Eq. (6.4.8), is assumed to apply. Hence a comparison of the number-state projected quantum equations obtained from Eq. (10.2.2.9) with the Floquet equations (10.2.2.4) permits one to identify the parameter E (the “characteristic exponent” of the Floquet system) with the total energy E of the corresponding quantum system (which justifies our anticipated notation). In the space of Fourier components (or in the photon number space) Eq. (10.2.2.7) has the infinite matrix representation

$$\begin{array}{ccccc} & n' = -2 & n' = -1 & n' = 0 & n' = 1 & n' = 2 \\ \begin{matrix} n = -2 \\ n = -1 \\ n = 0 \\ n = 1 \\ n = 2 \end{matrix} & \left[\begin{array}{ccccc} H_0 - 2\hbar\omega I - E & V^{(1)} & V^{(2)} & & \\ V^{(-1)} & H_0 - \hbar\omega I - E & V^{(1)} & V^{(2)} & \\ V^{(-2)} & V^{(-1)} & H_0 - E & V^{(1)} & V^{(2)} \\ & V^{(-2)} & V^{(-1)} & H_0 + \hbar\omega I - E & V^{(1)} \\ & & V^{(-2)} & V^{(-1)} & H_0 + 2\hbar\omega I - E \end{array} \right] & \begin{pmatrix} \phi_{-2} \\ \phi_{-1} \\ \phi_0 \\ \phi_1 \\ \phi_2 \end{pmatrix} & = & \begin{pmatrix} 0 \\ 0 \\ 0 \\ 0 \\ 0 \end{pmatrix} \end{array} \quad (10.2.2.12)$$

where each element of this infinite matrix corresponds to a J -dimensional block matrix in the atomic Hilbert space and I is the corresponding unit matrix.

We may expand the state vectors $\phi_n(\mathbf{x})$ in Eq. (10.2.2.4) on the basis of the eigenstates $|j\rangle \equiv |j(\mathbf{x})\rangle$ of H_0 :

$$\phi_n(\mathbf{x}) = \sum a_{jn} |j\rangle \quad (10.2.2.13)$$

Here, the summation over j must usually be truncated for practical reasons

but should be extended at least up to the point where the numerical convergence of the final results is ensured.

Substitution of expansion (10.2.2.13) in Eq. (10.2.2.4) provides an explicit set of algebraic equations for the determination of coefficients a_{jn} and energy E :

$$(E - E_j^n) a_{jn} = \sum_{j'} [V_{jj'}^{(1)} a_{j'n+1} + V_{jj'}^{(-1)} a_{j'n-1} + V_{jj'}^{(2)} a_{j'n+2} + V_{jj'}^{(-2)} a_{j'n-2}] \quad (10.2.2.14)$$

for $(j, j') = 1, 2, \dots, J$ and $n = 0, \pm 1, \pm 2, \dots, \pm \infty$, where we have set

$$E_j^n \equiv \varepsilon_j + n\hbar\omega + V^{(0)} \quad (10.2.2.15)$$

In this way the problem of solving the time-dependent Schrödinger equation (10.2.1.1) in the restricted J -dimensional Hilbert space of the atom is reduced to solving the infinite algebraic system of equations (10.2.2.14). For any finite truncation in both the $\{j\}$ and $\{n\}$ spaces, the algebraic equations may be solved by the usual method of diagonalization to obtain the eigenvalues E and the corresponding eigenvectors $a_{jn}(E)$. An example of actual calculations with such a truncated Hamiltonian is discussed in Section 10.2.7 and the theory of infinite-dimensional $\{n\}$ -space is developed in Section 10.2.8. We now consider the basic properties of the time-dependent solutions of the Floquet problem.

10.2.3. The Equivalent Solutions and the Independent Solutions

A fundamental characteristic of the Floquet Hamiltonian is its periodicity in the energy domain. Thus it is seen directly from Eq. (10.2.2.12) that it remains invariant under the twin transformations^(190,213)

$$\left. \begin{array}{l} E \rightarrow E + p\hbar\omega \\ \text{and} \\ n \rightarrow n + p \end{array} \right\} \quad (10.2.3.1)$$

where $p = 0, \pm 1, \pm 2, \dots, \pm \infty$. Transformation (10.2.3.1) merely shifts the “origin” $(n, n') = (0, 0)$ of the infinite system (10.2.2.12) without any other alteration. Hence, given a single eigenvalue $E = E_\lambda^0$ (say) of Eq. (10.2.2.14) there are infinitely many eigenvalues E_λ^p obtainable from E_λ^0 by the translation

$$E_\lambda^p = E_\lambda^0 + p\hbar\omega \quad (10.2.3.2)$$

Accordingly, if $a_{jn}(E_\lambda^0)$ is the (j, n) th component of the eigenvector

corresponding to E_λ^0 then, on account of relations (10.2.3.1) and (10.2.3.2), Eq. (10.2.2.14) is satisfied by the infinitely many equalities

$$a_{j,n+p}(E_\lambda^p) = a_{jn}(E_\lambda^0) \quad (10.2.3.3)$$

There are, however, only as many independent solutions of Eq. (10.2.2.14) as the number of independent basis states, namely J , used to represent the Hamiltonian $H(t)$ appearing in Eq. (10.2.1.1). Hence there exist only J independent eigenvalues E_λ^0 , and correspondingly only J independent sets of eigenvectors $a_{jn}(E_\lambda^0)$ with $\lambda = 1, 2, \dots, J$. We show below that the infinitely many time-dependent solutions of Eq. (10.2.1.1) that are related by Eqs. (10.2.3.2) and (10.2.3.3) differ at most by arbitrary phase factors. Therefore they are not only nonindependent but are equivalent. Thus there are J independent sets of time-dependent solutions of Eq. (10.2.1.1) each set consisting of infinitely many but equivalent individual solutions. Hence it is necessary and sufficient to choose one and only one solution from each such “equivalent set” to fully specify the system of interest.

The equivalence of the solutions of Eq. (10.2.1.1) subject to relations (10.2.3.2) and (10.2.3.3) is established by constructing the wave function $|\psi_\lambda(t)\rangle$ corresponding to the eigenvalue $E = E_\lambda^0$. On combining Eqs. (10.2.2.1) and (10.2.2.13) we obtain

$$|\psi_\lambda(t)\rangle = \exp(-iE_\lambda^0 t/\hbar) \sum_{j=1}^J \sum_{n=-\infty}^{\infty} a_{jn}(E_\lambda^0) e^{in(\omega t + \delta)} |j\rangle \quad (10.2.3.4)$$

Similarly, if the solution corresponding to $E = \tilde{E}_\lambda$ is $|\tilde{\psi}_\lambda(t)\rangle$,

$$|\tilde{\psi}_\lambda(t)\rangle = \exp(-i\tilde{E}_\lambda t/\hbar) \sum_{j=1}^J \sum_{n=-\infty}^{\infty} a_{jn}(\tilde{E}_\lambda) e^{in(\omega t + \delta)} |j\rangle \quad (10.2.3.5)$$

By substituting for $\tilde{E}_\lambda = E_\lambda^p$ and using relation (10.2.3.2) we obtain

$$|\tilde{\psi}_\lambda(t)\rangle = \sum_{j=1}^J \sum_{n=-\infty}^{\infty} \exp[-i(E_\lambda^0 + p\hbar\omega)t/\hbar] a_{jn}(E_\lambda^0) e^{in(\omega t + \delta)} |j\rangle \quad (10.2.3.6)$$

We now replace the summation index subject to $n \rightarrow n + p$ in Eq. (10.2.3.6), use (10.2.3.3) and combine the result with Eq. (10.2.3.4). This immediately yields

$$|\tilde{\psi}_\lambda(t)\rangle = |\psi_\lambda(t)\rangle \quad (10.2.3.7)$$

Thus $|\tilde{\psi}_\lambda(t)\rangle$ equals $|\psi_\lambda(t)\rangle$. Physically, this implies that the information contained in any one solution of the infinite number of solutions in an

“equivalent set” is identical to that contained in any other solution of the set.

10.2.4. The Biorthonormal Properties and “Stationary” Solutions

The J independent solutions of interest are given by Eq. (10.2.3.4) with $\lambda = 1, 2, 3, \dots, J$. From Eq. (10.2.1.10) and its complex conjugate, and assuming that $H(t) = H^+(t)$ (this may be always assured, if necessary, by properly choosing the phase of ϵ), it is easily seen that

$$\frac{\partial}{\partial t} \langle \psi_{\lambda}(\cdot)(t) | \psi_{\lambda}(t) \rangle = 0 \quad (10.2.4.1)$$

Hence we may normalize $\psi_{\lambda}(t)$ for all times t ,

$$\langle \psi_{\lambda}(t) | \psi_{\lambda}(t) \rangle = 1 \quad (10.2.4.2)$$

Therefore, with the aid of Eq. (10.2.3.4) we have

$$\begin{aligned} \langle \psi_{\lambda}(\cdot)(t) | \psi_{\lambda}(t) \rangle &= \\ \exp[-i(E_{\lambda}^0 - E_{\lambda}^0)t/\hbar] \sum_{p=-\infty}^{\infty} e^{-ip(\omega t + \delta)} \sum_{n=-\infty}^{\infty} \sum_{j=1}^J a_{j,n-p}^*(E_{\lambda}^0) a_{j,n}(E_{\lambda}^0) & \quad (10.2.4.3) \end{aligned}$$

where

$$p \equiv n - n'$$

Equation (10.2.4.1) requires that the left-hand side of Eq. (10.2.4.3) remain constant in time. This is assured provided

$$\sum_{n=-\infty}^{\infty} \sum_{j=1}^J a_{j,n-p}(E_{\lambda}^0) a_{j,n}(E_{\lambda}^0) = \delta_{\lambda' \lambda} \delta_{p_0} \quad (10.2.4.4)$$

An otherwise arbitrary constant factor on the right-hand side of this relation is fixed by the normalization condition (10.2.4.2) to be equal to unity.

We conclude from relations (10.2.4.4) and (10.2.4.2) that the J solutions $\psi_{\lambda}(\mathbf{x}, t)$, $\lambda = 1, 2, \dots, J$ provide an orthonormal set of solutions to Eq. (10.2.1.1). We observe that these solutions $\psi_{\lambda}(\mathbf{x}, t)$ are “stationary” in the sense that the probability density $\psi_{\lambda}^*(\mathbf{x}, t)\psi_{\lambda}(\mathbf{x}, t)$ integrated over all space is constant in time; in other words, once the system is in any of the states $\psi_{\lambda}(\mathbf{x}, t)$ at some initial time, it will remain in that state if undisturbed for all future times.

A second orthogonal property of the coefficients $a_{jn}(E_\lambda^0)$ is

$$\sum_{\lambda=1}^J \sum_{n=-\infty}^{\infty} a_{j'n-p}^*(E_\lambda^0) a_{jn}(E_\lambda^0) = \delta_{jj'} \delta_{p,0} \quad (10.2.4.5)$$

To prove this we rewrite the solutions (10.2.4.5) as

$$|\psi_\lambda(t)\rangle = \sum_{j=1}^J S_{\lambda j}(t) |j\rangle \quad (10.2.4.6)$$

where

$$S_{\lambda j}(t) = \sum_n a_{jn}(E_\lambda^0) \exp[iE_\lambda t/\hbar + in(\omega t + \delta)] \quad (10.2.4.7)$$

We note that $|j\rangle$ and $|\psi_\lambda(t)\rangle$ form two different sets of orthogonal basis vectors for the same J -dimensional vector space of interest. The transformation (10.2.4.7) therefore defines a unitary matrix $S(t)$ with elements $S_{\lambda j}$ at all times t such that

$$S^+(t)S(t) = 1 \quad (10.2.4.8)$$

Substituting from Eq. (10.2.4.7) into relation (10.2.4.8) and taking the (j', j) matrix element yields

$$\begin{aligned} \delta_{j'j} &= \sum_{\lambda} S_{\lambda j'}^*(t) S_{\lambda j}(t) \\ &= \sum_{p=-\infty}^{\infty} e^{-ip(\omega t + \delta)} \sum_{\lambda=1}^J \sum_{n=-\infty}^{\infty} a_{j'n-p}^*(E_\lambda^0) a_{jn}(E_\lambda^0) \end{aligned} \quad (10.2.4.9)$$

For this equality to be satisfied at all times t , we must have

$$\sum_{\lambda=1}^J \sum_{n=-\infty}^{\infty} a_{j'n-p}^*(E_\lambda^0) a_{jn}(E_\lambda^0) = \delta_{jj'} \delta_{p,0} \quad (10.2.4.10)$$

Equations (10.2.4.10) and (10.2.4.4) imply that $|\psi_\lambda(t)\rangle$, given by Eq. (10.2.3.4), forms a biorthonormal system of solutions to the Schrödinger equation (10.2.1.1) for all t :

$$\langle \psi_{\lambda'}(t) | \psi_\lambda(t) \rangle = \delta_{\lambda'\lambda} \quad (10.2.4.11)$$

and

$$\sum_{\lambda=1}^J |\psi_\lambda(t)\rangle \langle \psi_\lambda(t)| = 1 \quad (10.2.4.12)$$

10.2.5. The Evolution Matrix and the Transition Probabilities

Multiphoton transition probabilities from any given initial state are now obtained most conveniently with the help of the evolution matrix

$$U(t, t_0) \equiv \sum_{\lambda=1}^J |\psi_{\lambda}(t)\rangle\langle\psi_{\lambda}(t_0)| \quad (10.2.5.1)$$

which satisfies the usual properties of the evolution operator. Thus we have the time-transition property

$$U(t, t_0) = U(t, t_1)U(t_1, t_0) \quad (10.2.5.2)$$

as well as the unitary property

$$U^+(t, t_0) = U(t_0, t) = U^{-1}(t, t_0) \quad (10.2.5.3)$$

The normalization condition

$$U(t_0, t_0) = 1 \quad (10.2.5.4)$$

is satisfied at any time t_0 .

Equations (10.2.5.2)–(10.2.5.4) are easily verified on substitution from Eq. (10.2.5.1) and on utilizing relations (10.2.4.11) and (10.2.4.12).

A solution $\psi_i(t)$ of Eq. (10.2.1.1), obeying a given initial condition $|\phi_i(t_0)\rangle$ at $t = t_0$, is

$$|\psi_i(t)\rangle = U(t, t_0)|\phi_i(t_0)\rangle \quad (10.2.5.5)$$

Hence the desired transition amplitude between an initial unperturbed state $|\phi_i(t_0)\rangle = |i\rangle$ and a final unperturbed state $|\phi_f\rangle = |f\rangle$ is

$$\langle\phi_f|\psi_i(t)\rangle = \langle\phi_f|U(t, t_0)|\phi_i(t_0)\rangle \quad (10.2.5.6)$$

Equations (10.2.5.1) and (10.2.3.4) may be employed to express the right-hand side of Eq. (10.2.5.6) in the form

$$\begin{aligned} U_{i \rightarrow f}(t, t_0) &= \sum_{\lambda=1}^J \sum_{n,n'=-\infty}^{\infty} a_{f,n}(E_{\lambda}^0) \exp[-iE_{\lambda}^0 t/\hbar + in(\omega t + \delta)] \\ &\times a_{i,n'}^*(E_{\lambda}^0) \exp[+iE_{\lambda}^0 t_0/\hbar - in'(\omega t_0 + \delta)] \end{aligned} \quad (10.2.5.7)$$

This expression may be rewritten in various alternative ways. Thus, for

example, by setting $n' \rightarrow -l$ and using the periodic properties, we obtain

$$a_{i,-l}(E_\lambda^0) = a_{i,0}(E_\lambda^l) \quad \text{and} \quad a_{f,n}(E_\lambda^0) = a_{f,n+l}(E_\lambda^l) \quad (10.2.5.8)$$

and finally by putting $n \rightarrow n - l$, one obtains

$$U_{i \rightarrow f}(t, t_0) = \sum_{\lambda=1}^J \sum_{n,l=-\infty}^{\infty} a_{f,n}(E_\lambda^l) \exp[-iE_\lambda^l(t-t_0)/\hbar + in(\omega t + \delta)] a_{i,0}^*(E_\lambda^l) \quad (10.2.5.9)$$

The quantity $U_{i \rightarrow f}$ depends nontrivially on the initial phase δ , which is practically a random quantity. The probability of interest is often the one averaged over the distributions of δ . The simplest and most common assumption is that δ is uniformly distributed in the range $0 \leq \delta \leq 2\pi$. Hence

$$P_{i \rightarrow f}(t, t_0) = \frac{1}{2\pi} \int_0^{2\pi} |U(t, t_0)|^2 d\delta \quad (10.2.5.10)$$

$$= \sum_{n=-\infty}^{\infty} P_{i \rightarrow f}^{(n)}(t - t_0) \quad (10.2.5.11)$$

where

$$P_{i \rightarrow f}^{(n)}(t - t_0) = \left| \sum_{\lambda,l} a_{f,n}(E_\lambda^l) \exp[-iE_\lambda^l(t-t_0)/\hbar] a_{i,0}^*(E_\lambda^l) \right|^2 \quad (10.2.5.12)$$

As expected, the above transition probabilities depend only on the duration, $t - t_0$, of the interaction and not on t_0 and t independently. Averaging over the random phase is thus equivalent to averaging over the random initial instant t_0 , holding the elapsed time $t - t_0$ fixed.⁽¹¹⁶⁾ It is noteworthy that the use of a fixed δ ($= 0$) at the outset, and at the same time failing to average over the initial instants t_0 , may lead to significant differences in the calculated transition probabilities, particularly at higher intensities⁽²¹⁴⁾ where simple (phase-averaging-insensitive) approximations (such as the two-level RWA) may not be applicable.

10.2.6. The Floquet States and the “Floquet–Schrödinger Equation”

Let us denote by $|E_\lambda^l\rangle$ the orthonormal eigenvector of the Floquet matrix H^F belonging to the eigenvalue E_λ^l . Then the vector component $a_{jn}(E_\lambda^l)$ may be thought of as the projection of a state $|jn\rangle$ onto the eigenvector $|E_\lambda^l\rangle$:

$$a_{jn}(E_\lambda^l) \equiv \langle jn | E_\lambda^l \rangle \quad (10.2.6.1)$$

The state $|jn\rangle$ consists of the atomic state $|j\rangle$ and the Fourier component n ; it has been called⁽¹¹⁶⁾ a “Floquet state.”

In terms of relation (10.2.6.1), the phase-averaged transition probability equation (10.2.5.12) can be rewritten in the succinct form

$$P_{i \rightarrow f}^{(n)}(t - t_0) = \left| \sum_{\lambda,l} \langle f, n | E_\lambda^l \rangle \exp[-iE_\lambda^l(t - t_0)/\hbar] \langle E_\lambda^l | i, 0 \rangle \right|^2 \quad (10.2.6.2)$$

$$= |\langle fn | \exp[-iH^F(t - t_0)/\hbar] | i, 0 \rangle|^2 \quad (10.2.6.3)$$

where we have used the biorthogonal property of the eigenvectors $|E_\lambda^l\rangle$ [cf. Eqs. (10.2.4.10) and (10.2.4.4)]:

$$\sum_{\lambda,l} |E_\lambda^l\rangle \langle E_\lambda^l| = 1 \quad (10.2.6.4)$$

In view of the quantum-classical correspondence (in the “laser approximation”) one may interpret the Floquet state $|jn\rangle$ as the quantum product state $|j\rangle |n\rangle$. Equation (10.2.5.12) may then be interpreted as the probability of transition from the initial quantum state $|i\rangle |0\rangle$ to the final quantum state $|f\rangle |n\rangle$ with emission ($n > 0$) or absorption ($n < 0$) of n photons. Clearly the total probability (10.2.5.10) of exciting state $|f\rangle$ corresponds to the incoherent sum (10.2.5.11) of the n -photon emission and absorption probabilities (10.2.6.3).

We shall now show that the physically interesting transition probability (10.2.5.11) can be arrived at directly, without first obtaining the coherent amplitudes (10.2.5.9) and then averaging over the phase, from the solution of the “Floquet–Schrödinger equation”:

$$i\hbar \frac{\partial}{\partial t} |\psi^F(t)\rangle = H^F |\psi^F(t)\rangle \quad (10.2.6.5)$$

This equation is distinct from the original time-dependent Schrödinger equation (10.2.1.1). The solution of the stationary equation (10.2.6.5) satisfying any initial condition is

$$\psi^F(t) = U^F(t - t_0) \psi^F(t_0) \quad (10.2.6.6)$$

The evolution matrix associated with the stationary H^F is

$$U_0^F(t - t_0) = \exp[-iH^F(t - t_0)/\hbar] \quad (10.2.6.7)$$

which immediately gives the n -photon transition amplitude in the form

$$U_{fn,i0}^F(t - t_0) = \langle fn | \exp[-iH^F(t - t_0)/\hbar] | i, 0 \rangle \quad (10.2.6.8)$$

On the other hand, the transition amplitude containing full information of the initial phase, Eq. (10.2.5.9), can be rewritten as

$$U_{i \rightarrow f}(t, t_0) = \sum_{n=-\infty}^{\infty} \langle f n | \exp[-iH^F(t - t_0)/\hbar] | i 0 \rangle e^{in(\omega t + \delta)} \quad (10.2.6.9)$$

$$= \sum_{n=-\infty}^{\infty} U_{fn,i0}^F(t - t_0) e^{in(\omega t + \delta)} \quad (10.2.6.10)$$

Comparison of expressions (10.2.6.10) and (10.2.6.8) shows that the amplitudes $U_{i \rightarrow f}(t, t_0)$ generated by the original Schrödinger equation (10.2.1.1) consist of a coherent sum of the n -photon transition amplitudes, $U_{fn,i0}^F(t - t_0)$, generated by the Floquet–Schrödinger equation (10.2.6.5) weighted by phase factors $e^{in(\omega t + \delta)}$. The absence of phase information in the transition amplitudes obtained from the “Floquet–Schrödinger equation” is consistent with the complete indeterminacy of the field phase when the occupation number is known precisely (which is true for the number-state representation of the quantum field).

10.2.7. The Rovibrational Floquet Hamiltonian and the Multiphoton Infrared Excitation Spectra of CO

In this section we illustrate the truncated Floquet Hamiltonian method and obtain the multiphoton excitation probability of rovibrational states of small molecules. We discuss the structure of the truncated diatomic Floquet Hamiltonian, define the ensemble-averaged transition probabilities, and then give typical results^(215,216) for infrared multiphoton excitation spectra of CO.

For multiphoton infrared excitation from the ground vibrational level of diatomic molecules, the Floquet Hamiltonian is block multidiagonal in form. The dimension of this Hamiltonian depends not only on the number of vibrational levels included and the number of photon blocks retained, but also on the degree of occupation of the ground rotational states, i.e., on the rotational temperature T . All rotational states of the excited vibrational levels that couple to the ground rotational states via rovibrational selection rules must therefore be retained.

The block multidiagonal Floquet Hamiltonian for CO can be somewhat simplified (because of the quasi-harmonic structure of the rovibrational manifolds of a diatomic) by removing the photon blocks, which yield detunings greater than or equal to the laser frequency. Positions and widths of the individual rovibrational absorption lines calculated with and without this simplification have been found to agree to within a couple of percent for the line positions and to within a fraction of a percent for the

linewidths. The structure of the resulting Hamiltonian is shown schematically in Figure 39. The band structure of the matrix reflects the symmetry introduced by the rotational selection rules ($\Delta J = \pm 1$). An actual example is given in Figure 40, which results from $v = 0, 1, 2, 3$ and $J = 0, 1, 2$ in the initial, $v = 0$, level. The diagonal terms $\omega_{vJ}^v = \epsilon_{vJ} - v\omega$ refer to the particular v -photon detunings (ϵ_{vJ} is the vJ th rovibrational energy) and

$$\beta_{vJ,v'J'} = \frac{E}{2} \langle vJ | D_\lambda | v'J' \rangle \equiv \frac{E}{2} F_{JJ'} \langle v | D_\lambda | v' \rangle \quad (10.2.7.1)$$

are the off-diagonal rovibrational dipole coupling matrix elements. Here E

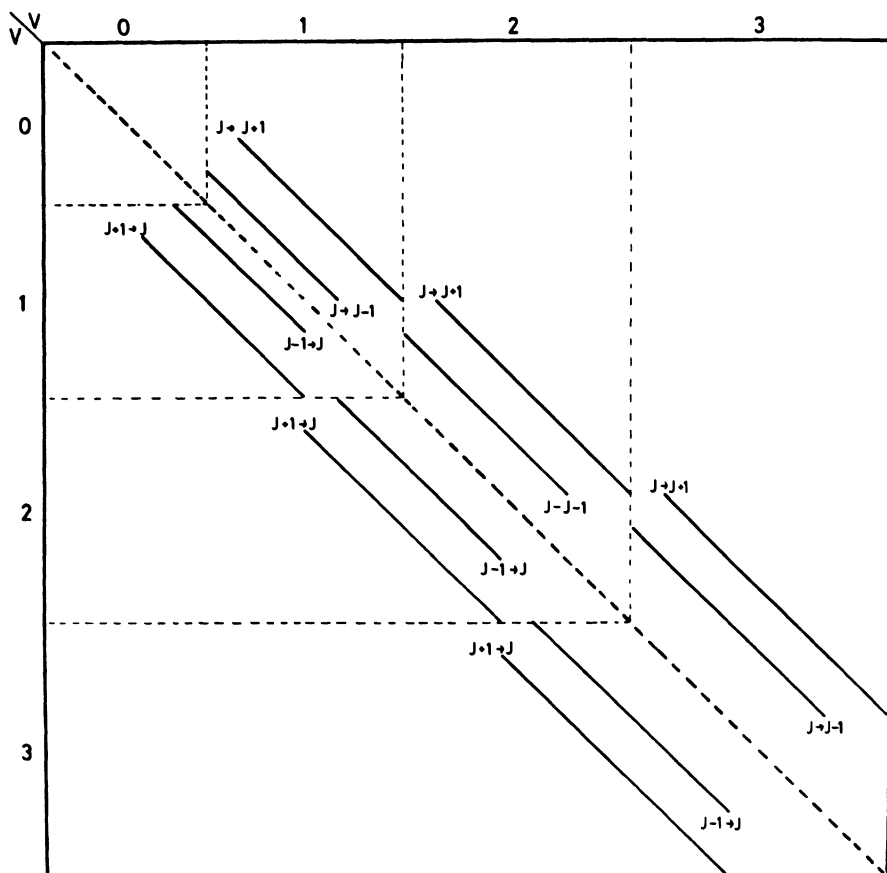


Figure 39. A schematic of the banded structure of the rovibrational Floquet Hamiltonian up to $v = 3$. Each vibrational block, enclosed by dotted lines, includes side bands due to rotational dipole couplings (from Moloney and Faisal⁽²¹⁵⁾).

$H =$

$$\begin{matrix} \omega_{00}^0 & 0 & 0 & \beta_{00,11} \\ 0 & \omega_{01}^0 & 0 & \beta_{01,10} \quad 0 & \beta_{01,12} \\ 0 & 0 & \omega_{02}^0 & 0 & \beta_{02,11} \quad 0 & \beta_{02,13} \\ 0 & \beta_{10,01} & 0 & \omega_{10}^1 & 0 & 0 & 0 & \beta_{10,21} \\ \beta_{11,00} & 0 & \beta_{11,02} & 0 & \omega_{11}^1 & 0 & 0 & \beta_{11,20} \quad 0 & \beta_{11,22} \\ \beta_{12,01} & 0 & 0 & 0 & \omega_{12}^1 & 0 & 0 & \beta_{12,21} \quad 0 & \beta_{12,23} \\ \beta_{13,02} & 0 & 0 & 0 & \omega_{13}^1 & 0 & 0 & \beta_{13,22} \quad 0 & \beta_{13,24} \\ 0 & \beta_{20,11} & 0 & 0 & \omega_{20}^2 & 0 & 0 & 0 & 0 & \beta_{20,31} \\ \beta_{21,10} & 0 & \beta_{21,12} & 0 & 0 & \omega_{21}^2 & 0 & 0 & 0 & \beta_{21,30} \quad 0 & \beta_{21,32} \\ \beta_{22,11} & 0 & \beta_{22,13} & 0 & 0 & \omega_{22}^2 & 0 & 0 & 0 & \beta_{22,31} \quad 0 & \beta_{22,33} \\ \beta_{23,12} & 0 & 0 & 0 & 0 & \omega_{23}^2 & 0 & 0 & 0 & \beta_{23,32} \quad 0 & \beta_{23,34} \\ \beta_{24,13} & 0 & 0 & 0 & 0 & \omega_{24}^2 & 0 & 0 & 0 & \beta_{24,33} \quad 0 & \beta_{24,35} \\ 0 & \beta_{30,21} & 0 & 0 & 0 & \omega_{30}^3 & 0 & 0 & 0 & 0 & 0 & 0 \\ \beta_{31,20} & 0 & \beta_{31,22} & 0 & 0 & 0 & \omega_{31}^3 & 0 & 0 & 0 & 0 & 0 \\ \beta_{32,21} & 0 & \beta_{32,23} & 0 & 0 & 0 & \omega_{32}^3 & 0 & 0 & 0 & 0 & 0 \\ \beta_{33,22} & 0 & \beta_{33,24} & 0 & 0 & 0 & 0 & \omega_{33}^3 & 0 & 0 & 0 & 0 \\ \beta_{34,23} & 0 & 0 & 0 & 0 & 0 & 0 & 0 & \omega_{34}^3 & 0 & 0 & 0 \\ \beta_{35,24} & 0 & 0 & 0 & 0 & 0 & 0 & 0 & 0 & 0 & \omega_{35}^3 & 0 \end{matrix} \quad \begin{matrix} 0 \\ 0 \end{matrix}$$

Figure 40. Rovibrational Floquet Hamiltonian for the ground electronic state of CO with $v = 0, 1, 2, 3$ and the coupling matrix elements arising from the initially occupied states ($v = 0$, $J = 0, 1, 2$). The diagonal elements $\omega_{vJ}^v = (\omega_{vJ} - v\omega)$ refer to the v -photon detunings with respect to vJ th rovibrational frequency ω_{vJ} and $\beta_{v,J,v',J'} = \frac{1}{2}\mathbf{E} \cdot \langle vJ | \mathbf{D} | vJ' \rangle$ (from Moloney and Faisal⁽²¹⁵⁾).

is the laser-field amplitude, $\langle v | D_\lambda | v' \rangle$ the rotationless $v \rightarrow v'$ dipole matrix element, and $F_{JJ'}$, the Herman–Wallis rotational factor.⁽²¹⁵⁾ We let the unity matrix $a_{l,k}$ diagonalize this finite Hamiltonian and let $E = \hbar\lambda_l$ be the resulting eigenvalues, where l (or k) runs over all $\{vJ\}$. Then the multiphoton rovibrational transition probability for a given transition from an initial vibrational level v to a final level v' (which is defined as an ensemble average over the occupied initial rotational states of v and a sum over the final rotational states of v') can be easily written down using Eq. (10.2.6.2),

$$P_{v \rightarrow v'}(\tau) = Q_R^{-1} \sum_J N_J \sum_{J'} a_{v'J',l} a_{v'J',k} a_{vJ,l} a_{vJ,k} \exp[-i(\lambda_l - \lambda_k)\tau] \quad (10.2.7.2)$$

where

$$N_J = (2J + 1) \exp[-\beta J(J + 1)hc/k_B T] \quad (10.2.7.3)$$

The quantity Q_R is the partition function and T is the rotational temperature (in K). Equation (10.2.7.2) yields the explicit transition probability at the interaction time $\tau = t - t_0$. For a continuously coherent operation of the laser, this reduces to its infinite-time-average stationary probability

$$\bar{P}_{v \rightarrow v'} = Q_R^{-1} \sum_J N_J \sum_{J',l,k} |a_{v'J',l}|^2 |a_{vJ,l}|^2 \quad (10.2.7.4)$$

If the coherent interaction of the laser with the molecule is of finite duration and is given by τ_c , then in place of expression (10.2.7.4) one obtains from Eq. (10.2.7.2)

$$\bar{P}_{v \rightarrow v'}^{T_c} = \bar{P}_{v \rightarrow v'} + Q_R^{-1} \sum_J N_J \sum_{v'J'l,k} \frac{a_{v'J',l} a_{v'J',k} a_{v,J,l} a_{vJ,k}}{1 + (\lambda_k - \lambda_l)^2 \tau_c^2} \quad (10.2.7.5)$$

It should be noted that for $\tau_c \gg |\lambda_k - \lambda_l|$ and all l and k , Eq. (10.2.7.5) reduces to Eq. (10.2.7.4), which describes a completely “saturated” system. In the example to follow this occurs for $\tau_c > 1$ ns. In the domain where $\tau_c < |\lambda_k - \lambda_l|$ for any pair of (“dressed” rovibrational) states k and l , the second term in Eq. (10.2.7.5) is negative and always reduces the induced transition probability, as expected, from its saturated value, given by Eq. (10.2.7.4). The quantity $|\lambda_k - \lambda_l|$ may be considered to play the role of a generalized “Rabi frequency” for a transition between the pair of dressed states.

The well-established molecular parameters and the rotationless dipole matrix elements of CO are used for the numerical calculation. We note that the multiphoton spectra can be computed from Eqs. (10.2.7.4) and (10.2.7.5) for different rotational temperatures T without the need for further diagonalization. Results are shown below only for the stationary transition probability, Eq. (10.2.7.4), for $T = 10$ K, which confines the significant Boltzmann population to the lowest five rovibrational states ($J = 0\text{--}4$) in the initial ground vibrational level, $v = 0$.

Multiphoton rovibrational spectra corresponding to excitation of one ($\bar{P}_{0 \rightarrow 1}$) and two ($\bar{P}_{0 \rightarrow 2}$) vibrational quanta for a laser intensity $I \approx 0.35$ GW cm⁻², over a frequency domain spanning 2097–2179 cm⁻¹, are shown in Figure 41. The positions of the individual unperturbed rovibrational transition frequencies are indicated by vertical dashed lines which, in turn, are labeled ($J-J'$) with the initial J and final J' quantum numbers. At the present field intensity the individual resonances in the single-quantum spectrum ($\bar{P}_{0 \rightarrow 1}$) tend to overlap strongly as a result of field-induced (power) broadening. The lines of the two-quantum spectrum, however, are well resolved and display a very strong Q-branch structure.

Two novel nonlinear features arise in these spectra in the vicinity of the $|v = 0, J = 1\rangle \rightarrow |v = 2, J = 3\rangle$ and $|v = 0, J = 3\rangle \rightarrow |v = 2, J = 1\rangle$ two-photon transition frequencies. Both features are associated with a “self-detected” power-splitting effect.⁽²¹⁶⁾

Figure 42 displays the multiphoton rovibrational spectra corresponding to the excitation with one ($\bar{P}_{0 \rightarrow 1}$), two ($\bar{P}_{0 \rightarrow 2}$), and three ($\bar{P}_{0 \rightarrow 3}$) vibrational quanta at a laser intensity $I \approx 8.7$ GW cm⁻² over the same frequency domain as in Figure 41. At this intensity, power broadening has completely smeared out the rovibrational structures in $\bar{P}_{0 \rightarrow 1}$ while those in

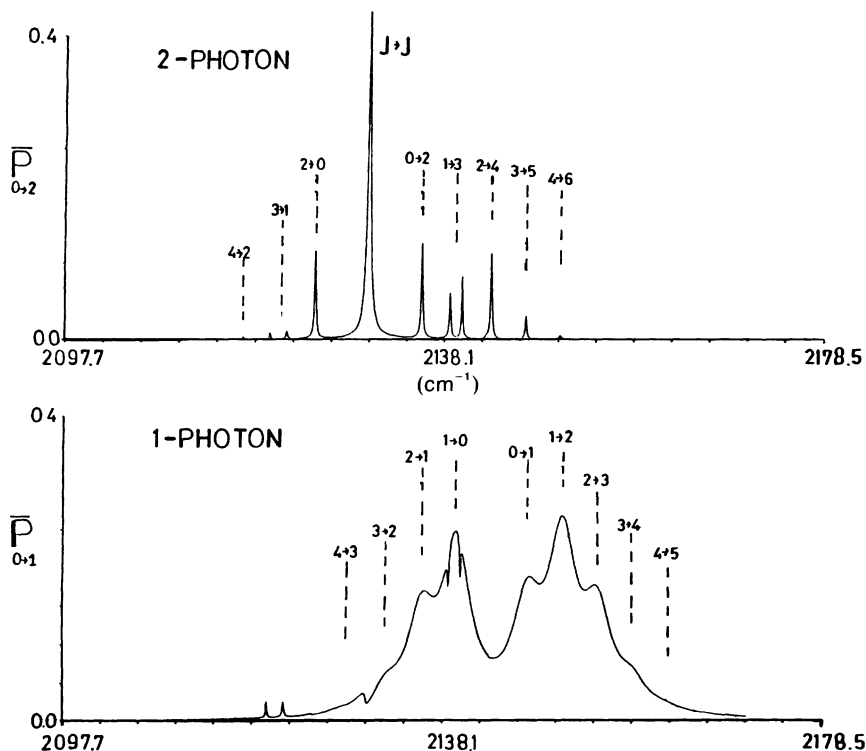


Figure 41. Infrared multiphoton rovibration excitation spectra for CO at a laser intensity $I = 0.35 \text{ GW cm}^{-2}$ and rotational temperature $T = 10 \text{ K}$. The steady-state excitation probabilities for one ($\bar{P}_{0 \rightarrow 1}$) and two ($\bar{P}_{0 \rightarrow 2}$) vibrational quanta are shown together with the rovibrational absorption line assignments ($J \rightarrow J'$). The self-induced hole burning in the single-quantum ($\bar{P}_{0 \rightarrow 1} : J = 1 \rightarrow J' = 0$) line and the splitting of the $J = 1 \rightarrow J' = 3$ and $J = 3 \rightarrow J' = 1$ two-quantum ($\bar{P}_{0 \rightarrow 2}$) lines are noteworthy (from Moloney and Faisal⁽²¹⁵⁾).

$\bar{P}_{0 \rightarrow 2}$ are still discernible but strongly perturbed. The three-quantum lines, however, are still resolved. The shift of the overall spectral envelope to lower frequencies with higher vibrational quantum excitation is a direct consequence of the anharmonicity of CO. Further nonlinear effects show up at this intensity. The low-frequency hump-like substructure in $\bar{P}_{0 \rightarrow 1}$ around the 4-3 unperturbed frequency mainly arises from a nonlinear contribution at the two-photon Q-branch ($J \rightarrow J$) transition frequency. This entails a process involving two-photon absorption followed by one-photon emission; this is also evident (though much weaker) at the reduced intensity in Figure 41. The very narrow resonances appearing in $\bar{P}_{0 \rightarrow 1}$ (labeled $0 \rightarrow 3, 1 \rightarrow 4$) that are not evident in Figure 41 are associated with

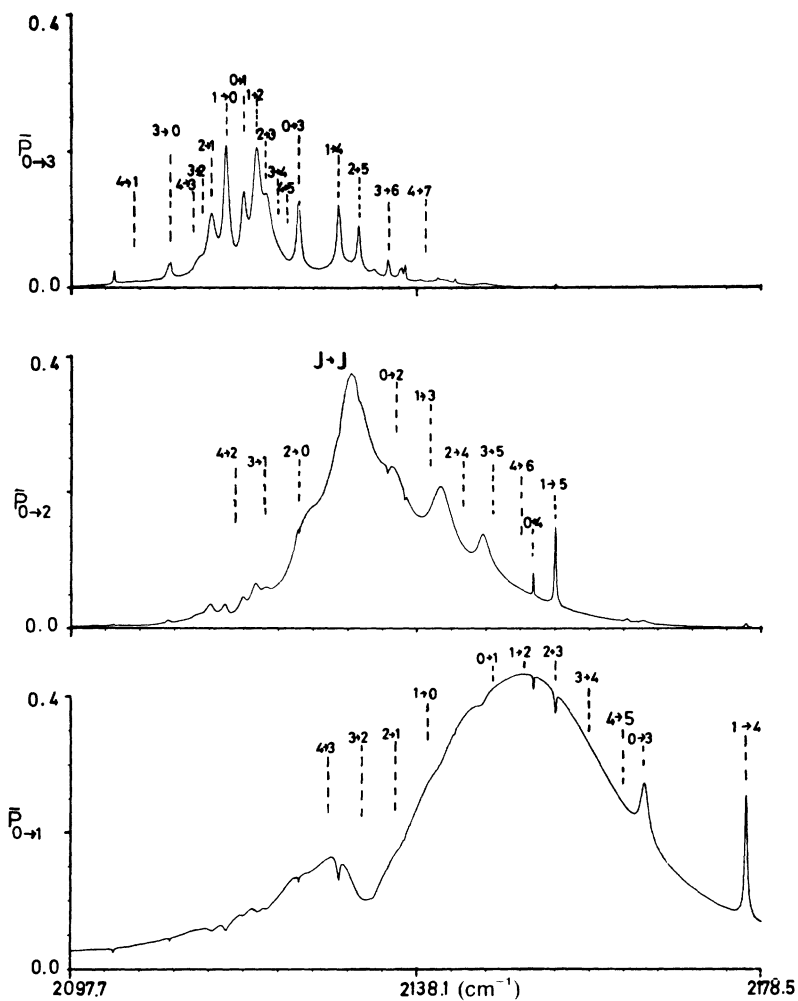


Figure 42. Infrared multiphoton rovibrational excitation spectra for CO at a laser intensity $I \approx 8.7 \text{ GW cm}^{-2}$ and rotational temperature $T = 10 \text{ K}$. The steady-state excitation probabilities for one ($\bar{P}_{0 \rightarrow 1}$), two ($\bar{P}_{0 \rightarrow 2}$), and three ($\bar{P}_{0 \rightarrow 3}$) vibrational quanta are shown together with the rovibrational absorption line assignments (from Moloney and Faisal⁽²¹⁵⁾).

higher-order nonlinear processes (mainly third-order) contributing to a lower-order (one-quantum) transition. The widths of these resonances are comparable to the third-order resonances appearing in $\bar{P}_{0 \rightarrow 3}$. The two narrow nonlinear structures in $\bar{P}_{0 \rightarrow 2}$ (labeled $0 \rightarrow 4$, $1 \rightarrow 5$) are similarly associated with fourth-order contributions to an otherwise second-order

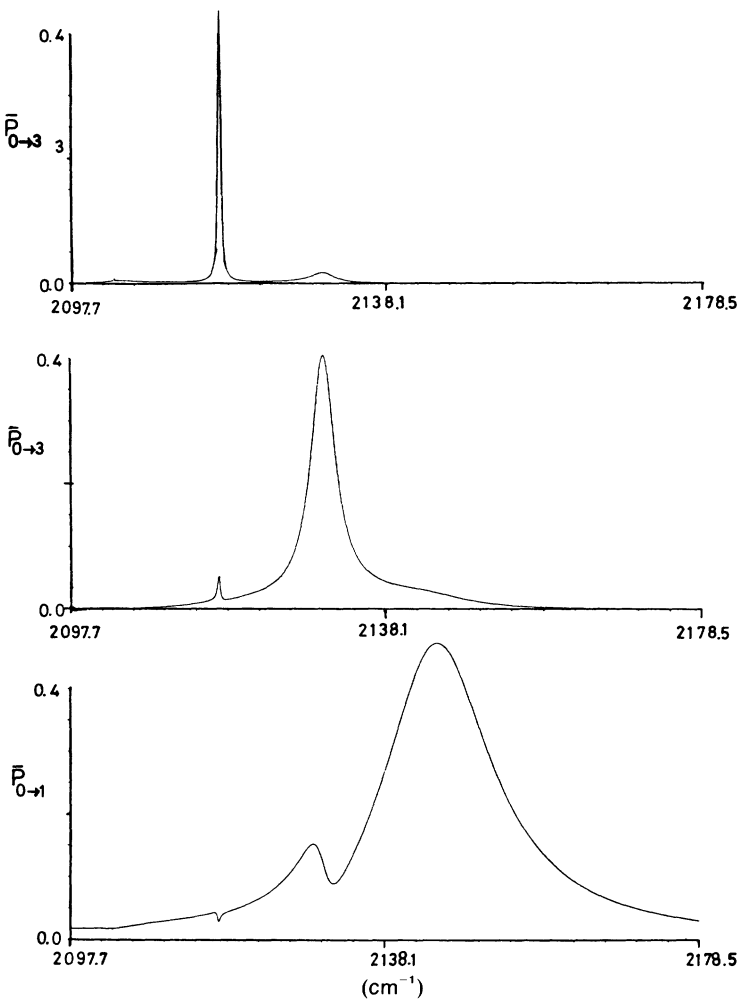


Figure 43. Infrared multiphoton rovibrational excitation spectra for CO neglecting the rotational structure, at a laser intensity $I = 8.7 \text{ GW cm}^{-2}$ and rotational temperature $T = 10 \text{ K}$. Excitation spectra of one (\bar{P}_{0-1}), two (\bar{P}_{0-2}), and three (\bar{P}_{0-3}) vibrational quanta shown here should be compared with the corresponding full spectra (including the rotational structure) shown in Figure 42 (from Moloney and Faisal⁽²¹⁵⁾).

transition process. The stability of the above spectra was not affected on including the $v = 4$ manifolds in the Floquet Hamiltonian.

We conclude this section by noting that care should be exercised in using any rotationless model for multiphoton vibrational excitation spectra of diatomics. Figure 43 presents vibrational excitation at an

intensity $I \approx 8.7 \text{ GW cm}^{-2}$, calculated by neglecting the associated rotational manifolds. This should be compared with the corresponding spectra shown in Figure 42 and obtained by retaining the rotational manifolds. For the low-lying transitions at this high field strength the rotationless model tends to reproduce the envelope of the full spectra, but the model clearly fails to reproduce the proper behavior for the higher excitations. Generally speaking, for a given field strength a rotationless model tends to give the spectral envelopes only for those transitions for which power broadening becomes comparable to or greater than the typical rotational-energy separations involved.

10.2.8. The Infinite System of Floquet Equations

The general problem of the interaction of a monomode radiation field with an atom, defined on a finite-dimensional atomic Hilbert space and on an infinite-dimensional photon space, has been reduced in Section 10.2 to the solution of an infinite system of algebraic equations (10.2.2.14). The crux of the problem is to determine the eigenvalues E_λ^0 , $\lambda = 1, 2, 3, \dots, J$. Once E_λ^0 are known the eigenvectors $a_{jn}(E_\lambda^0)$ may be determined with relative ease and the wave functions (10.2.3.4) or transition amplitudes (10.2.5.9) constructed as desired.

As in the case of Hill's equation,⁽²¹²⁾ we shall find it helpful in the subsequent development of our theory to recast the infinite secular determinant corresponding to Eq. (10.2.2.14) in the form of a generalized Hill-like determinant, by dividing each row of Eq. (10.2.2.14) by the corresponding element on the main diagonal. For analytic reasons we will find it also convenient to work in terms of the dimensionless characteristic exponents

$$z = E/\hbar\omega \quad (10.2.8.1)$$

defined in the complex E -plane. Similarly, we also define the dimensionless unperturbed energies

$$\alpha_i = \varepsilon_i/\hbar\omega \quad (10.2.8.2)$$

and coupling matrix elements

$$\beta_{ij}^{(p)} = -V_{ij}^{(p)}/\hbar\omega \quad (10.2.8.3)$$

where

$$(i, j) = 1, 2, \dots, J \quad \text{and} \quad p = \pm 1, \pm 2$$

Both α_i and $\beta_{ij}^{(p)}$ may be considered, in general, to be complex quantities. The structure of the infinite-order secular determinantal equation thus obtained is presented in display (10.2.8.4).

$$D(z) = \begin{vmatrix} & n' = -1 & n' = 0 & n' = 1 \\ \begin{matrix} & 1 & 0 & \frac{\beta_{11}^{(1)}}{z - \alpha_1 + 1} & \frac{\beta_{12}^{(1)}}{z - \alpha_1 + 1} & \frac{\beta_{11}^{(2)}}{z - \alpha_1 + 1} & \frac{\beta_{12}^{(2)}}{z - \alpha_1 + 1} \\ (n = -1) & 0 & 1 & \frac{\beta_{21}^{(1)}}{z - \alpha_2 + 1} & \frac{\beta_{22}^{(1)}}{z - \alpha_2 + 1} & \frac{\beta_{21}^{(2)}}{z - \alpha_2 + 1} & \frac{\beta_{22}^{(2)}}{z - \alpha_2 + 1} \\ & \frac{\beta_{11}^{(-1)}}{z - \alpha_1} & \frac{\beta_{12}^{(-1)}}{z - \alpha_1} & 1 & 0 & \frac{\beta_{11}^{(1)}}{z - \alpha_1} & \frac{\beta_{12}^{(1)}}{z - \alpha_1} \\ D(z) = (n = 0) & \frac{\beta_{21}^{(-1)}}{z - \alpha_2} & \frac{\beta_{22}^{(-1)}}{z - \alpha_2} & 0 & 1 & \frac{\beta_{21}^{(1)}}{z - \alpha_2} & \frac{\beta_{22}^{(1)}}{z - \alpha_2} \\ & \frac{\beta_{11}^{(-2)}}{z - \alpha_1 - 1} & \frac{\beta_{12}^{(-2)}}{z - \alpha_1 - 1} & \frac{\beta_{11}^{(-1)}}{z - \alpha_1 - 1} & \frac{\beta_{12}^{(-1)}}{z - \alpha_1 - 1} & 1 & 0 \\ (n = 1) & \frac{\beta_{21}^{(-2)}}{z - \alpha_2 - 1} & \frac{\beta_{22}^{(-2)}}{z - \alpha_2 - 1} & \frac{\beta_{21}^{(-1)}}{z - \alpha_2 - 1} & \frac{\beta_{22}^{(-1)}}{z - \alpha_2 - 1} & 0 & 1 \end{matrix} \end{vmatrix} = 0 \quad (10.2.8.4)$$

For the sake of brevity, we have explicitly indicated only two of the J basis states (in each block element).

The Floquet eigenvalue equation (10.2.8.4) is solved by generalizing the classical theory of Hill's determinant which we extend from the two-level^(217,218) system to an arbitrary J -level system.

10.2.9. Proof of the Existence of the Floquet Determinant and Its Analytic Properties

We may refer to the J -dimensional infinite-order determinant $D(z)$, of the form (10.2.8.4), as the Floquet determinant. The following properties of the Floquet determinant are of central importance for subsequent development of the theory.

1. The Floquet determinant $D(z)$ exists except at isolated pole singularities.

To establish this we first note the obvious pole singularities associated with each row of Eq. (10.2.8.4) at

$$z = \alpha_j + n \quad (10.2.9.1)$$

for $j = 1, 2, 3, \dots, J$ and $n = 0, \pm 1, \pm 2, \dots, \pm \infty$. Since multiplying a determinant by a factor is equivalent to multiplying each row by that factor, therefore $D(z)$ itself has only pole singularities at the infinitely many poles of the rows, given by expression (10.2.9.1). To prove the existence of the infinite determinant $D(z)$ at other values of z we make use of a theorem⁽²²⁰⁾ due to von Koch on infinite determinants, for the present case. If

$$D(z) \equiv \det[D_{ss'}] \quad (10.2.9.2)$$

with

$$(s, s') = -\infty \text{ to } +\infty$$

then by von Koch's theorem it is sufficient for $D(z)$ to exist that the diagonal elements satisfy

$$(a) \quad \prod_{s=-\infty}^{\infty} |D_{ss}| < \infty \quad (10.2.9.3)$$

and the off-diagonal elements satisfy

$$(b) \quad \sum_{s=-\infty}^{\infty} \sum_{s'(\neq s)=-\infty}^{\infty} |D_{ss'}|^2 < \infty \quad (10.2.9.4)$$

In our case, Eq. (10.2.8.4), $D_{ss} = 1$; hence clearly (a) is fulfilled. Furthermore, in the inner sum of (b), s' runs over only a finite number of nonvanishing terms of Eq. (10.2.8.4) while the outer sum (over s) falls off as $1/s^2$ when $|s| \rightarrow \infty$. Thus for Eq. (10.2.8.4) the left-hand side of (b) converges to a finite limit. Hence we conclude that the Floquet determinant $D(z)$ exists at all points z , other than the poles (10.2.9.1); $D(z)$ is a meromorphic function in the complex z -plane.

2. $D(z)$ is a periodic function of z with period unity.

This is clearly seen on shifting z by unity to $z + 1$ in Eq. (10.2.8.4) and observing that it does not change the value of $D(z)$; it merely shifts the position of the center block $(n, n') = (0, 0)$ of the infinite array.

3. Finally, $D(z)$ satisfies the limit

$$\lim_{\operatorname{Im} z \rightarrow \infty} D(z) = 1 \quad (10.2.9.5)$$

This follows from the fact that the off-diagonal elements of $D(z)$ tend to zero as $\operatorname{Im} z \rightarrow \infty$ and the diagonal elements are all unity.

10.2.10. The “Floquet Zones” and the Irreducible Set of Poles

It is useful to conceive of the complex z -plane as divided into infinitely many vertical “Floquet zones” of width unity. Because of the periodic property 2, the value of $D(z)$ at z in any zone is the same as the value $D(z')$ in another zone at a congruent point $z' = z \pmod{n}$. Thus although an (unperturbed) eigenvalue α , may lie in any of these zones, it may always be translated by a suitable integer n to find the corresponding pole [see Eq. (10.2.9.1)] in a given zone (say the first Floquet zone, which may be defined by $-\frac{1}{2} \leq \operatorname{Re} z \leq \frac{1}{2}$). Since there are J eigenvalues α_i , we may associate only J poles in the first zone, hence by congruence there are J poles in each Floquet zone. We shall call a set of J poles in a given zone an “irreducible set” of poles of $D(z)$.

10.2.11. Polynomial Reduction of the Infinite-Order Secular Equation

We are now in a position to reduce the infinite-order equation (10.2.8.4) for the determination of the characteristic exponents (eigenvalues) of the Floquet problem to an ordinary polynomial equation of order J .

We denote an irreducible set of poles of $D(z)$ (such as those in the first Floquet zone) by α'_j , $j = 1, 2, 3, \dots, J$, and introduce an auxiliary function

$$F^{(1)}(z - \alpha'_j) \equiv \pi \cot \pi(z - \alpha'_j) \quad (10.2.11.1)$$

From the elementary properties of $\cot z$ we easily find that $F^{(1)}(z - \alpha'_j)$ possesses the following properties:

1. $F^{(1)}(z - \alpha'_j)$ is a periodic function of z with period unity.
2. It is a meromorphic function of z with poles of order 1 at $z = \alpha'_j + n$.

$$3. \quad \lim_{z \rightarrow \alpha'_j} (z - \alpha'_j) F^{(1)}(z - \alpha'_j) = 1 \quad (10.2.11.2)$$

10.2.11.1. The Nondegenerate Secular Polynomial

This situation prevails for nonresonant multiphoton processes involving nondegenerate atomic states. In this case the irreducible set of J poles α'_j are all different. It can be seen directly from Eq. (10.2.8.4) that the poles

of the row elements are all of the simple kind. Function $D(z)$ may be factorized around a given pole α' , in the form

$$C_j^{(1)}/(z - \alpha') \quad (10.2.11.1.1)$$

where $C_j^{(1)}$ are for the moment assumed to be finite constants in the limit $z = \alpha'$ (the superscript on the constants C_j indicate the order of the corresponding poles α').

Let us consider the function

$$f(z) \equiv D(z) - \sum_{j=1}^J C_j^{(1)} F^{(1)}(z - \alpha') \quad (10.2.11.1.2)$$

In view of the properties of $D(z)$ and $F^{(1)}(z - \alpha')$, $f(z)$ has no pole at α' , and $f(z)$ is a periodic function of z with period unity. Therefore, $f(z)$ has no poles at any of the points $\alpha' + n$, $j = 1, 2, \dots, J$; $n = 0, \pm 1, \pm 2, \dots, \pm \infty$. Also, $f(z)$ is bounded as $\text{Im } z \rightarrow \pm \infty$ [cf. Eqs. (10.2.9.5) and (10.2.11.1)]. Thus all the requirements of Liouville's theorem⁽²²¹⁾ are fulfilled; hence $f(z)$ must be a constant. We take the limit $\text{Im } z \rightarrow \pm \infty$ in Eq. (10.2.11.1.2) and use relations (10.2.9.5) and (10.2.11.1) to find that $f(z) = 1 \mp i\pi \sum_{j=1}^J C_j^{(1)}$, hence $\sum_{j=1}^J C_j^{(1)} = 0$ and

$$f(z) = 1 \quad (10.2.11.1.3)$$

Thus from Eqs. (10.2.11.1.2), and (10.2.11.1.3), we conclude that

$$D(z) = 1 + \sum_{j=1}^J \pi C_j^{(1)} \cot \pi(z - \alpha') \quad (10.2.11.1.4)$$

The secular equation (10.2.8.4) therefore reduces to

$$1 + \sum_{j=1}^J \pi C_j^{(1)} \cot \pi(z - \alpha') = 0 \quad (10.2.11.1.5)$$

Equation (10.2.11.1.5) can be shown to agree with the secular equation for the nondegenerate problem originally obtained⁽²¹⁹⁾ in a somewhat different form by an alternative argument. To determine the constants $C_j^{(1)}$ we multiply Eq. (10.2.11.1.4) by $(z - \alpha')$, $j = 1, 2, 3, \dots, J$, one at a time, and take the limit $z = \alpha'$ to get

$$\lim_{z \rightarrow \alpha'} (z - \alpha') D(z) = C_j^{(1)}, \quad j = 1, 2, 3, \dots, J \quad (10.2.11.1.6)$$

In taking the limit for the right-hand side we have made use of the relation

$$\lim_{z \rightarrow 0} [\cot z - 1/z] = 0 \quad (10.2.11.1.7)$$

The left-hand side of relation (10.2.11.1.6) implies that the constant $C_j^{(1)}$ is nothing but the residue of $D(z)$ at $z = \alpha'_j$. It is in fact the determinant obtained from Eq. (10.2.8.4) at $z = \alpha'_j$, in which the denominator $(z - \alpha'_j)$ of the row elements of $D(z)$ corresponding to the pole $z = \alpha'_j$ are removed and the elements (of this row) containing no such denominator are put equal to zero. Thus, for example, $C_{j=2}^{(1)}$, associated with a pole $z = \alpha'_2 \equiv \alpha_2 - 1$, is given by determinant (10.2.11.1.8).

$$C_2^{(1)} = \begin{vmatrix} 1 & 0 & \frac{\beta_{11}^{(1)}}{\alpha_2 - \alpha_1} & \frac{\beta_{12}^{(1)}}{\alpha_2 - \alpha_1} & \frac{\beta_{11}^{(2)}}{\alpha_2 - \alpha_1} & \frac{\beta_{12}^{(2)}}{\alpha_2 - \alpha_1} \\ 0 & 0 & \beta_{21}^{(1)} & \beta_{22}^{(1)} & \beta_{21}^{(2)} & \beta_{22}^{(2)} \\ \frac{\beta_{11}^{(-1)}}{\alpha_2 - \alpha_1 - 1} & \frac{\beta_{12}^{(-1)}}{\alpha_2 - \alpha_1 - 1} & 1 & 0 & \frac{\beta_{11}^{(1)}}{\alpha_2 - \alpha_1 - 1} & \frac{\beta_{12}^{(1)}}{\alpha_2 - \alpha_1 - 1} \\ \frac{\beta_{21}^{(-1)}}{-1} & \frac{\beta_{22}^{(-1)}}{-1} & 0 & 1 & \frac{\beta_{21}^{(1)}}{-1} & \frac{\beta_{22}^{(1)}}{-1} \\ \frac{\beta_{11}^{(-2)}}{\alpha_2 - \alpha_1 - 2} & \frac{\beta_{12}^{(-2)}}{\alpha_2 - \alpha_1 - 2} & \frac{\beta_{11}^{(-1)}}{\alpha_2 - \alpha_1 - 2} & \frac{\beta_{12}^{(-1)}}{\alpha_2 - \alpha_1 - 2} & 1 & 0 \\ \frac{\beta_{21}^{(-2)}}{-2} & \frac{\beta_{22}^{(-2)}}{-2} & \frac{\beta_{21}^{(-1)}}{-2} & \frac{\beta_{22}^{(-1)}}{-2} & 0 & 1 \end{vmatrix} \quad (10.2.11.1.8)$$

The determinant $C_2^{(1)}$ given by Eq. (10.2.11.1.8), and similarly all $C_j^{(1)}$, $j = 1, 2, \dots, J$, are finite since by von Koch's theorem they are convergent determinants. Therefore they can be evaluated by the usual numerical means. The (quintidiagonal) banded structure of $C_j^{(1)}$ suggests that the triangular reduction should be very efficient for their evaluation. The computation time spent would be, for a large number of rows, essentially proportional to the number of rows retained (as opposed to its cube, which would be required for the computation of a general determinant of the same size). We note that in the dipole approximation all the quintidiagonal determinants appearing above reduce to mere tridiagonal determinants.

Equation (10.2.11.1.5) is a finite transcendental equation in z , possessing J principal roots corresponding to the J nondegenerate (unperturbed) eigenvalues α'_j . We observe parenthetically that as the coupling terms tend to zero the off-diagonal elements of $C_j^{(1)}$ [cf. Eq. (10.2.11.1.8)] tend toward zero and as there is (at least) one diagonal element which is

zero, the determinants $C_j^{(1)} \rightarrow 0$. Hence the solutions of Eq. (10.2.11.1.5) reduce, as expected, to $z = \alpha'_j$ for all $j = 1, 2, 3, \dots, J$, for vanishingly small field strengths.

It is possible to reduce Eq. (10.2.11.1.5) to a polynomial in terms of the complex variables

$$x \equiv e^{i2\pi z} \quad (10.2.11.1.9)$$

and

$$\kappa'_j \equiv e^{i2\pi\alpha'_j} \quad (10.2.11.1.10)$$

In terms of these variables

$$\cot \pi(z - \alpha'_j) = i \frac{x + \kappa'_j}{x - \kappa'_j} \quad (10.2.11.1.11)$$

Substitution of relation (10.2.11.1.11) in Eq. (10.2.11.1.4) yields the rational form

$$D(x) = 1 + i\pi \sum_{j=1}^J \left(\frac{x + \kappa'_j}{x - \kappa'_j} \right) C_j^{(1)} \quad (10.2.11.1.12)$$

Hence the secular equation (10.2.11.1.5) becomes

$$1 + i\pi \sum_{j=1}^J \left(\frac{x + \kappa'_j}{x - \kappa'_j} \right) C_j^{(1)} = 0 \quad (10.2.11.1.13)$$

Multiplication by the common factor

$$P_J(x) \equiv \prod_{j=1}^J (x - \kappa'_j) \quad (10.2.11.1.14)$$

shows immediately that the secular equation is in fact a polynomial in x of degree J :

$$P_J(x) + i\pi \sum_{j=1}^J (x + \kappa'_j) P_{j-1}^{(0)}(x) C_j^{(1)} = 0 \quad (10.2.11.1.15)$$

where $P_{j-1}^{(0)}(x)$ is a polynomial of degree $J - 1$ similar to Eq. (10.2.11.1.14) but with the j th factor $(x - \kappa'_j)$ omitted, namely

$$P_{j-1}^{(0)}(x) \equiv \prod_{s(s \neq j)=1}^J (x - \kappa'_s) \quad (10.2.11.1.16)$$

The solutions x_λ ($\lambda = 1, 2, \dots, J$) of Eq. (10.2.11.1.13) or (10.2.11.1.15)

provide the desired eigenvalues E'_λ [see Eqs. (10.2.11.1.9) and (10.2.8.11)], which correspond to and evolve from the unperturbed eigenvalues α'_λ . The other infinite number of congruent roots E''_λ are constructed trivially from

$$E''_\lambda = E'_\lambda + n\hbar\omega \quad (10.2.11.1.17)$$

this is a consequence of the periodicity of the Floquet matrix (in the energy domain).

10.2.12. The Solution Vectors

The eigenvector corresponding to a given eigenvalue E_λ may now be found from the system of homogeneous linear equations (10.2.2.14). To this end we first delete the equation corresponding to row $(j, n) = (i, 0)$ [i.e., we delete the entire $(i, 0)$ th row], then transfer the $(i, 0)$ th column on the right-hand side, and set $z = E_\lambda$ (in units of $\hbar\omega$) everywhere. Thus, for example, by choosing $(j, n) = (1, 0)$ one obtains [cf. Eq. (10.2.8.4)]

$$\begin{array}{c}
 \begin{matrix} (jn) & (1, -1) & (2, -1) & (2, 0) & (1, 1) & (2, 1) & a_{jn}(E) \\ (jn) & & & & & & \vdots \end{matrix} \\
 \begin{matrix} (1, -1) & \left[\begin{array}{ccccc} \ddots & & & & \\ & 1 & & & \\ & & 0 & & \\ & & & \frac{\beta_{12}^{(1)}}{E_\lambda - \alpha_1 + 1} & \\ & & & & \frac{\beta_{11}^{(2)}}{E_\lambda - \alpha_1 + 1} \\ & & & & \frac{\beta_{12}^{(2)}}{E_\lambda - \alpha_1 + 1} \end{array} \right] & \left[\begin{array}{c} a_{1,-1}(E_\lambda) \\ \vdots \\ a_{2,-1}(E_\lambda) \\ a_{2,0}(E_\lambda) \\ a_{1,1}(E_\lambda) \\ a_{2,1}(E_\lambda) \\ \vdots \end{array} \right] \\ (2, -1) & \left[\begin{array}{ccccc} 0 & & 1 & & \\ & & & \frac{\beta_{21}^{(1)}}{E_\lambda - \alpha_2 + 1} & \\ & & & & \frac{\beta_{21}^{(2)}}{E_\lambda - \alpha_2 + 1} \\ & & & & \frac{\beta_{22}^{(2)}}{E_\lambda - \alpha_2 + 1} \end{array} \right] & \left[\begin{array}{c} a_{1,-1}(E_\lambda) \\ \vdots \\ a_{2,-1}(E_\lambda) \\ a_{2,0}(E_\lambda) \\ a_{1,1}(E_\lambda) \\ a_{2,1}(E_\lambda) \\ \vdots \end{array} \right] \\ (2, 0) & \left[\begin{array}{ccccc} \frac{\beta_{21}^{(-1)}}{E_\lambda - \alpha_2} & & \frac{\beta_{22}^{(-1)}}{E_\lambda - \alpha_2} & & \\ & & 1 & & \\ & & & \frac{\beta_{21}^{(1)}}{E_\lambda - \alpha_2} & \\ & & & & \frac{\beta_{22}^{(1)}}{E_\lambda - \alpha_2} \end{array} \right] & \left[\begin{array}{c} a_{1,-1}(E_\lambda) \\ \vdots \\ a_{2,-1}(E_\lambda) \\ a_{2,0}(E_\lambda) \\ a_{1,1}(E_\lambda) \\ a_{2,1}(E_\lambda) \\ \vdots \end{array} \right] \\ (1, 1) & \left[\begin{array}{ccccc} \frac{\beta_{11}^{(-2)}}{E_\lambda - \alpha_1 + 1} & & \frac{\beta_{12}^{(-2)}}{E_\lambda - \alpha_1 + 1} & & \\ & & \frac{\beta_{11}^{(-1)}}{E_\lambda - \alpha_1 + 1} & & \\ & & & 1 & \\ & & & & 0 \end{array} \right] & \left[\begin{array}{c} a_{1,-1}(E_\lambda) \\ \vdots \\ a_{2,-1}(E_\lambda) \\ a_{2,0}(E_\lambda) \\ a_{1,1}(E_\lambda) \\ a_{2,1}(E_\lambda) \\ \vdots \end{array} \right] \\ (2, 1) & \left[\begin{array}{ccccc} \frac{\beta_{21}^{(-2)}}{E_\lambda - \alpha_2 - 1} & & \frac{\beta_{22}^{(-2)}}{E_\lambda - \alpha_2 + 1} & & \\ & & \frac{\beta_{21}^{(-1)}}{E_\lambda - \alpha_2 - 1} & & \\ & & & 0 & \\ & & & & 1 \\ & & & & \ddots \end{array} \right] & \left[\begin{array}{c} a_{1,-1}(E_\lambda) \\ \vdots \\ a_{2,-1}(E_\lambda) \\ a_{2,0}(E_\lambda) \\ a_{1,1}(E_\lambda) \\ a_{2,1}(E_\lambda) \\ \vdots \end{array} \right] \end{matrix} \\
 = \left[\begin{array}{c} \vdots \\ \frac{\beta_{11}^{(1)}}{E_\lambda - \alpha_1 + 1} a_{1,0}(E_\lambda) \\ \frac{\beta_{21}^{(1)}}{E_\lambda - \alpha_2 + 1} a_{1,0}(E_\lambda) \\ 0 \\ \frac{\beta_{11}^{(-1)}}{E_\lambda - \alpha_1 - 1} a_{1,0}(E_\lambda) \\ \frac{\beta_{21}^{(-1)}}{E_\lambda - \alpha_2 - 1} a_{1,0}(E_\lambda) \\ \vdots \end{array} \right] & (10.2.12.1)
 \end{array}$$

The solution for $a_{j,n}(E_\lambda)$ is easily found from Eq. (10.2.12.1) by Cramer's rule. Hence

$$\frac{a_{jn}(E_\lambda)}{a_{i,0}(E_\lambda)} = \frac{\Delta_{j,n \leftrightarrow i,0}(E_\lambda)}{\Delta(E_\lambda)}, \quad (jn) \neq i, 0 \quad (10.2.12.2)$$

where $\Delta(E_\lambda)$ is the (reduced) determinant $D(z)$ with its $(i,0)$ th row and $(i,0)$ th column deleted and the rest evaluated at $z = E_\lambda$ (in units of $\hbar\omega$) [e.g., the determinant of the coefficient matrix on the left-hand side of Eq. (10.2.12.1)]. Quantity $\Delta_{j,n \leftrightarrow i,0}(E_\lambda)$ is obtained from $\Delta(E_\lambda)$ in which the (j,n) th column is replaced by the $(i,0)$ th column [i.e., the coefficient column on the right-hand side of Eq. (10.2.12.1)]. The normalization condition

$$\sum_{jn} |a_{jn}(E_\lambda)|^2 = 1 \quad (10.2.12.3)$$

immediately yields

$$a_{i,0}(E_\lambda) = \left[\sum_{(j,n) \neq (i,0)} \left| \frac{\Delta_{j,n \leftrightarrow i,0}(E_\lambda)}{\Delta(E_\lambda)} \right|^2 + 1 \right]^{-1/2} \quad (10.2.12.4)$$

Equations (10.2.12.2) and (10.2.12.4) together provide all the eigenvector components $a_{j,n}(E_\lambda)$ in terms of the convergent determinants only. Clearly, any eigenvector of the system can be obtained in an exactly analogous way. The method of constructing the algebraic solutions of the infinite system of Floquet equations (defined on an arbitrary but finite Hilbert space) is thereby completed.

10.2.12.1. Alternative Forms of Polynomial Coefficients in the Vicinity of Resonances

In the nonresonant case all quantities $C_i^{(1)}$ can be calculated directly from Eq. (10.2.11.1.6). However, it may be practically more convenient, when the difference between two irreducible poles is small (as in the case of a near but not exact resonance), to calculate $C_1^{(1)}$ and $C_2^{(1)}$ in a slightly different manner. If $\alpha'_1 = \alpha'_2$ are the two near-resonant irreducible poles of $D(z)$, we may define

$$C_1^{(1)} \equiv \frac{1}{\alpha'_1 - \alpha'_2} C_1^{(1)} \quad (10.2.12.2.1)$$

and

$$C_2^{(1)} \equiv \frac{1}{\alpha'_1 - \alpha'_2} C_2^{(1)} \quad (10.2.12.2.2)$$

Clearly $C_{(1)}^{(1)}$ is obtained from the determinant $C_1^{(1)}$ by multiplying the α'_2 th row of the latter determinant by $(\alpha'_1 - \alpha'_2)$ [thereby removing the small differences $(\alpha'_1 - \alpha'_2)$ from its denominators]. Similarly $C_{(2)}^{(1)}$ is obtained from $C_2^{(1)}$ by multiplying the α'_1 th row of the latter by $(\alpha'_2 - \alpha'_1)$. The determinants $C_{(1)}^{(1)}$ and $C_{(2)}^{(1)}$ are evaluated as before. Since the modified determinants $C_{(1)}^{(1)}$ and $C_{(2)}^{(1)}$ contain only “large detunings” everywhere, they are expected to be insensitive to small changes in ω in the vicinity of the resonance frequency ω_r . To calculate the transition spectrum one generally needs to evaluate the transition amplitudes over a range of frequencies around ω_r . In view of the above insensitivity, $C_{(1)}^{(1)}$ and $C_{(2)}^{(1)}$ may be evaluated only once near ω_r (or, at most, at a few values of ω around ω_r and extended by simple extrapolation), and used over the spectral range $\Delta\omega \ll \omega$ near the resonance $\omega = \omega_r$.

In the neighborhood of a resonance, similar constructions apply for the determinants $\Delta(E_\lambda)$ and $\Delta_{j,n\leftrightarrow i,0}(E_\lambda)$. These considerations may also be easily generalized in the vicinity of several near-resonances. Thus, for example, in the presence of three nearly equal irreducible poles α'_1 , α'_2 , and α'_3 one may rewrite the constants $C_j^{(1)}$ ($j = 1, 2, 3$) in terms of the modified constants $C_{(j)}^{(1)}$ given by

$$C_1^{(1)} \equiv \frac{1}{(\alpha'_1 - \alpha'_2)(\alpha'_1 - \alpha'_3)} C_{(1)}^{(1)} \quad (10.2.12.2.3)$$

$$C_2^{(1)} \equiv \frac{1}{(\alpha'_2 - \alpha'_1)(\alpha'_2 - \alpha'_3)} C_{(2)}^{(1)} \quad (10.2.12.2.4)$$

and

$$C_3^{(1)} \equiv \frac{1}{(\alpha'_3 - \alpha'_1)(\alpha'_3 - \alpha'_2)} C_{(3)}^{(1)} \quad (10.2.12.2.5)$$

Again for $\Delta\omega/\omega_r \ll 1$, $C_{(j)}^{(1)}$ may be evaluated near the resonance frequency ω_r and treated as effective constants in the frequency range $\Delta\omega$ around ω_r .

10.3. The Time-Domain Floquet Method

10.3.1. Introduction

For multiphoton processes in a monomode field, a time-domain approach to the Floquet theory is also practicable. The Floquet theorem permits one to avoid direct numerical integration of the time-dependent Schrödinger equation (10.2.1.1) for any time t in favor, essentially, of numerical integration over the first period of the monomode Hamiltonian.

The solution, valid for any time t , may then be constructed from a knowledge of the solution in the first period alone.

It is convenient to work with the Schrödinger equation for the time-evolution operator $U(t, t_0)$,

$$i\hbar \frac{\partial}{\partial t} U(t, t_0) = H(t)U(t, t_0) \quad (10.3.1.1)$$

which satisfies the initial condition

$$U(t_0, t_0) = 1 \quad (10.3.1.2)$$

The evolution operator $U(t, t_0)$ reduces to a $J \times J$ matrix on a J -dimensional atomic Hilbert space. We recall that for a Hermitian Hamiltonian, $U(t, t_0)$ obeys the unitarity relation

$$U^+(t, t_0) = U^{-1}(t, t_0) = U(t_0, t) \quad (10.3.1.3)$$

where U^+ is the Hermitian adjoint of U . It also fulfills the time-transition relation

$$U(t, t_1)U(t_1, t_0) = U(t, t_0) \quad (10.3.1.4)$$

We may write the set of “stationary” or Floquet solutions of Eq. (10.3.1.1) as a $J \times J$ (solution) matrix of the form

$$S(t)\exp(-iE_D t/\hbar) \equiv U(t, t_0)S(t_0)\exp(-iE_D t_0/\hbar) \quad (10.3.1.5)$$

where $S(t_0)$ is a $J \times J$ constant unitary matrix and $S(t)$ is periodic in t with the period $\tau = 2\pi/\omega$ of the Hamiltonian. For example, at $t = \tau = 2\pi/\omega$ we have

$$S(\tau) = S(0) \quad (10.3.1.6)$$

We recall that the unitarity of $S(0)$ allows one to write

$$S^{-1}(0) = S^+(0) \quad (10.3.1.7)$$

where $S^+(0)$ is the Hermitian adjoint of $S(0)$. In relation (10.3.1.5) E_D is a diagonal matrix whose elements are the characteristic energies

$$E_\lambda \delta_{\lambda\lambda'}; \quad (\lambda, \lambda') = 1, 2, \dots, J \quad (10.3.1.8)$$

of the Floquet solutions. The right-hand side of Eq. (10.3.1.5) shows how a set of solutions is generated by the evolution operator acting on the initial set at any time t_0 . Let us choose $t_0 = 0$ in the relation (10.3.1.5) and evaluate it at $t = \tau = 2\pi/\omega$,

$$S(\tau)\exp(-iE_D\tau/\hbar) = U(\tau, 0)S(0) \quad (10.3.1.9)$$

By making use of relations (10.3.1.6) and (10.3.1.7) in Eq. (10.3.1.9) we are able to obtain the useful result⁽²²²⁾

$$\exp(-iE_D\tau/\hbar) = S^+(0)U(\tau, 0)S(0) \quad (10.3.1.10)$$

Hence as soon as $U(\tau, 0)$ is known, the $J \times J$ matrix equation (10.3.1.10) can be solved for the eigenvalues E_λ and the elements of $S(0)$. Function $U(\tau, 0)$ may be found by direct numerical integration up to $t = \tau$ of the evolution equation (10.3.1.1) with initial condition (10.3.1.2). When E_λ and $S(0)$ are known and the values of $U(t, 0)$ are available in the range $t = 0$ to τ [e.g., they may be stored at the increment points during integration of Eq. (10.3.1.1), needed to find $U(\tau, 0)$], then the unitary periodic matrix $S(t)$ may be constructed in the same interval $t = 0$ to τ , using Eq. (10.3.1.5) in the form

$$S(t) = U(t, 0)S(0)\exp(iE_Dt/\hbar), \quad \tau \leq t \leq 0 \quad (10.3.1.11)$$

The values of $S(t)$ thus found in $\tau \leq t \leq 0$ may now be Fourier analyzed to find the coefficients of the Fourier expansion of $S(t)$ in the first period and hence, by the periodicity, for any time t . Finally, the transition operator $U(t, 0)$ is obtained at any time t [in terms of the Fourier construction of $S(t)$] using the inverted form of Eq. (10.3.1.11), namely

$$U(t, 0) = S(t)\exp(-iE_Dt/\hbar)S(0) \quad (10.3.1.12)$$

The transition amplitudes are given by the elements of Eq. (10.3.1.12). One thus finds that the solution of the monomode Floquet problem at any t reduces essentially to the problem of integrating Eq. (10.3.1.1) only in the first period, $0 \leq t \leq \tau = 2\pi/\omega$.

10.3.2. Reduction of the Integration Interval

The numerical effort to integrate $U(\tau, 0)$ up to $t = \tau$ may be further reduced^(222,223) by employing the symmetry of the sinusoidal monomode Hamiltonian assumed in Eq. (10.3.1.1).

In the range $0 \leq t \leq \tau$, $H(t)$ is symmetric about $t = \tau/2$, i.e.,

$$H(\tau/2 - t) = H(\tau/2 + t) \quad (10.3.2.1)$$

One consequence of this is that

$$U(\tau/2 + t, \tau/2) = U^*(\tau/2 - t, \tau/2) \quad (10.3.2.2)$$

which may be seen by considering the integral form of Eq. (10.3.1.1):

$$U(t, t_0) = 1 - \frac{i}{\hbar} \int_{t_0}^t H(t') U(t', t_0) dt' \quad (10.3.2.3)$$

If we set $t_0 = \tau/2$, replace t by $t + \tau/2$, and change the variable of integration from t' to $t'' + \tau/2$, we obtain

$$U(\tau/2 + t, \tau/2) = 1 - \frac{i}{\hbar} \int_0^t H(\tau/2 + t'') U(\tau/2 + t'', \tau/2) dt'' \quad (10.3.2.4)$$

By changing t'' to t' , using relation (10.3.2.1), changing t to $-t$, and taking the complex conjugate of Eq. (10.3.2.4), we find that

$$U^*(\tau/2 - t, \tau/2) = 1 - \frac{i}{\hbar} \int_0^t H(\tau/2 + t') U^*(\tau/2 - t', \tau/2) dt' \quad (10.3.2.5)$$

Thus U and U^* in Eqs. (10.3.2.4) and (10.3.2.5) obey the same equations. Clearly they can be chosen to satisfy the same initial condition, $U(t_0, t_0) = U^*(t_0, t_0) = 1$ say at $t_0 = 0$. Hence they must be equal, and this proves Eq. (10.3.2.2). Next, one uses the time-transition relation to write

$$U(\tau/2 + t, \tau/2) U(\tau/2, 0) = U(\tau/2 + t, 0) \quad (10.3.2.6)$$

One may also rewrite Eq. (10.3.2.3) as

$$\begin{aligned} U(\tau/2 + t, \tau/2) &= U^*(\tau/2 - t, \tau/2) \\ &= U^*(\tau/2 - t, 0) U^*(0, \tau/2) \\ &= U^*(\tau/2 - t, 0) U^\dagger(\tau/2, 0) \end{aligned} \quad (10.3.2.7)$$

where the second line follows from the transitivity property, Eq. (10.3.1.4), and the third line from the unitarity property, Eq. (10.3.1.3).

Substitution of Eq. (10.3.2.7) in relation (10.3.2.6) finally gives

$$U(\tau/2 + t, 0) = U^*(\tau/2 - t, 0) U^\dagger(\tau/2, 0) U(\tau/2, 0) \quad (10.3.2.8)$$

Equation (10.3.2.8) expresses the values of U in the second half of the first period in terms of the values calculated in the first half of the first period. The effective numerical-integration effort is thereby reduced to nearly half of the original amount.

10.3.3. The Magnus Expansion of $U(t, 0)$

It is often desirable and reliable (up to moderately high intensities, say) to evaluate $U(t, 0)$ conveniently by systematic approximation means and thus to avoid direct numerical integration of Eq. (10.3.1.1). One way of doing this is to apply the Magnus approximation^(224,225) of the evolution operator $U(t, t_0)$. In this approximation $U(t, t_0)$ is expressed first in the (operator) exponential form

$$U(t, t_0) = \exp[A(t, t_0)] \quad (10.3.3.1)$$

in spite of the fact that $H(t)$ can be explicitly time-dependent.

In the next step Eq. (10.3.1.1) for $U(t, t_0)$ is replaced by an equivalent equation for $A(t, t_0)$, to be derived below, which is then solved by iterative integration. The result is an explicit matrix exponential approximation of $U(t, t_0)$ in the form (10.3.3.1), where $A(t, t_0)$ is obtained as the series

$$A(t, t_0) = \sum_{n=1}^{\infty} A_n(t, t_0) \quad (10.3.3.2)$$

In practice, this series is truncated at some convenient order $n = N$. To derive the Magnus form of $U(t, t_0)$, it is convenient to introduce⁽²²⁵⁾ the auxiliary operators

$$U(t, t_0 | \lambda) \equiv \exp[\lambda A(t, t_0)] \quad (10.3.3.3)$$

and

$$L(t, t_0 | \lambda) \equiv \frac{\partial U(t, t_0 | \lambda)}{\partial t} U^{-1}(t, t_0 | \lambda) \quad (10.3.3.4)$$

where λ is a real parameter (to be set equal to unity at the end). If derivatives of Eq. (10.3.3.3) are taken first with respect to t and with respect to λ and then in the reverse order, we get with the aid of Eq. (10.3.3.4)

$$\frac{\partial^2}{\partial \lambda \partial t} U = \frac{\partial L}{\partial \lambda} U + LAU \quad (10.3.3.5)$$

and

$$\frac{\partial^2}{\partial t \partial \lambda} U = \frac{\partial A}{\partial t} U + A U \quad (10.3.3.6)$$

By equating the right-hand sides we have

$$\frac{\partial L}{\partial \lambda} = \frac{\partial A}{\partial t} + [A, L] \quad (10.3.3.7)$$

where

$$[A, L] = AL - LA$$

is the commutator. The commutator may be written symbolically in terms of a linear operator C_A as

$$C_A L \equiv [A, L] \quad (10.3.3.8)$$

Substitution of relation (10.3.3.8) in Eq. (10.3.3.7) yields a linear equation for L . This equation can be readily integrated with respect to λ and gives

$$L(t, t_0 | \lambda) = \frac{\exp(\lambda C_A) - 1}{C_A} \frac{\partial A}{\partial t} \quad (10.3.3.9)$$

The truth of Eq. (10.3.3.9) may be immediately verified on substitution into Eq. (10.3.3.7) and remembering relation (10.3.3.8). The evolution equation (10.3.1.1) can be rewritten with the aid of definition (10.3.3.4) in the form

$$i\hbar L(t, t_0 | 1) \equiv i\hbar \frac{\partial U(t, t_0)}{\partial t} U^{-1}(t, t_0) = H(t) \quad (10.3.3.10)$$

Substitution of expression (10.3.3.9) into Eq. (10.3.3.10) therefore gives

$$\begin{aligned} i\hbar \frac{\partial A}{\partial t} &= \frac{C_A}{[\exp(C_A) - 1]} H(t) \\ &= \left(1 + \frac{C_A}{2!} + \frac{C_A^2}{3!} + \dots\right)^{-1} H(t) \\ &= H(t) - \frac{1}{2}[A, H(t)] + \frac{1}{12}[A, [A, H(t)]] - \dots \end{aligned} \quad (10.3.3.11)$$

The third line of this relation follows on expansion of the inverse series in powers of C_A and subsequent use of definition (10.3.3.8).

Equation (10.3.3.11) is now solved by systematic iteration to yield, for

example,

$$A_1(t, t_0) = -\left(\frac{i}{\hbar}\right) \int_{t_0}^t dt_1 H(t_1) \quad (10.3.3.12)$$

$$A_2(t, t_0) = -\left(\frac{i}{\hbar}\right)^2 \frac{1}{2} \int_{t_0}^t dt_2 \int_{t_0}^{t_2} dt_1 [H(t_1), H(t_2)] \quad (10.3.3.13)$$

The evolution operator in the N th-order Magnus approximation thus assumes the explicit form

$$U(t, t_0) = \exp \left[\sum_{n=1}^N A_n(t, t_0) \right] \quad (10.3.3.14)$$

Due to the various equivalent permutations possible in carrying out the multiple time integrations, the explicit choice may differ. Table 20 collects the first five orders of A_n as obtained elsewhere.⁽²²²⁾ In Table 20 the notation

$$\{ t^{t_{a_{n-1}}} \cdots t_{a_2} t_{a_1} [\quad] \}$$

denotes the integral

$$\int_{t_0}^t dt \int_{t_0}^{t_{a_{n-1}}} dt_{n-1} \cdots \int_{t_0}^{t_{a_2}} dt_2 \int_{t_0}^{t_{a_1}} dt_1 [\quad] \quad (10.3.3.15)$$

Table 20. First Five Orders of the Time-Dependent Matrices A Appearing in the Magnus Approximation $\exp(A) \approx \exp(A_1 + A_2 + A_3 + A_4 + A_5)$ for the Evolution Operator $U(t, t_0)$ (from Milfeld and Wyatt⁽²²²⁾)^a

$$A_1 \hbar = (-i) \{ H_i \}$$

$$A_2 \hbar^2 = (\frac{1}{2}) \{^6 H_1, H_2 \}$$

$$A_3 \hbar^3 = (i/4) \{^6 H_2 [[H_1, H_2] H_3] + (\frac{1}{3}) \{^6 H_3 [[H_1 [H_2, H_3]]]\}$$

$$A_4 \hbar^4 = -(\frac{1}{8}) \{^6 H_3 [[H_1, H_2] H_3] H_4] + (\frac{1}{3}) \{^6 H_4 [[H_1 [H_2, H_3]]] H_4] \\ + (\frac{1}{3}) \{^6 H_4 [[H_1 [[H_2, H_3] H_4]]] + (\frac{1}{2}) \{^6 H_4 [[H_1, H_2] [H_3, H_4]]\}$$

$$A_5 \hbar^5 = -(i/6) \{^6 H_4 [[[[H_1, H_2] H_3] H_4] H_5] + (\frac{1}{3}) \{^6 H_5 [[[[H_1 [H_2, H_3]]] H_4] H_5] \\ + (\frac{1}{2}) \{^6 H_5 [[H_1 [[H_2, H_3] H_4]]] H_5] + (\frac{1}{2}) \{^6 H_5 [[[[H_1, H_2] [H_3, H_4]]] H_5] \\ + (\frac{1}{3}) \{^6 H_5 [[H_1 [[[H_2, H_3] H_4] H_5]]] + (\frac{1}{3}) \{^6 H_5 [[H_1 [[H_2 [H_3, H_4]]] H_5]] \\ + (\frac{1}{3}) \{^6 H_5 [[H_1, H_2] [[H_3, H_4] H_5]] + (\frac{1}{3}) \{^6 H_5 [[[[H_1, H_2] H_3] [H_4, H_5]] \\ + (\frac{1}{6}) \{^6 H_5 [[[[H_1 [H_2, H_3]]] [H_4, H_5]] - (\frac{1}{25}) \{^6 H_5 [[H_1 [H_2 [H_3 [H_4, H_5]]]]\}$$

^a For notation see Eqs. (10.3.3.15) and (10.3.3.16).

Table 21. First Three Orders of the Magnus Time-Dependent Exponential Matrix Elements of A_1 , A_2 , A_3 , Evaluated for the Interaction-Picture Hamiltonian $[\exp(iH_0t/\hbar)V\exp(iH_0t/\hbar)\cos(\omega t)]$ with $U(t,0) = \exp(A) \simeq \exp(A_1 + A_2 + A_3)$ and $\hbar = 1$, and Matrix Element $\{A_3\}_{jn}$ of A_3 Is the Sum of Terms A_3^a and A_3^b (from Milfeld and Wyatt⁽²²²⁾)

$$\begin{aligned} \{A_1\}_j &= -V_j \left[\frac{e^{i(\alpha+1)T}-1}{\alpha+1} + \frac{e^{i(\alpha-1)T}-1}{\alpha-1} \right] / 2\omega \\ \{A_2\}_{jk} &= - \sum_i S_{ijk} \left| \left[\frac{1}{\alpha+1} - \frac{1}{\beta+1} \right] \left[\frac{e^{i(\alpha+\beta+2)T}-1}{\alpha+\beta+2} + (e^{i(\alpha+\beta)T}-1)D \right] \right. \\ &\quad + \left[\frac{1}{\alpha-1} - \frac{1}{\beta-1} \right] \left[\frac{e^{i(\alpha+\beta-2)T}-1}{\alpha+\beta-2} + (e^{i(\alpha+\beta)T}-1)D \right] \\ &\quad - \left[\frac{1}{(\alpha+1)(\beta+1)} \right] (-e^{i(\alpha+1)T} + e^{i(\beta+1)T}) \\ &\quad - \left[\frac{1}{(\alpha+1)(\beta-1)} \right] (-e^{i(\alpha+1)T} + e^{i(\beta-1)T}) \\ &\quad - \left[\frac{1}{(\alpha-1)(\beta+1)} \right] (-e^{i(\alpha-1)T} + e^{i(\beta+1)T}) \\ &\quad - \left[\frac{1}{(\alpha-1)(\beta-1)} \right] (-e^{i(\alpha-1)T} + e^{i(\beta-1)T}) \\ &\quad \left. - \left[\frac{1}{\alpha+1} + \frac{1}{\alpha-1} - \frac{1}{\beta+1} - \frac{1}{\beta-1} \right] \{iTZ\} \right| / 8\omega^2 \end{aligned}$$

For $i = k$, $D = 0$ and $Z = 1$ otherwise $D = 1/(\alpha + \beta)$ and $Z = 0$.

$$\begin{aligned} \{A_3\}_{jn} &= - \sum_k \sum_{r=1}^6 P_r(\alpha\beta\gamma) M_r S_{jkn} \left[\frac{1}{(\alpha+1)(\alpha+\beta+2)} \left[\frac{e^{i(\alpha+\beta+\gamma+3)T}-1}{\alpha+\beta+\gamma+3} + \frac{e^{i(\alpha+\beta+\gamma+1)T}-1}{\alpha+\beta+\gamma+1} \right] \right. \\ &\quad + \frac{1}{(\alpha-1)(\alpha+\beta-2)} \left[\frac{e^{i(\alpha+\beta+\gamma-3)T}-1}{\alpha+\beta+\gamma-3} + \frac{e^{i(\alpha+\beta+\gamma-1)T}-1}{\alpha+\beta+\gamma-1} \right] \\ &\quad + \frac{2\alpha B}{\alpha^2-1} \left[\frac{e^{i(\alpha+\beta+\gamma+1)T}-1}{\alpha+\beta+\gamma+1} + \frac{e^{i(\alpha+\beta+\gamma-1)T}-1}{\alpha+\beta+\gamma-1} \right] \\ &\quad - \frac{2\alpha}{(\alpha^2-1)(\beta+1)} \left[\frac{e^{i(\beta+\gamma+2)T}-1}{\beta+\gamma+2} + \frac{e^{i(\beta+\gamma)T}-1}{1/C} \right] \\ &\quad - \frac{2\alpha}{(\alpha^2-1)(\beta-1)} \left[\frac{e^{i(\beta+\gamma-2)T}-1}{\beta+\gamma-2} + \frac{e^{i(\beta+\gamma)T}-1}{1/C} \right] \\ &\quad - \left[\frac{1}{(\alpha+1)(\alpha+\beta+2)} + \frac{1}{(\alpha-1)(\alpha+\beta-2)} + \frac{2\alpha C}{\alpha^2-1} \right. \\ &\quad \left. - \frac{2\alpha}{(\alpha^2-1)(\beta+1)} - \frac{2\alpha}{(\alpha^2-1)(\beta-1)} \right] \\ &\quad \times \left[\frac{e^{i(\gamma+1)T}-1}{\gamma+1} + \frac{e^{i(\gamma-1)T}-1}{\gamma-1} \right] \Big/ 32\omega^3 \end{aligned}$$

For $i = k$, $B = 0$ otherwise $B = \frac{1}{\alpha + \beta}$.

For $j = n$, $C = 0$ otherwise $C = \frac{1}{\beta + \gamma}$.

Table 21 (continued)

$$\begin{aligned} \{A_3\}_{in} = & - \sum_{jk} \sum_{r=1}^6 P_r(\alpha\beta\gamma) N_r S_{ijkn} \\ & \times \left[\frac{1}{(\alpha+1)(\beta+1)} \left[\frac{e^{i(\alpha+\beta+\gamma+3)T}-1}{\alpha+\beta+\gamma+3} + \frac{e^{i(\alpha+\beta+\gamma+1)T}-1}{\alpha+\beta+\gamma+1} - \frac{e^{i(\alpha+\gamma+2)T}-1}{\alpha+\gamma+2} \right. \right. \\ & \quad \left. \left. - \frac{e^{i(\beta+\gamma+2)T}-1}{\beta+\gamma+2} - F - G + H \right] \right. \\ & + \frac{1}{(\alpha+1)(\beta-1)} \left[\frac{e^{i(\alpha+\beta+\gamma+1)T}-1}{\alpha+\beta+\gamma+1} + \frac{e^{i(\alpha+\beta+\gamma-1)T}-1}{\alpha+\beta+\gamma-1} - \frac{e^{i(\alpha+\gamma+2)T}-1}{\alpha+\gamma+2} \right. \\ & \quad \left. \left. - \frac{e^{i(\beta+\gamma-2)T}-1}{\beta+\gamma-2} - F - G + H \right] \right. \\ & + \frac{1}{(\alpha-1)(\beta+1)} \left[\frac{e^{i(\alpha+\beta+\gamma+1)T}-1}{\alpha+\beta+\gamma+1} + \frac{e^{i(\alpha+\beta+\gamma-1)T}-1}{\alpha+\beta+\gamma-1} - \frac{e^{i(\beta+\gamma+2)T}-1}{\beta+\gamma+2} \right. \\ & \quad \left. \left. - \frac{e^{i(\alpha+\gamma-2)T}-1}{\alpha+\gamma-2} - F - G + H \right] \right. \\ & + \frac{1}{(\alpha-1)(\beta-1)} \left[\frac{e^{i(\alpha+\beta+\gamma-3)T}-1}{\alpha+\beta+\gamma-3} + \frac{e^{i(\alpha+\beta+\gamma-1)T}-1}{\alpha+\beta+\gamma-1} - \frac{e^{i(\alpha+\gamma-2)T}-1}{\alpha+\gamma-2} \right. \\ & \quad \left. \left. - \frac{e^{i(\beta+\gamma-2)T}-1}{\beta+\gamma-2} - F - G + H \right] \right. \\ & - I \left[\frac{1}{(\alpha+1)(\beta+1)} + \frac{1}{(\alpha+1)(\beta-1)} + \frac{1}{(\alpha-1)(\beta+1)} \right. \\ & \quad \left. \left. + \frac{1}{(\alpha-1)(\beta-1)} \right] iT \right] / 96\omega^3 \end{aligned}$$

where $H = \frac{e^{i(\gamma+1)T}-1}{\gamma+1} + \frac{e^{i(\gamma-1)T}-1}{\gamma-1}$.

For $k=j$ and $i=n$, or $k=n$ and $i=j$, $F=0$ otherwise $F = \frac{e^{i(\alpha+\gamma)T}-1}{\alpha+\gamma}$.

For $j=n$, $G=0$ otherwise $G = \frac{e^{i(\beta+\gamma)T}-1}{\beta+\gamma}$.

If $F=0$ and $G \neq 0$ then $I=0$; if $F=0$ and $G=0$ then $I=2$ otherwise $I=1$.

$P_r(\alpha\beta\gamma)$					
r	α	β	γ	M_r	N_r
(b)					
1	$(E_i - E_j)/\omega$	$(E_j - E_k)/\omega$	$(E_k - E_n)/\omega$	1	1
2	$(E_i - E_j)/\omega$	$(E_k - E_n)/\omega$	$(E_j - E_k)/\omega$	0	-1
3	$(E_k - E_n)/\omega$	$(E_i - E_j)/\omega$	$(E_j - E_k)/\omega$	0	-1
4	$(E_j - E_k)/\omega$	$(E_i - E_j)/\omega$	$(E_k - E_n)/\omega$	-1	0
5	$(E_j - E_k)/\omega$	$(E_k - E_n)/\omega$	$(E_i - E_j)/\omega$	-1	0
6	$(E_k - E_n)/\omega$	$(E_i - E_k)/\omega$	$(E_i - E_j)/\omega$	1	1

^a $S_{ijk} = V_{ij}V_{jk}$ and $S_{ijkn} = V_{ij}V_{jk}V_{kn}$. For terms A_1 and A_2 , $\alpha = (E_i - E_j)/\omega$ and $\beta = (E_j - E_k)/\omega$. The values of α , β , and γ for terms A_3 are determined by $P_r(\alpha\beta\gamma)$, as listed above.

and the sequence of integrations is performed from right to left. The abbreviation

$$H_i \equiv H(t_i) \quad (10.3.3.16)$$

is also used.

Table 21 gives explicit expressions for the matrix elements of A_1 , A_2 , and A_3 between any pair of atomic basis states for the dipole Hamiltonian (in the interaction picture),

$$[e^{iH_0 t/\hbar} (V \cos \omega t)^{-iH_0 t/\hbar}] \quad (10.3.3.17)$$

10.3.4. An Example of a Time-Domain Floquet Calculation

The time-domain Floquet method has been applied^(222,226) to calculate multiphoton transition probabilities in the infrared domain in simple molecules. Below we illustrate some typical results⁽²²²⁾ of such calculations for the diatomic HF.

Figures 44 and 45 show the evolution of the transition probability for the transition of the rovibrational state ($v = 0, J = 0$) to the state ($v = 2, J = 2$) in the vicinity of a two-photon transition. The unperturbed energy difference of this transition lies at $\omega_0 = 2 \times (0.01793318)$ (au) and the field frequency is chosen at $\omega = 0.0179347$ (au).

The field intensity used corresponds to $I = 1.0 \times 10^{12}$ W cm⁻². In Figure 44 the evolution is depicted for the first 590 optical cycles (oc) corresponding to 5 ps of interaction time, while in Figure 45 it is shown over 50 ps. The quasi-periodic structures in the figures arise from the interference with states other than near-resonant. We note that the period corresponding to the longer time structure in Figure 45 is about 5.79 ps (684 oc) while the finer structure has a period of about 0.421 ps (49.7 oc). The frequency spectra for the same transition obtained from the time-averaged transition probability are given in Figure 46 at two field intensities, $I = 0.1 \times 10^{12}$ W cm⁻² and $I = 1.0 \times 10^{12}$ W cm⁻². It compares also the ($v = 0, J = 0$) \rightarrow ($v = 1, J = 1$) transition at the lower intensity. The expected broadening of the “two-photon” transition at the higher intensity is noteworthy. The spectra are also slightly asymmetric. The sharp structures in both transitions most probably have the same origin as the “higher-order” resonant peaks and dips observed in the spectra of CO, discussed in Section 10.2.7. Another quantity of interest is the difference of perturbed energies (the “eigenexponents”) corresponding to the unperturbed initial and final states. Such perturbed “transition energies” are shown in Figure 47 as a function of the incident frequency at the two field strengths $A = 10^{12}$

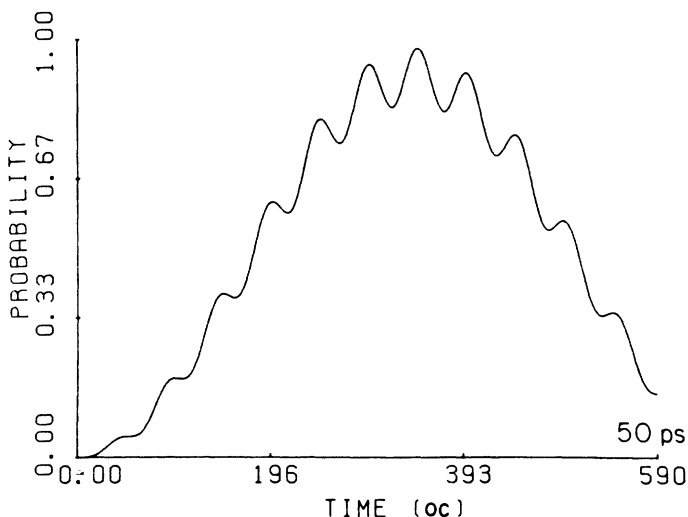


Figure 44. Short-time transition probability of the two-photon ($v = 0, J = 0 \rightarrow v = 2, J = 2$) transition in diatomic HF for 590 optical cycles (oc) or 5 ps. Field frequency $\omega = 0.0179347$ (au) is half the transition frequency and the field intensity $I = 10^{12} \text{ W cm}^{-2}$ (from Milfeld and Wyatt⁽²²²⁾).

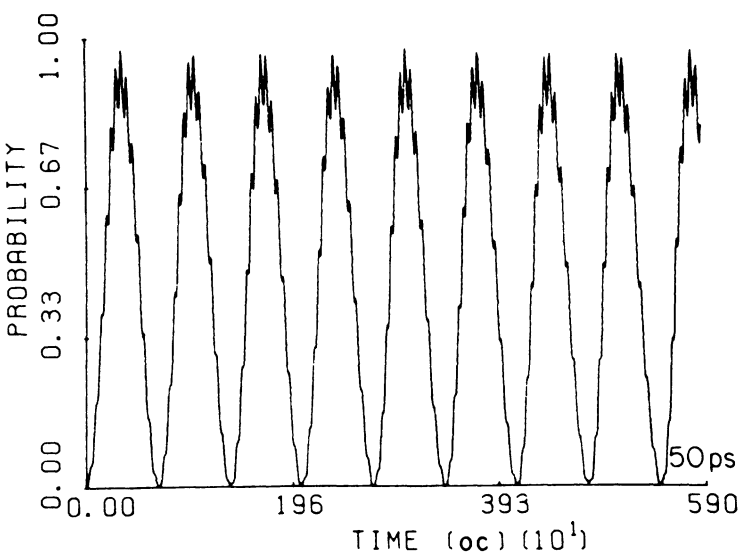


Figure 45. Time-dependent transition probability of the two-photon ($v = 0, J = 0 \rightarrow v = 2, J = 2$) transition in diatomic HF for 5900 optical cycles (oc) or 50 ps. Field frequency $\omega = 0.0179347$ (au) is half the transition frequency and the field intensity $I = 10^{12} \text{ W cm}^{-2}$ (from Milfeld and Wyatt⁽²²²⁾).

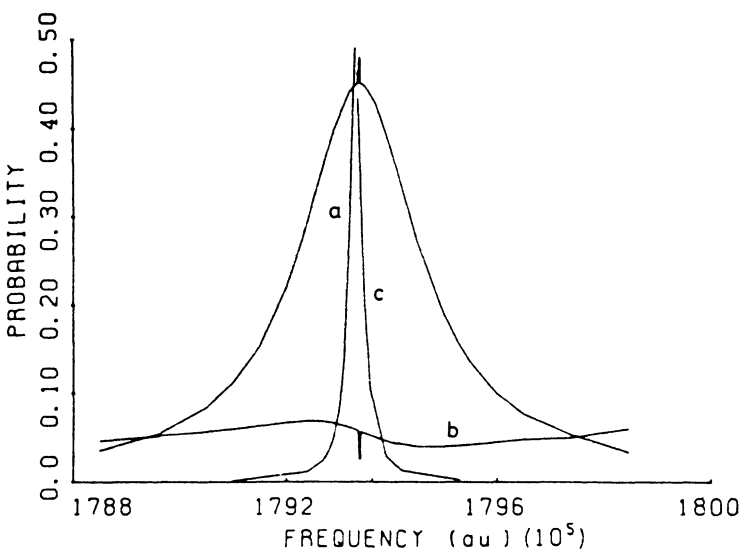


Figure 46. Two-photon excitation spectra for the $(v = 0, J = 0) \rightarrow (v = 2, J = 2)$ transition in diatomic HF at field intensity $I = 10^{12} \text{ W cm}^{-2}$ (curve a) and $I = 10^{11} \text{ W cm}^{-2}$ (curve c). The corresponding $(v = 0, J = 0) \rightarrow (v = 1, J = 1)$ transition at $I = 10^{12} \text{ W cm}^{-2}$ is shown by curve b, which indicates the presence of interaction between the one- and two-photon resonances (from Milfeld and Wyatt⁽²²²⁾).

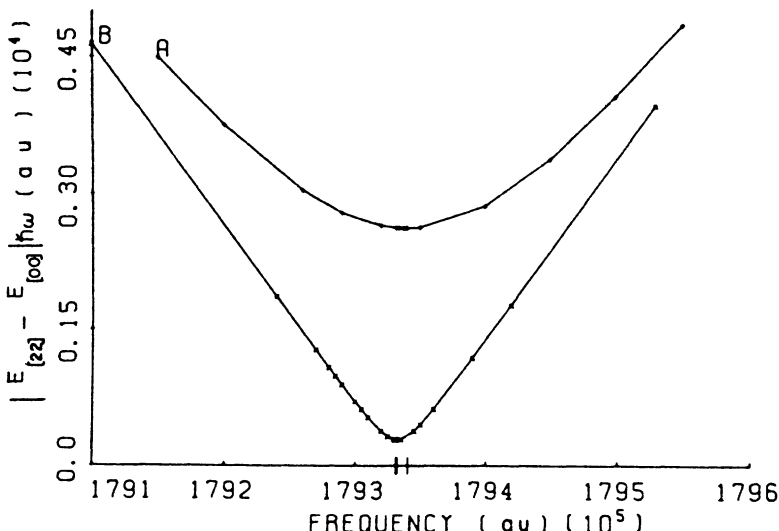


Figure 47. Floquet characteristic exponent (energy) differences $|E_{v=2, J=2} - E_{v=0, J=0}| \hbar\omega$, correlated to the unperturbed rovibrational energies, near the two-photon $(v = 0, J = 0) \rightarrow (v = 2, J = 2)$ transition in HF at intensity $I = 10^{12} \text{ W cm}^{-2}$ (curve A) or $I = 10^{11} \text{ W cm}^{-2}$ (curve B) (from Milfeld and Wyatt⁽²²²⁾).

W cm^{-2} and $B = 10^{11} \text{ W cm}^{-2}$ for the $(v = 0, J = 0) \rightarrow (v = 2, J = 2)$ transition. From the computational point of view it is worth noting that good agreement has been found⁽²²²⁾ between direct numerical integration and the second-order Magnus approximation of the evolution-operator matrix elements at these relatively high intensities.

11

Non-Hermitian Hamiltonian Theory of Multiphoton Transitions

11.1. Introduction

Under the action of the radiation field all atomic systems tend to make a transition (by absorption of one or more photons) into the decaying continuum. Thus, quite generally, atom-field interactions may be viewed from the standpoint of the general theory of decay of quantum systems. According to the Fock-Krylov theorem^(227,228) the necessary and sufficient condition for a quantum state to be a decaying state is that the energy distribution of the state be continuous. Such a state necessarily has a finite “lifetime” and hence its energy cannot be sharp. The resulting “width” can be related to the imaginary part of the complex eigenvalue of a class of non-Hermitian Hamiltonians, which may be systematically constructed from the given Hermitian Hamiltonian of the system. This can be done in more than one way. We shall consider two different methods of doing this: (a) the method of the “optical potential” and (b) the method of the complex coordinate (or dilatation) transformation. Both approaches when applied to the multiphoton problem lead to certain stationary non-Hermitian Hamiltonians whose eigenvalues and eigenvectors determine the multiphoton transition probabilities. In subsequent sections we discuss some of the useful general properties⁽²²⁹⁾ of non-Hermitian Hamiltonians, which can be employed for a consistent treatment of the time evolution of the transition probabilities and related distributions, and compare them with the properties of the more common Hermitian Hamiltonians.

11.2. Properties of Non-Hermitian Hamiltonians

We shall denote a non-Hermitian Hamiltonian by \hat{H} and a Hermitian one by H . Let

$$\hat{H} |\psi_i\rangle = \lambda_i |\psi_i\rangle \quad (11.2.1)$$

where $|\psi_i\rangle$ and λ_i are the eigenvectors and corresponding eigenvalues (which are in general complex) of \hat{H} . Quantities $|X_i\rangle$ and ε_i are the corresponding eigenvectors and eigenvalues satisfied by the concomitant adjoint Hamiltonian \hat{H}^+ :

$$\hat{H}^+ |X_i\rangle = \varepsilon_i |X_i\rangle \quad (11.2.2)$$

The adjoint of Eq. (11.2.2) is

$$\langle X_i | \hat{H} = \varepsilon_i^* \langle X_i | \quad (11.2.3)$$

where ε_i^* is the complex conjugate of ε_i and

$$|X_i\rangle^+ = \langle X_i | \quad (11.2.4)$$

The spectrum of \hat{H} is unique, so comparison of Eqs. (11.2.2) and (11.2.3) gives

$$\lambda_i = \varepsilon_i^* \quad \text{for all } i \quad (11.2.5)$$

The state vectors $|\psi_i\rangle$ and $|X_i\rangle$ are, however, in general different. We may now project with $\langle X_i |$ onto Eq. (11.2.1) and [changing i in Eq. (11.2.3) to j] project with $|\psi_i\rangle$ onto Eq. (11.2.3). Subtraction of the resulting expressions yields

$$(\lambda_i - \varepsilon_j^*) \langle X_i | \psi_i \rangle = 0 \quad (11.2.6)$$

Equations (11.2.5) and (11.2.6) permit one to orthonormalize; hence

$$\langle X_i | \psi_i \rangle = \delta_{ij} \quad \text{for all } i \text{ and } j \quad (11.2.7)$$

Equation (11.2.7) is the generalization of the usual orthonormal relation satisfied by the vectors of a Hermitian Hamiltonian. It clearly shows that now the orthonormal property follows not from the eigenvectors $|\psi_i\rangle$ or $|X_i\rangle$ on their own, but that it requires their simultaneous consideration. Similarly, the closure relation also requires both sets of vectors $|\psi_i\rangle$ and

Table 22. Comparison of Hermitian and Non-Hermitian Systems

	Hermitian	Non-Hermitian
1. Schrödinger equation	$i\hbar \frac{\partial}{\partial t} \psi\rangle = H \psi\rangle$	$i\hbar \frac{\partial}{\partial t} \psi\rangle = \hat{H} \psi\rangle$
2. Eigenvalue equations	$H \psi_i\rangle = E_i \psi_i\rangle$	$\hat{H} \psi_i\rangle = \lambda_i \psi_i\rangle$ $\hat{H}^+ X_i\rangle = \varepsilon_i X_i\rangle$
3. Eigenvalues	$E_i = E^*;$ (real)	$\lambda_i = \varepsilon^*;$ (complex)
4. Orthonormality	$\langle \psi_i \psi_j \rangle = \delta_{ij}$	$\langle X_i \psi_j \rangle = \delta_{ij}$
5. Closure	$\sum_i \psi_i\rangle \langle \psi_i = 1$	$\sum_i \psi_i\rangle \langle X_i = 1$
6. Resolvent	$G_E = \sum_i \frac{ \psi_i\rangle \langle \psi_i }{E - E_i}$	$G_E = \sum_i \frac{ \psi_i\rangle \langle X_i }{E - E_i}$
7. Diagonalization	H is always diagonalizable	\hat{H} can be diagonalized in the symmetric case and more generally if the eigenvalues are all distinct
8. Homogeneous boundary condition	$a\psi_s + b \frac{\partial\psi_s}{\partial\hat{n}} \Big _s = 0$	$\alpha\psi_s + \beta \frac{\partial\psi_s}{\partial\hat{n}} \Big _s = 0$ $\alpha X_s + \beta^* \frac{\partial X_s}{\partial\hat{n}} \Big _s = 0$

Notes to Item 7

If two or more eigenvalues are degenerate then, in principle, an infinitesimal perturbation of appropriate symmetry may be introduced to lift the degeneracy.

Notes to Item 8

This result is given in the space representation where \hat{n} is a normal to the boundary surface s and a, b, α, β are constants.

$|X_i\rangle$ and is given by

$$\sum_i |\psi_i\rangle \langle X_i| = 1 \quad (11.2.8)$$

All the relevant relations involving the non-Hermitian \hat{H} can be derived without difficulty by considering the set $\{|\psi_i\rangle\}$ and its concomitant set $\{|X_i\rangle\}$ in the theory. We list them in Table 22 and compare them with the Hermitian case.

11.3. The Solution Matrix

For specific computation it is convenient to express the abstract vectors $|\psi_i\rangle$ and $|X_i\rangle$ whenever possible in the matrix representation. We

let S be a similarity transformation matrix, which is no longer unitary, such that

$$HS = S\lambda \quad (11.3.1)$$

where λ is the diagonal complex-eigenvalue matrix. Let R be another nonunitary similarity transformation matrix satisfying

$$\hat{H}^T R = R\lambda \quad (11.3.2)$$

where \hat{H}^T is the (simple) transpose of \hat{H} . Quantity $|\psi\rangle$ denotes the whole set of vectors $|\psi_i\rangle$ (each $|\psi_i\rangle$ is a column of $|\psi\rangle$), i.e., $|\psi\rangle$ is the solution matrix. Similarly we let $|X\rangle$ be the concomitant solution matrix. If relation (11.3.1) is multiplied on the left by R^T and the transpose of Eq. (11.3.2) on the right by S and we subtract, then the equation

$$R^T S \lambda = \lambda R^T S \quad (11.3.3)$$

is obtained. Since λ is diagonal, therefore

$$R^T S = D \quad (11.3.4)$$

(this is diagonal but need not be the unit matrix). Thus

$$S^{-1} = D^{-1} R^T \quad (11.3.5)$$

Hence we may resolve the identity as

$$\begin{aligned} I &= SS^{-1} = SD^{-1}R^T \\ &= (SD^{-1/2})(D^{-1/2}R^T) = |\psi\rangle\langle X| \end{aligned} \quad (11.3.6)$$

and define the so-called right and left solution matrices by

$$|\psi\rangle = SD^{-1/2} \quad (11.3.7)$$

and

$$|X\rangle = R^*(D^{-1/2})^* \quad (11.3.8)$$

respectively. One easily verifies that

$$\langle X | \psi \rangle = (D^{-1/2}R^T)(SD^{-1/2}) = D^{-1/2}DD^{-1/2} = I \quad (11.3.9)$$

It is useful to note that when \hat{H} is symmetric, as in most, if not all, practical

applications, we can set $R = S$ and obtain the simpler relations

$$S^T S = D \quad (11.3.10)$$

$$|\psi\rangle = SD^{-1/2} \equiv U \quad (11.3.11)$$

and hence

$$|X\rangle = D^{-1/2} S^T = U^T \quad (11.3.12)$$

Hence one need only now diagonalize \hat{H} once and obtain both $|\psi\rangle$ and $|X\rangle$ from Eqs. (10.3.10)–(10.3.12), together with the (complex) eigenvalue matrix λ .

11.3.1. An Illustrative Case

Let us briefly illustrate the properties of the non-Hermitian Hamiltonian given above by a simple example. If

$$\hat{H} = \begin{pmatrix} z_1 & V_1 \\ V_2 & z_2 \end{pmatrix} \quad (11.3.1.1)$$

is a 2×2 non-Hermitian Hamiltonian, where at least z_1 and z_2 are complex, then the secular equation of matrix (11.3.1.1) is easily solved to obtain the two eigenvalues

$$\lambda_1 = \frac{z_1 + z_2}{2} - \left[\left(\frac{z_1 - z_2}{2} \right)^2 + V_1 V_2 \right]^{1/2} \quad (11.3.1.2)$$

and

$$\lambda_2 = \frac{z_1 + z_2}{2} + \left[\left(\frac{z_1 - z_2}{2} \right)^2 + V_1 V_2 \right]^{1/2} \quad (11.3.1.3)$$

We define a complex angle z by

$$\tan 2z \equiv \frac{(V_1 V_2)^{1/2}}{\frac{1}{2}(z_1 - z_2)} \quad (11.3.1.4)$$

The identities

$$\frac{\tan 2z}{1 - (1 + \tan^2 2z)^{1/2}} = -\cot z \quad (11.3.1.5)$$

and

$$\frac{\tan 2z}{1 + (1 + \tan^2 2z)^{1/2}} = \tan z \quad (11.3.1.6)$$

enable one to verify [cf. Eq. (11.3.1)] that

$$\begin{pmatrix} z_1 & V_1 \\ V_2 & z_2 \end{pmatrix} \begin{pmatrix} S_{11} & S_{12} \\ S_{21} & S_{22} \end{pmatrix} = \begin{pmatrix} S_{11} & S_{12} \\ S_{21} & S_{22} \end{pmatrix} \begin{pmatrix} \lambda_1 & 0 \\ 0 & \lambda_2 \end{pmatrix} \quad (11.3.1.7)$$

is satisfied by a nonunitary transformation matrix S given by

$$S \equiv \begin{pmatrix} S_{11} & S_{12} \\ S_{21} & S_{22} \end{pmatrix} = \begin{pmatrix} (V_1)^{1/2} \cos z & (V_1)^{1/2} \sin z \\ -(V_2)^{1/2} \sin z & (V_2)^{1/2} \cos z \end{pmatrix} \quad (11.3.1.8)$$

The concomitant equation (11.3.2) for the transposed system now takes the form

$$\begin{pmatrix} z_1 & V_2 \\ V_1 & z_2 \end{pmatrix} \begin{pmatrix} R_{11} & R_{12} \\ R_{21} & R_{22} \end{pmatrix} = \begin{pmatrix} R_{11} & R_{12} \\ R_{21} & R_{22} \end{pmatrix} \begin{pmatrix} \lambda_1 & 0 \\ 0 & \lambda_2 \end{pmatrix} \quad (11.3.1.9)$$

and is satisfied by the corresponding nonunitary transformation

$$R \equiv \begin{pmatrix} R_{11} & R_{12} \\ R_{21} & R_{22} \end{pmatrix} = \begin{pmatrix} (V_2)^{1/2} \cos z & (V_2)^{1/2} \sin z \\ -(V_1)^{1/2} \sin z & (V_1)^{1/2} \cos z \end{pmatrix} \quad (11.3.1.10)$$

Expressions (11.3.1.8) and (11.3.1.10) enable one to easily compute

$$R^T S = \begin{pmatrix} (V_1 V_2)^{1/2} & 0 \\ 0 & (V_1 V_2)^{1/2} \end{pmatrix} = D \quad (11.3.1.11)$$

which verifies Eq. (11.3.4). Thus, from relations (11.3.1.8) and (11.3.1.11), the desired right-hand solution matrix [cf. Eq. (11.3.7)] is given by

$$|\psi\rangle = SD^{-1/2} = \begin{pmatrix} (V_1/V_2)^{1/4} \cos z & (V_1/V_2)^{1/4} \sin z \\ (V_2/V_1)^{1/4} \sin z & (V_2/V_1)^{1/4} \cos z \end{pmatrix} \equiv U \quad (11.3.1.12)$$

The corresponding left-hand solution matrix [cf. Eq. (11.3.8)] assumes the form

$$\langle X | = D^{-1/2} R^T = \begin{pmatrix} (V_2/V_1)^{1/4} \cos z & -(V_2/V_1)^{1/4} \sin z \\ (V_1/V_2)^{1/4} \sin z & (V_1/V_2)^{1/4} \cos z \end{pmatrix} \equiv W \quad (11.3.1.13)$$

Hence, explicitly,

$$|X\rangle = W^+ = \begin{pmatrix} (V_2/V_1)^{1/4} \cos z & (V_2/V_1)^{1/4} \sin z \\ (V_1/V_2)^{1/4} \sin z & (V_1/V_2)^{1/4} \cos z \end{pmatrix}^* \quad (11.3.1.14)$$

It is easily seen from expressions (11.3.1.12) and (11.3.1.13) that

$$\langle X | \psi \rangle = WU = \begin{pmatrix} 1 & 0 \\ 0 & 1 \end{pmatrix} \quad (11.3.1.15)$$

and

$$| \psi \rangle \langle X | = UW = \begin{pmatrix} 1 & 0 \\ 0 & 1 \end{pmatrix} \quad (11.3.1.17)$$

This fulfills the biorthonormal properties (11.2.7) and (11.2.8).

In the case when the non-Hermitian Hamiltonian (11.3.1.1) is symmetric ($V_1 = V_2 \equiv V$), the fourth-root factors in Eqs. (11.3.1.12)–(11.3.1.14) clearly become unity and one can immediately verify the truth of the simpler relations (11.3.10)–(11.3.12). In the nonsymmetric case it is assumed that the elements of Hamiltonian (11.3.1.1) are such that all the above 2×2 matrices may exist.

11.4. Optical Potential Construction of Non-Hermitian Hamiltonians, Wave Functions, and Transition Amplitudes

A consistent derivation of a non-Hermitian equivalent of a Hermitian Hamiltonian $H = H_0 + V$ may be obtained by the projection-operator method of Section 7.5.1. One may choose the space p as belonging to the discrete part (including the initial state) of the spectrum of the unperturbed Hamiltonian H_0 and let $q = 1 - p$ contain the part including the continuum spectrum. The continuum part may first be projected out, imposing the causal (outgoing) boundary condition onto the resolvent, to obtain the reduced Hamiltonian H in the “discrete” p -space only. “Elimination” of the continuum q -space alters fundamentally the motion in the p -space. Due to the outgoing boundary condition in the q -space, the resulting Hamiltonian H becomes automatically non-Hermitian and the states in the “discrete” p -space exhibit true decaying behavior.

11.4.1. The Causal and Anticausal Wave Equations

We begin with the Schrödinger wave equation

$$i\hbar \frac{\partial}{\partial t} \psi(t) = H\psi(t) \quad (11.4.1.1)$$

where H is the stationary Hermitian Hamiltonian of interest [such as Eq. (1.9.25)], and easily derive (as shown in detail in Section 7.5.1) the equations for the projected wave functions

$$\psi_p(t) \equiv p\psi(t) \quad \text{and} \quad \psi_q(t) \equiv q\psi(t) \quad (11.4.1.2)$$

These equations are

$$i\hbar \frac{\partial}{\partial t} \psi_p(t) = H_{pp}\psi_p(t) + V_{pq}\psi_q(t) \quad (11.4.1.3)$$

and

$$i\hbar \frac{\partial}{\partial t} \psi_q(t) = H_{qq}\psi_q(t) + V_{qp}\psi_p(t) \quad (11.4.1.4)$$

Since H is stationary we may assume

$$\psi(t) = e^{-iEt/\hbar} |\psi\rangle \quad (11.4.1.5)$$

where E is the total energy of the system and $|\psi\rangle$ is stationary.

On projection with p or q Eq. (11.4.1.5) also yields

$$\psi_p(t) = e^{-iEt/\hbar} |\psi_p\rangle, \quad p |\psi\rangle = |\psi_p\rangle \quad (11.4.1.6)$$

and

$$\psi_q(t) = e^{-iEt/\hbar} |\psi_q\rangle, \quad q |\psi\rangle = |\psi_q\rangle \quad (11.4.1.7)$$

where $|\psi_p\rangle$ and $|\psi_q\rangle$ are thus also stationary. The equations satisfied by $|\psi_p\rangle$ and $|\psi_q\rangle$ are easily found by inserting expressions (11.4.1.6) and (11.4.1.7) in Eqs. (11.4.1.3) and (11.4.1.4). The resulting equations are the same as Eqs. (7.5.1.4) and (7.5.1.6), with $H_{pq} = V_{pq}$ and $H_{qp} = V_{qp}$. We may therefore proceed as in Section 7.5.1 and eliminate $|\psi_q\rangle$ in favor of $|\psi_p\rangle$ to obtain

$$|\psi_q\rangle = |\psi_q^0\rangle + G_{qq}(+i\eta)V_{qp}|\psi_p\rangle \quad (11.4.1.8)$$

where

$$G_{qq}(+i\eta) = \lim_{\eta \rightarrow 0^+} \frac{1}{E - H_{qq} + i\eta} = \frac{P}{E - H_{qq}} - i\pi\delta(E - H_{qq}) \quad (11.4.1.9)$$

is the propagator in the q -space satisfying the outgoing boundary condition and, in relation (11.4.1.8), $|\psi_q^0\rangle$ is the initial value of $|\psi_q\rangle$ in the absence of coupling with the p -space. Without loss of true generality we may always assume that the included initial state (or states) of the problem lies in the p -space and therefore set $|\psi_q^0\rangle = 0$.

On combining expression (11.4.1.8) with Eqs. (11.4.1.6) and (11.4.1.7) and substituting for $\psi_q(t)$ in Eq. (11.4.1.3) we derive

$$\begin{aligned} i\hbar \frac{\partial}{\partial t} \psi_p^{(+)}(t) &= [H_{pp} + V_{pq} G_{qq}(+i\eta) V_{qp}] \psi_p^{(+)}(t) \\ &= \hat{H}_{pp}^{(+)} \psi_p^{(+)}(t) \end{aligned} \quad (11.4.1.10)$$

where the superscript (+) attached to the wave function in the p -space reminds us of the outgoing boundary condition imposed on the q -space propagator (11.4.1.9). Equation (11.4.1.10) is a “causal wave equation” and describes the irreversible motion of the system in the time sector $t = [0, \infty]$ only. The solutions of Eq. (11.4.1.10) apply automatically and only for the whole class of initial-value problems. This situation is in marked contrast to the Schrödinger equation (11.4.1.1), which is completely time-reversal invariant and does not contain the causal (or for that matter, any) boundary condition built into it; the latter must be imposed subsequently onto the solutions of Eq. (11.4.1.1) when physical information is desired, e.g., for the initial-value problems. This point is of considerable interest in the general theory of irreversible dynamics. In fact we may also impose the ingoing (anticausal) boundary condition on the resolvent in the q -space:

$$G_{qq}(-i\eta) = \frac{P}{E - H_{qq}} + i\pi\delta(E - H_{qq}) \quad (11.4.1.11)$$

Equation (11.4.1.10) is now replaced by the “anticausal wave equation”

$$\begin{aligned} i\hbar \frac{\partial}{\partial t} \psi_p^{(-)}(t) &= [H_{pp} + V_{pq} G_{qq}(-i\eta) V_{qp}] \psi_p^{(-)}(t) \\ &\equiv \hat{H}_{pp}^{(-)} \psi_p^{(-)}(t) \end{aligned} \quad (11.4.1.12)$$

where $\hat{H}_{pp}^{(-)}$ differs from $\hat{H}_{pp}^{(+)}$ only in the ingoing character of the propagator. Equation (11.4.1.12) describes the motion of the system in the irreversible time sector $t = [-\infty, 0]$ and is applicable to all final-value problems (e.g., in the Prigoginian sense⁽²³⁰⁾).

A stationary boundary condition could also have been imposed on the resolvent, but this would have left the Hamiltonian Hermitian and a description of the decay process would have been indirect; for example, the outgoing-wave decaying states would be obtained via a construction from the linear combination of the standing-wave states. The latter approach would be similar, for example, to the well-known Fano theory⁽¹²⁰⁾ of autoionization. We note here also that the non-Hermitian character of $\hat{H}_{pp}^{(\pm)}$ depends crucially on the existence of the continuum part of the spectrum of the original H . This allows the delta functional distribution to be defined meaningfully as an integration operator. The total energy E must therefore be degenerate with the continuum in order that the delta integration becomes nonvanishing, which alone makes $\hat{H}_{pp}^{(\pm)}$ non-Hermitian. The necessity of the continuum for the existence of the decaying states, as required by the Fock–Krylov theorem, is thus incorporated directly in the present formalism.

We note that not only do the wave equations (11.4.1.10) and (11.4.1.12) themselves incorporate the “causality conditions” [unlike the Schrödinger Eq. (11.4.1.1)], but also the “causality conditions” are incorporated in a local (or pointwise-differential) sense!⁽²³¹⁾

11.4.2. The Causal Wave Functions

The solution of Eq. (11.4.1.10) satisfying a given initial condition may be first expressed in the operator exponential form

$$|\psi_p^+(t)\rangle = \exp(-i\hat{H}_{pp}^{(+)}t/\hbar)|\psi_p^+(0)\rangle \quad (11.4.2.1)$$

where the non-Hermitian Hamiltonian of interest

$$\hat{H}_{pp}^{(+)} \equiv H_{pp} + V_{pq} \frac{P}{E - H_{qq}} V_{qp} - i\pi\delta(E - H_{pp}) \quad (11.4.2.2)$$

is a symmetric matrix in the p -space. For practical purposes it is useful to diagonalize it in terms of the (nonunitary) transformation matrix U ,

$$\hat{H}_{pp}^{(+)}U = U\lambda \quad (11.4.2.3)$$

where λ (diagonal) is the complex eigenvalue matrix, and the identity

$$I = UU^\top \quad (11.4.2.4)$$

Substitution of expression (11.4.2.4) in Eq. (11.4.2.1) with allowance for relation (11.4.2.3) yields a useful form of the wave function in the p -space,

namely

$$|\psi_p^+(t)\rangle = \sum_B U |B\rangle \exp(-i\lambda_B t/\hbar) \langle B|U^\dagger|B_0\rangle \quad (11.4.2.5)$$

where $\{|B\rangle\}$ is the unperturbed set of product states (in the p -space) and we have set $|\psi_p^+(0)\rangle = |B_0\rangle$, the initial state. Obviously Eq. (11.4.2.5) determines the physical properties of the system at all times $t > 0$, but in the p -space. The description of the system in the whole space can be completed by obtaining the wave function in the q -space. This will now be derived.

Since $|\psi_p^+(t)\rangle$ is known we may use Eq. (11.4.1.4) to find $|\psi_q^+(t)\rangle$. To this end we consider first the equation of the time-dependent outgoing propagator $G_{qq}^+(t, t')$ in the q -space. This quantity satisfies the Green's equation

$$\left(i\hbar \frac{\partial}{\partial t} - H_{qq}\right) G_{qq}^+(t, t') = \delta(t - t') \quad (11.4.2.6)$$

The unique solution (satisfying the causal condition) is

$$G_{qq}^+(t, t') = \frac{-i}{\hbar} \theta(t - t') \exp[-iH_{qq}(t - t')/\hbar] \quad (11.4.2.7)$$

where

$$\theta(t - t') = \begin{cases} 1, & t > t' \\ 0, & t < t' \end{cases} \quad (11.4.2.8)$$

Equation (11.4.2.7) can be easily verified by direct substitution in Eq. (11.4.2.6) and remembering that the derivative of the step function is the delta function, namely

$$\frac{\partial}{\partial t} \theta(t - t') = \delta(t - t') \quad (11.4.2.9)$$

In terms of expressions (11.4.2.7) and (11.4.2.1) the required solution of Eq. (11.4.1.4) can be written as

$$|\psi_q^+(t)\rangle = |\psi_q^+(0)\rangle + \int_0^\infty dt' G_{qq}^+(t, t') V_{qp} |\psi_p^+(t')\rangle \quad (11.4.2.10)$$

$$= |\psi_q^+(0)\rangle - \frac{i}{\hbar} \exp(-iH_{qq}t/\hbar) \int_0^t dt' \exp(iH_{qq}t'/\hbar) \times V_{qp} \exp(-i\hat{H}_{pp}^{(+)}t'/\hbar) |B_0\rangle \quad (11.4.2.11)$$

where $|B_0\rangle = |\psi_p^+(0)\rangle$ is the initial state. For explicit computations it is necessary to diagonalize the Hermitian matrix H_{qq} in the q -space by the unitary matrix s such that

$$H_{qq}s = s\xi \quad (11.4.2.12)$$

with the real eigenvalue matrix ξ (diagonal), and the identity

$$ss^+ = I \quad (11.4.2.13)$$

where s^+ is the Hermitian adjoint of s .

By introducing the resolutions of identity (11.4.2.4) and (11.4.2.13) in the integral of expression (11.4.2.11), and making use of Eqs. (11.4.2.3) and (11.4.2.12), we may easily express the transformation matrices in the unperturbed representation and carry out the time integration in expression (11.4.2.11) to obtain the final form of the solution:

$$\begin{aligned} |\psi_q^+(t)\rangle &= |\psi_q^+(0)\rangle + \sum_{cc'B'B} s |C\rangle \exp(-i\xi_c t/\hbar) \langle C| s |C'\rangle \\ &\quad \times \langle C' | V | B'\rangle \langle B' | U | B\rangle \frac{\exp[i(\lambda_B - \xi_c)t/\hbar] - 1}{\lambda_B - \xi_c} \langle B | U^\dagger | B_0\rangle \end{aligned} \quad (11.4.2.14)$$

where ($|C\rangle, |C'\rangle$) are the unperturbed product states in the q -space while ($|B\rangle, |B'\rangle$) are the unperturbed product states in the p -space.

11.4.3. Amplitudes for Bound–Bound and Bound–Free Transitions

The time-dependent transition amplitude at time t for a bound–bound transition from the initial state $|B_0\rangle$ to a final state $|B\rangle \exp(-iE_B t/\hbar)$ is readily obtained from the wave function (11.4.2.5) in the form

$$A_{B_0 \rightarrow B_f}(t) \equiv \exp(iE_B t/\hbar) \langle B_f | \psi_p^+(t)\rangle = \sum_B U_{B_f B} \exp[-i(\lambda_B - E_B)t/\hbar] U_{B_0 B} \quad (11.4.3.1)$$

where

$$U_{B' B} = \langle B' | U | B\rangle \quad (11.4.3.2)$$

On the other hand, for a transition from the bound initial state $|B_0\rangle$ to a final continuum state $|C_f\rangle \exp(-iE_c t/\hbar)$ we must use the wave function

(11.4.2.14). Hence

$$\begin{aligned} A_{B_0 \rightarrow C_f}^q(t) &\equiv \exp(iE_{c_f}t/\hbar)\langle C_f | \psi_q^+(t) \rangle \\ &= \exp(iE_{c_f}t/\hbar)\langle C_f | \psi_q^+(0) \rangle + \sum_{BB'CC'} s_{CfC} \exp[-i(\xi_c - E_{c_f})t/\hbar] s_{C'C}^* \\ &\quad \times V_{C'B'} U_{B'B'} \frac{\exp[-i(\lambda_B - \xi_c)t/\hbar] - 1}{\lambda_B - \xi_c} U_{B_0B} \end{aligned} \quad (11.4.3.3)$$

where the matrix elements of s , s^+ , and V are expressed in an obvious notation, similar to relation (11.4.3.2). In Eq. (11.4.3.3) the first term $\langle C_f | \psi_q^+(0) \rangle = 0$ since, as usual, we have defined the initial state in the p -space. Amplitudes (11.4.3.1) and (11.4.3.3) completely describe the evolution of the system, which is initially in state $|B_0\rangle$, into all future times.

It is noteworthy that, for not too large intensities or for stable final states, the influence of the further continuum–continuum transition onto a given bound–bound or bound–free transition may be small and neglected. Formally, this amounts to letting $s_{cc'} \rightarrow \delta_{cc'}$ and $\xi_c \rightarrow E_c$, where E_c is the unperturbed continuum energy. Thus, for example, in this approximation Eq. (11.4.3.3) simplifies to

$$A_{B_0 \rightarrow C_f}^q(t) = \sum_{BB'} V_{C_fB'} U_{B'B'} \frac{\exp[-i(\lambda_B - E_{c_f})t/\hbar] - 1}{\lambda_B - E_{c_f}} U_{B_0B} \quad (11.4.3.4)$$

11.4.4. Total Probability of Multiphoton-Induced Decay

We note that since the total probability of finding the system anywhere in the $(p+q)$ -space is unity, the probability of decay (or ionization) in the continuum (q -space) can be found conveniently from the relation

$$P_{\text{decay}}(t) = 1 - \sum_{B_f} |A_{B_0 \rightarrow B_f}^p(t)|^2 \quad (11.4.4.1)$$

where the sum runs over all states in the bound-like p -space. The very detailed information obtained from a multiphoton ionization decay experiment, namely the probability of finding the ionized electron with a given kinetic energy, propagating in a given direction, after a given interaction time t , is given by the corresponding double differential ionization probability

$$\frac{d^2}{dk_{C_f} d\varepsilon_{C_f}} P_{\text{decay}}(t) = |A_{B_0 \rightarrow C_f}^q(t)|^2 \quad (11.4.4.2)$$

where $d\hat{k}_{C_f}$ is the element of solid angle in the direction of the decaying electron's momentum vector \mathbf{k}_{C_f} in the final state, $|C_f\rangle$, and $d\varepsilon_{C_f}$ is the element of energy of the decaying electron between ε_{C_f} and $\varepsilon_{C_f} + d\varepsilon_{C_f}$, where $\varepsilon_{C_f} = (\hbar^2 k_{C_f}^2)/2\mu + \hbar n_{C_f}\omega$. We have assumed that the final state $|C_f\rangle$ has the form $|\mathbf{k}_{C_f}\rangle^{(-)} \otimes |n_{C_f}\rangle$ where $|\mathbf{k}_{C_f}\rangle^{(-)}$ is the directed ingoing-type continuum wave function [cf. Eq. (5.2.4)] of the decaying electron and $|n_{C_f}\rangle$ is the final-state field occupation number. The total decay or induced multiphoton ionization probability must also equal the sum of the probabilities of occupying all possible states in the continuum space. Thus from Eq. (11.4.3.3) we also get

$$P_{\text{decay}}(t) = \sum_{C_f} \int d\hat{k}_{C_f} d\varepsilon_{C_f} |A_{B_0 \rightarrow C_f}(t)|^2 \quad (11.4.4.3)$$

Although it is usually more convenient to compute $P_{\text{decay}}(t)$ from the expression (11.4.4.1) rather than (11.4.4.3), it is noteworthy that a simultaneous calculation of the two expressions, at least in one instance, should provide a useful check on the consistency of the computational procedure adopted for any particular system.

11.4.5. Time Dependence of Multiphoton Transitions in Hydrogen

As an example of the application of the method we present in this section typical time-dependent results of numerical calculations⁽²²⁹⁾ using expressions (11.4.3.1), (11.4.3.4), (11.4.4.1), and (11.4.4.2) for two- and three-photon ionization decay of the ground-state hydrogen atom.

11.4.5.1. Two-Photon Transitions

Figure 48a shows the total resonance-ionization probability $P_{\text{ion}}(\tau)$ for a hydrogen atom initially in the state H(1s) as a function of the interaction time τ . The frequency of the radiation is $\omega = 0.375$ (au) (corresponding to the $1s \rightarrow 2p$ resonance frequency of the atom). The field amplitude ε_0 is 10^{-3} (au) or 5.14×10^6 V/cm. It would seem that the ionization probability at first grows steadily with time and then saturates toward the value unity. The relevant scale of time is given by $1/\gamma = 0.09$ ns, where γ is the width of the ground state due to the ionization and corresponds roughly to the rate of ionization in the domain where the dependency of $P_{\text{ion}}(\tau)$ is linear in τ .

In Figure 48b the (survival) probability $P_{1s}(t)$ of finding the electron in the ground state is shown as a function of the interaction time. Starting from $P_{1s}(0) = 1$, it exhibits an overall irreversible decay with time. However, the instantaneous probability is a highly oscillatory function of time. On the other hand, the corresponding ionization probability in Figure 48a

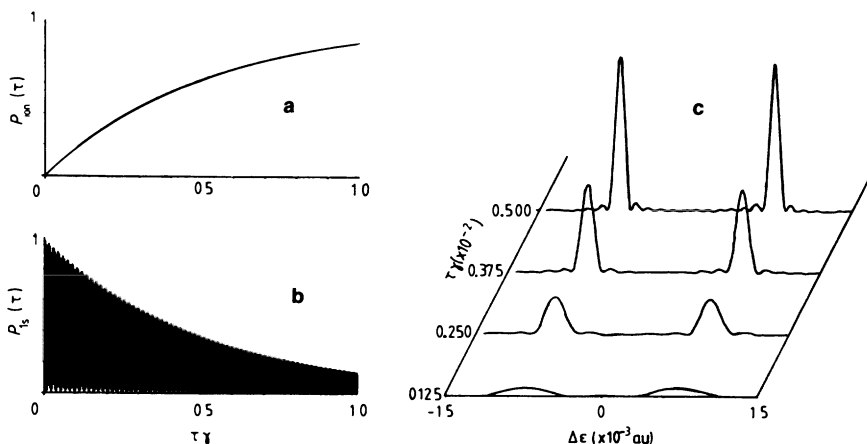


Figure 48. Time dependence of one-photon resonant two-photon ionization of the H(1s) state. Shown are (a) the total ionization probability, (b) the survival probability of the H(1s) state, and (c) the time evolution of the energy spectrum (at the first ionization continuum) of the ionized electron. Photon energy $\hbar\omega = 0.375$ (au) equals the $1s-2p$ transition energy. The characteristic time scale is given by the inverse of the field-induced width γ of the ground state: $\gamma^{-1} = 0.09$ ns. The corresponding peak field strength $E_0 = 10^3$ (au) = 5.142×10^6 V/cm (from Faisal and Moloney⁽²²⁹⁾).

shows no such oscillation. This is due to the fact that the probability distribution of the one-photon resonant $2p$ -state also oscillates rapidly but in nearly opposite phase to that of the ground state and effectively cancels the oscillating contribution of the ground state to the total probability. (The occupation probability of the nonresonant states, although entering systematically in the computation, is numerically very small compared to that of the resonant states.) The oscillations observed above are damped Rabi oscillations⁽¹⁴⁰⁾ in photoionization. Their presence has been noted and studied extensively^(109,232-239) with the help of simple models.

Figure 48c shows the energy spectra of the ionized electron at the first ionization continuum assumed to be stable at different times. The first thing one notes about these spectra is their doublet structure, which is a consequence of splitting^(240,241) of the intermediate resonant $2p$ -state under the influence of the dynamic Stark effect induced by the field (an Autler-Townes effect⁽¹⁹⁰⁾). The doublet is seen to be placed symmetrically around the “unperturbed energy” $\varepsilon_k = 2\hbar\omega - E_{\text{ion}}$, where E_{ion} is the ionization threshold. One notes further that the $1s-2p$ resonant doublet structure grows as well as narrows with increasing time. The height of the doublet is 15-fold greater at $\gamma\tau = 0.125$ than at $\gamma\tau = 0.5$, while the widths have shrunk by more than a factor of 3 during the same time interval. This

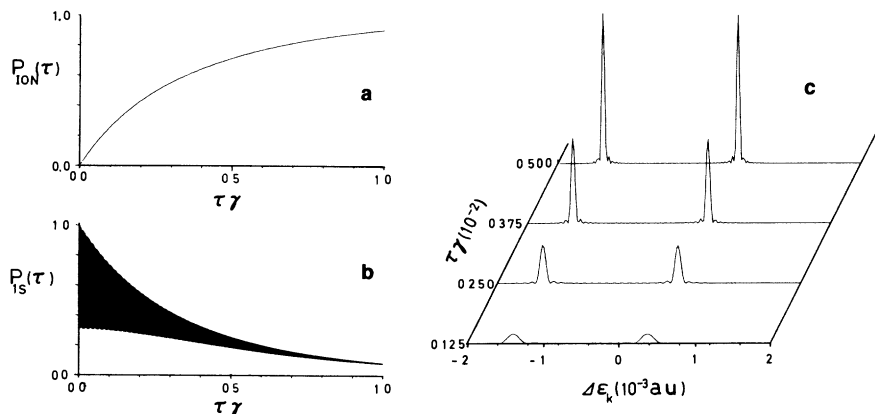


Figure 49. Time dependence of off-resonant two-photon ionization of the H(1s) state. Shown are (a) the total ionization probability, (b) the survival probability of the H(1s) state, and (c) the time evolution of the energy spectrum (at the first ionization continuum) of the ionized electron. Photon energy $\hbar\omega = 0.376$ (au) is 0.001 (au) off-resonant with respect to the $1s-2p$ transition energy. The time scale of evolution of the system is given by the inverse of the field-induced width γ of the ground state: $\gamma^{-1} = 0.22$ ns. The corresponding peak field strength $E_0 = 10^{-3}$ (au) = 5.142×10^6 V/cm (from Faisal and Moloney⁽²²⁹⁾).

is understood qualitatively as the increase in probability of ionization with diminishing “rate” at time progresses.

Figure 49a shows the total ionization probability for two-photon ionization at a nonresonant frequency. The frequency is $\omega = 0.376$ (au) corresponding to a detuning $\Delta = 0.001$ (au) from the (near-resonant) $2p$ -state. We note that the general growth of the ionization is similar to the resonant case (cf. Figure 48a), but to attain the same degree of ionization now requires a longer time than in the resonant case. This is reflected by the characteristic time $1/\gamma = 0.02$ ns, compared to 0.09 ns in the resonant case.

Figure 49b exhibits the corresponding probability of finding the electron in the ground state. This result differs from that of the resonant case (cf. Figure 48b) in that the rapid oscillations are confined mostly above the minimum value of zero, reflecting the general fact of incomplete Rabi oscillation for a finite detuning from the resonance. However, the probability envelope shows as before an irreversible decay with increasing time.

Figure 49c shows the nonresonant ionization spectrum. Unlike the spectrum in the resonant case (cf. Figure 48c), the Autler–Townes doublet is here placed asymmetrically around the electron energy $\epsilon_k = 2\hbar\omega - E_{\text{ion}} = 0.252$ (au). Qualitatively, the width of the spectrum indicates the rapidity with which the system ionizes. The spectrum is significantly more narrow compared to the resonant case for the same $(\gamma\tau)$ values, reflecting a relatively slower decay in the nonresonant situation. The characteristic time in this case is $1/\gamma = 0.22$ ns.

11.4.5.2. Three-Photon Transitions

Figure 50a shows the probability of resonant three-photon ionization of the H(1s) state. The frequency is $\omega = 0.1875$ (au) so that there is a two-photon resonance with respect to the intermediate 2s-state. The ionization probability at the early times passes through points of inflection and then settles down to uniform growth toward the saturation value unity. In this circumstance the usual constant rate of transition, which requires a linear variation of probability with time, ceases to be a meaningful parameter of the process (see Section 7.4).

Figure 50b shows the decay with time of the probability of occupying the ground state. The decay here shows only a gentle modulation, in contrast to the rapid oscillations in the corresponding two-photon resonant case in Figure 48b. This is due to the difference in coupling strengths between the ground and the resonant state, and that between the resonant state and the ionization continuum. The two-photon resonant 1s–2s coupling

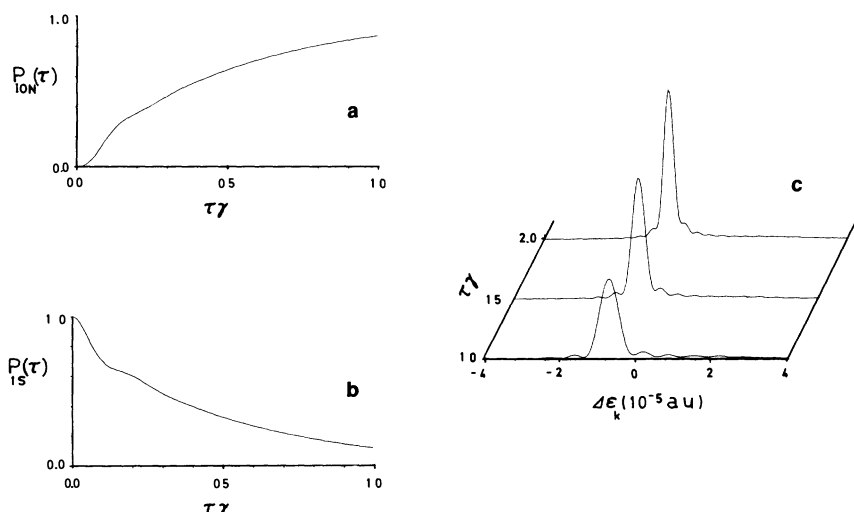


Figure 50. Time dependence of two-photon resonant three-photon ionization of the H(1s) state. Shown are (a) the total ionization growth probability, (b) the survival probability of the initial 1s-state, and (c) the time evolution of the energy spectrum (at the first ionization continuum) of the ionized electron. Photon energy $\hbar\omega = 0.1875$ (au) equals half of the 1s–2p transition energy. The time scale of evolution of the system is given by the inverse of the field-induced width γ of the ground state: $\gamma^{-1} = 0.02$ ns. The corresponding peak field strength $E_0 = 10^{-3}$ (au) = 5.142×10^6 V/cm (from Faisal and Moloney⁽²²⁹⁾).

strength is comparable to the coupling strength to the continuum from the $2s$ -level, both being of the order of E_0^2 (E_0 is the peak field strength). Ionization therefore competes with the bound–bound Rabi oscillation and effectively inhibits the latter. The one-photon resonant $1s$ – $2s$ coupling is much stronger ($\propto E_0$) than the corresponding coupling to the $2p$ -continuum ($\propto E_0^2$) and hence allows many Rabi oscillations to occur before ionization becomes effective. The severe inhibition of the Rabi oscillation due to competition with ionization decay is also revealed by the qualitative change in the doublet structures of the electron energy spectrum (Figures 48c and 49c) into the singlet structure in Figure 50c. It shows indirectly the absence of Autler–Townes splitting of the resonant state, due to lack of sufficient Rabi oscillations. Perhaps the most significant influence of the inhibition of Rabi oscillations and the consequent prevalence of irreversible ionization in the three-photon resonant-ionization process shows up in the highly reduced characteristic time for the ionization, $1/\gamma = 0.02$ ns, compared to the longer characteristic time ($1/\gamma = 0.09$ ns) of the two-photon resonant-ionization process shown in Figure 48a (at the same field strength $E_0 = 5.142 \times 10^6$ V/cm).

11.4.5.3. Field-Induced Quantum Beats in Multiphoton Ionization of H

Multiphoton quantum beats in ionization have been studied theoretically⁽²⁴²⁾ and observed⁽²⁴³⁾ experimentally for beating between intermediate-state fine or hyperfine structures, influencing the ionization signals. The accidental l -degeneracy of a hydrogen atom can also lead to photoionization quantum beats between two different l -states⁽²²⁹⁾ of the same shell. Consider the three-photon ionization of H($1s$) via the intermediate l -degenerate $3s$ - and $3d$ -states. In this case, a sequence of quantum beats appears in the total ionization probability (Figure 51a) and in the ground-state survival probability (Figure 51b). The corresponding photoelectron energy spectrum is shown in Figure 51c. Physically, the beats may be understood to arise as follows: Due to the accidental l -degeneracy the unperturbed energy difference is $\varepsilon_{3s} - \varepsilon_{3d} = 0$, but due to coupling of the field with the $3s$ - and $3d$ -states and due to the difference in strength of the coupling for the two states, the corresponding field-modified (or “dressed”) energies of the two states become different. During the ionization process, therefore, an interference between the two amplitudes associated with the modified ε'_{3s} and ε'_{3d} states gives rise to a beat frequency $\Omega \approx (\varepsilon'_{3s} - \varepsilon'_{3d})/\hbar$ with finite period $T = 2\pi/\Omega$, as seen in Figures 51a and 51b. Finally, Figure 51d shows a typical angular distribution of the ionized electron for the two-photon resonant three-photon ionization, for an interaction time $\tau = 1.4$ ns, at $\omega = 0.22222$ (au) = 6.044 eV and peak field strength $E_0 = 5.142 \times 10^6$ V/cm.

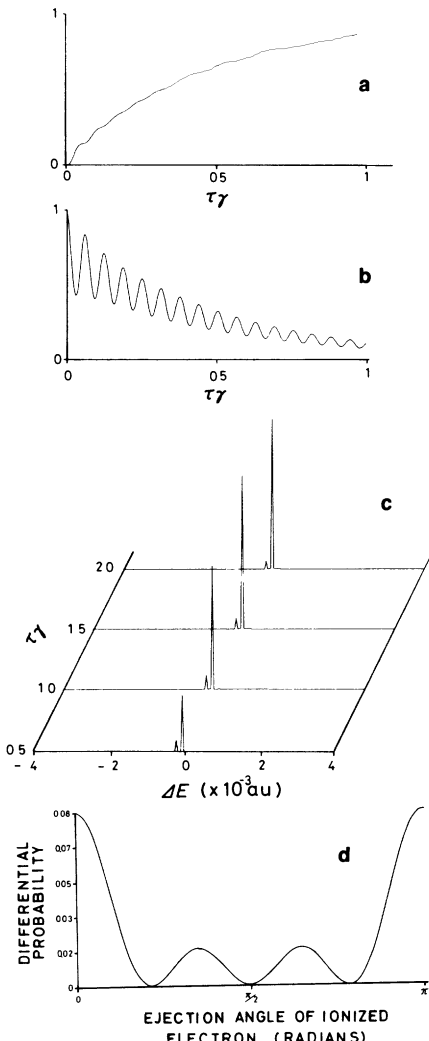


Figure 51. Time dependence of two-photon (doubly) resonant three-photon ionization of the $H(1s)$ state, giving rise to l -degenerate quantum beats in the ionization signal. Shown are (a) the total growth probability of ionization showing typical beat modulations, (b) the survival probability of the initial $H(1s)$ state showing marked beating, (c) the time evolution of the energy spectrum (at the first ionization continuum) of the ionized electron and (d) the angular distribution of the ionized electron for an interaction time $\tau = 1.4$ ns. Photon energy $\hbar\omega = 0.22222$ (au) leads to two-photon intermediate resonances to the two degenerate transitions, $1s-3s$ and $1s-3d$. The time scale of evolution of the system is given by the inverse of the field-induced width γ of the ground state: $\gamma^{-1} = 0.15$ ns. The corresponding peak field strength $E_0 = 10^{-3}$ (au) = 5.142×10^6 V/cm. The beats occur with period $T = 2\pi/\Omega$, where $\hbar\Omega \approx (\epsilon'_{3s} - \epsilon'_{3d})$ is the difference of the perturbed (dressed) energies of the initially degenerate ($\epsilon_{3s} = \epsilon_{3d}$) even-parity states of the $n = 3$ shell (after Faisal and Moloney⁽²²⁹⁾).

11.5. The Multiphoton Non-Hermitian Hamiltonian Generated by Rotation of Coordinates

The basic idea of this method is to transform a Hermitian Hamiltonian H given in the coordinate representation into a non-Hermitian one, by introducing a unitary complex scale transformation of the radial coordi-

nates:

$$r \rightarrow u(\theta)r = e^{i\theta}r, \quad |\theta| \leq \pi/2 \quad (11.5.1)$$

Atomic N_a -electron Hamiltonians of the form

$$H_{\text{atom}} = \text{KE} + \text{PE}$$

where KE and PE are the kinetic- and potential-energy parts, respectively, transform under rotation (11.5.1) into

$$H_{\text{atom}}(\theta) = e^{-2i\theta} \text{KE} + e^{-i\theta} \text{PE} \quad (11.5.2)$$

This has the consequence of rotating by 2θ the continuum spectrum of H about the branch point (bound–continuum threshold) from the positive real axis into the lower half of the complex energy plane (as depicted in Figure 52) while the bound-state poles on the negative real E -axis remain unaffected. Some of the basic spectral properties of $H_{\text{atom}}(\theta)$ are as follows.^(244,245)

1. The bound-state energies of $H_{\text{atom}}(\theta)$ are identical to those of H_{atom} and do not depend on θ for $|\theta| < \pi/2$.
2. The branch points at the (bound–continuum) thresholds of $H_{\text{atom}}(\theta)$ and H are the same and do not depend on θ for $|\theta| < \pi/2$.
3. The positive energy cuts of H_{atom} are rotated in the lower-half complex E -plane by 2θ revealing possible complex eigenvalues of $H_{\text{atom}}(\theta)$ in the sector

$$-2\theta \leq \arg(E - E_{\text{threshold}}^{\min}) \leq 0$$

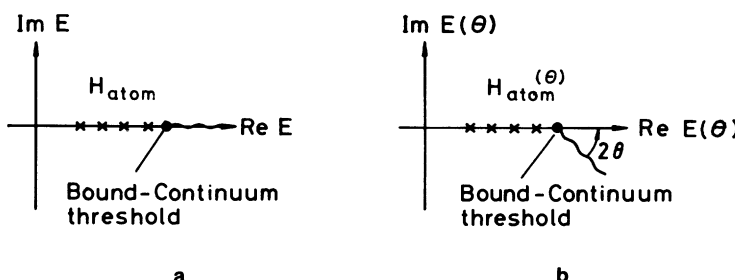


Figure 52. Schematic diagrams illustrating the rotation of the continuum energy cut of H on the real axis (a) into the cut of the rotated $H(\theta)$ (b) in the lower-half complex E -plane along a line rotated by 2θ about the fixed bound–continuum threshold (branch point) of both H and $H(\theta)$. Crosses indicate bound-state poles, which remain unaffected (like the threshold) by the rotation.

where $E_{\text{threshold}}^{\min}$ is the lowest (bound–continuum) threshold of H and E complex; the corresponding eigenfunctions are square-integrable.

4. The discrete eigenvalues (real and complex) of $H_{\text{atom}}(\theta)$ are of finite multiplicity except perhaps at the thresholds (branch points).

These (and several other properties) apply to the class of Hamiltonians with so-called “dilatation analytic”⁽²⁴⁶⁾ interactions (potentials), which include the (many-body) Coulomb interaction and the “atom + electric field” interaction in the dipole approximation. From the calculational point of view the significant fact is that quantities such as the spectrum or resolvent associated with $H_{\text{atom}}(\theta)$ are now free from the continuum cuts along the positive real axis. Consequently, the coordinate representation of $H_{\text{atom}}(\theta)$ may be replaced by its projection onto the space of L^2 -functions only.

11.5.1. Rotated Hydrogenic Floquet Hamiltonian

The first study⁽²⁴⁷⁾ of multiphoton processes by rotated Hamiltonians was conducted in this prototype system. Transformation (11.5.1) when applied to the Hermitian atom + field Hamiltonian H for the hydrogenic problem

$$H = -\frac{\hbar^2}{2\mu} \nabla_r^2 - \frac{Ze^2}{r} + \hbar\omega a^+ a - e\boldsymbol{\epsilon} \cdot \mathbf{r} \left(\frac{2\pi\hbar\omega}{L^3} \right)^{1/2} (a^+ + a) \quad (11.5.1.1)$$

with $F = (8\pi\hbar\omega n_0/L^3)^{1/2}$ as the peak field strength, gives the non-Hermitian dilated Hamiltonian

$$\begin{aligned} H(\theta) &= \left[e^{-2i\theta} \left(-\frac{\hbar^2}{2\mu} \nabla_r^2 \right) + e^{-i\theta} \left(-\frac{Ze^2}{r} \right) \right] \\ &\quad + \hbar\omega a^+ a + \left[e^{i\theta} (-e) \left(\frac{2\pi\hbar\omega}{L^3} \right)^{1/2} \boldsymbol{\epsilon} \cdot \mathbf{r} (a^+ + a) \right] \quad (11.5.1.2) \end{aligned}$$

$$= H_{\text{atom}}(\theta) + \hbar\omega a^+ a + V(\theta) \quad (11.5.1.3)$$

where $H_{\text{atom}}(\theta)$ and $V(\theta)$ are defined by the first and second pairs of square brackets on the right-hand side of Eq. (11.5.1.2). The presence of the field Hamiltonian $\hbar\omega a^+ a$ with eigenvalues $n\hbar\omega$ indicates that now there is a sequence of (bound–continuum) thresholds corresponding to the absorption of 1, 2, 3, ..., etc., photons from the field. It is assumed that each of the continuum cuts beginning at these thresholds of the dilated unperturbed Hamiltonian

$$H_0(\theta) \equiv H_{\text{atom}}(\theta) + \hbar\omega a^+ a \quad (11.5.1.4)$$

will be similarly rotated into the lower-half complex E -plane (Figure 53).

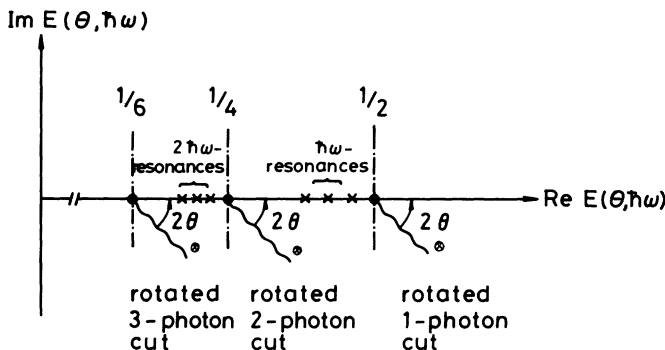


Figure 53. Schematic diagram illustrating rotations of the multiphoton continuum cuts on the real axis (associated with the Hermitian “atom + field” Hamiltonian H) into the lower-half complex E -plane, associated with the rotated non-Hermitian Hamiltonian $H(\theta)$. Energy with respect to the ground state of the “hydrogen atom + field” system is schematized, for a fixed θ , in the frequency variable. Crosses are associated with the bound-state poles. These poles and the threshold branch points are shown to remain unaffected by the rotation. Circles with crosses indicate possible exposed complex poles of $H(\theta)$ when the cuts are rotated beyond them.

Discretization of $H(\theta)$ in Eq. (11.5.1.3) is most conveniently obtained by projection onto the L^2 product space $|J\rangle = |j\rangle \otimes |n_0 + n\rangle$, constructed from a set of L^2 -basis functions $|j\rangle$ in the space of the atom and the number states $|n_0 + n\rangle$ in the space of the photons. This results in a typical block-tridiagonal rotated Floquet matrix $H_F(\theta)$, which represents $H(\theta)$ (see Figure 54). The main diagonal of the matrix $H_F(\theta)$ corresponds to the n -photon states and the upper and lower diagonals represent coupling to the $(n \pm 1)$ -photon states. Each block element consists of a submatrix involving the dipole matrix elements between the L^2 -basis functions. An economic organization of the submatrices, paying attention to the angular-momentum symmetry, yields the forms A and B illustrated in Figure 54. Perhaps the most convenient basis functions to use for Coulomb-like systems are generalized Laguerre (or so-called Sturmian) functions (cf. Section 4.3.1.3) for each angular-momentum symmetry (l, m) :

$$\{|j\rangle\} = \{e^{-\lambda r/2} r^{l+1} L_j^{2l+2}(\lambda r) Y_{lm}(\hat{r})\} \quad (11.5.1.5)$$

where $j = 1, 2, 3, \dots, J$ are integers and λ is an arbitrary real positive parameter; $L_j^{2l+2}(\lambda r)$ are Laguerre polynomials. The set (11.5.1.5) in fact renders the radial Coulomb Hamiltonian into a tridiagonal (or Jacobi-matrix) form for each l , and generates a Gauss–Pollaczek quadrature⁽²⁴⁸⁾ of the Coulomb continuum.

$$\begin{aligned}
 H(\theta) &= \boxed{\begin{array}{ccccc} A+4\omega I & B & 0 & 0 & 0 \\ B^T & A+2\omega I & B & 0 & 0 \\ 0 & B^T & A & B & 0 \\ 0 & 0 & B^T & A-2\omega I & B \\ 0 & 0 & 0 & B^T & A-4\omega I \end{array}} \\
 A &= \boxed{\begin{array}{ccccc} S & V_{sp} & 0 & 0 & 0 \\ V_{ps} & P-\omega I & V_{pd} & 0 & 0 \\ 0 & V_{dp} & D & V_{df} & 0 \\ 0 & 0 & V_{fd} & F-\omega I & V_{fg} \\ 0 & 0 & 0 & V_{gf} & G \end{array}} \\
 B &= \boxed{\begin{array}{ccccc} 0 & 0 & 0 & 0 & 0 \\ V_{ps} & 0 & V_{pd} & 0 & 0 \\ 0 & 0 & 0 & 0 & 0 \\ 0 & 0 & V_{fd} & 0 & V_{fg} \\ 0 & 0 & 0 & 0 & 0 \end{array}}
 \end{aligned}$$

Figure 54. Floquet matrix arranged for convenience of computation. In this form only the submatrices A and B need be stored and the tridiagonal structure may still be utilized (from Chu and Reinhardt⁽²⁴⁷⁾).

11.5.2. Transition Amplitudes from the Rotated Hamiltonian

To obtain the transition probabilities of interest we first consider the integral representation (3.2.10) of the total wave function (3.2.7) governed by the original Hermitian Hamiltonian (11.5.1.1) and express it as a contour integral in the complex E -plane,

$$|\Psi(t)\rangle = e^{-iHt/\hbar} |B_0\rangle \quad (11.5.2.1)$$

$$= \frac{1}{2\pi i} \int_c dE \frac{e^{-iEt/\hbar}}{E - H} |B_0\rangle \quad (11.5.2.2)$$

where C runs parallel to the real E -axis in an anticlockwise sense in the upper-half plane, and $|B_0\rangle$ is a bound-like initial state of

$$H^0 = H_{\text{atom}} + \hbar\omega a^\dagger a$$

The transition amplitude to a final bound-like state $|B\rangle$ is simply

$$A_{B_0 \rightarrow B}(t) \equiv \langle B | e^{-iHt/\hbar} | B_0 \rangle = \frac{1}{2\pi i} \int_c \langle B | \frac{dE e^{-iEt/\hbar}}{E - H} | B_0 \rangle \quad (11.5.2.3)$$

The matrix element of the resolvent of H is now given by

$$\begin{aligned} \langle B | \frac{1}{E - H} | B_0 \rangle &= \langle B | u^{-1}(\theta)u(\theta) \frac{1}{E - H} u^{-1}(\theta)u(\theta) | B_0 \rangle \\ &= \langle B(\theta) | \frac{1}{E - H(\theta)} | B_0(\theta) \rangle \end{aligned} \quad (11.5.2.4)$$

where we have introduced the unitary dilatation transformation $u(\theta)$ so that

$$B_0(\theta) = u(\theta) |B_0\rangle, \quad B(\theta) = u(\theta) |B\rangle \quad (11.5.2.5)$$

and

$$H(\theta) = u(\theta) H u^{-1}(\theta) \equiv H(re^{i\theta}) \quad (11.5.2.6)$$

is the rotated Hamiltonian (11.5.1.2).

In view of the spectral properties of $H(\theta)$, noted in the previous section, the right-hand side of Eq. (11.5.1.7) provides an analytic continuation of the left-hand side into the lower-half complex E -plane. By introducing relation (11.5.2.4) in Eq. (11.5.2.3) and deforming the contour C , one obtains the new integral representation of the amplitude in terms of

the rotated Hamiltonian:

$$A_{B_0 \rightarrow B}(t) = \frac{1}{2\pi i} \int_{C'} \langle B(\theta) | \frac{dE e^{-iEt/\hbar}}{E - H(\theta)} | B_0(\theta) \rangle \quad (11.5.2.7)$$

where the contour C' is deformed to go round the complex poles of $H(\theta)$ and to run parallel to the real E -axis in an anticlockwise sense in the lower-half complex E -plane. "Integration" [cf. Eqs. (11.5.2.1) and (11.5.2.2)] yields the useful result⁽²⁴⁹⁾

$$A_{B_0 \rightarrow B}(t) = \langle B(\theta) | e^{-iH(\theta)t/\hbar} | B_0(\theta) \rangle \quad (11.5.2.8)$$

$$= \langle B(\theta) | \Psi_\theta(t) \rangle \quad (11.5.2.9)$$

where the total wave function in the new representation is

$$| \Psi_\theta(t) \rangle = e^{-iH(\theta)t/\hbar} | B_0(\theta) \rangle \quad (11.5.2.10)$$

We assume (see the next section) that the eigenvalue problem defined by the discretized $H_F(\theta)$

$$H_F(\theta) \mathbf{x}_i = \lambda_i \mathbf{x}_i \quad (11.5.2.11)$$

can be solved to obtain the right-hand eigenvectors, say \mathbf{x}_i , and the corresponding complex eigenvalues λ_i . If the discretized $H_F(\theta)$ is assumed to be symmetric, then the resolution of the identity (see Section 11.3) can be expressed in the form

$$\sum_i \mathbf{x}_i \mathbf{x}_i^T = 1 \quad (11.5.2.12)$$

where \mathbf{x}_i^T is the simple transpose of \mathbf{x}_i . With the aid of relations (11.5.2.11) and (11.5.2.12), the computational form (11.5.2.8) of the transition amplitude becomes

$$A_{B_0 \rightarrow B}(t) = \sum_i \mathbf{B}^T \mathbf{x}_i \exp(-i\lambda_i t/\hbar) \mathbf{x}_i^T \mathbf{B}_0 \quad (11.5.2.13)$$

where \mathbf{B}_0 and \mathbf{B} are vectors of overlaps $\langle j | B_0(\theta) \rangle$ and $\langle j | B(\theta) \rangle$, with respect to the basis set $\{|j\rangle\}$, of the rotated initial and final states, respectively. The corresponding transition probability

$$P_{B_0 \rightarrow B}(t) = \left| \sum_i \mathbf{B}^T \mathbf{x}_i \exp(-i\lambda_i t/\hbar) \mathbf{x}_i^T \mathbf{B}_0 \right|^2 \quad (11.5.2.14)$$

is properly interpreted as the probability averaged over the initial phase of the field, assumed to be a statistical variable which is distributed uniformly (see Sections 10.2.5 and 10.2.6).

The complex eigenvalues λ , correspond to the decaying dressed states of the system. The imaginary part of the particular λ_i , which adiabatically (as the field strength $F \rightarrow 0$) connects to the initial states, can therefore be related to the half-width of that state and hence (under nonresonant conditions) also to the “rate,” or generalized cross section, of (multi-) photoionization of the initial state.

The time evolution of the total ionization probability may be obtained from knowledge of excitation probabilities of the bound states and probability conservation:

$$P_{\text{ion}}(t) = 1 - \sum_B P_{B_0 \rightarrow B}(t) \quad (11.5.2.15)$$

This expression is particularly useful for near- (or at) resonant ionization when the significant probabilities $P_{B_0 \rightarrow B}(t)$ tend to be confined to a few (or at most a finite number of) bound states.

This method of calculating the total probability of multiphoton ionization (or dissociation) cannot give more detailed information, such as the angular distribution of the ionized electron. This can be calculated if the amplitudes for transitions into partial wave continuum states (see, e.g., Section 6.8.4) can be determined. However, since the ordinary atomic continuum states consist asymptotically of linear combinations of both ingoing and outgoing spherical waves, any attempt to rotate them would cause them to explode due to unbounded asymptotic growth of one or other spherical wave. We merely remark here that indirect means within the dilatation transformation method can be employed to avoid this difficulty.

11.5.3. The Multiphoton Eigenvalue Problem and Inverse Iteration

It is often possible to investigate either the generalized total cross sections for nonresonant multiphoton processes or the time dependence of resonant processes with the help of only a few explicit eigenvalues and vectors of $H_F(\theta)$. In that event it is useful to apply the method of inverse iteration for such a determination. Here we outline an algorithm,⁽²⁴⁹⁾ which takes special advantage of the banded structure of the space matrix $H_F(\theta)$. This algorithm begins with a zeroth-order estimate α_i (say, an unperturbed eigenvalue) of the desired complex eigenvalue λ_i of $H_F(\theta)$ and solves successively the set of linear equations

$$[H_F(\theta) - \alpha_i I] \mathbf{X}_n = \mathbf{X}_{n-1}, \quad n = 1, 2, 3, \dots \quad (11.5.3.1)$$

where I is a unit matrix and X_n is the corresponding vector in the n th iteration. Thus

$$X_n = [H_F(\theta) - \alpha_i I]^{-n} X_0 \quad (11.5.3.2)$$

where X_0 is an arbitrary starting vector, which should not be orthogonal to the eigenvectors ϕ_i of $H_F(\theta)$ [$[H_F(\theta)]\phi_i = \lambda_i \phi_i$]. One may choose $x_0 = (1, 1, 1, \dots)$ followed by normalization. Completeness of the vectors ϕ_i [of the complex symmetric Hamiltonian $H_F(\theta)$], namely

$$\sum_i \Phi_i \Phi_i^T = I \quad (11.5.3.3)$$

enables Eq. (11.5.3.1) to be expressed in the form

$$X_n = \sum_i \frac{1}{(\lambda_i - \alpha_i)^n} \Phi_i (\Phi_i^T X_0) \quad (11.5.3.4)$$

Provided α_i is closer to λ_i than to any other eigenvalue of $H_F(\theta)$, then for sufficiently large n Eq. (11.5.3.4) may be approximated by

$$X_n \approx \frac{1}{(\lambda_i - \alpha_i)^n} \Phi_i N_i \quad (11.5.3.5)$$

where $N_i = (\Phi_i^T X_0)$ is a normalization constant.

In the multiphoton problem we have the Hamiltonian structure (see Figure 54)

$$[H_F(\theta) - \alpha_i I] \equiv \begin{pmatrix} H_1 & V^T & 0 & 0 \\ V & H_2 & V^T & 0 \\ 0 & V & H_3 & V^T \\ 0 & 0 & V & \vdots \end{pmatrix} \quad (11.5.3.6)$$

where H_n and V are submatrices, each of size $(J \times J)$, where J is the number of L^2 basis functions retained. The (block) tridiagonal form permits convenient factorization of Eq. (11.5.3.6) into the upper (U) and lower (L) (block-) triangular matrices. To this end we define iteratively two auxiliary sets of submatrices

$$\begin{aligned} \Lambda_1 &= H_1 & \text{and} & U_1 = (\Lambda_1)^{-1} V^T \\ \Lambda_2 &= H_2 - VU_1 & \text{and} & U_2 = (\Lambda_2)^{-1} V^T \\ && \vdots & \\ \Lambda_i &= H_i - VU_{i-1} & \text{and} & U_i = (\Lambda_i)^{-1} V^T \end{aligned} \quad (11.5.3.7)$$

for all $i = 1, 2, 3, \dots$.

It is easily verified now that

$$[H_F(\theta) - \alpha_i I] = LU \quad (11.5.3.8)$$

where

$$U \equiv \begin{pmatrix} 1 & U_1 & 0 & 0 \\ 0 & 1 & U_2 & 0 \\ 0 & 0 & 1 & U_3 \end{pmatrix} \quad (11.5.3.9)$$

and

$$L \equiv \begin{pmatrix} \Lambda_1 & 0 & 0 & 0 \\ V & \Lambda_2 & 0 & 0 \\ 0 & V & \Lambda_3 & 0 \\ \vdots & & & \ddots \end{pmatrix} \quad (11.5.3.10)$$

In terms of Eqs. (11.5.3.8)–(11.5.3.10), Eq. (11.5.3.1) can be written as

$$LU\mathbf{X} = \mathbf{f} \quad (11.5.3.11)$$

where \mathbf{f} is a known vector (at each stage of iteration starting with X_0).

Equation (11.5.3.11) is solved in two steps. First, one solves for the vector \mathbf{g} from the equation

$$L\mathbf{g} = \mathbf{f} \quad (11.5.3.12)$$

and second, for \mathbf{X} from the equation

$$U\mathbf{X} = \mathbf{g} \quad (11.5.3.13)$$

We note that Eq. (11.5.3.12) has the structure

$$\left. \begin{array}{l} \Lambda_1 g_1 = f_1 \\ Vg_1 + \Lambda_2 g_2 = f_2 \\ Vg_2 + \Lambda_3 g_3 = f_3 \\ \vdots \\ Vg_{i-1} + \Lambda_i g_{i+1} = f_i \end{array} \right\} \quad (11.5.3.14)$$

while Eq. (11.5.3.13) has the structure

$$\left. \begin{array}{l} X_1 + U_1 X_2 = g_1 \\ X_2 + U_2 X_3 = g_2 \\ X_3 + U_3 X_4 = g_3 \\ \vdots \\ X_i + U_i X_{i+1} = g_i \\ X_N = g_N \end{array} \right\} \quad (11.5.3.15)$$

It is seen from the sets (11.5.3.7) that U_i may be obtained from the solution of the set of linear equations $\Lambda_i U_i = V^T$, and the Λ_i constructed from (11.5.3.10) and used in Eq. (11.5.3.12) to solve for g_i . By using g_i and the stored values of U_i , x_i may be generated, starting with the last relation in Eqs. (11.5.3.15). We point out that one needs to store only the values of U_i and not Λ_i for this sequence of operations. Also, the inverses in Eqs. (11.5.3.7) do not need to be calculated directly.

Having calculated the quantities x_n , the eigenvalues λ_i and vectors ϕ_i can be determined easily from relation (11.5.3.5) and the normalization condition

$$\sum_{p=1}^{p_{\max}} U_i(p) U_i(p) = 1 \quad (11.5.3.16)$$

where $U_i(p)$ is the p th component of vector U_i and $p = 1, 2, 3, \dots, p_{\max}$. For every given value of the field strength $F = (8\pi\hbar\omega n_0/L^3)^{1/2}$ and frequency ω , the eigenvalues λ_i are to be tested for numerical convergence with respect to changes in all the arbitrary variables: number (and angular symmetry) of basis functions, number of Floquet (photon) blocks N , basis scale parameter λ [see Eq. (11.5.1.5), not to be confused with eigenvalues λ_i], and finally the values of the rotation angle θ . Table 23 shows an example of the convergence of the complex eigenvalue (to five figures in the imaginary part $\Gamma/2$) as a function of these variables.

Table 23. Overall View of Convergence of the Complex Eigenvalue λ_{1s} Corresponding to the $1s$ State for an H Atom in a Laser Field of Strength F (rms) = 0.025 (au) = 0.12856×10^9 V/cm² and at (1s-2p) Resonance Frequency $\omega = 0.375$ (au) as a Function of Number (and Angular Symmetry) of Atomic Basis Functions, Basis Scale Parameter λ , Rotation Angle θ , and Number of Floquet (Photon) Blocks N (from Maquet *et al.*⁽²⁴⁹⁾)^a

Basis	λ	θ (rad)	N	λ_{1s}
15(s)15(p)15(d)	1.2	0.45	3	$-0.511946 - i1.3464 \cdot 10^{-4}$
	1.5	0.5236	3	$-0.511946 - i1.3464 \cdot 10^{-4}$
15(s)15(p)15(d)15(f)	1.2(1.5)	0.45	4	$-0.511923 - i1.3827 \cdot 10^{-4}$
	1.2(1.5)	0.5236	4	$-0.511923 - i1.3827 \cdot 10^{-4}$
10(s)10(p)10(d)10(f)10(g)	1.2(1.5)	0.45	5	$-0.511923 - i1.3824 \cdot 10^{-4}$
13(s)13(p)13(d)13(f)13(g)	1.2(1.5)	0.45	5	$-0.511923 - i1.3827 \cdot 10^{-4}$
15(s)15(p)15(d)15(f)15(g)	1.2(1.5)	0.45	5	$-0.511923 - i1.3827 \cdot 10^{-4}$
	1.2(1.5)	0.45	5	$-0.511923 - i1.3827 \cdot 10^{-4}$

^a Change in the scale parameter is indicated as 1.2(1.5) and does not affect the figures shown.

For the illustrative calculation⁽²⁴⁹⁾ with the largest basis set and $N = 5$, the dimension of the $H_F(\theta)$ matrix has been taken as 375×375 . However, results within 3% accuracy for $\Gamma/2$ have been obtained for an $N = 3$ calculation with matrix dimension 54×54 and optimized values of θ and λ . Large-scale calculations are apparently only needed to check convergence or to obtain high-precision results.

In Figure 55, the generalized two-photon dominated ionization cross section of the H(1s) state near the one-photon (1s-2p) and (1s-3p) intermediate resonances (identified by the adiabatic relation of the width of the complex dressed state reducing to the 1s-state as $F \rightarrow 0$) is exhibited for high to very high field strengths.

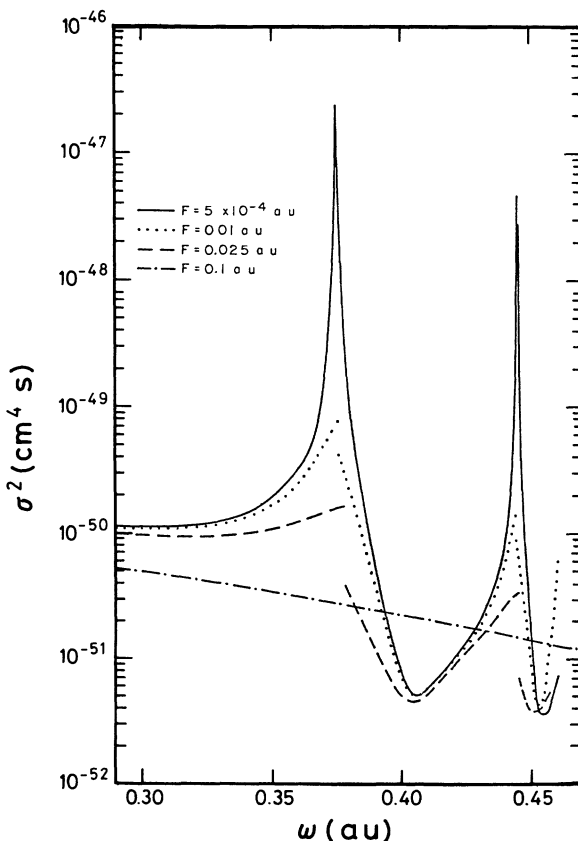


Figure 55. Intensity-dependent generalized cross section $\sigma^{(2)} \equiv \Gamma_{1s}(I)/I^2$ [$\Gamma_{1s}(I)/2$ is the imaginary part of the decaying dressed-state eigenvalue λ_{1s} , adiabatically associated with the unperturbed 1s-state energy] in units of cm^4s , for the two-photon dominated ionization of H(1s) in the region of one-photon (1s-2p) and (1s-3p) resonances, shown at four different field strengths F (from Maquet *et al.*⁽²⁴⁹⁾).

For field strengths F (rms) $< 10^{-3}$ (au) we obtain the second-order perturbation theoretical result (see Section 5.2.1). We note the progressive power-broadening of the two resonances until at $F = 0.1$ (au) $\approx 3.5 \times 10^{14}$ W/cm² they are completely quenched.

11.5.4. An Effective Hamiltonian Generated by the Non-Hermitian Floquet Method

A simple but useful application of the non-Hermitian $H_F(\theta)$ for resonant multiphoton problems is found⁽²⁵⁰⁾ in the construction of the effective Hamiltonians for the reduced (or near-resonant) p -space. This provides a nonperturbative method of constructing such Hamiltonians by invoking intuitive physical assumptions. We illustrate this for the rather ubiquitous case of atomic multiphoton transitions with one (intermediate) resonance plus possible transition into the ionization continuum. From the theory of effective Hamiltonians (see Section 7.5.2) we know that for an N -photon-induced near-resonant or resonant transition, the Hamiltonian in the space of the two “resonating states” may be given by a 2×2 effective Hamiltonian in which the off-resonant and ionizing states are implicitly “folded in.” The Hamiltonian is assumed to have the form

$$H = \begin{pmatrix} h_{11} & h_{12} \\ h_{21} & h_{22} \end{pmatrix} \quad (11.5.4.1)$$

where all h_{ij} are generally complex but symmetric ($h_{12} = h_{21}$). In the atom-field product space the resonating states may be designated by

$$|1\rangle \equiv |1, 0\rangle \quad \text{and} \quad |2\rangle \equiv |2, -N\rangle \quad (11.5.4.2)$$

where the initial field occupation number n_0 is scaled to zero, for convenience of notation. For the N -photon resonant coupling case, the matrix elements in Eq. (11.5.4.1) are assumed to have the form [cf. Eqs. (8.5.14)]

$$\begin{aligned} h_{11} &= \hbar(\omega_1 + \delta_1 - \frac{1}{2}i\gamma_1) \\ h_{22} &= \hbar(\omega_2 - N\omega + \delta_2 - \frac{1}{2}i\gamma_2) \\ h_{12} &= h_{21} = H'_{12} - \frac{1}{2}i\hbar\gamma_{12} \equiv -\hbar(\Omega + \frac{1}{2}i\beta) \end{aligned} \quad (11.5.4.3)$$

where ω_1 and ω_2 are the Bohr frequencies of the unperturbed atomic states. We note the physical significance of the parameters appearing in Eqs. (11.5.4.3) as well as their field dependence, as governed by the lowest nonvanishing-order perturbation theory [cf. Eqs. (8.5.1.5)–(8.5.1.12)].

Thus:

1. δ_1 and $\delta_2 \propto F^2$; dynamic Stark-shifts of states 1 and 2, respectively.
2. $\gamma_1 \propto F^{2(N+p)}$; ($N + p$)-photon ionization width of the lower state 1.
3. $\gamma_2 \propto F^{2p}$; p -photon ionization width of the upper state 2 (most often, for atomic targets, $p = 1$ dominates).
4. $\Omega_{12} \propto F^N$; real part of the coupling strength between the resonating states (dominated by direct N -photon coupling).
5. $\gamma_{12} \propto F^{N+2p}$; imaginary part of the coupling strength between the resonating states arising from ($N + 2p$)-photon indirect coupling via the ionization continuum.

The transition amplitudes governed by the rotated non-Hermitian Floquet Hamiltonian between states $|1\rangle \equiv |1, 0\rangle$ and $|2\rangle \equiv |2, -N\rangle$ can be written as

$$\begin{aligned} a_{1 \rightarrow 2}(t) &= \langle 2, -N | \exp(-iH_F(\theta)t/\hbar) | 1, 0 \rangle \\ &= \sum_i \langle 2, -N | \lambda_i \rangle \exp(-i\lambda_i t/\hbar) \langle \lambda_i^* | 1, 0 \rangle \end{aligned} \quad (11.5.4.4)$$

where $|\lambda_i\rangle$ and $\langle \lambda_i^*|$ ($= |\lambda_i\rangle^T$) are the set of right and left eigenvectors (with eigenvalues λ_i) of the rotated Floquet Hamiltonian $H_F(\theta)$.

We let λ_1 and λ_2 be the complex eigenvalues, which evolve from (and hence correlate to) the unperturbed eigenvalues of $|1\rangle \equiv |1, 0\rangle$ and $|2\rangle \equiv |2, -N\rangle$, respectively. In view of the resonant character of the unperturbed states $|1\rangle$ and $|2\rangle$, one expects the amplitudes of these two states to dominate over the amplitudes of all the other (off-resonant) discrete states. It is also expected that the “perturbed” eigenstates $|\lambda_1\rangle$ and $|\lambda_2\rangle$, which correlate to the unperturbed states $|1\rangle$ and $|2\rangle$ respectively, should also dominate in a like manner. To the extent that this expectation is justified, one may approximate the right-hand side of Eq. (11.5.4.4) by retaining only states $|\lambda_1\rangle$ and $|\lambda_2\rangle$ in the intermediate sums

$$\begin{aligned} a_{1 \rightarrow 2}(t) &= \langle 2, -N | \lambda_1 \rangle \exp(-i\lambda_1 t/\hbar) \langle \lambda_1^* | 1, 0 \rangle \\ &\quad + \langle 2, -N | \lambda_2 \rangle \exp(-i\lambda_2 t/\hbar) \langle \lambda_2^* | 1, 0 \rangle \end{aligned} \quad (11.5.4.5)$$

On the other hand, the solution of the transition amplitude governed by Hamiltonian (11.5.4.1) for transition $|1\rangle \rightarrow |2\rangle$ may be directly obtained in the form

$$b_{1 \rightarrow 2}(t) = \frac{\hbar_{12}}{E_+ - E_-} (e^{-iE_+ t/\hbar} - e^{-iE_- t/\hbar}) \quad (11.5.4.6)$$

Table 24. Two-Level Effective Hamiltonian Parameters in Atomic Units for Photon Ionization of H(1s) for Several Detunings and Field Strengths (from Holt *et al.*⁽²⁵⁰⁾)^a

ω	Δ	Ω	β	γ_1	γ_2	δ_1	δ_2
<i>F</i> = 0.001 au							
0.350	-2.500(-2)	7.450(-4)	3.1(-9)	7.4(-11)	3.53(-7)	-9.33(-7)	3.36(-6)
0.360	-1.500(-2)	7.449(-4)	2.7(-9)	7.6(-11)	3.12(-7)	-9.79(-7)	3.18(-6)
0.370	-5.004(-3)	7.449(-4)	2.5(-9)	1.3(-10)	2.77(-7)	-1.04(-6)	3.01(-6)
0.375	-3.982(-6)	7.449(-4)	2.9(-9)	6.0(-10)	2.61(-7)	-1.07(-6)	2.92(-6)
0.380	4.996(-3)	7.449(-4)	3.2(-9)	1.0(-10)	2.46(-7)	-1.11(-6)	2.84(-6)
0.390	1.500(-2)	7.449(-4)	2.8(-9)	4.5(-11)	2.20(-7)	-1.21(-6)	2.70(-6)
0.400	2.500(-2)	7.449(-4)	2.4(-9)	3.3(-11)	1.97(-7)	-1.25(-6)	2.57(-6)
<i>F</i> = 0.005 au							
0.350	-2.511(-2)	3.727(-3)	3.9(-7)	4.6(-8)	8.80(-6)	-2.91(-5)	8.38(-5)
0.360	-1.510(-2)	3.726(-3)	3.5(-7)	4.8(-8)	7.77(-6)	-2.42(-5)	7.91(-5)
0.370	-5.099(-3)	3.725(-3)	3.2(-7)	6.8(-8)	6.87(-6)	-2.51(-5)	7.43(-5)
0.375	-9.711(-5)	3.723(-3)	3.6(-7)	9.1(-8)	6.45(-6)	-2.54(-5)	7.17(-5)
0.380	4.903(-3)	3.721(-3)	3.9(-7)	5.7(-8)	6.12(-6)	-2.70(-5)	7.03(-5)
0.390	1.490(-2)	3.720(-3)	3.4(-7)	2.9(-8)	5.48(-6)	-2.99(-5)	6.72(-5)
0.400	2.490(-2)	3.720(-3)	3.0(-7)	2.2(-8)	4.91(-6)	-3.34(-5)	6.40(-5)
<i>F</i> = 0.01 au							
0.350	-2.542(-2)	7.459(-3)	3.1(-6)	7.2(-7)	3.49(-5)	-8.95(-5)	3.32(-4)
0.360	-1.540(-2)	7.457(-3)	2.8(-6)	7.2(-7)	3.07(-5)	-9.25(-5)	3.12(-4)
0.370	-5.385(-3)	7.448(-3)	2.7(-6)	8.4(-7)	2.71(-5)	-9.43(-5)	2.91(-4)
0.375	-3.767(-4)	7.436(-3)	2.8(-6)	8.8(-7)	2.55(-5)	-9.59(-5)	2.81(-4)
0.380	4.624(-3)	7.423(-3)	2.9(-6)	7.3(-7)	2.41(-5)	-1.02(-4)	2.75(-4)
0.390	1.462(-2)	7.415(-3)	2.7(-6)	4.7(-7)	2.17(-5)	-1.16(-4)	2.65(-4)
0.400	2.462(-2)	7.412(-3)	2.4(-6)	3.5(-7)	1.95(-5)	-1.31(-4)	2.53(-4)

^a ω denotes laser frequency, Δ detuning, Ω Rabi frequency, β “imaginary” Rabi frequency, γ_1 , γ_2 ionization widths of $|1\rangle$ and $|2\rangle$, δ_1 , δ_2 dynamic Stark shifts of $|1\rangle$ and $|2\rangle$, F electric field amplitude. A field strength of $F = 1.0$ au corresponds to an intensity of 3.51×10^{16} W/cm²; a circular frequency of 1.0 au corresponds to 4.134×10^{16} rad/s. The entry -2.500(-2) is an abbreviation for -2.500×10^{-2} , etc.

where E_{\pm} are the eigenvalues of Hamiltonian (11.5.4.1) given by

$$E_{+} = \frac{h_{11} + h_{22}}{2} + \left[\left(\frac{h_{11} - h_{22}}{2} \right)^2 + h_{12}^2 \right]^{1/2} \quad (11.5.4.7)$$

and

$$E_{-} = \frac{h_{11} + h_{22}}{2} - \left[\left(\frac{h_{11} - h_{22}}{2} \right)^2 + h_{12}^2 \right]^{1/2} \quad (11.5.4.8)$$

Since with the onset of the field E_{+} evolves from the unperturbed

Table 25. Two-Level Effective Hamiltonian Parameters in Atomic Units for Three-Photon Ionization of H(1 s) for Several Detunings and Field Strengths (from Holt *et al.*⁽²⁵⁰⁾)^a

ω	Δ	Ω	β	γ_2	δ_1	δ_2
<i>F</i> = 0.001 au						
0.18500	-5.009(-3)	3.98(-6)		6.70(-6)	-1.42(-6)	7.65(-6)
0.18650	-2.009(-3)	3.95(-6)		6.52(-6)	-1.43(-6)	7.54(-6)
0.18700	-1.009(-3)	3.95(-6)		6.47(-6)	-1.43(-6)	7.50(-6)
0.18725	-5.089(-4)	3.93(-6)		6.44(-6)	-1.43(-6)	7.48(-6)
0.18745	-1.089(-4)	3.94(-6)		6.42(-6)	-1.42(-6)	7.46(-6)
0.18750	-8.891(-6)	3.93(-6)		6.41(-6)	-1.43(-6)	7.47(-6)
0.18775	4.911(-4)	3.93(-6)		6.38(-6)	-1.43(-6)	7.45(-6)
0.18800	9.911(-4)	3.94(-6)		6.36(-6)	-1.43(-6)	7.42(-6)
<i>F</i> = 0.005 au						
0.1850	-5.227(-3)	9.94(-5)	2.3(-7)	1.67(-4)	-3.55(-5)	1.91(-4)
0.1865	-2.224(-3)	9.84(-5)	2.2(-7)	1.63(-4)	-3.56(-5)	1.89(-4)
0.1870	-1.223(-3)	9.81(-5)	2.3(-7)	1.62(-4)	-3.57(-5)	1.88(-4)
0.1875	-2.225(-4)	9.78(-5)	2.2(-7)	1.60(-4)	-3.58(-5)	1.87(-4)
0.1880	7.785(-4)	9.80(-5)	2.6(-7)	1.59(-4)	-3.58(-5)	1.86(-4)
0.1885	1.779(-3)	9.83(-5)	2.5(-7)	1.58(-4)	-3.59(-5)	1.85(-4)
0.1900	4.782(-3)	9.93(-5)	2.4(-7)	1.54(-4)	-3.60(-5)	1.82(-4)
0.1950	1.479(-2)	1.03(-4)	2.1(-7)	1.41(-4)	-3.66(-5)	1.73(-4)
<i>F</i> = 0.010 au						
0.1850	-5.909(-3)	3.93(-4)	3.9(-6)	6.72(-4)	-1.42(-4)	7.67(-4)
0.1865	-2.898(-3)	3.89(-4)	3.4(-6)	6.54(-4)	-1.43(-4)	7.55(-4)
0.1870	-1.895(-3)	3.88(-4)	3.4(-6)	6.49(-4)	-1.43(-4)	7.52(-4)
0.1875	-8.925(-3)	3.87(-4)	3.4(-6)	6.43(-4)	-1.44(-4)	7.49(-4)
0.1880	1.129(-4)	3.86(-4)	3.9(-6)	6.33(-4)	-1.43(-4)	7.44(-4)
0.1885	1.117(-3)	3.87(-4)	4.0(-6)	6.31(-4)	-1.43(-4)	7.44(-4)
0.1900	4.126(-3)	3.91(-4)	3.9(-6)	6.16(-4)	-1.44(-4)	7.29(-4)
0.1950	1.416(-2)	4.05(-4)	3.3(-6)	5.66(-4)	-1.47(-4)	6.95(-4)
$\gamma_1 = 5.7 \times 10^{-8}$ ($\omega = 0.185$, $F = 0.01$)						
$\gamma_1 = 5.0 \times 10^{-8}$ ($\omega = 0.195$, $F = 0.01$)						

^a ω denotes laser frequency, Δ detuning, Ω Rabi frequency, β “imaginary” Rabi frequency, γ_2 ionization widths of $|2\rangle$, δ_1 , δ_2 dynamic Stark shifts of $|1\rangle$ and $|2\rangle$, F electric field strength. A field strength of $F = 1.0$ au corresponds to an intensity of 3.51×10^{16} W/cm²; a circular frequency of 1.0 au corresponds to 4.134×10^{16} rad/s. The entry -5.009(-3) is an abbreviation for -5.009×10^{-3} , etc.

eigenvalue of state $|1\rangle$ and E_- from that of $|2\rangle$, one may identify eigenvalues λ_1 and λ_2 as

$$\lambda_1 = E_+ \quad \text{and} \quad \lambda_2 = E_- \quad (11.5.4.9)$$

The solution of Eqs. (11.5.4.7)–(11.5.4.9) easily gives the diagonal matrix

elements in terms of the eigenvalues and h_{12} :

$$h_{11} = \frac{\lambda_1 + \lambda_2}{2} + \left[\left(\frac{\lambda_1 - \lambda_2}{2} \right)^2 - h_{12}^2 \right]^{1/2} \quad (11.5.4.10)$$

$$h_{22} = \frac{\lambda_1 + \lambda_2}{2} - \left[\left(\frac{\lambda_1 - \lambda_2}{2} \right)^2 - h_{12}^2 \right]^{1/2} \quad (11.5.4.11)$$

Comparison of amplitudes (11.5.4.5) and (11.5.4.6) for the same transition $|1\rangle \rightarrow |2\rangle$ also yields h_{12} :

$$\begin{aligned} h_{12} = & (\lambda_1 - \lambda_2) \langle 2, -N | \lambda_1 \rangle \langle \lambda_1^* | 1, 0 \rangle \\ & + (\lambda_2 - \lambda_1) \langle 2, -N | \lambda_2 \rangle \langle \lambda_2^* | 1, 0 \rangle \end{aligned} \quad (11.5.4.12)$$

Table 26. Two-Level Effective Hamiltonian Parameters in Atomic Units for Four-Photon Ionization of H(1s) for Several Detunings and Field Strengths (from Holt *et al.*⁽²⁵⁰⁾)^a

ω	Δ	Ω	β	γ_2	δ_1	δ_2
<i>F</i> = 0.0010 au						
0.14810	-1.582(-4)	2.71(-8)		3.31(-6)	-1.30(-6)	1.24(-5)
0.14812	-9.816(-5)	2.67(-8)		3.31(-6)	-1.30(-6)	1.24(-5)
0.14884	-3.816(-5)	2.69(-8)		3.31(-6)	-1.30(-6)	1.24(-5)
0.14816	2.184(-5)	2.68(-8)		3.30(-6)	-1.30(-6)	1.24(-5)
0.14817	5.184(-5)	2.69(-8)		3.30(-6)	-1.30(-6)	1.24(-5)
0.14820	1.418(-4)	2.69(-8)		3.30(-6)	-1.30(-6)	1.24(-5)
<i>F</i> = 0.0050 au						
0.14790	-1.083(-3)	3.27(-6)	1.6(-8)	8.27(-5)	-3.24(-5)	3.07(-4)
0.14822	-1.222(-4)	3.24(-6)	1.7(-8)	8.20(-5)	-3.24(-5)	3.05(-4)
0.14825	-3.208(-5)	3.24(-6)	1.7(-8)	8.19(-5)	-3.24(-5)	3.05(-4)
0.14828	5.804(-5)	3.23(-6)	1.6(-8)	8.19(-5)	-3.24(-5)	3.05(-4)
0.14830	1.181(-4)	3.23(-6)	1.6(-8)	8.19(-5)	-3.24(-5)	3.05(-4)
0.14860	1.019(-3)	3.20(-6)	1.7(-8)	8.12(-5)	-3.25(-5)	3.04(-4)
<i>F</i> = 0.010 au						
0.1482	-1.092(-3)	2.32(-5)	4.9(-7)	3.20(-4)	-1.30(-4)	1.12(-3)
0.1484	-4.903(-4)	2.31(-5)	4.9(-7)	3.19(-4)	-1.30(-4)	1.12(-3)
0.1485	-1.893(-4)	2.30(-5)	4.9(-7)	3.18(-4)	-1.30(-4)	1.11(-3)
0.1487	4.134(-4)	2.29(-5)	4.8(-7)	3.16(-4)	-1.30(-4)	1.11(-3)
0.1488	7.144(-4)	2.28(-5)	4.8(-7)	3.16(-4)	-1.30(-4)	1.11(-3)
0.1491	1.618(-3)	2.26(-5)	4.7(-7)	3.13(-4)	-1.30(-4)	1.11(-3)

^a ω denotes laser frequency, Δ detuning, Ω Rabi frequency, β “imaginary” Rabi frequency, γ_2 ionization widths of $|2\rangle$, δ_1 , δ_2 dynamic Stark shifts of $|1\rangle$ and $|2\rangle$, F electric field strength. A field strength of $F = 1.0$ au corresponds to an intensity of 3.51×10^{16} W/cm²; a circular frequency of 1.0 au corresponds to 4.1341×10^{-6} rad/s. The entry -1.582(-4) is an abbreviation for -1.582×10^{-4} , etc.

Equations (11.5.4.10)–(11.5.4.12) show that knowledge of the eigenvalues λ_1 and λ_2 of $H_F(\theta)$ and the eigenvector components $\langle 2, -N | \lambda_i \rangle$ and $\langle \lambda_i^* | 1, 0 \rangle$, $i = 1, 2$, suffices to determine all the matrix elements h_{ij} of the effective Hamiltonian (11.5.4.1). Finally, by equating the real and imaginary parts of Eqs. (11.5.4.9)–(11.5.4.12) with those of Eqs. (11.5.4.3) one may explicitly determine the values of all the parameters δ_1 , δ_2 , γ_1 , γ_2 , Ω , and β as a function of the field variables.

Once they are known the transition probability for the resonant excitation, the survival probability of the initial state, as well as the ionization probability (both time-dependent and steady-state) can be obtained immediately from the explicit expressions (7.4.4), (7.4.13), (7.4.15), and (7.4.17), respectively. Tables 24–26 present numerical values⁽²⁵⁰⁾ of these parameters obtained from the roots and vectors of $H_F(\theta)$ for two-, three-, and four-photon ionization of H(1s), for a number of frequencies ω , detunings Δ where

$$\Delta \equiv N\omega - (\omega_2 + \delta_2 - \omega_1 - \delta_1) \quad (11.5.4.13)$$

and for a set of (peak) field strengths F .

12

Theory of Radiative Electron–Atom Scattering

12.1. Introduction

By radiative scattering we simply mean scattering of electrons from atomic targets in the presence of the radiation field. The relative complexity and richness of the theory of radiative scattering is due primarily to the fact that for every channel of scattering in the absence of the field, there arises a multitude of subchannels corresponding to real and virtual multiphoton emission and absorption processes. Generally, both the projectile electron and the target atom take part in the emission and absorption process during the scattering. A systematic theory of radiative scattering, comparable to the theory of ordinary electron–atom scattering, must therefore be able to account for these channels in a manageable way. Another special circumstance associated with radiative electron–atom scattering is the problem of the initial distributions of the states of the system. Unlike ordinary scattering, the projectile electron may find the target atom not just in the thermal-equilibrium state but rather in a certain superposition of field-modified states (usually far from thermal equilibrium). This situation is further complicated by the possibility that such a superposition state of the target atom may also decay due, among other things, to the incoherent influence of spontaneous emission and (multiphoton) ionization. The problem of how to relate the scattering amplitudes, as defined with respect to a given pair of “initial” and “final” states, to the observable differential scattering signals is treated subsequently.

In principle, radiative scattering theory can be formulated either in the (semiclassical) time-dependent formalism or in the stationary number-state formalism. In the “laser approximation” they are equivalent. Since a stationary formulation permits a description closely resembling the usual

electron-atom scattering theory, we shall mainly adopt such a description; explicit time dependence will be recovered easily whenever deemed necessary.

We shall also find it convenient to adopt the “velocity form” of the interaction Hamiltonian and assume that the A^2 term has been properly removed by the renormalization procedure, as shown in Section 1.11.

Before we develop the general theory of radiative electron-atom scattering we consider the simpler problem of radiative potential scattering. This will help define, among other things, the notion of the asymptotic states of the scattering electron inside the field and certain basic properties of the corresponding scattering amplitudes.

12.2. Potential Scattering in a Laser Field

The stationary Hamiltonian of a free electron in the presence of the field is

$$H = H^0 + V(\mathbf{r}) \quad (12.2.1)$$

where

$$H^0 = -\frac{\hbar^2 \nabla^2}{2\mu} + \hbar\omega a^+ a + \frac{ie\hbar}{\mu c} \nabla \cdot \mathbf{A} \quad (12.2.2)$$

and $V(\mathbf{r})$ is the scattering potential. The vector-potential operator in the dipole approximation is

$$\mathbf{A} = \begin{cases} \left(\frac{8\pi\hbar c^2}{L^3\omega}\right)^{1/2} \frac{\varepsilon_z}{2} (a^+ + a) & \text{(linear polarization)} \end{cases} \quad (12.2.3)$$

$$\mathbf{A} = \begin{cases} \left(\frac{8\pi\hbar c^2}{L^3\omega}\right)^{1/2} \frac{1}{2}[(\varepsilon_x + i\varepsilon_y)a^+ + (\varepsilon_x - i\varepsilon_y)a] & \text{(circular polarization)} \end{cases} \quad (12.2.4)$$

where ε_x , ε_y , and ε_z are unit polarization vectors in the indicated directions. We introduce the usual “laser approximation,” namely Eq. (6.4.8), for the field \mathbf{A} , which is assumed to have a large initial occupation number n_0 , and count all photon occupation numbers n from n_0 . Thus

$$A_0 = \frac{c}{\omega} F_0 = \left(\frac{8\pi\hbar c^2 n_0}{L^3\omega}\right)^{1/2} \quad (12.2.5)$$

is the peak strength of the vector potential and F_0 is the peak electric field.

12.2.1. The Floquet Equation for Radiative Potential Scattering

We expand the solution of the Schrödinger equation of the scattering electron

$$H^0 |\psi\rangle = V(\mathbf{r}) |\psi\rangle \quad (12.2.1.1)$$

in the form

$$|\psi\rangle = \sum_{n=-\infty}^{\infty} F_n(\mathbf{r}) |n\rangle \quad (12.2.1.2)$$

and project on the state $|n\rangle$ to obtain (in the ordinary space)

$$[E - H_n^{(0)}] F_n(\mathbf{r}) = V(\mathbf{r}) F_n(\mathbf{r}) \quad (12.2.1.3)$$

where

$$H_n^{(0)} = \begin{cases} -\frac{\hbar^2 \nabla^2}{2\mu} + n\hbar\omega + i\hbar \frac{\omega}{2} \alpha_0 \nabla_z (s_n^+ + s_n^-) & \text{(linear polarization)} \\ -\frac{\hbar^2 \nabla^2}{2\mu} + n\hbar\omega + \frac{i\hbar\omega}{2} \alpha_0 (\nabla^- s_n^+ + \nabla^+ s_n^-) & \text{(circular polarization)} \end{cases} \quad (12.2.1.4)$$

with

$$\nabla^\pm = \nabla_x \pm i\nabla_y \quad (12.2.1.6)$$

The quantity $\alpha_0 = (eF_0)/(\mu\omega^2)$ is a “radius of vibration” of the electron in the field. The “index shifters” are defined by

$$s_n^\pm F_n \equiv F_{n\pm1} \quad (12.2.1.7)$$

12.2.2. Asymptotic Wave Functions

We shall first consider solutions of Eq. (12.2.1.3) without $V(\mathbf{r})$, namely

$$[E - H_n^{(0)}] F_n^{(0)}(\mathbf{r}) = 0 \quad (12.2.2.1)$$

such that the wave function $|\psi(\mathbf{r})\rangle$ satisfies the scattering boundary condition in the asymptotic region. We verify that a solution of Eq. (12.2.2.1) is given by

$$F_n^{(0)}(\mathbf{r}) = e^{i\mathbf{k}\cdot\mathbf{r}} J_n(k_z \alpha_0) \quad \text{(linear polarization)} \quad (12.2.2.2)$$

or

$$F^{(0)}(\mathbf{r}) = e^{i\mathbf{k}\cdot\mathbf{r}} J_n(k^\perp \alpha_0) e^{in\phi_k} \quad (\text{circular polarization}) \quad (12.2.2.3)$$

The functions J_n are the usual Bessel functions of integral order n , $k_z = \cos \theta_k$, and $k^\perp = k \sin \theta_k$; the direction of the wave vector \mathbf{k} is denoted by (θ_k, φ_k) .

Substitution of expression (12.2.2.2) in Eq. (12.2.2.1) yields

$$(E - H_n^{(0)}) F_n(\mathbf{r}) = \left[E - \left(\frac{\hbar^2 k^2}{2\mu} + n\hbar\omega \right) \right] e^{i\mathbf{k}\cdot\mathbf{r}} J_n(\alpha_0 \cdot \mathbf{k}) + \frac{\hbar\omega}{2} (\alpha_0 k_z) e^{i\mathbf{k}\cdot\mathbf{r}} [J_{n+1}(\mathbf{k} \cdot \boldsymbol{\alpha}_0) + J_{n-1}(\mathbf{k} \cdot \boldsymbol{\alpha}_0)] \quad (12.2.2.4)$$

We may simplify the quantity in the second set of square brackets by using the Bessel identity

$$J_{p+1}(x) + J_{p-1}(x) = \frac{2p}{x} J_p(x) \quad (12.2.2.5)$$

Hence the right-hand side of expression (12.2.2.4) vanishes provided

$$E = \frac{\hbar^2 k^2}{2\mu} \quad (12.2.2.6)$$

is the kinetic energy of the free electron. On combining Eqs. (12.2.2.1) and (12.2.1.2) we immediately find the solution of wave equation (12.2.1.1) without the potential,

$$|\psi^{(0)}\rangle = e^{i\mathbf{k}\cdot\mathbf{r}} \sum_{n=-\infty}^{\infty} J_n(\mathbf{k} \cdot \boldsymbol{\alpha}_0) |n\rangle \quad (12.2.2.7)$$

In view of the equivalence of $H_n^{(0)}$ with the Floquet Hamiltonian we may write down the semiclassical version of Eq. (12.2.2.7) by using the “substitution rule”

$$|n\rangle \rightarrow e^{in(\omega t + \delta) - iEt/\hbar} \quad (12.2.2.8)$$

Thus the time-dependent solution is

$$\psi^{(0)}(\mathbf{r}, t) = e^{i\mathbf{k}\cdot\mathbf{r}} \sum_{n=-\infty}^{\infty} J_n(\mathbf{k} \cdot \boldsymbol{\alpha}_0) e^{in(\omega t + \delta) - iEt/\hbar} \quad (12.2.2.9)$$

which should be compared with Eq. (1.7.1.1.4).

Solution (12.2.2.7) would constitute an appropriate scattering state provided it passes over adiabatically to the standard plane-wave state outside the field. If we note the usual relation between the Bessel function and the Kronecker delta,

$$J_p(0) = \delta_{p,0} \quad (12.2.2.10)$$

it is seen that as the field strength $F_0 \rightarrow 0$ (across the boundary), Eq. (12.2.2.7) goes over to the plane wave $e^{i\mathbf{k}\cdot\mathbf{r}}$, as required. We observe that the external radiation field of interest is of macroscopic dimension ($\geq 10^6$ Bohr radii, e.g., for a usual laser beam or pulse). Consequently these states (even when inside the field) satisfy the asymptotic condition insofar as the (scattering) potential is concerned, since the latter is of microscopic extension (say, 10 Bohr radii).

12.2.3. Green's Function for an Electron in a Dipole Radiation Field

In the development of the scattering amplitude it is useful to obtain an explicit expression for Green's function G^0 of the electron inside the field, where by definition

$$(E_0 - H^0)G^0 = \delta(\mathbf{r} - \mathbf{r}')I \quad (12.2.3.1)$$

H^0 is defined by expression (12.2.2) and I is the unit operator in the occupation number space

$$I = \sum_n |n\rangle\langle n| \quad (12.2.3.2)$$

We first introduce the expansion

$$G^0 = \sum_{n,n'=-\infty}^{\infty} |n\rangle G_{nn'}^0(\mathbf{r}, \mathbf{r}')\langle n'| \quad (12.2.3.3)$$

Substitution of Eq. (12.2.3.3) in relation (12.2.3.1) and projection from the left on $\langle n |$ and from the right on $| n' \rangle$ give the equation governing Green's function $G_{nn'}^0(\mathbf{r}, \mathbf{r}')$:

$$[E - H_n^{(0)}]G_{nn'}^0(\mathbf{r}, \mathbf{r}') = \delta(\mathbf{r} - \mathbf{r}')\delta_{nn'} \quad (12.2.3.4)$$

where $H_n^{(0)}$ is defined in Eq. (12.2.1.4) or (12.2.1.5). The solution of Eq. (12.2.3.4) is

$$G_{nn'}^0(\mathbf{r}, \mathbf{r}') = \sum_{\mathbf{k}} \sum_{N=-\infty}^{\infty} \frac{J_{n-N}(\mathbf{k} \cdot \boldsymbol{\alpha}_0) e^{i\mathbf{k} \cdot (\mathbf{r}-\mathbf{r}')}}{E - \varepsilon_k - N\hbar\omega} J_{n'-N}(\mathbf{k} \cdot \boldsymbol{\alpha}_0) \quad (12.2.3.5)$$

(linear polarization)

$$G_{nn'}^0(\mathbf{r}, \mathbf{r}') = \sum_{\mathbf{k}} \sum_{N=-\infty}^{\infty} \frac{J_{n-N}(\alpha_0 k \sin \theta_k) e^{in\phi_k} e^{i\mathbf{k}\cdot(\mathbf{r}-\mathbf{r}')}}{E - \epsilon_k - N\hbar\omega} e^{-in'\phi_k} J_{n'-N}(\alpha_0 k \sin \theta_k)$$

(circular polarization) (12.2.3.6)

We use the abbreviation

$$\sum_{\mathbf{k}} \equiv \left(\frac{1}{2\pi} \right)^3 \int d\mathbf{k} \quad (12.2.3.7)$$

throughout this chapter. The validity of Green's function (12.2.3.5), and hence of expansion (12.2.3.3), can be verified by substitution in Eq. (12.2.3.4) and noting that

$$\sum_{\mathbf{k}, N} J_{n-N}(x) e^{i\mathbf{k}\cdot(\mathbf{r}-\mathbf{r}')} J_{n'-N}(x) = \delta_{nn'} \delta(\mathbf{r} - \mathbf{r}') \quad (12.2.3.8)$$

This relation follows from the summation theorem of Bessel functions

$$\sum_{p=-\infty}^{\infty} J_{n-p}(t) J_{n'-p}(z) = J_{n-n'}(t-z) \quad (12.2.3.9)$$

and

$$\sum_{\mathbf{k}} e^{i\mathbf{k}\cdot(\mathbf{r}-\mathbf{r}')} = \delta(\mathbf{r} - \mathbf{r}') \quad (12.2.3.10)$$

The validity of Green's function (12.2.3.6) in the case of circular polarization is easily established in an analogous way.

The corresponding time-dependent Green's function is defined by the equation

$$\left\{ i\hbar \frac{\partial}{\partial t} - \left[-\frac{\hbar^2}{2\mu} \nabla^2 - \frac{ie}{\mu c} \mathbf{p} \cdot \mathbf{A}(t) \right] \right\} G^0(\mathbf{r}, \mathbf{r}'; t, t') = \delta(\mathbf{r} - \mathbf{r}') \delta(t - t') \quad (12.2.3.11)$$

The substitution rule (12.2.2.7) and the stationary Green's function (12.2.3.5) enable the solution of Eq. (12.2.3.11) to be immediately written down in the form

$$\begin{aligned} G^0(\mathbf{r}, \mathbf{r}'; t, t') &= \frac{1}{2\pi\hbar} \int_{-\infty}^{\infty} e^{-iE(t-t')/\hbar} \sum_{n, n'=-\infty}^{\infty} e^{in(\omega t + \delta)} G_{nn'}^0(\mathbf{r}, \mathbf{r}'; E) e^{-in'(\omega t' + \delta)} dE \\ &= -\frac{i}{\hbar} \theta(t - t') \sum_{\mathbf{k}} \exp \left[-\frac{i\hbar k^2}{2\mu} (t - t') \right] \end{aligned} \quad (12.2.3.12)$$

$$\times \exp \{ i\mathbf{k} \cdot (\mathbf{r} - \mathbf{r}') + i\mathbf{k} \cdot \boldsymbol{\alpha}_0 [\sin(\omega t + \delta) - \sin(\omega t' + \delta)] \} \quad (12.2.3.13)$$

where we have used the integral representation of the step function

$$\theta(t - t') = -\frac{1}{2\pi i} \int_{-\infty}^{\infty} d\lambda \frac{e^{-i\lambda(t-t')}}{\lambda + i\varepsilon} \quad (12.2.3.14)$$

$$= \begin{cases} 1, & t > t' \\ 0, & t < t' \end{cases} \quad (12.2.3.15)$$

12.2.4. The Scattered Wave and the Scattering Amplitude

The scattering wave function $F_n(\mathbf{r})$ satisfying Eq. (12.2.1.3) can be written with the help of expression (12.2.3.5) in the form

$$F_n(\mathbf{r}) = F_n^{(0)}(\mathbf{r}) + \sum_n \int d\mathbf{r}' G_{nn'}^0(\mathbf{r}, \mathbf{r}') V(\mathbf{r}') F_{n'}(\mathbf{r}') \quad (12.2.4.1)$$

To find the scattering amplitude we first take the limit $r \rightarrow \infty$ and integrate over $d\mathbf{k}$ in Eq. (12.2.3.5) to obtain

$$\lim_{r \rightarrow \infty} G_{nn'}^0(\mathbf{r}, \mathbf{r}') = \sum_{N=-\infty}^{\infty} \frac{e^{ik_N r}}{r} J_{n-N}(\boldsymbol{\alpha}_0 \cdot \mathbf{k}_N) \left(-\frac{\mu}{2\pi\hbar^2} \right) J_{n'-N}(\boldsymbol{\alpha}_0 \cdot \mathbf{k}_N) e^{i\mathbf{k}_N \cdot \mathbf{r}'} \quad (12.2.4.2)$$

where $\mathbf{k}_N = k_N \Omega$ with $k_N^2 = (E - N\hbar\omega)^2/2\mu/\hbar^2$ and Ω is a unit vector in the scattering direction: $\Omega = (\theta, \phi)$. If relation (12.2.4.2) is substituted in Eq. (12.2.4.1), we obtain the asymptotic form of the spatial part of the scattered wave:

$$\begin{aligned} F_n(\mathbf{r}) &= e^{i\mathbf{k}_0 \cdot \mathbf{r}} J_n(\boldsymbol{\alpha}_0 \cdot \mathbf{k}_0) + \sum_{N=-\infty}^{\infty} \frac{e^{ik_N r}}{r} J_{n-N}(\boldsymbol{\alpha}_0 \cdot \mathbf{k}_N) \\ &\times \sum_{n'=-\infty}^{\infty} \left(-\frac{\mu}{2\pi\hbar^2} \right) J_{n'-N}(\boldsymbol{\alpha}_0 \cdot \mathbf{k}_N) \langle e^{i\mathbf{k}_N \cdot \mathbf{r}'} | V(\mathbf{r}') | F_{n'}(\mathbf{r}') \rangle \end{aligned} \quad (12.2.4.3)$$

On combining this equation with expression (12.2.1.2), we find that the total wave vector is given by

$$\begin{aligned} |\psi\rangle &= e^{i\mathbf{k}_0 \cdot \mathbf{r}} \sum_{n=-\infty}^{\infty} J_n(\boldsymbol{\alpha}_0 \cdot \mathbf{k}_0) |n\rangle \\ &+ \sum_{N=-\infty}^{\infty} \frac{e^{ik_N r}}{r} \sum_n J_{n-N}(\boldsymbol{\alpha}_0 \cdot \mathbf{k}_N) |n\rangle f_N(\mathbf{k}_0 \rightarrow \mathbf{k}_N) \end{aligned} \quad (12.2.4.4)$$

where we have introduced the notation

$$f_N(\mathbf{k}_0 \rightarrow \mathbf{k}_N) \equiv \sum_{n=-\infty}^{\infty} \left(-\frac{\mu}{2\pi\hbar^2} \right) J_{n-N}(\boldsymbol{\alpha}_0 \cdot \mathbf{k}_N) \langle e^{i\mathbf{k}_N \cdot \mathbf{r}'} | V(\mathbf{r}') | F_{n'}(\mathbf{r}') \rangle \quad (12.2.4.5)$$

We observe that Eq. (12.2.4.4) enables the scattering amplitude to be defined in two different ways. The first term in Eq. (12.2.4.4) is clearly the incident plane wave “dressed” by the field, while each term of the sum over N is associated with an outgoing spherical wave $e^{ik_N r}/r$, also “dressed” by the field. Clearly, with respect to the ratio of the “dressed” incident and “dressed” outgoing wave for each N , the scattering amplitude is just $f_N(\mathbf{k}_0 \rightarrow \mathbf{k})$ and is given by Eq. (12.2.4.5). This corresponds to the amplitude for emission or absorption of N photons and the change of electron momentum from \mathbf{k}_0 to \mathbf{k} . This definition is consistent with respect to the field-modified (“dressed”) asymptotic states defined earlier. On the other hand, one may still like to define the scattering amplitude in the usual manner, namely with respect to the ratio of the unperturbed (“bare”) spherical waves to the unperturbed (“bare”) plane waves. It is noteworthy in this context that the average flux associated with the incident wave (or the scattered waves) in both representations is identical. This follows from the identity

$$\left[\sum_{n=-\infty}^{\infty} J_{n-N}(\mathbf{k} \cdot \boldsymbol{\alpha}_0) |n\rangle \right]^+ \left[\sum_{n'=-\infty}^{\infty} J_{n'-N}(\mathbf{k} \cdot \boldsymbol{\alpha}_0) |n'\rangle \right] = \sum_{n=-\infty}^{\infty} J_{n-N}^2(\mathbf{k} \cdot \boldsymbol{\alpha}_0) = 1 \quad (12.2.4.6)$$

Hence the cross sections are not affected by this difference in the representations of the asymptotic reference states. The cross sections are

$$\frac{d\sigma_N(\mathbf{k}_0 \rightarrow \mathbf{k})}{d\Omega} = \frac{k_N}{k_0} |f_N(\mathbf{k}_0 \rightarrow \mathbf{k}_N)|^2 \quad (12.2.4.7)$$

with $f_N(\mathbf{k}_0 \rightarrow \mathbf{k}_N)$ given by expression (12.2.4.5).

12.2.5. Existence of the Stationary Cross Section in a Semiclassical Field

It is also interesting to enquire whether a stationary cross section exists for electron scattering in a time-dependent (semiclassical) field, Eq. (1.6.2), or whether one is necessarily required to consider some kind of averaging in time, such as a cycle averaging, to define them.

The asymptotic form of the time-dependent total Floquet wave function may be obtained using the asymptotic form (12.2.4.4) and the substitution rule (12.2.2.8)

$$\begin{aligned} |\psi(\mathbf{r}, t)\rangle &= e^{i\mathbf{k}_0 \cdot \mathbf{r}} \sum_{n=-\infty}^{\infty} J_n(\mathbf{k}_0 \cdot \boldsymbol{\alpha}_0) e^{in(\omega t + \delta) - iEt/\hbar} \\ &\quad + \sum_{N=-\infty}^{\infty} \frac{e^{ik_N r}}{r} \sum_{n=-\infty}^{\infty} J_{n-N}(\mathbf{k}_N \cdot \boldsymbol{\alpha}_0) e^{in(\omega t + \delta) - iEt/\hbar} f_N(\mathbf{k}_0 \rightarrow \mathbf{k}_N) \end{aligned} \quad (12.2.5.1)$$

Use of the Jacobi-Anger formula (1.7.1.1.3) allows one to conclude that the sum associated with the scattered wave

$$\sum_{n=-\infty}^{\infty} J_{n-N}(\mathbf{k}_N \cdot \boldsymbol{\alpha}_0) e^{in(\omega t + \delta)} = \exp[i\mathbf{k}_N \cdot \boldsymbol{\alpha}_0 \sin(\omega t + \delta) + iN(\omega t + \delta)] \quad (12.2.5.2)$$

is a purely time-dependent phase factor. The same is true for the sum

$$\sum_{n=-\infty}^{\infty} J_n(\mathbf{k}_0 \cdot \boldsymbol{\alpha}_0) e^{in(\omega t + \delta)} = \exp[i\mathbf{k}_0 \cdot \boldsymbol{\alpha}_0 \sin(\omega t + \delta)] \quad (12.2.5.3)$$

corresponding to the incident plane wave. Thus if we adopt the usual definition of the scattering amplitude and take the ratio of the amplitude of a “bare” outgoing wave to that of the “bare” incident wave in Eq. (12.2.5.1), we get a time-dependent scattering amplitude given by

$$f_N(\mathbf{k}_0 \rightarrow \mathbf{k}; t) = \frac{\exp[i\mathbf{k}_N \cdot \boldsymbol{\alpha}_0 \sin(\omega t + \delta) + iN(\omega t + \delta)] f_N(\mathbf{k}_0 \rightarrow \mathbf{k}_N)}{\exp[i\mathbf{k}_0 \cdot \boldsymbol{\alpha}_0 \sin(\omega t + \delta)]} \quad (12.2.5.4)$$

This shows explicitly that the scattering amplitude in the time-dependent field differs merely by an overall time-dependent phase factor from that obtained by the stationary theory. The stationarity of the cross sections is therefore ensured independently of any time averaging.

12.2.6. Radiative Scattering from a Pseudopotential

An exactly solvable (closed-form) example of radiative scattering amplitude is the scattering of electrons from an arbitrary separable pseudopotential in the presence of a circularly polarized laser field. At low energy where s -wave scattering dominates, the scattering process may be modeled by a one-term pseudopotential whose parameters may be determined from known empirical data, such as the electron affinity. If the pseudopotential is

$$V = -V_0 |U(r)\rangle\langle U(r)| \quad (12.2.6.1)$$

with any $U(r)$ and constant V_0 , then the scattering equation (12.2.1.3) with the aid of Eq. (12.2.1.5) now becomes

$$\begin{aligned} & \left[E - \left(-\frac{\hbar^2}{2\mu} \nabla^2 + n\hbar\omega + i\hbar\omega\alpha_{02}^{-1}(\nabla^+ s^-_n + \nabla^- s^+_n) \right) \right] |F_n(\mathbf{r})\rangle \\ &= -V_0 |U(r)\rangle\langle U(r)| F_n(\mathbf{r}) \end{aligned} \quad (12.2.6.2)$$

The solutions $F_n(\mathbf{r})$ are given by Eqs. (12.2.3.6) and (12.2.4.1),

$$\begin{aligned} |F_n(\mathbf{r})\rangle &= J_n(k_0^\perp \alpha_0) e^{in\phi_0} |e^{i\mathbf{k}_0 \cdot \mathbf{r}}\rangle \\ &- V_0 \sum_{n'} \sum_{N\mathbf{k}} |e^{i\mathbf{k} \cdot \mathbf{r}}\rangle \frac{J_{n-N}(k^\perp \alpha_0) e^{i(n-n')\phi_k} J_{n'-N}(k^\perp \alpha_0)}{E - \varepsilon_k - N\hbar\omega + i0} \\ &\times \langle e^{i\mathbf{k} \cdot \mathbf{r}} | U(r)\rangle \langle U(r) | F_{n'}(\mathbf{r})\rangle \end{aligned} \quad (12.2.6.3)$$

where $k^\perp \equiv k \sin(\theta_k)$ and \mathbf{k}_0 is the incident wave vector. We note that since $U(r)$ is centrally symmetric, then

$$\langle e^{i\mathbf{k} \cdot \mathbf{r}} | U(r)\rangle \equiv U(k) \quad (12.2.6.4)$$

is also centrally symmetric. We project $\langle U(r) |$ onto expression (12.2.6.3) and rewrite the result to obtain

$$\langle U(r) | F_n(\mathbf{r})\rangle = \frac{J_n(k_0^\perp \alpha_0) e^{in\phi_0} \langle U(r) | e^{i\mathbf{k}_0 \cdot \mathbf{r}}\rangle}{1 + V_0 \sum_N \sum_{\mathbf{k}} \frac{J_{n-N}^2(k^\perp \alpha_0) |U(k)|^2}{E - \varepsilon_k - N\hbar\omega + i0}} \quad (12.2.6.5)$$

where the orthogonality, $\delta_{nn'}$, implied by the ϕ_k integration is used. Substitution of this relation into the right-hand side of Eq. (12.2.6.3) yields the exact “Floquet wave function” of the problem,

$$\begin{aligned} |F_n(\mathbf{r})\rangle &= J_n(k_0^\perp \alpha_0) e^{in\phi_0} |e^{i\mathbf{k}_0 \cdot \mathbf{r}}\rangle \\ &- V_0 \sum_{N\mathbf{k}} \sum_{n'} |e^{i\mathbf{k} \cdot \mathbf{r}}\rangle J_{n-N}(k^\perp \alpha_0) U^*(k) J_{n'-N}(k^\perp \alpha_0) e^{i(n-n')\phi_k} \frac{1}{E - \varepsilon_k - N\hbar\omega + i0} \\ &\times \frac{J_n(k_0^\perp \alpha_0) e^{in\phi_0} U(k_0)}{1 + V_0 \sum_N \sum_{\mathbf{k}} \frac{J_{n-N}^2(k^\perp \alpha_0) |U(k)|^2}{E - \varepsilon_k - N\hbar\omega + i0}} \end{aligned} \quad (12.2.6.6)$$

We take the asymptotic limit $r \rightarrow \infty$ and perform the $\Sigma_{\mathbf{k}}$ summation in Eq. (12.2.6.6) to obtain

$$\begin{aligned} F_n(\mathbf{r}) &= \lim_{r \rightarrow \infty} J_n(k_0^\perp \alpha_0) e^{in\phi_0} |e^{i\mathbf{k}_0 \cdot \mathbf{r}}\rangle \\ &+ \sum_{N=-\infty}^{\infty} \frac{e^{ik_N r}}{r} J_{n-N}(k_N^\perp \alpha_0) e^{in\phi} f_N(\mathbf{k}_0 \rightarrow \mathbf{k}_N) \end{aligned} \quad (12.2.6.7)$$

with the exact radiative scattering amplitude

$$\begin{aligned} f_N(\mathbf{k}_0 \rightarrow \mathbf{k}_N) &= \frac{\mu}{2\pi\hbar^2} V_0 \sum_{n=-\infty}^{\infty} J_{n-N}(k_N^\perp \alpha_0) J_n(k_0^\perp \alpha_0) \\ &\times \frac{e^{in(\phi_0 - \phi)} U^*(k_N) U(k_0)}{1 + V_0 \sum_{s=-\infty}^{\infty} \sum_{\mathbf{k}} \frac{J_{n-s}^2(k^\perp \alpha_0) |U(k)|^2}{E - \varepsilon_k - s\hbar\omega + i0}} \end{aligned} \quad (12.2.6.8)$$

where φ is the azimuth of \mathbf{k}_N and

$$k_N = \left[\frac{2\mu(E - N\hbar\omega)}{\hbar^2} \right]^{1/2}$$

is the scattered wave number for absorption ($N < 0$) or emission ($N > 0$) of N photons. In the limit $\alpha_0 \rightarrow 0$, the above Bessel-function factors become Kronecker-delta functions of their orders and Eq. (12.2.6.8) reduces to

$$f(\mathbf{k}_0 \rightarrow \mathbf{k}) = + \frac{\mu}{2\pi\hbar^2} \frac{(V_0)|U(k_0)|^2}{1 + \sum_{\mathbf{k}} \frac{|V_0| |U(k)|^2}{E - \varepsilon_k + i0}} \quad (12.2.6.9)$$

which is the exact scattering amplitude for ordinary elastic scattering.

We note that the denominator of Eq. (12.2.6.8) contains the effect of electron propagation through the intermediate (virtual or off-shell) states. If the effect of electron “dressing” in the virtual states is assumed to be negligible, then one may approximate

$$J_{n-s}^2(k^\perp \alpha_0 \rightarrow 0) = \delta_{n-s} \quad (12.2.6.10)$$

in the denominator of Eq. (12.2.6.8) and assume $|N|\omega \ll E$ to obtain

$$f_N(\mathbf{k}_0 \rightarrow \mathbf{k}_N) = \sum_{n=-\infty}^{\infty} J_{n-N}(K_N^\perp \alpha_0) f(E - n\hbar\omega) J_n(k_0^\perp \alpha_0) e^{in(\phi_0 - \phi)} \quad (12.2.6.11)$$

where $f(E - n\hbar\omega)$ is the exact field-free elastic amplitude (12.2.6.9) evaluated at the shifted energies ($E - n\hbar\omega$). Relation (12.2.6.11), or its minor variations, for any scattering potential and any field polarization is usually referred to as the “low-frequency approximation” to the radiative scattering amplitude and has been studied extensively.⁽²⁵¹⁻²⁵⁷⁾ The low-frequency formula for the case of linear polarization is given by

$$f_N(\mathbf{k}_0 \rightarrow \mathbf{k}_N) = \sum_{n=-\infty}^{\infty} J_{n-N}(\mathbf{k}_N \cdot \boldsymbol{\alpha}_0) f(E - n\hbar\omega) J_n(\mathbf{k}_0 \cdot \boldsymbol{\alpha}_0) \quad (12.2.6.12)$$

where $f(E - n\hbar\omega)$ is the true elastic scattering amplitude evaluated at $(E - n\hbar\omega)$. It is of some interest to note that if $|n|\hbar\omega \ll E$, for all n which may contribute significantly to the cross section of interest, then $f(E - n\hbar\omega)$ may be replaced approximately by $f(E)$ and the Bessel identity (12.2.3.9) used in Eq. (12.2.6.12) to write

$$f_N(\mathbf{k}_0 \rightarrow \mathbf{k}_N) \approx f(E) J_N(\mathbf{q}_N \cdot \boldsymbol{\alpha}_0) \quad (12.2.6.13)$$

where $\mathbf{q}_N \equiv (\mathbf{k}_0 - \mathbf{k}_N)$ is the momentum transfer. Use of this latter approxi-

mation shows that the sum of radiative cross sections for all N , namely

$$\sum_{N=-\infty}^{\infty} \frac{d}{d\Omega} \sigma_N(\mathbf{k}_0 \rightarrow \mathbf{k}_N) \approx |f(E)|^2 \sum_{N=-\infty}^{\infty} J_N^2(\mathbf{q}_N \cdot \mathbf{a}_0) \approx |f(E)|^2 \quad (12.2.6.14)$$

is approximately equal^(259,260) to the ordinary elastic differential cross

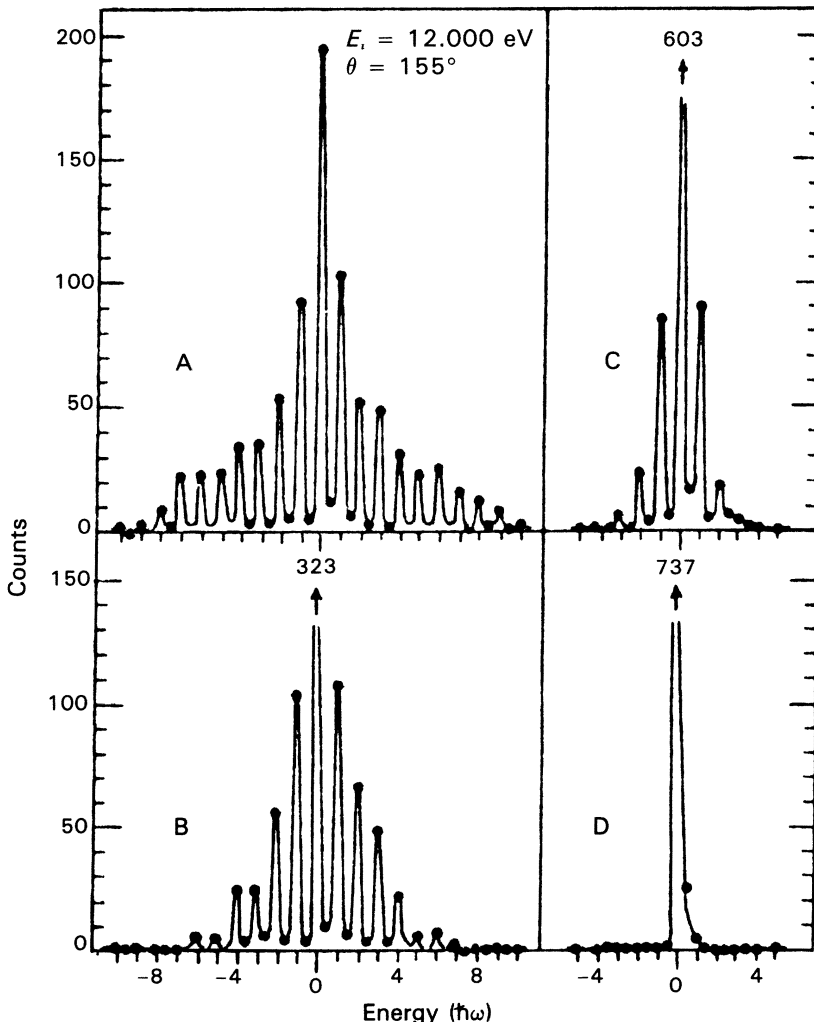


Figure 56. High-field energy loss-gain spectra observed during electron scattering with argon atoms in a CO_2 laser field ($\hbar\omega = 0.117$ eV) at 12.000 eV incident electron energy. The number of photons emitted and absorbed by the electron is seen to increase from curves C to B to A, which correspond to increasing strength of the applied field. The signal in the absence of the field is shown by curve D (from Weingartshofer *et al.*⁽²⁶⁰⁾).

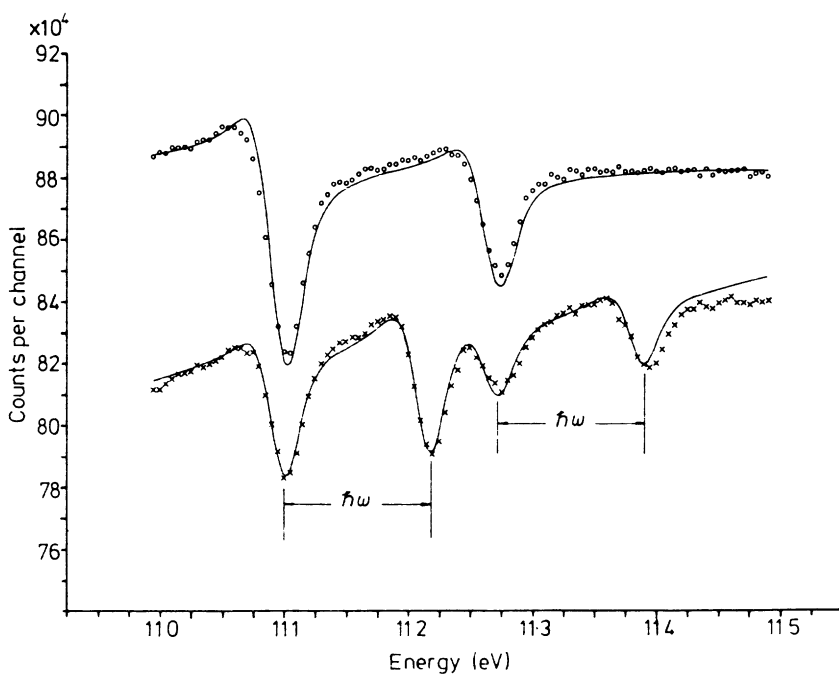


Figure 57. Low-field electron-argon scattering near the 11.098 eV and 11.270 eV elastic resonances in the presence of a CO₂ laser field ($\hbar\omega = 0.117$ eV). Circles refer to experimental elastic scattering data in the absence of the field, crosses to experimental data in the presence of the field; the upper solid curve refers to calculated cross sections using known phase shifts, the lower solid curve to calculated cross sections using the weak-field limit of the low-frequency formula. The elastic resonances reappear in the one-photon absorption channel occurring at energies shifted by $\hbar\omega$ (from Langhans⁽²⁶²⁾).

section in the absence of the field. Neglect of dressing in the virtual states appears to be a good approximation at high energy, low frequency, and not too large intensities for nonresonant scattering energies. “Elastic” scattering of electrons with argon atoms in a “low-frequency” field (CO₂ laser, $\hbar\omega = 0.117$ eV) with emission and absorption of one or more photons has been observed at high-field,⁽²⁵⁷⁻²⁶⁰⁾ nonresonant and resonant collision energies and at low-field,^(261,262) resonant collision energies. Figure 56 shows typical energy loss-gain spectra observed during scattering of 12.000 eV electrons from argon atoms in a CO₂ laser field. Multiphoton emission and absorption of up to ten photons are discernible in this data at the highest field strength (curve A). The total area under an energy loss-gain spectrum has been found practically equal to the elastic signal in the absence of the field (curve D); this may be regarded as consistent with the approximate sum rule (12.2.6.14). Figure 57 demonstrates clearly how the resonant

behavior of the ordinary electron–argon scattering in the elastic channel near 11.098 eV and 11.270 eV are repeated in the new scattering channels (at energies shifted by $\hbar\omega$) corresponding to the absorption of a (CO₂ laser) photon. This result is consistent with the weak-field limit of the low-frequency formula when careful use is made⁽²⁶²⁾ of the known elastic amplitudes (phase shifts). As regards the interesting process of photon absorption by electrons, for which the initial and final electron energies correspond to two such resonances, no reliable data are available; in this case the low-frequency formula is likely to break down⁽²⁵³⁾ even for small incident frequencies.

In the next section we develop more general theories of radiative electron–atom scattering taking into account the internal structure of the target atom.

12.3. Multichannel Electron–Atom Scattering in a Laser Field

The internal structure of atoms is generally affected by the field during scattering. Taking this into consideration we write the total Hamiltonian of “electron + atom + radiation field” in the presence of electron–atom collision as

$$H = H_a - \frac{\hbar^2}{2\mu} \nabla_r^2 + \hbar\omega a^\dagger a + \frac{ie\hbar}{\mu c} (\mathbf{A} \cdot \nabla_a + \mathbf{A} \cdot \nabla_r) + V(\mathbf{r}, \mathbf{x}_a) \quad (12.3.1)$$

In writing this equation we have assumed that the A^2 term has already been removed by the renormalization process shown in detail in Section 1.9, and the field may be interpreted as consisting of the renormalized modes. The quantity

$$H_a = \sum_i |\phi_i\rangle \epsilon_i \langle \phi_i| \quad (12.3.2)$$

is a multistate atomic Hamiltonian, $V(\mathbf{r}, \mathbf{x}_a)$ is the electron–atom interaction, \mathbf{r} denotes the coordinates of the scattering electron, and \mathbf{x}_a is the set of coordinates of the N_a atomic electrons. Similarly,

$$-i\hbar\nabla_r \quad \text{and} \quad -i\hbar\nabla_a \quad (12.3.3)$$

are the momentum operators of the scattering electron and of the sum of atomic electrons, respectively. The vector potential \mathbf{A} is given by expression (12.2.3) or (12.2.4). We shall consider the initial field density n_0/L^3 to be large enough so that A_0 is given by relation (12.2.5) and is virtually independent of the change in occupation number of the field during the whole course of the collision.

12.3.1. The Floquet Equation for Scattering

The Schrödinger equation of the system “electron + atom + field” is

$$H |\psi\rangle = E |\psi\rangle \quad (12.3.1.1)$$

where E is the total energy. We expand $|\psi\rangle$ as

$$|\psi\rangle = \sum_n \psi_n(\mathbf{r}, \mathbf{x}_a) |n\rangle \quad (12.3.1.2)$$

If this expansion is substituted in Eq. (12.3.1.1) and we project onto $\langle n |$, then we obtain the “Floquet equations” (entirely in the coordinate space)

$$(E - H_n^{(0)})\psi_n(\mathbf{r}, \mathbf{x}_a) = V(\mathbf{r}, \mathbf{x}_a)\psi_n(\mathbf{r}, \mathbf{x}_a) \quad (12.3.1.3)$$

for all $n = 0, \pm 1, \pm 2, \dots, \pm \infty$. The unperturbed Hamiltonian is

$$H_n^{(0)} = H_a + n\hbar\omega - \frac{\hbar}{2\mu} \nabla_r^2 + H'_n \quad (12.3.1.4)$$

where H'_n is the sum of the interaction Hamiltonians (of the scattering electron and atomic electrons) with respect to the field and is given by

$$H'_n = i\hbar\omega \frac{\alpha_0}{2} (\nabla_z^a + \nabla_z^e)(s_n^- + s_n^+) \quad (\text{linear polarization}) \quad (12.3.1.5)$$

or

$$H'_n = i\hbar\omega \frac{\alpha_0}{2} [(L_a^+ + L_e^+)s_n^- + (L_a^- + L_e^-)s_n^+] \quad (\text{circular polarization}) \quad (12.3.1.6)$$

We have denoted the z -component of the sum of momentum operators of the atomic electrons by ∇_z^a and that of the scattering electron by ∇_z^e . Similarly, we have defined

$$L_a \equiv -i[\nabla_x^a \pm i\nabla_y^a] \quad (12.3.1.7)$$

$$L_e \equiv -i(\nabla_x^e \pm i\nabla_y^e) \quad (12.3.1.8)$$

and

$$s_n^\pm \psi_n \equiv \psi_{n\pm 1} \quad (12.3.1.9)$$

The Floquet equations (12.3.1.3) provide a bridge between the time-dependent treatment and the number-state treatment of the “radiative

scattering” of interest. Part of the convenience of using the Floquet equations lies in not having to deal explicitly either with the time dependence or with the number-state dependence and yet (as will be seen below) both the time dependence and number-state dependence of the scattering amplitudes can be recovered whenever required, easily and explicitly. Another useful point to note is that the Floquet equations (12.3.1.3) are exactly analogous to the Schrödinger equations governing the usual⁽²⁶³⁾ multichannel electron–atom scattering equations; the only difference is the appearance of an extra channel index “ n ” (which can be incorporated in the set of channel quantum numbers that arise in the absence of the field). This analogy is useful, since with its help virtually all methods developed for the treatment of ordinary multichannel scattering problems may be adopted systematically for the present problem of radiative scattering.

12.3.2. Eigenfunctions of the Reference Hamiltonian

When solving Eq. (12.3.1.3) it is convenient to obtain first the eigenfunctions χ_n of the reference Hamiltonian $H_n^{(0)}$:

$$[E - H_n^{(0)}]\chi_n = 0 \quad (12.3.2.1)$$

The reference Hamiltonian (12.3.1.4) includes via H' a coupling between the isolated atom and free electron due to the radiation field. We therefore expect that the eigenvectors of Eq. (12.3.1.3) will not be given by a single product of eigenfunctions of the “atom + field” subsystem and the electron eigenfunction in the field but rather by suitable linear combinations of them.

In the case of linear polarization we therefore set

$$\chi_n = \sum_j \sum_{m=-\infty}^{\infty} J_{n-m}(\alpha_0 \cdot \mathbf{k}) e^{i\mathbf{k} \cdot \mathbf{r}} a_{jm} |j(\mathbf{x}_a)\rangle \quad (12.3.2.2)$$

where a_{jm} are constants to be determined and $|j(\mathbf{x})\rangle$ denotes the eigenfunctions of the atomic Hamiltonian H_a . By operating with $H_n^{(0)}$ on Eq. (12.3.2.2) and proceeding as in Section 12.2.2 one finds that

$$H_n^{(0)}\chi_n = \sum_j \sum_{m=-\infty}^{\infty} J_{n-m}(\alpha_0 \cdot \mathbf{k}) e^{i\mathbf{k} \cdot \mathbf{r}} \times \left[\varepsilon_k + H_a + m\hbar\omega + i\hbar\omega \frac{\alpha_0}{2} (\nabla_z^a)(s_m^- + s_m^+) \right] a_{jm} |j(\mathbf{x}_a)\rangle \quad (12.3.2.3)$$

If we substitute expression (12.3.2.3) in Eq. (12.3.2.1), multiply by $J_{n-m}(\alpha_0 \cdot \mathbf{k}) \langle j'(\mathbf{x}_a) |$, sum over n , integrate over \mathbf{x}_a , and make use of the

Bessel-function identity (12.2.2.5), then we obtain

$$[(E - \varepsilon_k) - (\varepsilon_j + n\hbar\omega)]a_{jm} = i\hbar\omega \frac{\alpha_0}{2} (\nabla_z)_j [a_{j'm-1} + a_{j'm+1}] \quad (12.3.2.4)$$

for all $m = 0, \pm 1, \pm 2, \pm 3, \dots, \pm \infty$, where subscripts m and m' and j and j' are interchanged for convenience.

Equation (12.3.2.4) is essentially the Floquet equation for the “atom + field” subsystem discussed in Section 10.2. Thus $a_{jm}(\lambda_p)$ corresponds to the (jm) th component of the eigenvector with eigenvalue λ_p , which is related to E by $E = \lambda_p + \varepsilon_k$, where $p = 1, 2, \dots, J$ (J being the maximum dimension of the atomic Hilbert space retained in a particular calculation). We recall the orthogonality relation

$$\sum_{m,p} a_{jm}(\lambda_p) a_{j'm-s}^*(\lambda_p) = \delta_{jj'} \delta_{s,0} \quad (12.3.2.5)$$

and the periodicity relation

$$a_{jm}(\lambda_p) = a_{jm+n}(\lambda_p) \quad (12.3.2.6)$$

with

$$\lambda_p^n = \lambda_p + n\hbar\omega \quad (12.3.2.7)$$

where $p = 1, 2, \dots, J$ and $n = 0, \pm 1, \pm 2, \dots, \pm \infty$. In terms of the Floquet coefficient $a_{jm}(\lambda_p)$ we therefore obtain explicitly⁽²⁶⁴⁾ the eigenfunctions (12.3.2.2) of the reference Hamiltonian $H_n^{(0)}$ corresponding to eigenvalues λ_p with total energy $E = \lambda_p + \varepsilon_k$,

$$\chi_n(\mathbf{k}, \lambda_p; \mathbf{r}, \mathbf{x}) = \sum_j \sum_m J_{n-m}(\boldsymbol{\alpha}_0 \cdot \mathbf{k}) e^{i\mathbf{k} \cdot \mathbf{r}} a_{jm}(\lambda_p) |j(\mathbf{x}_a)\rangle \quad (12.3.2.8)$$

12.3.3. Green's Function for the Reference Hamiltonian

The desired scattering amplitudes can be derived by solving for the Green's function of the Hamiltonian (12.3.1.4). This function is defined by

$$(E - H_n^{(0)}) G_{nn'}^{(0)} = \delta_{nn'} \delta(\mathbf{r} - \mathbf{r}') \delta(\mathbf{x}_a - \mathbf{x}'_a) \quad (12.3.3.1)$$

for all $(n, n') = 0, \pm 1, \pm 2, \pm 3, \dots, \pm \infty$. In terms of Eq. (12.3.2.8) the desired solution of Eq. (12.3.3.1) can be immediately expressed in the form

$$\begin{aligned} G_{nn'}^{(0)} &\equiv G_{nn'}^{(0)}(\mathbf{r}, \mathbf{r}'; \mathbf{x}_a, \mathbf{x}'_a) \\ &= \sum_{\mathbf{k}Np} \frac{\chi_{n-N}(\mathbf{k}, \lambda_p; \mathbf{r}, \mathbf{x}_a) \chi_{n'-N}^*(\mathbf{k}, \lambda_p; \mathbf{r}', \mathbf{x}'_a)}{E - \lambda_p^N - \varepsilon_k} \end{aligned} \quad (12.3.3.2)$$

where

$$\lambda_p^N \equiv \lambda_p + N\hbar\omega, \quad \varepsilon_k \equiv \hbar^2 k^2 / 2\mu \quad (12.3.3.3)$$

$$N = 0, \pm 1, \pm 2, \dots, \pm \infty \quad \text{and} \quad p = 1, 2, 3, \dots, J.$$

Solution (12.3.3.2) is readily verified by substitution in Eq. (12.3.3.1) with allowance for the orthogonality relation

$$\sum_{\mathbf{k} \neq \mathbf{k}'} \chi_{n-N}(\mathbf{k}, \lambda_p; \mathbf{r}, \mathbf{x}_a) \chi_{n'-N}^*(\mathbf{k}, \lambda_p; \mathbf{r}', \mathbf{x}'_a) = \delta_{nn'} \delta(\mathbf{r} - \mathbf{r}') \delta(\mathbf{x}_a - \mathbf{x}'_a) \quad (12.3.3.4)$$

In obtaining this equation use has been made of the Bessel identity (12.2.3.8) and relations (12.3.2.5) and (12.3.2.6) for $a_{jm}(\lambda_p)$.

Green's function $G_{nn'}^{(0)}$ in the case of circular polarization is given by Eq. (12.3.3.2), provided wave functions χ_n are suitably modified. Eigenvalues λ_p and coefficients $a_{jm}(\lambda_p)$ must now be obtained from the Floquet equations

$$\begin{aligned} & [\lambda_p - (\varepsilon_j + n\hbar\omega)] a_{jm}(\lambda_p) \\ &= \hbar\omega \frac{\alpha_0}{2} \sum_{j'} \sum_m [(L_a^+)_m a_{j'm-1}(\lambda_p) + (L_a^-)_m a_{j'm+1}(\lambda_p)] \end{aligned} \quad (12.3.3.5)$$

On combining the eigenvectors $a_{jm}(\lambda_p)$ of Eq. (12.3.3.5) with the coefficients corresponding to the free-electron wave function (12.2.2.3), we obtain the required eigenfunctions of $H_n^{(0)}$ in the form

$$\chi_n(\mathbf{k}, \lambda_p; \mathbf{r}, \mathbf{x}_a) = \sum_{mj} J_{n-m}(k\alpha_0 \sin \theta_k) e^{i(n-m)\phi_k} a_{jm}(\lambda_p) e^{i\mathbf{k} \cdot \mathbf{r}} | j(\mathbf{x}_a) \rangle \quad (12.3.3.6)$$

Equations (12.3.3.2) and (12.3.3.6) define the desired Green's function in the case of circular polarization.

12.3.4. Wave Functions of the Total System and the Scattering Amplitude

Green's function (12.3.3.2) now enables us to obtain the solution of the Floquet equation in the form

$$\begin{aligned} \psi_n^{(i)} &= \chi_n(\mathbf{k}_i, \lambda_i) + \sum_n G_{nn'}^{(0)} V | \psi_{n'}^{(i)} \rangle \\ &= \chi_n(\mathbf{k}_i, \lambda_i) + \sum_{\mathbf{k} \neq \mathbf{k}' \neq \mathbf{k}'} \chi_{n-N}(\mathbf{k}, \lambda_p) \frac{1}{E - \lambda_p^N - \varepsilon_k} \langle \chi_{n'-N}(\mathbf{k}, \lambda_p) | V | \psi_{n'}^{(i)} \rangle \end{aligned} \quad (12.3.4.1)$$

where \mathbf{k}_i and λ_i correspond to the initial asymptotic momentum state of the scattering electron and the energy of the dressed atom, respectively. In Eq. (12.3.4.1) we have omitted the coordinate arguments and added the index i to remind us of the specified initial condition. Finally, substitution of solution (12.3.4.1) in expansion (12.3.1.2) yields the state vector of the total system:

$$\begin{aligned} |\psi_i\rangle &= \sum_n |\psi_n^{(i)}\rangle |n\rangle \\ &= \sum_n \chi_n(\mathbf{k}_i, \lambda_i) |n\rangle + \sum_{kpN} \sum_n \chi_n(\mathbf{k}, \lambda_p) |n\rangle \frac{1}{E - \lambda_p^N - \epsilon_k} \\ &\quad \times \sum_n \langle \chi_{n'-N}(\mathbf{k}, \lambda_p) | V | \psi_n^{(i)} \rangle \end{aligned} \quad (12.3.4.2)$$

The scattering amplitude is obtained by taking the asymptotic limit $r \rightarrow \infty$ in Eq. (12.3.4.2). Hence

$$\begin{aligned} \lim_{r \rightarrow \infty} |\psi_i\rangle &= \left(\sum_n \chi_n(\mathbf{k}_i, \lambda_i) |n\rangle \right) \\ &\quad + \sum_{Np} \left(\sum_n \chi_n(\mathbf{k}_{pN}, \lambda_p) |n\rangle \right) \frac{e^{ik_{pN}r}}{r} f(\lambda_i \mathbf{k}_i \rightarrow \lambda_f \mathbf{k}_{pN}) \end{aligned} \quad (12.3.4.3)$$

where

$$f(\lambda_i \mathbf{k}_i \rightarrow \lambda_f \mathbf{k}_{pN}) \equiv -\frac{\mu}{2\pi\hbar^2} \sum_{n=-\infty}^{\infty} \langle \chi_n(\mathbf{k}_{pN}, \lambda_p) | V | \psi_n^{(i)} \rangle \quad (12.3.4.4)$$

The direction of the incident momentum \mathbf{k}_i is $\Omega_0 = (\theta_0, \phi_0)$ and the direction of the scattered momentum \mathbf{k}_{pN} , $\Omega = (\theta, \phi)$. The magnitude of \mathbf{k}_{pN} is fully determined by the conservation of the perturbed energy of the system:

$$\frac{\hbar^2 k_{pN}^2}{2\mu} + \lambda_p + N\hbar\omega = \frac{\hbar^2 k_i^2}{2\mu} + \lambda_i \quad (12.3.4.5)$$

The states

$$\sum_n \chi_n(\mathbf{k}, \lambda_p) |n\rangle \equiv |\mathbf{k}, \lambda_p\rangle \quad (12.3.4.6)$$

appearing in Eq. (12.3.4.2) are the collision-free eigenstates of the atom + electron system interacting with the field. An alternative form of relation (12.3.4.6), derived in Section 12.4 below, shows explicitly its dependence on

the dressed eigenstates of the target atom:

$$|\mathbf{k}, \lambda_p\rangle = \sum_n \sum_{jm} J_{n-m}(\mathbf{k} \cdot \boldsymbol{\alpha}_0) e^{i\mathbf{k} \cdot \mathbf{r}} a_{jm}(\lambda_p) |j(\mathbf{x}_a)\rangle |n\rangle \quad (12.3.4.7)$$

$$= \sum_n J_n(\mathbf{k} \cdot \boldsymbol{\alpha}_0) e^{i\mathbf{k} \cdot \mathbf{r}} |\lambda_p^n; \mathbf{x}_a\rangle \quad (12.3.4.8)$$

where

$$|\lambda_p^n; \mathbf{x}_a\rangle \equiv \sum_{jm} a_{jm}(\lambda_p^n) |j(\mathbf{x}_a)\rangle |m\rangle \quad (12.3.4.9)$$

are the dressed eigenstates of the “target + field” subsystem, with eigenvalues

$$\lambda_p^n = \lambda_p + n\hbar\omega \quad (12.3.4.10)$$

The radiation field of interest is usually of a macroscopic dimension (such as a laser beam). Consequently, the electron can be far away (on the microscopic or atomic scale) from the scattering center while remaining within the field. Equation (12.3.4.3) defines an appropriate set of asymptotic states, which are connected adiabatically to the field-free states of the atom and the plane-wave state of the electron outside ($\alpha_0 = 0$) the field. Hence relation (12.3.4.3) enables one to identify

$$f(\lambda_i \mathbf{k}_i \rightarrow \lambda_f \mathbf{k}_{fN}) = -\frac{\mu}{2\pi\hbar^2} \sum_n \langle \chi_{n-N}(\mathbf{k}_{fN}, \mathbf{k}_f; \mathbf{r}, \mathbf{x}_a) | V(\mathbf{r}, \mathbf{x}_a) | \psi_n^{(i)}(\mathbf{r}, \mathbf{x}_a) \rangle \quad (12.3.4.11)$$

as the radiative direct-scattering amplitude associated with the transition

$$|\mathbf{k}_i, \lambda_i\rangle \rightarrow |\mathbf{k}_{fN}, \lambda_f\rangle \quad (12.3.4.12)$$

On substituting Eq. (12.3.2.8) in Eq. (12.3.4.11) we obtain, for the case of linear polarization,

$$\begin{aligned} f(\lambda_i \mathbf{k}_i \rightarrow \lambda_f \mathbf{k}_{fN}) &= -\frac{\mu}{2\pi\hbar^2} \sum_n \sum_{mj} J_{n-m-N}(\mathbf{k}_{fN} \cdot \boldsymbol{\alpha}_0) a_{jm}(\lambda_f) \\ &\times \langle e^{i\mathbf{k}_{fN} \cdot \mathbf{r}} | \langle j(\mathbf{x}_a) | V(\mathbf{r}, \mathbf{x}_a) | \psi_n^{(i)}(\mathbf{r}, \mathbf{x}_a) \rangle \rangle \end{aligned} \quad (12.3.4.13)$$

A similar expression is obtained by substituting Eq. (12.3.3.6) in Eq. (12.3.4.11), for the case of circular polarization. Equation (12.3.4.2) and (12.3.2.8) in conjunction with Eq. (12.3.4.11) can be used to develop a

systematic expansion of the radiative scattering amplitude in powers of the potential $V(\mathbf{r}, \mathbf{x}_a)$, which is a direct generalization of the usual Born series. As in the case of ordinary scattering the higher-order terms of this series could become very difficult to use in practice. Below we briefly discuss the amplitude structure of only the first two terms of the series, which help to reveal some properties of the full expression (12.3.4.13).

12.3.4.1. The Radiative First Born Amplitude

Some insight into the nature of Eq. (12.3.4.13) can be obtained by considering the scattering amplitude in the lowest order of $V(\mathbf{r}, \mathbf{x}_a)$ (which corresponds to the usual first Born approximation). Thus by neglecting the influence of $V(\mathbf{r}, \mathbf{x}_a)$ on the wave function $\psi_n^{(i)}(\mathbf{r}, \mathbf{x}_a)$, given in Eq. (12.3.4.1), we have

$$\begin{aligned} \psi_n^{(i)}(\mathbf{r}, \mathbf{x}_a) &\rightarrow \chi_n(\mathbf{k}_i, \lambda_i) \\ &= \sum_{m'm} J_{n-m'}(k_i \alpha_0 \cos \theta_0) a_{m'm}(\lambda_i) |j(\mathbf{x}_a)\rangle e^{i\mathbf{k}_i \cdot \mathbf{r}} \end{aligned} \quad (12.3.4.1.1)$$

If relation (12.3.4.1.1) is substituted in Eq. (12.3.4.13), we obtain the first-order amplitude

$$\begin{aligned} f^{(1)}(\lambda_i \mathbf{k}_i \rightarrow \lambda_f \mathbf{k}_{fN}) &= -\frac{\mu}{2\pi\hbar^2} \sum_{njm'm'} J_{n-m'-N}(\mathbf{k}_{fN} \cdot \boldsymbol{\alpha}_0) a_{m'm}^*(\lambda_f) \\ &\times T_{jj'}^B(\mathbf{k}_i \rightarrow \mathbf{k}_{fN}) J_{n-m}(\mathbf{k}_i \cdot \boldsymbol{\alpha}_0) a_{jm}(\lambda_i) \end{aligned} \quad (12.3.4.1.2)$$

where

$$T_{jj'}^B(\mathbf{k}_i \rightarrow \mathbf{k}_{pN}) \equiv \langle e^{i\mathbf{k}_{pN} \cdot \mathbf{r}} | \langle j' | V(\mathbf{r}, \mathbf{x}_a) | j \rangle | e^{i\mathbf{k}_i \cdot \mathbf{r}} \rangle \quad (12.3.4.1.3)$$

This is the inelastic Born matrix element between the unperturbed atomic states $|j\rangle$ and $|j'\rangle$ and the electron momenta \mathbf{k}_i and \mathbf{k}_{pN} . We note, however, that the corresponding electron energies $\hbar k_i^2/(2\mu)$ and $\hbar k_{pN}^2/2\mu$ satisfy Eq. (12.3.4.5) and are therefore in general “off shell” with respect to the field-free transitions $|j\rangle \rightarrow |j'\rangle$. The Bessel identity (12.2.3.9) may be employed to simplify Eq. (12.3.4.4) to the form

$$\begin{aligned} f^{(1)}(\lambda_i \mathbf{k}_i \rightarrow \lambda_f \mathbf{k}_{fN}) &= -\frac{\mu}{2\pi\hbar^2} \sum_{mm'm'} a_{m'm}^*(\lambda_f) a_{jm}(\lambda_i) J_{m'-m+N}(\mathbf{q}_{fN} \cdot \boldsymbol{\alpha}_0) T_{jj'}^B(\mathbf{k}_i \rightarrow \mathbf{k}_{fN}) \\ &\quad (12.3.4.1.4) \end{aligned}$$

where

$$\mathbf{q}_{fN} = \mathbf{k}_i - \mathbf{k}_{fN} \quad (12.3.4.1.5)$$

is the momentum transfer. It should be noted from Eq. (12.3.4.1.4) that even in the lowest order of scattering potential the influence of the field on the target atom and on the scattering electron gives rise to contributions due to interference between different atomic states in the cross section,

$$\frac{d\sigma_{i \rightarrow f}}{d\Omega} = \frac{k_{fN}}{k_i} |f(\lambda_i \mathbf{k}_i \rightarrow \lambda_f \mathbf{k}_{fN})|^2 \quad (12.3.4.1.6)$$

However, if the interaction of the field with the target atom is negligible (such as in the off-resonant weak-field case) then

$$\begin{aligned} a_{jm}(\lambda_f) &\rightarrow \delta_{jf}\delta_{m,0} \quad \text{and} \quad a_{j'm'}(\lambda_i) \rightarrow \delta_{j'i}\delta_{m'0} \\ \lambda_f &\rightarrow \varepsilon_f \quad \text{and} \quad \lambda_i \rightarrow \varepsilon_i \end{aligned} \quad (12.3.4.1.7)$$

and the first-order scattering amplitude (12.3.4.1.4) reduces to the relation^(251,265–268)

$$f^{(1)}(\lambda_i \mathbf{k}_i \rightarrow \lambda_f \mathbf{k}_{fN}) = J_N(\mathbf{q}_{fN} \cdot \boldsymbol{\alpha}_0) T_{if}^B(\mathbf{k}_i \rightarrow \mathbf{k}_{fN}) \quad (12.3.4.1.8)$$

where now the final energy of the electron is given by the unperturbed energy relation

$$\frac{\hbar^2 k_{fN}^2}{2\mu} = \frac{\hbar^2 k_i^2}{2\mu} + \varepsilon_i - (N\hbar\omega + \varepsilon_f) \quad (12.3.4.1.9)$$

Finally, if the projectile is a neutral (or inert) particle, we may neglect its interaction with the field. Thus by setting $\alpha_0 = 0$ in Eq. (12.3.4.1.4) we obtain

$$f^{(1)} = -\frac{\mu}{2\pi\hbar^2} \sum_{n'} \sum_m a_{j'm-N}^*(\lambda_f) a_{jm}(\lambda_i) T_{n'}^B(\mathbf{k}_i \rightarrow \mathbf{k}_{fN}) \quad (12.3.4.1.10)$$

In principle, therefore, the distortion of the target atom by the field can influence the scattering probability even at high energies.

12.3.4.2. The Radiative Second Born Amplitude

The second-order amplitude is obtained by replacing $|\psi_n^{(1)}\rangle$ on the right-hand side of Eq. (12.3.4.13) by the first-order wave function [from Eq. (12.3.4.1)]

$$\psi_n^{(1)} \approx \chi_n(\mathbf{k}_i, \lambda_i) + \sum_n G_{nn'}^{(0)} V |\chi_{n'}(\mathbf{k}_i, \lambda_i)\rangle \quad (12.3.4.2.1)$$

Substitution of the second part of expression (12.3.4.2.1) in Eq. (12.3.4.13) gives the second-order contribution to the scattering amplitude,

$$f^{(2)}(\lambda_i \mathbf{k}_i \rightarrow \lambda_f \mathbf{k}_{fN}) = -\frac{\mu}{2\pi\hbar^2} \sum_n \sum_{n'} \langle \chi_{n-N}(\mathbf{k}_{fN}, \lambda_f) | V G_{nn'}^{(0)} V | \chi_n(\mathbf{k}_i, \lambda_i) \rangle \quad (12.3.4.2.2)$$

When functions χ_n and $G_{nn'}^{(0)}$ are replaced by expressions (12.3.2.8) and (12.3.3.2), the second-order scattering amplitude is derived in the form

$$\begin{aligned} f^{(2)}(\lambda_i \mathbf{k}_i \rightarrow \lambda_f \mathbf{k}_{fN}) &= -\frac{\mu}{2\pi\hbar^2} \sum' \sum_{\mathbf{k}} J_{n-m_f-N}(\mathbf{k}_{fN} \cdot \boldsymbol{\alpha}_0) a_{jm_f}^*(\lambda_f) a_{jm-s}(\lambda_p) J_{n-m}(\mathbf{k} \cdot \boldsymbol{\alpha}_0) \\ &\times \langle \mathbf{k}_{fN} | \langle j_f | V | j \rangle | \mathbf{k} \rangle \frac{1}{E - \lambda_p^s - \varepsilon_{\mathbf{k}}} \langle j' | \langle \mathbf{k} | V | j_i \rangle | \mathbf{k}_i \rangle \\ &\times J_{n'-m'}(\mathbf{k} \cdot \boldsymbol{\alpha}_0) a_{j'm'-s}(\lambda_p) a_{j,m_i}(\lambda_i) J_{n'-m_i}(\mathbf{k}_i \cdot \boldsymbol{\alpha}_0) \end{aligned} \quad (12.3.4.2.3)$$

where Σ' denotes summation over the whole set of photon indices $\{m_f, n, m, s, m', n', m_i\} = 0, \pm 1, \pm 2, \dots, \pm \infty$, and the set of atomic-state indices $\{j_f, j, p, j', j_i\} = 1, 2, \dots, J, \dots$.

The sums over n and n' can be carried out using the Bessel relation (12.2.3.9), but this is not particularly useful due to the required integration over $d\mathbf{k}$. We observe that the first and third lines of expression (12.3.4.2.3) contain most of the information about the interaction of the scattering system with the field; the second line is essentially a linear combination of the ordinary second-order but “off-shell” Born amplitudes. In practice, the main difficulty of exact evaluation of expression (12.3.4.2.3) is essentially of the same kind as that encountered in the absence of the field, namely determination of the intermediate sums over the infinite set of atomic states and integration over $d\mathbf{k}$. The following special cases of Eq. (12.3.4.2.3) should be noted.

1. For scattering of neutral (or inert) projectiles, we can simply set $\boldsymbol{\alpha}_0 = 0$ in Eq. (12.3.4.2.3) and use rule (12.2.2.8) to obtain

$$\begin{aligned} f^{(2)} &= -\frac{\mu}{2\pi\hbar^2} \sum' \sum_{\mathbf{k}} a_{jm_f}^*(\lambda_f) a_{jN+m_f-s}(\lambda_p) \\ &\times \langle \mathbf{k}_{fN} | \langle j_f | V | j \rangle | \mathbf{k} \rangle \frac{1}{E - \lambda_p^s - \varepsilon_{\mathbf{k}}} \langle j' | \langle \mathbf{k} | V | j_i \rangle | \mathbf{k}_i \rangle a_{j',m_i-s}(\lambda_p) a_{j,m_i}(\lambda_i) \end{aligned} \quad (12.3.4.2.4)$$

where now Σ' is only taken over (j_f, j, j', j_i) and (m_f, s, m_i) .

2. If the interaction of the field with the target can be neglected (such

as weak-field off-resonant interaction with the target) then the limiting values of $a_{jm}(\lambda_p)$ given by relation (12.3.4.1.7) are approximately true and expression (12.3.4.2.3) yields

$$f^{(2)} = -\frac{\mu}{2\pi\hbar^2} \sum_{nn'sj} \sum_{\mathbf{k}} J_{n-N}(\mathbf{k}_{fN} \cdot \boldsymbol{\alpha}_0) J_{n-s}(\mathbf{k} \cdot \boldsymbol{\alpha}_0) \langle \mathbf{k}_{fN} | \langle f | V | j \rangle | \mathbf{k} \rangle \\ \times \frac{1}{E - \lambda_j^s - \varepsilon_k} \langle j | \langle \mathbf{k} | V | i \rangle | \mathbf{k}_i \rangle J_{n'-s}(\mathbf{k} \cdot \boldsymbol{\alpha}_0) J_{n'}(\mathbf{k}_i \cdot \boldsymbol{\alpha}_0) \quad (12.3.4.2.5)$$

Again the sums over n and n' can be carried out, if desired, using relation (12.2.3.9).

3. If it is further assumed in case 2 that the interaction of the electron with the field in the intermediate (virtual) states is negligible (plausibly, due to the very short, about 10^{-16} s duration of collisions, compared to the time spent in the asymptotic domain), then one may use the limits

$$J_{n-s}(\mathbf{k} \cdot \boldsymbol{\alpha}_0 \rightarrow 0) \rightarrow \delta_{n,s} \quad \text{and} \quad J_{n'-s}(\mathbf{k} \cdot \boldsymbol{\alpha}_0 \rightarrow 0) \rightarrow \delta_{n',s} \quad (12.3.4.2.6)$$

in expression (12.3.4.2.5) and obtain

$$f^{(2)} = -\frac{\mu}{2\pi\hbar^2} \sum_{n=-\infty}^{\infty} J_{n-N}(\mathbf{k}_{fN} \cdot \boldsymbol{\alpha}_0) T_{i \rightarrow f}^{B2}(E - n\hbar\omega) J_n(\mathbf{k}_i \cdot \boldsymbol{\alpha}_0) \quad (12.3.4.2.7)$$

where $T_{i \rightarrow f}^{B2}(E - n\hbar\omega)$ is the usual second-order Born amplitude but evaluated at the off-shell energy $E - n\hbar\omega$:

$$T_{i \rightarrow f}^{B2}(E - n\hbar\omega) = \sum_{jk} \langle \mathbf{k}_{fN} | \langle f | V | j \rangle | \mathbf{k} \rangle \frac{1}{E - n\hbar\omega - \varepsilon_j - \varepsilon_k} \langle j | \langle \mathbf{k} | V | \mathbf{k}_i \rangle | i \rangle \quad (12.3.4.2.8)$$

4. Finally, if the atom-field interaction is significant (e.g., near the optical resonance frequencies) but the electron-field interaction in the intermediate (virtual) states is weak [as in case 3], then one may use the limits

$$a_{jm-s}(\lambda_p) J_{n-m}(\mathbf{k} \cdot \boldsymbol{\alpha}_0 \rightarrow 0) = a_{jn-s}(\lambda_p) \delta_{nm} \quad \text{and} \quad (12.3.4.2.9)$$

$$a_{jm'-s}(\lambda_p) J_{n'-m'}(\mathbf{k} \cdot \boldsymbol{\alpha}_0 \rightarrow 0) = a_{jn'-s}(\lambda_p) \delta_{n'm'}$$

in Eq. (12.3.4.2.3) and obtain a correspondingly simplified second-order amplitude.

12.3.5. Target State Distributions for Radiative Scattering

In the presence of the field, in general, the state of the target from which the electrons scatter is not the thermal ground state but rather originates from a certain distribution of target states, which depend significantly on the field parameters. Depending on whether or not the atom-field interaction time T is shorter or longer than the typical relaxation or decay time (t_{relax} or t_{decay}) of the excited states of the target, the relevant distribution can be determined under suitable conditions, to be specified below.

Suppose prior to $t = 0$ there is effectively no interaction of the atom with the field. Under the action of the field the density matrix $\rho(t)$ of the atomic states becomes a function of time. If the instant of collision between an atom and electron is t_c and the atom-field density matrix at this instant is $\rho(t_c)$, then for a given colliding pair of target + projectile the instant t_c is essentially a random quantity. Hence the distribution corresponding to the target states, from the standpoint of collisions, is given by the average of $\rho(t_c)$ with respect to the probability distribution of t_c . On the assumption that t_c is distributed uniformly, the target state distribution of interest is

$$\bar{\rho}(T) = \frac{1}{T} \int_0^T \rho(t_c) dt_c \quad (12.3.5.1)$$

where T is the duration of the atom-field interaction. For example, for a pulsed laser of pulse length τ_p , T can be set equal to τ_p . On the other hand, for a cw laser T may be allowed to approach the limit $T \rightarrow \infty$. Generally speaking, for (short-pulse) lasers with

$$\tau_p \ll t_{\text{relax}}, t_{\text{decay}} \quad (12.3.5.2)$$

$\rho(T)$ is expected to be a “pure-state” density matrix, which will exhibit the presence of coherence between the target states generated by the field. On the other hand, if

$$\tau_p \gg t_{\text{relax}}, t_{\text{decay}} \quad (12.3.5.3)$$

then such coherence will tend to be destroyed and $\rho(T)$ will be an “incoherent mixture” (see Section 8.2). Finally, for long pulses or cw lasers, even in the presence of decay or losses, the possibility exists that the relevant distribution will become a steady-state distribution ρ_s , provided of course that there is also a steady supply of fresh target atoms in the interaction region. This is provided, for example, by the atomic beams in crossed-beam scattering experiments.

Once the distribution $\rho(T)$ or ρ_s is found it can be combined with the appropriate fundamental amplitude matrix f , an element of which consists of a typical radiative scattering amplitude. The differential scattering signal into the element of solid angle $d\Omega$ (around the scattering direction Ω) is then given by the expectation value

$$\frac{dS}{d\Omega} = \text{Tr}[f\bar{\rho}f^+] \quad (12.3.5.4)$$

where f^+ is the adjoint of f and Tr denotes the trace operation. To illustrate the above procedure simply, we consider the structure of the elastic signal for scattering from an atomic target in a near- or on-resonant field (within a two-state approximation).

12.3.5.1. State Distribution: Pulsed Laser

We restrict ourselves to the two (near-degenerate) eigenstates of the Floquet equations (12.3.2.4), ($j = a, n = 0$) and ($j = b, n = -1$) in the “quasi-on-shell” (or RWA) approximation. The corresponding solutions for $a_m(\lambda_p)$ are

$$\begin{pmatrix} a_{1,0}(\lambda_1) = \cos \theta & a_{2,-1}(\lambda_1) = \sin \theta \\ a_{1,0}(\lambda_2) = -\sin \theta & a_{2,-1}(\lambda_2) = \cos \theta \end{pmatrix} \quad (12.3.5.1.1)$$

with eigenvalues

$$\hbar\lambda_1 = \hbar \left(\omega_a + \frac{\Delta}{2} - \frac{\Omega}{2} \right) \rightarrow \hbar\omega_a \quad \text{as } \beta \rightarrow 0 \quad (\Delta > 0) \quad (12.3.5.1.2)$$

and

$$\hbar\lambda_2 = \hbar \left(\omega_a + \frac{\Delta}{2} + \frac{\Omega}{2} \right) \rightarrow \hbar\omega_b - \hbar\omega \quad \text{as } \beta \rightarrow 0 \quad (\Delta > 0) \quad (12.3.5.1.3)$$

They are reversed for $\Delta < 0$. Quantity $\Omega = (\Delta^2 + \beta^2)^{1/2}$ is the effective Rabi frequency, Δ is the effective detuning $\omega_b - \omega_a - \omega$, and β is the effective coupling matrix element. We note that the Rabi frequency equals the separation between the dressed energies, $\Omega = \lambda_1 - \lambda_2$. Finally, $\tan 2\theta = \beta/\Delta$, with $-\pi/4 \leq \theta \leq \pi/4$. Hence the two dressed states of interest are

$$|\lambda_1\rangle = \cos \theta |a\rangle |0\rangle + \sin \theta |b\rangle |-1\rangle \quad (12.3.5.1.4)$$

and

$$|\lambda_2\rangle = -\sin \theta |a\rangle |0\rangle + \cos \theta |b\rangle |-1\rangle \quad (12.3.5.1.5)$$

where the atomic states $|a\rangle$ and $|b\rangle$ have energies $\hbar\omega_a$ and $\hbar\omega_b$; $|0\rangle$ and $| -1\rangle$ are the number states (with occupation numbers measured from the initial occupation number $|n_0\rangle$). If the wave function of the atom + field system prior to the interaction is $|\psi(0)\rangle$, then after an interaction time t it evolves into

$$\psi(t) = e^{-i\lambda_1 t} |\lambda_1\rangle \langle \lambda_1 | \psi(0) \rangle + e^{-i\lambda_2 t} |\lambda_2\rangle \langle \lambda_2 | \psi(0) \rangle \quad (12.3.5.1.6)$$

To be specific we now let $|\psi(0)\rangle = |a\rangle|0\rangle$ be the wave function prior to the field interaction, so that

$$\langle \lambda_1 | \psi(0) \rangle = \cos \theta \quad \text{and} \quad \langle \lambda_2 | \psi(0) \rangle = -\sin \theta \quad (12.3.5.1.7)$$

12.3.5.2. Reduction of the Pure State to a Mixture

The density matrix of the target at the instant of collision t_c is found immediately from Eqs. (12.3.5.1.6) and (12.3.5.1.7) to be

$$\rho(t_c) = \begin{pmatrix} \cos^2 \theta & e^{i\Omega t_c} \cos \theta \sin \theta \\ e^{-i\Omega t_c} \cos \theta \sin \theta & \sin^2 \theta \end{pmatrix} \quad (12.3.5.2.1)$$

At this time, clearly $[\rho(t_c)]^2 = \rho(t_c)$ and the target is at a coherent superposition of states (a “pure state”). But the instant t_c for all pairs of target atom + projectile electron is, as already stated, essentially a random quantity. Hence assuming a uniform probability distribution of t_c , the average distribution (12.3.5.1) is obtained in the form

$$\bar{\rho}(T) = \begin{pmatrix} \cos^2 \theta & -i \frac{1}{\Omega T} (e^{i\Omega T} - 1) \cos \theta \sin \theta \\ i \frac{1}{\Omega T} (e^{-i\Omega T} - 1) \cos \theta \sin \theta & \sin^2 \theta \end{pmatrix} \quad (12.3.5.2.2)$$

It is hence seen explicitly that the off-diagonal correlation between the dressed states $|\lambda_1\rangle$ and $|\lambda_2\rangle$ is significant so long as the pulse interaction time $T < O(1/\Omega)$, but it becomes negligible for long pulses ($T \gg 1/\Omega$). In fact, if the pulse interaction time is longer than the spontaneous relaxation times, then we may take $T \rightarrow \infty$ in matrix (12.3.5.2.2) and obtain

$$\begin{aligned} \bar{\rho} &\equiv \lim_{T \rightarrow \infty} \bar{\rho}(T) \\ &= \begin{pmatrix} \cos^2 \theta & 0 \\ 0 & \sin^2 \theta \end{pmatrix} \end{aligned} \quad (12.3.5.2.3)$$

In this limit the coherence between states $|\lambda_1\rangle$ and $|\lambda_2\rangle$ is destroyed and distribution (12.3.5.2.3) describes an incoherent mixture of these states. This is because now

$$[\bar{\rho}]^2 \neq [\bar{\rho}] \quad (12.3.5.2.4)$$

It should be noted that the effects of decay or spontaneous emission do not appear explicitly in expression (12.3.5.2.3). This restricts its use to the class of experiments in which the spontaneous width γ_s and ionization decay width γ_{ion} are small in comparison with the Rabi frequency Ω , i.e,

$$\Omega \gg \gamma_s, \gamma_{\text{ion}} \quad (12.3.5.2.5)$$

We shall see in Section 12.3.5.6 that for the steady-state distribution required to analyze crossed-beam experiments in cw lasers, inequality (12.3.5.2.5) is not a necessary restriction.

12.3.5.3. The Radiative “Elastic” Scattering Signal

We are now in a position to obtain the elastic signal from distribution (12.3.5.2.3) and the corresponding fundamental amplitude matrix

$$\hat{f} = \begin{pmatrix} f_{\lambda_1 \rightarrow \lambda_2}(\mathbf{k}_0 \rightarrow \mathbf{k}) & \left(\frac{k_{21}}{k_0}\right) f_{\lambda_2 \rightarrow \lambda_1}(\mathbf{k}_0 \rightarrow \mathbf{k}_{21}) \\ \left(\frac{k_{12}}{k_0}\right) f_{\lambda_1 \rightarrow \lambda_2}(\mathbf{k}_0 \rightarrow \mathbf{k}_{12}) & f_{\lambda_2 \rightarrow \lambda_2}(\mathbf{k}_0 \rightarrow \mathbf{k}) \end{pmatrix} \quad (12.3.5.3.1)$$

where \mathbf{k}_0 is the incident wave vector; the scattered wave vectors in the scattering direction \hat{n} are

$$\begin{aligned} \mathbf{k}_{21} &= \left(k_0^2 + \frac{2\mu}{\hbar} \Omega \right)^{1/2} \hat{n} \\ \mathbf{k}_{12} &= \left(k_0^2 - \frac{2\mu}{\hbar} \Omega \right)^{1/2} \hat{n} \\ \mathbf{k} &= k_0 \hat{n} \end{aligned} \quad (12.3.5.3.2)$$

For resonant pulsed excitation, the elastic scattering signal is obtained by substituting expressions (12.3.5.3.1) and (12.3.5.2.3) in Eq. (12.3.5.4). One finds that the “elastic signal” splits into three closely spaced components, separated by $\hbar\Omega$ from each other:

$$\frac{dS}{d\Omega} = \frac{dS_{\text{el}}}{d\Omega} + \frac{dS_{\lambda_1 \rightarrow \lambda_2}}{d\Omega} + \frac{dS_{\lambda_2 \rightarrow \lambda_1}}{d\Omega} \quad (12.3.5.3.3)$$

where the central peak at the incident energy has intensity

$$\frac{dS_{\text{el}}}{d\Omega} = \cos^2 \theta \frac{d\sigma_{\lambda_1 \rightarrow \lambda_1}(\mathbf{k}_0 \rightarrow \mathbf{k})}{d\Omega} + \sin^2 \theta \frac{d\sigma_{\lambda_2 \rightarrow \lambda_2}(\mathbf{k}_0 \rightarrow \mathbf{k})}{d\Omega} \quad (12.3.5.3.4)$$

and the intensities of the two “side bands” are

$$\frac{dS_{\lambda_1 \rightarrow \lambda_2}}{d\Omega} = \cos^2 \theta \frac{d\sigma_{\lambda_1 \rightarrow \lambda_2}(\mathbf{k}_0 \rightarrow \mathbf{k}_{12})}{d\Omega} \quad (12.3.5.3.5)$$

and

$$\frac{dS_{\lambda_2 \rightarrow \lambda_1}}{d\Omega} = \sin^2 \theta \frac{d\sigma_{\lambda_2 \rightarrow \lambda_1}(\mathbf{k}_0 \rightarrow \mathbf{k}_{21})}{d\Omega} \quad (12.3.5.3.6)$$

We see that the actual signal in the radiative “elastic” scattering is obtainable in terms of suitable combinations [Eqs. (12.3.5.3.4)–(12.3.5.3.6)] of the basic cross sections,

$$\frac{d\sigma_{\lambda_i \rightarrow \lambda_j}(\mathbf{k}_0 \rightarrow \mathbf{k}_y)}{d\Omega} = \frac{k_y}{k_0} |f_{\lambda_i \rightarrow \lambda_j}(\mathbf{k}_0 \rightarrow \mathbf{k}_y)|^2 \quad (12.3.5.3.7)$$

with $(i, j) = 1, 2$. For pulses of finite duration in which $\Omega T \approx 1$, analogous results are obtained by substituting expressions (12.3.5.3.1) and (12.3.5.2.2) in Eq. (12.3.5.4), thus reflecting the effect of pulse duration on the signal. Furthermore, for short pulses satisfying

$$\left(\frac{\Omega T}{2}\right)^2 \ll 1 \quad (12.3.5.3.8)$$

the density matrix (12.3.5.2.2) remains virtually fully coherent since now

$$[\bar{\rho}(T)]^2 = [\bar{\rho}(T)] \quad (12.3.5.3.9)$$

to within inequality (12.3.5.3.8), and the elastic signal is influenced by the off-diagonal correlation terms in $\rho(T)$.

12.3.5.4. The Scattering Signal for Adiabatic and Sudden Excitations

If the pulse rise time $t_{\text{rise}} < 1/\Omega$, which is often the case at resonance ($|\Delta| = 0$), the atom–field interaction may be thought of as being switched on suddenly at $t = 0$. In this case, generally speaking, all the dressed eigenstates of the target will be superpositioned in the total wave function satisfying the initial condition. In the present example this corresponds to

the solution (12.3.5.1.6) and to the density matrices (12.3.5.2.1) and (12.3.5.2.2). If, on the other hand, $t_{\text{rsc}} > 1/\Omega$, which occurs in general for off-resonant interactions ($|\Delta| \gg \text{ linewidths}$), the pulse may be considered as switched on adiabatically. Consequently, according to the adiabatic theorem⁽²⁶⁹⁾ the dressed eigenstate corresponding to the initial bare state $|\lambda\rangle$, such as $|\lambda_1\rangle$ (for $\Delta > 0$), will be occupied while the other eigenstates, such as $|\lambda_2\rangle$, will remain empty. Therefore, for the adiabatic case (in the Floquet representation) we obtain

$$\bar{\rho}(t_c) = \begin{pmatrix} 1 & 0 \\ 0 & 0 \end{pmatrix} = \bar{\rho}(T) \quad (12.3.5.4.1)$$

Substitution of expressions (12.3.5.4.1) and (12.3.5.3.1) in Eq. (12.3.5.4) yields the corresponding elastic signal

$$\frac{dS_{\text{ad}}}{d\Omega} = \frac{d\sigma_{\lambda_1 \rightarrow \lambda_1}(\mathbf{k}_0 \rightarrow \mathbf{k})}{d\Omega} + \frac{d\sigma_{\lambda_1 \rightarrow \lambda_2}(\mathbf{k}_0 \rightarrow \mathbf{k}_{12})}{d\Omega} \quad (12.3.5.4.2)$$

It should be noted that this result may also be obtained as a limiting case of Eq. (12.3.5.3.3). Indeed, in the off-resonant limit $|\Delta| \gg \beta$, $\sin \theta \approx 0$ and $\cos \theta \approx 1$ and the “sudden signal” (12.3.5.3.3) approaches the “adiabatic signal” (12.3.5.4.2). We should also remember that for $\Delta < 0$, the roles of eigenstates $|\lambda_1\rangle$ and $|\lambda_2\rangle$ are reversed [see Eqs. (12.3.5.1.2) and (12.3.5.1.3)]. Hence the scattering signals for $\Delta < 0$ are given by the same expressions given above for $\Delta > 0$, except that their subscripts 1 and 2 are interchanged.

12.3.5.5. Steady-State Distribution: Continuous-Wave Case

In crossed-beam experiments in a near-resonant cw laser field the characteristic time parameters controlling the nature of the target-state distribution are, for example,^(270–272)

$$\left. \begin{array}{l} t_{\text{rlx}}(\text{spontaneous relaxation}) \approx 10^{-8} \text{ s} \\ t_{\text{coll}}(\text{electron + atom collision}) < 10^{-14} \text{ s} \\ s_{\text{suc}}(\text{successive collision}) > (10-100) \times 10^{-8} \text{ s} \\ \quad (\text{e.g., electron energy} > 0.01 \text{ eV}) \\ t_{\text{rsp}}(\text{atomic response}) > 10^{-13} \text{ s} \\ T(\text{atom-field interaction}) \approx \infty \text{ (cw laser)} \end{array} \right\} \quad (12.3.5.5.1)$$

In the above situation the electron–atom collision time is generally much shorter than the atom–field response time. In other words, the collisions can be considered to occur in the impact limit⁽²⁷³⁾

$$t_{\text{coll}} < t_{\text{rsp}} \quad (12.3.5.5.2)$$

Furthermore

$$t_{\text{suc}} > t_{\text{rlx}}, t_{\text{res}} \quad (12.3.5.5.3)$$

which permits one to view the individual electron + atom collision as occurring from an ensemble of target atoms and reaching a steady state (with respect to atom + field interaction) between successive collisions with the incident electrons. Thus condition (12.3.5.5.2) allows one to calculate the steady-state scattering signal in two independent steps; first, the field-dependent distribution ρ_s of the steady-state ensemble of the beam atoms is obtained in the unperturbed representation of the atom (as opposed to the fully dressed state representation), and second, by constructing the fundamental amplitude matrix f in the same unperturbed representation. The scattering signal is again given by Eq. (12.3.5.4) with $\bar{\rho} \Rightarrow \rho_s$. The state of the scattering electron does not generally reach a steady state with respect to the field during the collision and is given, as before, by the dressed scattering state (12.2.2.7).

In the presence of any loss and decay (and relaxation) of the target beam atoms, on the one hand, and the steady supply of fresh beam atoms in the interaction region, on the other, the distribution of the states of the target ensemble of beam atoms in the field can be obtained from the slowly varying density matrix equation (see Section 8.4)

$$\frac{\partial \rho}{\partial t} = -\frac{i}{\hbar} [H, \rho] - \frac{i}{2} [\Gamma, \rho]_+ + \Lambda \quad (12.3.5.5.4)$$

where H is the effective atom + field Hamiltonian, Γ is the decay (or loss) matrix, and Λ is the “supply” matrix. The condition for the steady state is simply

$$\frac{\partial \rho}{\partial t} = 0 \quad (12.3.5.5.5)$$

12.3.5.6. A Typical Steady-State Distribution

For the simple but instructive case of the two-level system considered above (treated below in RWA and in the unperturbed atomic-state

representation) and in the presence of loss decay, relaxation, and supply, we have

$$H = \begin{pmatrix} -\frac{\Delta}{2} & \beta \\ \beta & \frac{\Delta}{2} \end{pmatrix}, \quad \Gamma = \begin{pmatrix} \gamma_1 & 0 \\ 0 & \gamma_2 \end{pmatrix},$$

$$\Lambda = \begin{pmatrix} \lambda_1 + \gamma_s \rho_{22} & 0 \\ 0 & 0 \end{pmatrix} \quad (12.3.5.6.1)$$

where γ_s is the spontaneous width of level 2 and

$$\gamma_1 = \frac{1}{T_1} \quad \text{and} \quad \gamma_2 = \gamma_s + \gamma_{\text{ion}} + \frac{1}{T_1} \quad (12.3.5.6.2)$$

In the above relations, λ_1 is the rate at which beam atoms enter the interaction region, γ_1 is the loss rate of the ground-state beam atoms from the interaction region due to a finite transit time T_1 , γ_2 is the total loss rate of the upper level 2 and equals the sum of the spontaneous emission, (multiphoton) ionization, and transit-time losses. Substitution of expressions (12.3.5.6.1) in Eq. (12.3.5.5.4) and use of the steady-state condition (12.3.5.5.5) give rise to a pair of algebraic equations, which can easily be solved to obtain the desired 2×2 distribution ρ_s . The steady-state probability of ionization in the continuum is then obtained from $\rho_{cc} = \rho_{22} \gamma_{\text{ion}} / \lambda_1$. Thus the normalized ensemble state distribution is

$$\rho_{11} = \frac{\Delta^2 + \beta'^2 + \gamma_{12}^2}{D}, \quad \rho_{12} = -\frac{\beta(\Delta + i\gamma)_{12}}{D}$$

$$\rho_{21} = \rho_{12}^*, \quad \rho_{22} = \frac{\beta'^2}{D}, \quad \rho_{cc} = \frac{\gamma_{\text{ion}} \cdot \beta'^2}{\lambda_1 D} \quad (12.3.5.6.3)$$

with

$$D = \left(2 + \frac{\gamma_{\text{ion}}}{\lambda_1}\right) \beta'^2 + \Delta^2 + \gamma_{12}^2 \quad (12.3.5.6.4)$$

$$\beta'^2 = (\beta/2)^2 \left(1 + \frac{\gamma_1}{\gamma_2}\right), \quad \gamma_{12} = \frac{\gamma_1 + \gamma_2}{2} \quad (12.3.5.6.5)$$

Here, elements ρ_{2c} and ρ_{c2} are absent, reflecting the assumption that the ensemble ionization is an incoherent decay process. The distribution

(12.3.5.6.3) contains a number of special cases,^(264,270,271) which apply to resonance fluorescence⁽²⁷⁴⁾ and the radiative scattering signal in the absence of decay. We note that, as expected, in the absence of the supply rate ($\lambda_1 = 0$) the atoms in the interaction volume are ionized, in the long run, with certainty. Furthermore, if the supply rate λ_1 is so high that $\gamma_{\text{ion}}/\lambda_1 \ll 1$ then the presence of the ionizing component in the ensemble becomes negligibly small. Finally, the fact that the set (12.3.5.6.3) is not diagonal in the present unperturbed representation reveals the presence of a finite induced (dipole) polarization⁽²⁷⁵⁾ of the ensemble of beam atoms. It is clear from relations (12.3.5.6.3) that at or near the optical resonance ($\Delta = 0$) the two bound states can be populated significantly and therefore both may take part in determining the scattering signal. For the sake of simplicity, we consider the case $\gamma_{\text{ion}}/\lambda_1 \ll 1$, so that the effect of ionization in the elastic signal remains negligible. The electron scattering cross section at the optical resonance is then given by

$$\frac{d\sigma}{d\Omega} = \rho_{11}(\sigma_{1,0 \rightarrow 1,0} + \sigma_{1,0 \rightarrow 2,1}) + \rho_{22}(\sigma_{2,0 \rightarrow 2,0} + \sigma_{2,0 \rightarrow 1,-1}) \quad (12.3.5.6.6)$$

where $f_{i,0 \rightarrow j,n}$ are cross sections for the atomic transition $|\phi_i\rangle \rightarrow |\phi_j\rangle$ that are associated with the steady-state target distribution ρ_s , and are accompanied by the absorption ($n < 0$) or emission of n photons by the electron. The corresponding scattering amplitudes $f_{i,0 \rightarrow j,n}$ are derived in the next section.

12.3.6. The Amplitude Matrix in the Steady-State Case

When the atom–field interaction reaches a steady state, certain simplifications for radiative electron–atom scattering occur. In the steady state, all information on the atom–field interaction may be assumed to be contained in the distribution ρ_s of the states of the target atom, and hence we need only consider the scattering system

$$\text{"bare atom" + "dressed electron"} \quad (12.3.6.1)$$

to determine the amplitude matrix \hat{f} . The scattering signal is then obtained from the relation

$$\frac{ds}{d\Omega} = \text{Tr}[\hat{f}\rho_s\hat{f}]^+ \quad (12.3.6.2)$$

Below, we briefly obtain the typically simplified system of scattering amplitudes f in the steady-state case.

The Schrödinger equation associated with system (12.3.6.1) is

$$[E - H^0] |\psi\rangle = V(\mathbf{r}, \mathbf{x}) |\psi\rangle \quad (12.3.6.3)$$

where for illustration we assume a circularly polarized field so that

$$H^0 = -\frac{\hbar^2}{2\mu} \nabla_r^2 + \hbar\omega a^+ a + \beta(L_e^+ a + L_e^- a^+) + H_a(\mathbf{x}_a) \quad (12.3.6.4)$$

where

$$\beta = \left(\frac{2\pi\hbar c^2}{L^3 \omega} \right)^{1/2}$$

If the state $|\psi\rangle$ is expanded in the form

$$|\psi\rangle = \sum_n \phi_n(\mathbf{x}_a) F_{nn'}(\mathbf{r}) |n\rangle \quad (12.3.6.5)$$

and projected onto $\langle n |$ and $\langle \phi_n(\mathbf{x}) |$, then

$$[E - (H_n^0 + \epsilon_j)] F_{nj}(\mathbf{r}) = \sum_{j'} V_{jj'}(\mathbf{r}) F_{j'n}(\mathbf{r}) \quad (12.3.6.6)$$

where

$$H_n^0 = -\frac{\hbar^2}{2\mu} \nabla_r^2 + n\hbar\omega + \frac{1}{2}i\hbar\omega\alpha_0(L_e^+ s_n^- + L_e^- s_n^+) \quad (12.3.6.7)$$

The Green's function $G'_{nn'}(\mathbf{r}, \mathbf{r}')$, defined by

$$[E - (H_n^0 + \epsilon_j)] G'_{nn'}(\mathbf{r}, \mathbf{r}') = \delta_{nn'} \delta(\mathbf{r} - \mathbf{r}') \quad (12.3.6.8)$$

has the exact solution [cf. Eq. (12.3.3.6)]

$$\begin{aligned} G'_{nn'}(\mathbf{r}, \mathbf{r}') &= \sum_{N=-\infty}^{\infty} \sum_{\mathbf{k}} J_{n-N}(k\alpha_0 \sin \theta_k) e^{-in\phi_k} \\ &\times \frac{e^{i\mathbf{k} \cdot (\mathbf{r}-\mathbf{r}')}}{E - \epsilon_j - N\hbar\omega - \hbar^2 k^2 / 2\mu} e^{in'\phi_k} J_{n'-N}(k\alpha_0 \sin \theta_k) \end{aligned} \quad (12.3.6.9)$$

This expression may be used to solve Eq. (12.3.6.6):

$$\begin{aligned} F_{jn}^{(t)}(\mathbf{r}) &= e^{i\mathbf{k}_0 \cdot \mathbf{r}} J_n(k_0 \alpha_0 \sin \theta_0) e^{-in\phi_0} \\ &+ \sum_{j'n'} \int d\mathbf{r}' G'_{nn'}(\mathbf{r}, \mathbf{r}') V_{jj'}(\mathbf{r}') F_{j'n'}^{(t)}(\mathbf{r}) \end{aligned} \quad (12.3.6.10)$$

On taking the limit $r \rightarrow \infty$ the scattered wave in the second term of Eq. (12.3.6.10) becomes

$$\sum_{jN} J_{n-N}(k_{jN}\alpha_0 \sin \theta_k) e^{-im\phi_{kN}} \frac{e^{ik_{jN}r}}{r} f_{i,0 \rightarrow i,N}(\Omega_0, \Omega) \quad (12.3.6.11)$$

whence the desired system of scattering amplitudes is given by

$$f_{i,0 \rightarrow jN}(\Omega_0, \Omega) = -\frac{\mu}{2\pi\hbar^2} \sum_{j'n'} J_{n'-N}(k_{jN}\alpha_0 \sin \theta_k) e^{-im'\phi_{kN}} \times \langle e^{i\mathbf{k}_{jN}\mathbf{r}} | V_{jj'}(\mathbf{r}) | F_{j'n'}^{(i)}(\mathbf{r}) \rangle \quad (12.3.6.12)$$

12.3.7. A Multichannel Pseudopotential Model

Characteristically new scattering phenomena in radiative “electron + atom” scattering occur at low electron energies E_i , which include the region in which the electron energy could be comparable to or even less than the photon energy, namely $E_i \leq \hbar\omega$. In this situation neither the Born approximation nor the low-frequency approximation is expected to be applicable. Considerable physical insight into these processes can be gained in the absence of elaborate computations from a multichannel pseudopotential scattering model, with parameters determined semiempirically from known data on low-energy scattering in the absence of the field. Such a simple model is essentially of pedagogic interest; it permits the analysis to be carried out exactly to the end.

In this model we approximate the scattering potential as

$$V(\mathbf{r}, \mathbf{x}) = \sum_{jj'} |j(\mathbf{x})\rangle U_{jj'}(\mathbf{r}) \langle j'(\mathbf{x})| \quad (12.3.7.1)$$

where $U_{jj'}(\mathbf{r})$ are the interchannel pseudopotentials, which we determine semiempirically assuming the very simple Breit-Zilsel form^(276,277)

$$U_{jj'}(\mathbf{r}) = W_{jj'} \delta(\mathbf{r}) \frac{\partial}{\partial r} r \quad (12.3.7.2)$$

For the present example we restrict (j, j') to only two states, $(j, j') = 1, 2$, with energies $\epsilon_1 = 0$ and $\epsilon_2 = 10.2$ eV (corresponding to the $n = 2$ level of the hydrogen atom). There is no difficulty (except for lengthy algebra) in solving this system for an arbitrary but finite number of states $(j, j') = 1, 2, 3, \dots, J$. The constants $W_{jj'}$ are determined from the known data on low-energy electron-hydrogen scattering in the absence of the field. We

choose

$$W_{11} = 29.23 \text{ (au)}, \quad W_{22} = 30.79 \text{ (au)}, \quad W_{12} = W_{21} = 7.67 \text{ (au)} \quad (12.3.7.3)$$

The low-energy field-free elastic scattering cross section [cf. Eq. (12.3.7.4)] obtained using the two-level parameters (12.3.7.3) is shown in Figures 58 and 59. It is seen that the model reproduces the experimentally observed⁽²⁷⁸⁾ electron–hydrogen scattering resonance ('S) at 9.6 eV and also the width 0.04 eV (see Figure 59). The same pseudopotential yields the H⁻ (negative-ion) bound-state energy at -0.75 eV (not shown in the figures). The elastic cross section at zero energy is seen to be comparable with the actual two-state close-coupling calculation,⁽²⁷⁹⁾ which gives $\sigma(E=0) \approx 254.75 \text{ } a_0^2$. Thus the above semiempirical two-state model fits the known low-energy electron–hydrogen scattering data correctly from a physical standpoint. This model can be easily extended to obtain the steady-state transition amplitudes in a circularly polarized cw laser field. To obtain the amplitudes explicitly we must solve for $F_{j,n}^{(i)}(\mathbf{r})$, appearing Eq. (12.3.6.12). To this end we substitute the interaction (12.3.7.1) and (12.3.7.2) in Eq. (12.3.6.10), operate on the left with $\langle j(\mathbf{x}_a) | \delta(\mathbf{r})(\partial/\partial r)r, \text{ and integrate over } \mathbf{r} \text{ and } \mathbf{x}_a \text{ to obtain a set of } J \text{ algebraic equations, where } J$

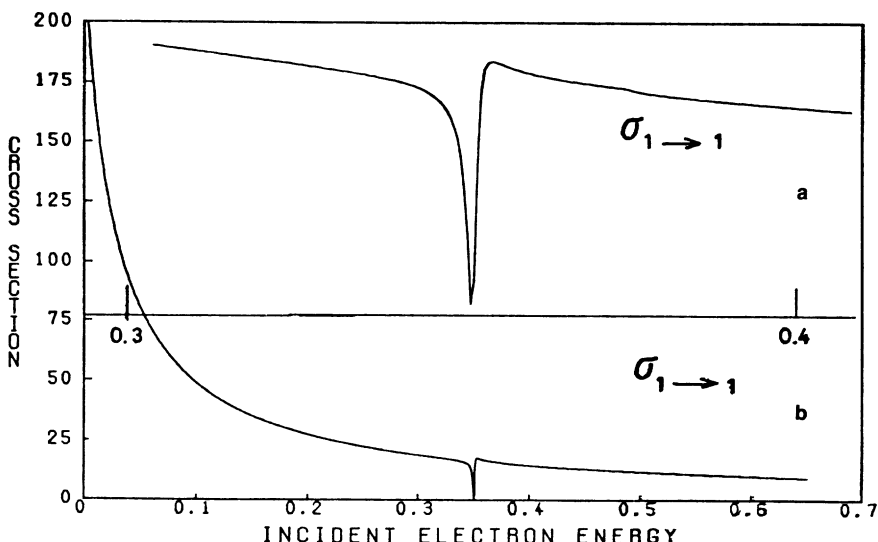


Figure 58. Low-energy electron–hydrogen elastic cross section calculated according to the pseudopotential model. The '¹S' resonance is reproduced near 9.558 eV (width 0.04 eV). The scales are in atomic units.

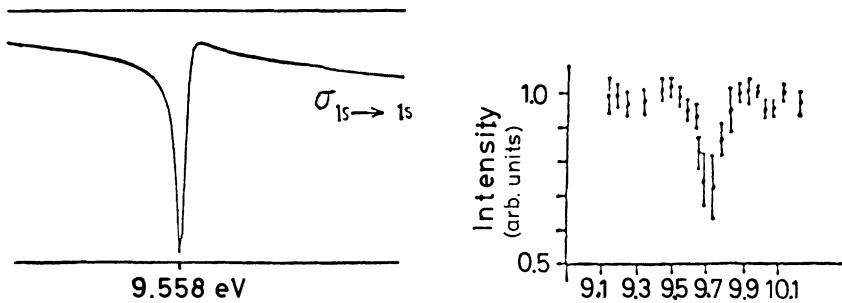


Figure 59. Comparison of experimentally measured 1S resonance at about 9.6 eV with the pseudopotential-model calculation (diagram on the left-hand side). The experimental result is from Kleinpoppen and Riable.⁽²⁷⁸⁾

equals the number of target states retained. For a finite number of states this set is easily solved, and resubstitution of the result back into Eq. (12.3.6.10) yields the final explicit expressions for the amplitudes (12.3.6.12). For the two-level scattering problem of interest we easily derive

$$f_{i,0 \rightarrow j,N}(\Omega_0, \Omega_k) = -\frac{\mu}{2\pi\hbar^2} \sum_n J_n(k_0 \alpha_0 \sin \theta_0) e^{in(\phi_0 - \phi_{kN})} J_{n-N}(k_{jN} \alpha_0 \sin \theta_k) g_{i \rightarrow j}^{(n)}(E_i) \quad (12.3.7.4)$$

where

$$g_{i \rightarrow j}^{(n)}(E_i) = \begin{cases} W_{j1}(1 + i(1 - \alpha)R_{2n}\delta_{j1})/d_n(E_i), & i = 1 \\ W_{j2}(1 + i(1 - \alpha)R_{1n}\delta_{j2})/d_n(E_i), & i = 2 \end{cases} \quad (12.3.7.5)$$

$$R_{jn} = \frac{\mu}{2\pi\hbar^2} W_{jn} s_{jn} \quad (12.3.7.6)$$

$$s_{jn} = \sum_m k_{jm} \frac{1}{2} \int_0^\pi d\theta \sin \theta J_{m-n}^2(k_{mj} \sin \theta \alpha_0) \quad (12.3.7.7)$$

$$d_n(E_i) = (1 + iR_{1n})(1 + iR_{2n}) + \alpha R_{1n} R_{2n} \quad (12.3.7.8)$$

$$\alpha = \frac{W_{12} W_{21}}{W_{11} W_{22}} \quad (12.3.7.9)$$

The amplitude (12.3.7.4) corresponds to scattering of electrons incident in the direction $\Omega_0 = (\theta_0, \phi_0)$ with momentum $k_0 = [(2\mu/\hbar^2)(E_i - \varepsilon_i)]^{1/2}$ to a final state in the direction $\Omega = (\theta, \phi)$ with momentum $k_{jN} = [(2\mu/\hbar^2)(E_i - \varepsilon_i - N\hbar\omega)]^{1/2}$. The result contains rather a considerable amount of information. To get some insight into the result we first consider a few limiting cases.

12.3.7.1. The Scattering Singularities

If we neglect all interactions with the radiation field, then Eq. (12.3.7.4) yields the scattering amplitude for ordinary scattering. Thus, for example, the field-free elastic amplitude is obtained:

$$f_{1 \rightarrow 1}(E_i) = -\frac{\mu}{2\pi\hbar^2} W_{11}[1 + i(1 - \alpha)R_2]/d(E_i) \quad (12.3.7.1.1)$$

where

$$d(E) = (1 + iR_1)(1 + iR_2) + \alpha R_1 R_2 \quad (12.3.7.1.2)$$

and

$$R_i = \frac{\mu}{2\pi\hbar^2} W_{ii} k_i \quad (12.3.7.1.3)$$

The scattering poles are seen to occur at the zeros of function (12.3.7.1.2), which is a quartic in the total energy E and generally gives four roots. For small reduced coupling strength α , given by Eq. (12.3.7.9), they reduce to a real root and a complex root yielding a true compound state and a decaying resonance, respectively. Another type of singularity is due to the presence of inelastic thresholds. The elastic scattering cross sections near the vicinity of the threshold $k_2^2 = 0$ is easily found from Eq. (12.3.7.1.1) by expanding it around $k_2^2 = 0$ in the form

$$\sigma_{1 \rightarrow 1}(k_2^2 \rightarrow 0) = \frac{4\pi R_i^2}{1 + R_i^2} \left[1 - \frac{2\alpha}{(1 + R_i^2)^{1/2}} R'_2 h(\theta_1) \right] / (k_1^i)^2 \quad (12.3.7.1.4)$$

where

$$h(\theta_1) = \begin{cases} \sin \theta_1 & \text{for } k_2^2 > 0 \\ \cos \theta_1 & \text{for } k_2^2 < 0 \end{cases} \quad (12.3.7.1.5)$$

$$\theta_1 = \operatorname{tg}^{-1}[R_i]$$

and

$$R_i = \frac{\mu W_{11}}{2\pi\hbar^2} k_1^i, \quad R'_2 = \frac{\mu W_{22}}{2\pi\hbar^2} |k_2|, \quad k_1^i = k_1 \quad \text{at } k_2^2 = 0 \quad (12.3.7.1.6)$$

This result illustrates explicitly the four types of Wigner–Baz cusp singularities⁽²⁸⁰⁾ associated with the value of θ_1 in the first, second, third, and fourth quadrants. We may ask how the poles and cusp singularities are affected in the presence of the laser field. The answer depends, strictly speaking, on the particularities of the field parameters. Qualitatively, the

result may be summarized as a “propensity rule”^(257,264): All scattering singularities occurring at a given channel in the absence of the radiation field tend to be repeated in the new channels at energies shifted by multiples of the photon energy. We should also note that in the presence of the field all scattering singularities will be shifted and broadened by the field.

12.3.7.2. Potential Scattering in a Laser Field

It is also of some interest to take the limit of Eq. (12.3.7.4) in which the internal structure of the atom is altogether neglected. This is equivalent to making the so-called static approximation,⁽²⁸¹⁾ in which only one atomic state is retained and all laser–atom interactions are neglected. In this limit the amplitude $f_{i,0 \rightarrow j,N}(\Omega)$ reduces to

$$f_{i,0 \rightarrow j,N}^I(\Omega) = -\frac{\mu W_{11}}{2\pi\hbar^2} \sum_n J_n(k_1 \sin \theta_0 \alpha_0) e^{in(\phi_0 - \phi_{k_N})} J_{n-N}(k_{1N} \sin \theta \alpha_0) \frac{1}{h_n} \quad (12.3.7.2.1)$$

with

$$h_n = 1 + i \frac{\mu W_{11}}{2\pi\hbar^2} s_{jn} \quad (12.3.7.2.2)$$

Equation (12.3.7.2.1) has been used to discuss stimulated bremsstrahlung in potential scattering.⁽²⁷⁷⁾

12.3.7.3. The Low-Frequency Limit

The exact model amplitude (12.3.7.4) is reminiscent of the low-frequency amplitude, where one neglects the effect of radiation field on the electron motion in the intermediate states. However, it differs from the latter in one important respect. The quantity $g_{i \rightarrow j}^{(n)}(E)$ in Eq. (12.3.7.4) is seen to represent the same function as the exact scattering amplitude in the absence of the radiation field but evaluated at the “dressed momenta” s_{jn} . The low-frequency approximation^(251–257) effectively uses the unperturbed momenta k_{jn} in place of s_{jn} . The dressed momenta s_{jn} are seen from expression (12.3.7.7) to represent the weighted sum of the unperturbed momenta, weighted by their probability of occurrence in the wave function of the “dressed electron” in the field. It is also interesting to observe that in the opposite limit of “high frequency” such that $\langle k_{1N} \alpha_0 \rangle \ll 1$, the dressed momenta s_{jn} again approach the unperturbed momenta k_{jn} . Below, we point out a number of new scattering phenomena with specific reference to low-energy electron–hydrogen scattering, calculated using Eq. (12.3.7.4).

12.3.7.4. The Resonant Influence of Ground State H^- on Elastic Scattering

Consider electron-hydrogen scattering at energies far below the $n = 2$ threshold energy $E_{th} = 10.2$ eV, and at field photon frequency $\hbar\omega = 0.05$ au. Figure 60 shows the result for the elastic cross section. Comparison with Figure 58 shows a dramatic change in the field-modified elastic cross section $\sigma_{1,0 \rightarrow 1,0}$ (with no net emission or absorption of photons); it exhibits a sharp structure, which “reflects” the bound H^- negative ion state into the elastic channel. This is because at $E_i \approx 0.0224$ (au) the photon energy $\hbar\omega = 0.05$ (au) matches approximately the binding energy of H^- , $E_B = -0.0276$ (au), and we have a resonant capture of the scattering electron in the H^- state (as it loses the energy of one photon by the stimulated emission). However, the captured electron can also reabsorb a laser photon and return to its positive-energy elastic channel; the delay caused by the temporary “capture and escape” episodes shows up as a new resonance in the elastic channel. We note that a smaller two-photon “capture-escape” resonance is also discernible at an electron energy which is $\hbar\omega = 0.05$ (au) above the primary one-photon resonance. Clearly, the main resonance may be used to infer the electron affinity by elastic scattering in the field. Figure 61 shows a similar “capture-escape” resonance in the field of a Nd laser with $\hbar\omega = 1.17$ eV (= 0.043 au) and peak field strength $F_0 = 0.0005$ au. It

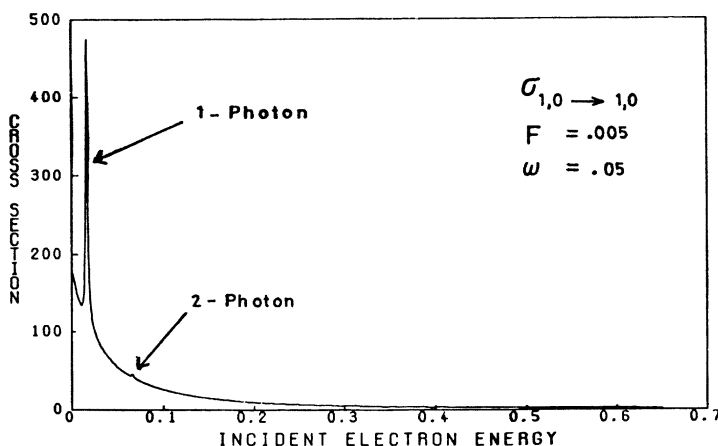


Figure 60. Low-energy cross section for radiative electron-hydrogen scattering. $\sigma_{1,0 \rightarrow 1,0}$ is the model $1s-1s$ cross section in the presence of the field (with no net emission or absorption of photons). Peak field strength $F_0 = 0.005$ au ($I = 0.85 \times 10^{12} \text{ cm}^{-2}$) and $\hbar\omega = 1.35$ eV. The sharp structure at about 0.6 eV is one-photon “capture-escape” resonance due to temporary capture of the scattering electron in the bound H^- state (at -0.75 eV). The small peak at about 1.95 eV is due to two-photon resonance with the H^- state. The scales are in atomic units.

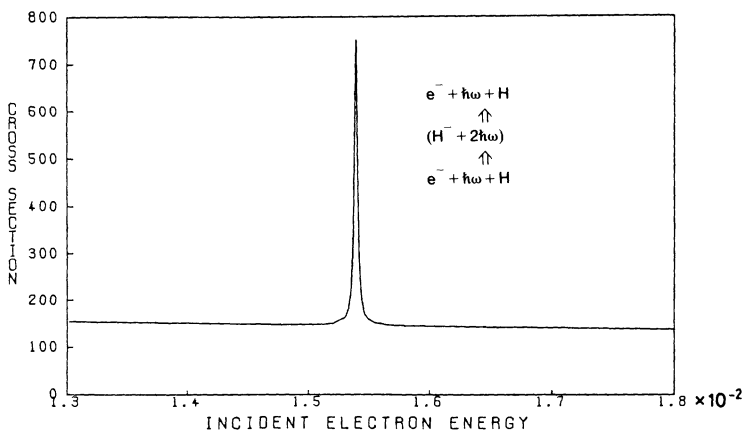
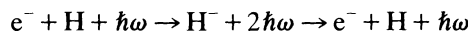


Figure 61. Field-modified electron-hydrogen elastic scattering cross section (with no net emission or absorption of photons) in a Nd-laser field. Field strength $F_0 = 0.0005$ au, $\hbar\omega = 1.17$ eV. The sharp structure is field-induced “capture-escape” resonance due to temporary capture of the scattering electron in the H^- bound state. The scales are in atomic units.

may be schematized as a “reaction”:



12.3.7.5. Target Excitation by Subthreshold Scattering

Another interesting phenomenon, at electron energies below the first inelastic excitation threshold of the hydrogen atom, is the resonant excitation of the $n = 2$ level by the subthreshold electrons. This process may permit one to probe experimentally a portion of the off-shell electron-scattering amplitude. With the subthreshold electrons the only excitation mechanism⁽²⁷²⁾ is the “off-shell” scattering.⁽²⁸²⁻²⁸⁴⁾ Diagram (a) in Figure 62 exhibits a typical result of such an excitation cross section $\sigma_{1,0 \rightarrow 2,-1}$, in which the electron borrows a photon from the field and excites the upper state of the atom by the collisional transfer of its enhanced kinetic energy to the atom. What is more, the process becomes resonant in nature due to the presence of the elastic scattering resonance (at about 9.6 eV). We also note the existence of a threshold cusp (at approximately 10.2 eV) and a secondary resonance at about 0.35 (au). The calculated values are for $\hbar\omega = 0.15$ au and peak field strength $F_0 = 0.035$ au. We should emphasize that the resonant subthreshold excitation is not, of course,

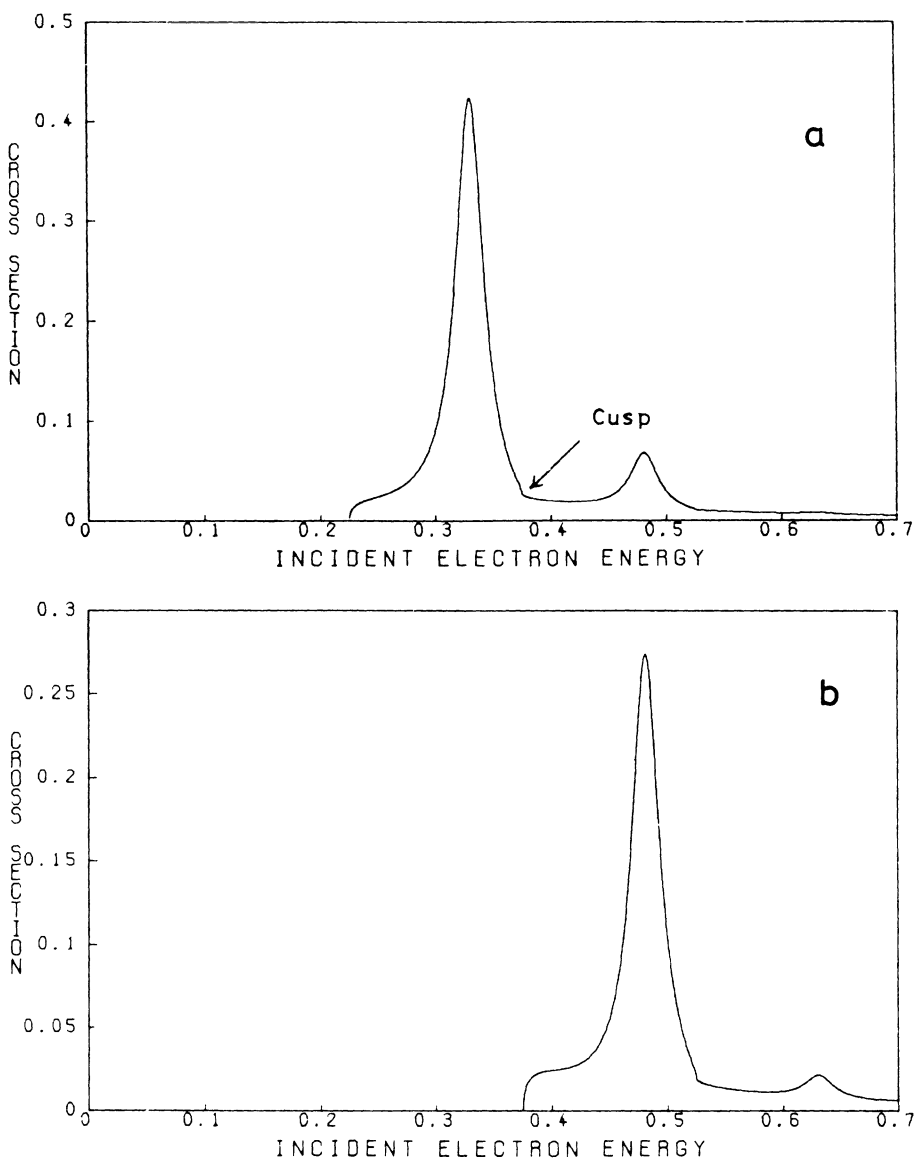


Figure 62. Low-energy radiative inelastic electron-hydrogen scattering. Diagram (a) shows subthreshold excitation via 1S resonance (at about 9.6 eV) and absorption of a photon. $\sigma_{10 \rightarrow 2-1}$ is the corresponding model $1s\rightarrow 2s$ excitation cross section with net absorption of a photon. In diagram (b) $\sigma_{10 \rightarrow 20}$ is the model $1s\rightarrow 2s$ excitation cross section with no net exchange of photons. The main peak is due to intermediate or temporary one-photon emission resonance with respect to the elastic 1S resonance (at about 9.6 eV), the second peak is due to temporary two-photon emission resonance. In diagram (c) $\sigma_{10 \rightarrow 2,1}$ is the model $1s\rightarrow 2s$ excitation cross section with net emission of one photon. Peak field strength $F_0 = 0.035$ au ($I = 4.2 \times 10^{13} \text{ W cm}^{-2}$), $\hbar\omega = 0.15$ au. The scales are in atomic units.

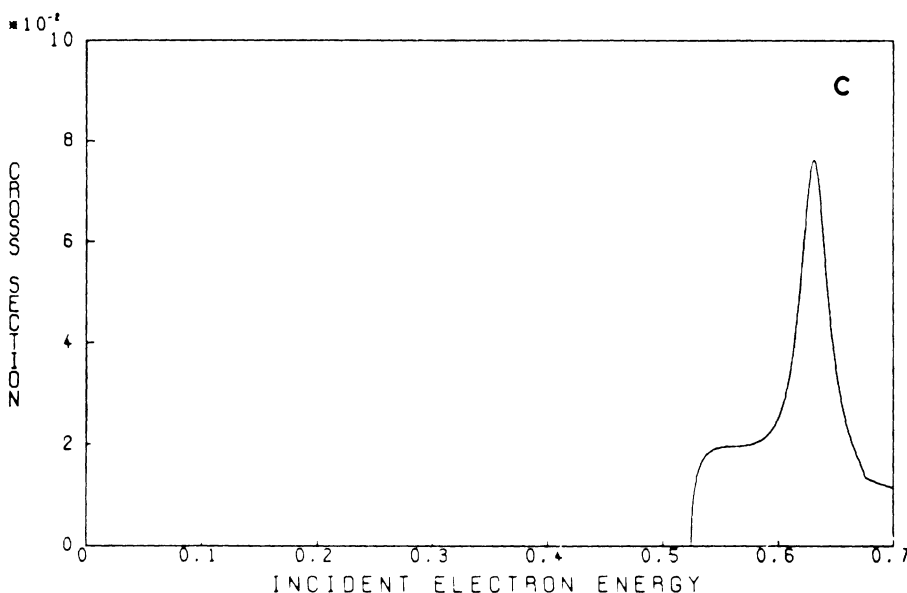


Figure 62 (continued)

specific to electron-hydrogen scattering but should occur in other systems as well. Excitation of vibrational states of diatomic molecules, such as H₂ and N₂, by very-low-energy electrons in the presence of a strong infrared laser (such as a CO₂ laser at $\hbar\omega = 0.117$ eV) should also exhibit the resonant subthreshold excitation phenomena.

12.3.7.6. The Inelastic and Emission Cross Sections

Diagram (b) in Figure 62 shows the direct 1s-2s excitation cross section $\sigma_{1,0 \rightarrow 2,0}$ in the presence of the field with no net emission or absorption of photons. Beginning at the threshold ($E/\hbar = 0.375$ au = 10.2 eV) these cross sections also show the resonance and cusp structures associated with the elastic ¹S resonance. We note that a secondary (two-photon) resonance structure also occurs at this high field strength ($F_0 = 0.035$ au). These resonances are similar to the "capture-escape" resonances except that they are associated not with respect to the sharp H⁻ state but rather with respect to the broader ¹S elastic resonance. Diagram (c) in Figure 62 shows the inelastic 1s-2s excitation cross section accompanied by the net emission of a photon. The cross section naturally arises from the threshold lying $\hbar\omega$ above the ordinary excitation threshold, and exhibits the ¹S resonance in its turn. Comparison of diagrams (a), (b), and

(c) in Figure 62 supports the aforementioned propensity rule regarding the tendency toward repetition of all resonant and singular structures in the absence of the field, in all new channels opened up by the presence of the field.

12.3.7.7. Photon Amplification by Scattering

Just as the electron can borrow energy from the field, the field may also gain energy from the electron during the collision. At specific electron energies the field may gain more energy from the electron than the other way around, which could lead to an amplification of the field intensity. In Figure 63 we show the coefficient $\alpha(E_i)$ defined by the net absorption of photons by the scattering system, as a function of the incident electron energy E_i for a fixed field frequency $\omega = 0.05$ au, where both elastic scattering and atomic excitation are taken into account. Figure 63 clearly exhibits how at preferred electron energies the “absorption coefficient” becomes negative and hence changes into a “gain coefficient.” We observe also that the “gain resonance” deepens, broadens, as well as shifts toward lower energies, as the field strength increases from $F_0 = 0.001$ (au) ($= 5.1 \times 10^6$ V/cm), through 0.0025 (au), to 0.005 (au). Here we have a case of photon amplification by the radiative scattering of electrons.

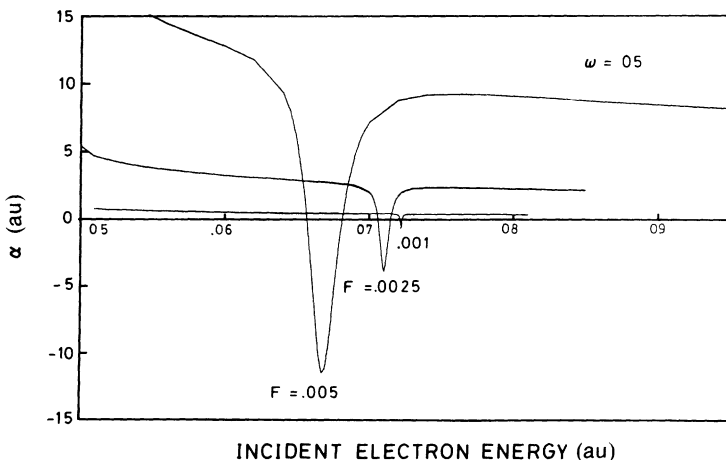


Figure 63. Calculated net photon-absorption coefficient $\alpha(E_i)$ vs. incident electron energy E_i for radiative electron–hydrogen scattering at $\hbar\omega = 0.05$ au and at three different field strengths $F_0 = 0.001$, 0.0025, and 0.005 au. “Negative absorption” (or photon gain) occurs resonantly due essentially to “capture–escape” resonance with respect to the temporary formation of bound state H^- . We note that the position and width of the gain resonance shifts and broadens respectively with increasing field strengths. The scales are in atomic units (from Faisal⁽²⁷²⁾).

12.3.7.8. Low-Energy Angular Distribution

The field can affect the differential scattering cross sections due to both symmetry and dynamic reasons. In the absence of the field, the scattering process maintains its cylindrical symmetry about the incident-beam direction, which leads to the usual azimuthal invariance of the angular distributions of the scattered electrons. The very presence of the field destroys this invariance, since in general it provides an extra quantization direction in the laboratory (except perhaps if the polarization direction lies along the incident electron-beam direction). Besides, the distribution with respect to the polar angle in a given azimuthal plane can also be overwhelmingly modified. Figure 64 shows an example of the change in low-energy ($E_i = 0.05$ au) spherically symmetric angular distribution for electron–hydrogen scattering due to the presence of the field ($\hbar\omega = 0.05$ au, peak field strength $F_0 = 0.005$ au) when a circularly polarized photon beam is directed (a) along the incident electron-beam direction (left panel), (b) at 45° (middle panel) and (c) perpendicular (right panel) to the electron-beam direction. The outer circles in these panels correspond to the spherical distribution of the scattered low-energy electrons when the field is off.

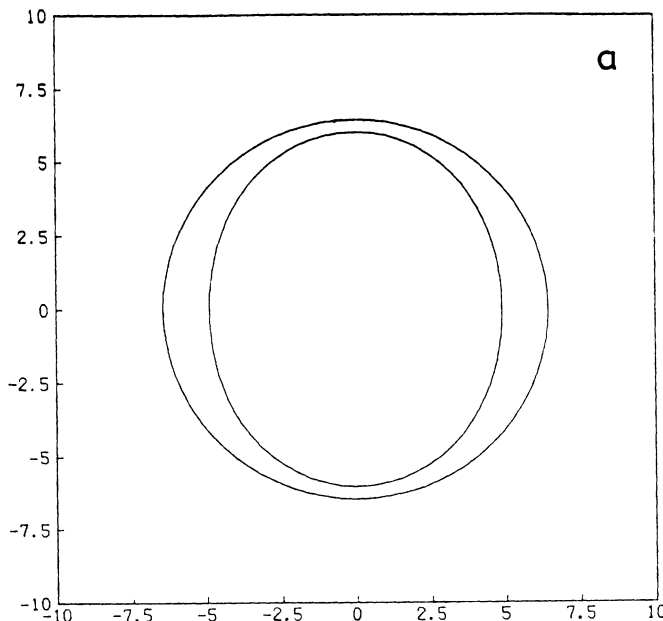


Figure 64. Modification of low-energy spherically symmetric angular distribution (in the absence of the field) due to radiative scattering in a circularly polarized field (propagation along the z -axis). The incident electron beam is directed along $\theta_i = 0^\circ$ (a), 45° (b), and 90° (c), with respect to the z -axis. The final azimuth angle is fixed at $\phi_f = 45^\circ$. Incident electron energy $E_i = 0.05$ au.

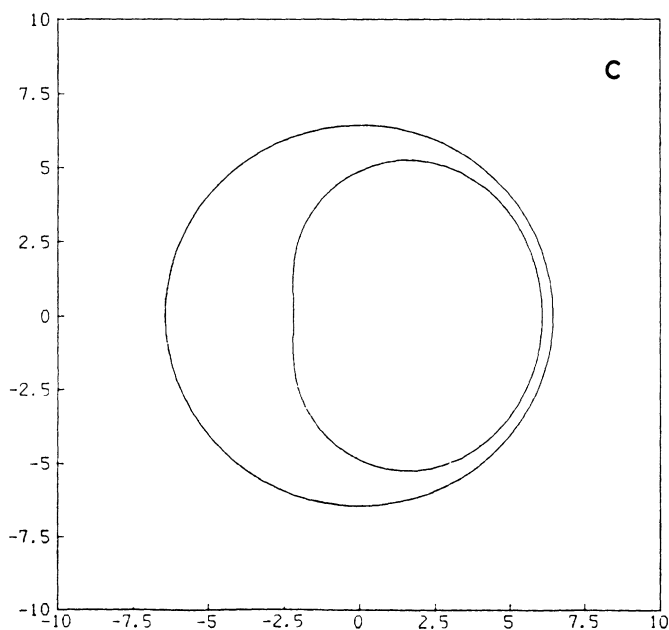
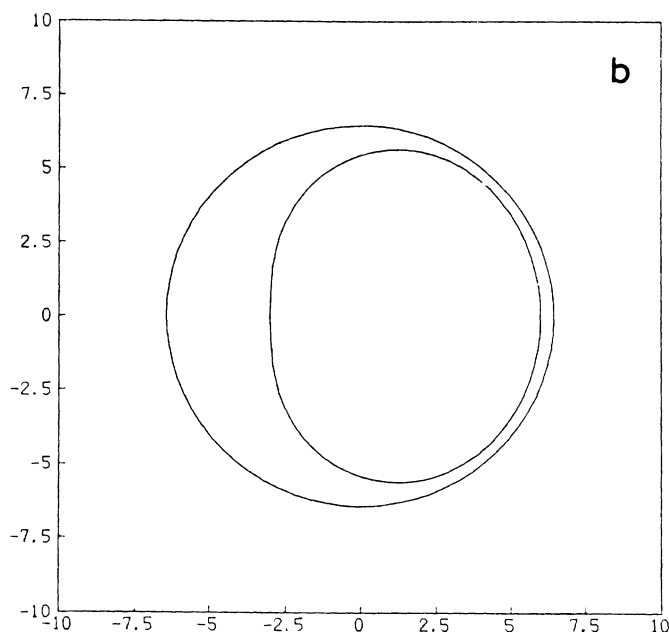


Figure 64 (continued)

12.4. Direct, Rearrangement, and Fully Symmetrized Radiative Scattering Amplitudes

In this section we develop the fully symmetrized $(N_a + 1)$ -electron radiative scattering amplitudes in terms of the simpler unsymmetrized direct and rearrangement amplitudes. Within the present stationary treatment this can be achieved by generalizing the method^(285,286) used in the absence of the field.

As before we define the scattering potential

$$V(\mathbf{r}, \mathbf{x}) = H - H_0 \quad (12.4.1)$$

as the perturbation, so that the reference Hamiltonian is

$$H_0 = H_a + \hbar\omega a^+ a + \beta_x(a^+ + a) - \frac{\hbar^2}{2\mu} \nabla_{\mathbf{r}}^2 + \beta_{\mathbf{r}}(a^+ + a) \quad (12.4.2)$$

where

$$\beta_x \equiv s \frac{ie\hbar}{2\mu c} \nabla_{\mathbf{z}}^a \quad \text{and} \quad \beta_{\mathbf{r}} \equiv s \frac{ie\hbar}{2\mu c} \nabla_z^e \quad \text{with } s \equiv \left(\frac{8\pi\hbar c^2}{\omega L^3} \right)^{1/2}$$

The Green's function G_0 corresponding to Eq. (12.4.2) satisfies

$$G_0 = \frac{I}{E - H_0 + i0} \quad (12.4.3)$$

where the identity operator has the explicit representation

$$I = \delta(\mathbf{r} - \mathbf{r}')\delta(\mathbf{x} - \mathbf{x}') \sum_n |n\rangle\langle n| \quad (12.4.4)$$

The eigenstates of reference Hamiltonian (12.4.2) associated with eigenvalue

$$\Lambda_{pN}^k = \lambda_p + \varepsilon_k + N\hbar\omega \quad (12.4.5)$$

are, from Eq. (12.3.2.8),

$$\begin{aligned} |\mathbf{k}, \lambda_p^N\rangle &\equiv \sum_n \chi_{n-N}(\mathbf{k}, \lambda_p) |n\rangle \\ &= \sum_n \sum_{jm} J_{n-m-N}(\mathbf{k} \cdot \boldsymbol{\alpha}_0) e^{i\mathbf{k} \cdot \mathbf{r}} a_{jm}(\lambda_p) |j\rangle |n\rangle \end{aligned} \quad (12.4.6)$$

For the present purpose it is useful to derive an alternative form of $|\mathbf{k}, \lambda_p^n\rangle$ that relates it directly to the product of the eigenstates of the dressed atom and dressed electron. We show below that the desired form can be obtained in two steps:

$$|\mathbf{k}, \lambda_p^n\rangle = \sum_n J_{n-N}(\mathbf{k} \cdot \boldsymbol{\alpha}_0) e^{i\mathbf{k} \cdot \mathbf{r}} \sum_{jm} a_{jm}(\lambda_p^n) |j\rangle |m\rangle \quad (12.4.7)$$

$$= \sum_n J_{n-N}(\mathbf{k} \cdot \boldsymbol{\alpha}_0) e^{i\mathbf{k} \cdot \mathbf{r}} |\lambda_p^n; \mathbf{x}\rangle \quad (12.4.8)$$

where

$$|\lambda_p^n; \mathbf{x}\rangle \equiv \sum_{jm} a_{jm}(\lambda_p^n) |j(\mathbf{x})\rangle |m\rangle \quad (12.4.9)$$

are the dressed-atom eigenstates (with eigenvalues $\lambda_p^n = \lambda_p + n\hbar\omega$) belonging to the atom + field sub-Hamiltonian

$$\hat{H}_a \equiv H_a + \hbar\omega a^+ a + \beta_x(a^+ + a) \quad (12.4.10)$$

with

$$\beta_x \equiv s \frac{ie\hbar}{2\mu e} \nabla_z^a \quad (12.4.11)$$

Equation (12.4.7) is obtained from Eq. (12.4.6) by first shifting the summation index $n \rightarrow n + m$ and then shifting $m \rightarrow m - n$ in the resulting equation. This gives

$$\sum_n J_{n-N}(\mathbf{k} \cdot \boldsymbol{\alpha}_0) e^{i\mathbf{k} \cdot \mathbf{r}} \sum_{jm} a_{jm-n}(\lambda_p) |j\rangle |m\rangle \quad (12.4.12)$$

We may replace $a_{jm-n}(\lambda_p)$ in the second summation of expression (12.4.12) by $a_{jm}(\lambda_p^n)$ because of the periodicity relation (12.3.2.6), namely

$$a_{jm-n}(\lambda_p) = a_{jm}(\lambda_p^n) \quad (12.4.13)$$

and arrive at the result (12.4.8).

Equation (12.4.8) can be used to define the initial state, with eigenvalue

$$A_{i,0} = \frac{\hbar^2}{2\mu} k_i^2 + \lambda_i \quad (12.4.14)$$

and incident momentum \mathbf{k}_i , as

$$|\mathbf{k}_i, \lambda_i\rangle = \sum_n J_n(\mathbf{k}_i \cdot \boldsymbol{\alpha}_0) e^{i\mathbf{k}_i \cdot \mathbf{r}} |\lambda_i^n; \mathbf{x}\rangle \quad (12.4.15)$$

Similarly, we define the final state, with eigenvalue

$$\Lambda_{f,N}^{k_f} = \frac{\hbar^2}{2\mu} k_{fN}^2 + \lambda_f \quad (12.4.16)$$

and scattered momentum k_{fN} , where

$$\frac{\hbar^2}{2\mu} k_{fN}^2 \equiv \left(\frac{\hbar^2}{2\mu} k_f^2 + N\hbar\omega \right) \quad (12.4.17)$$

as

$$|\mathbf{k}_{fN}, \lambda_f\rangle = \sum_n J_{n-N}(\mathbf{k}_{fN} \cdot \boldsymbol{\alpha}_0) e^{i\mathbf{k}_{fN} \cdot \mathbf{r}} |\lambda_f^n; \mathbf{x}\rangle \quad (12.4.18)$$

Definition (12.4.18) corresponds to the directly scattered final state. For the final state of rearrangement collision in which the projectile coordinate \mathbf{r} and an atomic electron coordinate \mathbf{x} are exchanged, we must define

$$|\mathbf{k}_{fN}, \lambda_f\rangle^e = \sum_n J_{n-N}(\mathbf{k}_{fN} \cdot \boldsymbol{\alpha}_0) e^{i\mathbf{k}_{fN} \cdot \mathbf{x}} |\lambda_f^n; \mathbf{r}\rangle \quad (12.4.19)$$

In the present representation Green's function (12.4.3), given by

$$G_0 = \sum_{pN} \sum_{\mathbf{k}} \frac{|\mathbf{k}, \lambda_p^N\rangle \langle \mathbf{k}, \lambda_p^N|}{E - \Lambda_{p,N}^k} \quad (12.4.20)$$

takes the form

$$G_0(\mathbf{r}, \mathbf{x}; \mathbf{r}', \mathbf{x}') = \sum_{nn'} \sum_{pNk} |\lambda_p^n; \mathbf{x}\rangle J_{n-N}(\mathbf{k} \cdot \boldsymbol{\alpha}_0) e^{i\mathbf{k} \cdot (\mathbf{r}-\mathbf{r}')} J_{n'-N}(\mathbf{k} \cdot \boldsymbol{\alpha}_0) |\lambda_p^{n'}; \mathbf{x}'\rangle \quad (12.4.21)$$

12.4.1. Direct and Rearrangement Amplitudes

The total wave function $|\psi_i^+\rangle$ satisfying the initial-state boundary condition can be written as

$$|\psi_i^+\rangle = |\mathbf{k}_i, \lambda_i\rangle + G_0 V |\psi_i^+\rangle \quad (12.4.1.1)$$

The direct transition amplitude is obtained by projecting function (12.4.1.1) to the final state $\langle \mathbf{k}_{fN}, \lambda_f |$:

$$\langle \mathbf{k}_{fN}, \lambda_f | \psi_i^+ \rangle = \langle \mathbf{k}_{fN}, \lambda_f | \mathbf{k}_i, \lambda_i \rangle + \frac{1}{E - \Lambda_{f,N}^{k_f} + i0} \langle \mathbf{k}_{fN}, \lambda_f | V | \psi_i^+ \rangle \quad (12.4.1.2)$$

Hence the transition matrix is

$$T_{i \rightarrow f} = \langle \mathbf{k}_{fN}, \lambda_f | V | \psi_i^+ \rangle \quad (12.4.1.3)$$

provided, of course, the total energy E coincides with the (field-normalized) initial-state and final-state energies:

$$E = \Lambda_{i,0}^{k_i} = \lambda_i + \frac{\hbar^2 k_i^2}{2\mu} = \lambda_f + \frac{\hbar^2 k_{fN}^2}{2\mu} \quad (12.4.1.4)$$

Equation (12.4.13) corresponds exactly, as it must, to the direct scattering amplitude (12.3.4.13).

12.4.2. The Radiative Rearrangement Scattering Amplitude

In a rearrangement collision, the projectile particle coalesces with the target while a target particle emerges as a scattered particle in the final states. Unlike definition (12.4.1) for the collisional perturbation $V(\mathbf{r}, \mathbf{x})$ (which is appropriate for all direct channel scattering processes), we now need to define the (collisional) perturbation in the “rearrangement channel”:

$$V' \equiv H - H'_0 \quad (12.4.2.1)$$

where

$$V'(\mathbf{r}, \mathbf{x}) = V(\mathbf{x}, \mathbf{r}) \quad (12.4.2.2)$$

and the corresponding Hamiltonian

$$H'_0 = H_a(\mathbf{r}) + \hbar\omega a^+ a + \beta_r(a^+ + a) - \frac{\hbar^2}{2\mu} \nabla_x^2 + \beta_x(a^+ + a) \quad (12.4.2.3)$$

We have the set of eigenfunctions of Eq. (12.4.2.3) in the form

$$|\mathbf{k}, \lambda_p\rangle^e = \sum_n J_n(\mathbf{k} \cdot \boldsymbol{\alpha}_0) e^{i\mathbf{k} \cdot \mathbf{x}} |\lambda_p^n; \mathbf{r}\rangle \quad (12.4.2.4)$$

The corresponding Green's function of H'_0 is

$$G'_0 = \frac{1}{E - H'_0 + i0} \quad (12.4.2.5)$$

$$= \sum_{pN\mathbf{k}} \frac{|\mathbf{k}, \lambda_p\rangle^e \langle \mathbf{k}, \lambda_p|}{E - \Lambda_{p,N}^k} \quad (12.4.2.6)$$

With the aid of definitions (12.4.2.5) and (12.4.20) and the identity

$$G_0 - G'_0 = G_0(V' - V)G'_0 \quad (12.4.2.7)$$

it is now a matter of simple algebra to show that the wave function (12.4.1.1) can be rewritten as

$$|\psi_i^+\rangle = |\mathbf{k}_i, \lambda_i\rangle - G'_0(V' - V)|\mathbf{k}_i, \lambda_i\rangle + G'_0V'|\psi_i^+\rangle \quad (12.4.2.8)$$

The first two terms can be combined as follows:

$$R \equiv [1 - G'_0(H_0 - H'_0)]|\mathbf{k}_i, \lambda_i\rangle \quad (12.4.2.9)$$

$$\begin{aligned} &= \left[1 - \frac{1}{E - H'_0 + i0} (\Lambda_{i0}^{k_i} - H'_0) \right] |\mathbf{k}_i, \lambda_i\rangle \\ &= 0 \end{aligned} \quad (12.4.2.10)$$

The last line follows in view of the (renormalized) energy relation (12.4.1.4). Thus we obtain the useful result

$$|\psi_i^+\rangle = G'_0V'|\psi_i^+\rangle \quad (12.4.2.11)$$

The transition amplitude for the rearrangement collision is now conveniently obtained by projecting the wave function (12.4.2.11) onto the final rearrangement state (12.4.2.4):

$${}^c\langle \mathbf{k}_{fN}, \lambda_f | \psi_i^+ \rangle = \frac{1}{E - \Lambda_{fN}^{k_i} + i0} {}^c\langle \mathbf{k}_{fN}, \lambda_f | V' | \psi_i^+ \rangle \quad (12.4.2.12)$$

This relation enables the rearrangement transition matrix element to be identified as

$$T_{i \rightarrow f}^c = {}^c\langle \mathbf{k}_{fN}, \lambda_f | V' | \psi_i^+ \rangle \quad (12.4.2.13)$$

12.4.3. The Fully Symmetrized Radiative Scattering Amplitude

We shall assume that the N_a -electron target-atom wave functions are already given and antisymmetrized. Our interest is to account for the required antisymmetry of the “projectile + target” system and its influence on the radiative scattering amplitude. This can be done most economically in terms of the (simpler) unsymmetrized direct and rearrangement amplitudes derived above. To this end we define

$$x_\alpha \equiv (\mathbf{r}_\alpha, \sigma_\alpha), \quad \alpha = 1, 2, \dots, N_a \quad (12.4.3.1)$$

for the coordinate and spin of the α th atomic electron. We assume that the set of properly antisymmetrized atomic eigenfunctions is denoted by

$$|j(x_1, x_2, \dots, x_{N_a})\rangle, \quad j = 1, 2, \dots, J \quad (12.4.3.2)$$

Therefore, the set of antisymmetrized dressed-atom eigenstates belonging to the dressed energy $\{\lambda_p^n\}$ is

$$|\lambda_p^n; x_1, x_2, \dots, x_{N_a}\rangle = \sum_{jm} a_{jm}(\lambda_p^n) |j(x_1, x_2, \dots, x_{N_a})\rangle |m\rangle \quad (12.4.3.3)$$

(We shall assume that the laser field does not directly affect the spin of an electron; in the dipole approximation, the magnetic component of the field is identically zero.) If the projectile electron, denoted by “0,” were distinguishable then we could express the initial reference state in the form

$$|i; x^0\rangle \equiv |\mathbf{k}_i, \lambda_i, \mu'_0; x^0\rangle \equiv \sum_n J_n(\mathbf{k}_i \cdot \boldsymbol{\alpha}_0) U_{\mathbf{k}_i}(x_0) |\lambda_i^n; x_1, x_2, \dots, x_{N_a}\rangle \quad (12.4.3.4)$$

where we have defined

$$U_{\mathbf{k}_i}(x_0) = e^{i\mathbf{k}_i \cdot \mathbf{r}_0} \eta(\mu'_0 | \sigma_0) \quad (12.4.3.5)$$

Here

$$\eta(\mu | \sigma) = \begin{cases} 1, & \sigma = \mu \\ 0, & \sigma \neq \mu \end{cases} \quad (12.4.3.6)$$

are the orthonormal electron-spin functions:

$$\sum_{\sigma=-1/2}^{+1/2} \eta(\mu | \sigma) \eta(\mu' | \sigma) = \delta_{\mu\mu'} \quad (12.4.3.7)$$

The Pauli principle is accounted for by introducing the antisymmetrizing operator

$$A \equiv (N_a + 1)^{-1/2} \left[1 - \sum_{\alpha=1}^{N_a} P_{\alpha 0} \right] \quad (12.4.3.8)$$

where $P_{\alpha 0}$ interchanges x_α and x_0 . For example,

$$\begin{aligned} P_{\alpha\beta} |\lambda_p^n; x_1, \dots, x_\alpha, \dots, x_\beta, \dots, x_{N_a}\rangle &= |\lambda_p^n; x_1, \dots, x_\beta, \dots, x_\alpha, \dots, x_{N_a}\rangle \\ &= - |\lambda_p^n; x_1, \dots, x_\alpha, \dots, x_\beta, \dots, x_{N_a}\rangle \end{aligned} \quad (12.4.3.9)$$

The last line follows from the antisymmetry of the dressed states. Therefore, the fully antisymmetric ($N_a + 1$)-electron reference eigenfunction has the form

$$\begin{aligned} A |\mathbf{k}, \lambda_p, \mu; x^0\rangle &= \sum_n J_n(\mathbf{k} \cdot \boldsymbol{\alpha}_0) \{ U_{\mathbf{k}}(x_0) |\lambda_p^n; x_1, x_2, \dots, x_{N_a}\rangle \\ &\quad - [U_{\mathbf{k}}(x_1) |\lambda_p^n; x_0, x_2, \dots, x_{N_a}\rangle + U_{\mathbf{k}}(x_2) |\lambda_p^n; x_1, x_0, \dots, x_{N_a}\rangle \\ &\quad + U_{\mathbf{k}}(x_3) |\lambda_p^n; x_1, x_2, x_0, \dots, x_{N_a}\rangle + \dots] \} \end{aligned} \quad (12.4.3.10)$$

Let us denote the total wave function [see Eq. (12.4.1.1)] in which the electron “0” is considered free by

$$|\psi_i^+(x^0)\rangle = |i; x^0\rangle + \frac{1}{E - H_0(x^0) + i0} V(x^0) |\psi_i^+(x^0)\rangle \quad (12.4.3.11)$$

where $H_0(x^0)$ is the reference Hamiltonian with the projectile electron distinguished as “0” and $V(x^0)$ is the corresponding projectile-target interaction given by

$$V(x^0) \equiv H - H_0(x^0) \quad (12.4.3.12)$$

We observe that the total Hamiltonian H is fully symmetric among ($N_a + 1$) electrons and hence H commutes with A . The fully symmetrized transition amplitude is obtained from the overlap between the antisymmetric total wave function (satisfying the initial condition) and the antisymmetrized final state, i.e., between

$$A |\psi_i^+(x^0)\rangle \quad \text{and} \quad A |f; x^0\rangle \quad (12.4.3.13)$$

This overlap is

$$\begin{aligned} \langle f; x^0 | A, A | \psi_i^+(x^0)\rangle &= (N_a + 1)^{1/2} \langle f; x^0 | A | \psi_i^+(x^0)\rangle \\ &= \langle x^0; f | \left(1 - \sum_{\alpha=1}^{N_a} p_{\alpha 0} \right) | \psi_i^+(x^0)\rangle \end{aligned} \quad (12.4.3.14)$$

The second equality follows from the identity

$$A^2 |f; x^0\rangle = (N_a + 1)^{1/2} A |f; x^0\rangle \quad (12.4.3.15)$$

Furthermore

$$\sum_{\alpha=1}^{N_a} P_{\alpha 0} |f; x^0\rangle = N_a |f; x^1\rangle \quad (12.4.3.16)$$

because all terms of the left-hand sum here are exactly equal due to the fact that both $|f; x^0\rangle$ and $|\psi_i^+(x^0)\rangle$ contain antisymmetric combinations of the bound electrons $\alpha = 1, 2, \dots, N_a$. Hence by combining relations (12.4.3.14) and (12.4.3.16) we obtain the useful result

$$\langle x^0; f | A, A | \psi_i^+(x^0)\rangle = \langle x^0; f | \psi_i^+(x^0)\rangle - N_a \langle x^0; f | \psi_i^+(x^1)\rangle \quad (12.4.3.17)$$

This shows that the fully symmetrized transition amplitude for the radiative scattering between an electron and an (N_a -electron) atom is given by the difference between the unsymmetrized direct amplitude and N_a times the unsymmetrized rearrangement amplitude. Consequently, the corresponding fully symmetrized T-matrix can be expressed as

$$\tau_{i \rightarrow f} = \tau_{i \rightarrow f}^d - N_a \tau_{i \rightarrow f}^{ex} \quad (12.4.3.18)$$

where $\tau_{i \rightarrow f}^d$ and $\tau_{i \rightarrow f}^{ex}$ are the direct and exchange T-matrices containing both the spatial and spin parts:

$$\tau_{i \rightarrow f}^d = \langle x^0; f | V(x^0) | \psi_i^+(x^0)\rangle \quad (12.4.3.19)$$

$$= \langle x^0; f | \tau | i; x^0\rangle \quad (12.4.3.20)$$

where

$$\begin{aligned} \tau &= V(x^0) + V(x^0)G_0V(x^0) + \dots \\ &= V(x^0) + V(x^0)G_0\tau \end{aligned} \quad (12.4.3.21)$$

Equation (12.4.3.21) is obtained by substituting expression (12.4.1.1) in Eq. (12.4.3.19) and iterating; quantity $|i; x^0\rangle$ is defined by relation (12.4.3.4) and

$$\begin{aligned} |f, x^0\rangle &= |\mathbf{k}_{fN}, \lambda_f, \mu_f; x_0\rangle \\ &= \sum_n J_n(\mathbf{k}_{fN} \cdot \boldsymbol{\alpha}_0) e^{i\mathbf{k}_{fN} \cdot \mathbf{r}_0} \eta(\mu_f | \sigma_0) | \lambda_p^n; x_1, x_2, \dots, x_{N_a}\rangle \end{aligned} \quad (12.4.3.22)$$

The exchange transition matrix is

$$\tau_{i \rightarrow f}^{ex} = \langle x^1; f | V(x^1) | \psi_i^+(x^0)\rangle \quad (12.4.3.23)$$

$$= \langle x^1; f | \tau^{ex} | i; x^0\rangle \quad (12.4.3.24)$$

where

$$\tau^{ex} = V(x^1) + V(x^1)G_0V(x^0) + V(x^1)G_0V(x^0)G_0V(x^0) + \dots \quad (12.4.3.25)$$

Equation (12.4.3.25) is obtained by iterating function (12.4.2.11) and

substituting the resulting expression in Eq. (12.4.3.23). The exchanged final state is defined by

$$\begin{aligned} |f; x^1\rangle &= |k_{fn}, \lambda_f, l_f; x^1\rangle \\ &= \sum_n J_n(\mathbf{k}_{fn} \cdot \boldsymbol{\alpha}_0) e^{i\mathbf{k}_{fn} \cdot \mathbf{r}_1} \eta(\mu_f | \sigma_1) |\lambda_p^n; x_0, x_2, \dots, x_{N_0}\rangle \end{aligned} \quad (12.4.3.26)$$

Finally, the fully symmetrized radiative differential scattering cross sections are obtained from

$$\frac{d\sigma_{i \rightarrow f}^{(N)}}{d\Omega} = \frac{k_{fn}}{k_i} \left(\frac{\mu}{2\pi\hbar^2} \right)^2 |\tau_{i \rightarrow f}^d - N_a \tau_{i \rightarrow f}^{\text{ex}}|^2 \quad (12.4.3.27)$$

12.4.4. Spin-Flip and Related Amplitudes

The present method is illustrated by considering the spin-flip and other spin-specific amplitudes in radiative scattering from a one-electron atom.

In this case, the initial state is

$$|i; x^0\rangle = \sum_n J_n(\mathbf{k}_{i0} \cdot \boldsymbol{\alpha}_0) e^{i\mathbf{k}_{i0} \cdot \mathbf{r}_0} \eta(\mu'_0 | \sigma_0) \eta(\mu'_1 | \sigma_1) |\lambda_i^n; \mathbf{r}_1\rangle \quad (12.4.4.1)$$

For the final state of direct scattering we have

$$|f; x^0\rangle = \sum_n J_n(\mathbf{k}_{fn} \cdot \boldsymbol{\alpha}_0) e^{i\mathbf{k}_{fn} \cdot \mathbf{r}_0} \eta(\mu'_0 | \sigma_1) \eta(\mu'_1 | \sigma_1) |\lambda_f^n; \mathbf{r}_1\rangle \quad (12.4.4.2)$$

In the final state of exchange scattering

$$|f; x^1\rangle = \sum_n J_n(\mathbf{k}_{fn} \cdot \boldsymbol{\alpha}_0) e^{i\mathbf{k}_{fn} \cdot \mathbf{r}_0} \eta(\mu'_0 | \sigma_1) \eta(\mu'_1 | \sigma_0) |\lambda_f^n; \mathbf{x}_0\rangle \quad (12.4.4.3)$$

If expressions (12.4.4.1) and (12.4.4.2) are substituted in Eq. (12.4.3.20), then with the aid of the orthogonality relation (12.4.3.7), we obtain

$$\tau_{if}^d = \delta_{\mu'_0, \mu'_0} \cdot \delta_{\mu'_1, \mu'_1} \cdot T_{if}^d \quad (12.4.4.4)$$

where T_{if}^d is the T-matrix defined by the space parts of relations (12.4.4.1) and (12.4.4.2) alone. Similarly, substitution of expressions (12.4.4.1) and (12.4.4.3) in Eq. (12.4.3.24) yields

$$\tau_{if}^{\text{ex}} = \delta_{\mu'_0, \mu'_0} \cdot \delta_{\mu'_1, \mu'_1} \cdot T_{if}^{\text{ex}} \quad (12.4.4.5)$$

T_{if}^{ex} is defined by the space part of expressions (12.4.4.1) and (12.4.4.3)

alone. The fully symmetrized transition amplitude for arbitrarily given spin orientations in the initial and final states is therefore given by

$$\tau_{if} = [\delta_{\mu_0^i, \mu_0^f} \cdot \delta_{\mu_1^i, \mu_1^f} \cdot T_{if} - \delta_{\mu_0^i, \mu_0^f} \cdot \delta_{\mu_1^i, \mu_0^f} \cdot T_{if}^{\text{ex}}] \quad (12.4.4.6)$$

If the spin orientations of the two electrons are denoted by arrows, then Eq. (12.4.4.6) yields the spin-flip amplitude in the form

$$\tau_{if} (\uparrow \rightarrow \downarrow) = -T_{if}^{\text{ex}} \quad (12.4.4.7)$$

Thus, as expected, only the exchange amplitude contributes to the spin-flip process,

$$\frac{d\sigma(\text{flip})}{d\Omega} = \frac{k_{FN}}{k_i} \left(\frac{\mu}{2\pi\hbar^2} \right)^2 |T_{if}^{\text{ex}}|^2 \quad (12.4.4.8)$$

Similarly, we may obtain the radiative analogs of other measurable spin-specific scattering amplitudes. Thus in the process in which the initially parallel spins remain unaltered by the scattering, the amplitude is

$$\tau_{if} (\uparrow \rightarrow \uparrow) = T_{if}^d - T_{if}^{\text{ex}} \quad (12.4.4.9)$$

If initially the incident and bound electrons have opposite orientations, then

$$\tau_{if} (\uparrow \rightarrow \uparrow) = T_{if}^d \quad (12.4.4.10)$$

In this case the exchange amplitude is zero. For experiments with unpolarized spin we must sum over the final spin states and average over the initial spin states. This gives from Eq. (12.4.4.6)

$$\frac{d\sigma}{d\Omega} = \frac{k_{FN}}{k_i} \left(\frac{\mu}{2\pi\hbar^2} \right)^2 \frac{1}{2} [|T_{if}^{\text{ex}}|^2 + |T_{if}^d - T_{if}^{\text{ex}}|^2 + |T_{if}^d|^2] \quad (12.4.4.11)$$

$$= \frac{k_{FN}}{k_i} \left(\frac{\mu}{2\pi\hbar^2} \right)^2 \left[\frac{1}{4} |T_{if}^d + T_{if}^{\text{ex}}|^2 + \frac{3}{4} |T_{if}^d - T_{if}^{\text{ex}}|^2 \right] \quad (12.4.4.12)$$

The last line expresses the same result in terms of the familiar weighted cross section for singlet scattering and triplet scatterings.

12.5. Radiative Close-Coupling Equations

In this section we develop a system of close-coupling equations, which correspond to a generalization of the close-coupling equations, widely

employed in low-energy electron-atom scattering calculations without the field, to the problem of radiative scattering. Expansion of the total wave function in the eigenfunctions of the target atom plays a fundamental role in the usual close-coupling method.^(263,287) In the present case this role is played by the dressed eigenstates of the target.

For the sake of algebraic economy and clarity we explicitly consider only the case of a two-electron system, consisting of free-electron scattering from a one-electron atom, in the presence of the field. The Schrödinger equation of this system can be written as

$$[E - H(\mathbf{r}, \mathbf{r}')] |\psi(\mathbf{r}, \mathbf{r}')\rangle = 0 \quad (12.5.1)$$

where

$$H(\mathbf{r}, \mathbf{r}') = \hat{H}_a(\mathbf{r}') - \frac{\hbar^2}{2\mu} \nabla_r^2 + \beta_r(a^+ + a) + V(\mathbf{r}, \mathbf{r}') \quad (12.5.2)$$

with

$$\beta_r \equiv \frac{ie\hbar}{2\mu c} \nabla_z \quad (12.5.3)$$

and where

$$\hat{H}_a(\mathbf{r}') = -\frac{\hbar^2}{2\mu} \nabla_{r'}^2 - \frac{e^2}{r'} + \hbar\omega a^+ a + \beta_r(a^+ + a) \quad (12.5.4)$$

is the atom + field Hamiltonian and

$$V(\mathbf{r}, \mathbf{r}') = -\frac{e^2}{r} + \frac{e^2}{|\mathbf{r} - \mathbf{r}'|} \quad (12.5.5)$$

is the collisional interaction. We expand the state vector of the total system, which satisfies the Schrödinger equation (12.5.1), in terms of the dressed states of the atom, $|\lambda_p^n; \mathbf{r}\rangle$ [see Eq. (12.4.9)], which satisfy

$$\hat{H}_a(\mathbf{r}) |\lambda_p^n; \mathbf{r}\rangle = \lambda_p^n |\lambda_p^n; \mathbf{r}\rangle \quad (12.5.6)$$

as follows:

$$|\psi(\mathbf{r}, \mathbf{r}')\rangle = \sum_{pn} [F_{pn}^{(\pm)}(\mathbf{r}) |\lambda_p^n; \mathbf{r}'\rangle \pm F_{pn}^{(\pm)}(\mathbf{r}') |\lambda_p^n; \mathbf{r}\rangle] \quad (12.5.7)$$

where $F_{pn}^{(\pm)}$ refer to the singlet (+) or triplet (-) scattering waves.

In order to derive the independent set of coupled equations for the scattering wave functions $F_{pn}^{(\pm)}(\mathbf{r})$ that will provide the desired generalization of the close-coupling equations in the radiative case, we first consider

the effect of H , given by Eq. (12.5.2), on the first sum in Eq. (12.5.7). We have (on temporarily omitting superscripts of functions F)

$$\begin{aligned} H(\mathbf{r}, \mathbf{r}') \sum_{pn} F_{pn}(\mathbf{r}) &| \lambda_p^n; \mathbf{r}' \rangle \\ = \sum_{pn} \left\{ F_{pn}(\mathbf{r}) H_a(\mathbf{r}') | \lambda_p^n; \mathbf{r}' \rangle + \left[-\frac{\hbar^2}{2\mu} \nabla_{\mathbf{r}}^2 + \beta_r(a^+ + a) V(\mathbf{r}, \mathbf{r}') \right] F_{pn}(\mathbf{r}) | \lambda_p^n; \mathbf{r}' \rangle \right\} \end{aligned} \quad (12.5.8)$$

In view of Eq. (12.5.6), the first part on the right-hand side of Eq. (12.5.8) immediately simplifies to

$$\sum_{pn} \lambda_p^n | \lambda_p^n; \mathbf{r}' \rangle F_{pn}(\mathbf{r}) \quad (12.5.9)$$

The second part on the right-hand side of Eq. (12.5.8) consists of two sums over $\{pn\}$:

$$\sum_{pn} | \lambda_p^n; \mathbf{r}' \rangle \left[-\frac{\hbar^2}{2\mu} \nabla_{\mathbf{r}}^2 + V(\mathbf{r}, \mathbf{r}') \right] F_{pn}(\mathbf{r}) + \sum [\beta_r(a^+ + a)] | \lambda_p^n; \mathbf{r}' \rangle F_{pn}(\mathbf{r}) \quad (12.5.10)$$

Substitution for $| \lambda_p^n; \mathbf{r}' \rangle$ from Eq. (12.4.9) yields for the second sum

$$\sum_{pn} \sum_j \beta_r F_{pn}(\mathbf{r}) \sum_m a_{jm}(\lambda_p^n) | j(\mathbf{r}') \rangle [| m+1 \rangle + | m-1 \rangle] \quad (12.5.11)$$

In this expression we now shift the summation index $m \rightarrow m-1$ and $n \rightarrow n-1$ for the term with $| m+1 \rangle$, and similarly shift $m \rightarrow m+1$ and $n \rightarrow n-1$ for the term with $| m-1 \rangle$. Hence we obtain

$$\sum_{pn} \sum_{jm} [\beta_r [F_{pn-1}(\mathbf{r}) a_{jm-1}(\lambda_p^{n-1}) + F_{pn+1}(\mathbf{r}) a_{jm+1}(\lambda_p^{n+1})]] | j(\mathbf{r}') \rangle \quad (12.5.12)$$

From the Floquet-periodicity rule (12.3.2.6) and (12.3.2.7) we obtain

$$a_{jm-1}(\lambda_p^{n-1}) = a_{jm+1}(\lambda_p^{n+1}) = a_{jm}(\lambda_p^n) \quad (12.5.13)$$

Substitution of this relation in expression (12.5.12) simplifies the latter to

$$\begin{aligned} \sum_{pn} \sum_{jm} \beta_r [F_{pn-1}(\mathbf{r}) + F_{pn+1}(\mathbf{r})] a_{jm}(\lambda_p^n) | j(\mathbf{r}') \rangle \\ = \sum_{pn} | \lambda_p^n; \mathbf{r}' \rangle [\beta_r (F_{pn-1}(\mathbf{r}) + F_{pn+1}(\mathbf{r}))] \end{aligned} \quad (12.5.14)$$

where in the last line we have used definition (12.4.9). We now combine relations (12.5.14), (12.5.10), and (12.5.9) together with (12.5.8) to obtain

$$\begin{aligned} H(\mathbf{r}, \mathbf{r}') \sum_{pn} F_{pn}(\mathbf{r}) &| \lambda_p^n, \mathbf{r}' \rangle \\ &= \sum_{pn} | \lambda_p^n, \mathbf{r}' \rangle \left[-\frac{\hbar^2}{2\mu} \nabla_{\mathbf{r}}^2 + \lambda_p^n + \beta_{\mathbf{r}}(s_n^- + s_n^+) + V(\mathbf{r}, \mathbf{r}') \right] F_{pn}(\mathbf{r}) \end{aligned} \quad (12.5.15)$$

where, as usual,

$$s_n^\pm F_{pn}(\mathbf{r}) \equiv F_{pn\pm 1}(\mathbf{r}) \quad (12.5.16)$$

The action of $H(\mathbf{r}, \mathbf{r}')$ on the second part of Eq. (12.5.7) can be obtained from the symmetry of the Hamiltonian, $H(\mathbf{r}, \mathbf{r}') = H(\mathbf{r}', \mathbf{r})$, as follows. On interchanging the role of \mathbf{r} and \mathbf{r}' in Eq. (12.5.15) we derive

$$\begin{aligned} H(\mathbf{r}', \mathbf{r}) \sum_{pn} F_{pn}(\mathbf{r}') &| \lambda_p^n; \mathbf{r} \rangle \\ &= \sum_{pn} | \lambda_p^n; \mathbf{r} \rangle \left[-\frac{\hbar^2}{2\mu} \nabla_{\mathbf{r}}^2 + \lambda_p^n + \beta_{\mathbf{r}'}(s_n^- + s_n^+) + V(\mathbf{r}', \mathbf{r}) \right] F_{pn}(\mathbf{r}') \end{aligned} \quad (12.5.17)$$

Since $H(\mathbf{r}, \mathbf{r}') = H(\mathbf{r}', \mathbf{r})$, the left-hand side of Eq. (12.5.17) also equals the action of $H(\mathbf{r}, \mathbf{r}')$ on the second part of expression (12.5.7). We may now combine Eqs. (12.5.17) and (12.5.15) with relation (12.5.7) and obtain

$$\begin{aligned} H(\mathbf{r}, \mathbf{r}') &| \psi(\mathbf{r}, \mathbf{r}') \rangle \\ &= \sum_{pn} | \lambda_p^n; \mathbf{r}' \rangle \left[-\frac{\hbar^2}{2\mu} \nabla_{\mathbf{r}}^2 + \lambda_p^n + \beta_{\mathbf{r}}(s_n^+ + s_n^-) + V(\mathbf{r}, \mathbf{r}') \right] F_{pn}(\mathbf{r}) \\ &\quad + \sum_{pn} | \lambda_p^n; \mathbf{r} \rangle \left[-\frac{\hbar^2}{2\mu} \nabla_{\mathbf{r}}^2 + \lambda_p^n + \beta_{\mathbf{r}'}(s_n^+ + s_n^-) + V(\mathbf{r}', \mathbf{r}) \right] F_{pn}(\mathbf{r}') \end{aligned} \quad (12.5.18)$$

Finally, we substitute expression (12.5.18) in Eq. (12.5.1), project onto the dressed states $\langle \lambda_p^{n'}; \mathbf{r}' |$, and multiply by $2\mu/\hbar^2$ (after restoring the superscripts to F) to obtain the radiative close-coupling equations:

$$\begin{aligned} &\left[\nabla_{\mathbf{r}}^2 + k_{p'n'}^2 - \frac{2\mu}{\hbar^2} \beta_{\mathbf{r}}(s_{n'}^+ + s_{n'}^-) \right] F_{p'n'}^{(\pm)}(\mathbf{r}) \\ &= \sum_{pn} U_{p'n'}^{pn}(\mathbf{r}) F_{pn}^{(\pm)}(\mathbf{r}) \pm \sum_{pn} \int d\mathbf{r}' W_{p'n'}^{pn}(\mathbf{r}, \mathbf{r}') F_{pn}^{(\pm)}(\mathbf{r}') \end{aligned} \quad (12.5.19)$$

where

$$k_{p'n'} = [2\mu(E - \lambda_p^{n'})/\hbar^2]^{1/2} \quad (12.5.20)$$

We have also defined the “direct potentials”

$$U_{pn}^{p'n'}(\mathbf{r}) \equiv \frac{2\mu}{\hbar^2} |\lambda_p^{n'}; \mathbf{r}'| - \frac{e^2}{r} + \frac{e^2}{|\mathbf{r} - \mathbf{r}'|} |\lambda_p^n; \mathbf{r}| \quad (12.5.21)$$

and “exchange potentials”

$$\begin{aligned} W_{pn}^{p'n'}(\mathbf{r}, \mathbf{r}') &\equiv -\frac{2\mu}{\hbar^2} |\lambda_p^n; \mathbf{r}\rangle \langle \lambda_p^{n'}; \mathbf{r}'| \\ &\times \left[[E - \lambda_p^{n'} - H_a(\mathbf{r}')] - \left(\beta_r(s_n^+ + s_n^-) + \frac{e^2}{|\mathbf{r}' - \mathbf{r}|} \right) \right] \end{aligned} \quad (12.5.22)$$

Use of the dressed wave functions (12.4.9) gives the more explicit relations

$$U_{pn}^{p'n'}(\mathbf{r}) = \frac{2\mu}{\hbar^2} \sum_{j'm} a_{j'm}^*(\lambda_p^{n'}) a_{jm}(\lambda_p^n) \langle j'(\mathbf{r}') | - \frac{e^2}{r} + \frac{e^2}{|\mathbf{r} - \mathbf{r}'|} | j(\mathbf{r}) \rangle \quad (12.5.23)$$

and

$$\begin{aligned} W_{pn}^{p'n'}(\mathbf{r}, \mathbf{r}') &= -\frac{2\mu}{\hbar^2} \sum_{j'm} | j(\mathbf{r}) \rangle \langle a_{j'm}^*(\lambda_p^{n'}) a_{jm}(\lambda_p^n) \\ &\times \langle j'(\mathbf{r}') | \left[(E - \lambda_p^{n'} - \varepsilon_{j'}) - \left(\beta_r(s_n^+ + s_n^-) + \frac{e^2}{|\mathbf{r}' - \mathbf{r}|} \right) \right] \end{aligned} \quad (12.5.24)$$

We observe that the radiative close-coupling equations (12.5.19) are formally analogous to the usual close-coupling equations in the absence of the field, except that a new channel quantum number $n = 0, \pm 1, \pm 2, \dots$ must now be incorporated in the usual set of quantum numbers and that the direct and exchange potentials ought to be augmented as above in Eqs. (12.5.23) and (12.5.24). The direct and exchange potentials differ from the corresponding potentials in the field-free case due to the appearance of the Floquet coefficients, which incorporate the persistent influence of the dynamic polarization of the target by the field. It shows that the modification of the scattering potentials due to the field is not entirely a transient phenomena but is rather reminiscent of the persistent effect of the perturbation in the field theory.

The radiative scattering amplitudes can be found by solving the close-coupling equations (12.5.19) subject to the outgoing-wave boundary condition as $r \rightarrow \infty$. In this limit the exchange and direct potentials will tend to zero (the latter mostly vanish exponentially while the former vanish as inverse powers of the distance). Equations (12.5.19) then reduce to

$$\left[\nabla^2 + k_{p'n'}^2 - 2 \frac{\mu}{\hbar^2} \beta_r(s_n^- + s_n^+) \right] F_{p'n'}(\mathbf{r}) \rightarrow 0 \quad (12.5.25)$$

which have the asymptotically plane-wave solutions of the form

$$J_{n'-N}(\mathbf{k}_{p'N} \cdot \boldsymbol{\alpha}_0) e^{i\mathbf{k}_{p'N} \cdot \mathbf{r}} \quad (12.5.26)$$

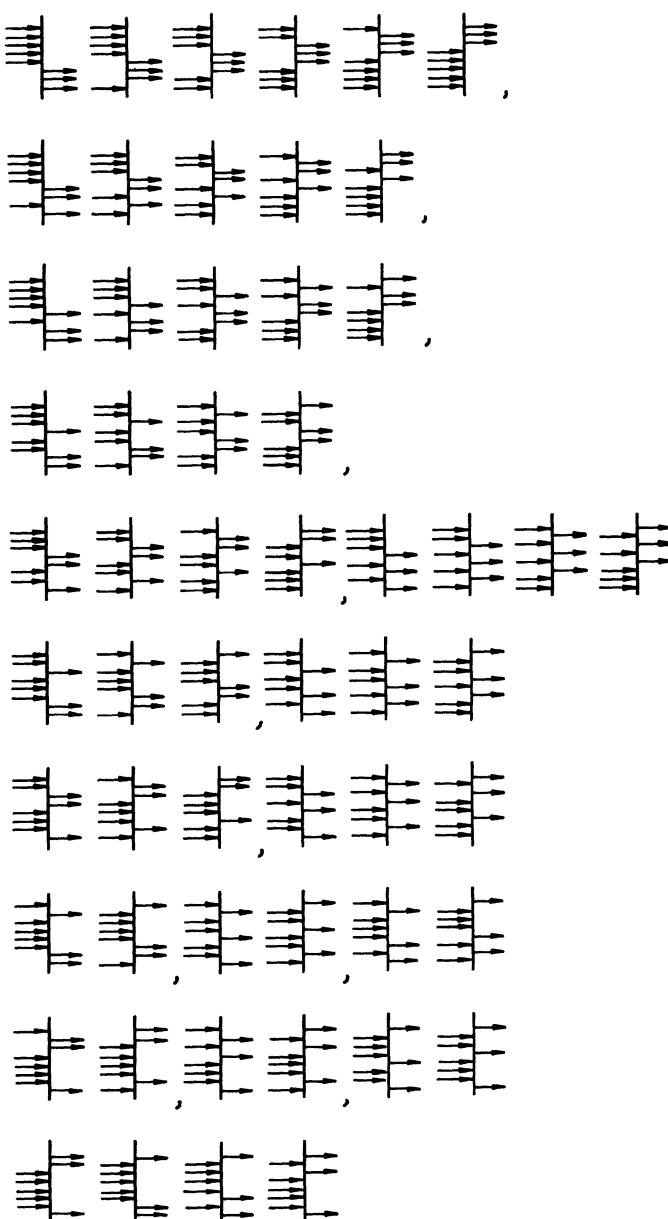
for all n' , N , and p' . Consistent with the asymptotic condition, therefore, the boundary conditions governing the channel-wave functions $F_{p'n'}(\mathbf{r})$ for the solution of differential equations (12.5.19) assume the form

$$\begin{aligned} F_{p'n'}(\mathbf{r}) &= \lim_{r \rightarrow \infty} J_{n'-N}(\mathbf{k}_{p'N} \cdot \boldsymbol{\alpha}_0) e^{i\mathbf{k}_{p'N} \cdot \mathbf{r}} \delta_{p',i} \delta_{N,0} \\ &+ \sum_{N=-\infty}^{\infty} J_{n'-N}(\mathbf{k}_{p'n'} \cdot \boldsymbol{\alpha}_0) \frac{e^{i\mathbf{k}_{p'N} \cdot \mathbf{r}}}{r} f_{i,0 \rightarrow p',N}^{(\pm)}(\Omega_0, \Omega) \end{aligned} \quad (12.5.27)$$

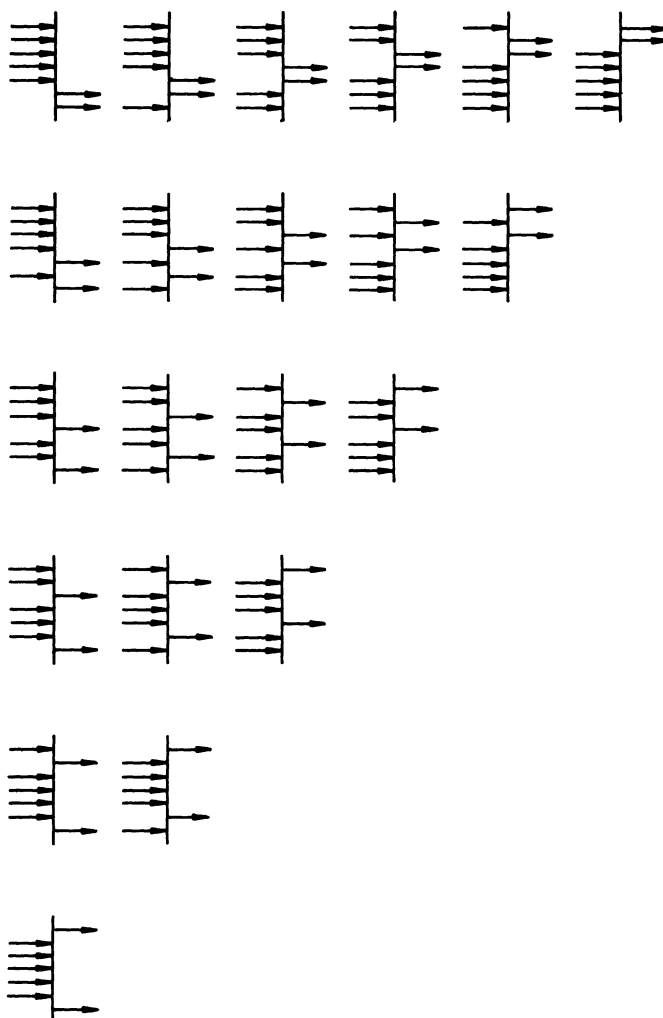
where $f_{i,0 \rightarrow p',N}^{(\pm)}(\Omega_0, \Omega)$ are identified with the singlet (+) and triplet (-) electron-atom scattering amplitudes for the scattering of the electron from the initial momentum state $\mathbf{k}_{i,0}$ in the direction Ω_0 , to the final momentum state $\mathbf{k}_{p'N}$ in the direction Ω , accompanied by the emission ($N > 0$) or absorption ($N < 0$) of N photons.

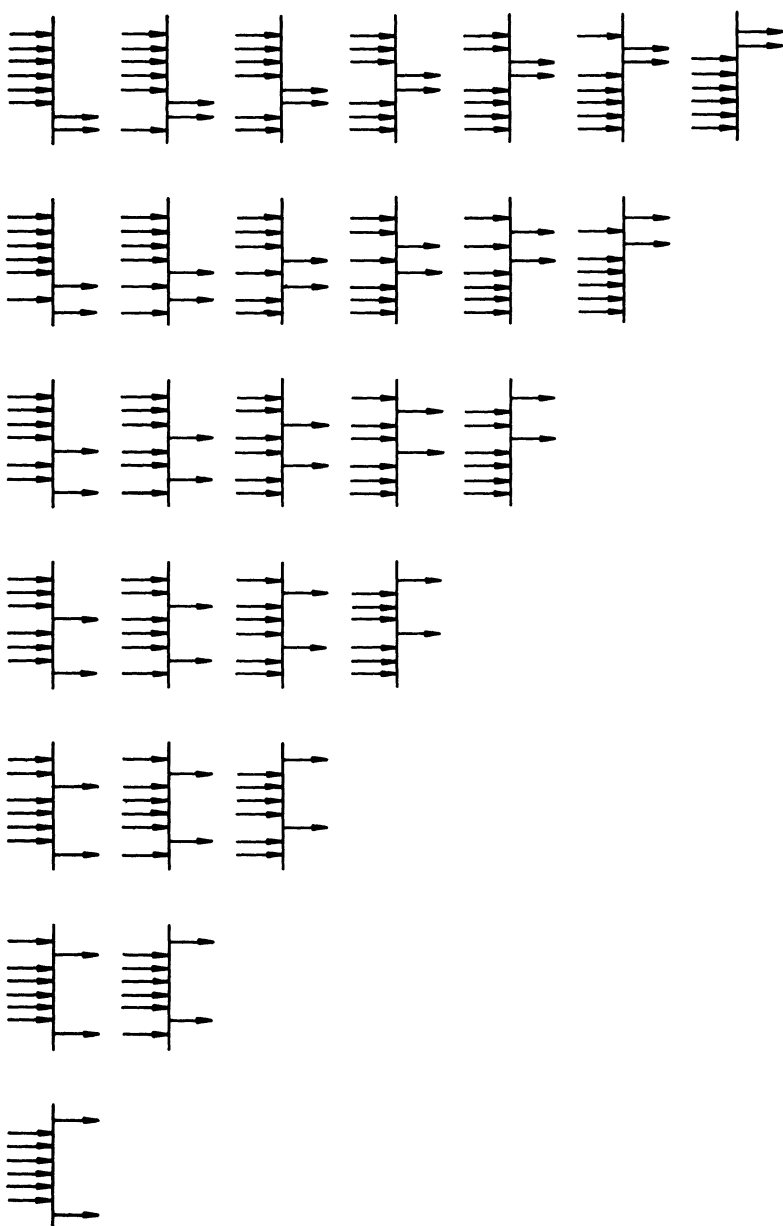
Appendices

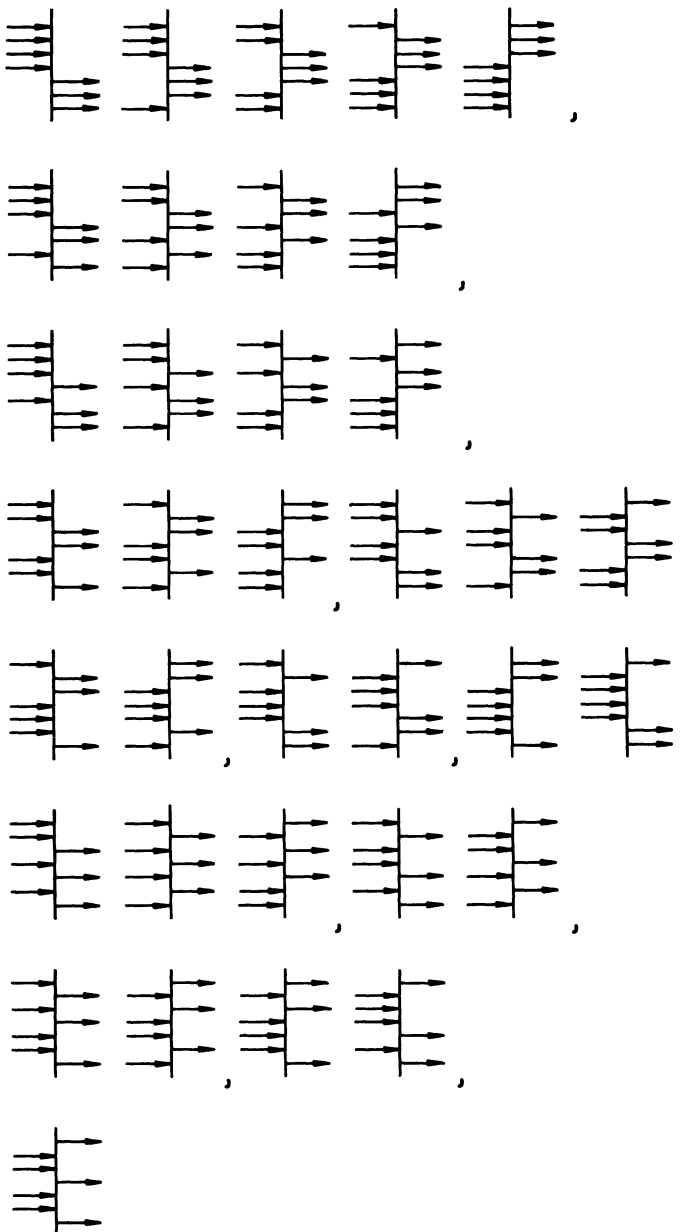
Appendix 1a. The Fifty-Six Topologically Distinct Eighth-Order Diagrams Which Provide the Third Correction to Two-Photon Absorption



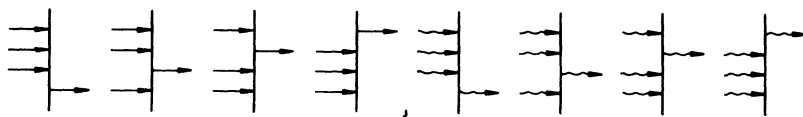
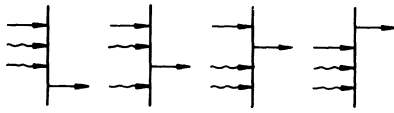
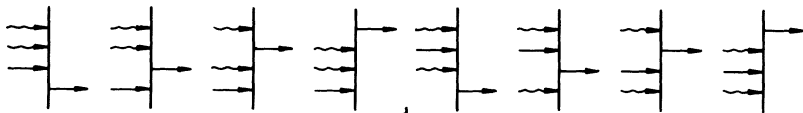
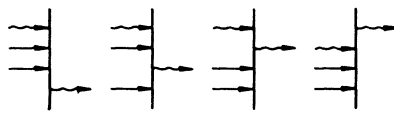
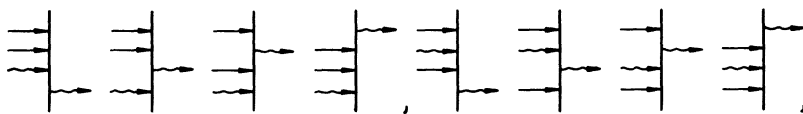
Appendix 1b. The Twenty-One Topologically Distinct Seventh-Order Diagrams Which Provide the Second Correction to Three-Photon Absorption



Appendix 1c. The Twenty-Eight Topologically Distinct Eighth-Order Diagrams Which Provide the Second Correction to Four-Photon Absorption

Appendix 1d. The Thirty-Five Topologically Distinct Seventh-Order Diagrams Which Provide the Third Correction to One-Photon Absorption

Appendix 1e. Forty Additional Diagrams Which Contribute in the Fourth Order to the Two-Photon Absorption Amplitude for a Two-Mode Field When the Modes Are Distinct but Their Frequencies Are Degenerate



Appendix 2. Two-Photon Matrix Elements τ for Hydrogen
(from S. Jetzke, personal communication)^a

$ i\rangle$	$ f\rangle$	$l = 0$	$l = 2$	$l = 4$	$l = 6$
$ 1s\rangle$	$ 2s\rangle$	0.471219(02)	0.472197(02)	0.475152(02)	0.480146(02)
$ 1s\rangle$	$ 3s\rangle$	0.128437(02)	0.128512(02)	0.128729(02)	0.129061(02)
$ 1s\rangle$	$ 4s\rangle$	0.657216(01)	0.656907(01)	0.655870(01)	0.653745(01)
$ 1s\rangle$	$ 5s\rangle$	0.420584(01)	0.420105(01)	0.418564(01)	0.415629(01)
$ 1s\rangle$	$ 6s\rangle$	0.300937(01)	0.300465(01)	0.298959(01)	0.296129(01)
$ 1s\rangle$	$ 3d\rangle$	-0.526232(02)	-0.523240(02)	-0.514190(02)	-0.498858(02)
$ 1s\rangle$	$ 4d\rangle$	-0.320766(02)	-0.319948(02)	-0.317537(02)	-0.313669(02)
$ 1s\rangle$	$ 5d\rangle$	-0.223177(02)	-0.223011(02)	-0.222575(02)	-0.222075(02)
$ 1s\rangle$	$ 6d\rangle$	-0.167438(02)	-0.167491(02)	-0.167714(02)	-0.168308(02)
$ 2s\rangle$	$ 3s\rangle$	0.157844(04)	0.158142(04)	0.159041(04)	0.160560(04)
$ 2s\rangle$	$ 4s\rangle$	0.997702(02)	0.966991(02)	0.871256(02)	0.698843(02)
$ 2s\rangle$	$ 5s\rangle$	-0.562817(02)	-0.613273(02)	-0.775368(02)	-0.108703(03)
$ 2s\rangle$	$ 6s\rangle$	-0.882718(02)	-0.947681(02)	-0.116534(03)	-0.162670(03)
$ 2s\rangle$	$ 3d\rangle$	0.853623(05)	0.854874(05)	0.858649(05)	0.865021(05)
$ 2s\rangle$	$ 4d\rangle$	-0.411964(05)	-0.417451(05)	-0.434422(05)	-0.464522(05)
$ 2s\rangle$	$ 5d\rangle$	-0.387582(05)	-0.395057(05)	-0.418919(05)	-0.464230(05)
$ 2s\rangle$	$ 6d\rangle$	-0.328278(05)	-0.337363(05)	-0.367622(05)	-0.431046(05)
$ 3s\rangle$	$ 4s\rangle$	0.133712(05)	0.133956(05)	0.134695(05)	0.135942(05)
$ 3s\rangle$	$ 5s\rangle$	-0.208823(04)	-0.216976(04)	-0.242797(04)	-0.290919(04)
$ 3s\rangle$	$ 6s\rangle$	-0.400971(04)	-0.435360(04)	-0.569462(04)	-0.100705(05)
$ 3s\rangle$	$ 4d\rangle$	0.181399(06)	0.182313(06)	0.185073(06)	0.189734(06)
$ 3s\rangle$	$ 5d\rangle$	-0.120022(07)	-0.121889(07)	-0.127781(07)	-0.138687(07)
$ 3s\rangle$	$ 6d\rangle$	-0.125896(07)	-0.133413(07)	-0.162655(07)	-0.257695(07)

^a $\tau = \langle f | rG(E_i + \omega; r, r')r' | i \rangle + \langle f | rG(E_f - \omega; r, r')r' | i \rangle$. The photon energy is chosen in the following way: $\omega = (\epsilon_f - \epsilon_i) \times (0.5 - 0.01 \times l)$. Data are given in au; the entry 0.471219(02) is an abbreviation for 0.471219×10^2 , etc.

References

1. W. Heitler, *Quantum Theory of Radiation*, 3rd edn., Chapter 1, Clarendon Press, Oxford (1954).
2. A. Erdélyi, ed., *Higher Transcendental Functions*, Vol. 2, p. 7, McGraw-Hill book Company, Inc., New York (1953).
3. A. S. Davydov, *Quantum Mechanics*, Section 33, Pergamon Press, Oxford (1965).
4. G. N. Lewis, *Nature* **118**, 874 (1926).
5. W. Heitler, *Quantum Theory of Radiation*, 3rd edn., p. 20, Clarendon Press, Oxford (1954).
6. E. A. Power and S. Zienau, *Philos. Trans. R. Soc. London, Ser. A* **251**, 427 (1959).
7. P. A. M. Dirac, *Proc. R. Soc. London, Ser. A* **112**, 661 (1926); **114**, 243 (1927).
8. Y. Gontier, N. K. Rahman, and M. Trahin, *Phys. Rev. Lett.* **34**, 774 (1975); *Phys. Rev. A* **14**, 2109 (1976).
9. P. Lambropoulos, in: *Advances in Atomic and Molecular Physics* (D. R. Bates and B. Bederson, eds.). Vol. 12, pp. 87–164, Eq. (20), Academic Press, New York (1976).
10. M. L. Goldberger and K. M. Watson, *Collision Theory*, Chapter 8, pp. 424–509, John Wiley and Sons, Inc., New York (1964).
11. H. P. Kelly, in: *Advances in Theoretical Physics* (K. A. Brueckner, ed.), Vol. 2, pp. 75–169, Academic Press, New York (1968).
12. E. T. Whittaker and G. N. Watson, *A Course of Modern Analysis*, Section 7.32, pp. 132–133, Cambridge University Press, Cambridge (1962).
13. W. Heitler, *Quantum Theory of Radiation*, 3rd edn., Section 1b, pp. 163–174, Clarendon Press, Oxford (1954).
14. A. Erdélyi, ed., *Higher Transcendental Functions*, Vol. 1, pp. 248–264, McGraw-Hill Book Company, Inc., New York (1953).
15. E. C. Titmarch, *Eigenfunction Expansions Associated with Second Order Differential Equations*, Vol. 2, Section 15.15, Oxford University Press, London (1958).
16. L. S. Rodberg and R. M. Thaler, *Introduction to the Quantum Theory of Scattering*, Chapter 4, pp. 73–126, Academic Press, New York (1967).
17. M. Abramowitz and I. A. Stegun, *Handbook of Mathematical Functions*, 5th printing, Eqs. (13.1.32), (13.1.33), (13.6.9), and (13.6.27), pp. 505–510, Dover Publications, Inc., New York (1968).
18. V. A. Davidkin, B. A. Zon, N. L. Manakov, and L. P. Rapoport, *Zh. Eksp. Theor. Fiz.* **60**, 124 (1971); *Sov. Phys. JETP (Engl. Transl.)* **33**, 70 (1971).
19. M. J. Seaton, *Mon. Not. R. Astron. Soc.* **118**, 504 (1958).
20. A. Burgess and M. J. Seaton, *Mon. Not. R. Astron. Soc.* **120**, 121 (1960).

21. G. E. Norman, *Opt. Spektrosk. (USSR)* **12**, 333 (1962); *Opt. Spectrosc. (USSR) (Engl. Transl.)* **12**, 183 (1962).
22. L. Hostler, *J. Math. Phys.* **5**, 591 (1964).
23. H. Buchholz, *Die Konfluente Hypergeometrische Funktion*, Springer-Verlag, Berlin (1953).
24. I. S. Gradshtyn and I. M. Ryzhik, *Tables of Integrals, Series and Products*, p. 729, Eq. (4), Academic Press, New York (1965).
25. L. P. Rapoport and B. A. Zon, *Phys. Lett.* **11**, 564 (1968).
26. S. Klarsfeld, *Lett. Nuovo Cimento* **1**, 682 (1969); **2**, 548 (1969).
27. L. Hostler, *J. Math. Phys.* **11**, 2966 (1970).
28. S. V. Khristenko and S. I. Vetchinkin, *Opt. Spektrosk. (USSR)* **31**, 503 (1971); *Opt. Spectrosc. (USSR) (Engl. Transl.)* **31**, 269 (1971).
29. B. Podolsky, *Proc. Natl. Acad. Sci. U.S.A.* **14**, 253 (1928).
30. B. Podolsky and V. Rojanski, *Phys. Rev.* **34**, 1367 (1929).
31. M. Rotenberg, *Ann. Phys. (N.Y.)* **19**, 262 (1962).
32. N. L. Manakov and L. P. Rapoport, *Opt. Spektrosk. (USSR)* **33**, 998 (1972); *Opt. Spectrosc. (USSR) (Engl. Transl.)* **33**, 547 (1972).
33. N. L. Manakov, V. D. Ovsyannikov, and L. P. Rapoport, *Opt. Spektrosk. (USSR)* **38**, 206 (1975); *Opt. Spectrosc. (USSR) (Engl. Transl.)* **38**, 115 (1975).
34. A. Erdélyi, ed., *Higher Transcendental Functions*, Vol. 2, p. 189, Eq. (20), McGraw-Hill Book Company, Inc., New York (1953).
35. A. Erdélyi, ed., *Higher Transcendental Functions*, Vol. 2, p. 189, Eq. (14), McGraw-Hill Book Company, Inc., New York (1953).
36. L. Hostler, *J. Math. Phys.* **8**, 642 (1967).
37. B. J. Laurenzi, *J. Chem. Phys.* **52**, 3049 (1970).
38. L. Hostler, *J. Math. Phys.* **5**, 1235 (1964).
39. S. Okubo and D. Feldman, *Phys. Rev.* **117**, 292 (1960).
40. V. G. Gorshkov, *Zh. Eksp. Theor. Fiz.* **47**, 352 (1964); *Sov. Phys. JETP (Engl. Transl.)* **20**, 234 (1965).
41. J. Schwinger, *J. Math. Phys.* **5**, 1606 (1964).
42. M. Gavrila, *Phys. Rev.* **163**, 147 (1967).
43. B. J. Laurenzi, D. G. Williams, and G. S. Bhatia, *J. Chem. Phys.* **61**, 2079 (1974).
44. M. Gavrila, *Lett. Nuovo Cimento* **2**, 180 (1969); *Phys. Rev. A* **6**, 1348 (1972).
45. A. Maquet, *Phys. Rev. A* **15**, 1088 (1977).
46. G. Simons, *J. Chem. Phys.* **55**, 756 (1971).
47. V. Avilova and L. I. Podlubny, *Opt. Spektrosk. (USSR)* **38**, 1059 (1975); *Opt. Spectrosc. (USSR) (Engl. Transl.)* **38**, 613 (1975).
48. E. Yurtsever and F. H. M. Faisal, *Chem. Phys. Lett.* **66**, 104 (1979).
49. R. M. Sternheimer, *Phys. Rev.* **84**, 244 (1951).
50. A. Dalgarno and J. J. Lewis, *Proc. Phys. Soc. A* **233**, 70 (1955).
51. C. Schwartz and J. J. Tiemann, *Ann. Phys. (N.Y.)* **6**, 178 (1959).
52. M. H. Mittleman and F. A. Wolf, *Phys. Rev.* **128**, 2686 (1962).
53. W. Zernik, *Phys. Rev.* **132**, 320 (1963).
54. W. Zernik, *Phys. Rev.* **135**, A 51 (1964).
55. Y. Gontier and M. Trahin, *Phys. Rev.* **172**, 83 (1968); *Phys. Rev. A* **4**, 1896 (1971); **14**, 1935 (E) (1976).
56. M. Aymar and M. Crance, *J. Phys. B* **14**, 3585 (1981).
57. I. I. Sobelman, *Atomic Spectra and Radiative Transitions*, Section 4.2, pp. 40–74, Springer-Verlag, Berlin (1979).
58. I. Cacelli, R. Moccia, and V. Carravetta, in: *Collisions and Half-Collisions with Lasers* (N. K. Rahman and C. Guidotti, eds.), pp. 229–248, Harwood Academic Publishers, London (1984).

59. H. B. Bebb, *Phys. Rev.* **149**, 25 (1966); **153**, 23 (1967).
60. P. Lambropoulos and M. R. Teague, *J. Phys. B* **9**, 587 (1976).
61. M. R. Teague and P. Lambropoulos, *J. Phys. B* **9**, 1251 (1976).
62. P. Lambropoulos, in: *Advances in Atomic and Molecular Physics* (D. R. Bates and B. Bederson, eds.), Vol. 12, Section 5, Academic Press, New York (1976).
63. S. Klarsfeld, *Lett. Nuovo Cimento* **3**, 395 (1970).
64. W. Zernik and R. W. Klopffenstein, *J. Math. Phys.* **6**, 262 (1965).
65. J. Morellec, D. Normand, and G. Petite in: *Advances in Atomic and Molecular Physics* (D. R. Bates and B. Bederson, eds.), Vol. 18, pp. 96–165, Academic Press, New York (1982).
66. F. T. Chan and C. L. Tang, *Phys. Rev.* **185**, 42 (1969).
67. Y. Gontier and M. Trahin, *Phys. Rev. A* **4**, 1896 (1971).
68. S. Klarsfeld, *Lett. Nuovo Cimento* **2**, 548 (1969).
69. S. V. Khristenko and S. I. Vetchinkin, *Opt. Spectrosc. (USSR)* **40**, 417 (1976); *Opt. Spectrosc. (USSR) (Engl. transl.)* **40**, 239 (1976).
70. E. Karule, *J. Phys. B* **11**, 441 (1978).
71. G. Laplanche, A. Durrieu, Y. Flank, M. Jaouen, and A. Rachman, *J. Phys. B* **9**, 1263 (1976).
72. E. Karule, *J. Phys. B* **4**, L 67 (1971).
73. E. Karule, in: *Atomic Processes*, p. 5, Latvian Academy of Sciences, Riga (1975) (in Russian), quoted in ref. 9.
74. W. Gordon, *Ann. Phys. (Leipzig)* **2**, 1031 (1929).
75. W. J. Karzas and R. Latter, *Astrophys. J. Suppl.* **6**, 167 (1961).
76. E. Karule, *J. Phys. B* **11**, 444 (1977).
77. S. Klarsfeld and A. Maquet, *Phys. Lett. A* **78**, 40 (1980).
78. M. Aymar and M. Crance, *J. Phys. B* **13**, L 287 (1980).
79. S. Klarsfeld and A. Maquet, *J. Phys. B* **12**, L 553 (1979).
80. Y. Gontier and M. Trahin, *J. Phys. B* **13**, 4383 (1980).
81. H. B. Bebb, *Phys. Rev.* **149**, 25 (1966).
82. N. L. Manakov, V. D. Ovsannikov, and L. P. Rapoport, *Proc. Int. Conf. Phenom. Ioniz. Gases*, 11th, p. 29 (1973).
83. N. L. Manakov, V. D. Ovsannikov, M. A. Preobrazhenki, and L. P. Rapoport, *J. Phys. B* **11**, 245 (1978).
84. E. J. McGuire, *Phys. Rev. A* **23**, 186 (1981).
85. G. Laplanche, Y. Flank, M. Jaouen, and A. Rachman, *Phys. Lett. A* **58**, 223 (1976).
86. B. A. Zon, N. L. Manakov, and L. P. Rapoport, *Zh. Eksp. Theor. Fiz.* **61**, 968 (1971); *Sov. Phys. JETP (Engl. Transl.)* **34**, 515 (1972).
87. J. Bakos, N. B. Delone, A. Kiss, N. L. Manakov, and M. L. Nagaera, *Zh. Eksp. Theor. Fiz.* **71**, 511 (1976); *Sov. Phys. JETP (Engl. Transl.)* **44**, 268 (1976).
88. T. Olsen, P. Lambropoulos, S. Weatley, and S. Rountree, *J. Phys. B* **11**, 4167 (1978).
89. R. K. Sharma and K. C. Mathur, *IEEE J. Quantum Electron.* **QE-14**, 771 (1978).
90. K. C. Mathur, *Phys. Rev. A* **18**, 2170 (1978).
91. L. A. Lompré, G. Mainfray, B. Mathieu, G. Watel, M. Aymar, and M. Crance, *J. Phys. B* **13**, 1799 (1980).
92. M. Aymar and M. Crance, *J. Phys. B* **13**, 2527 (1980).
93. M. S. Pindzola and H. P. Kelly, *Phys. Rev. A* **11**, 1543 (1975).
94. E. J. McGuire, *Phys. Rev. A* **24**, 835 (1981).
95. R. Moccia, N. K. Rahman, and A. Rizzo, *J. Phys. B* **16**, 2737 (1983).
96. G. S. Voronov and N. B. Delone, *Zh. Eksp. Theor. Fiz.* **50**, 78 (1966); *Sov. Phys. JETP (Engl. Transl.)* **23**, 54 (1966).
97. D. Normand and I. Morellec, *J. Phys. B* **13**, 1551 (1980).
98. M. R. Cervenan, R. H. C. Chan, and N. R. Isenor, *Can J. Phys.* **53**, 1573 (1975).

99. T. V. Arslanbekov, V. A. Grinchuk, G. A. Delone, and K. B. Petrosyan, *Sov. Phys., Lebedev Inst. Rep.* **10**, 29 (1975).
100. T. U. Arslanbekov and N. B. Delone, *Sov. Phys., Lebedev Inst. Rep.* **11**, 33 (1976).
101. M. Aymar and M. Crance, *J. Phys. B* **12**, L 667 (1979).
102. J. Morellec, D. Normand, G. Mainfray, and C. Manus, *Phys. Rev. Lett.* **44**, 1394 (1980).
103. A. Declémé, A. Rachman, M. Jaouen, and G. Laplanche, *Phys. Rev. A* **23**, 1823 (1981).
104. M. R. Teague, P. Lambropoulos, D. Goodmanson, and D. W. Norcross, *Phys. Rev. A* **14**, 1057 (1976).
105. M. Aymar and M. Crance, *J. Phys. B* **15**, 719 (1982).
106. C. Bottcher, *J. Phys. B* **4**, 1140 (1971).
107. J. Mizuno, *J. Phys. B* **6**, 314 (1973).
108. P. Lambropoulos, *Phys. Rev. A* **9**, 1992 (1974).
109. B. L. Beers and L. Armstrong, Jr., *Phys. Rev. A* **12**, 2447 (1975).
110. Y. Gontier, N. K. Rahman, and M. Trahin, *Phys. Rev. A* **14**, 2109 (1976).
111. F. H. M. Faisal, *J. Phys. B* **9**, 3009 (1976).
112. Shi-I Chu and W. P. Reinhardt, *Phys. Rev. Lett.* **39**, 1195 (1977).
113. C. Cohen-Tannoudji, in: *Cargese Lectures in Physics* (M. Levy, ed.), Vol. 2, pp. 347–393, Gordon and Breach, New York (1968).
114. L. Mower, *Phys. Rev.* **142**, 799 (1966).
115. W. Heitler and S. T. Ma, *Proc. Roy. Ir. Acad.* **52**, 109 (1949).
116. I. H. Shirley, *Phys. Rev.* **138**, B 979 (1965); G. Oliver, *Lett. Nuovo Cimento* **2**, 1075 (1971).
117. M. Born, W. Heisenberg, and P. Jordan, *Z. Phys.* **35**, 557 (1926).
118. I. Bialynicki-Birula and Z. Bialynicka-Birula, *Phys. Rev. A* **14**, 1101 (1976).
119. K. O. Friedrichs, *Comm. Pure Appl. Math.* **1**, 361 (1948).
120. U. Fano, *Phys. Rev.* **124**, 1866 (1961).
121. C. D. Cantrell, V. S. Letokov, and A. A. Manakov, in: *Coherent Nonlinear Optics: Recent Advances* (M. S. Feld and V. S. Letokov, eds.), pp. 165–269, Springer-Verlag, Berlin (1980), and references cited therein.
122. P. Agostini, F. Fabre, G. Mainfray, G. Petite, and N. K. Rahman, *Phys. Rev. Lett.* **42**, 1127 (1979).
123. F. Fabre, P. Agostini, and G. Petite, *Phys. Rev. A* **27**, 1682 (1983).
124. R. Hipppler, H. J. Humpert, H. Schwier, S. Jetzke, and H. O. Lutz, *J. Phys. B* **16**, L 713 (1983).
125. L. A. Lompré, A. L'Huillier, G. Mainfray, and J. Y. Fan, *J. Phys. B* **18**, L 817 (1984).
126. P. Kruit, J. Kimmer, H. G. Muller, and M. J. Van der Wiel, *Phys. Rev. A* **28**, 248 (1983); *J. Phys. B* **16**, 937 (1983).
127. A. Dohdhy, R. N. Compton, and J. A. D. Stockdall, *Phys. Rev. Lett.* **54**, L 22 (1985).
128. M. Aymar and M. Crance, *J. Phys. B* **13**, L 421 (1980).
129. H. G. Muller, A. Tip, and M. J. Van der Wiel, *J. Phys. B* **16**, L 679 (1983).
130. Z. Bialynicka-Birula, *J. Phys. B* **17**, 3091 (1984).
131. M. Edwards, L. Pan, and L. J. Armstrong, *J. Phys. B* **17**, L 515 (1984).
132. M. Crance, *J. Phys. B* **17**, L 355 (1984).
133. Z. Deng and J. H. Eberly, *Phys. Rev. Lett.* **53**, 1810 (1984).
134. Z. Deng and J. H. Eberly, *J. Opt. Soc. Am. B* **2**, 486 (1985).
135. Z. Deng and J. H. Eberly, *J. Phys. B* **18**, L 287 (1985).
136. K. Rzżewski and R. Grobe, *Phys. Rev. Lett.* **54**, 1729 (1985).
137. L. Armstrong, Jr., L. B. Beers, and S. Feneuille, *Phys. Rev. A* **12**, 1303 (1975).
138. S. Feneuille and L. Armstrong, Jr., *J. Phys. Lett.* **36**, 2447 (1975).
139. M. Crance, *J. Phys. B* **11**, 1931 (1978).
140. I. Rabi, *Phys. Rev.* **51**, 652 (1937).

141. D. Normand, G. Petite, and J. Morellec, *Phys. Lett. A* **65**, 652 (1978).
142. M. Crance and M. Aymar, *J. Phys. B* **12**, 3665 (1979).
143. B. R. Judd, *Operator Techniques in Atomic Spectroscopy*, p. 41, McGraw-Hill Book Company, Inc., New York (1963).
144. H. Feshbach, *Ann. Phys. (N.Y.)* **5**, 357 (1958); **19**, 287 (1962).
145. E. Arnous, J. Bastian, and A. Maquet, *Phys. Rev. A* **27**, 977 (1983).
146. A. M. Bonch-Bruevich and V. A. Khodovoi, *Usp. Fiz. Nauk* **93**, 71 (1967); *Sov. Phys. Usp. (Engl. Transl.)* **10**, 637 (1968).
147. A. Schabert, R. Keil, and P. E. Toschek, *Opt. Commun.* **13**, 265 (1975).
148. P. F. Liao and J. E. Bjorkholm, *Phys. Rev. Lett.* **34**, 1 (1975).
149. J. E. Bjorkholm and P. F. Liao, *Opt. Commun.* **21**, 132 (1977).
150. M. Crance and M. Aymar, *J. Phys. B* **13**, L 421 (1980).
151. N. B. Delone, I. I. Bondar, V. V. Suran, and B. A. Zon, *Opt. Commun.* **40**, 268 (1982).
152. D. Feldmann, H. J. Krautwald, and K. H. Welge, *J. Phys. B* **15**, L 529 (1982).
153. P. Agostini and G. Petite, in: *Multiphoton Processes* (P. Lambropoulos and S. J. Smith, eds.), pp. 13–30, Springer-Verlag, Berlin (1980) and references cited therein.
154. P. Lambropoulos, *Appl. Opt.* **19**, 3926 (1980).
155. K. Rzżewski and J. H. Eberly, *Phys. Rev. Lett.* **47**, 408 (1981).
156. P. Lambropoulos and P. Zoller, *Phys. Rev. A* **24**, 379 (1981).
157. G. S. Agarwal, S. L. Haan, K. Burnett, and J. Cooper, *Phys. Rev. Lett.* **48**, 1164 (1982).
158. Y. S. Kim and P. Lambropoulos, *Phys. Rev. Lett.* **49**, 1698 (1982).
159. M. Crance and L. A. Armstrong, *J. Phys. B* **15**, 3191 (1982).
160. A. M. F. Lau and C. K. Rhodes, *Phys. Rev. A* **15**, 1570 (1977); **16**, 2392 (1977).
161. A. Lami and N. K. Rahman, *Nuovo Cimento B* **63**, 407 (1981).
162. A. Lami and N. K. Rahman, *Phys. Rev. A* **26**, 3360 (1982).
163. M. H. Mittleman, *J. Phys. B* **12**, 1781 (1972).
164. F. H. M. Faisal, A. Lami, and N. K. Rahman, *J. Phys. B* **14**, L 569 (1981); A. Lami, N. K. Rahman, and F. H. M. Faisal, *Phys. Rev.* **30**, 2433 (1984).
165. G. S. Agarwal, *Quantum Statistical Theories of Spontaneous Emission and their Relation to Other Approaches*, Springer-Verlag, Berlin (1974).
166. G. S. Agarwal, *Phys. Rev. A* **1**, 1445 (1970).
167. J. H. Eberly, in: *Laser Spectroscopy IV* (H. Walter and K. W. Rothe, eds.), p. 80, Springer-Verlag, Berlin (1979), and references cited therein.
168. A. T. Georges and P. Lambropoulos, *Adv. Electron. Electron Phys.* **34**, 190–240 (1980), Section VIII, and references cited therein.
169. P. Zoller, in: *Multiphoton Processes* (P. Lambropoulos and S. J. Smith, eds.), pp. 68–75, Springer-Verlag, Berlin (1984), and references cited therein.
170. P. Zoller, *J. Phys. B* **10**, L 321 (1977).
171. D. R. Cox and H. D. Miller, *The Theory of Stochastic Processes*, Chapter 5, Chapman and Hill Ltd., London (1972).
172. P. Avan and C. Cohen-Tannoudji, *J. Phys. B* **10**, 155 (1977).
173. P. Zoller, *Phys. Rev. A* **19**, 1151 (1979).
174. R. T. Glauber, in: *Quantum Optics and Electronics* (C. de Witt, ed.), p. 63, Gordon and Breach, New York (1965).
175. N. G. Van Kampen, *Stochastic Processes in Physics and Chemistry*, Chapter XV, North-Holland Publ. Co., Amsterdam (1983).
176. M. C. Wang and G. E. Uhlenbeck, in: *Selected Topics in Noise and Stochastic Processes* (N. Wax, ed.), Dover, New York (1954).
177. R. Kubo, *J. Math. Phys.* **4**, 174 (1963).
178. H. Risken, *The Fokker-Planck Equation, Methods of Solutions and Applications*, Springer-Verlag, Berlin (1984).

179. S. N. Dixit, P. Zoller, and P. Lambropoulos, *Phys. Rev. A* **21**, 1289 (1980).
180. H. Haken, in: *Handbuch der Physik* (S. Fluegge, ed.), Vol. XXV/2C, Springer-Verlag, Berlin (1969).
181. G. S. Agarwal, *Phys. Rev. A* **18**, 1490 (1978).
182. K. Wodkiewicz, *Phys. Rev. A* **19**, 1686 (1979).
183. J. L. Debethune, *Nuovo Cimento B* **12**, 101 (1972).
184. P. Zoller and P. Lambropoulos, *J. Phys. B* **13**, 69 (1980).
185. W. H. Louisell, *Quantum Statistical Properties of Radiation*, John Wiley and Sons, New York (1973).
186. P. Agostini, A. T. Georges, S. E. Wheatley, P. Lambropoulos, and M. D. Levenson, *J. Phys. B* **11**, 1133 (1978).
187. J. Morellec, D. Normand, and G. Petite, *Phys. Rev. A* **14**, 3002 (1976).
188. M. Crance, *J. Phys. B* **13**, 101 (1980).
189. Y. Gontier, N. K. Rahman, and M. Trahin, *Phys. Lett. A* **54**, 341 (1975).
190. S. H. Autler and C. H. Townes, *Phys. Rev.* **100**, 703 (1955).
191. S. Stenholm and W. E. Lamb, Jr., *Phys. Rev.* **181**, 618 (1969).
192. S. Stenholm, *J. Phys. B* **5**, 878 (1972).
193. S. Swain, *J. Phys. A* **8**, 1277 (1975).
194. S. Swain, *J. Phys. A* **9**, 1811 (1976).
195. S. Swain, *J. Phys. A* **10**, 155 (1977).
196. S. Yeh and P. Stehle, *Phys. Rev. A* **15**, 213 (1977).
197. A. Maquet, S. I. Chu, and W. P. Reinhardt, *Phys. Rev. A* **27**, 2946 (1983).
198. Y. Gontier, N. K. Rahman, and M. Trahin, *Phys. Rev. A* **24**, 3102 (1981).
199. K. Smith, R. J. W. Henny, and P. G. Burke, *Phys. Rev.* **147**, 21 (1966).
200. C. Lanczos, *J. Res. Natl. Bur. Stand.* **45**, 255 (1950).
201. R. Haydock, *J. Phys. A* **7**, 2120 (1974).
202. R. Haydock, *Solid State Phys.* **35**, 215 (1980).
203. A. Nauts and R. E. Wyatt, *Phys. Rev. Lett.* **51**, 2238 (1983); *Phys. Rev. A* **30**, 872 (1984).
204. E. J. Heller and H. A. Yamani, *Phys. Rev. A* **9**, 1201, 1209 (1974).
205. H. A. Yamani and L. Fishman, *J. Math. Phys.* **16**, 410 (1975).
206. E. J. Heller, *Phys. Rev. A* **12**, 122 (1975).
207. J. T. Broad and W. P. Reinhardt, *Phys. Rev. A* **14**, 2159 (1976).
208. J. T. Broad, *Phys. Rev. A* **26**, 3078 (1982).
209. G. Szegő, *Orthogonal Polynomials*, 3rd edn., Am. Math. Soc., Providence (1967).
210. H. S. Wall, *Analytical Theory of Continued Fractions*, Van Nostrand, New York (1948).
211. M. Floquet, *Ann. Ecole Norm. Sup. (2)* **XII**, 47 (1883).
212. E. T. Whittaker and G. N. Watson, *A Course of Modern Analysis*, 4th edn., Chapter XIX, Cambridge University Press, Cambridge (1962).
213. W. W. Hicks, R. A. Hess, and W. S. Cooper, *Phys. Rev. A* **5**, 490 (1972).
214. J. V. Moloney and W. J. Meath, *J. Phys. B* **11**, 2641 (1978).
215. J. V. Moloney and F. H. M. Faisal, *J. Phys. B* **12**, 2829 (1979).
216. J. V. Moloney and F. H. M. Faisal, *Opt. Commun.* **29**, 62 (1979).
217. N. Ashby, in: *Proc. of Boulder Inst. Theor. Phys.*, p. 599, Boulder, Colorado (1968).
218. D. R. Dion and J. O. Hirschfelder in: *Advances in Chemical Physics* (I. Prigogine and S. A. Rice, eds.), Vol. XXXV, pp. 265–350, John Wiley and Sons, New York (1976).
219. H. E. Meadow, *Bell Syst. Tech. J.* **41**, 1275 (1962).
220. H. von Koch, *Rend. Circ. Mat. Palermo* **28**, 255 (1909).
221. E. T. Whittaker and G. N. Watson, *A Course of Modern Analysis*, 4th edn., pp. 105–106, Cambridge University Press, Cambridge (1962).
222. K. F. Milfeld and R. E. Wyatt, *Phys. Rev. A* **27**, 72 (1983).
223. J. V. Moloney and W. J. Meath, *Mol. Phys.* **30**, 171 (1975).

224. W. Magnus, *Commun. Pure Appl. Math.* **7**, 649 (1954).
225. D. W. Robinson, *Helv. Phys. Acta* **36**, 140 (1963).
226. S. C. Leisure, K. F. Milfeld, and R. E. Wyatt, *J. Chem. Phys.* **74**, 6197 (1981).
227. V. A. Fock and S. N. Krylov, *Zh. Eksp. Theor. Fiz.* **17**, 93 (1947).
228. A. S. Davydov, *Quantum Mechanics*, Section 80, Pergamon Press, Oxford (1965).
229. F. H. M. Faisal and J. V. Moloney, *J. Phys. B* **4**, 3603 (1981); (Corrigendum) **16**, 3109 (1983).
230. I. Prigogine, in: *The Physicists Conception of Nature* (J. Mehra, ed.), pp. 561–593, Reidel, Boston (1973).
231. A. Einstein and W. Ritz, *Phys. Z.* **10**, 323 (1909).
232. J. R. Ackerhalt and J. H. Eberly, *Phys. Rev. A* **14**, 1705 (1976).
233. B. W. Shore and J. R. Ackerhalt, *Phys. Rev. A* **15**, 1640 (1977).
234. M. Crance and S. Feneuille, *Phys. Rev. A* **16**, 1587 (1977).
235. M. V. Fedorov and A. E. Kazakov, *Opt. Commun.* **22**, 42 (1977).
236. P. L. Knight, *Opt. Commun.* **22**, 173 (1977).
237. S. Geltman, *J. Phys. B* **10**, 831 (1977).
238. J. R. Ackerhalt, *Phys. Rev. A* **17**, 293 (1978).
239. E. J. Austin, *J. Phys. B* **12**, 4045 (1979).
240. P. L. Knight, *J. Phys. B* **11**, L 511 (1978).
241. S. Geltman, *J. Phys. B* **13**, 115 (1980).
242. A. T. Georges and P. Lambropoulos, *Phys. Rev. A* **18**, 1072 (1978).
243. G. Leuchs, S. J. Smith, E. Khawaja, and H. Walther, *Opt. Commun.* **31**, 313 (1979).
244. B. R. Junker, *Adv. At. Mol. Phys.* **18**, 207 (1982), and references cited therein.
245. W. P. Reinhardt, *Ann Rev. Phys. Chem.* **33**, 223 (1982), and references cited therein.
246. M. Reed and B. Simon, *Methods of Modern Mathematical Physics*, Vol. 4, pp. 51–60, Academic Press, New York (1978).
247. S.-I. Chu and W. P. Reinhardt, *Phys. Rev. Lett.* **39**, 1195 (1977).
248. H. A. Yamani and W. P. Reinhardt, *Phys. Rev. A* **11**, 1144 (1975).
249. A. Maquet, S.-I. Chu and W. P. Reinhardt, *Phys. Rev. A* **27**, 2946 (1983).
250. C. R. Holt, M. G. Raymer, and W. P. Reinhardt, *Phys. Rev. A* **27**, 2971 (1983).
251. N. M. Kroll and K. M. Watson, *Phys. Rev. A* **8**, 804 (1973).
252. H. Krüger and C. Jung, *Phys. Rev. A* **17**, 1706 (1978).
253. C. Jung and H. Krüger, *Z. Phys. A* **287**, 7 (1978).
254. M. H. Mittleman, *Phys. Rev. A* **20**, 1965 (1979); **21**, 79 (1980).
255. G. Ferrante, *Nuovo Cimento B* **52**, 229 (1979); *Phys. Rev. A* **22**, 2529 (1980).
256. L. Rosenberg, *Phys. Rev. A* **21**, 157 (1980); **23**, 2283 (1981).
257. C. Jung and H. S. Taylor, *Phys. Rev. A* **23**, 1115 (1981).
258. A. Weingartshofer, J. K. Holmes, G. Caudle, E. M. Clarke, and H. Krüger, *Phys. Rev. Lett.* **39**, 269 (1977).
259. A. Weingartshofer, E. M. Clark, J. K. Holmes, and C. Jung, *Phys. Rev. A* **19**, 2371 (1979).
260. A. Weingartshofer, J. K. Holmes, J. Sabagh, and S. L. Chin, *J. Phys. B* **16**, 1805 (1983).
261. D. Andrick and L. Langhans, *J. Phys. B* **9**, L 459 (1976); **11**, 2355 (1978).
262. L. Langhans, *J. Phys. B* **11**, 2361 (1978).
263. N. F. Mott and H. S. W. Massey, *The Theory of Atomic Collisions*, 3rd edn., Chapter 15 and pp. 524–526, Clarendon Press, Oxford (1965).
264. F. H. M. Faisal, in: *Laser Assisted Collision and Related Topics* (N. K. Rahman and C. Guidotti, eds.), pp. 287–301, Harwood Academic Publishers, New York (1982).
265. F. V. Bunkin and M. V. Fedorov, *Zh. Eksp. Theor. Fiz.* **49**, 1215 (1965); *Sov. Phys. JETP (Engl. Transl.)* **22**, 844 (1966).
266. H. Brehme, *Phys. Rev. C* **3**, 837 (1971).

267. F. H. M. Faisal, *J. Phys. B* **6**, L 312 (1973).
268. N. K. Rahman, *Phys. Rev. A* **10**, 440 (1974).
269. A. Messiah, *Quantum Mechanics*, Vol. II, p. 740, North-Holland Publ. Co., Amsterdam (1970) (Engl. Transl.).
270. I. V. Hertel and W. Stoll, *J. Phys. B* **7**, 570 (1974).
271. M. H. Mittleman, *Phys. Rev. A* **14**, 1338 (1976); **15**, 1355 (E) (1979).
272. F. H. M. Faisal, *Comments At. Mol. Phys.* **15**, 119 (1984).
273. I. I. Sobelman, L. A. Vainstein, and E. A. Yukov, *Excitation of Atoms and Broadening of Spectral Lines*, p. 241, Springer-Verlag, Berlin (1981).
274. B. R. Mollow, *Phys. Rev.* **188**, 1969 (1969).
275. M. Sergeant, M. O. Scully, and W. E. Lamb, Jr., *Laser Physics*, Chapter 8, Addison Wesley, London (1974).
276. L. Dimou and F. H. M. Faisal, in: *Collisions and Half-Collisions with Atoms* (N. K. Rahman and C. Guidotti, eds.), pp. 121–136, Harwood Academic Publishers, New York (1984).
277. I. J. Berson, *J. Phys. B* **8**, 3078 (1975).
278. H. Kleinpoppen and V. Riable, *Phys. Lett.* **18**, 24 (1965).
279. N. F. Mott and H. S. W. Massey, *The Theory of Atomic Collisions*, 3rd edn., p. 530, Clarendon Press, Oxford (1965).
280. L. D. Landau and E. M. Lifschitz, *Quantum Mechanics*, p. 518, Pergamon Press, Oxford (1975).
281. N. F. Mott and H. S. W. Massey, *The Theory of Atomic Collisions*, 3rd edn., p. 522, Clarendon Press, Oxford (1965).
282. N. K. Rahman and F. H. M. Faisal, *J. Phys. B* **9**, L 275 (1976); **11**, 2003 (1978); *Phys. Lett. A* **57**, 426 (1976).
283. A. Lami and R. K. Rahman, *J. Phys. B* **14**, L 523 (1981); **16**, L 201 (1983).
284. S. Jetzke, F. H. M. Faisal, R. Hippler, and H. O. Lutz, *Z. Phys. A* **315**, 271 (1984).
285. M. L. Goldberger and K. M. Watson, *Collision Theory*, Section 4.5, John Wiley and Sons, Inc., New York (1964).
286. L. S. Rodberg and R. M. Thaler, *Introduction to the Quantum Theory of Scattering*, pp. 205–210, Academic Press, New York (1967).
287. P. G. Burke and M. J. Seaton, in: *Methods in Computational Physics* (B. Alder, S. Fernbach, and M. Rotenberg, eds.), Vol. 10, pp. 1–81, Academic Press, New York 1971).

Index

- Above threshold ionization (ATI), 101, 102, 137
- Absorption, 32
- amplitude, 32–34
 - four-photon, 39, 89, 388
 - multiphoton, 119, 213, 217, 220, 253
 - single-photon, 32, 40, 145, 261, 389
 - three-photon, 39, 41, 145, 387
 - two-photon, 34, 36, 41, 46, 47, 120, 386, 390
- Adjoint, 88
- Hamiltonian, 288
- Amplification, 366
- photon, 366
- Amplitude, 8, 12, 22
- operator, 31
 - probability, 30
 - matrix, 355
 - resolvent, 213
 - scattering, 323, 324, 329–333, 340, 359, 369
 - spin-flip, 377
 - transition, 31, 62, 243–245, 310
- Angular
- distribution, 140, 367, 368
 - part, 68
- Angular momentum, 138, 148, 154, 227
- states, 232
- Anticausal wave equation, 294–296
- Approximation
- dipole, 1, 8, 18, 45, 245
 - generalized rotating wave, 190
 - Markov–Born rotating wave, 189
 - memoryless, 203
 - quasi-energy shell, 190
 - random phase (RPA), 103
- Approximation (*continued*)
- rotating wave, 348
 - single electron, 73
- Asymptotic
- series, 77
 - wavefunction, 325
- Atom, 1, 18
- field Hamiltonian, 18–28, 121
 - hydrogen, 90–102
 - nonhydrogenic, 102–117
 - target, 67
- Atomic
- core, 74
 - frequency, 63
 - Green’s function, 68
 - Hilbert space, 217, 249
- Autler–Townes effect, 301, 302
- Average, marginal, 196, 197
- Bessel
- function, 74, 326
 - generalized-function, 11
 - identity, 326, 333, 339, 340, 343
- Biorthonormal
- properties, 252, 256
 - system, 253
- Bohr
- frequency, 317
 - radius, 327
- Born
- first-amplitude, 343
 - first-approximation, 343, 344
 - matrix element, 343
 - second-amplitude, 344–346
 - Breit–Zelz form, 357
- Brillouin–Wigner perturbation expansion, 224

- Canonical
 coordinates, 2–4
 momenta, 2–4
 variables, 14–16
- Causal, 294
 wave equation, 294–296
 wave function, 296–298
- Chain Hamiltonian, 237–244
- Charged particles, 1
- Coherence time, 209
- Coherent, 183
 superposition, 183
- Commutation relation, 24
- Commutator, 15
- Complex Rabi frequency, 149
- Continued-fraction, 213–218
 matrix, 202
 perturbation theory, 213
 representation, 214, 221, 227
- Continuum, 67, 145
 p -wave, 67, 145
 states, 67, 137, 147, 300
- Coordinate
 normal, 23, 24
 rotation of, 305–307
- Coulomb, 69, 78
 continuum state, 90
 phase shift, 74, 90, 93
 problem, 74, 96
 radial-Green's function, 69–74, 96, 97
- Sturmian, 78
 system, 67
 wave function, 93
- Coupled inhomogeneous radial equation, 226–228
- Cross section, 67, 92–97
 differential, 92, 330
 inelastic, 365
 ionization, 92–95, 96–116
 radiative, 334
 stationary, 330
- Dalgarno–Lewis IDE method, 224, 225, 228, 230
- Decay probability, 287, 299
 multiphoton-induced, 299, 300
- Delta function, 122
 energy conserving, 32, 33, 48, 54
- Density matrix, 183–185, 189–191, 347
- Density of states, 49, 66, 145, 148
- Denumerable set, 67
- Detuning, 120
- Diagram, 34, 35
 rules for constructing, 35–44
 topologically distinct, 37
- Diagrammatic method, 34
- Differential, 67
 inhomogeneous equation (IDE), 67–68, 79–82, 89, 96, 103
 ionization cross-section, 92–95
 stochastic-equation, 194
- Dipole
 approximation, 1, 8–10, 18, 45, 245, 248, 307
 operator, 32, 45, 55, 67
 radiation field, 327
- Dilatation, 287, 310
- Distribution
 angular, 367, 368
 probability, 137–140, 347
 steady-state, 352–355
 target-state, 347–352
- Doppler effect, 157
- Dressed
 frequency, 25–27
 oscillator, 18–25
- Dynamic
 Stark effect, 180, 197
 Stark shift, 34, 192, 224, 318
- E*-plane, 306, 310, 311
- Effect
 photoelectric, 73
 Stark, 180, 197
- Effective
 alkali-like one-electron atoms, 73
 Hamiltonian, 62, 143, 157, 161, 166–168, 170, 175, 176, 317–321
- Eigenenergy, 75
- Eigenstates, 186, 245
- Eigenvalue, 245
 equation, 16
- Einstein A coefficient, 188
- Elastic
 resolvent, 216
 scattering processes, 35
- Electron, 1
 field interaction, 4
 free, 10–12
 gas, 20
- Emission, 32
 amplitude, 32–34, 220

- Emission (*continued*)
multiphoton, 217, 220, 256
single-photon, 32, 220, 261
spontaneous, 183, 188
stimulated, 44
two-photon, 34
- Energy, 13
bound state, 75
domain, 245, 250
excitation, 15
interaction, 143
photon, 21, 26
shift, 60–63
spectrum, 78
zero-point, 16
- Evolution
matrix, 254
operator, 254
- Excitation, 183
continuous, 152
- Expansion, linked-cluster, 57, 58
- Expectation value, quantum, 184
- Fano asymmetry parameter, 151
- Field
electric, 2, 18, 32
electron-interaction, 4
external-strength, 143
high-strength, 213
laser, 7, 10–12, 324, 336
magnetic, 2
momentum, 14–17
photon, 12
radiation, 1, 3, 15–17
stationary, 143
stochastic, 194
time-dependent, 143
two-mode, 25, 41
vacuum, 16, 183
- Floquet
determinant, 755
equation, 247, 250, 264, 272, 337–341, 348
Hamiltonian, 123, 126, 127, 245, 248, 250, 257, 263, 307, 317–322
method, 213, 245, 273–275, 282
Schrödinger equation, 255–257
states, 256
theorem, 247, 265
zones, 267
- Fluctuation, laser, 183
- Fock–Krylov Theorem, 287, 296
- Fokker–Planck equation, 199, 205
- Fourier
expansion, 275
series, 247
transform, 56
- Fraction, polarization, 117
- Friedrichs–Fano model, 140, 141
- Function
Bessel, 11, 74, 326
confluent hypergeometric, 70, 72, 78
delta, 32, 33, 48, 54, 122
gamma, 69, 70
hypergeometric (Gauß), 71, 93
line shape, 49
periodic, 246
Whittaker, 69, 76, 77
- Gamma function, 69, 70
- Gauge
Coulomb, 6
invariance, 5, 6
length, 12, 31
radiation, 6
transformation, first kind, 5
transformation, second kind, 6, 9
transverse gauge, 6
velocity, 8, 10, 111
- Gaunt factor, 94
- Gaussian
Doppler profile, 157
fluctuation, 194
forces, 205
Markov assumption, 206
process, 194–205
random force, 198
- Gauss–Pollaczek quadrature, 308
- Green's function, 327, 328, 339, 340, 356, 371, 372
outgoing, 74
pseudopotential, 77–79
radial coulomb, 68–74
- Hamiltonian, 1, 4, 6, 70, 121, 235, 238
atom-field, 18–28, 121
effective, 62, 143–144, 161, 166–168, 170, 175, 176, 317–322
Floquet, 123, 126, 127, 245, 248, 250, 257, 263
- Friedrichs–Fano, 132
- interaction, 8, 9, 131

- Hamiltonian (*continued*)**
- model, 68, 131
 - multiphoton, 143
 - non-Hermitian, 288, 289, 291, 293
 - operator, 15
 - N*-particle, 246
 - reference, 338
 - rotated, 307–312
 - unperturbed, 214, 307
- Harmonic, 11**
- expansion, 12
 - oscillator, 14–16
 - spherical, 68, 77
 - third, 42
- Heisenberg picture, 17
- Herman–Wallis rotational factor, 259
- Hermite polynomials, 201
- Hermitian Hamiltonian, 186
- Hilbert space, 264, 272
- atomic, 217, 249
- Hill
- determinant, 265
 - equation, 264
- Hille–Hardy formula, 72
- Hydrogen atom, 89
- multiphoton ionization, 90–92
- Hydrogenic
- energy values, 70
 - Hamiltonian, 307
 - orbitals, 71
 - wave function, 70
- Hypergeometric function
- confluent, 70, 72, 78
 - Gauss, 71
 - generalized, 93
- Incoherent, mixture, 184
- Inelastic, resolvant, 217
- Infrared, excitation spectra of CO, 257–264
- Integral representation, 64
- Interaction, 63
- atom-field, 346, 347
 - energy (mean), 247
 - Hamiltonian, 8, 9
 - operator, 18, 23, 28
 - picture, 30, 31
 - stationary, 143
 - time, 63
 - time-dependent, 143
- Intermediate
- detuning, 63
- Intermediate (*continued*)**
- picture, 129
 - resonance, 144, 234, 235
 - state, 54
- Ionization, 89**
- cross section, 92–95, 96–116
 - multiphoton, 49, 90–92
 - nonresonant multiphoton, 89
 - probability, 152, 299, 300
 - rate, 50, 152
 - three-photon, 97–102
 - threshold-energy, 89
 - two-photon, 92–97, 111
- Iteration, inverse, 316**
- Jacobi–Anger formula, 11
- Jacobi tridiagonal form, 240
- J-level system, 264
- J-matrix, 241, 308
- Kubo–Liouville equation, 195, 196, 206
- Lagrange expansion, 61
- Laguerre polynomial, 72, 208, 308
- Lamb shift, 188, 189, 193
- Lanczos method, 237, 238
- Langevin equation, 199, 205
- Laplace transform, 56, 202–205
- Laser
- approximation, 128, 130, 249, 256, 323, 324
 - constant amplitude, 7
 - continuous-wave, 352
 - field, 18–28, 324, 336
 - fluctuation, 183
 - monomode, 7, 8, 18, 48, 198
 - multimode, 22–25
 - pulsed, 8, 252
 - two-mode, 25–27
- Length
- form, 9, 27
 - gauge, 12, 31
- Light field, 14
- Level-shift operator, 223, 226, 237
- Limit
- long-time, 65
 - low-frequency, 361
- Limiting property, 64
- Line shape function, 49
- Linked-cluster expansion, 57, 58
- Liouville’s theorem, 268

- Lorentz
 equation, 2
 force, 2
 Lorentzian, 199
- Magnus expansion, 277–282
- Marginal averages, 196
- Markov Born rotating wave approximation (RWA), 189
 process, 195, 205
- Master
 equation, 189, 195, 205
 operator, 197
- Matrix
 evolution, 254
 unitary, 253
- Method
 chain Hamiltonian, 237–244
 density matrix, 183
 diagrammatic, 34
 Floquet, 213, 317–322
 of inhomogenous differential equations (IDE), 67, 68, 79–82, 89, 96, 224–228, 230
 J-matrix, 241
 Lanczos, 237–238
 of pseudocontinuum basis, 79–85, 89
 recursive-iterative solution, 222
 resolvant equation, 119
 truncated summation, 85–87
- Minimal-coupling prescription, 1–4, 18
- Mixture, 349
 incoherent, 183
- Mode, 23
 two-field, 25–27
 two-problem, 235–237
- Model, 130, 131
 Friedrichs–Fano, 140–141
 monomode laser field, 198, 199
 multimode laser field, 205, 206
 resonance, 199–205
- Momentum, 1, 14
 field, 16
 operator, 17, 246, 336
 transfer, 333
- Multichannel electron-atom scattering, 336
- Multimode laser, 22, 205, 206
- Multiphoton
 absorption, 119
 eigenvalue problem, 222, 312–317
 Hamiltonian, 119, 305
- Multiphoton (*continued*)
 ionization of hydrogen, 89–102, 300–305
 ionization of non-hydrogenic atoms, 102–117
 process, 119, 245
 resonant-processes, 119, 191, 245
 wave vector, 213
- Nondegenerate secular equation, 268–270
- Non-Hermitian
 Hamiltonian, 186–190, 287–289, 291, 293
 Floquet method, 317–322
- Nonresonant
 path, 144, 154
 state, 143, 159
- Normalization
 Volume L^3 , 6, 17, 22, 137, 147
- Observable, 184
- One-resonance resolvant equation, 147–149
- Operator, 15
 annihilation, 15–18, 21, 25, 33
 creation, 15–18, 21, 25, 33
 evolution, 31, 254
 Hamiltonian, 15
 interaction, 18, 23, 38
 level-shift, 223–226, 237
 momentum, 246, 336
 multipole, 71
 noncommutable, 15
 projection, 159, 213
- Optical potential, 287, 293–296
- Oscillator
 dressed, 18–27
 harmonic, 14, 16
 quantum, 15
 vacuum, 16
- Partial wave, 138
- Particle, charged, 1
- Partition function, 259
- Path
 nonresonant, 144
 quasi-resonant, 144
- Periodic function, 246
- Perturbation
 breakdown of theory, 119–121
 Brillouin–Wigner thoery, 224
 continued fraction theory, 213
 series, 32

- Perturbation (*continued*)

 theory, 119, 213

 time-dependent theory, 29–34, 172
- Phase, 7, 11, 12, 246

 factor, 6, 30

 random, 255

 shift, 74
- Photon, 12

 absorption coefficient, 366

 field, 12–18

 flux, 38, 50, 92
- Photoelectric effect, ordinary, 73
- Plane wave, 6–7
- Plasma frequency, 20, 21
- Polarization

 circular, 8, 11, 81, 91, 324–328, 331, 337, 338

 linear, 8, 10, 81, 91, 92, 324–328, 337, 338, 342

 vector, 7, 22, 26, 33, 235, 246, 324
- Potential

 effective, 69

 scalar, 1, 2

 scattering, 324, 325

 vector, 1, 2, 6, 7, 10, 13, 17–19, 22, 27, 246, 336
- Poynting vector, 14
- Prescription, minimal coupling, 1–4, 18
- Probability

 distribution, 137–141, 176–181, 301

 of multiphoton-induced decay, 299, 300
- Process

 multiphoton, 1, 9, 19, 29, 34, 40, 143

 nonresonant, 63

 resonant, 143
- Projection operator, 159, 213
- Propagation

 of light, 6–8

 vector, 7, 246
- Propagator, 34, 176
- Pseudocontinuum-basis, 67
- Pseudopotential, 331

 Green's function, 77–79
- Pure state, 183, 349
- Quantization, 4

 first, 4

 second, 14–18

 volume, 22
- Quantized

 field strengths, 17
- Quantized (*continued*)

 vector potential, 17
- Quantum

 beats, 304

 defect, 73

 defect method (QDM), 73–77

 expectation value, 184

 number, 246

 principal number, 72, 73, 78
- Quasi-quantum

 envelope equation, 170
- Quasi-resonant

 level, 145

 path, 144

 state, 143–145, 160, 162
- Rabi

 formula, 150

 frequency, 149, 150, 260, 348, 350

 oscillation, 153, 301, 302, 304
- Radial

 Coulomb Green's function, 69–72

 equations, 226, 233, 236
- Radiation

 dipole-field, 327

 field, 1, 13, 15–17

 gauge, 6
- Radiative

 Born amplitudes, 343, 344

 elastic scattering, 350

 scattering amplitudes, 369–373
- Radius of vibration, 11, 325
- Random phase approximation (RPA), 103
- Rate equation, 181
- Recurrence relation, 213

 three-term, 214, 219
- Recursive-iterative wave equations, 228–231
- Reduced

 chain, 244

 T -matrix, 66
- Relaxation, spontaneous, 183, 186
- Renormalization

 energy, 60–62

 perturbation, 53–55, 172
- Renormalized

 rate, 62, 65

 T -matrix, 59
- Representation

 closed-form, 73

 integral, 71

- Representation (continued)**
- Sturmian, 71–73
 - Resolvent, 55–56, 213–215, 231
 - elastic, 216
 - equations, 119, 127, 134, 147, 214
 - inelastic, 217
 - semiclassical, 126
 - Resonance, 119–121, 199
 - intermediate, 144, 234, 235
 - path, 144, 154
 - Resonant
 - process, 143
 - states, 159
 - Retardation, 247–249
 - effects, 71
 - Retarded Hamiltonian, 133
 - Rotating wave approximation, 348
 - generalized, 190
 - Markov–Born, 189
 - Rovibrational Floquet Hamiltonian, 257–264
 - Rule
 - for diagrams, 35–45
 - for transition amplitudes, 45–47
 - golden, 48
 - Rydberg
 - energy levels, 70, 100
 - formula, 73, 75
 - Scaling law, 96
 - Scattering
 - amplitude, 323, 324, 329–332, 340
 - elastic, 333, 362
 - electron-atom, 323, 324, 336, 383
 - potential, 324, 325, 357, 361
 - radiative, 323–325, 331, 338, 347, 369, 373, 382
 - subthreshold, 363
 - Scattered
 - wave, 329, 330
 - wave number, 333
 - Schrödinger
 - equation, 4–6, 27, 28, 121–124, 173, 174, 221, 222, 237, 240, 245, 248–250, 274, 337, 356, 379
 - picture, 17
 - representation, 17, 121
 - time-dependent-equation, 158
 - Secular equation, nondegenerate, 268–270
 - Selection rules, angular momentum, 89
 - Semiclassical
 - approximation, 4
 - Semiclassical (continued)
 - field, 121, 330
 - interaction, 9
 - interaction operator, 213
 - Set, denumerable, 67
 - Shift
 - energy, 60, 61
 - Lamb, 188, 189, 193
 - level-operators, 223–226, 237
 - phase, 74
 - Stark, 34, 192, 193, 211, 224, 318
 - Singular ζ -function, 63
 - Signal radiative elastic scattering, 350, 351
 - Slater orbitals, 71
 - Spectrum
 - energy, 78
 - experimental, 79
 - Spherical harmonics, 68, 77
 - Spontaneous
 - emission, 183, 188, 189
 - relaxation, 183, 188, 191
 - State
 - continuum, 67
 - discrete, 66, 67
 - intermediate, 144
 - nonresonant, 143
 - pure, 183, 349
 - quasi-resonant, 143
 - resonant, 144
 - vector, 213
 - Stark
 - dynamic-shift, 34, 155, 192, 252, 253
 - effect, 180, 197
 - Stationary
 - equation, 256
 - solution, 207, 252, 253
 - state, 33
 - Statistical weights, 184
 - Steady-state, 350–355
 - Stimulated emission, 44
 - Stochastic
 - differential equations, 194
 - fields, 194
 - Sturmian
 - Green's function, 97, 100
 - representation, 71–73
 - Superposition, 6
 - coherent, 183
 - System, isolated, 183–184
 - Target
 - excitation, 363

- Target** (*continued*)
 state distribution, 347, 352
- Third harmonic**, 42
- Time-varying effective Hamiltonian**, 168–170
- Time-dependence of H-atom transitions**, 300–305
- Topologically distinct diagrams**, 37–44, 386–390
- Transform**
 Fourier, 56
 Laplace, 56, 202–205
- Transformation**
 twin, 250
 unitary, 27
- Transition**
 amplitude, 31, 45, 62, 67, 243, 293, 298, 310, 311
 continuum-continuum, 218
 dipole, 188
 energy, 4
 multiphoton, 47, 62, 63, 67, 194
 operator, 47, 58
 probability, 63, 213, 256
 process, 45
 rate, 47, 49, 63–66, 304
 rearrangement-matrix, 373
 rules, 45, 46
 three-photon, 303
 time-dependent amplitude, 298
 two-photon radiative, 71
- T-matrix**, 57–59, 218, 377
 element, 79
 reduced, 219
- Types of physical transitions**, 134, 141
 bound-bound (excitation), 134, 141, 149, 152, 298, 299
 bound-free (ionization), 134, 137, 141, 149, 298, 299
 free-bound (capture), 134, 141
- Types of physical transitions** (*continued*)
 free-free (scattering), 134, 141
- Unitary matrix**, 253
- Unitary transformation**, 27
- Unperturbed**
 Hamiltonian, 214
 resolvent, 218
- Vacuum field**, 16, 183
- Vector**
 multiphoton wave, 213
 Poynting, 14
 solution, 271
- Velocity**, 2–4
 gauge, 8, 10
- Volume normalization- L^3** , 6, 17, 22, 137, 147
- von Koch's theorem**, 266, 269
- Wave**
 Maxwell's equation, 6
 discrete-function, 75
 function, 4, 6, 10–12, 30, 55, 71–73, 183–186, 229, 247, 251, 295
 light, 6–8, 12–14
 multiphoton-vector, 213, 222
 partial-expansion, 138
 plane, 6, 7
 scattered, 329
 stationary-function, 221
- White noise**, 198
- Whittaker**
 irregular-function, 69, 76, 77
 regular-function, 69
 standard form, 69
- Width**, 135, 287
- Zero-point energy**, 16